

Development of a Metabolically Innocuous Aniline Isostere Enabled by Photoredox Catalysis

by

Taylor Marie Sodano

A dissertation submitted in partial fulfillment
of the requirements for the degree of
Doctor of Philosophy
(Chemistry)
in the University of Michigan
2020

Doctoral Committee:

Professor Corey R. J. Stephenson, Chair
Associate Professor R. Keith Duncan
Professor Melanie S. Sanford
Associate Professor Corinna S. Schindler

Taylor Marie Sodano

tsodano@umich.edu

ORCID iD: 0000-0001-7040-0331

© Taylor Marie Sodano 2020

DEDICATION

*To my grandmothers,
who have always been models of remarkable
strength, resilience, and love.*

Acknowledgements

It should go without saying that none of the work presented in this thesis would be possible without the continued support and guidance of my committee: Prof. Corey Stephenson, Prof. Melanie Sanford, Prof. Corinna Schindler, and Prof. Keith Duncan. Corey was the one to call me to inform me that I had been accepted to Michigan for graduate school, and he was also kind enough to let me come to not one, but two visitation weekends. Throughout my rotation and dissertation work, Corey has always been supportive of my interests and let me explore whatever research direction I thought was necessary to advance the project. I would be remiss if I did not thank Melanie for always willing to share her vast knowledge to better focus my research efforts, and for being especially supportive during the job application process. I must thank Corinna for allowing me to complete my winter rotation in her lab and for always having an open door to discuss anything on my mind. Of course, last but not least, I am so grateful to not only have Keith on my committee, but for taking on a secondary advisor role to me. Keith also placed an inordinate amount of trust in me, whether that was to not contaminate the shared cell culture room or mentor undergraduates in his lab. There aren't words to describe how much I learned from him and how valuable our collaboration was to my development as a scientist and as a human being.

While my committee has been invaluable to my graduate work, those who scientifically supported me prior to graduate school have played a large role in this story. My very first chemistry

lesson was with Mr. Doug Smith in high school, who I thought was joking when he said “stoichiometry” was a real word. Despite that, he sponsored me in a work-study program my senior year, in which I prepared reagents for demos in his classroom, and then nominated me for a substantial scholarship to attend the University of Rochester. Once I was a junior at Rochester, I attended a seminar in which the third-year graduate students gave talks about their research, and I not only thoroughly enjoyed a particular talk about the total synthesis of FK-506, but I recognized the speaker as Kyle Biegasiewicz. Prior to this moment, I only knew Kyle as a frequent customer of mine at Starbucks, and it only took me several weeks to gather the courage to tell him I intrigued by his talk and was interested in undergraduate research opportunities. Through Kyle, I connected with his Ph.D. advisor, Prof. Robert Boeckman, Jr., and completed a summer REU and my senior thesis in his lab.

I would not be the scientist I am today without the support from everyone I worked with in the Stephenson lab: Dr. Verner Lofstrand, Dr. Xu Zhu, Dr. Markus Kaerkaes, Dr. Irene Bosque-Martinez, Dr. Dirk Alpers, Dr. Daryl Staveness, Dr. Logan Combee, Dr. Maddie Snowden, Dr. Mitch Keylor, Dr. Joel Beatty, Dr. Tim Monos, Martin Sevrin, Theresa Williams, Dr. Gabe Magallanes, Dr. Rory McAtee, Dr. Alex Sun, Dr. Kevin Romero, Matt Galliher, Ted McClain, James Collins, Efrey Noten, Anthony Allen, Cheng Yang, Bec Roldan, Alex Harmata, and Alan Wortman. For undergraduates on Team AminoNB, I have to thank the incredible hard work of Annika Tharp, Alyiah Chmiel, and Alexander Levashkevich. I learned and grew from individual discussions on a daily basis, but also from weekly group meetings where I absorbed so much information about the disparate areas of research within the lab.

I have a special shout-out to Alex, Rory, and Kevin, who were in my cohort and always supplied a sympathetic ear to whatever was going on over the last 5 years. Daryl was my mentor

and was overall a good match because we each have perfectionist tendencies and high personal expectations. He also made me into a flash column chromatography wizard. All other members of the “middle bay” are acknowledged for their respective contributions. Specifically, I felt like I never had to go see a movie because Matt has an exceptional repertoire of pop culture that he is more than happy to enact out. With Efrey, I was never behind on the most current meme, which I assuredly (and embarrassingly) found hilarious. I think the addition of Bec to the “middle bay” will create the perfect storm of Millennial/GenZ humor and I look forward to hearing about their future shenanigans and successes.

How do I write a section to acknowledge the unconditional, unquestioning support of my family? I know I am so lucky to have a family that accepts me no matter what. So, Mom and Dad, thank you so much for always nurturing my love of science, emotionally and financially enabling me to become a first-generation college student, and consistently providing encouragement to be the best that I can be. Kyle, Nicholina, and little GiGi - I am so happy to have you in my life, and I cannot wait to start reading “Organic Chemistry for Babies” to my niece and making mud pies in the driveway together. A new addition to my family since starting graduate school is my partner, Christopher, and our two cats, Hendricks and Harper. Christopher gave me strength every step of the way, always believed in me, and at times was more confident in my abilities than I was. He has been unrelenting with his support and has offered his expert judgement on my ChemDraws countless times. I look forward to this new chapter of our life and the continuation of dressing cats up in sweaters together.

Table of Contents

DEDICATION.....	ii
ACKNOWLEDGEMENTS	iii
LIST OF FIGURES	xi
LIST OF TABLES	xvii
ABSTRACT.....	xviii
Chapter 1. Recent Advances and Outlook for the Isosteric Replacement of Anilines	1
1.1 Introduction to Aniline Isosterism.....	1
1.2 Current Approaches to Aniline Isosterism	3
1.3 Outlook.....	6
1.4 References	8
Chapter 2. Providing a New Aniline Isostere Through the Photochemical Production of 1-Aminonorbornanes	11
2.1 Introduction	11
2.1.1 Introducing sp ³ -Content in Pharmaceutical Development	11
2.1.2 Previous Approaches to AminoNBs.....	12
2.1.3 Background and Synthetic Utility of Amine Oxidation.....	13
2.2 Results and Discussion.....	16

2.2.1 Optimization	16
2.2.2 Differential Pulse Voltammetry	19
2.2.3 Quantum Yield Measurements	24
2.2.4 Stern-Volmer Luminescence Quenching Analysis	25
2.2.5 Reaction Scope	27
2.2.6 Continuous Flow Processing	32
2.3 Conclusion.....	37
2.4 Experimental Procedures and Characterization of Compounds.....	38
2.4.1 General Methods	38
2.4.2 Reaction Optimization.....	40
2.4.3 Differential Pulse Voltammetry	47
2.4.4 Quantum Yield Calculations	50
2.4.5 Excited State Quenching Studies.....	53
2.4.6 Batch and Continuous Flow Processing.....	57
2.4.7 Experimental Methods.....	71
2.5 References	241
Chapter 3. Examining Multiple Modes of Diastereoselectivity in the Synthesis of 1-	
Aminonornornanes	247
3.1 Introduction.....	247
3.2 Results and Discussion.....	250
3.2.1 C3 Diastereoselectivity.....	250
3.2.2 C7 Diastereoselectivity.....	251
3.3 Conclusion.....	258

3.4 Experimental Procedures and Characterization of Compounds.....	259
3.4.1 General Methods	259
3.4.2 Reaction Optimization.....	261
3.4.3 Preparation of AminoCPs.....	266
3.4.4 Photochemical Conversion of AminoCPs to AminoNBs.....	276
3.4.5 Mechanistic Studies.....	293
3.5 References	299
Chapter 4. Re-Engineering the Acrylamide S1 Scaffold by Substitution of 1-	
Aminonorbornanes in Metabolic Hotspot	302
4.1 Introduction	302
4.2 Synthesis of C7 Analogs 4.10 and 4.11	307
4.2.1 First-Generation Synthesis	307
4.2.2 Second-Generation Synthesis.....	312
4.2.3 Third-Generation Synthesis.....	316
4.3 Synthesis of C3-Axial Analogs 4.12 and 4.13	318
4.4 Efforts Towards the Synthesis of C3-Equatorial Analogs 4.16 and 4.17	321
4.5 Efforts Towards the Synthesis of C7-Methylene, C3-Axial Analogs 4.14 and 4.15	324
4.6 Synthesis of C4 Analog 4.18	328
4.7 Efforts Towards the Synthesis of C2 Analogs 4.19 , 4.20 , 4.21 , and 4.22	329
4.8 Future Directions: Developing a Second-Generation Library	331
4.9 Experimental Procedures and Characterization of Compounds.....	334
4.9.1 General Methods	334
4.9.2 Synthesis of C7 Analogs and Intermediates.....	337

4.9.3 Synthesis of C3-Axial Analogs and Intermediates.....	367
4.9.4 Synthesis of C3-Equatorial Analog Intermediates	373
4.9.5 Synthesis of C3-Axial, C7-Methylene Analog Intermediates	380
4.9.6 Synthesis of C4 Analog and Intermediates	384
4.9.7 Synthesis of C2 Analog Intermediates	396
4.9.8 X-Ray Crystallographic Data	401
4.10 References	427
Chapter 5. Evaluation of Metabolic Stability and KCNQ Agonism Activity of 1-	
Aminonorbornane Analogs.....	430
5.1 Metabolic Behavior of Anilines	430
5.1.1 Metabolic Processing of Acrylamide S1	431
5.2 Evaluation of AminoNB Metabolic Stability.....	434
5.2.1 Microsomal Stability Assays and Metabolite Identification on AminoNB Model Systems	434
5.2.2 Microsomal Stability Assay and Metabolite Identification of AminoNB Analogs	436
5.3 Evaluating AminoNB Analogs for KCNQ Agonism Activity.....	439
5.3.1 Background on KCNQ Ion Channels: Physiology and Role in Disease	439
5.3.2 Overview of Whole Cell Electrophysiology.....	444
5.3.3 KCNQ Agonism Activity of Acrylamide S1	446
5.3.4 Preliminary Evaluation of AminoNB Analogs as KCNQ Agonists	447
5.3.5 Future Directions	451
5.4 Experimental Procedures and Characterization of Compounds.....	453
5.4.1 Preparation of Compounds	453

5.4.2 Evaluation of Metabolic Stability	461
5.4.3 Manual Whole Cell Electrophysiology.....	478
5.5 References	481

List of Figures

Figure 1.1. Meta-analysis of reactions appearing in <i>J. Med. Chem.</i> in 2014.....	2
Figure 1.2. Examples of (A) bicyclo[1.1.1]pentane, (B) bicyclo[2.2.2]octane, and (C) cubane in benzene isosterism efforts in drug discovery and lead optimization	4
Figure 1.3. (A) Saturated isosteres of aniline to overcome metabolic liability; (B) Strain-driven photochemical synthesis of aminoNBs.....	6
Figure 2.1. Previous synthetic approaches towards aminoNBs.....	12
Figure 2.2. Examples of (A) Heterolytic and (B) Homolytic decomposition pathways of amine radical cations	14
Figure 2.3. Select examples of strain-driven homolysis of aminoCPs	15
Figure 2.4. Proposed mechanism for the synthesis of aminoNBs from aminoCPs	16
Figure 2.5. Summary of reaction optimization	17
Figure 2.6. Initial hypothesis for the mechanistic role of Lewis acids	19
Figure 2.7. Summary of voltammetry data for various trialkyl amines.....	20
Figure 2.8. Measured peak oxidation potentials of aminoCP 2.14 in the presence and absence of LiBF ₄	23
Figure 2.9. (A) Emission spectra of photocatalyst 2.16 in the presence of varying concentrations of aminoCP 2.14 ± 20 mol% LiBF ₄ ; (B) Stern-Volmer luminescence quenching analysis	26
Figure 2.10. Scope of trialkylamines	27
Figure 2.11. Substitution accessible on the norbornane core.....	28
Figure 2.12. Proposed pathway toward bicyclo[3.2.0]heptane by-product 2.38	30

Figure 2.13. Stereochemical model for the high diastereoselectivity observed in allylic-substituted aminoCPs.....	31
Figure 2.14. Results and stereochemical model for aminoCPs of form 2.49	32
Figure 2.15. (A) Adaption of small-scale batch reaction to continuous flow processing; (B) Comparison of batch and flow reactors on gram scale	34
Figure 2.16. Effects of LiBF ₄ on the oxidation potential of morpholine-derived systems	48
Figure 2.17. Effects of LiBF ₄ on the oxidation potential of piperidine, piperazine, and prolinol scaffolds	49
Figure 2.18. Summary of differential pulse voltammetry data (vs. Ag/AgCl values).....	50
Figure 2.19. Summary of excited state quenching data for photocatalyst 2.16 and aminoCP 2.14	53
Figure 2.20. Excited state quenching data	55
Figure 2.21. Continuous flow processing equipment	58
Figure 2.22. Full flow apparatus	59
Figure 2.23. Continuous flow reaction vessel.....	60
Figure 2.24. Large-scale batch processing apparatus	61
Figure 2.25. Small-scale batch processing equipment.....	62
Figure 2.26. Small-scale evaluations of formal [3+2] cycloadditions in continuous flow	63
Figure 2.27. Large-scale batch processing results	67
Figure 3.1. Stereochemical models for chiral induction via substrate control.....	249
Figure 3.2. (A) Mechanism of [3+2] photochemical cyclization of aminoCPs to aminoNBs....	250
Figure 3.3. Computational evaluation of C3 diastereoselectivity (CBS-QB3).....	251
Figure 3.4. (A) AminoCPs evaluated to probe diastereomeric outcomes; (B) Proposed transition state model for observed diastereoselectivity	252
Figure 3.5. Unfavorable gauche interaction towards <i>7R,8R</i> product hinders electrostatic interaction	252

Figure 3.6. Relationship between electron donating ability of the C8 substituent and diastereomeric ratio of aminoNB products	253
Figure 3.7. Energy coordinate diagram with two transition state models.....	254
Figure 3.8. (A) ¹ H NMR observation of reversibility between 3.18-7R and 3.18-7S ; (B) Attempted reversibility between 3.22-7R and 3.22-7S	257
Figure 3.9. Plot of percent yield of aminoNB 3.31 over time as determined by ¹ H NMR.....	262
Figure 3.10. Proposed pathway for the formation of tetracycle 3.32	264
Figure 3.11. (A) Structure of photocatalyst; (B) Side and top view of reaction set up	277
Figure 3.12. ¹ H NMR spectra monitoring reversibility of photochemical cyclization of aminoNB 3.18-7R over 3 h	296
Figure 3.13. ¹ H NMR spectra monitoring reversibility of photochemical cyclization for aminoNB 3.22-7R over 2 h.....	298
Figure 4.1. Discovery of acrylamide S1 (AS1).....	302
Figure 4.2. Synthesis of AS1	303
Figure 4.3. SAR study of AS1 active pharmacophore.....	305
Figure 4.4. Overlay of energy minimized structure of AS1 and C3 aminoNB 4.12	305
Figure 4.5. First-generation library of AS1 aminoNB analogs.....	306
Figure 4.6. Synthesis of <i>7S</i> , <i>8R</i> aminoNB 4.30	307
Figure 4.7. Alcohol 4.30 is resistant to substitution due to blocked backside approach	308
Figure 4.8. Incorporation of amine functionality prior to photochemical cyclization.....	309
Figure 4.9. Completion of analogs 4.36 and 4.10	310
Figure 4.10. Comparison of ¹ H NMR spectra of AS1 and 4.36	311
Figure 4.11. Computational modeling of low energy conformers of 4.36 and 4.37	312
Figure 4.12. (A) Retrosynthetic analysis of first-generation approach; (B) Proposed disconnection for second-generation synthesis.....	313

Figure 4.13. (A) Synthesis of PTS 4.39 ; (B) Synthesis of aldehyde 4.40 and results of the modified Julia-Kocienski olefination.....	314
Figure 4.14. (A) Photochemical cyclization generates both C7 diastereomers; (B) Removal of Boc group and failed attempts at debenzoylation.....	315
Figure 4.15. (A) Third-generation synthesis employing 2,5-dimethylpyrrole as a nitrogen protecting group; (B) Pyrrole deprotection and completion of 4.11 synthesis.....	317
Figure 4.16. Comparison of x-ray crystal structures of 4.35 and 4.60	318
Figure 4.17. Branched olefins will not undergo ligand exchange to form substituted aminoCPs.....	318
Figure 4.18. Synthesis of aminoCPs 4.65 and 4.66 for C3-axial aminoNBs.....	319
Figure 4.19. Second half of C3-axial analog syntheses (A) 3 <i>R</i> 4.12 and (B) 3 <i>S</i> 4.13	320
Figure 4.20. Epimerization strategy to access C3-equatorial substitution.....	321
Figure 4.21. (A) Preliminary studies towards C3-equatorial analogs; (B) Selectivity in the reduction of 4.78 is partially controlled by substrate.....	323
Figure 4.22. (A) Example of C7 decarboxylation to access C7 methylene aminoNB; (B) Retrosynthetic analysis for synthesis of C3-axial, C7-methylene aminoNB analog.....	325
Figure 4.23. Preliminary studies towards C3-axial, C7-methylene analogs.....	326
Figure 4.24. Synthesis of C4 analog 4.18	329
Figure 4.25. Studies toward the synthesis of C2 analogs.....	330
Figure 4.26. (A) p <i>K</i> _a values of protonated tertiary amines and their corresponding %ionization at pH = 7.4; (B) Experimental determination of p <i>K</i> _a and log <i>D</i> (at pH = 7.4) for propranolol derivatives with electron-withdrawing groups.....	332
Figure 5.1. General scheme for the metabolic processing of anilines by CYP450s.....	430
Figure 5.2. Structure-metabolism studies of AS1 identifies aniline as source of reactive metabolite formation.....	433
Figure 5.3. Panel of anilines and aminoNBs evaluated in microsomal stability assays; graphical depiction of compound retention after 45 min incubation in the presence of RLMs or HLMs.	435
Figure 5.4. Metabolite identification of 5.13	436

Figure 5.5. Results of microsomal stability assay of RTG , AS1 scaffolds, and C3-axial aminoNB analogs.....	437
Figure 5.6. Metabolite identification of aminoNB analog 5.22	438
Figure 5.7. Schematic representation of a generic potassium ion channel	440
Figure 5.8. Introduction to the KCNQ family of voltage-gated potassium ion channels	441
Figure 5.9. Graph of cell membrane potential over the course of an action potential.....	442
Figure 5.10. The effect of a KCNQ agonist (RTG) and antagonist (XE 991) on neuronal excitability. Figure reproduced from <i>Ref. 24</i>	443
Figure 5.11. Overview of electrophysiology – whole cell configuration	444
Figure 5.12. Mechanism of KCNQ agonism by (A) leftward shift of $V_{1/2}$ and/or (B) increase in conductance.....	445
Figure 5.13. Representative whole cell recording from an (A) untransfected HEK239A cell in extracellular solution of (B) HEK293A cell transiently transfected with hKCNQ2 wt in 0.1% DMSO; (C) Analysis of tail currents from the final voltage step to 0 mV against proceeding test potentials as a normalized I-V Boltzmann curve for 0.1% DMSO and 100 μ M AS1 ; (D) Immunohistochemistry results staining fixed preparations for anti-KCNQ2 and counterstained with Hoechst to reveal cell nuclei.....	448
Figure 5.14. Summary bar graphs representing (A) half-activation ($V_{1/2}$) and (B) I_{max} of hKCNQ2 wt currents calculated from I-V Boltzmann curves at controls and compound treatment groups.....	450
Figure 5.15. Validation of Microsome Source.....	465
Figure 5.16. Complete Microsomal Stability Data Set.....	466
Figure 5.17. Tabular Metabolite Fragmentation Data.....	469
Figure 5.18. HPLC traces of aminoNB 5.13 upon incubation with RLMs and validation of formamide 5.17 identity.....	470
Figure 5.19. Glutathione trials with aminoNB 5.13	470
Figure 5.20. LC/MS/MS trace identifying metabolite 5.23 in RLMs.....	474
Figure 5.21. LC/MS/MS trace identifying metabolite 5.22 in RLMs.....	474
Figure 5.22. LC/MS/MS trace identifying metabolite 5.25 in RLMs.....	475

Figure 5.23. LC/MS/MS trace identifying metabolite 5.24 in RLMs.....	475
Figure 5.24. LC/MS/MS trace identifying metabolite 5.26A in RLMs.....	476
Figure 5.25. LC/MS/MS trace identifying metabolite 5.26B in RLMs.....	476
Figure 5.26. LC/MS/MS trace identifying metabolite 5.26C in RLMs.....	477

List of Tables

Table 3.1. Summary of $\Delta\Delta G^\ddagger$ for identified transition states.....	256
Table 3.2. Results of reaction optimization.....	261
Table 3.3. Summary of stereochemical outcomes.....	265
Table 4.1. Screen of cross metathesis conditions.....	327
Table 5.1. Side-by-side comparison of pharmacokinetic parameters of AS1 and 5.1	432
Table 5.2. (A) CYP450 inhibitory potential of AS1 ; (B) Results of TDI studies of AS1 and 5.1	432
Table 5.3. Reaction mix for metabolite identification	471
Table 5.4. Summary of metabolite identification trials in RLMs, HLMs, and control experiments.....	472
Table 5.5. Final reaction mixture for metabolite identification experiments	473

Abstract

Many promising drug candidates and pharmaceutical compounds fail due to idiosyncratic adverse drug reactions, often arising from the formation of reactive metabolites (RM). Among the many “structural alerts” responsible for these toxicity issues, anilines are well-known to undergo deleterious metabolic processing, yet the ease with which these systems are prepared often outweighs the risks. One common approach to ameliorate RM formation has been to replace the problematic functionality with an isostere that will not undergo adverse metabolic processing while maintaining therapeutic activity. Saturated carbocycles represent an attractive option for the isosteric replacement of anilines as they are more resistant to RM formation. The synthetic challenges presented by densely functionalized saturated architectures generally prohibit their evaluation. The overarching theme of this body of work is the development and application of new and enabling photocatalytic methods for the preparation of compounds capable of mimicking aniline motifs commonly found in drug molecules.

Chapter 1 provides an overview of aniline metabolism and currently available isosteric scaffolds. Many of these reported strategies are limited in application, scope, and diversity. As a response to this problem, our group sought to employ the mild reactivity of photoredox catalysis in the synthesis of a new aniline isostere. Leveraging single electron oxidation of aminocyclopropanes, we were able to efficiently access the 1-aminonorbornane (aminoNB)

scaffold, a saturated bicyclic ring system that offers similar spatial occupancy to that of anilines. Chapter 2 outlines the optimization, functional group compatibility, and scalability of this reaction platform.

During the course of the initial reaction development, several unique mechanistic features were noted, and an in-depth study of the reaction mechanism is presented in Chapter 3. In agreement with experimental studies and computational analysis, C7-diastereoselectivity is controlled by a mode of 1,2-asymmetric induction hinging on an intramolecular electrostatic interaction in the transition-state of the *5-exo-trig* cyclization. A discussion on the role of ZnCl₂ in the reaction mechanism is included, with experimental observations supporting the theory that Lewis acids may operate in multiple capacities to benefit the efficiency of the reaction.

To demonstrate the viability of the aminoNB as an aniline isostere hypothesis, a KCNQ agonist scaffold in preclinical development that has previously been shown to suffer from adverse metabolic processing was re-engineered by incorporating differentially substituted aminoNBs. Using the knowledge obtained from the methodology development and mechanistic study, a first-generation analog library is in development using a modular synthetic approach. Chapter 4 discusses these synthetic efforts and proposes future directions for a second-generation library.

Collaborative efforts to assess the metabolic profile and KCNQ agonism behavior of the analogs are described in Chapter 5. Both model systems and final aminoNB analogs demonstrate enhanced metabolic stability in a standard microsomal stability assay, and preliminary metabolite identification suggests limited propensity for RM formation. KCNQ agonism activity was investigated by manual whole cell electrophysiology, and initial studies reveal promising results.

Taken together, the work presented in this thesis culminates in proof-of-concept for aminoNBs to enact as metabolically innocuous aniline isosteres. Future work will focus on further

optimization of the aminoNB analogs, and biological studies will incorporate a high-throughput screening platform to detect KCNQ agonism activity and selectivity. Given the ubiquity of the aniline motif, similar isosteric strategies could be applied to an array of scaffolds encompassing established drugs to preclinical leads, thereby potentially impacting a wide range of diseases.

Chapter 1

Recent Advances and Outlook for the Isosteric Replacement of Anilines

Portions of this chapter have been adapted from the following publication with permission: Sodano, T.M.; Combee, L.A.; Stephenson, C.R.J. *ACS Med. Chem. Lett.* **2020** DOI.10.1021/acsmchemlett.9b00687. Copyright 2020 American Chemical Society.

1.1 Introduction to Aniline Isosterism

In the last two decades, advancements in automation, technology, and reaction science have shifted the landscape of pharmaceutical development. Among these shifts, the ability to rapidly evaluate chemical entities in high-throughput formats has become standard practice due to enabling technologies in both the synthesis and analysis of new compounds. C-N bond forming protocols have been particularly transformative for discovery efforts. In a meta-analysis of the 20 most common reactions reported in *J. Med. Chem.* publications in 2014, amines appear as ubiquitous reagents (Figure 1.1).¹ Amide bond couplings were the most prevalent class of all reactions tabulated, appearing in 50% of the papers analyzed. Other high usage reactions employing amines include S_NAr (30%) and sulfonamide formation (13%). Buchwald-Hartwig cross couplings are reported in nearly 10% of manuscripts and rank as the 11th (out of 26) most used reaction in the final step of a synthetic sequence. The operational simplicity, high

chemoselectivity, and commercial availability of the required synthetic precursors for these reactions have contributed to the enrichment of Csp² content in pharmaceutical chemical space.

As a result, aryl amines have become a prevalent substructure in high-throughput screening

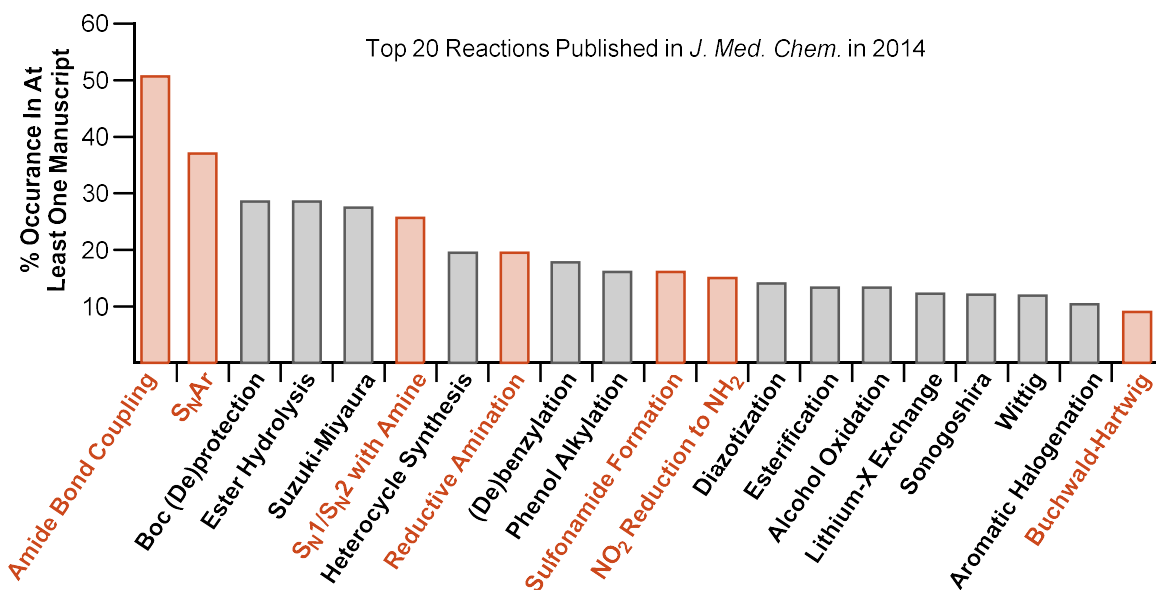


Figure 1.1. Meta-analysis of reactions appearing in *J. Med. Chem.* in 2014

libraries but have proven to be particularly disruptive in late-stage pharmaceutical development due to their propensity for reactive metabolite (RM) formation (Chapter 5). Cytochrome P450 (CYP450)-mediated oxidation of the aniline motif affords highly electrophilic species (i.e. quinone-imines) that form covalent linkages to bystander proteins or CYP450s themselves in an indiscriminate fashion, leading to increased risk for drug-drug interactions or idiosyncratic adverse drug reactions (IADR).² Nearly one-third of drugs with IADRs that have been labeled with black-box-warnings or completely withdrawn from the market contain the aniline functionality, and many of these examples have evidence for aniline bioactivation and RM formation.³⁻⁵

This association of anilines as precursors to RMs prompted our own group to consider effective strategies for mitigating aniline-derived toxicity such that failed drug candidates could be re-engineered with preserved efficacy but enhanced safety. As such, the use of isosteres

represents an attractive approach to address this issue, as isosteric replacement aims to closely mimic the efficacy of a lead compound while improving physicochemical properties. With respect to anilines, available isosteres are limited in application, scope, and diversity. The work presented herein discusses current approaches to aniline isosterism and offers an outlook on new structures to serve as metabolically innocuous aniline isosteres.

1.2 Current Approaches to Aniline Isosterism

As benzene itself is a structural alert susceptible to RM formation, benzene isosterism has been targeted in a number of different applications. The unifying feature of these approaches has been the use of small, saturated carbocycles to supplant the arene, and the appeal of this strategy is multifaceted. Saturated carbocycles increase F_{sp^3} and three-dimensionality,^{6,7} are more resistant to RM formation and CYP-inhibition,⁸ and often represent novel intellectual property. The most common examples of benzene isosteres are bicyclo[1.1.1]pentane (BCP),⁹⁻¹¹ bicyclo[2.2.2]octane (BCO),¹²⁻¹⁴ and cubane (CUB),¹⁵ although several alternative structures have been proposed recently but have yet to be realized synthetically¹⁶ or applied in a biological setting (Figure 1.2).^{17,18} Conversely, despite the well-known metabolic liabilities of anilines, a subclass of substituted benzenes, examples of aniline isosterism are sparsely reported in the literature. Among compounds containing these motifs, it is difficult to quantify the number of pharmaceutical entities that have been intentionally modified with a saturated structure to improve ADME properties and those that simply incorporate these motifs as *de novo* building blocks.

Broad comparison of physical parameters of aminoBCP, aminoBCO, aminoCUB, and aminonorborene (aminoNB) against the analogous aniline reveals that these isosteres provide

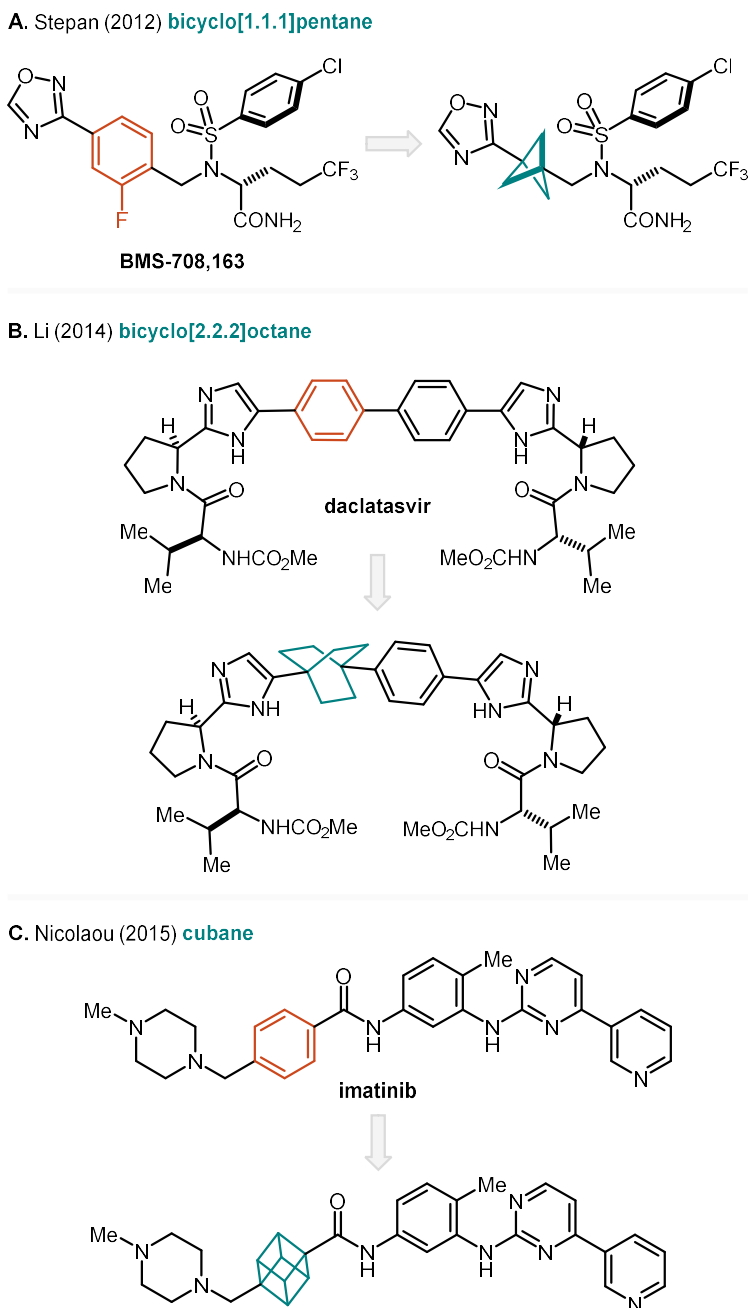


Figure 1.2. Examples of (A) bicyclo[1.1.1]pentane, (B) bicyclo[2.2.2]octane, and (C) cubane in benzene isosterism efforts in drug discovery and lead optimization

general spatial approximations to the parent structure (Figure 1.3A).¹⁹ Out of the 198 patents disclosing 1-aminoBCPs, all structures were exclusively mono- or di-substituted at the bridgehead position, resulting in linear structures. This substitution pattern is prevalent in the other scaffolds as well. Out of 310 patents containing either 1-aminoNBs or 1-aminoBCOs, only 6 patents contain

structures with a substitution pattern other than “para” despite having 11 and 13 unique sites for substitution, respectively.²⁰ This analysis of the patent literature highlights an important limitation of these carbocycles: despite having multiple sites available for substitution, the vast majority of reported structures are only functionalized at the bridgehead position. The reason for this void of chemical diversity within the field of aniline (and more generally, benzene) isosterism lies in the limited number of synthetic methods available to prepare and functionalize these saturated hydrocarbon scaffolds.

Current synthetic methods only allow access to para-substituted mimics of anilines, but this only represents a fraction of drugs which contain considerably more diversity. Of the 200 top selling drugs of 2018, 48 contain an aniline motif, but among these only 12 are solely para-substituted. To address this limitation, our laboratory became engaged in developing flexible and scalable synthetic protocols to access diversely substituted 1-aminoNBs to leverage in aniline isosteric applications. Efforts within our group have resulted in facile synthetic access to the aminoNB scaffold via a robust photochemical cyclization strategy. Two distinct methods have been developed, providing entry into uniquely decorated aminoNB cores. The first approach employs photoredox catalysis, an emerging technology within drug discovery programs,²¹ and the second exploits direct photochemical excitation of imines using visible light as the sole reagent necessary to enact the transformation (Figure 1.3B).²² The mild nature of these reactions tolerates a wide array of functional groups, have proven to be scalable in continuous flow processing, and importantly, all sites of substitution are diversifiable with these approaches. Initial stability assays in rat and human liver microsomes, in addition to metabolite identification, have demonstrated that the aminoNBs generally have improved metabolic profiles compared to their aniline counterparts. These new methods can be easily translated to medicinal chemistry applications, and our hope is

that these innovative building blocks will be incorporated into existing therapeutics to yield improved safety profiles and re-invigorate promising leads.

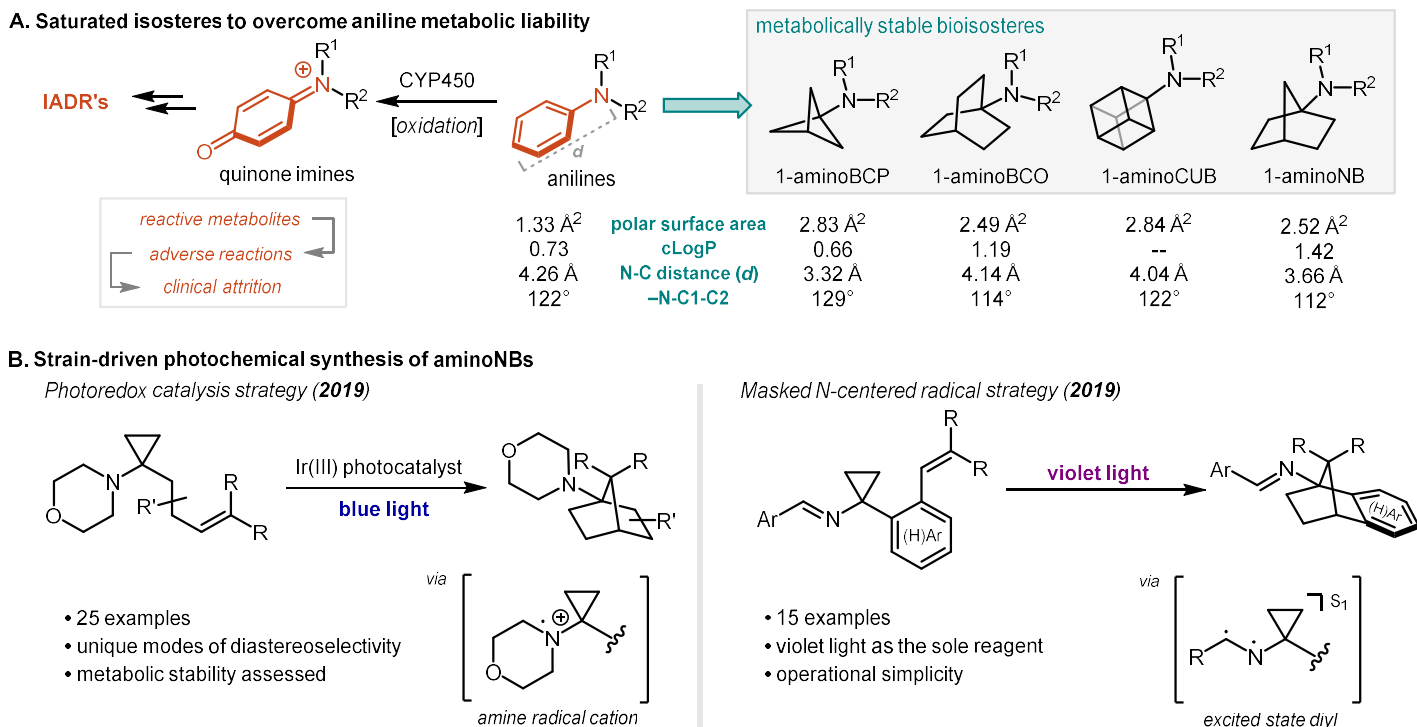


Figure 1.3. (A) Saturated isosteres of aniline to overcome metabolic liability; (B) Strain-driven photochemical synthesis of aminoNBs

1.3 Outlook

Despite the recent advances in accessing diversely substituted carbocyclic structures, a number of challenges remain for the isosteric replacement of anilines to be broadly applicable. The ability to selectively synthesize and strategically manipulate small carbocyclic frameworks remains limited. Lack of imaginative new methods and commercial availability of precursors (e.g. BCP and CUB bridgehead dicarboxylates) has considerably narrowed the region of chemical space being interrogated for pharmaceutical applications. Due to the increased complexity of saturated carbocycles compared to planar anilines, these isosteres have the potential to be more versatile

than their aromatic precursors. Only advancements in synthetic technology will be able to provide the structural diversity and scrupulous control over physicochemical properties required to mimic densely functionalized anilines.

Even meeting these criteria, careful considerations need to be made to select an appropriate isostere for any given application; exchanging an aryl amine to an alkyl amine has the potential to significantly perturb protonation state and removal of arenes may disrupt π - π stacking interactions within the binding pocket. However, conscientious design can prevent these issues. Inductive withdrawing groups can modulate the pK_a of alkyl amines, and access to a large library of isosteres of varying sizes, shapes, and bond angles will increase the likelihood of achieving an optimal fit within a binding pocket, recouping or even improving upon the energetic contributions of π -stacking.

Anilines have persisted as staple components of drug development libraries due to their accessibility and ease of handling despite being stereotyped as the most “notorious” of all structural alerts.²³ It is unsurprising then that a significant fraction of drugs labeled with black box warnings or completely withdrawn from the market contain the aniline motif, and some of the consequences of bioactivation have been as severe as patient death.³ However, pharmaceutical compounds containing this predictable liability continue to be overlooked as these toxicities are tolerated in patients with traditionally poor outcomes and for areas of unmet medical need. Instead, can advancements in reaction science and investment in aniline isosterism overcome this bias to continue to incorporate anilines into new therapies? We foresee a great benefit from developing rationally designed, inert structures with multiple sites for diversification that complement the current armamentarium of aniline isosteres and hope to see further advancements in this area in the near future.

1.4 References

1. Brown, D.G.; Boström, J. "Analysis of Past and Present Synthetic Methodologies on Medicinal Chemistry: Where Have All the New Reactions Gone?" *J. Med. Chem.* **2016**, *59*, 4443-4458.
2. Walsh, J.S.; Miwa, G.T. "Bioactivation of Drugs: Risk and Drug Design." *Annu. Rev. Pharmacol. Toxicol.* **2011**, *51*, 145-167.
3. Stepan, A.F.; Walker, D.P.; Bauman, J.; Price, D.A.; Baillie, T.A.; Kalgutkar, A.S.; Aleo, M.D. "Structural Alert/Reactive Metabolite Concept as Applied in Medicinal Chemistry to Mitigate the Risk of Idiosyncratic Drug Toxicity: A Perspective Based on the Critical Examination of Trends in the Top 200 Drugs Marketed in the United States." *Chem. Res. Toxicol.* **2011**, *24*, 1345-1410.
4. Kalgutkar, A.S. "Should the Incorporation of Structural Alerts be Restricted in Drug Design? An Analysis of Structure-Toxicity Trends with Aniline-Based Drugs." *Curr. Med. Chem.* **2015**, *22*, 438-464.
5. Orr, S.T.M.; Ripp, S.L.; Ballard, T.E.; Henderson, J.L.; Scott, D.O.; Obach, R.S.; Sun, H.; Kalgutkar, A.S. "Mechanism-Based Inactivation (MBI) of Cytochrome P450 Enzymes: Structure-Activity Relationships and Discovery Strategies to Mitigate Drug-Drug Interaction Risks." *J. Med. Chem.* **2012**, *55*, 4896-4933.
6. Ritchie, T.J.; Macdonald, S.J.F. "The impact of aromatic ring count on compound developability – are too many aromatic rings a liability in drug design?" *Drug Discov. Today* **2009**, *14*, 1011.
7. Lovering, F.; Bikker, J.; Humblet, C. "Escape from Flatland: Increasing Saturation as an Approach to Improving Clinical Success." *J. Med. Chem.* **2009**, *52*, 6752-6756.
8. Lovering, F. "Escape from Flatland 2: complexity and promiscuity." *Med. Chem. Commun.* **2013**, *4*, 515-519.
9. Stepan, A.F.; Subramanyam, C.; Efremov, I.V.; Dutra, J.K.; O'Sullivan, T.J.; DiRico, K.J.; McDonald, W.S.; Won, A.; Dorff, P.H.; Nolan, C.E.; Becker, S.L.; Pustilnik, L.R.; Riddell, D.R.; Kauffman, G.W.; Kormos, B.L.; Zhang, L.; Lu, Y.; Capetta, S.H.; Green, M.E.; Karki, K.; Sibley, E.; Atchison, K.P.; Hallgren, A.J.; Oborski, C.E.; Robshaw, A.E.; Sneed, B.; O'Donnell, C.J. "Application of the Bicyclo[1.1.1]pentane Motif as a Nonclassical Phenyl Ring Bioisostere in the Design of a Potent and Orally Active γ -Secretase Inhibitor." *J. Med. Chem.* **2012**, *55*, 3414-3424.
10. Nicolaou, K.C.; Vourloumis, D.; Totokotsopoulos, S.; Papakyriakou, A.; Karsunky, H.; Fernando, H.; Gavrilyuk, J.; Webb, D.; Stepan, A.F. "Synthesis and Biopharmaceutical Evaluation of Imatinib Analogues Featuring Unusual Structural Motifs." *ChemMedChem* **2016**, *11*, 31-37.
11. Meason, N.D.; Down, K.D.; Hirst, D.J.; Jamieson, C.; Manas, E.S.; Patel, V.K.; Somers, D.O. "Investigation of a Bicyclo[1.1.1]pentane as a Phenyl Replacement within a LpPLA2 Inhibitor." *ACS. Med. Chem. Lett.* **2017**, *8*, 43-48.

12. Auberson, Y.P.; Brocklehurst, C.; Furegati, M.; Fessard, T.C.; Koch, G.; Decker, A.; La Vecchia, L.; Briard, E. "Improving Nonspecific Binding and Solubility: Bicycloalkyl Groups and Cubanes as *para*-Phenyl Bioisosteres." *ChemMedChem* **2017**, *12*, 590-598.
13. Zhong, M.; Peng, E.; Huang, N.; Huang, Q.; Huq, A.; Lau, M.; Colonna, R.; Li, L. "Discovery of functionalized bisimidazoles bearing cyclic aliphatic-phenyl motifs as HCV NS5A inhibitors." *Bioorg. Med. Chem. Lett.* **2014**, *24*, 5731-3737.
14. Aguilar, A.; Lu, J.; Liu, L.; Du, D.; Bernard, D.; McEachern, D.; Przybranowski, S.; Li, X.; Luo, R.; Wen, B.; Sun, D.; Wang, H.; Wen, J.; Wang, G.; Zhai, Y.; Guo, M.; Yang, D.; Wang, S. "Discovery of 4-((3'R,4'S,5'R)-6"-Chloro-4'-(3-chloro-2-fluorophenyl)-1'-ethyl-2'-oxodispiro[cyclohexane-1,2'-pyrrolidine-3',3"-indoline]-5'-carboxamido)bicyclo[2.2.2]octane-1-carboxylic Acid (AA-115/APG-115): A Potent and Orally Active Murine Double Minute 2 (MDM2) Inhibitor in Clinical Development." *J. Med. Chem.* **2017**, *60*, 2819-2839.
15. Chalmers, B.A.; Xing, H.; Houston, S.; Clark, C.; Ghassabian, S.; Kuo, A.; Cao, B.; Reitsma, A.; Murray, C-E. P.; Stok, J.E.; Boyle, G.M.; Pierce, C.J.; Littler, S.W.; Winkler, D.A.; Bernhardt, P.V.; Pasay, C.; De Voss, J.J.; McCarthy, J.; Parson, P.G.; Walter, G.H.; Smith, M.T.; Cooper, H.M.; Nilsson, S.K.; Tsanktsidis, J.; Savage, G.P.; Williams, C.M. "Validating Eaton's Hypothesis: Cubane as a Benzene Bioisostere." *Angew. Chem. Int. Ed.* **2016**, *55*, 3580-3585.
16. Mykhailiuk, P.K. "Saturated bioisosteres of benzene: where to go next?" *Org. Biomol. Chem.* **2019**, *17*, 2839-2849.
17. Bychek, R.M.; Hutskalova, V.; Bas, J.P.; Zaporozhets, O.A.; Zozulia, S.; Levterov, V.V.; Mykhailiuk, P.K. "Difluoro-substituted bicyclo[1.1.1]pentanes as Novel Motifs for Medicinal Chemistry: Design, Synthesis and Characterization." *J. Org. Chem.* **2019**, *84*, 15106-15117.
18. Levterov, V.; Panasyuk, Y.; Pivnytska, V.; Mykhailiuk, P.K. "Water-soluble non-classical benzene mimics." *Angew. Chem. Int. Ed.* **2020**, *59*, 7161-7167.
19. Values were calculated from ground state equilibrium geometries using ω B97x-D G-31 G* level of theory in Spartan.
20. 198 patents containing aminoBCPs, 207 patents containing aminoBCO, 103 patents containing aminoNBs, and 20 patents containing CUBs have been registered since 2000. The search was performed in December 2019 in Reaxys DB.
21. Staveness, D.; Sodano, T.M.; Li, K.; Burnham, E.A.; Jackson, K.D.; Stephenson, C.R.J. "Providing a New Aniline Bioisostere through the Photochemical Production of 1-Aminonorbornanes." *Chem.* **2019**, *5*, 215-226.
22. Staveness, D.; Collins, J.L. III.; McAtee, R.C.; Stephenson, C.R.J. "Exploiting Imine Photochemistry for Masked N-Centered Radical Reactivity." *Angew. Chem. Int. Ed.* **2019**, *131*, 19176-19182.

23. Kalgutkar, A.S.; Dalvie, D. “Predicting Toxicities of Reactive Metabolite-Positive Drug Candidates.” *Annu. Rev. Pharmacol. Toxicol.* **2015**, *55*, 35-54.

Chapter 2

Providing a New Aniline Isostere Through the Photochemical Production of 1-Aminonorbornanes

Portions of this chapter have been adapted from the following publications (no permissions required): (1) Staveness, D.; Sodano, T.M.; Li, K.; Burnham, E.A.; Jackson, K.D.; Stephenson, C.R.J. “Providing a New Aniline Bioisostere through the Photochemical Production of 1-Aminonorbornanes.” *Chem*, **2019**, *5*, 215-226.; (2) Staveness, D.; Sodano, T.M.; Stephenson, C.R.J *ChemRxiv*, **2017**, DOI:10.26434/chemrxiv.5437255.v1

2.1 Introduction

2.1.1 Introducing sp³-Content in Pharmaceutical Development

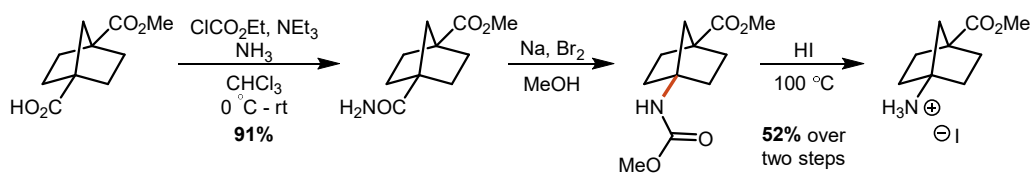
Recent analyses of pharmaceutical libraries have indicated that approved drugs are enriched in saturated content (higher Fsp³) relative to the average high-throughput screening compound,¹⁻³ and this revelation has sparked an increasing demand for new, saturated building blocks for use in drug discovery efforts.⁴ Further incentive arises from the fact that saturated substructures are generally less susceptible to adverse metabolic processing events than their aromatic congeners⁵ while also offering more potential sites of diversification. Thus, the introduction of new sp³-rich motifs will not only generate novel intellectual property and access unique chemical space, but also promote improved drug safety by reducing the likelihood of metabolism-derived toxicities⁶⁻⁹ (e.g. drug-induced liver injury¹⁰). However, these saturated

systems tend to require more involved syntheses, and ease of handling and broad commercial availability remains a central reason for the bias toward aromatic systems¹¹ in modern commercial screening libraries. Diversifying the medicinal chemistry toolbox from its current arene-rich state therefore requires the development of efficient methods for the preparation of complex, saturated substructures. This work provides one solution to this challenge, offering a robust and operationally simple method for the synthesis of diversely substituted 1-aminonorbornanes (aminoNBs) via a visible light-mediated transformation.

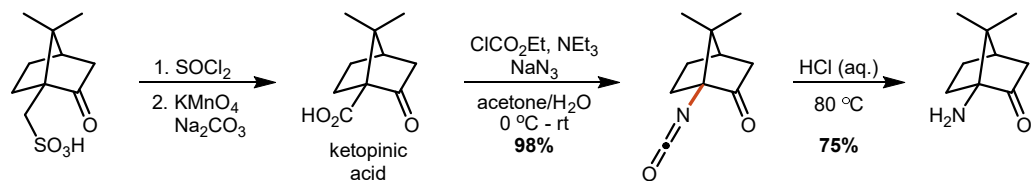
2.1.2. Previous Approaches to AminoNBs

Despite receiving little attention in recent times, aminoNBs were central to delineating the basic principles of S_N1 and S_N2 reactivity,¹² as illustrated by the landmark report from Bartlett and Knox¹³ in which bridgehead-substituted 1-apocamphanes were used as negative controls for S_N2 reactivity supporting the Walden inversion mechanism.¹⁴⁻¹⁶ These classical accounts¹⁷⁻²¹ as well

A. Wilcox (1968) Hofmann Rearrangement



B. Braslau (1996) Curtius Rearrangement



C. Knill (1994) Radical Closure

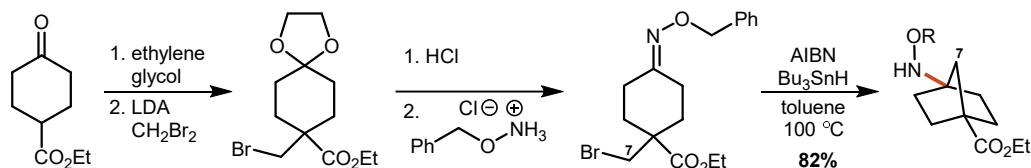


Figure 2.1. Previous synthetic approaches towards aminoNBs

as more recent approaches²²⁻²⁵ largely generate the bridgehead amine via Hofmann or Curtius rearrangements of bridgehead carboxylates within terpene derivatives or from downstream products of cyclopentadiene-based Diels-Alder reactions (Figure 2.1A and 2.1B). One radical-based closure exists from Della and Knill,²⁶ cyclizing a C7-radical into an oxime after traditional tin-based initiation conditions (Figure 1C). The lack of structural diversity available through these strategies has likely contributed to the minimal utilization of aminoNB-based scaffolds within medicinal chemistry,²¹ yet these substructures aptly address the needs of Fsp³-centric drug discovery.

2.1.3. Background and Synthetic Utility of Amine Oxidation

Single-electron oxidation of amines can be readily-achieved through the reductive quenching of excited state photocatalysts such as [Ru(bpy)₃]Cl₂, reactivity that was first observed by Whitten and co-workers in 1977 for both anilines and trialkylamines.²⁷ Kellogg²⁸ and Mariano²⁹ provided some of the earliest reports that capitalized on the synthetic utility of the resultant amine radical cations. The recent rise of photoredox catalysis both in academia^{30,31} and industry³² has led to a multitude of new methods employing amine radical cation intermediates,³³⁻³⁵ including our group's 2010 report of visible light-mediated aza-Henry reactions (Figure 2.2A).³⁶ The majority of these methods still operate through the classically-studied heterolytic mode of decomposition,^{37,38} fragmenting α -C-R bonds to access α -amino radicals.

Homolytic decomposition modes are far less common,³⁹ though only small amounts of ring strain are necessary to drive C-C bond homolysis, as seen in our efforts converting catharanthine into *Aspidosperma* and *Iboga* alkaloids (Figure 2.2B).⁴⁰ Photochemical amine oxidation of (+)-catharanthine (**2.1**) cleaves the C16-C21 bond, releasing 4.23 kcal/mol of ring strain and forming a distonic radical cation in which the resultant iminium is trapped by cyanide. Further elaboration

of common intermediate **2.2** yields pseudovincadifformine (**2.3**), pseudotabersonine (**2.4**), and coronaridine (**2.5**) in the highest yields known to date, requiring no more than 3 steps for each semi-synthesis. Computational and experimental investigations revealed the thermodynamic importance of ring strain in this transformation. When less-strained (+)-coronaridine (**2.5**) and (+)-dihydrocatharanthine (**2.6**) (0.00 and +0.08 kcal/mol strain, respectively) were subjected to the

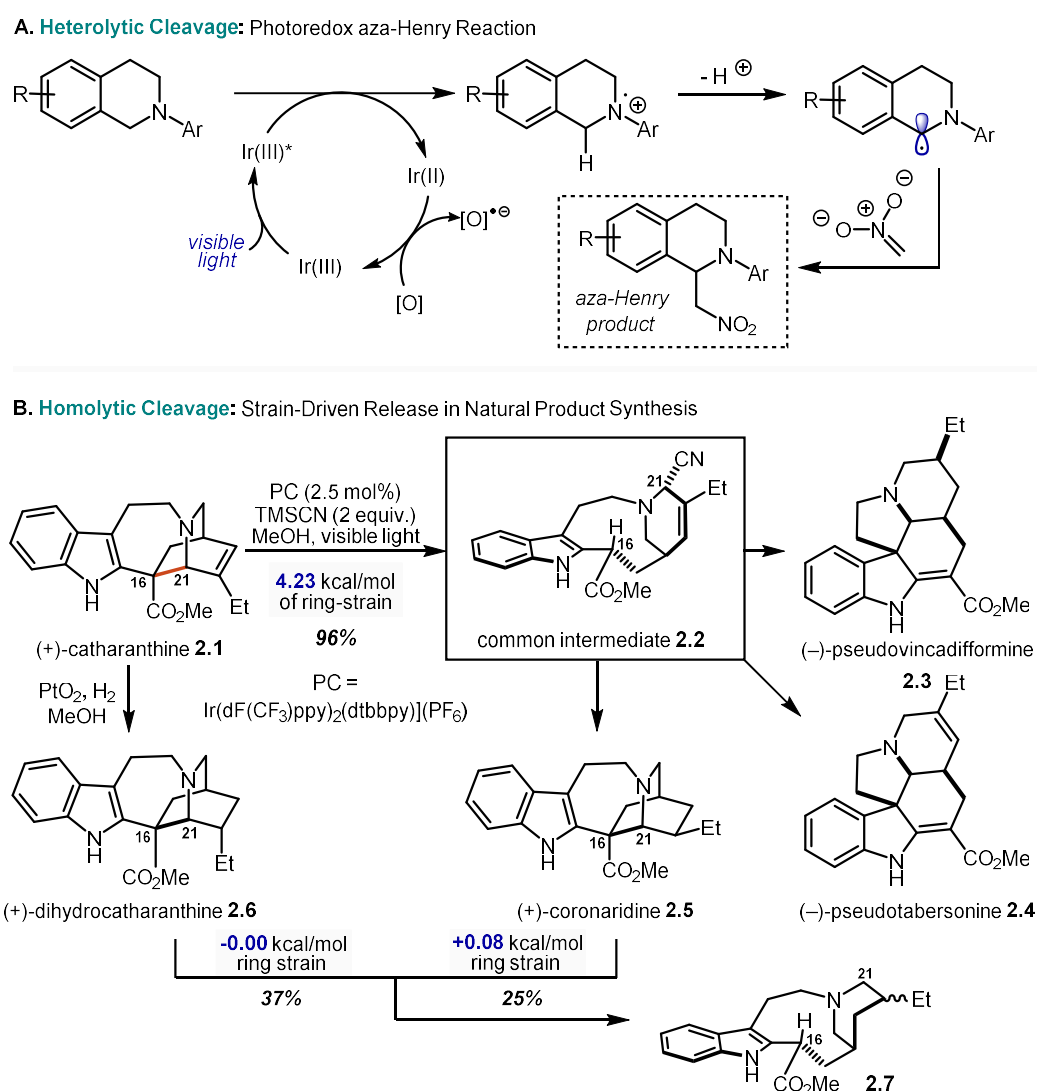


Figure 2.2. Examples of (A) Heterolytic and (B) Homolytic decomposition pathways of amine radical cations

photocatalytic conditions, the reaction required heating and longer times to achieve even modest yields of the ring-opened product **2.7**.

Strain-driven ring-opening facilitated by single electron oxidation of aminoCPs has previously been employed in the literature for the formation of carbocycles. Early examples relied on harsh, superstoichiometric oxidants such as ceric ammonium nitrate (CAN)⁴¹ or high-energy irradiation,⁴² severely limiting functional group tolerance (Figure 2.3A). Zheng *et al.* have exploited the mild conditions afforded by visible light photoredox catalysis for the intermolecular

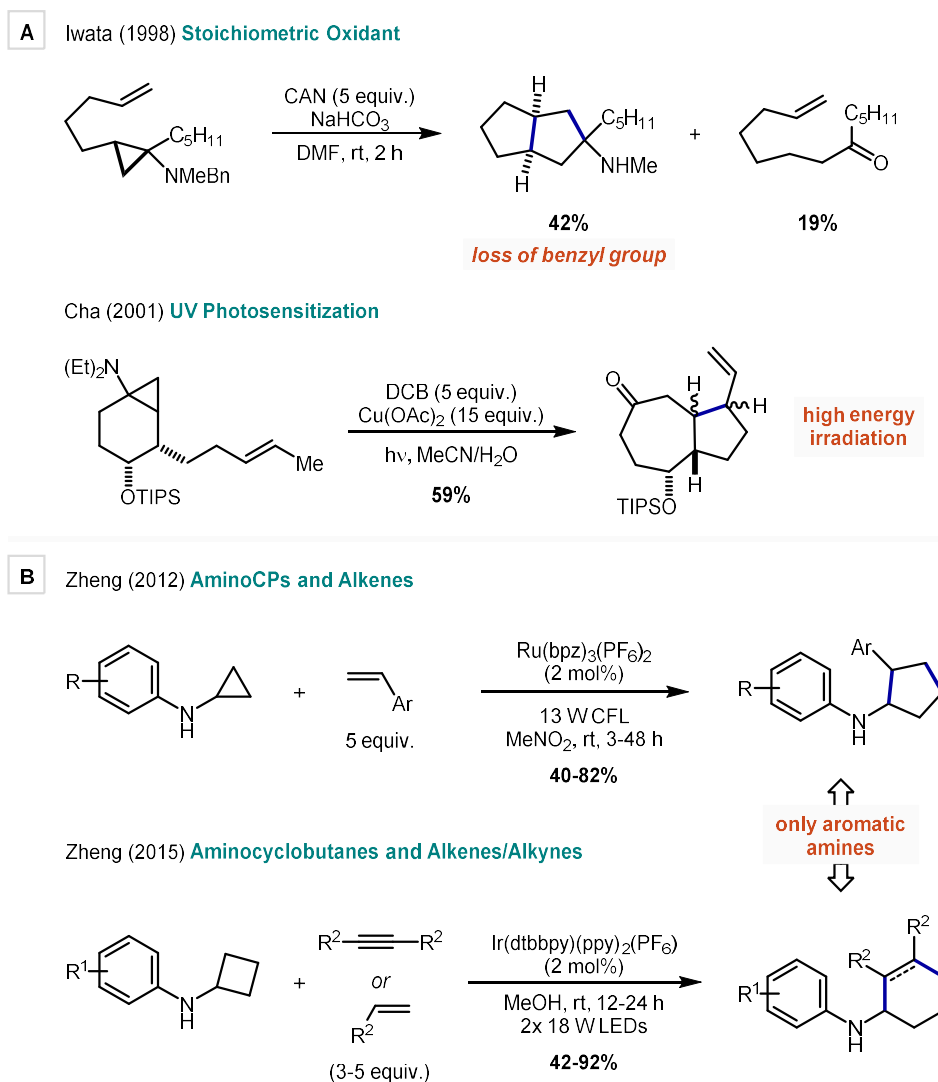


Figure 2.3. Select examples of strain-driven homolysis of aminoCPs

[3+2] cycloaddition of aminoCPs with alkenes (Figure 2.3B). Since this initial report,⁴³ the scope of this reaction platform has been expanded to include both internal and terminal alkynes as coupling partners and have additionally shown that aminocyclobutanes have sufficient ring strain to afford analogous [4+2] cycloadditions with alkenes or alkynes.^{44,45} While these methods have now been extended to a variety of styrenes, arylacetylenes,⁴⁶ diynes, and enynes⁴⁷ to yield a number of polycyclic carbon skeletons with good diastereoselectivity, they all stem from aryl substrates. The goal of this work was to harness the unique capabilities of photoredox catalysis to generate aminoNBs from alkyl amines as a means of addressing the need for new, saturated building blocks in drug discovery. The following describes the optimization, preliminary mechanistic studies, scope, and performance in continuous flow of this formal [3+2] cycloaddition toward aminoNBs.

2.2 Results and Discussion

2.2.1 Optimization

Our approach to the synthesis of aminoNBs sought to generate the norbornane core through serialized radical cyclizations initiated from a photochemically-generated amine radical cation

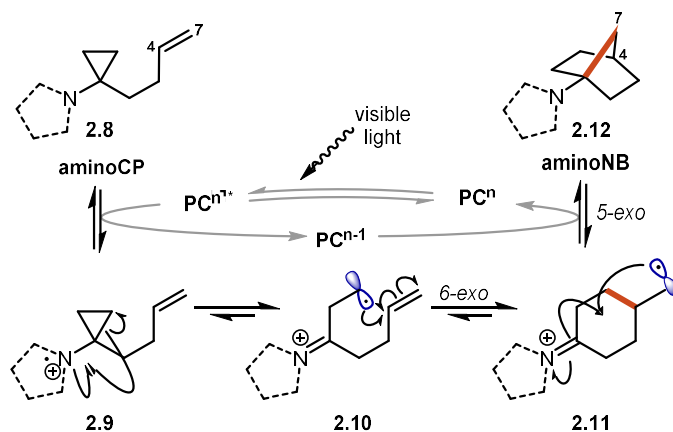
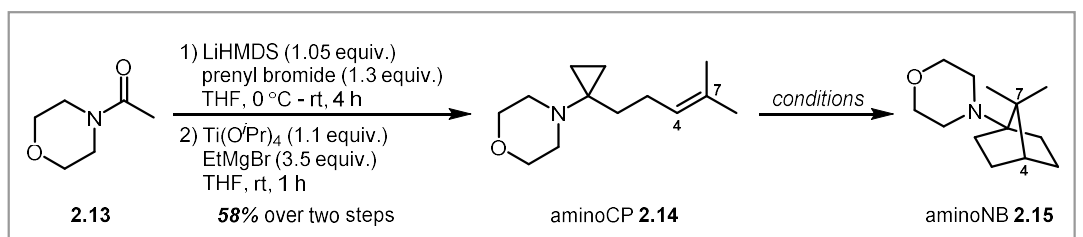


Figure 2.4. Proposed mechanism for the synthesis of aminoNBs from aminoCPs

intermediate (Figure 2.4). Single-electron oxidation of 1-homoallyl-1-aminocyclopropanes (aminoCPs) (**2.8**) by the excited state of a photocatalyst would provide amine radical cation **2.9**. Rapid β -scission would generate distonic radical cation **2.10**, thereby enabling serial *6-exo-trig* and *5-exo-trig* radical cyclizations to forge the norbornane core. Reduction to the neutral aminoNB product **2.12** closes the catalytic cycle (or propagates the chain) without the need for exogenous sacrificial additives.

Initial optimization was performed with 7,7-dimethyl aminoCP **2.14**, prepared by alkylation of *N*-acetyl morpholine (**2.13**) with prenyl bromide and subsequent Kulinkovich



Reactions Conditions:
2x 4.4 W Blue LEDs, degassed MeCN, 15-25 °C, 12 h

Entry	Catalyst (2 mol%)	Additive (20 mol%)	Isolated Yield
1	[Ir(dF(CF ₃)ppy) ₂ (dtbbpy)](PF ₆)	--	63%
2	[Ir(dF(CF ₃)ppy) ₂ (dtbbpy)](PF ₆)	ZnCl ₂	84%
3	[Ir(dF(CF ₃)ppy) ₂ (dtbbpy)](PF ₆)	LiBF ₄	79%
4	[Ir(dF(CF ₃)ppy) ₂ (dtbbpy)](PF ₆)	NaBF ₄	66%
5	[Ir(dF(CF ₃)ppy) ₂ (dtbbpy)](PF ₆)	Me ₂ AlCl	59%
6	[Ir(dF(CF ₃)ppy) ₂ (dtbbpy)](PF ₆)	BF ₃ ·OEt ₂	69%
7	[Ir(dF(CF ₃)ppy) ₂ (dtbbpy)](PF ₆)	MgBr ₂ ·OEt ₂	75%
8	[Ir(dF(CF ₃)ppy) ₂ (dtbbpy)](PF ₆)	CuBr ₂	20%
9	[Ir(dF(CF ₃)ppy) ₂ (dtbbpy)](PF ₆)	NiCl ₂	49%

10	[Ru(bpy) ₃](Cl ₂)·6H ₂ O	--	0%
11	[Ru(bpy) ₃](Cl ₂)·6H ₂ O	ZnCl ₂	34%

12	--	ZnCl ₂	0%
13	[Ir(dF(CF ₃)ppy) ₂ (dtbbpy)](PF ₆)	ZnCl ₂	0% *no light
14	--	--	0% *80 °C, dark

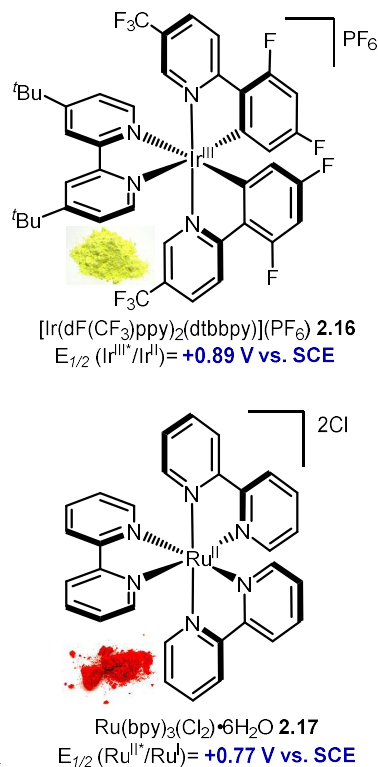


Figure 2.5. Summary of reaction optimization

cyclopropanation⁴⁸ of the corresponding amide. Heteroleptic polyfluorinated Ir(III) photocatalyst [Ir(dF[CF₃]ppy)₂(dtbbpy)](PF₆)⁴⁹ (**2.16**) was quickly identified as the optimal photocatalyst. Further evaluation of reaction parameters determined degassed MeCN and 12 h of irradiation with 2x 4.4 W blue LEDs to be the optimized solvent, time, and light source, affording 63% of aminoNB **2.15** (Figure 2.5, Entry 1). While trying to further enhance productive conversion, it was found that simple Lewis acidic salts increased the yield of the reaction even at sub-stoichiometric loadings (20 mol%). ZnCl₂ and LiBF₄ proved to be the most effective, yielding 84% and 79% of aminoNB **2.15**, respectively (Entries 2-3). Other Lewis acids provided little enhancement (NaBF₄; Entry 4) or facilitated degradation pathways (Me₂AlCl, BF₃·OEt₂, MgBr₂·OEt₂; Entries 5-7), while redox non-innocent metal salts inhibited reactivity (CuBr₂, NiCl₂; Entries 8-9). Of note, ZnCl₂ is not necessarily redox-innocent under these conditions given the studies of Bernhard and co-workers, though only the most inefficient substrates afforded a grey precipitate that could indicate reduction to Zn⁰.⁵⁰ When the less oxidizing photocatalyst [Ru(bpy)₃](Cl₂)·6H₂O (**2.17**) was employed (Entries 10-11; Ru(II)*³⁴/Ru(I) $E_{1/2} = +0.77$ V vs. SCE³⁴; Ir(III)*⁴⁷/Ir(II) $E_{1/2} = +0.89$ V vs. SCE⁴⁷), no aminoNB product was observed and only starting aminoCP **2.14** was recovered (Entry 10). However, when 20 mol% ZnCl₂ was used in conjunction with [Ru(bpy)₃](Cl₂)·6H₂O, aminoNB **2.15** was isolated in 34% yield with overall good mass recovery (Entry 11). The reaction did not proceed to any extent in the absence of photocatalyst, without light, or under purely thermal conditions and starting material was recovered in >95% yield (Entries 12-14).

The specific mechanistic role of ZnCl₂ and LiBF₄ in this reaction was unclear, and we initially hypothesized that certain Lewis acids were facilitating product formation by interacting with the morpholine oxygen. Short C-O and C-N bonds force morpholines into more staggered chair structures than one would find with cyclohexanes, and *in silico* analysis of *N*-methyl

morpholine (NMM) estimates a dihedral angle of 58° in addition to a typical pyramidal amine geometry (Figure 2.6). If a Lewis acid were coordinated to the oxygen, the C-O bonds should elongate, decreasing the dihedral angle and facilitating planarization of the nitrogen center. It is a well-known trend that nitrogen centers with a lower barrier to planarity are more readily oxidized,⁵¹ as is demonstrated by the smaller dihedral angle and lower oxidation potential of *N*-methylpiperidine (NMP), and we set out to test the validity of this hypothesis by measuring the

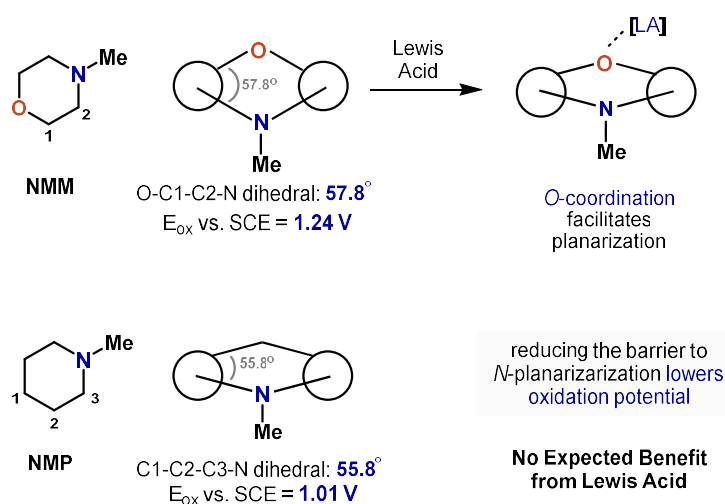


Figure 2.6. Initial hypothesis for the mechanistic role of Lewis acids

oxidation potential of various amines in the presence and absence of Lewis acid additives.

2.2.2 Differential Pulse Voltammetry

Differential pulse voltammetry (DPV) is a sensitive electrochemical technique used to quantify redox potentials of different substances. To measure the redox potentials of select trialkylamines, aminoCPs, and aminoNBs, oxidative voltages were applied and current output measured. We chose to use stoichiometric quantities (1.2 equiv.) of Lewis acid to saturate any coordinative species that might be present in solution, and LiBF_4 was selected over ZnCl_2 due to the formation of heterogeneous mixtures at the increased catalyst loading with the latter. Full experimental details are provided in Section 2.4.3.

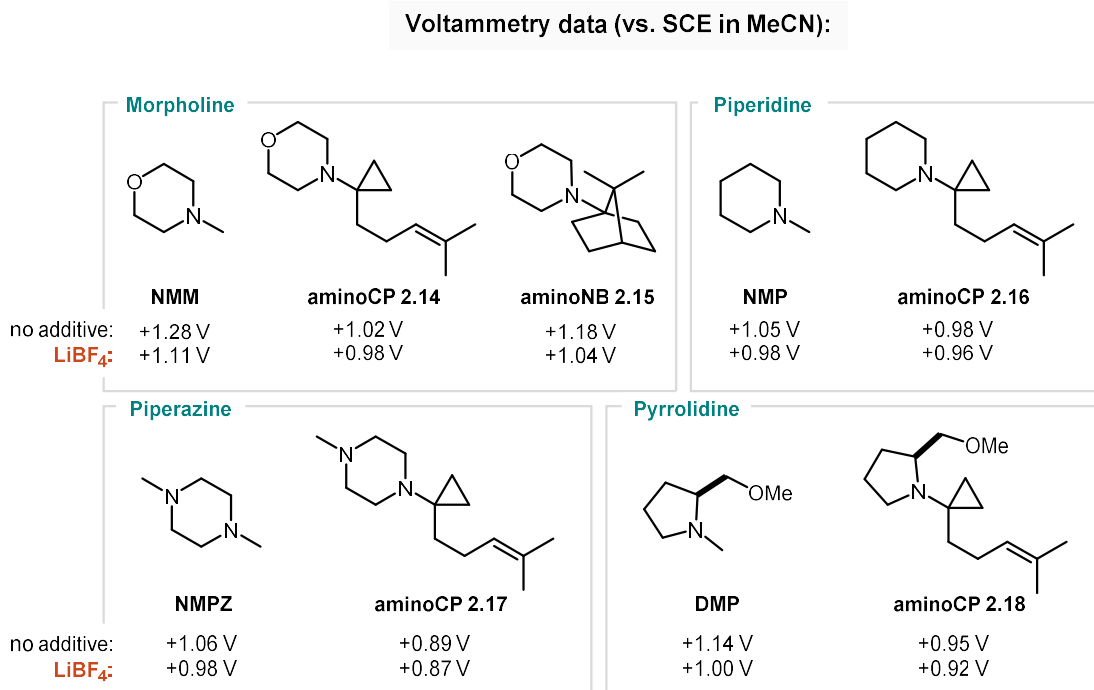


Figure 2.7. Summary of voltammetry data for various trialkyl amines; NMM = *N*-methyl morpholine; NMP = *N*-methyl piperidine; NMPZ = *N*-methyl piperazine; DMP = dimethyl pyrrole

A summary of these experiments is provided in Figure 2.7, and the results suggest that the Lewis acidic salts are eliciting an effect on reaction outcome through modulation of amine oxidation potential. Morpholines are unusually difficult to oxidize relative to other *N,N*-dialkylamines (NMM $E_p = +1.28$ V,⁵² NMP $E_p = +1.05$ V vs. SCE), thus prior morpholine oxidation efforts in the field have necessitated the use of an Ir(ppy)₃/O₂-based oxidative quenching cycle⁵³ or the development of new Ir(III) photocatalysts with excited state oxidizing power that vastly exceeds that of photocatalyst **2.16**.⁵⁴ Based on this data, morpholine oxidation appears more facile in the presence of LiBF₄, decreasing by 170 mV for NMM, 40 mV for aminoCP **2.14**, and 140 mV for aminoNB **2.15**. These results supported the proposed *O*-coordination model, but further investigation revealed that the impact of the Lewis acids was not limited to morpholines. Piperidine, piperazine, azetidine (not shown), and pyrrolidine all showed decreases in oxidation

potential in the presence of LiBF₄, nullifying the *O*-coordination hypothesis as the predominant mechanism for decrease in oxidation potential.

To our knowledge, there is no definitive explanation in the literature for the observed phenomenon of Lewis acidic salts decreasing the oxidation potential of amine-containing heterocycles. An explanation invoking direct Lewis acid coordination to the nitrogen is initially counter-intuitive in that drawing electron density away from a heteroatom should result in an increase in oxidation potential. However, the impact of conformation changes arising from *N*-coordination should be considered, as oxidation could conceivably be made easier if the σ_{C-C} and n_N orbitals were aligned, allowing for better donation into the respective anti-bonding orbitals. Experimentally, ¹H NMR analysis of aminoCP **2.14** at room temperature revealed minimal perturbation upon introduction of LiBF₄ (data not shown), suggesting that the conformational flexibility is similar with and without Lewis acid present. Alternatively, it is also possible that the metal center is acting via *N*-coordination and serving as an electron relay catalyst.

Other explanations beyond *N*-coordination should be considered, and it is conceivable that the Lewis acids are altering processes other than the electron transfer event, such as the rate of back-electron transfer or the rate of a given radical cyclization. Altering the kinetic profile of a reaction is known to impact the measured redox potential (*vide infra*), thus any impact downstream of the electron transfer, such as enhancing the rate of the *5-exo-trig* cyclization, would affect the measurement (see aminoCP **2.65**). This kinetic argument would not explain the impact of the salts on the methylated amines, but the same concept could apply should the deprotonation of the amine radical cation to an α -amino radical be facilitated by the presence of the Lewis acids.

At this stage, we believe multiple factors are likely contributing to different extents across the substrates studied. It is important to keep in mind that the chemistry occurring at the surface

of the electrode in this analysis is not necessarily representative of the reaction in solution, and further studies are needed to probe the role of Lewis acids in this reaction manifold. Additional experiments and discussion on this topic can be found in Chapter 3.4.2.

The DPV measurements offers other key mechanistic insights beyond elucidating the role of the Lewis acids. The E_p of aminoNB **2.15** is significantly higher than that of the aminoCP **2.14** (+160 mV), offering a comfortable margin of selectivity for oxidation of the starting material over the product by excited state photocatalyst **2.16**. The data also reveals a general trend between the oxidation potential of the *N*-methyl amines and the aminoCPs. In each case, the aminoCP is significantly easier to oxidize than the cooresponding *N*-methyl amine. These discrepancies in oxidation potential ($\Delta E_p = -260$ mV for aminoCP **2.14** and NMM) can be rationalized by the facile post-oxidation fragmentation pathway in the aminoCP, as single-electron transfer processes with amines are highly influenced by post-oxidation reactivity. A particularly informative and concise review³⁷ from Mariano and co-workers provides a few key general statements regarding the driving forces for amine oxidation:

“Owing to the large driving force for SET in the electronic excited vs. ground states [of metal species], radical ion formation is often one of the most efficient pathways for excited-state deactivation. Consequently, in contrast to classical photochemical reactions, SET-promoted excited-state processes are controlled by *the nature and rates of secondary reactions of charged radical intermediates.*”

“In all cases, the driving force for fragmentation of the aminium radical is provided by a combination of factors, including (1) delocalization of the *N*-centered positive charge

density into the α -C-H, α -C-C, or α -C-SiR₃ σ -bonds, and (2) the thermodynamics associated with [the formation of the fragmentation products].”

As it pertains to the work herein, the amine oxidation via photocatalyst **2.16** largely depends on the available homolytic decomposition process - the cyclopropane ring-opening via β -scission. Not only is this fragmentation known to proceed rapidly ($8.6 \times 10^{-7} \text{ s}^{-1}$ for the isoelectronic cyclopropylmethyl radical),⁵⁵ but it is also thermodynamically favorable due to the considerable relief of ring strain (28 kcal/mol in cyclopropane). As this fragmentation pathway is not available to the *N*-methylamines, their oxidation is less favorable as represented by higher oxidation potentials.

One final observation from the DPV experiments is the presence of a second oxidation peak observed in the voltammograms of the aminoCP starting materials. As represented by the traces for aminoCP **2.14**, the second oxidation peak is observed at 1.36 V for the no additive trial

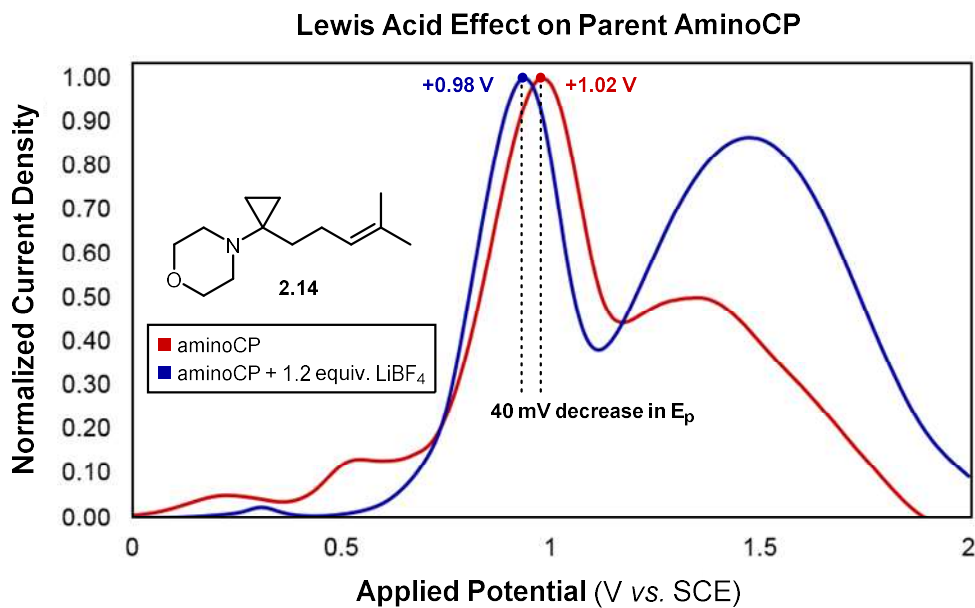


Figure 2.8. Measured peak oxidation potentials of aminoCP **2.14** in the presence and absence of LiBF₄

(red line) and at 1.47 V for the LiBF₄ trial (blue line) (Figure 2.8). Interestingly, there is a significant increase in current intensity for the second oxidation in the LiBF₄ trial compared to the no additive trial, suggesting that this oxidation occurs more readily in the presence of Lewis acid (despite the 110 mV increase in E_p). This downstream oxidation event is suspected to be the oxidation of the tertiary radical that forms after the *6-exo-trig* cyclization (analogous to **2.11**) to the corresponding tertiary cation. Both experimental and theoretical studies place the oxidation of the *tert*-butyl radical around 500-600 mV higher than that of simple trialkylamines,^{56,57} which is in close alignment to the values obtained here (+380 mV for no additive, +530 mV for LiBF₄). The lack of this peak in the aminoNB **2.15** and NMM voltammograms also supports this conclusion.

2.2.3 Quantum Yield Measurements

The quantum yield of the photochemical cyclization was measured to provide further information about the reaction mechanism. A quantum yield <1 indicates that a reaction required more than one photon for every molecule of product that was generated, implying that a portion of photons were wasted through non-productive or deleterious pathways (e.g. phosphorescence, back-electron transfer, non-radiative relaxation, off-cycle reactivity).⁵⁸ The quantum yield for the reaction of aminoCP **2.14** was calculated to be only 0.39, a number usually representative of a non-propagative process. This result was unexpected given the thermodynamic driving force for oxidation of a second equivalent of starting material by the oxidized aminoNB intermediate following *5-exo-trig* cyclization. Additionally, there are kinetic challenges associated with a closed catalytic cycle of two low concentration species - both the Ir(II) catalyst intermediate and oxidized aminoNB have maximum theoretical concentrations of just 2 mM. Additionally, the high quenching efficiency of aminoCP **2.14** (see Section 2.2.4) and the presence of a post-oxidation

fragmentation pathway to putatively minimize back-electron transfer limits the impact of two common explanations for artificially low quantum yields.⁵⁹ However, the large range of quantum yields that have been reported for many different classes of photochemical reactions makes it difficult to differentiate between chain- and non-chain processes, especially for measured quantum yields ~ 1 . A recent study from Chen, Zheng, and co-workers discloses a new method for detecting radical chain-processes employing ESI/MS coupled with online laser irradiation.⁶⁰ While a direct comparison between this new analytical technique and traditional quantum yield measurements has yet to be reported, Chen and Zheng provide evidence for a radical chain mechanism for anilinocyclopropane-based formal [3+2] cycloadditions toward cyclopentanes.

Importantly, the low measured quantum yield does not preclude the involvement of propagative pathways, but it does suggest that non-productive pathways are significant if this process is predominantly operating via a radical chain mechanism. One hypothesis is that the 5-*exo-trig* cyclization, suspected to be the rate-determining step, is sufficiently slow relative to the electron transfer processes that it renders the measured quantum yield < 1 due to photons lost during the lifetime of distonic radical cation **2.11**. The lifetime of **2.11** is time in which neither propagative nor closed cycle pathways are progressing, necessarily representing a window of time in which all irradiation is non-productive and accounting for a quantum yield < 1 .

2.2.4 Stern-Volmer Luminescence Quenching Analysis

To further build upon the quantum yield measurement, Stern-Volmer luminescence quenching experiments were performed. Upon irradiation with visible light, the emission spectrum of photocatalyst **2.16** was recorded in the presence of variable concentrations of aminoCP **2.14** with and without 20 mol% LiBF₄ (Figure 2.9A). Control experiments showed that LiBF₄ alone does not quench photocatalyst **2.16** (data not shown). Subsequent Stern-Volmer analysis showed

a modest increase in quenching rate in the presence of 20 mol% LiBF₄, but this increase was not statistically significant (no additive $k_q = 2.34 \times 10^7 \text{ M}^{-1}\cdot\text{s}^{-1}$; 20 mol% LiBF₄ $k_q = 2.62 \times 10^7 \text{ M}^{-1}\cdot\text{s}^{-1}$) (Figure 2.9B).

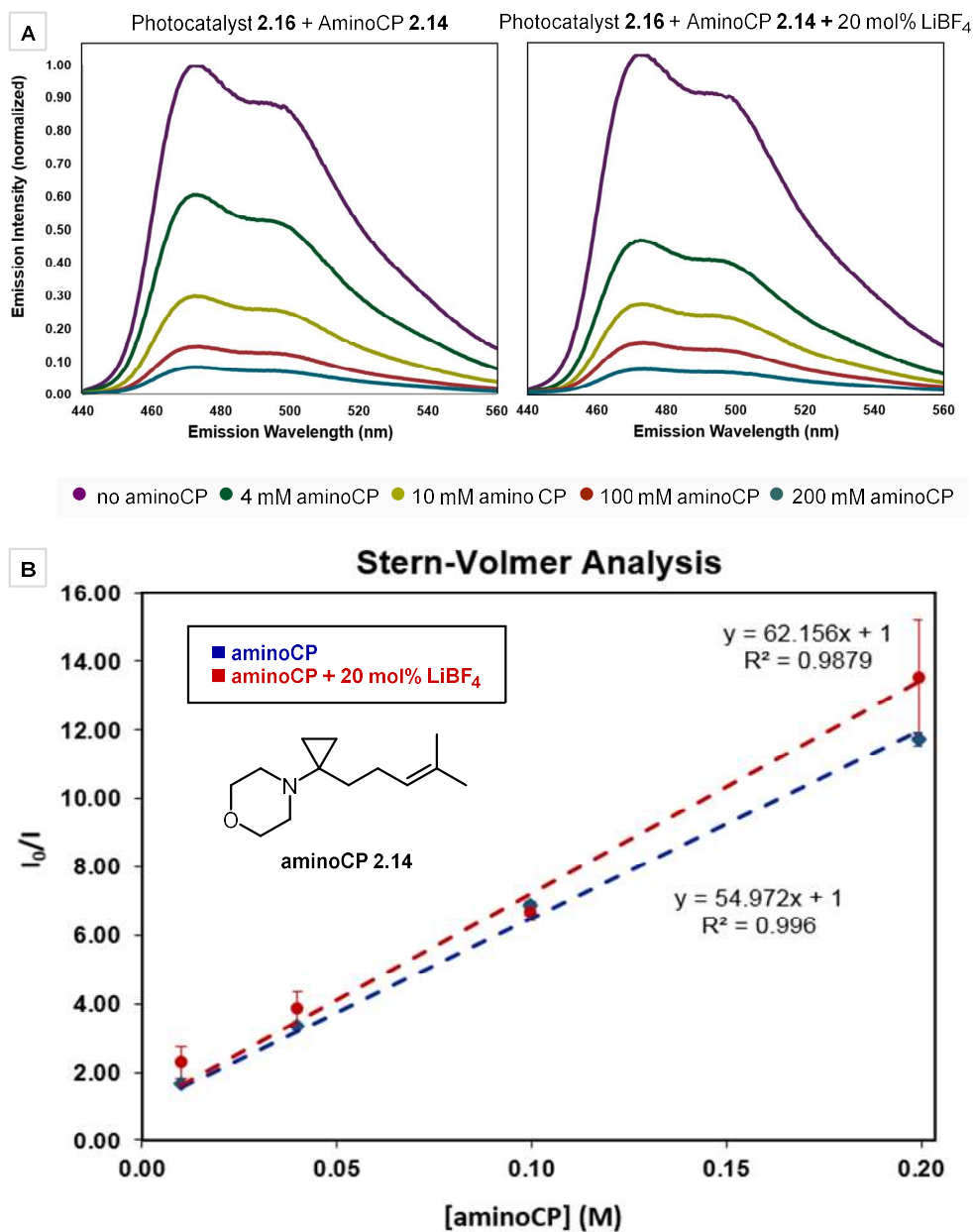


Figure 2.9. (A) Emission spectra of photocatalyst **2.16** in the presence of varying concentrations of aminoCP **2.14** ± 20 mol% LiBF₄; (B) Stern-Volmer luminescence quenching analysis

While it appears as though LiBF₄ is not significantly contributing the rate of the initial single electron transfer event, aminoCP is a competent quencher of the photocatalyst, suggesting that inefficient quenching is not an explanation for the low quantum yield observed above.

2.2.5 Reaction Scope

To achieve our goal of providing robust access to differentially substituted aminoNBs through the [3+2] photochemical cyclization, we first prepared a number of aminoCPs varying the identity of the amine. Due to the necessity of employing the Kulinkovich-de Meijere cyclopropanation to synthesize the aminoCPs, only trialkylamines were evaluated. Aryl amides, common amine protecting-groups (e.g. -Boc, -CBz), or coordinating species (-OTs, -OH) are not well-tolerated under the cyclopropanation conditions, but an alternative photochemical approach to accessing free-amine aminoNBs has been developed by our group.⁶¹ In addition to morpholine, piperidine **2.19**, *N*-methyl piperazine **2.20**, chiral pyrrolidine **2.21**, and fluorinated azetidine **2.22** aminoNBs were prepared (Figure 2.10). In all cases, the addition of 20 mol% ZnCl₂ enhanced the yield of the reaction. The modest yields of *N*-methyl piperazine **2.20** (no additive 33%; ZnCl₂

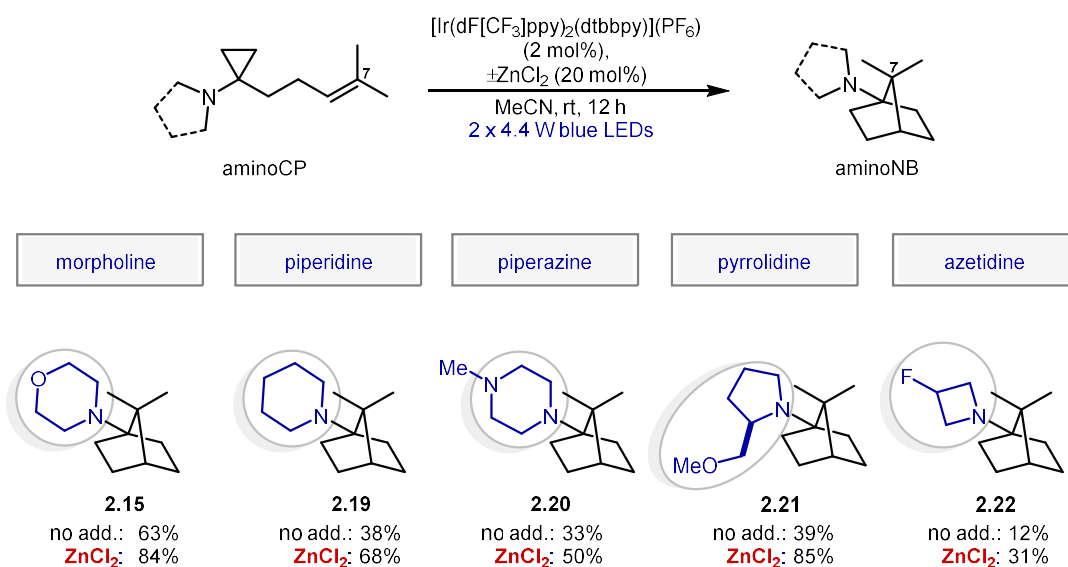


Figure 2.10. Scope of trialkylamines

50%) are a particularly demonstrative result in that the oxidation of the cyclopropylamine is somewhat selective in the presence of other trialkylamines due to the post-fragmentation pathway.

In addition to enabling the use of various nitrogen heterocycles, this methodology proved effective for substituting all sites on the norbornane core, generating C2-, C3-, C4-, and C7-substituted scaffolds (Figure 2.11). Presence of C2-methyl substitution led to preferential formation of the C2-axial isomer in a 4:1 *dr* and 71% yield as seen with aminoNB **2.23**. A C2-prenyl substituent was less well-tolerated due to competing cyclization and C-H abstraction pathways, and aminoNB **2.24** was isolated in only 21% yield and low (1.5:1 *dr*). Moderate selectivity for the equatorial C3-methyl aminoNB **2.25** was observed when the methyl substitution

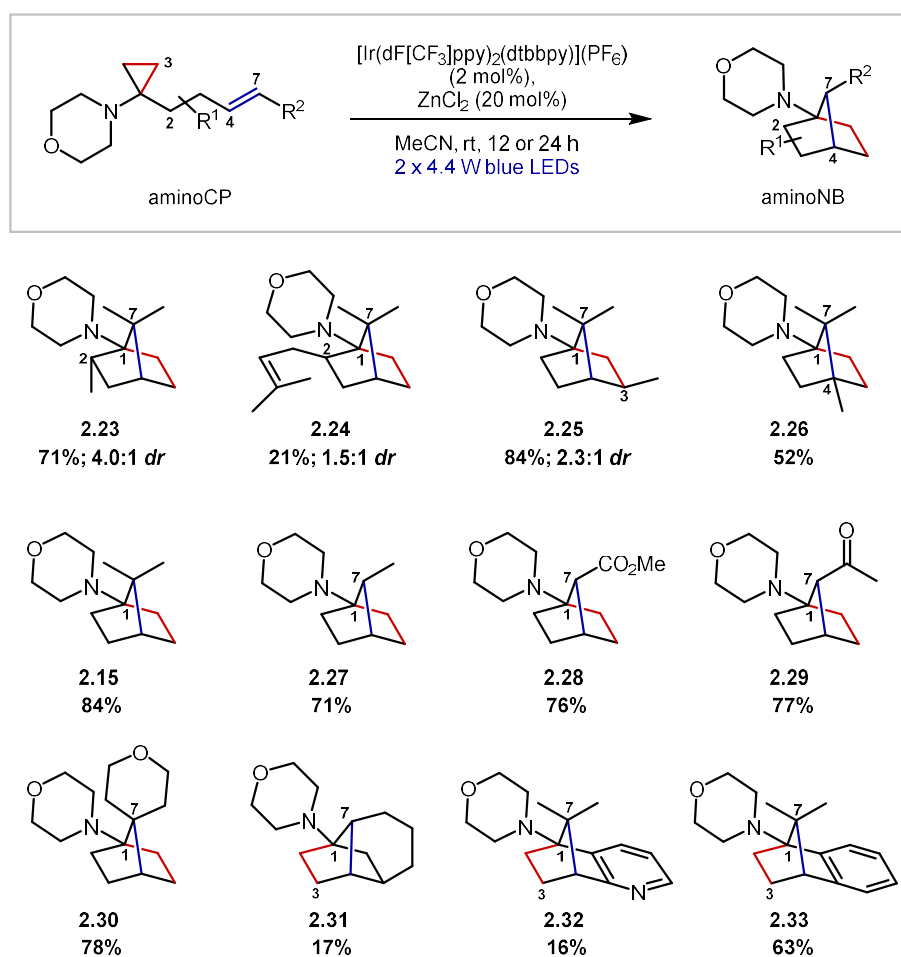


Figure 2.11. Substitution accessible on the norbornane core

arose from substitution off of the cyclopropane ring (2.3:1 *dr*), while allylic functionality proceeded with high selectivity for axial C3-substitution (*vide infra*). C7 mono- and di-methyl aminoNBs **2.15** and **2.27** were prepared in 84% and 71% yield, respectively, but terminal alkene aminoCPs were unable to generate C7 methylene aminoNBs (see **2.39** and **2.67**). However, both acrylate- and enone-based aminoCPs were efficiently converted to C7-substituted aminoNBs **2.28** and **2.29** (76% and 77% yield, respectively). Further annulated aminoNBs were also accessible via this strategy, as evidenced by C7 spirocyclic aminoNB **2.30** (78% yield after 24 h) and C3-C7-propyl-bridged aminoNB **2.31**. This bridged system was low-yielding (17%) regardless of irradiation time, presumably due to unfavorable torsional strain during the radical cyclizations. C2-C3 (hetero)aryl-fused aminoNBs **2.32** and **2.33** necessitated an extended reaction time (24 h) likely due to the competing photosensitization of the styrenyl functionality in the aminoCP substrate.

C4-methyl aminoNB **2.26** was prepared in a modest 52% yield, but the analogous C4-phenyl system afforded bicyclo[3.2.0]heptane **2.38** in 21% yield with 51% recovered starting material (**2.34**) (Figure 2.12). This byproduct arises from an initial *7-endo-trig* cyclization to provide highly stabilized tertiary benzylic radical **2.36** before *4-exo-trig* cyclization into the iminium. This mechanistic pathway likely predominates over the typical radical cyclization sequence as the *6-exo-trig* cyclization would yield high energy primary radical intermediate **2.41**. We postulate that the lifetime of this radical is not sufficiently long-lived enough for the cyclohexane to undergo a conformational change from chair **2.41** to the boat **2.42** required for the final radical ring closure. Instead, if the barrier for the *6-exo-trig* cyclization is even low enough to proceed at room temperature, radical intermediate **2.41** reverts back to pre-cyclized species **2.40** or aminoCP **2.34** and funnels through the *7-exo-trig* pathway.

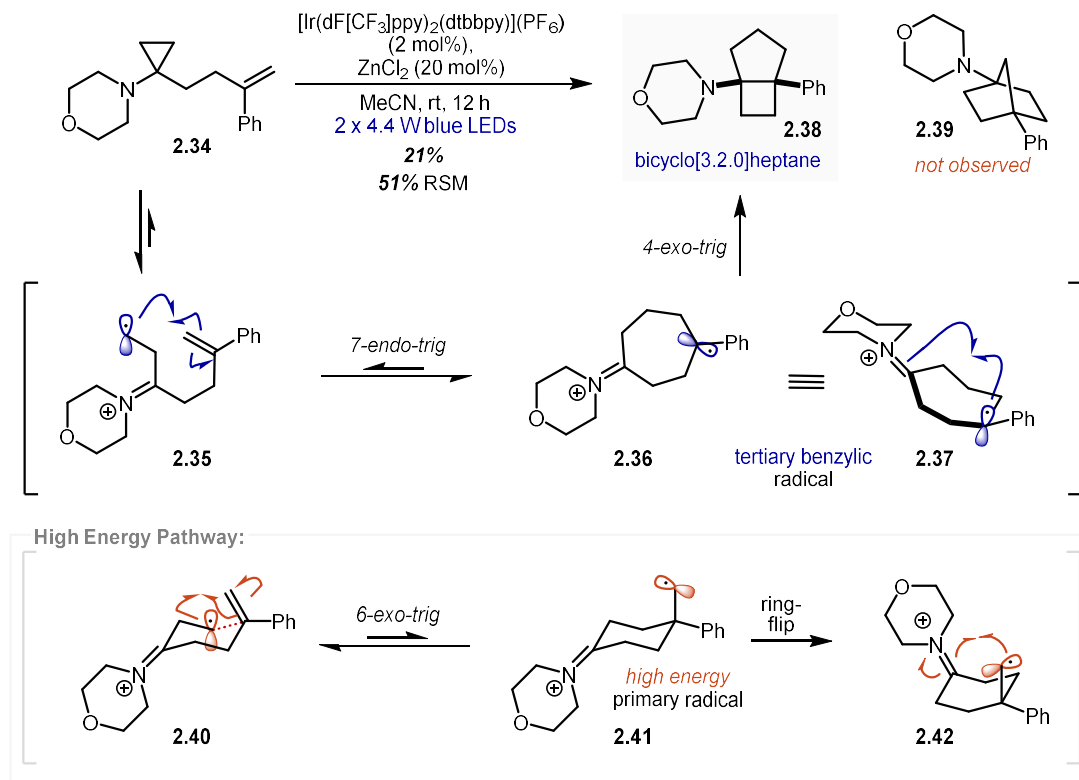


Figure 2.12. Proposed pathway toward bicyclo[3.2.0]heptane by-product **2.38**

During the course of these studies, high levels of diastereoselectivity were observed for two classes of substrates. Significantly, the two series of aminoCPs discussed below further highlights the robust functional group tolerance of this strategy, incorporating alcohol, acyloxy, amide, and carbamate motifs in good to high yields while featuring unique stereochemical qualities of this reaction platform.

Substrates with allylic substitution of the form **2.43** could potentially yield C3-equatorial (**2.47**) and C3-axial (**2.48**) aminoNBs (Figure 2.13). However, in all cases, >20:1 diastereoselectivity was observed favoring the axial substitution. This outcome arises from minimization of $A_{1,3}$ strain in intermediate **2.44** before the *6-exo-trig* cyclization, placing the large group equatorial. Preceding the *5-exo-trig*, the large substituent is placed axially after a ring-flip from a chair (**2.45**) to a boat conformation (**2.46**), ultimately giving rise to the observed selectivity.

The divergent axial vs. equatorial selectivities of cyclopropane-substituted (**2.74** and **2.75**) and allylic-substituted (**2.43**) aminoCPs offers complementary forms of diastereocontrol at the C3 position, avoiding the necessity of developing elements of exogenous asymmetric induction.

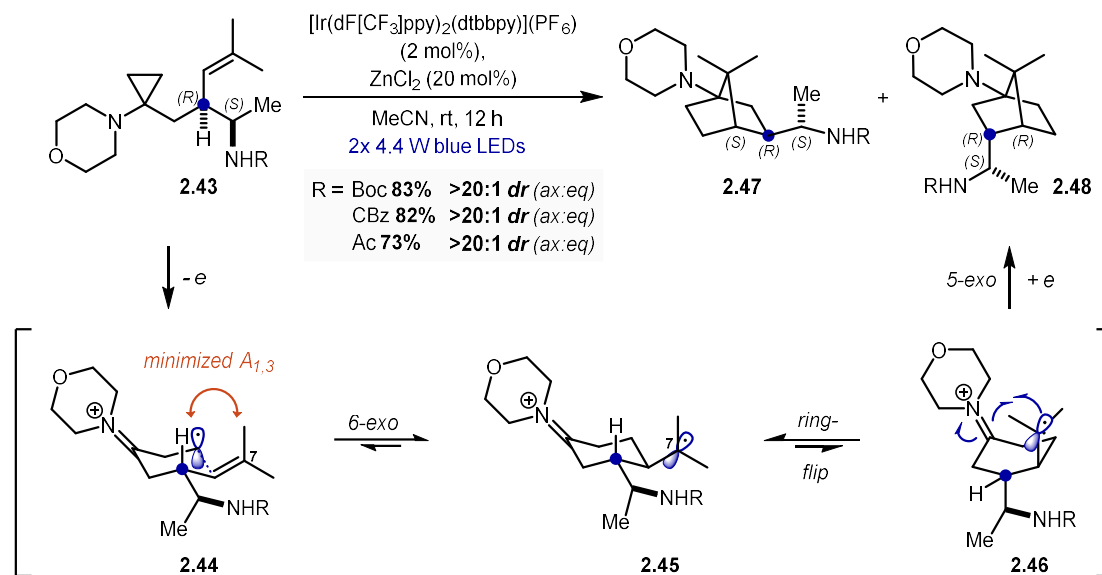


Figure 2.13. Stereochemical model for the high diastereoselectivity observed in allylic-substituted aminoCPs

The second diastereoselective variant concerns aminoCPs bearing a chiral center at the C8 position (**2.49**) (Figure 2.14). These substrates were predicted to yield diastereomeric aminoNBs **2.50** and **2.51**, and it was discovered that varying degrees of diastereoselectivity were observed depending on the identity of the C8-substituent. Complete control for the 7*S*,8*R* isomer was obtained when employing free alcohol aminoCP **2.52**, but this selectivity was eroded upon differential protection of the alcohol. The increasing availability of the oxygen lone pairs (both in steric and electronic terms; -OH > -OBn > -OAc > -OTBS) was positively correlated with selectivity for the 7*S*,8*R* diastereomer. Our hypothesis for these observations is that the oxygen lone pairs are donating into the antibonding orbital of the iminium species in the earliest phases of the transition state for the formation of the C1-C7 bond, a donation that is readily accomplished toward the favored 7*S*-epimer (**2.56**) but impeded by steric encumbrance *en route* to the disfavored

7*R*-epimer (**2.57**). When the oxygen lone pairs are less accessible, this interaction cannot occur and the reaction proceeds through alternative transition states (e.g. **2.58** and **2.59**) which are not energetically differentiated to favor either the 7*S* or the 7*R* product. A detailed investigation of this proposed stereochemical model was carried out and the results of which are reported in Chapter 3.

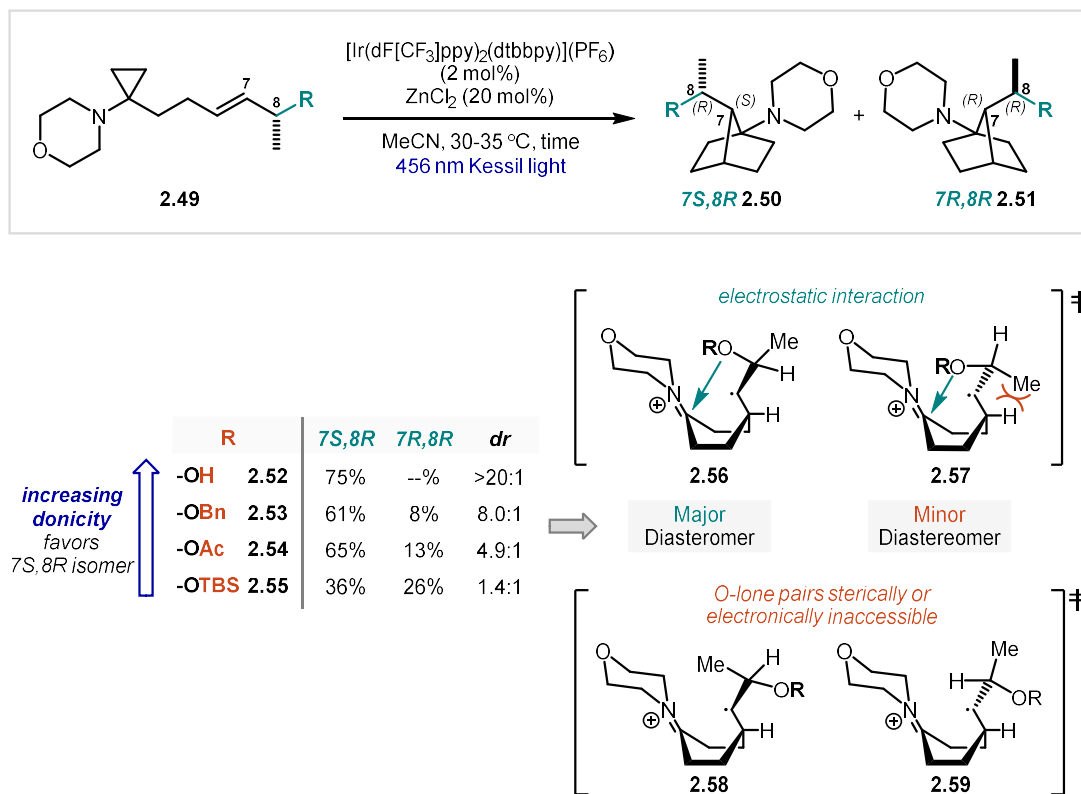


Figure 2.14. Results and stereochemical model for aminoCPs of form **2.49**

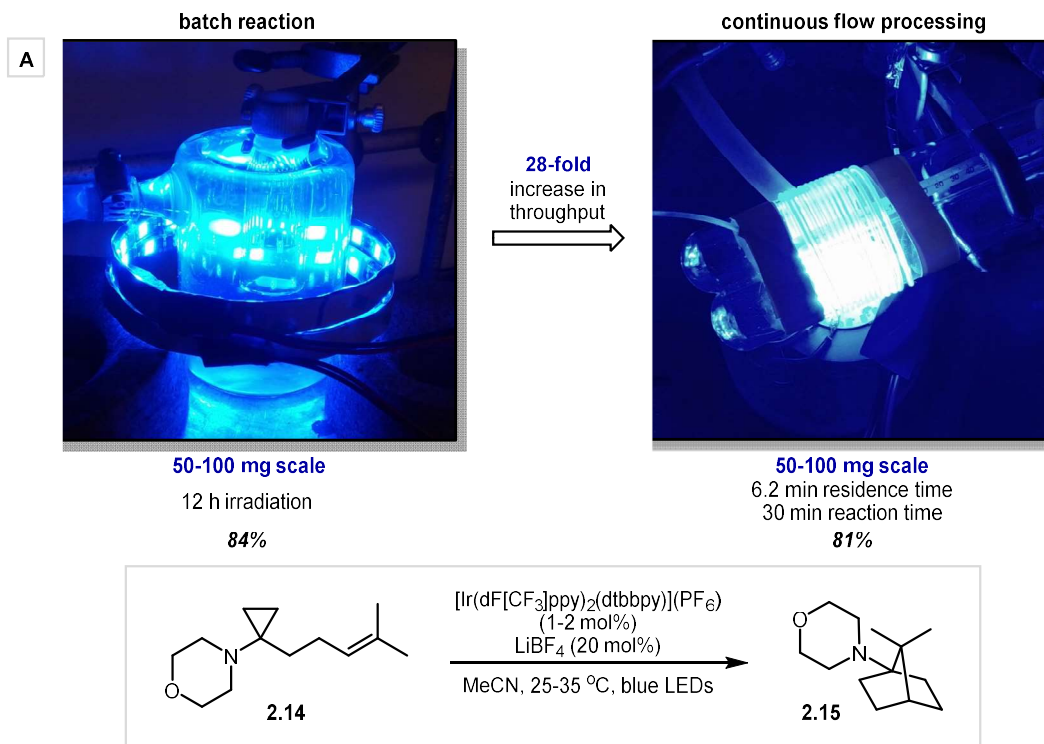
2.2.6 Continuous Flow Processing

One of the attractions of photochemical reactions is their potential to be readily translated to larger scales via continuous flow processing. Efforts from our group have demonstrated the benefits of adapting photoredox methodologies to continuous flow systems, such as decreased catalyst loadings and increased reaction efficiency. Although we have developed this [3+2] photochemical cyclization with the intention of application in a medicinal chemistry setting, we

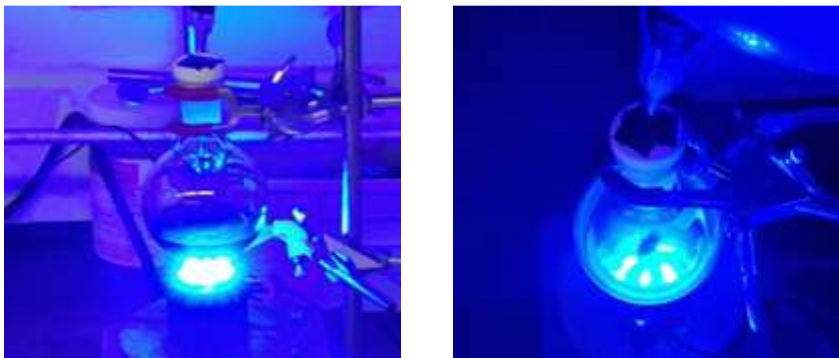
wanted to show that this methodology is also amenable to large-scale processing relevant to industrial settings.

The set-up for the standard batch reaction and flow reactor is pictured in Figure 2.15A. On 50-100 mg scale, a 2-dram vial containing the reaction mixture is placed in a jacketed water bath with circulating water to maintain constant reaction temperature and irradiated by 2x 4.4 W blue LED strips. We constructed the flow reactor in-house by wrapping PFA tubing around two test tubes and placing over blue LEDs mounted onto a heat sink. Optimization identified that a 6.2 min residence time was required to consume all of the aminoCP, and 20 mol% of LiBF₄ was employed as the Lewis acid additive to alleviate concerns of clogging related to slight heterogeneity of reaction mixtures with ZnCl₂. Attempts were made to lower the catalyst loading from 2 mol%, but the reaction efficiency significantly suffered (see Figure 2.26). Under these conditions, the flow reaction of aminoCP **2.14** provided aminoNB **2.15** in 81% yield in only 30 min, directly comparable to the 12 h batch reaction result of 84% yield.

Increasing the scale of the reaction to one gram (Figure 2.15B), the flow reaction provided 70% of aminoNB **2.15** with 11% recovered starting material (81% total mass recovery) after 7.2 h total reaction time (Entry 1). To keep time constant, the gram-scale batch reaction was also irradiated for 7.2 h using the same light source as the flow reaction, and aminoCP **2.14** was fully consumed to produce aminoNB **2.15** in 65% yield (Entry 2). However, due to the low mass recovery and concerns of product decomposition, an additional batch reaction was performed in which aminoCP was irradiated for half of the prescribed time (3.6 h) with 1 mol% photocatalyst **2.16**. AminoNB **2.15** was isolated in 73% yield along with 14% recovered starting material (87% total mass recovery) (Entry 3).



B Gram-Scale Reactions:



Entry	Processing	Time (h)	Catalyst Loading	Yield	Recovered SM	Throughput
1	flow	7.2	2 mol%	70%	11%	0.008 mmol/min
2	batch	7.2	2 mol%	65%	0%	0.007 mmol/min
3	batch	3.6	1 mol%	73%	14%	0.016 mmol/min

Figure 2.15. (A) Adaption of small-scale batch reaction to continuous flow processing; (B) Comparison of batch and flow reactors on gram scale

The table in Figure 2.15B clearly shows an improvement in throughput in batch processing relative to flow processing (2x increase in throughput between flow Entry 1 and batch Entry 3), a

result that runs contrary to the *status quo* of photoredox catalysis flow reactions. This data is thought to be largely a consequence of reactor design rather than factors inherent to the reaction itself. In Figure 2.15A, the image on the right shows that a substantial amount of light is passing directly through the flow reactor. To prevent overexposure of the image, this picture was taken while operating the lights at 30 mA rather than at the working current for the reaction. Comparing this to the pictures of the gram-scale batch reaction in Figure 2.15B, where the lights are operating at 700 mA (over 20-fold increase in light output), the background of the image is darker suggesting less light scattering. Despite the dramatic increase in light intensity, the large-scale batch reaction is actually letting less light penetrate through the reaction mixture. The simple consequence of this discrepancy is that the reaction in flow is absorbing fewer photons/second because of all the light passing through the dead space not containing the reaction mixture. Importantly, typical discussions of flow processing will reference “enhanced light penetration,” yet this does not speak to the number of photons delivered but the homogeneity with which they are delivered across the reaction mixture. For the experiments presented, the number of photons absorbed is sufficiently different between the batch and flow reactions such that the benefits of more uniform irradiation are made insignificant. More quantitatively, this flow system only suspends 715 μL of reaction mixture above the light source at a given time, while the batch setup places the entirety of the mixture (50 mL) above the LEDs for the entire duration of the reaction. In flow, this setup necessarily imposes the limitation that only $\sim 1.4\%$ of photocatalyst has access to light at any given time ($0.715 \text{ mL}/50 \text{ mL} = 1.4\%$). The batch system may not boast the same evenness of light penetration, but it places the full catalyst loading in the path of the light throughout the course reaction, assuredly leading to more total excitation events. Thus, the unexpected reversal of

efficiency for this batch vs. flow comparison may be a result of using a relatively small flow reactor.

In addition to the above engineering-based issue, the choice of photocatalyst could also be playing a role in the unusually high efficiency of the batch reaction. Many of the initial and current applications of visible light photoredox catalysis in flow employ Ru(bpy)₃²⁺ salts (such as **2.17**) as the photocatalyst rather than the Ir(III) catalyst **2.16** used in this methodology. The most common Ru(II) photocatalysts tend to produce dark reaction mixtures over time, presumably the result of various catalyst decomposition pathways.⁶² These colored byproducts necessarily absorb some of the light, reducing the number of photons reaching the active catalyst. With the prolonged reaction times of batch processing, this darkening can become a major issue, giving strong impetus for switching to flow.⁶³ The Ir(III) photocatalysts will also suffer decomposition under certain conditions,⁶⁴ but with the method reported herein, these do not significantly darken the reaction mixture, allowing light to penetrate the batch setup as efficiently at the end of the reaction as it does at the outset. Additionally, Ir(III) photocatalysts tend to have substantially lower extinction coefficients than Ru(II) systems at ~450 nm (as much as two orders of magnitude⁶⁵), necessarily meaning that light can reach deeper into batch reactions with catalysts such as photocatalyst **2.16**. Collectively, this suggests that the choice of Ir(III) photocatalyst **2.16** could place limits on the benefit that can be achieved in flow when compared to the benefits available to analogous Ru(II)-catalyzed methods. It is also possible that the nature of the mechanism (propagative vs. closed cycle) plays a role; empirically, one can observe that many of the reactions that have proven highly efficient in flow involve chain processes. The presence of a slow rate-determining step that does not involve an electron transfer with the photocatalyst (as is suspected to be the case with this method) could also impact the efficiency in batch and in flow differently. Work in the group is

currently evaluating several reaction types, photocatalysts, and commercial flow reactors to develop a more robust and nuanced understanding of continuous flow photochemistry, which will ideally facilitate the transitions from batch to flow and from discovery to industrial scales. Importantly, this work still demonstrates that this reaction can be adapted to a continuous flow process, and subsequent optimization has resulted in improved reaction efficiency (see Chapter 4).

2.3 Conclusion

This report details the most efficient and flexible access to aminoNBs to date in an effort to provide the medicinal chemistry community with a valuable new saturated building block. Reaction optimization revealed a beneficial but mechanistically complex role of Lewis acid catalysts that may have implications beyond this methodology. Through this photochemical approach, a wide variety of substitution patterns have been readily prepared, many incorporating functional handles for further diversification. These include enantiomerically pure aminoNBs via diastereoselective variants, a central requirement for drug discovery purposes, as well as bridged, fused, and spirocyclic structures for exploration of unique chemical space. This methodology operates well in continuous flow, including gram-scale preparations, suggesting that this chemistry can translate beyond discovery scale. Future investigations will seek to demonstrate the value of these substructures for generating bioactive leads.

2.4 Experimental Procedures and Characterization of Compounds

2.4.1 General Methods

Unless otherwise noted, all reactions were run under a nitrogen atmosphere in flame-dried glassware. Reactions were stirred using Teflon-coated magnetic stir bars. Reactions were monitored by thin layer chromatography (TLC) using glass-backed plates pre-coated with 230–400 mesh silica gel (250 μm thickness) with fluorescent indicator F254, available from EMD Millipore (cat. #1.05715.0001). Plates were visualized by treatment with UV, acidic *p*-anisaldehyde stain, KMnO_4 stain, or aqueous ceric ammonium molybdate (Hanessian's stain) with gentle heating. Products were purified by flash column chromatography using the solvent systems indicated. Silica gel was purchased from SiliCycle, specifically using SiliaFlash P60, 40–63 μm , 230–400 mesh (cat. #: R12030B).

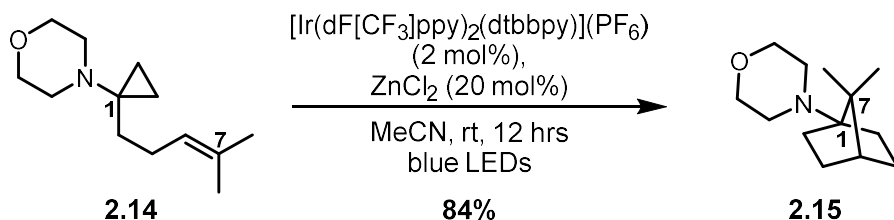
Organic solvents (acetonitrile, dichloromethane, diethyl ether, dimethylformamide, dimethyl sulfoxide, methanol, tetrahydrofuran, toluene) and amine bases (triethylamine, pyridine, *N,N*-diisopropylethylamine, and diisopropylamine) were purified prior to use by the method of Grubbs and co-workers⁶⁶ using a Phoenix Solvent Drying System (for organic solvents, available from JC-Meyer Solvent Systems) or PureSolv Micro amine drying columns (for amine bases, available from Innovative Technology/Inert) under positive argon pressure; all were supplied by Fisher Scientific. Titanium isopropoxide was obtained from Alfa-Aesar, distilled immediately upon receipt, and stored in a clean sure-seal bottle under inert atmosphere. Unless otherwise noted, all other reagents were purchased from Sigma-Aldrich, stored as recommended by the supplier, and used without any additional purification.

NMR spectra were measured on a Varian INOVA 500 (^1H at 500 MHz), a Varian VNMR 500 (^1H at 500 MHz, ^{13}C at 126 MHz), or a Varian VNMR 700 MHz (^1H at 700 MHz, ^{13}C at 176

MHz) magnetic resonance spectrometer. ^1H chemical shifts are reported relative to the residual solvent peak (chloroform = 7.26 ppm; benzene = 7.16 ppm) as follows: chemical shift (δ) (multiplicity [s = singlet, d = doublet, t = triplet, quart. = quartet, quint. = quintet, hept. = heptet, b = broad, *app* = apparent], integration, coupling constant(s) in Hz, proton ID [when available, designated by carbon number]). Deuterated solvents were obtained from Cambridge Isotope Laboratories, Inc. Proton assignments were made via 2D spectroscopy (COSY, HSQC, HMBC, and/or NOESY) and/or analogy to related systems. ^{13}C chemical shifts are reported relative to the residual deuterated solvent ^{13}C signals (CDCl_3 = 77.16 ppm, C_6D_6 = 128.1 ppm). Infrared spectra were recorded on either a Perkin-Elmer Spectrum BX or a Nicolet iS50 FT-IR spectrophotometer using an ATR mount with a ZnSe crystal and are reported in wavenumbers (cm^{-1}). Optical rotation data were obtained using a JASCO P-2000 Polarimeter and are reported as $[\alpha]_{\text{D}}^{\text{T}}$ (c = grams/100 mL), where D indicates the sodium D line (589 nm) and T indicates temperature (all optical rotation values were obtained at ambient operating temperature, ca. 22-28 °C). High resolution mass spectra were obtained using a Micromass AutoSpec Ultima Magnetic Sector mass spectrometer using electrospray ionization (ESI), positive ion mode, or electron impact ionization (EI); we thank Dr. James Windak and Dr. Paul Lennon at the University of Michigan Department of Chemistry instrumentation facility for conducting these experiments.

2.4.2 Reaction Optimization

The optimization of the visible light-mediated formal [3+2] cycloaddition was performed with 7,7-dimethyl aminoCP **2.14** on ~250 μmol scale in the fashion described below. The results of these trials are summarized in Figure 2.5.



General Procedure

In a dry vial under nitrogen, aminoCP **2.14** (51.6 mg, 247 μmol) was dissolved in 2.5 mL dry MeCN before adding $[\text{Ir}(\text{dF}[\text{CF}_3]\text{ppy})_2(\text{dtbbpy})](\text{PF}_6)$ (5.5 mg, 4.9 μmol) then ZnCl_2 (1.0 M in ether, 49 μL , 49 μmol) in one portion each. Reaction mixture is bright yellow, but slightly cloudy from the Zn salt. Reaction mixture was degassed with three freeze-pump-thaw cycles. The reaction was performed by stirring at room temp (as controlled with jacketed water bath, temp maintained between 18-23 $^\circ\text{C}$) while irradiating with two strips of 4.4 W blue LEDs for 12 hrs. Mixture appeared somewhat cloudier than it did prior to irradiation and perhaps slightly darker yellow. A 25 μL aliquot was removed and diluted into 450 μL MeCN + 25 μL of a dodecane standard solution (5 mM in MeCN) both prior to degassing (total volume = MeCN volume) and after 12 hrs (5 mL total volume; reaction mixture diluted with ether in 5 mL vol. flask); these samples were run on the GC/MS to measure starting material conversion. The diluted mixture was added to 10 mL 1:1 sat. NaHCO_3 :water containing 1 mL of 50% NaOH to ensure aqueous phase pH ~14, then diluted further with 5 mL hexanes. Phases were separated, and the aqueous phase was extracted

with 10 mL 1:1 ether:hexanes three times. Combined organics were washed with 10 mL brine, dried over anhydrous magnesium sulfate, filtered to remove solids, and concentrated *in vacuo*. The crude residue was purified via flash chromatography over silica (4 to 28% ethyl acetate:hexanes, increasing in 4% increments; residue loaded with PhMe).

- GCMS conversion: 94%

- Recovered starting material: 4.0 mg; clear, colorless oil, but ^1H NMR revealed minor impurities; ~8% recovery

- Product: 42.8 mg (46.8 mg collected, 91.5 wt% with ethyl acetate by ^1H NMR); clear, colorless oil; 84.2% yield

Additional Trials with Varied Additives

No Additive (Entry 1)

Following the general procedure outlined above, 51.4 mg of aminoCP **2.14** (246 μmol) were dissolved in 2.5 mL dry MeCN along with 5.5 mg of $[\text{Ir}(\text{dF}[\text{CF}_3]\text{ppy})_2(\text{dtbbpy})](\text{PF}_6)$ (4.9 μmol) prior to irradiation. Isolation provided the following:

- GCMS conversion: 79%

- Recovered starting material: 12.2 mg (12.5 mg collected, 97.3 wt% with pentane); clear, colorless oil; 24.1% recovery

- Product: 32.1 mg; clear, colorless oil; 63.4% yield, 83.5% BORSM

LiBF₄ (entry 3)

Following the general procedure outlined above, 52.6 mg of aminoCP **2.14** (251 μmol) were dissolved in 2.5 mL dry MeCN along with 5.6 mg of $[\text{Ir}(\text{dF}[\text{CF}_3]\text{ppy})_2(\text{dtbbpy})](\text{PF}_6)$ (5.0

μmol) and 4.7 mg of LiBF_4 (50 μmol) prior to irradiation. Isolation provided the following:

- GCMS conversion: 93%
- Recovered starting material: 8.0 mg; clear, colorless oil, but ^1H NMR revealed minor impurities; ~15% recovery
- Product: 41.0 mg (42.0 mg collected, 97.4 wt% with ethyl acetate); slightly yellow oil; 79.1% yield

NaBF₄ (entry 4)

Following the general procedure outlined above, 52.6 mg of aminoCP **2.14** (251 μmol) were dissolved in 2.5 mL dry MeCN along with 5.6 mg of $[\text{Ir}(\text{dF}[\text{CF}_3]\text{ppy})_2(\text{dtbbpy})](\text{PF}_6)$ (5.0 μmol) and 5.5 mg of NaBF_4 (50 μmol) prior to irradiation. Isolation provided the following:

- GCMS conversion: 87%
- Recovered starting material: 9.7 mg; clear, colorless oil; 18.7% recovery
- Product: 34.3 mg; clear, colorless oil; 66.2% yield, 81.4% BORSM

Me₂AlCl (entry 5)

Following the general procedure outlined above, 54.2 mg of aminoCP **2.14** (259 μmol) were dissolved in 2.5 mL dry MeCN along with 5.8 mg of $[\text{Ir}(\text{dF}[\text{CF}_3]\text{ppy})_2(\text{dtbbpy})](\text{PF}_6)$ (5.2 μmol) and 52 μL of Me_2AlCl (1.0 M in hexanes, 52 μmol) prior to irradiation. Reaction mixture was bright orange after irradiation. Isolation provided the following:

- GCMS conversion: 78%
- Recovered starting material: 10.9 mg; clear, colorless oil; 20.4% recovery
- Product: 31.4 mg; clear, colorless oil; 58.8% yield, 73.9% BORSM

BF₃·OEt₂ (entry 6)

Following the general procedure outlined above, 52.4 mg of aminoCP **2.14** (250 μmol) were dissolved in 2.5 mL dry MeCN along with 5.6 mg of [Ir(dF[CF₃]ppy)₂(dtbbpy)](PF₆) (5.0 μmol) and 6.2 μL of BF₃·OEt₂ (50 μmol) prior to irradiation. Reaction mixture was bright orange after irradiation. Isolation provided the following:

- GCMS conversion: 92%
- Recovered starting material: 5.6 mg; clear, colorless oil, but ¹H NMR revealed minor impurities;
~11% recovery
- Product: 35.4 mg; slightly yellow oil; 68.6% yield

MgBr₂·OEt₂ (entry 7)

Following the general procedure outlined above, 52.6 mg of aminoCP **2.14** (251 μmol) were dissolved in 2.5 mL dry MeCN along with 5.6 mg of [Ir(dF[CF₃]ppy)₂(dtbbpy)](PF₆) (5.0 μmol) and 13.0 mg of MgBr₂·OEt₂ (50 μmol) prior to irradiation. Salt remained a white precipitate at outset of reaction; post-irradiation, reaction still had white precipitate, but the clear yellow solution above the salt had become slightly cloudy and somewhat orange. Isolation provided the following:

- GCMS conversion: 97%
- Recovered starting material: 2.7 mg; clear, colorless oil, but ¹H NMR revealed minor impurities;
~5% recovery
- Product: 38.9 mg; clear, colorless oil; 75.1% yield

CuBr₂ (entry 8)

Following the general procedure outlined above, 52.3 mg of aminoCP **2.14** (250 μmol) were dissolved in 2.5 mL dry MeCN along with 5.6 mg of $[\text{Ir}(\text{dF}[\text{CF}_3]\text{ppy})_2(\text{dtbbpy})](\text{PF}_6)$ (5.0 μmol) and 11.2 mg of CuBr_2 (50 μmol) prior to irradiation. Reaction mixture was red-orange at outset and turned dark red after irradiation (color potentially precluded efficient excitation of photocatalyst). Isolation provided the following:

- GCMS conversion: 47%
- Recovered starting material: 19.9 mg; clear, colorless oil; 38.6% recovery
- Product: 10.5 mg; clear, colorless oil; 20.4% yield, 33.2% BORSM

NiCl₂ (entry 9)

Following the general procedure outlined above, 53.1 mg of aminoCP **2.14** (254 μmol) were dissolved in 2.5 mL dry MeCN along with 5.7 mg of $[\text{Ir}(\text{dF}[\text{CF}_3]\text{ppy})_2(\text{dtbbpy})](\text{PF}_6)$ (5.1 μmol) and 6.6 mg of NiCl_2 (51 μmol) prior to irradiation. The reaction was heterogeneous at outset of reaction, and after irradiation, reaction mixture was very cloudy, orange, and contained some grey precipitate. Isolation provided the following:

- GCMS conversion: 53%
- Recovered starting material: not isolated (overlapped with impurity)
- Product: 25.6 mg; clear, colorless oil; 48.9% yield

Ru(bpy)₃²⁺ trial, no additive (entry 10)

Following the general procedure outlined above, 52.4 mg of aminoCP **2.14** (250 μmol) were dissolved in 2.5 mL dry MeCN along with 3.8 mg of $[\text{Ru}(\text{bpy})_3]\text{Cl}_2 \cdot 6\text{H}_2\text{O}$ (5.0 μmol) prior

to irradiation. Reaction mixture was clear, red solution pre-irradiation, then turned a dark purple over the course of reaction. Isolation provided the following:

- GCMS conversion: 7%
- Recovered starting material: 45.5 mg; clear, colorless oil; 88.1% recovery
- Product: none detected

Ru(bpy)₃²⁺ trial, ZnCl₂ (entry 11)

Following the general procedure outlined above, 51.4 mg of aminoCP **2.14** (246 μmol) were dissolved in 2.5 mL dry MeCN along with 3.7 mg of [Ru(bpy)₃]Cl₂·6H₂O (4.9 μmol) and 49 μL of ZnCl₂ (1.0 M in ether, 49 μmol) prior to irradiation. Reaction mixture was slightly cloudy, red solution at pre-irradiation; post-irradiation, the mixture was slightly cloudier, but the red-orange color was consistent with the initial reaction mixture. Isolation provided the following:

- GCMS conversion: 48%
- Recovered starting material: 26.4 mg; clear, colorless oil; 52.1% recovery
- Product: 17.2 mg; clear, colorless oil; 34.0% yield, 71.0% BORSM

No photocatalyst control (entry 12)

Following the general procedure outlined above, 51.1 mg of aminoCP **2.14** (244 μmol) were dissolved in 2.5 mL dry MeCN along with 49 μL of ZnCl₂ (1.0 M in ether, 49 μmol) prior to irradiation. Reaction mixture was colorless and slightly cloudy at outset, becoming only faintly yellow over the course of reaction. Isolation provided the following:

- GCMS conversion: 1%
- Recovered starting material: 48.2 mg; clear, colorless oil; 95.8% recovery

- Product: none detected

No light control (entry 13)

Following the general procedure outlined above, 52.3 mg of aminoCP **2.14** (250 μmol) were dissolved in 2.5 mL dry MeCN along with 5.6 mg of $[\text{Ir}(\text{dF}[\text{CF}_3]\text{ppy})_2(\text{dtbbpy})](\text{PF}_6)$ (5.0 μmol) and 50 μL of ZnCl_2 (1.0 M in ether, 50 μmol) prior to stirring for 12 hrs at room temp without exposure to light (vial wrapped in foil). Isolation provided the following:

- GCMS conversion: <1%

- Recovered starting material: 51.1 mg; clear, colorless oil; 99.2% recovery

- Product: none detected

Control for thermal reactivity (entry 14)

Following the general procedure outlined above, 51.4 mg of aminoCP **2.14** (246 μmol) were dissolved in 2.5 mL dry MeCN then heated to 80 $^\circ\text{C}$ for 12 hrs without exposure to light (vial wrapped in foil). Isolation provided the following:

- GCMS conversion: <1%

- Recovered starting material: 48.4 mg; clear, colorless oil; 95.6% recovery

- Product: none detected

2.4.3 Differential Pulse Voltammetry

Differential pulse voltammetry was employed to determine whether or not the Lewis acid additives were facilitating the conversion of starting material (at least in part) by lowering the oxidation potential of the substrate. A representative procedure for obtaining these measurements is detailed below:

A stock solution of electrolyte was prepared by dissolving tetrabutylammonium tetrafluoroborate (1.65 g, 5.0 mmol) in 50 mL dry MeCN. This mixture was degassed with three freeze-pump-thaw cycles and stored under nitrogen for continued use. The substrates of interest were all freshly purified via chromatography, and pre-aliquoted into ~300 μ mol portions. Each substrate was dissolved in ~3.0 mL degassed electrolyte solution (100 mM substrate stock solution), before adding 1.2 equivalent of the additive in question. The resultant mixture was sonicated for 2 min before being transferred into the electrochemical cell and evaluated.

The equipment employed is as follows: CHI620E potentiostat from CH Instruments running through an HP laptop; platinum wire as the counter electrode; glassy carbon with 3 mm² electrode surface (polished with 0.05 micron Micro-Polish powder from CH Instruments before and after each use); Ag/AgCl reference electrode; standard electrochemical cell, sealed under positive pressure of Ar for each trial. All trials collected data sweeping from 0 to +2.0 V (4 mV increments; amplitude = 50 mV; pulse width = 0.05 s; sample width = 0.0167 s; pulse period = 0.5 s).

This setup was used to evaluate the effects of LiBF₄ on the oxidation potential of morpholine-based aminoCP **2.14**, 1-aminoNB **2.15**, and *N*-methylmorpholine (NMM) (see Figure 2.16 for voltammograms). Similar comparison was also made for the piperidine, piperazine, and prolinol scaffolds (see Figure 2.17 for voltammograms). The data is summarized in Figure 2.18.

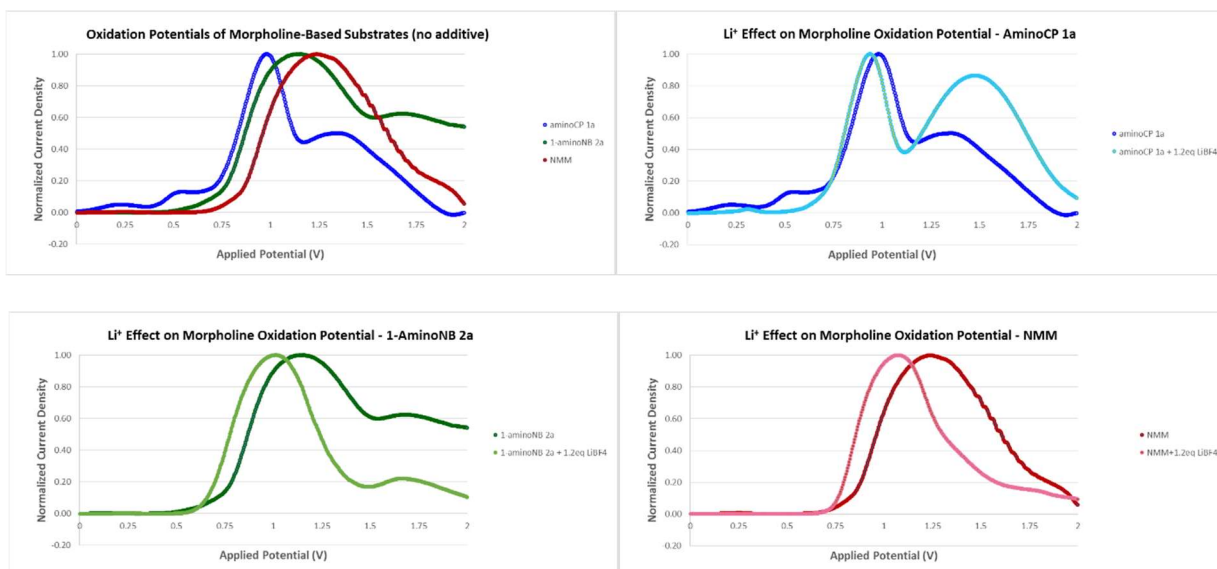


Figure 2.16. Effects of LiBF₄ on the Oxidation Potential of Morpholine-Derived Systems
 Top Left: Voltammograms of aminoCP **2.14**, 1-aminoNB **2.15**, and NMM without LiBF₄;
 Top Right: Voltammogram of aminoCP **2.14** with and without LiBF₄;
 Bottom Left: Voltammogram of 1-aminoNB **2.15** with and without LiBF₄;
 Bottom Right: Voltammogram of *N*-methylmorpholine (NMM) with and without LiBF₄.

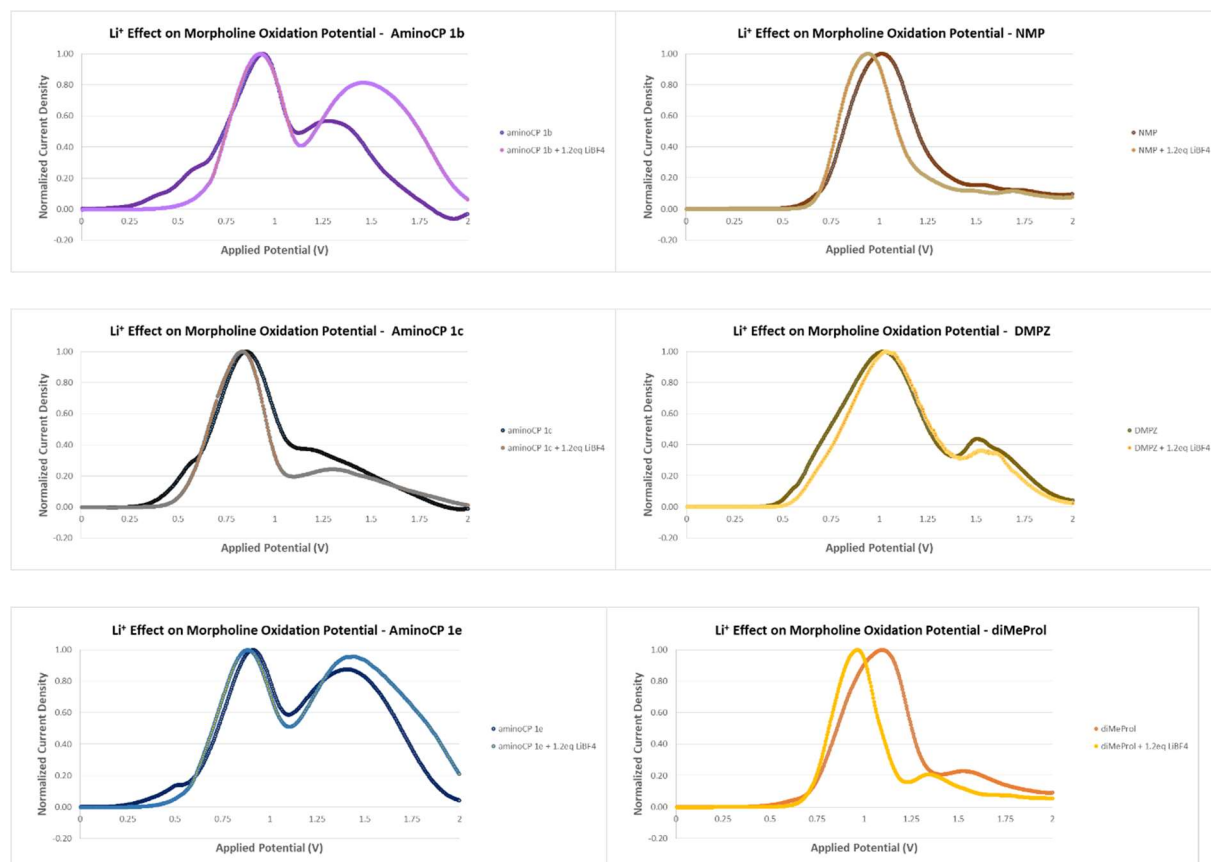


Figure 2.17. Effects of LiBF₄ on the Oxidation Potential of Piperidine, Piperazine, and Prolinol scaffolds

Top Left: Voltammogram of piperidine aminoCP **2.13** with and without LiBF₄;

Top Right: Voltammogram of *N*-methylpiperidine (NMP) with and without LiBF₄;

Middle Left: Voltammogram of piperazine-based aminoCP **2.17** with and without LiBF₄;

Middle Right: Voltammogram of *N,N'*-dimethylpiperazine (DMPZ) with and without LiBF₄;

Bottom Left: Voltammogram of prolinol-based aminoCP **2.18** with and without LiBF₄;

Bottom Right: Voltammogram of *N,O*-dimethylprolinol (diMeProl) with and without LiBF₄.

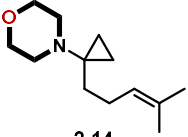
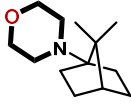
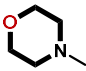
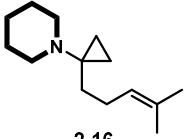
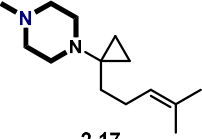
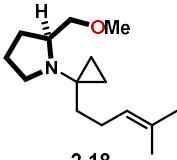
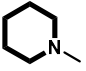
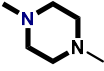
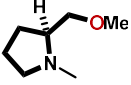
		
2.14	2.15	NMM
no additive: +0.98 V; +1.36 V	+1.14 V	+1.24 V
LiBF ₄ : +0.94 V; +1.47 V	+1.00 V	+1.07 V
<hr/>		
		
2.16	2.17	2.18
no additive: +0.94 V	+0.85 V	+0.91 V
LiBF ₄ : +0.92 V	+0.83 V	+0.88 V
		
NMP	DMPZ	diMeProl
no additive: +1.01 V	+1.02 V	+1.10 V
LiBF ₄ : +0.94 V	+1.03 V	+0.96 V

Figure 2.18. Summary of Differential Pulse Voltammetry Data (vs. Ag/AgCl values)

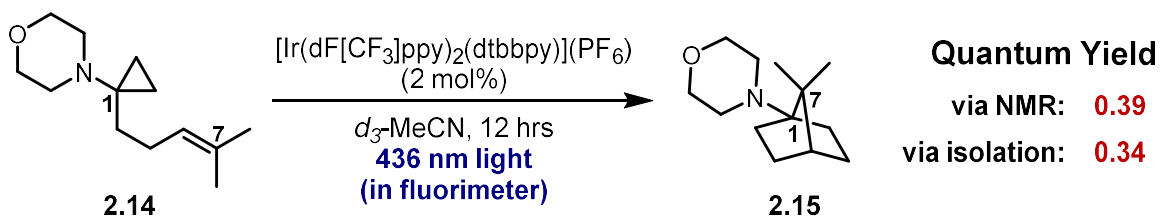
Note: All values provided above are the peak potentials directly measured against a Ag/AgCl reference electrode; for more direct comparison to the field, the values in the text are reported as vs. SCE and were calculated using the following equation: $V_{\text{SCE}} = V_{\text{Ag/AgCl}} + (0.241 - 0.197 \text{ V})$

2.4.4 Quantum Yield Calculations

This experiment followed closely to the report of Cismesia and Yoon.⁵⁹ The only modification was the use of a 0.1 cm path length cuvette for the UV/Vis data during the calculation of the photon flux, a modification made during recent investigations into our photochemical radical trifluoromethylation chemistry.⁶⁷

The light source employed was a 150 W Xenon Arc lamp within a Fluoromax-2 Fluorimeter. UV/Vis data was collected on a Shimadzu UV-1601 UV-Vis Spectrometer. The photon flux of this specific fluorimeter had previously been determined within the group to be 5.46×10^{-9} einstein/s at 436 nm (1 einstein = 1 mol photons). The experiment was repeated as is detailed in the Supplementary Information of our recent report²² to obtain a photon flux of 5.55×10^{-9} einstein/s at 436 nm; this value was used in the following calculations. Specific details for the

experimental determination of the quantum yield for the transformation of aminoCP **2.14** to aminoNB **2.15** are provided below:



Procedure for quantum yield calculation

In a dry vial under nitrogen, aminoCP **2.14** (53.2 mg, 254 μmol) was dissolved in 2.5 mL $d_3\text{-MeCN}$ before adding $[\text{Ir}(\text{dF}[\text{CF}_3]\text{ppy})_2(\text{dtbbpy})](\text{PF}_6)$ (5.7 mg, 5.1 μmol) in one portion. Reaction mixture was bright yellow. Reaction mixture was degassed with three freeze-pump-thaw cycles then 2.3 mL of the reaction mixture was quickly transferred via syringe into a dry quartz cuvette (1 cm path length) previously flushed with Ar. The cuvette was flushed with Ar, capped, and sealed. The reaction was irradiated for 12 hrs (43200 s) in the fluorimeter (excitation wavelength = 436 nm; excitation slit width = 10 nm) with stirring. Care was taken to avoid exposure to light before or after this irradiation interval. Mixture appears slightly orange after irradiation. A stock of trimethoxybenzene (17.3 mg, 103 μmol) in 1.0 mL $d_3\text{-MeCN}$ was prepared to serve as the internal NMR standard. An NMR sample was prepared using 200 μL of the internal standard stock solution and 260 μL of the reaction mixture, and ^1H NMR was used to determine conversion and yield: 1-aminoNB **2.15** = 92.2 μmol , 40.1% yield; aminoCP **2.14** = 137 μmol , 59.7% recovery. The NMR sample was then combined with the bulk reaction, which was then added to 10 mL 1:1 sat. NaHCO_3 :1 M NaOH to ensure aqueous phase pH \sim 14 and diluted with 10 mL 1:1 ether:hexanes. Phases were separated, and the aqueous phase was extracted with 10 mL

portions of 1:1 ether:hexanes three times. Combined organics were washed with 10 mL brine, dried over anhydrous magnesium sulfate, filtered to remove solids, and concentrated *in vacuo*. The crude residue was purified via flash chromatography over silica (3 to 5 to 7 to 10 to 15 to 21 to 28 to 40% ethyl acetate:hexanes; residue loaded with PhMe). Isolated 17.0 mg of 1-aminoNB **2.15** as a clear, colorless oil (81.2 μmol ; 35.3% yield) and recovered 28.2 mg of aminoCP **2.14** as a clear, colorless oil (135 μmol ; 58.6% recovery); both materials pure by ^1H NMR.

The quantum yield was determined using the relationship below (Eq. 1) for both the NMR-derived yield (Eq. 2) and the isolated yield (Eq. 3): flux = photon flux; t = time of irradiation (s); f = fraction of light absorbed = $1 - 10^{-A}$, where A = absorbance. As seen in other reports, the absorbance of these systems is substantial (>3), leading to $f \sim 1$. For the purposes of this calculation, f is assumed to equal 1, implying that all light was absorbed. Importantly, this time point was taken well before full conversion to the product (~40% consumption of aminoCP **2.14**), thus the quantum yield is not artificially decreased by prolonged irradiation.

$$\text{Quantum Yield} = \Phi = \frac{\text{mol product}}{\text{flux} \cdot t \cdot f} \quad (1)$$

$$\text{via NMR: } \Phi = \frac{92.2 \mu\text{mol}}{(5.55 \times 10^{-9} \text{ einstein/s}) \cdot (43200 \text{ s}) \cdot (1)} = 0.386 \quad (2)$$

$$\text{via isolation: } \Phi = \frac{81.2 \mu\text{mol}}{(5.55 \times 10^{-9} \text{ einstein/s}) \cdot (43200 \text{ s}) \cdot (1)} = 0.339 \quad (3)$$

2.4.5 Excited State Quenching Studies

Standard Stern-Volmer analysis was applied to this system in order to determine the quenching efficiency of our aminoCP substrates (represented by aminoCP **2.14**) alone and in the presence of LiBF₄.

The light source employed was a 150 W Xenon Arc lamp within a Fluoromax-2 Fluorimeter. Specific details for the experimental determination of the quantum yield for the transformation of aminoCP **2.14** to 1-aminoNB **2.15** are provided below:

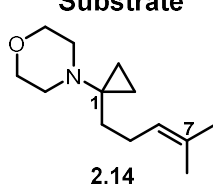
Substrate	Quenching Rate	Quenching Fraction	Chain Length
 2.14	no additive: $2.34 \times 10^7 \text{ M}^{-1}\text{s}^{-1}$	0.84	0.40
	20 mol% LiBF ₄ : $2.62 \times 10^7 \text{ M}^{-1}\text{s}^{-1}$	0.86	0.39

Figure 2.19. Summary of Excited State Quenching Data for Photocatalyst **2.16** and AminoCP **2.14**

Procedure for excited state quenching determination

MeCN (50 mL) was degassed by sparging with argon for 30 min; this solvent was used for all subsequent solution preparations. In a dry vial under Ar, aminoCP **2.14** (452 mg, 2.16 mmol) was dissolved in 4.3 mL degassed MeCN to generate a 0.5 M stock solution. In a separate dry vial under Ar, [Ir(dF[CF₃]ppy)₂(dtbbpy)](PF₆) (12.3 mg, 110 μmol) was dissolved in 11 mL degassed MeCN to generate a 1.0 mM stock solution. In a separate dry vial under Ar, LiBF₄ (18.8 mg, 0.20 mmol) was dissolved in 1.0 mL degassed MeCN to generate a 0.2 M stock solution. All stocks were sonicated for 2 min prior to use and stored under Ar while preparing the samples. A series of trial samples were generated from these stocks, providing the following series of aminoCP **2.14** concentrations both with and without 20 mol% LiBF₄ with a constant 400 μM concentration of

photocatalyst **2.16**: 0, 10, 40, 100, 200 mM; all trial samples were sonicated for 1 min immediately prior to recording emission measurements. Upon transferring to a quartz cuvette under Ar via syringe, each sample was irradiated with 432 nm light (slit widths: excitation = 2 nm; emission = 2 nm); emission data was collected via right-angle detection over 440-560 nm range of light, obtaining data points every 0.5 nm with a 0.05 s integration time. Under our experimental conditions, maximum emission intensity was observed at 473 nm (reported value = 470 nm), with an additional side emission band at ~510 nm. Three emission spectra were collected for each trial. The data points between 471-475 nm were averaged to compensate for signal-to-noise variability; this average was used to determine I_0/I (normalized emission intensity of photocatalyst **2.16** alone divided by normalized emission intensity of trial in question) for each set of data, which was then plotted against concentration of aminoCP **2.14** (see Figure 2.20).

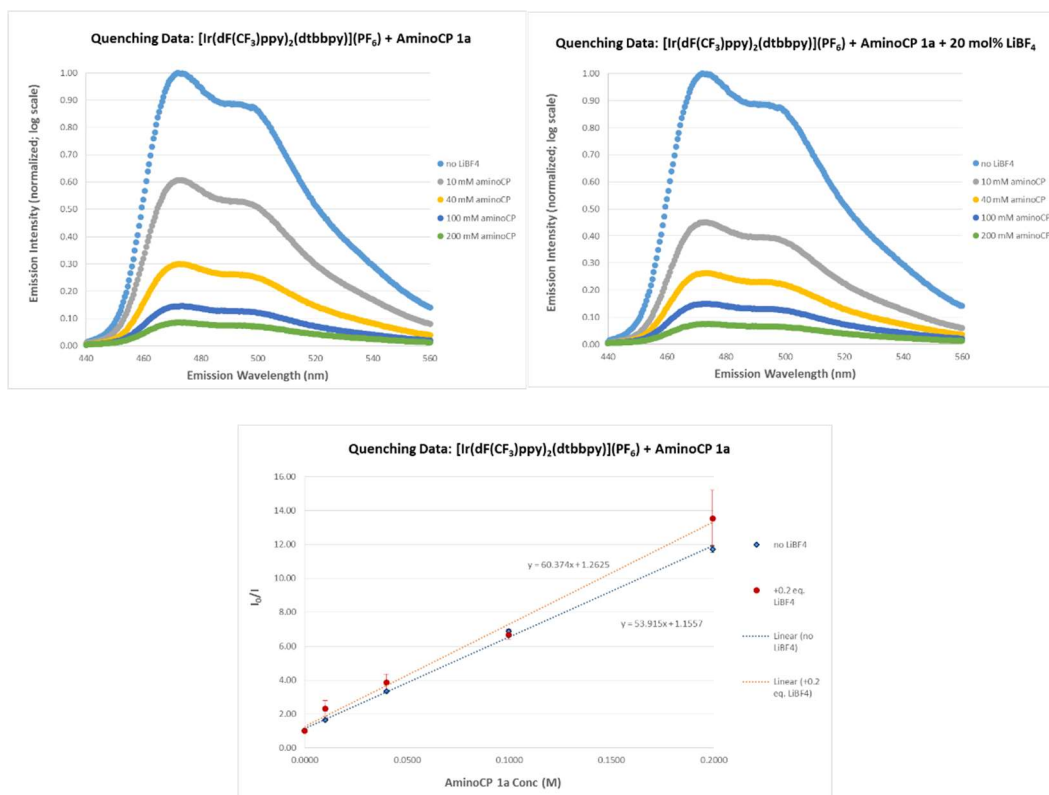


Figure 2.20. Excited State Quenching Data

Top Left: Emission spectra upon irradiating photocatalyst **2.16** in the presence of varying concentrations of aminoCP **2.14**;

Top Right: Emission spectra upon irradiating photocatalyst **2.16** in the presence of varying concentrations of aminoCP **2.14** with 20 mol% LiBF₄;

Bottom: Stern-Volmer plot for quenching photocatalyst **2.16** with aminoCP **2.14** with and without 20 mol% LiBF₄.

The equations used to determine the quenching rate (k_q), quenching efficiency (Q), and chain length (CL) are presented below (Eq. 4-6, respectively) and were derived from those presented by Cismesia and Yoon:⁵⁹

$$\frac{I_0}{I} = k_q \cdot \tau_0 \cdot [1a] + 1 \quad \Rightarrow \quad k_q = \frac{\text{slope}}{\tau_0} \quad (4)$$

$$Q = \frac{k_q \cdot [1a]}{\frac{1}{\tau_0} + (k_q \cdot [1a]) + (\text{other processes})} \quad (5)$$

$$\text{chain length} = \frac{\Phi}{Q} \quad (6)$$

<i>No additive</i>	<i>20 mol% LiBF₄</i>
$k_q = \frac{(53.92 \text{ M}^{-1})}{(2.3 \text{ } \mu\text{s})} = 2.34 \times 10^7 \text{ M}^{-1}\text{s}^{-1}$	$k_q = \frac{(60.37 \text{ M}^{-1})}{(2.3 \text{ } \mu\text{s})} = 2.62 \times 10^7 \text{ M}^{-1}\text{s}^{-1}$ (7,8)
$Q = \frac{(2.34 \times 10^7 \text{ M}^{-1}) \cdot (0.1 \text{ M})}{\frac{1}{(2.3 \text{ } \mu\text{s})} + (2.34 \times 10^7 \text{ M}^{-1}\text{s}^{-1}) \cdot (0.1 \text{ M})} = 0.84$	$Q = \frac{(2.62 \times 10^7 \text{ M}^{-1}) \cdot (0.1 \text{ M})}{\frac{1}{(2.3 \text{ } \mu\text{s})} + (2.62 \times 10^7 \text{ M}^{-1}\text{s}^{-1}) \cdot (0.1 \text{ M})} = 0.86$ (9,10)
$\text{chain length} = \frac{(0.34)}{(0.84)} = 0.40$	$\text{chain length} = \frac{(0.34)}{(0.86)} = 0.39$ (11,12)

This data demonstrates that inefficient quenching is not an explanation for the low quantum yield observed above. Of note, the quenching fraction calculation does not delineate mode of quenching (i.e. electron transfer vs. photosensitization), though there is no obvious path for energy transfer. No quenching was observed with lithium tetrafluoroborate (LiBF₄ does not quench photocatalyst **2.18** either). Conceivably, a term for the lifetime of the distonic radical cation intermediate could be incorporated into the calculation for Q to compensate for photons lost during the radical cyclization processes.

2.4.6 Batch and Continuous Flow Processing

Figures 2.21-2.23 present the specific equipment and the apparatus used while performing the formal [3+2] cycloadditions in continuous flow. This setup was used for both small- (250 μ mol) and large-scale (5 mmol) trials.

The LED assembly was obtained from Luxeon StarLEDs (Model No.: SP-02-V4, consisting of a series of seven LXML-PR02-A900 Royal Blue Luxeon Rebel ES LEDs mounted to a SinkPad-II base; <http://www.luxeonstar.com/royal-blue-447.5nm-sinkpad-ii-40mm-7-led-round-led-1030mw>) and was adhered to a heat sink to dissipate heat from the LED (Luxeon, 60 mm round x 45 mm high alpha heat sink; <http://www.luxeonstar.com/60mm-round-3.9-degree-cw-alpha-heat-sink>). This was powered with a Costway DC power supply (Model No.: EP20570-110V), with both constant current (0-5 A) and constant voltage (0-30 V) capabilities. The light source was operated at 700 mA (unless otherwise noted); the manufacturer lists this as the optimal operating current.

Material was pumped through the system with an IPC-04 Ismatec peristaltic pump (Model No.: ISM930C, 4 channel pump) with a range of 32.2 μ L/min up to 3.2 mL/min. Material was flowed through Teflon PFA tubing (0.030" inner diameter, 1/16" outer diameter) which was obtained from IDEX Health & Science (Part No.: 1514L; <https://www.idex-hs.com/fluidic-connections/dupontr-pfa-tubing-natural-1-16-od-x-030-id-x-50ft.html>).



Figure 2.21. Continuous Flow Processing Equipment

Left: Luxeon SP-02-V4 Royal Blue LED mounted to heat sink;

Middle: Ismatec peristaltic pump;

Right: Costway DC controller.

At the entry point of the tubing, the needle from a 22-gauge hypodermic needle was removed and inserted into the tube. The starting reaction mixture was kept under a positive pressure of inert atmosphere in a rubber septum-capped vial, charging the flow system via the 22-gauge needle. Beyond the peristaltic pump, the tubing was wrapped around two 18x150mm borosilicate test tubes and secured in place with tape. Aluminum foil was taped around the tubing at the points outside of the intended irradiation window as this would define the “reaction vessel”. The reaction vessel itself was suspended 1 cm above the light source (see Figure 2.22). Finally, the end of the tubing was threaded through a rubber septum which was fitted onto a flame-dried vial prior to each run; a balloon of Ar was applied as well as a vent line to ensure dissipation of any pressure build-up while maintaining an inert atmosphere. During each run, a cardboard box lined with aluminum foil was placed over the light source and reaction vessel to minimize irradiation of the starting material vessel or the collection vessel.

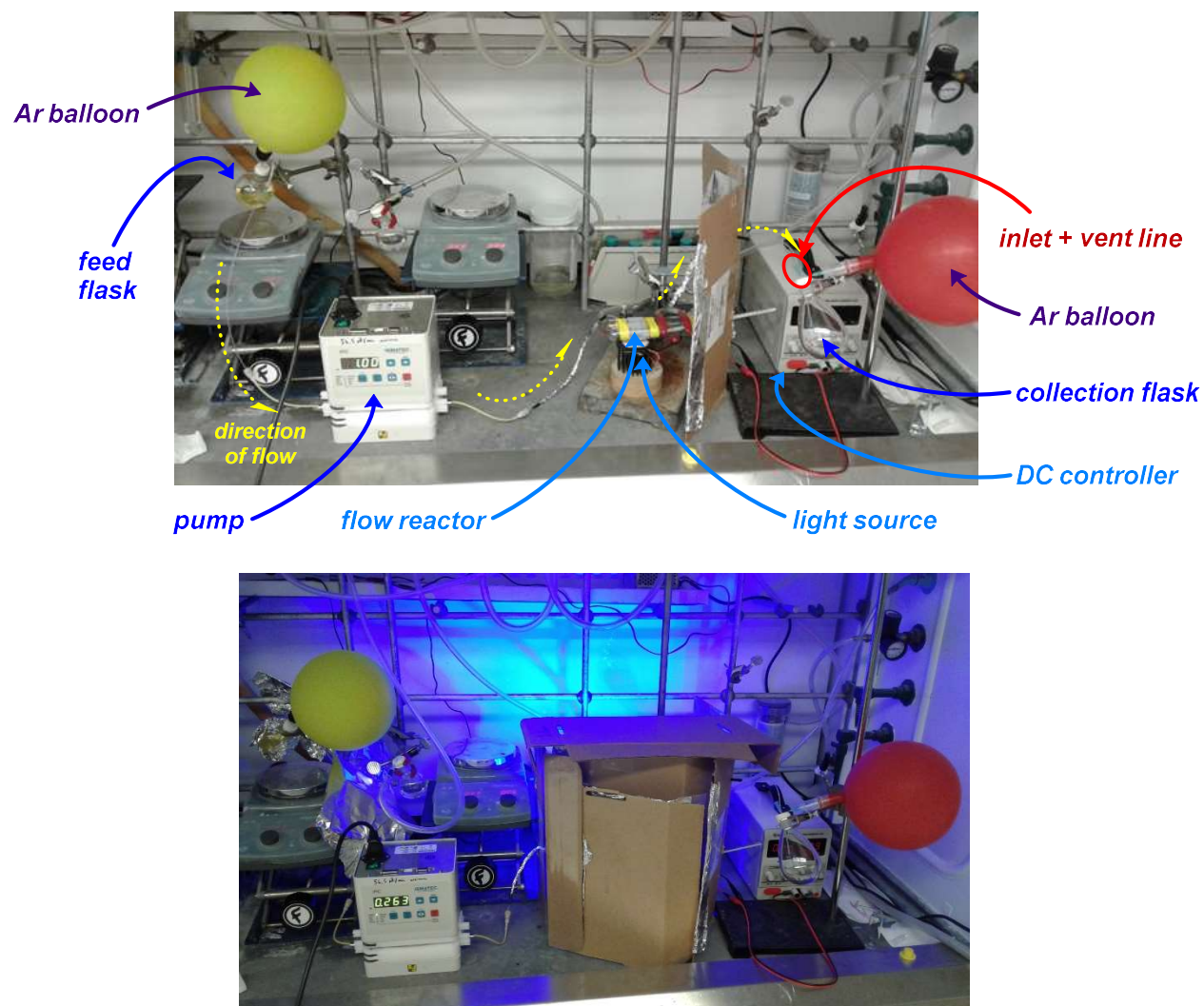


Figure 2.22. Full Flow Apparatus

Top: Full apparatus with key parts labeled;

Bottom: Apparatus in use (note: pump currently displaying 263 $\mu\text{L}/\text{min}$ flow rate; calibration of this instrument determined that the 263 $\mu\text{L}/\text{min}$ setting was equivalent to 115 $\mu\text{L}/\text{min}$).

To get an estimate of the reaction mixture temperature, a thermometer was placed inside one of the borosilicate test tubes (see Figure 2.23). As the light source tends to generate heat even when attached to the heat sink, a stream of compressed air was blown between the LEDs and the tubing to keep the temperature near room temp. The light source was turned on at least a few

minutes before each run to ensure the reaction vessel equilibrated to the steady state temperature (generally 32-35 °C).

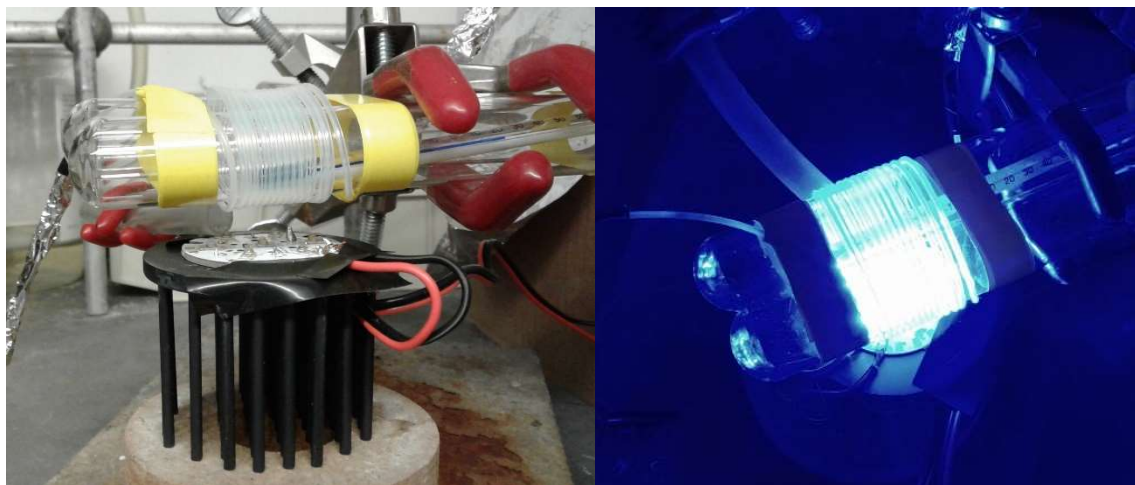


Figure 2.23. Continuous Flow Reaction Vessel

Left: Side view of reaction vessel displaying orientation of compressed air hose;
Right: Reaction vessel in use.

For the large-scale batch reactions (ca. 1 g, 5 mmol of aminoCP **2.14**), the reaction setup mimicked the flow apparatus. Thus, the reaction vessel was placed under a positive pressure of inert atmosphere and was suspended 1 cm above the light source, which was cooled with a stream of compressed air (see Figure 2.24).

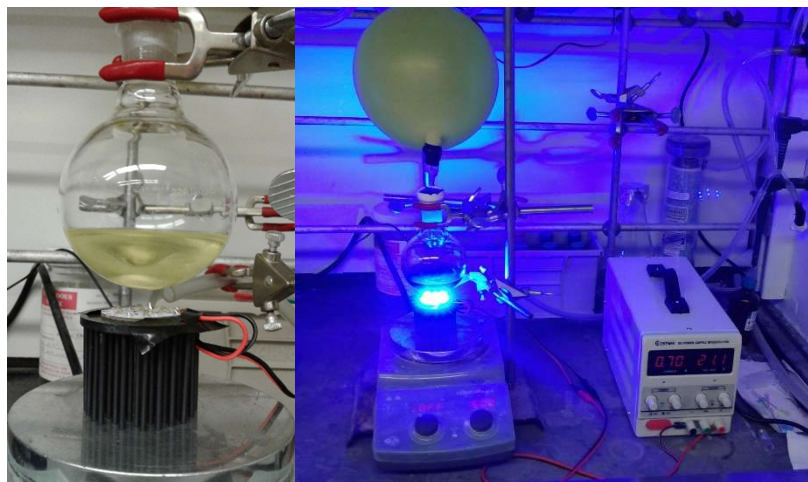


Figure 2.24. Large-Scale Batch Processing Apparatus

Left: Reaction suspended 1 cm above light source with cooling air stream;
Right: Reaction vessel in use.

Small-scale batch reactions, as used in the reaction optimization and evaluation of substrate scope, employed an alternative apparatus (see Figure 2.25). The general setup employed two 4.4 W LED strips as the light source, obtained from Creative Lighting Solutions (Product code: CL-FRS5050-12WP-12V; 12” Flex LED Strip 5050-High Density-12vDC, Waterproof, Black PCB, Sapphire Blue; <http://www.creativelightings.com/Flex-LED-Strip-5050-High-Output-12IN-WP-p/cl-frs5050-12wp-12v.htm?1=1&CartID=1>). These were taped into a circle and placed around a jacketed water bath connected to constantly flowing cold water supply, allowing for maintenance of the water bath temperature between 18-23 °C. The lights were connected to a 12V DC power source (constant voltage, max power output = 25 W) via JST connectors; no more than four LED strips were run off the power source at a given time to ensure full light output from each strip.



Figure 2.25. Small-Scale Batch Processing Equipment

Top Left: 4.4 W LED strip used to irradiate sample;

Top Right: Two 4.4 W LED strips around jacketed water bath as used for each formal [3+2] cycloaddition detailed below; Bottom Left: 12 V DC power source wired to JST connectors; Bottom Right: Full apparatus in use.

Preliminary Evaluation of Continuous Flow Processing (~250 μmol scale)

The visible light-mediated formal [3+2] cycloaddition with 7,7-dimethyl aminoCP **2.14** was used to evaluate the amenability of this methodology to continuous flow processing. Calibration of the apparatus revealed the reaction vessel to have a 715 μL capacity. Preliminary evaluation in flow identified a 115 $\mu\text{L}/\text{min}$ flow rate to be optimal, corresponding to a 6.2 min residence time. All trials employed this flow rate. A subset of the reaction optimization screen was repeated within this manifold both to compare the effectiveness of flow to batch and to determine if the small-scale batch trials could faithfully predict performance in flow. This strategy was also used to evaluate the dependence on catalyst loading. This data is summarized below in Figure 2.26, followed by the specific details of each reaction.

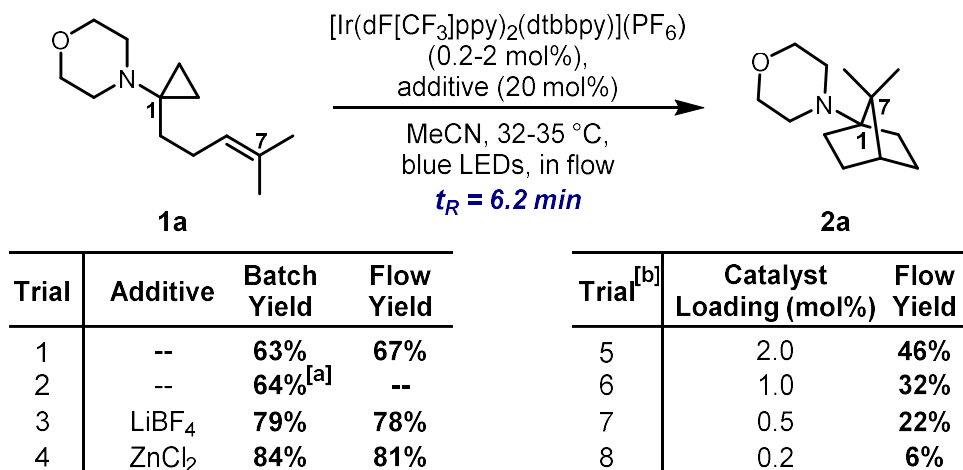


Figure 2.26. Small-Scale Evaluations of Formal [3+2] Cycloadditions in Continuous Flow
^[a]Trial run in batch using the same light source as the flow setup rather than the LED strips

In a dry vial under nitrogen, aminoCP **2.14** was dissolved in dry MeCN before adding [Ir(dF[CF₃]ppy)₂(dtbbpy)](PF₆) then the additive in one portion each. Reaction mixture was degassed with three freeze-pump-thaw cycles. The reaction mixture was then flowed through the flow apparatus under a positive pressure of Ar at 115 μL/min, providing a 6.2 min residence time. Upon completion of the irradiation, the reaction mixture was quenched, and the product was isolated in the same manner as described above for the reaction optimization.

No Additive (entry 1)

Following the general procedure outlined above, 51.8 mg of aminoCP **2.14** (247 μmol) were dissolved in 2.5 mL dry MeCN along with 5.6 mg of [Ir(dF[CF₃]ppy)₂(dtbbpy)](PF₆) (5.0 μmol) prior to irradiation in flow. Isolation provided the following:

- Recovered starting material: 11.1 mg; clear, colorless oil; 21.4% recovery
- Product: 34.9 mg; clear, colorless oil; 67.4% yield, 85.7% BORSM

No Additive - batch control (entry 2)

Following the general procedure outlined above, 51.7 mg of aminoCP **2.14** (247 μmol) were dissolved in 2.5 mL dry MeCN along with 5.5 mg of $[\text{Ir}(\text{dF}[\text{CF}_3]\text{ppy})_2(\text{dtbbpy})](\text{PF}_6)$ (4.9 μmol). This reaction mixture was not flowed through the apparatus; instead, the reaction vial was stored under a positive pressure of Ar, suspended 1 cm above the light source (cooling air stream in place), and irradiated for 22.2 min (intended to replicate length of reactions in flow). Isolation provided the following:

- Recovered starting material: 13.5 mg; clear, colorless oil; 26.1% recovery
- Product: 32.9 mg; slightly yellow oil; 63.6% yield, 86.1% BORSM

LiBF₄ (entry 3)

Following the general procedure outlined above, 52.5 mg of aminoCP **2.14** (251 μmol) were dissolved in 2.5 mL dry MeCN along with 5.6 mg of $[\text{Ir}(\text{dF}[\text{CF}_3]\text{ppy})_2(\text{dtbbpy})](\text{PF}_6)$ (5.0 μmol) and 4.7 mg of LiBF₄ (50 μmol) prior to irradiation in flow. Isolation provided the following:

- Recovered starting material: 7.0 mg; clear, colorless oil; 13.3% recovery
- Product: 40.7 mg; slightly yellow oil; 77.5% yield, 89.5% BORSM

ZnCl₂ (entry 4)

Following the general procedure outlined above, 52.7 mg of aminoCP **2.14** (252 μmol) were dissolved in 2.5 mL dry MeCN along with 5.7 mg of $[\text{Ir}(\text{dF}[\text{CF}_3]\text{ppy})_2(\text{dtbbpy})](\text{PF}_6)$ (5.0 μmol) and 50 μL of ZnCl₂ (1.0 M in ether, 50 μmol) prior to irradiation in flow. Isolation provided the following:

- Recovered starting material: 3.6 mg; yellow oil, ^1H NMR reveals several small impurities; <7% recovery

- Product: 42.6 mg; slightly yellow oil; 80.8% yield

In a dry vial under nitrogen, aminoCP **2.14** (previously aliquoted into four equal portions) was dissolved in dry MeCN before adding 20 mol% LiBF_4 and the desired amount of $[\text{Ir}(\text{dF}[\text{CF}_3]\text{ppy})_2(\text{dtbbpy})](\text{PF}_6)$; both reagents were prepared as stock solutions in dry, degassed MeCN (50 mM and 5.0 mM respectively). Reaction mixture was degassed with three freeze-pump-thaw cycles. The reaction mixture was then flowed through the flow apparatus under a positive pressure of Ar at 115 $\mu\text{L}/\text{min}$, providing a 6.2 min retention time. Upon completion of the irradiation, the reaction mixture was quenched, and the product was isolated in the same manner as described above for the reaction optimization.

2.0 mol% photocatalyst (entry 5)

Following the general procedure outlined above, 52.2 mg of aminoCP **2.14** (249 μmol) were dissolved in 0.5 mL dry MeCN. To this solution, 1.0 mL 50 mM LiBF_4 (5.0 μmol) and 1.0 mL 5.0 mM $[\text{Ir}(\text{dF}[\text{CF}_3]\text{ppy})_2(\text{dtbbpy})](\text{PF}_6)$ (5.0 μmol) were added respectively, prior to irradiation in flow. Isolation provided the following:

- Recovered starting material: 22.4 mg; clear, colorless oil; 42.9% recovery

- Product: 23.8 mg; clear, colorless oil; 45.6% yield, 79.9% BORSM

1.0 mol% photocatalyst (entry 6)

Following the general procedure outlined above, 52.2 mg of aminoCP **2.14** (249 μmol)

were dissolved in 1.0 mL dry MeCN. To this solution, 1.0 mL 50 mM LiBF₄ (5.0 μmol) and 0.5 mL 5.0 mM [Ir(dF[CF₃]ppy)₂(dtbbpy)](PF₆) (2.5 μmol) were added respectively, prior to irradiation in flow. Isolation provided the following:

- Recovered starting material: 29.3 mg; clear, colorless oil; 57.1% recovery
- Product: 16.3 mg; clear, colorless oil; 31.8% yield, 74.1% BORSM

0.5 mol% photocatalyst (entry 7)

Following the general procedure outlined above, 52.2 mg of aminoCP **2.14** (249 μmol) were dissolved in 1.25 mL dry MeCN. To this solution, 1.0 mL 50 mM LiBF₄ (5.0 μmol) and 250 μL 5.0 mM [Ir(dF[CF₃]ppy)₂(dtbbpy)](PF₆) (1.3 μmol) were added respectively, prior to irradiation in flow. Isolation provided the following:

- Recovered starting material: 37.6 mg; clear, colorless oil; 73.4% recovery
- Product: 11.2 mg; clear, colorless oil; 21.9% yield, 82.4% BORSM

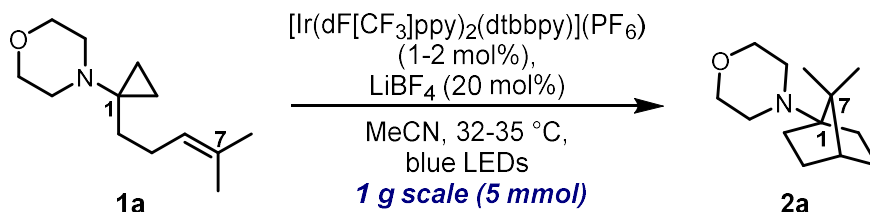
0.2 mol% photocatalyst (entry 8)

Following the general procedure outlined above, 52.2 mg of aminoCP **2.14** (249 μmol) were dissolved in 1.4 mL dry MeCN. To this solution, 1.0 mL 50 mM LiBF₄ (5.0 μmol) and 100 μL 5.0 mM [Ir(dF[CF₃]ppy)₂(dtbbpy)](PF₆) (0.5 μmol) were added respectively, prior to irradiation in flow. Isolation provided the following:

- Recovered starting material: 42.2 mg; clear, colorless oil; 82.4% recovery
- Product: 3.3 mg; clear, colorless oil; 6.4% yield, 36.7% BORSM

Large Scale (~1 g) Batch and Continuous Flow Reactions

To evaluate the scalability of the visible light-mediated formal [3+2] cycloaddition, a series of 1 g reactions (5 mmol, 20-fold increase relative to small-scale) were run both in flow and in batch. The data is summarized below in Figure 2.27 and highlighted in the text in Figure 2.15.



Trial	Processing	Time (hrs)	Catalyst Loading	Isolated Yield	Recov. SM ^[a]
1	<i>flow</i>	7.2	2 mol%	70%	~11%
2	<i>batch</i>	7.2	2 mol%	65%	0%
3	<i>batch</i>	3.6	1 mol%	73%	14%



Figure 2.27. Large-Scale Batch Processing Results

Top: Generic reaction scheme; Middle: Table of results from 1 g scale formal [3+2] cycloadditions;

Bottom Left: Flow reactor under irradiation, lights operating at 30 mA;

Bottom Center: Batch reactor under irradiation (side view), lights operating at 700 mA;

Bottom Right: Batch reactor, top view. ^[a]Recov. SM = recovered starting material, trial 1 is listed as ~11% because of minor impurities seen in the ¹H NMR.

Entry 1

In a dry flask under nitrogen, aminoCP **2.14** (1.03 g, 4.92 mmol) was dissolved in 50 mL dry MeCN before adding $[\text{Ir}(\text{dF}[\text{CF}_3]\text{ppy})_2(\text{dtbbpy})](\text{PF}_6)$ (110 mg, 98 μmol) then LiBF_4 (92 mg, 0.98 mmol) in one portion each. Reaction mixture was bright yellow and clear. Reaction mixture was degassed with three freeze-pump-thaw cycles. The reaction mixture was then processed through the flow apparatus under a positive pressure of Ar at 115 $\mu\text{L}/\text{min}$, providing a 6.2 min retention time. Mixture was dark orange-red immediately upon exiting flow reactor; collection vessel slowly turned to dark red and eventually black over the course of the reaction (likely indicating moderate exposure to oxygen, a likely source for the slight reduction in yield between small and large scale flow trials). The reaction was quenched with 100 mL 1:1 sat. NaHCO_3 :1 M NaOH to ensure aqueous phase pH ~ 14 , then diluted further with 100 mL ether. Phases were separated, and the aqueous phase was extracted with 100 mL portions of ether three times. Combined organics were washed with 100 mL brine, dried over anhydrous magnesium sulfate, filtered to remove solids, and concentrated *in vacuo*. The crude residue was purified via flash chromatography over silica (3 to 5 to 7 to 10 to 15 to 20 to 28 to 35% ethyl acetate:hexanes; residue loaded with PhMe); residual MeCN dragged some product through the column, mixing with the still eluting starting material. The mixed fractions were exposed to a second round of chromatography (4 to 6 to 8 to 12 to 16 to 21 to 30 to 40% ethyl acetate:hexanes; loaded residue with PhMe). Combined amounts from the two columns listed below:

- Recovered starting material: 109 mg; slightly yellow liquid, revealed to be a mix with the C1 ethyl ketone byproduct; would be 10.6% recovery if it had been recovered cleanly
- Product: 723 mg; yellow oil; 70.2% yield

Entry 2

In a dry flask under nitrogen, aminoCP **2.14** (1.03 g, 4.92 mmol) was dissolved in 50 mL dry MeCN before adding $[\text{Ir}(\text{dF}[\text{CF}_3]\text{ppy})_2(\text{dtbbpy})](\text{PF}_6)$ (110 mg, 98 μmol) then LiBF_4 (92 mg, 0.98 mmol) in one portion each. Reaction mixture was bright yellow and clear. Reaction mixture was degassed with three freeze-pump-thaw cycles. The reaction mixture was irradiated in a fashion that most closely mimicked the flow apparatus under a positive pressure of Ar. Total irradiation time was 7.2 hrs, as this corresponds to the total length of irradiation for the large-scale flow reaction. Mixture was yellow-orange, still clear. As above, the reaction was quenched with 100 mL 1:1 sat. NaHCO_3 :1 M NaOH to ensure aqueous phase pH ~ 14 , then diluted further with 100 mL ether. Phases were separated, and the aqueous phase was extracted with 100 mL portions of ether three times. Combined organics were washed with 100 mL brine, dried over anhydrous magnesium sulfate, filtered to remove solids, and concentrated *in vacuo*. The crude residue was purified via flash chromatography over silica (5 to 10 to 20 to 30 to 40% ethyl acetate:hexanes; residue loaded with PhMe) to afford:

- Recovered starting material: none detected
- Product: 670 mg (obtained 681 mg that was 98.2 wt% with water); yellow-orange liquid; 65.0% yield

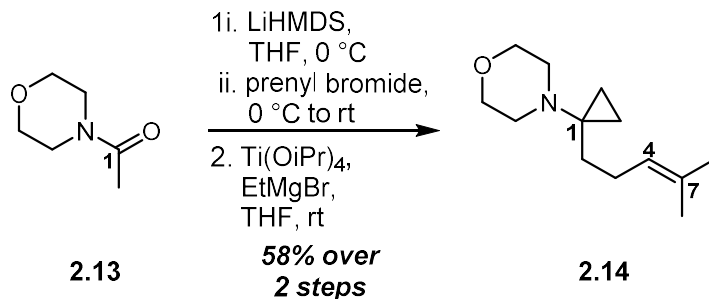
Entry 3

In a dry flask under nitrogen, aminoCP **2.14** (1.03 g, 4.92 mmol) was dissolved in 50 mL dry MeCN before adding $[\text{Ir}(\text{dF}[\text{CF}_3]\text{ppy})_2(\text{dtbbpy})](\text{PF}_6)$ (55 mg, 49 μmol) then LiBF_4 (92 mg, 0.98 mmol) in one portion each. Reaction mixture was bright yellow and clear. Reaction mixture was degassed with three freeze-pump-thaw cycles. The reaction mixture was irradiated in a fashion that most closely mimicked the flow apparatus under a positive pressure of Ar. Total irradiation

time was 3.6 hrs, half the time employed for the two proceeding trials. Mixture was yellow-orange, still clear. The reaction was quenched with 200 mL 1:1 sat. NaHCO₃:1 M NaOH to ensure aqueous phase pH ~14, then diluted further with 100 mL 1:1 ether:hexanes. Phases were separated, and the aqueous phase was extracted with 100 mL portions of 1:1 ether:hexanes three times. Combined organics were washed with 100 mL brine, dried over anhydrous magnesium sulfate, filtered to remove solids, and concentrated *in vacuo*. The crude residue was purified via flash chromatography over silica (3 to 5 to 7 to 10 to 15 to 25 to 40 to 60% ethyl acetate:hexanes; residue loaded with PhMe) to afford:

- Recovered starting material: 144 mg; light yellow oil; 14.0% recovery
- Product: 752 mg; yellow-orange liquid; 73.0% yield, 84.9% BORSM

2.4.7. Experimental Methods



N-Acetyl morpholine (**2.13**, 1.50 mL, 13.0 mmol) was dissolved in 35 mL dry THF in a dry flask under N₂, before cooling to 0 °C (ice/water). LiHMDS (1.0 M in THF, 13.6 mL, 13.6 mmol) was added dropwise down the side of the vial over 5 min, then the reaction mixture was allowed to stir at 0 °C for 1 hr. In a separate dry flask kept under inert atmosphere, prenyl bromide (2.0 mL, 17.5 mmol) was dissolved in 10 mL dry THF. The enolate solution was then cannulated into the bromide solution slowly down the side of the vial over the course of 2.5 hrs. Transfer was quantified with two rinses of 2.5 mL dry THF. After the addition was complete, the mixture was stirred at room temp for 30 min before quenching with 100 mL 1:1 sat. NaHCO₃:sat. Na₂S₂O₃. The mixture was diluted with 100 mL ether, and the phases were separated. The aqueous phase was then extracted with 100 mL portions of ether three times. Combined organics were washed with 100 mL brine, dried over anhydrous magnesium sulfate, filtered to remove solids, and concentrated *in vacuo* to afford a slightly yellow oil. This crude residue was purified by flash chromatography over silica (20 to 70% ethyl acetate:hexanes, increasing in 10% increments; residue was loaded with PhMe). Two major spots were present by TLC analysis; both were collected cleanly after chromatography. The first was obtained as a clear, colorless oil and determined to be the *bis*-prenylated amide by ¹H NMR (447 mg, 13.0% yield). The second spot was revealed to be the desired mono-prenylated product by ¹H NMR, affording 1.97 g of a clear, colorless oil (77.1% yield).

¹H NMR (CDCl₃, 500 MHz): δ = 5.06 (t, 2H, *J* = 7.3 Hz, vinyl CH's), 3.65-3.60 (m, 6H, morph.), 3.51-3.47 (m, 2H, morph.), 2.60 (quint., 1H, *J* = 6.9 Hz, C2), 2.29 (dt, 2H, *J* = 14.1, 6.8 Hz, allyl CH₂), 2.18 (dt, 2H, *J* = 14.4, 7.5 Hz, allyl CH₂), 1.68 (s, 6H, Me, Me), 1.58 (s, 6H, Me, Me) ppm
R_f = 0.55 (60% EtOAc in hexanes), one yellow spot, KMnO₄

¹H NMR (CDCl₃, 500 MHz): δ = 5.15-5.10 (m, 1H, C4), 3.68-3.64 (m, 4H, morph.), 3.64-3.60 (m, 2H, morph.), 3.46 (*app* t, 2H, *J* = 4.6 Hz, morph.), 2.33 (*app*. d, 4H, *J* = 2.9 Hz, C2, C3), 1.69 (s, 3H, C7-Me), 1.63 (s, 3H, C7-Me) ppm

R_f = 0.20 (60% EtOAc in hexanes), one yellow spot, KMnO₄

The mono-prenylated amide from above (1.97 g, 10.0 mmol) was dissolved in 165 mL dry THF under inert atmosphere, followed by addition of titanium isopropoxide (3.3 mL, 11.0 mmol). The reaction vessel was submerged in a water bath at ambient temp to serve as a heat sink. Ethylmagnesium bromide (1.0 M in THF, 35.0 mL, 35 mmol) was added dropwise via syringe over the course of 15 min. A vent line was added to account for gas evolution (note: gas evolution can be quite vigorous along with substantial heat generation if addition is too rapid). The reaction mixture (clear, colorless at outset of addition) undergoes a series of color changes, first turning a bright yellow with initial drops, then transitioning to orange and red hues, and ultimately turning a dark red-brown (almost black) upon complete addition of EtMgBr. Vent line was removed, and the reaction mixture was stirred at room temp for 1 hr, at which point starting material had been consumed as revealed by TLC analysis. The reaction was quenched with 100 mL sat. Rochelle salt and stirred vigorously for 10 min. The mixture was then diluted with 150 mL sat. Rochelle salt, 50 mL brine, and 200 mL ether. Phases were separated. The aqueous phase was extracted with 100 mL portions of ether three times. The combined organics were then washed with 100 mL brine,

dried over anhydrous sodium sulfate, filtered to remove solids, and concentrated *in vacuo*. The crude residue was purified via flash chromatography over silica (5 to 30% ethyl acetate:hexanes, increasing in 5% increments; residue was loaded with PhMe). Obtained aminoCP **2.14** as clear, colorless liquid, 1.47 g, clean by ^1H NMR (70.3%; 54.2% over 2 steps), along with some mixed fractions. A second round of chromatography (3 to 21% ethyl acetate:hexanes, increasing in 3% increments, mixture loaded with PhMe) afforded an additional 97 mg of aminoCP **2.14**, bringing final yield to 74.9% (57.6% over two steps).

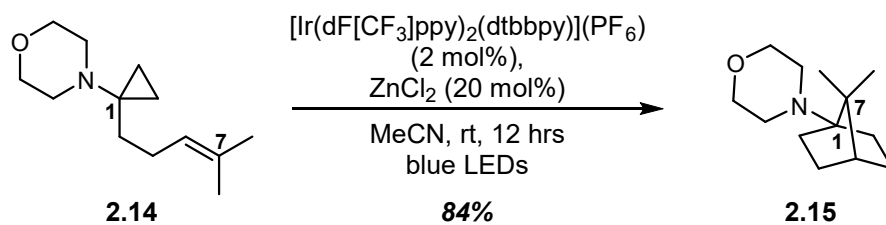
^1H NMR (CDCl_3 , 500 MHz): δ = 5.06 (*app.* t, 1H, J = 7.1 Hz, C4), 3.62-3.59 (m, 4H, morph.), 2.67-2.64 (m, 4H, morph.), 1.94-1.88 (m, 2H, C2), 1.67 (s, 3H, C7-Me), 1.59 (s, 3H, C7-Me), 1.56-1.51 (m, 2H, C3), 0.54-0.50 (m, 2H, CP), 0.45-0.41 (m, 2H, CP) ppm

^{13}C NMR (CDCl_3 , 125 MHz): δ = 131.3, 124.7, 67.9, 49.9, 44.2, 30.0, 25.9, 25.8, 17.8, 12.9 ppm

IR (neat): 2926, 2851, 1450, 1374, 1264, 1116, 1012, 984, 857 cm^{-1}

HRMS (ES⁺, m/z) calculated for $\text{C}_{13}\text{H}_{24}\text{NO}^+$: 210.1852, Found: 210.1855

R_f = 0.40 (20% EtOAc in hexanes), one yellow spot, KMnO_4



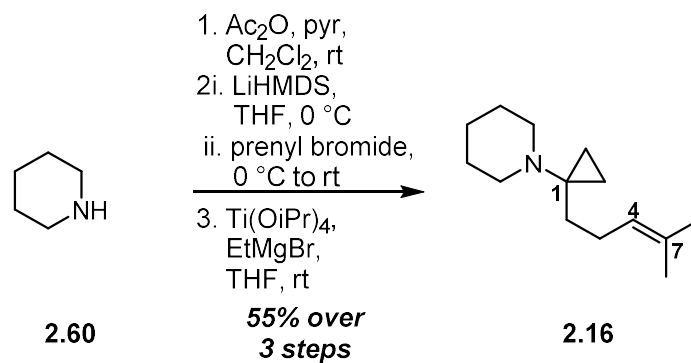
^1H NMR (CDCl_3 , 500 MHz): δ = 3.70-3.65 (m, 4H, morph.), 2.59-2.55 (m, 4H, morph.), 1.85-1.75 (m, 4H, C2_{eq} , C6_{eq} , C3_{eq} , C5_{eq}), 1.44-1.39 (m, 3H, C4 , C2_{ax} , C6_{ax}), 1.25-1.18 (m, 2H, C3_{ax} , C5_{ax}), 1.03 (s, 6H, C7-Me , C7-Me) ppm

^{13}C NMR (CDCl_3 , 126 MHz): δ = 70.2, 67.8, 49.0, 47.0, 46.8, 29.2, 27.4, 21.6 ppm

IR (neat): 2952, 2877, 1449, 1385, 1367, 1318, 1273, 1157, 1119, 1037, 902, 884 cm^{-1}

HRMS (ES^+ , m/z) calculated for $\text{C}_{13}\text{H}_{24}\text{NO}^+$: 210.1852, Found: 210.1852

R_f = 0.15 (20% EtOAc in hexanes), one yellow spot, KMnO_4



Piperidine (**2.60**; 1.16 mL, 11.7 mmol) was dissolved in 20 mL dry CH₂Cl₂ in a dry flask under inert atmosphere. Pyridine (1.18 mL, 14.7 mmol) then acetic anhydride (1.22 mL, 12.9 mmol) were added in one portion each. The reaction was stirred for 28 hrs at room temp before quenching by pouring into 40 mL sat. NaHCO₃. Phases were separated. The aqueous phase was extracted with 40 mL portions of CH₂Cl₂ three times. The combined organics were then washed with 100 mL 1 M HCl, dried over anhydrous magnesium sulfate, filtered to remove solids, and concentrated *in vacuo*. Obtained 1.36 g of a clear, faintly yellow oil (90.8% yield).

A portion of the *N*-Acetyl piperidine from above (365 mg, 2.87 mmol) was subsequently dissolved in 6.0 mL dry THF in a dry flask under N₂, before cooling to 0 °C (ice/water). LiHMDS (1.0 M in THF, 3.0 mL, 3.0 mmol) was added dropwise down the side of the vial over 2.5 min, then the reaction mixture was allowed to stir at 0 °C for 30 min before adding prenyl bromide (0.23 mL, 1.91 mmol; this serves as the limiting reagent for this transformation) dropwise down the side of the vial via syringe over the course of 3 min. The mixture was stirred 1 hr while allowing to slowly come to room temp before quenching with 15 mL 1:1 sat. NaHCO₃:sat. Na₂S₂O₃. The mixture was diluted with 15 mL ether, and the phases were separated. The aqueous phase was then extracted with 15 mL portions of ether three times. Combined organics were washed with 15 mL brine, dried over anhydrous magnesium sulfate, filtered to remove solids, and concentrated *in vacuo*. This crude residue was purified by flash chromatography over silica (5 to 30% ethyl

acetate:hexanes, increasing in 5% increments; residue was loaded with PhMe). Obtained the desired alkylation product as a clear, colorless oil; 284 mg, 76.0% yield.

¹H NMR (CDCl₃, 500 MHz): δ = 5.14 (br s, 1H, C4), 3.58-3.51 (m, 2H, piperidine-C2), 3.43-3.36 (m, 2H, piperidine-C2), 2.37-2.27 (m, 4H, C2, C3), 1.69 (s, 3H, C7-Me), 1.66-1.61 (m, 2H, piperidine-C4), 1.63 (s, 3H, C7-Me), 1.57-1.50 (m, 4H, piperidine-C3) ppm

R_f = 0.50 (50% EtOAc in hexanes), one yellow spot, KMnO₄

The prenylated amide (281 mg, 1.44 mmol) was dissolved in 25 mL dry THF under inert atmosphere, followed by addition of titanium isopropoxide (0.47 mL, 1.58 mmol). The reaction vessel was submerged in a water bath at ambient temp to serve as a heat sink. Ethylmagnesium bromide (1.0 M in THF, 5.0 mL, 5.0 mmol) was added dropwise via syringe over the course of 5 min. A vent line was added to account for gas evolution (note: gas evolution can be quite vigorous along with substantial heat generation if addition is too rapid). The reaction mixture (clear, colorless at outset of addition) undergoes a series of color changes, first turning a bright yellow with initial drops, then transitioning to orange and red hues, and ultimately turning a dark red-brown (almost black) upon complete addition of EtMgBr. Vent line was removed, and the reaction mixture was stirred at room temp for 45 min. An aqueous solution containing 75 mL sat. Rochelle salt, 25 mL brine, and 2 mL of 50% NaOH was prepared. The reaction was quenched with 50 mL of this aqueous mixture, and stirred vigorously for 30 min. The mixture was then diluted with the remainder of the quenching solution and 100 mL ether. The phases were separated. The aqueous phase was extracted with 100 mL portions of ether three times. The combined organics were then washed with 100 mL brine, dried over anhydrous magnesium sulfate, filtered to remove solids, and concentrated *in vacuo*. The crude residue was purified via flash chromatography over silica

(10 to 15 to 25% ethyl acetate:hexanes; the residue was loaded with PhMe). Collected aminoCP **2.16** in two portions. The central fractions afforded 116 mg as a clear, colorless oil, while the shoulder fractions totaled 122 mg of a faintly yellow oil. Both portions were clean by ^1H NMR, bringing the total yield of aminoCP **2.16** to 238 mg (79.7% yield; 55.0% over 3 steps).

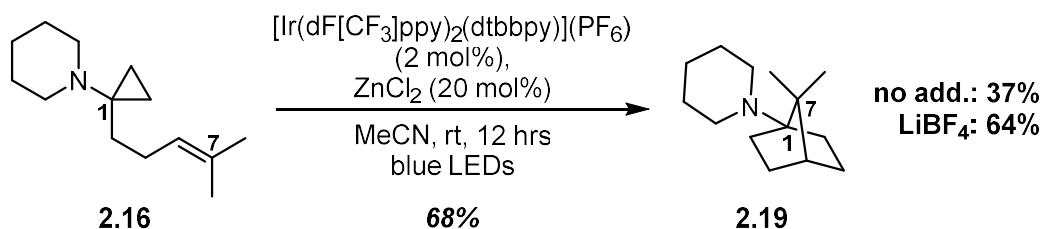
^1H NMR (CDCl_3 , 500 MHz): δ = 5.06 (t, 1H, J = 7.1 Hz, C4), 2.62 (*app.* t, 4H, J = 5.3 Hz, piperidine-C2), 1.87 (dt, 2H, J = 8.8, 7.6 Hz, C2), 1.67 (s, 3H, C7-Me), 1.59 (s, 3H, C7-Me), 1.56-1.51 (m, 2H, piperidine-C4), 1.50-1.44 (m, 4H, piperidine-C3), 1.42-1.36 (m, 2H, C3), 0.50-0.46 (m, 2H, CP), 0.45-0.41 (m, 2H, CP) ppm

^{13}C NMR (CDCl_3 , 126 MHz): δ = 131.2, 125.0, 50.8, 44.5, 29.2, 26.9, 26.1, 25.8, 25.1, 17.8, 13.5 ppm

IR (neat): 2929, 2853, 2791, 1441, 1378, 1342, 1269, 1239, 1035, 1011, 862 cm^{-1}

HRMS (ES⁺, m/z) calculated for $\text{C}_{14}\text{H}_{26}\text{N}^+$: 208.2060, Found: 208.2062

R_f = 0.50 (20% EtOAc in hexanes), one yellow spot, KMnO_4



In a dry vial under nitrogen, aminoCP **2.16** (65.8 mg, 317 μmol) was dissolved in 3.2 mL dry MeCN before adding $[\text{Ir}(\text{dF}[\text{CF}_3]\text{ppy})_2(\text{dtbbpy})](\text{PF}_6)$ (7.1 mg, 635 μmol) then ZnCl_2 (1.0 M in ether, 64 μL , 64 μmol) in one portion each. Reaction mixture is bright yellow, but starting material is sparingly soluble in MeCN. Sonicated mixture for 2 min to generate a slightly cloudy but homogeneous mixture. Reaction mixture was degassed with three freeze-pump-thaw cycles. The reaction was performed by stirring at room temp (as controlled with jacketed water bath, temp maintained between 18-23 $^\circ\text{C}$) while irradiating with two strips of 4.4 W blue LEDs for 12 hrs; stirred vigorously to help maintain homogeneity. Mixture appeared yellow-green and was clearer than before irradiation. The mixture was added to 10 mL 1:1 sat. NaHCO_3 :1 M NaOH , then diluted further with 5 mL hexanes and 5 mL ether. Phases were separated, and the aqueous phase was extracted with 10 mL portions of 1:1 ether:hexanes three times. Combined organics were washed with 10 mL brine, dried over anhydrous MgSO_4 . Solids and some catalyst byproducts were removed by filtering through a pad of basic alumina, eluting with 200 mL 50% ether:hexanes. Sample was then concentrated *in vacuo*, and the crude residue was purified via flash chromatography over silica (2 to 5 to 10 to 15 to 25% ethyl acetate:hexanes; residue loaded with PhMe; silica was pre-neutralized with 2% ethyl acetate:hexanes + 1% NET_3). Collected:

- Recovered starting material: 13.7 mg; clear, colorless oil, but ^1H NMR reveals minor impurities; ~21% recovery
- Product: 44.7 mg; slightly yellow oil; 67.9% yield

¹H NMR (C₆D₆, 700 MHz): δ = 2.50 (br s, 4H, piperidine-C2), 1.85-1.73 (m, 4H, norbornane core), 1.56 (*app.* quint., 4H, *J* = 5.6 Hz, piperidine-C3), 1.39-1.33 (m, 5H, piperidine-C4, norbornane core [2H], C4), 1.17-1.12 (m, 2H, norbornane core), 1.06 (s, 6H, C7-Me, C7-Me) ppm

¹³C NMR (C₆D₆, 176 MHz): δ = 70.7, 49.9, 47.1, 47.1, 29.7, 27.8, 27.5, 25.4, 21.9 ppm

IR (neat): 2926, 2873, 2785, 1467, 1450, 1440, 1382, 1366, 1274, 1260, 1164, 1128, 1077, 1021, 880 cm⁻¹

HRMS (ES+, *m/z*) calculated for C₁₄H₂₆N⁺: 208.2060, Found: 208.2057

R_f = 0.20 (20% EtOAc in hexanes on basic alumina plate), one yellow spot, KMnO₄

Additional Trials with Varied Additives

No Additive

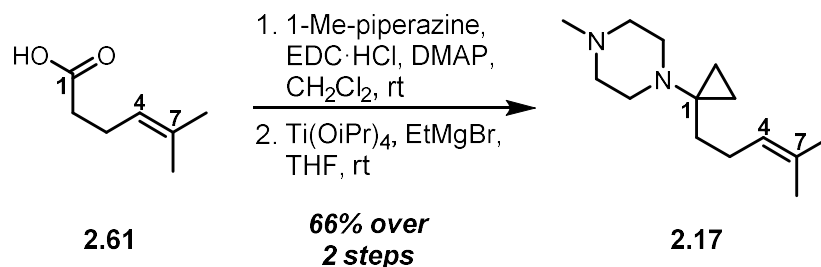
Following the general procedure outlined above, 53.8 mg of aminoCP **2.16** (259 μmol) was dissolved in 2.6 mL dry MeCN along with 5.8 mg of [Ir(dF[CF₃]ppy)₂(dtbbpy)](PF₆) (5.2 μmol) prior to irradiation. Isolation provided the following:

- Recovered starting material: 15.5 mg; clear, colorless liquid; 28.8% recovery
- Product: 20.4 mg; slightly yellow oil; 37.4% yield, 53.3% BORSM

LiBF₄

Following the general procedure outlined above, 65.9 mg of aminoCP **1b** (318 μmol) were dissolved in 3.2 mL dry MeCN along with 7.1 mg of [Ir(dF[CF₃]ppy)₂(dtbbpy)](PF₆) (6.4 μmol) and 6.0 mg of LiBF₄ (64 μmol) prior to irradiation. Isolation provided the following:

- Recovered starting material: 14.7 mg; clear, colorless oil, but ¹H NMR reveals minor impurities; ~22% recovery
- Product: 42.3 mg; slightly yellow oil; 64.2% yield



In a dry flask under inert atmosphere, carboxylic acid⁶⁸ **2.61** (325 mg, 2.54 mmol) was dissolved in 12.5 mL dry CH₂Cl₂. DMAP (31 mg, 0.25 mmol) and EDC·HCl (730 mg, 3.81 mmol) in one portion each, respectively, followed by dropwise addition of *N*-methyl piperazine (0.42 mL, 3.81 mmol). The reaction was stirred at room temp for 21 hours, at which point it was orange in color. The mixture was quenched by pouring into 50 mL sat. sodium bicarbonate solution and diluting with 50 mL CH₂Cl₂. The layers were separated, and the aqueous layer was extracted with three 50 mL portions of CH₂Cl₂. The combined organic layers were washed with 50 mL brine, dried over anhydrous MgSO₄, filtered, and concentrated *in vacuo*. The crude residue was purified by flash column chromatography over silica (1 to 5% MeOH:CH₂Cl₂ + 1% NH₄OH, increasing in 1% increments; loaded residue with PhMe), providing 473 mg of the desired amide as a slightly orange oil (88.7% yield).

¹H NMR (CDCl₃, 500 MHz): δ = 5.13 (br s, 1H, C4), 3.63 (br s, 2H, piperazine), 3.47 (*app.* t, 2H, *J* = 5.2 Hz, piperazine), 2.42-2.34 (m, 4H, C2, C3), 2.35-2.31 (m, 4H, piperazine), 2.30 (s, 3H, piperazine-Me), 1.68 (s, 3H, C7-Me), 1.62 (s, 3H, C7-Me) ppm

R_f = 0.50 (5% MeOH in CH₂Cl₂ + 1% NH₄OH), one yellow spot, KMnO₄

A portion of the amide prepared above (279 mg, 1.33 mmol) was dissolved in 22 mL dry THF under inert atmosphere, followed by addition of titanium isopropoxide (0.43 mL, 1.46 mmol). The reaction vessel was submerged in a water bath at ambient temp to serve as a heat sink.

Ethylmagnesium bromide (1.0 M in THF, 4.64 mL, 4.64 mmol) was added dropwise via syringe over course of 3 min. A vent line was added to account for gas evolution (note: gas evolution can be quite vigorous along with substantial heat generation if addition is too rapid). Reaction mixture (clear, colorless at outset of addition) undergoes a series of color changes, first turning a bright yellow with initial drops, then transitioning to orange and red hues, and ultimately turning a dark red-brown (almost black) upon complete addition of EtMgBr. The vent line was removed, and the reaction mixture was stirred at room temp for 1 hr. An aqueous solution containing 60 mL sat. Rochelle salt and 20 mL 1 M NaOH was prepared. The reaction was quenched with 25 mL of this aqueous mixture and stirred vigorously for 15 min at room temperature. The mixture was then diluted with the remainder of the quenching solution and 50 mL ether. The layers were separated, and the aqueous layer was extracted with 50 mL portions of ether three times. The combined organics were then washed with 50 mL brine, dried over anhydrous MgSO₄, filtered to remove solids, and concentrated *in vacuo*. The crude residue was purified via flash column chromatography over silica (5 to 10 to 15 to 25 to 35 to 60% acetone:CH₂Cl₂; silica was pre-neutralized with 5% acetone:CH₂Cl₂ + 1% NEt₃; the residue was loaded with PhMe), and the product was collected in two portions. The central fractions afforded 130 mg as clear, colorless oil, while the shoulder fractions totaled 120 mg of a yellow oil. Over the course of a few hrs, the latter separated into biphasic mixture; 90 mg of a clear, colorless oil were removed from the top and were identified as the desired product, while the residual brown oil was suspected to be the demethylated aminoCP byproduct based on NMR analysis (totalling 30 mg). Overall, 220 mg of aminoCP **2.17** were collected (74.6% yield or 66.2% yield over two steps).

¹H NMR (CDCl₃, 500 MHz): δ = 5.03 (t, 1H, *J* = 7.1 Hz, C4), 2.71 (*app.* t, 4H, *J* = 4.8 Hz, piperazine), 2.43-2.28 (br s, 4H, piperazine), 2.26 (s, 3H, piperazine-Me), 1.94-1.88 (m, 2H, C3),

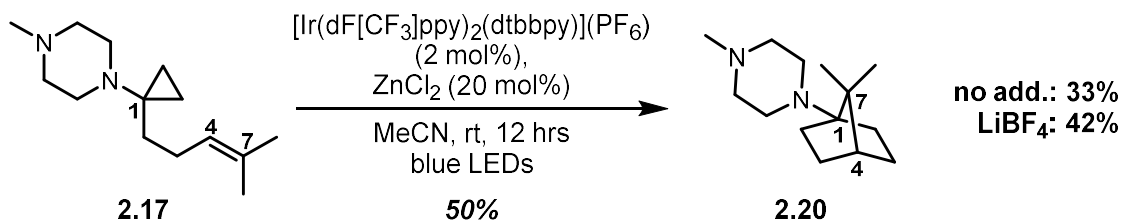
1.65 (s, 3H, C7-Me), 1.57 (s, 3H, C7-Me), 1.55-1.50 (m, 2H, C2), 0.52-0.48 (m, 2H, CP), 0.44-0.40 (m, 2H, CP) ppm

¹³C NMR (CDCl₃, 126 MHz): δ = 131.3, 124.8, 56.0, 49.2, 46.3, 43.8, 30.0, 26.2, 25.8, 17.8, 13.4 ppm

IR (neat): 2955, 2874, 2820, 1450, 1384, 1315, 1214, 1196, 1111, 1070, 969, 912 cm⁻¹

HRMS (ES⁺, *m/z*) calculated for C₁₄H₂₇N₂⁺: 223.2169, Found: 223.2170

R_f = 0.50 (40% acetone in CH₂Cl₂ + NH₄OH), one yellow spot, KMnO₄



In dry vial under nitrogen, aminoCP **2.17** (55.2 mg, 248 μmol) was dissolved in 2.5 mL dry MeCN before adding $[\text{Ir}(\text{dF}[\text{CF}_3]\text{ppy})_2(\text{dtbbpy})](\text{PF}_6)$ (5.6 mg, 5.0 μmol) then ZnCl_2 (1.0 M in ether, 50 μL , 50 μmol) in one portion each. Reaction mixture was clear and bright yellow (almost yellow-green). Reaction mixture was degassed with three freeze-pump-thaw cycles. The reaction was performed by stirring at room temp (as controlled with jacketed water bath, temp maintained between 18-23 $^\circ\text{C}$) while irradiating with two strips of 4.4 W blue LEDs for 12 hrs. Mixture became slightly orange and a little cloudy. Quenched the reaction mixture by pouring into 10 mL 1 M HCl, then diluted with 40 mL ether and 5 mL CH_2Cl_2 . Phases were separated, and the organic phase was extracted with 10 mL 0.25 M HCl two times; no starting material or product was visible in the organic phase by TLC analysis. Aqueous phase was cooled with ice (one scoopula's worth), then basified with 15 mL 3 M NaOH (added slowly with swirling); mixture becomes cloudy. A 10 mL portion of ether was added, and the phases were separated; the aqueous phase pH was ~ 14 . The aqueous phase was extracted with 10 mL ether three times. Combined organics were washed with 10 mL brine, dried over anhydrous magnesium sulfate, filtered to remove solids, and concentrated *in vacuo*. The crude residue was purified via flash chromatography over silica (20 to 30 to 40 to 50 to 70 to 90% acetone: CH_2Cl_2 + 0.1% triethylamine; pre-neutralized silica with 20% acetone: CH_2Cl_2 + 1% triethylamine). Both the starting material and product could be collected, but both as mixtures. The starting material was mixed with a small amount of what is suspected to be the *N*-demethylated starting material; this

byproduct phase separates from the starting material as a brown oil that can be removed via syringe, leaving clean starting material (though not for the ZnCl₂ trial). The product co-elutes with a white solid (suspected to be the salt of a 1-aminoNB-derived byproduct), but this is easily removed through trituration from 1:1 ether:pentane and decanting; three rounds of trituration were performed, and the combined organics were concentrated to reveal the desired product. Collected the following:

- Recovered starting material: 11.3 mg; yellow oil, ¹H NMR reveals mostly starting material contaminated with a number of minor impurities; ~15% recovery

- Product: 27.3 mg; slightly yellow oil; 49.5% yield

¹H NMR (CDCl₃, 500 MHz): δ = 2.62 (br s, 4H, piperazine), 2.41 (br s, 4H, piperazine), 2.26 (s, 3H, piperazine-Me), 1.85-1.74 (m, 4H, C2-eq, C6-eq, C3-eq, C5-eq), 1.47-1.39 (m, 3H, C4, C2-ax, C6-ax), 1.23-1.17 (m, 2H, C3-ax, C5-ax), 1.03 (s, 6H, C7-Me, C7-Me) ppm

¹³C NMR (CDCl₃, 176 MHz): δ = 70.2, 56.1, 48.2, 47.0, 46.9, 46.3, 29.5, 27.4, 21.7 ppm

IR (neat): 2954, 2931, 2877, 2790, 1451, 1376, 1292, 1275, 1169, 1144, 1086, 1039, 1013, 872, 791 cm⁻¹

HRMS (ES⁺, *m/z*) calculated for C₁₄H₂₇N₂⁺: 223.2169, Found: 223.2169

R_f = 0.30 (50% acetone in CH₂Cl₂), one yellow spot, KMnO₄

Additional Trials with Varied Additives

No Additive

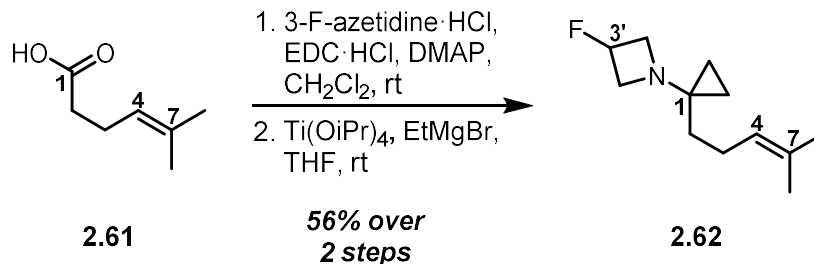
Following the general procedure outlined above, 53.6 mg of aminoCP **2.17** (241 μmol) were dissolved in 2.4 mL dry MeCN along with 5.4 mg of [Ir(dF[CF₃]ppy)₂(dtbbpy)](PF₆) (4.8 μmol) prior to irradiation. Isolation provided the following:

- Recovered starting material: 26.5 mg; clear, colorless oil; 49.4% recovery
- Product: 17.8 mg; slightly yellow oil; 33.2% yield, 65.7% BORSM

LiBF₄

Following the general procedure outlined above, 53.1 mg of aminoCP **2.17** (239 μmol) were dissolved in 2.4 mL dry MeCN along with 5.4 mg of $[\text{Ir}(\text{dF}[\text{CF}_3]\text{ppy})_2(\text{dtbbpy})](\text{PF}_6)$ (4.8 μmol) and 4.5 mg of LiBF_4 (48 μmol) prior to irradiation. Isolation provided the following:

- Recovered starting material: 19.5 mg; slightly yellow oil; 36.7% recovery
- Product: 22.2 mg; slightly yellow oil; 41.8% yield, 66.1% BORSM



In a dry flask under inert atmosphere, carboxylic acid **2.61** (207 mg, 1.61 mmol) was dissolved in 10 mL dry CH₂Cl₂. DMAP (99 mg, 0.81 mmol), EDC·HCl (464 mg, 2.42 mmol), and 3-fluoroazetidine·HCl (270 mg, 2.42 mmol) were added sequentially, each in one portion. Triethylamine (0.34 mL, 2.42 mmol) was added and the reaction was stirred at room temperature for 23 hours, at which point the reaction was homogeneous and slightly yellow in color. The reaction was quenched by pouring into 40 mL sat. sodium bicarbonate solution and diluting with 40 mL CH₂Cl₂. The layers were separated, and the aqueous layer was extracted three times with 40 mL portions of CH₂Cl₂. The combined organic layers were washed with 40 mL brine, dried over anhydrous MgSO₄, filtered, and concentrated *in vacuo*. The crude residue was purified by flash column chromatography over silica (20 to 70% ethyl acetate:hexanes, increasing in 10% increments; the residue was loaded with PhMe), providing 262 mg of a slightly yellow oil.

¹H NMR (CDCl₃, 500 MHz): δ = 5.30 (dtt, 1H, *J* = 56.4, 6.1, 3.4 Hz, C3'), 5.10 (t, 1H, *J* = 7.3 Hz, C4), 4.40-4.04 (m, 4H, C2', C4'), 2.34-2.26 (m, 2H, C3), 2.14-2.08 (m, 2H, C2), 1.69 (s, 3H, C7-Me), 1.62 (s, 3H, C7-Me) ppm

¹⁹F NMR (CDCl₃, 376 MHz): δ = -181.3 to -181.7 (m) ppm

R_f = 0.30 (70% EtOAc in hexanes), one yellow spot, KMnO₄

A portion of the amide generated above (159 mg, 0.86 mmol) was dissolved in 12 mL dry THF under inert atmosphere, followed by addition of titanium isopropoxide (0.28 mL, 0.94 mmol).

The reaction vessel was submerged in a water bath at ambient temp to serve as a heat sink. Ethylmagnesium bromide (1.0 M in THF, 2.99 mL, 2.99 mmol) was added dropwise via syringe over course of 2 min. A vent line was added to account for gas evolution (note: gas evolution can be quite vigorous along with substantial heat generation if addition is too rapid). Reaction mixture (clear, colorless at outset of addition) undergoes a series of color changes, first turning a bright yellow with initial drops, then transitioning to orange and red hues, and ultimately turning a dark red-brown (almost black) upon complete addition of EtMgBr. The vent line was removed, and the reaction mixture was stirred at room temp for 1 hr. An aqueous solution containing 50 mL sat. Rochelle salt, 20 mL brine, and 2 mL 6 M NaOH was prepared. The reaction was quenched with 40 mL of this aqueous mixture and stirred vigorously for 15 min at room temperature. The mixture was then diluted with the remainder of the quenching solution and 50 mL ether. The layers were separated, and the aqueous layer was extracted with 50 mL portions of ether three times. The combined organics were then washed with 50 mL brine, dried over anhydrous MgSO₄, filtered to remove solids, and concentrated *in vacuo*. The crude residue was purified via flash column chromatography over silica (2 to 8% EtOAc/hexanes, increasing in 2% increments; residue was loaded with PhMe), affording aminoCP **2.62** as a clear, colorless oil, 107.3 mg, 63.3% yield or 55.5% yield over two steps.

¹H NMR (CDCl₃, 500 MHz): δ = 5.09 (t, 1H, *J* = 7.3 Hz, C4), 5.07 (d of *app.* pent, *J* = 57.9, 5.4 Hz, C3'), 3.50-3.43 (m, 2H, C2', C4'), 3.09-3.00 (m, 2H, C2', C4'), 2.05 (dt, 2H, *J* = 8.8, 7.3 Hz, C3), 1.67 (s, 3H, C7-Me), 1.60 (s, 3H, C7-Me), 1.43-1.38 (m, 2H, C2), 0.64-0.61 (m, 2H, CP), 0.32-0.29 (m, 2H, CP) ppm

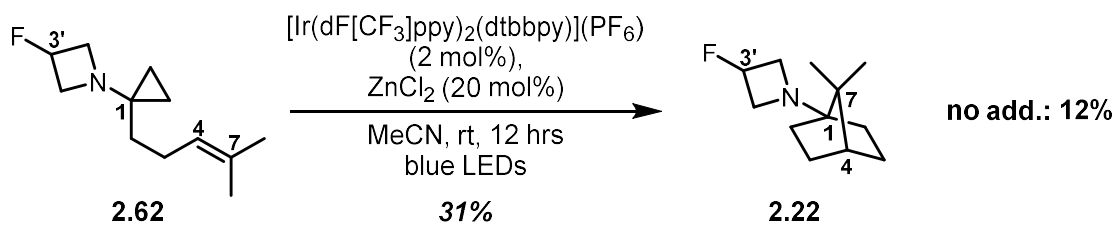
¹³C NMR (CDCl₃, 126 MHz): δ = 131.6, 124.6, 81.9 (d, *J* = 204.1 Hz, C3'), 57.0 (d, *J* = 20.0 Hz, C2', C4'), 42.5, 35.6, 25.8, 25.2, 17.8, 7.0 ppm

^{19}F NMR (CDCl_3 , 376 MHz): $\delta = -179.3$ to -179.7 (m) ppm

IR (neat): 2957, 2931, 2876, 1713, 1684, 1453, 1365, 1316, 1275, 1177, 1074, 624 cm^{-1}

HRMS (ES^+ , m/z) calculated for $\text{C}_{12}\text{H}_{21}\text{FN}^+$: 198.1653, Found: 198.1652

R_f = 0.30 (20% ethyl acetate in hexanes), one yellow spot, KMnO_4



In dry vial under nitrogen, aminoCP **2.62** (33.7 mg, 171 μmol) was dissolved in 1.7 mL dry MeCN before adding $[\text{Ir}(\text{dF}[\text{CF}_3]\text{ppy})_2(\text{dtbbpy})](\text{PF}_6)$ (3.8 mg, 3.4 μmol) then ZnCl_2 (1.0 M in ether, 34 μL , 34 μmol) in one portion each. Reaction mixture was clear and bright yellow (almost yellow-green). Reaction mixture was degassed with three freeze-pump-thaw cycles. The reaction was performed by stirring at room temp (as controlled with jacketed water bath, temp maintained between 18-23 $^\circ\text{C}$) while irradiating with two strips of 4.4 W blue LEDs for 12 hrs. Mixture has turned orange but is still clear. Quenched the reaction mixture with 20 mL 1:1 sat bicarb:1M NaOH to ensure aq phase pH \sim 14, then diluted further with 10 mL ether. Phases were separated, and the aqueous phase was extracted with 10 mL 1:1 ether:hexanes three times. Combined organics were washed with 10 mL brine, dried over anhydrous magnesium sulfate, filtered to remove solids, and concentrated *in vacuo*. The crude residue was purified via flash chromatography (2 to 5 to 8 to 12 to 20 to 30% ethyl acetate:hexanes; residue loaded with PhMe; pre-neutralized silica with 2% ethyl acetate:hexanes + 1% triethylamine). Collected the following:

- Recovered starting material: 4.9 mg; yellow oil; 14.5% recovery
- Product: 10.5 mg; slightly yellow oil; 30.6% yield, 35.8% BORSM

$^1\text{H NMR}$ (CDCl_3 , 500 MHz): δ = 5.14 (d of *app.* pent., 1H, J = 57.9, 5.6 Hz, C3'), 3.58-3.53 (m, 2H, C2', C4'), 3.41-3.35 (m, 2H, C2', C4'), 1.85-1.79 (m, 2H, norbornane core), 1.79-1.73 (m, 2H, norbornane core), 1.49 (t, 1H, J = 4.4 Hz, C4), 1.35-1.30 (m, 2H, norbornane core), 1.29-1.24 (m, 2H, norbornane core), 0.92 (s, 6H, C7-Me, C7-Me) ppm

¹³C NMR (CDCl₃, 176 MHz): δ = 83.1 (d, *J* = 203.7 Hz, C3'), 68.7, 57.4 (d, *J* = 20.4 Hz, C2', C4'), 47.3, 44.9, 28.0, 27.5, 20.0 ppm

¹⁹F NMR (CDCl₃, 376 MHz): δ = -177.4 to -177.8 (m) ppm

IR (neat): 2955, 2928, 2875, 1713, 1452, 1384, 1366, 1317, 1276, 1162, 1092 cm⁻¹

HRMS (ES⁺, *m/z*) calculated for C₁₂H₂₁FN⁺: 198.1653, Found: 198.1652

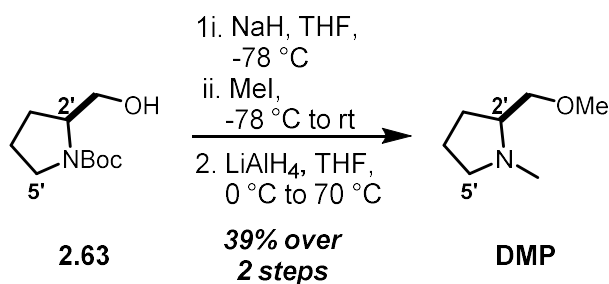
R_f = 0.20 (20% ethyl acetate in hexanes), one yellow spot, KMnO₄

Additional Trials with Varied Additives

No Additive

Following the general procedure outlined above, 38.1 mg of aminoCP **2.62** (193 μmol) were dissolved in 2.0 mL dry MeCN along with 4.3 mg of [Ir(dF[CF₃]ppy)₂(dtbbpy)](PF₆) (3.9 μmol) prior to irradiation. Isolation provided 20.5 mg of a clear, colorless oil that proved to be 3.4:1 recovered starting material:product based on ¹H NMR, indicating the following:

- Recovered starting material: 15.9 mg; 41.7% recovery
- Product: 4.6 mg; 12.1% yield, 20.7% BORSM



In a dry flask under inert atmosphere, NaH (60% dispersion in mineral oil; 358 mg, 9.0 mmol) was washed with three 5 mL portions of pentane before drying with a gentle stream of nitrogen. The washed NaH was suspended in 60 mL dry THF, then cooled to -78 °C. In a separate dry flask under nitrogen, Boc-prolinol (**2.63**; 1.45 g, 7.2 mmol) was dissolved in 15 mL dry THF; this solution was added to the NaH suspension via syringe, dropwise down the side of the flask over 3.5 min; a vent line was in place during the addition to compensate for the H₂ generation. After stirring at -78 °C for 1 hr, methyl iodide (0.58 mL, 9.4 mmol) was added dropwise over 1 min. The reaction was allowed to stir for 23 hrs while slowly coming to room temp. The reaction mixture was quenched by slowly pouring into 100 mL sat. NH₄Cl before diluting with 100 mL ether. The layers were separated, and the aqueous phase was extracted with three 100 mL portions of ether. The combined organics were washed with 75 mL water then 100 mL brine, dried over anhydrous magnesium sulfate, filtered to remove solids, and concentrated under vacuum. The crude residue was purified via flash chromatography over silica (4 to 20% ethyl acetate:hexanes, increasing in 4% increments; loaded residue with PhMe). The desired *O*-methyl Boc-prolinol⁶⁹ (**2.64**) was obtained as a clear, slightly yellow oil (1.20 g, 77.5%).

A portion of the methylated material was exposed to reduction conditions. In a dry flask under an inert atmosphere, lithium aluminum hydride (331 mg, 8.7 mmol) was suspended in 60 mL dry THF then cooled to 0 °C. *O*-methyl Boc-prolinol (750 mg, 3.5 mmol) was dissolved in 10 mL dry THF in a separate flask under nitrogen; this solution was added to the LiAlH₄ suspension

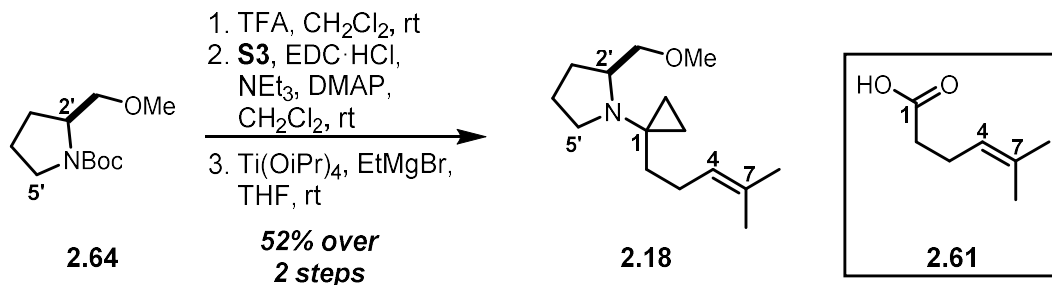
via syringe, dropwise down the side of the flask over 1.5 min. The ice bath was removed, and a reflux condenser was attached. The reaction mixture was then heated to 70 °C for 12 hrs. Upon cooling to room temp, the mixture was again cooled to 0 °C prior to quenching with 60 mL of sat. Rochelle salt. After diluting with 60 mL ether, the layers were separated, and the aqueous phase was extracted with three 60 mL portions of ether. The combined organics were washed with 60 mL brine, dried over magnesium sulfate, filtered to remove solids and carefully concentrated under reduced pressure. This provided 225 mg of *N,O*-dimethyl prolinol **DMP** as a slightly yellow oil (50.0% yield or 38.7% yield over two steps).

¹H NMR (CDCl₃, 500 MHz): δ = 3.41 (dd, 1H, *J* = 9.5, 5.4 Hz, CH₂OMe), 3.36 (s, 3H, -OMe), 3.32 (dd, 1H, *J* = 9.5, 5.6 Hz, CH₂OMe), 3.05 (ddd, 1H, *J* = 9.3, 7.3, 1.7 Hz, C2'), 2.39 (s, 3H, -NMe), 2.38-2.32 (m, 1H, C5'), 2.20 (dt, 1H, *J* = 9.5, 7.6 Hz, C5'), 1.94-1.86 (m, 1H, C3'), 1.81-1.65 (m, 2H, C3', C4'), 1.65-1.57 (m, 1H, C4') ppm

¹³C NMR (CDCl₃, 100 MHz): δ = 75.9, 65.0, 59.3, 57.9, 41.7, 28.7, 22.9 ppm

IR (neat): 2966, 2934, 2881, 2837, 2790, 2743, 1451, 1372, 1286, 1157, 1013 cm⁻¹

HRMS (ES⁺, *m/z*) calculated for C₇H₁₆NO⁺: 130.1226, Found: 130.1225



Prolinol derivative **2.64** (an intermediate en route to *N,O*-dimethyl prolinol (547 mg, 2.54 mmol) was dissolved in 12 mL dry CH₂Cl₂ in a dry flask under inert atmosphere. The solution was cooled to 0 °C in an ice bath and TFA (1.89 mL, 25.4 mmol) was added dropwise down the side of the flask over 1 min with a vent line in place. The vent line was removed after the addition was complete. The reaction was warmed to room temperature and stirred for 2 hr. CH₂Cl₂ was removed under reduced pressure and the resultant 1.27 g of orange residue was used in the next reaction without further purification.

¹H NMR (CDCl₃, 500 MHz): δ = 3.87 (br s, 1H, C2'), 3.63 (dd, 1H, *J* = 10.4, 3.5 Hz, CH₂-OMe), 3.51 (dd, 1H, *J* = 10.4, 6.2 Hz, CH₂-OMe), 3.42-3.30 (m, 2H, C5') 3.37 (s, 3H, -OMe), 2.20-1.98 (m, 3H, C3', C3', C4'), 1.87 (*app.* dq, 1 H, *J* = 13.1, 8.3 Hz, C4') ppm

The resultant TFA salt (assumed 2.54 mmol) was dissolved in 17 mL dry CH₂Cl₂ in a dry flask under inert atmosphere. The solution was cooled to 0 °C before adding NEt₃ (1.20 mL, 8.63 mmol) down the side of the flask over 1 min. The ice bath was removed, followed by sequential addition of DMAP (155 mg, 1.27 mmol), carboxylic acid **2.61** (391 mg, 3.05 mmol), and EDC·HCl (828 mg, 4.32 mmol) in one portion each. The reaction was stirred for 48 hrs at room temp before quenching by pouring into 60 mL 1 M HCl. The mixture was further diluted with 60 mL CH₂Cl₂, and the layers were separated. The aqueous layer was extracted with three 60 mL portions of CH₂Cl₂, and the combined organic layers were washed with 60 mL sat. sodium bicarbonate, 60

mL brine, dried over anhydrous MgSO₄, filtered to remove solids, and concentrated *in vacuo*. The crude material was purified by flash column chromatography over silica (20 to 60% EtOAc:hexanes, increasing in 10% increments; the crude residue was loaded with toluene), affording 535 mg of the desired amide as a slightly yellow, clear oil (**R_f** = 0.30 [60% EtOAc in hexanes], one yellow spot, KMnO₄).

A portion of amide intermediate (311 mg, 1.38 mmol) was dissolved in 20 mL dry THF in a dry flask under inert atmosphere, followed by the addition of titanium isopropoxide (0.45 mL, 1.52 mmol). The reaction vessel was submerged in a water bath at ambient temperature to serve as a heat sink. Ethylmagnesium bromide (1.0 M in THF, 4.83 mL, 4.83 mmol) was added dropwise via syringe over the course of 2 min. A vent line was added to account for gas evolution (note: gas evolution can be quite vigorous along with substantial heat generation if addition is too rapid). The reaction mixture (clear, colorless at the outset of the addition) undergoes a series of color changes, first turning a bright yellow with initial drops, then transitioning to orange and red hues, and ultimately turning a dark red-brown (almost black) upon complete addition of EtMgBr. The vent line was removed, and the reaction mixture was stirred at room temperature for 1 hr. An aqueous solution containing 100 mL Rochelle salt, 40 mL brine, and 4 mL 6 M NaOH was prepared. The reaction was quenched with 70 mL of this aqueous solution and stirred vigorously for 30 min. The mixture was then poured into the remaining quenching solution and further diluted with 20 mL ether. The layers were separated and the aqueous layer was extracted three 20 mL portions of ether. The combined organic layers were washed with 20 mL brine, dried over anhydrous MgSO₄, filtered to remove solids, and concentration *in vacuo*. The crude residue was purified by flash column chromatography over silica (3 to 15% EtOAc:hexanes, increasing in 3% increments; the residue was loaded with toluene). The middle fractions provided 171 mg of aminoCP **2.18** as a

slightly yellow, clear oil. The end fractions (38.5 mg) were subjected to another round of flash column chromatography over silica identical to the first, affording an additional 11 mg of the desired product. The total yield of aminoCP **2.18** was thus 182 mg (51.9% over three steps).

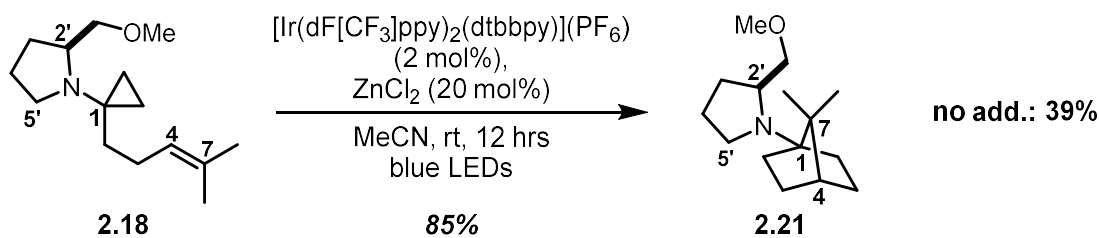
¹H NMR (CDCl₃, 500 MHz): δ = 5.08 (t, 1H, J = 7.0 Hz, C4), 3.45 (dd, 1H, J = 9.1 Hz, 3.5 Hz, CH₂-OMe) 3.34 (s, 3H, -OMe), 3.19 (dd, 1H, J = 8.9, 7.9 Hz, CH₂-OMe), 3.04-2.98 (m, 1H, C5'), 2.97-2.89 (m, 1H, C5'), 2.74 (dd, 1H, J = 16.3, 8.3 Hz, C2'), 1.97-1.79 (m, 3H, C3', C3', C4'), 1.73-1.62 (m, 4H, C3, C2), 1.67 (s, 3H, C7-Me), 1.59 (s, 3H, C7-Me), 1.42 (ddd, 1H, J = 13.9, 11.1, 5.8 Hz, C4'), 0.62 – 0.53 (m, 2H, CP), 0.48-0.40 (m, 2 H, CP) ppm

¹³C NMR (CDCl₃, 176 MHz): δ = 131.4, 124.8, 75.7, 59.2, 58.1, 50.5, 38.5, 31.1, 29.5, 25.8, 25.6, 22.9, 17.8, 13.3, 11.5 ppm

IR (neat): 2965.3, 2918.25, 2823.45, 2808.1, 1449.7, 1375.8, 1332.7, 1282.9, 1196.8, 1112.8, 1012.8, 969.4 cm⁻¹

HRMS (ES⁺, m/z) calculated for C₁₅H₂₉NO⁺: 238.2165, Found: 238.2166

R_f = 0.45 (20% EtOAc in hexanes), one yellow spot, KMnO₄



In dry vial under nitrogen, aminoCP **2.18** (60.2 mg, 254 μmol) was dissolved in 2.5 mL dry MeCN before adding $[\text{Ir}(\text{dF}[\text{CF}_3]\text{ppy})_2(\text{dtbbpy})](\text{PF}_6)$ (5.7 mg, 5.1 μmol) then ZnCl_2 (1.0 M in ether, 51 μL , 51 μmol) in one portion each. Reaction mixture was bright yellow. Reaction mixture was degassed with three freeze-pump-thaw cycles. The reaction was performed by stirring at room temp (as controlled with jacketed water bath, temp maintained between 18-23 $^\circ\text{C}$) while irradiating with two strips of 4.4 W blue LEDs for 12 hrs. Mixture appeared slightly cloudy and had turned a light orange color. A 25 μL aliquot was removed and diluted into 450 μL MeCN + 25 μL of a dodecane standard solution (5 mM in MeCN) both prior to degassing (total volume = MeCN volume) and after 12 hrs (5 mL total volume; reaction mixture diluted with ether in 5 mL vol. flask). The mixture was poured into with 20 mL 1:1 sat. NaHCO_3 :1M NaOH to ensure aq phase pH \sim 14, then diluted further with 5 mL ether. Phases were separated, and the aqueous phase was extracted with 10 mL ether three times. Combined organics were washed with 10 mL brine, dried over anhydrous sodium sulfate, filtered to remove solids, and concentrated *in vacuo*. The crude residue was purified via flash chromatography (5 to 10 to 15 to 20 to 30 to 50 to 70% ethyl acetate:hexanes; silica was pre-neutralized with 5% ethyl acetate:hexanes + 1% NEt_3 ; starting at 20%, 0.1% NEt_3 was added to each increment; residue loaded with PhMe).

- GCMS conversion: *[data of insufficient quality]*

- Recovered starting material: 3.5 mg; 5.9% recovery

- Product: 53.8 mg; 84.8% yield, 90.1% BORSM

¹H NMR (CDCl₃, 700 MHz): δ = 3.33 (s, 3H, -OMe), 3.25 (ddd, 1H, *J* = 9.0, 3.6, 1.0 Hz, CH₂-OMe), 3.16-3.12 (m, 1H, C2'), 3.02 (dd, 1H, *J* = 9.9, 9.2 Hz, CH₂-OMe), 2.86-2.83 (m, 1H, C5'), 2.69-2.64 (m, 1H, C5'), 1.89-1.73 (m, 5H, C2, C3-eq, C5-eq, C4', C6), 1.72-1.67 (m, 2H, C3', C3'), 1.57-1.48 (m, 2H, C4', C6), 1.42 (t, 1H, *J* = 4.4 Hz, C4), 1.42-1.38 (m, 1H, C2), 1.26-1.20 (m, 2H, C5-ax, C3-ax), 1.02 (s, 3H, C7-Me), 1.01 (s, 3H, C7-Me) ppm

¹³C NMR (CDCl₃, 176 MHz): δ = 77.7, 69.9, 59.1, 57.7, 50.1, 47.4, 46.2, 30.1, 29.8, 29.2, 27.6, 27.6, 24.1, 21.1, 20.5 ppm

IR (neat): 2955, 2873, 2820, 1450, 1384, 1315, 1215, 1196, 1111, 1070, 969, 912 cm⁻¹

HRMS (ES⁺, *m/z*) calculated for C₁₅H₂₈NO⁺: 238.2165, Found: 238.2166

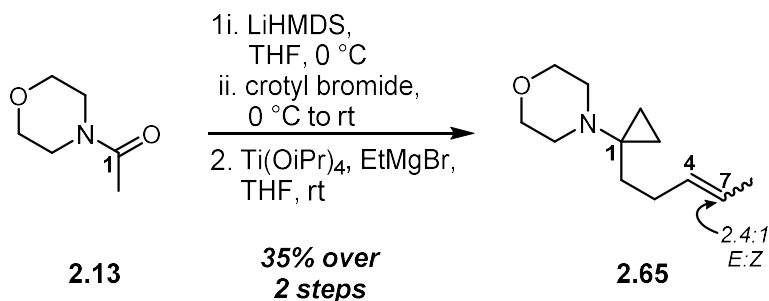
R_f = 0.15 (70% ethyl acetate:hexanes), one yellow spot, KMnO₄

Additional Trials with Varied Additives

No Additive

Following the general procedure outlined above, 58.3 mg of aminoCP **1e** (246 μmol) were dissolved in 2.5 mL dry MeCN along with 5.5 mg of [Ir(dF[CF₃]ppy)₂(dtbbpy)](PF₆) (4.9 μmol) prior to irradiation. Isolation provided:

- Recovered starting material: 30.4 mg; yellow oil; 52.9% recovery
- Product: 22.5 mg; clear, colorless oil; 39.2% yield, 83.2% BORSM



N-Acetyl morpholine (**2.13**, 360 μ L, 3.1 mmol) was dissolved in 8 mL dry THF in a dry flask under N₂ before cooling to 0 °C (ice/water). LiHMDS (1.0 M in THF, 3.25 mL, 3.25 mmol) was added dropwise down the side of the vial over 2 min, then the reaction mixture was allowed to stir at 0 °C for 1 hr. In a separate dry flask kept under inert atmosphere, crotyl bromide (0.51 mL, 4.2 mmol) was dissolved in 5 mL dry THF. The enolate solution was then cannulated into the bromide solution slowly down the side of the vial over the course of 2 hrs. Transfer was quantified with two rinses of 2 mL dry THF. The mixture was stirred at room temp for 30 min before quenching with 20 mL 1:1 sat. NaHCO₃:sat. Na₂S₂O₃. Mixture was diluted with 20 mL ether, and the phases were separated. The aqueous phase was then extracted with 20 mL portions of ether three times. Combined organics were washed with 20 mL brine, dried over anhydrous magnesium sulfate, filtered to remove solids, and concentrated *in vacuo* to afford a slightly yellow oil. This crude residue was purified by flash chromatography over silica (15 to 75% ethyl acetate:hexanes, increasing in 15% increments; residue was loaded with PhMe). The desired mono-alkylated product was afforded as a clear, colorless oil (359 mg, 63.3% yield; R_f = 0.30 in 60% EtOAc:hexanes, one yellow spot, KMnO₄) as a mixture of the *E* and *Z* olefin isomers, along with 56 mg of the bis-crotylated species (7.6%). The mono-alkylated product was moved on without further purification.

The mixture of amides from above (324 mg, 1.77 mmol) was dissolved in 35 mL dry THF under inert atmosphere, followed by addition of titanium isopropoxide (0.58 mL, 1.94 mmol). The

reaction vessel was submerged in a water bath at ambient temp to serve as a heat sink. Ethylmagnesium bromide (1.0 M in THF, 6.2 mL, 6.2 mmol) was added dropwise via syringe over the course of 4 min. A vent line was added to account for gas evolution (note: gas evolution can be quite vigorous along with substantial heat generation if addition is too rapid). Reaction mixture (clear, colorless at outset of addition) undergoes a series of color changes, first turning a bright yellow with initial drops, then transitioning to orange and red hues, and ultimately turning a dark red-brown (almost black) upon complete addition of EtMgBr. Vent line was removed, and the reaction mixture was stirred at room temp for 1 hr before quenching with 50 mL sat. Rochelle salt and stirred vigorously for 20 min. The mixture was then diluted with 25 mL sat. Rochelle salt, 25 mL brine, and 50 mL ether. Phases were separated. The aqueous phase was extracted with 50 mL portions of ether three times. The combined organics were then washed with 50 mL brine, dried over anhydrous sodium sulfate, filtered to remove solids, and concentrated *in vacuo*. The crude residue was purified via flash chromatography over silica (4 to 20% ethyl acetate:hexanes, increasing in 4% increments; residue was loaded with PhMe). Obtained aminoCP **2.65** as clear, colorless liquid (190 mg, 55.0%, 34.8% over two steps). The olefin isomers were inseparable (2.4:1 *E:Z*) and were thus characterized as a mixture. This mixture is inconsequential for subsequent transformations detailed herein.

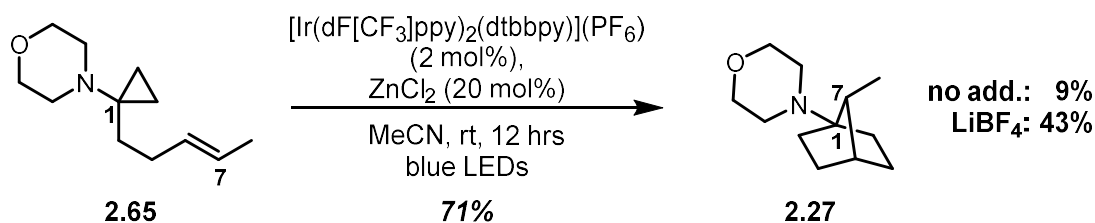
¹H NMR (CDCl₃, 500 MHz): δ = 5.46-5.31 (m, 2H-*E*, 2H-*Z*, C4, C7), 3.65-3.55 (m, 4H-*E*, 4H-*Z*, morph.), 2.69-2.60 (m, 4H-*E*, 4H-*Z*, morph.), 2.02-1.95 (m, 2H-*Z*, C3), 1.95-1.89 (m, 2H-*E*, C3), 1.67-1.62 (m, 3H-*E*, 3H-*Z*, C7-Me), 1.61-1.54 (m, 2H-*E*, 2H-*Z*, C2), 0.56-0.49 (m, 2H-*E*, 2H-*Z*, CP), 0.47-0.40 (m, 2H-*E*, 2H-*Z*, CP) ppm

¹³C NMR (CDCl₃, 126 MHz): δ = 131.4 (*E*), 130.6 (*Z*), 124.8 (*E*), 123.9 (*Z*), 67.9 (*E/Z*), 49.9 (*Z*), 49.8 (*E*), 44.1 (*E/Z*), 30.4 (*E*), 29.8 (*Z*), 29.8 (*E*), 24.8 (*Z*), 18.0 (*E/Z*), 12.9 (*E/Z*) ppm

IR (thin film): 2930, 2852, 1450, 1263, 1115, 1013, 984, 963, 856 cm^{-1}

HRMS (ES+, m/z) calculated for $\text{C}_{12}\text{H}_{22}\text{NO}^+$: 196.1696, Found: 196.1696

R_f = 0.35 (20% EtOAc in hexanes), one yellow spot, KMnO_4



In dry vial under nitrogen, aminoCP **2.65** (2.8:1 mix of olefin isomers; 65.0 mg, 333 μmol) was dissolved in 3.3 mL dry MeCN before adding $[\text{Ir}(\text{dF}[\text{CF}_3]\text{ppy})_2(\text{dtbbpy})](\text{PF}_6)$ (7.5 mg, 6.66 μmol) then ZnCl_2 (1.0 M in ether, 66.6 μL , 66.6 μmol) in one portion each. Reaction mixture is bright yellow, but slightly cloudy from the Zn salt. Reaction mixture was degassed with three freeze-pump-thaw cycles. The reaction was performed by stirring at room temp (as controlled with jacketed water bath, temp maintained between 18-23 $^\circ\text{C}$) while irradiating with two strips of 4.4 W blue LEDs for 12 hrs. Mixture appears somewhat cloudier than it did prior to irradiation and perhaps slightly darker yellow. A 25 μL aliquot was removed and diluted into 450 μL MeCN + 25 μL of a dodecane standard solution (5 mM in MeCN) both prior to degassing (total volume = MeCN volume) and after 12 hrs (5 mL total volume; reaction mixture diluted with ether in 5 mL vol. flask); these samples were run on the GCMS to measure starting material conversion. The diluted mixture was added to 10 mL 1:1 NaHCO_3 :water containing 1 mL of 50% NaOH to ensure aqueous phase pH ~ 14 , then diluted further with 5 mL hexanes. Phases were separated, and the aqueous phase was extracted with 10 mL 1:1 ether:hexanes three times. Combined organics were washed with 10 mL brine, dried over anhydrous magnesium sulfate, filtered to remove solids, and concentrated *in vacuo*. The crude residue was purified via flash chromatography (4 to 32% ethyl acetate:hexanes, increasing in 4% increments; residue loaded with PhMe).

- GCMS conversion: 94%

- Recovered starting material: 3.8 mg; slightly yellow oil, but ^1H NMR reveals a number of minor impurities; <6% recovery

- Product: 45.8 mg; slightly yellow oil; 71.3% yield:

¹H NMR (CDCl₃, 500 MHz): δ = 3.75-3.65 (m, 4H, morph.), 2.55 (dt, 2H, *J* = 11.3, 4.7 Hz, morph.), 2.45 (dt, 2H, *J* = 11.7, 4.9 Hz, morph.), 1.89-1.80 (m, 1H, C3), 1.79 (*app.* t, 1H, *J* = 4.4 Hz, C4), 1.71 (*app.* t, 1H, *J* = 6.3 Hz, C7), 1.70-1.66 (m, 1H, C6), 1.63-1.54 (m, 1H, C5), 1.51-1.46 (m, 2H, C2, C2), 1.35-1.29 (m, 2H, C5, C3), 1.15 (ddd, 1H, *J* = 11.0, 9.8, 4.7 Hz, C6), 0.83 (d, 3H, *J* = 6.6 Hz, C7-Me) ppm

¹³C NMR (CDCl₃, 126 MHz): δ = 70.9 (C1), 67.3 (morph.), 48.5 (morph.), 43.6 (C7), 39.4 (C4), 32.0 (C2), 29.1 (C5), 27.9 (C3), 23.7 (C6), 10.1 (C7-Me) ppm

IR (thin film): 2950, 2870, 2810, 1449, 1377, 1327, 1274, 1248, 1167, 1156, 1117, 1070, 1038, 1027, 1004, 967, 920, 891, 847, 688 cm⁻¹

HRMS (ES⁺, *m/z*) calculated for C₁₂H₂₂NO⁺: 196.1696, Found: 196.1700

R_f = 0.20 (20% EtOAc in hexanes), one yellow spot, KMnO₄

Additional Trials with Varied Additives

No Additive

Following the general procedure outlined above, 55.8 mg of aminoCP **2.65** (286 μmol) were dissolved in 2.8 mL dry MeCN along with 5.7 mg of [Ir(dF[CF₃]ppy)₂(dtbbpy)](PF₆) (5.3 μmol) prior to irradiation. Isolation provided the following:

- GCMS conversion: *[data not collected]*

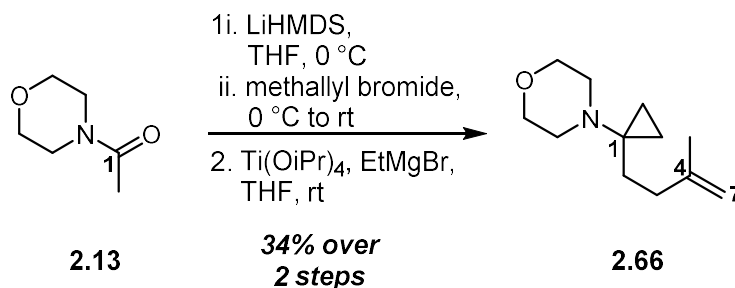
- Recovered starting material: 31.1 mg; clear, colorless oil; 55.7% recovery

- Product: 5.0 mg; clear, colorless oil; 9.0% yield, 20.9% BORSM

LiBF₄

Following the general procedure outlined above, 54.2 mg of aminoCP **2.65** (278 μmol) were dissolved in 2.8 mL dry MeCN along with 6.2 mg of $[\text{Ir}(\text{dF}[\text{CF}_3]\text{ppy})_2(\text{dtbbpy})](\text{PF}_6)$ (5.6 μmol) and 5.2 mg of LiBF_4 (56 μmol) prior to irradiation. Isolation provided the following:

- GCMS conversion: 60%
- Recovered starting material: 18.1 mg; clear, colorless oil, but ^1H NMR reveals a number of minor impurities; ~34% recovery
- Product: 22.8 mg; yellow oil; 42.1% yield



N-Acetyl morpholine (**2.13**, 0.31 mL, 2.66 mmol) was dissolved in 3.3 mL dry THF in a dry flask under N₂, before cooling to 0 °C (ice/water). LiHMDS (1.0 M in THF, 2.8 mL, 2.8 mmol) was added dropwise down the side of the vial over 2 min, then the reaction mixture was allowed to stir at 0 °C for 1 hr. In a separate dry flask kept under inert atmosphere, methallyl bromide (0.36 mL, 3.59 mmol) was dissolved in 10 mL dry THF. The enolate solution was then cannulated into the bromide solution slowly down the side of the vial over the course of 2.5 hrs. Transfer was quantified with two rinses of 1 mL dry THF. The mixture was stirred at room temp for 30 min before quenching with 20 mL 1:1 sat. NaHCO₃:sat. Na₂S₂O₃. The mixture was diluted with 20 mL ether, and the phases were separated. The aqueous phase was then extracted with 20 mL portions of ether three times. Combined organics were washed with 20 mL brine, dried over anhydrous magnesium sulfate, filtered to remove solids, and concentrated *in vacuo* to afford a slightly yellow oil. This crude residue was purified by flash chromatography over silica (20 to 70% ethyl acetate:hexanes, increasing in 10% increments; residue was loaded with PhMe). The desired mono-alkylated product was afforded as a yellow oil (231 mg, 47.4% yield).

¹H NMR (CDCl₃, 500 MHz): δ = 4.76 (s, 1H, C7), 4.69 (s, 1H, C7), 3.70-3.65 (m, 4H, morph.), 3.65-3.60 (m, 2H, morph.), 3.51-3.46 (m, 2H, morph.), 2.48-2.43 (m, 2H, C2), 2.37-2.32 (m, 2H, C3), 1.76 (s, 3H, C4-Me) ppm

R_f = 0.35 (60% EtOAc in hexanes), one yellow spot, KMnO₄

The amide from above (ca. 1.3 mmol) was dissolved in 20.5 mL dry THF under inert atmosphere, followed by addition of titanium isopropoxide (0.41 mL, 1.39 mmol). The reaction vessel was submerged in a water bath at ambient temp to serve as a heat sink. Ethylmagnesium bromide (1.0 M in THF, 4.4 mL, 4.4 mmol) was added dropwise via syringe over the course of 4 min. A vent line was added to account for gas evolution (note: gas evolution can be quite vigorous along with substantial heat generation if addition is too rapid). Reaction mixture (clear, colorless at outset of addition) undergoes a series of color changes, first turning a bright yellow with initial drops, then transitioning to orange and red hues, and ultimately turning a dark red-brown (almost black) upon complete addition of EtMgBr. Vent line was removed, and the reaction mixture was stirred at room temp for 1 hr, at which point starting material had been consumed as revealed by TLC analysis. Reaction was quenched with 20 mL sat. Rochelle salt and stirred vigorously for 15 min. The mixture was then diluted with 10 mL sat. Rochelle salt, 10 mL brine, and 20 mL ether. Phases were separated. The aqueous phase was extracted with 20 mL portions of ether three times. The combined organics were then washed with 20 mL brine, dried over anhydrous sodium sulfate, filtered to remove solids, and concentrated *in vacuo*. The crude residue was purified via flash chromatography over silica (4 to 20% ethyl acetate:hexanes, increasing in 4% increments; residue was loaded with PhMe). Obtained aminoCP **2.66** as clear, colorless liquid (178 mg, 34.2% over 2 steps).

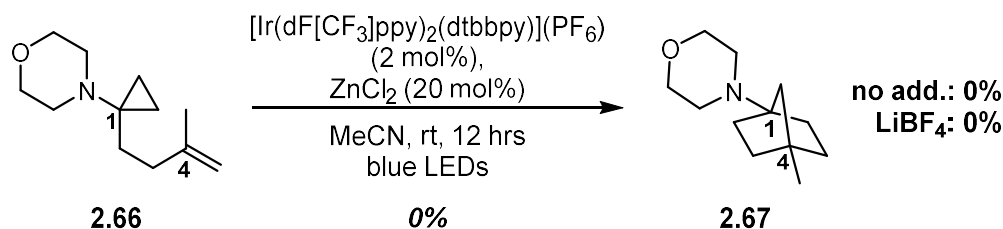
¹H NMR (CDCl₃, 500 MHz): δ = 4.68 (s, 1H, C7), 4.65 (s, 1H, C7), 3.64-3.57 (m, 4H, morph.), 2.71-2.64 (m, 4H, morph.), 1.98-1.92 (m, 2H, C3), 1.71 (s, 3H, C4-Me), 1.69-1.64 (m, 2H, C2), 0.57-0.53 (m, 2H, CP), 0.46-0.42 (m, 2H, CP) ppm

¹³C NMR (CDCl₃, 126 MHz): δ = 146.3, 109.6, 67.9, 49.9, 44.2, 35.4, 28.2, 22.8, 12.9 ppm

IR (neat): 2935, 2853, 1449, 1264, 1115, 1013, 986, 884, 857 cm⁻¹

HRMS (ES⁺, *m/z*) calculated for C₁₂H₂₂NO⁺: 196.1696, Found: 196.1698

R_f = 0.50 (20% EtOAc in hexanes), one yellow spot, KMnO₄



In a dry vial under nitrogen, aminoCP **2.66** (44.4 mg, 227 μmol) was dissolved in 2.3 mL dry MeCN before adding $[\text{Ir}(\text{dF}[\text{CF}_3]\text{ppy})_2(\text{dtbbpy})](\text{PF}_6)$ (5.1 mg, 4.6 μmol) then ZnCl_2 (1.0 M in ether, 46 μL , 46 μmol) in one portion each. Reaction mixture is bright yellow, but slightly cloudy from the Zn salt. Reaction mixture was degassed with three freeze-pump-thaw cycles. The reaction was performed by stirring at room temp (as controlled with jacketed water bath, temp maintained between 18-23 $^\circ\text{C}$) while irradiating with two strips of 4.4 W blue LEDs for 12 hrs. The mixture appears substantially cloudier than prior to irradiation, with some grey precipitate adhering to the walls of the vial. A 25 μL aliquot was removed and diluted into 450 μL MeCN + 25 μL of a dodecane standard solution (5 mM in MeCN) both prior to degassing (total volume = MeCN volume) and after 12 hrs (5 mL total volume; reaction mixture diluted with ether in 5 mL vol. flask); these samples were run on the GCMS to measure starting material conversion. The diluted mixture was added to 10 mL 1:1 sat. NaHCO_3 :water containing 1 mL of 50% NaOH to ensure aq phase pH \sim 14, then diluted further with 5 mL hexanes. Phases were separated, and the aqueous phase was extracted with 10 mL portions of 1:1 ether:hexanes three times. Combined organics were washed with 10 mL brine, dried over anhydrous magnesium sulfate, filtered to remove solids, and concentrated *in vacuo*. Only starting material could be detected by ^1H NMR of the crude residue, but this material was not recovered. GCMS revealed 53% consumption of the starting material.

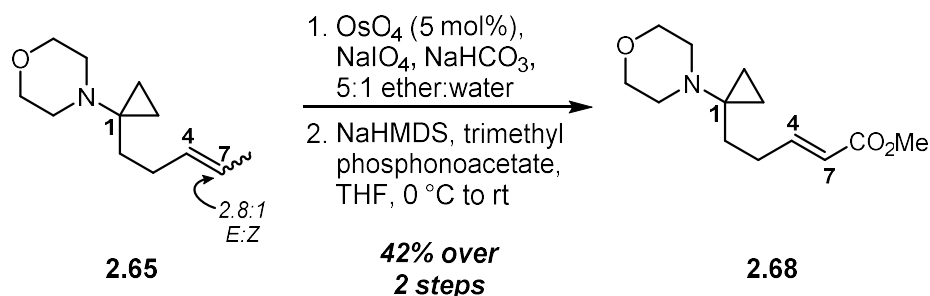
Additional Trials with Varied Additives

No Additive

Following the general procedure outlined above, 55.3 mg of aminoCP **2.66** (283 μmol) were dissolved in 2.8 mL dry MeCN along with 6.3 mg of $[\text{Ir}(\text{dF}[\text{CF}_3]\text{ppy})_2(\text{dtbbpy})](\text{PF}_6)$ (5.6 μmol) prior to irradiation. No product observed. Starting material was recovered via flash chromatography over silica (4 to 28% ethyl acetate:hexanes, increasing in 4% increments; loaded crude residue with PhMe). Recovered 42.5 mg of the starting material (78% recovery); GCMS data was of insufficient quality to report.

LiBF₄

Following the general procedure outlined above, 53.7 mg of aminoCP **2.66** (275 μmol) were dissolved in 2.8 mL dry MeCN along with 6.2 mg of $[\text{Ir}(\text{dF}[\text{CF}_3]\text{ppy})_2(\text{dtbbpy})](\text{PF}_6)$ (5.5 μmol) and 5.2 mg of LiBF_4 (55 μmol) prior to irradiation. No product observed. Starting material not isolated. GCMS revealed 35% conversion.



Homocrotyl aminoCP **2.65** (2.8:1 mix of olefin isomers, 453 mg, 2.32 mmol) was dissolved in 23 mL ether under an inert atmosphere followed by addition of 4.6 mL water. While stirring vigorously at room temp, OsO₄ (0.2 M in PhMe, 580 μL, 116 μmol) was added in one portion. After 5 min at room temp, the brown biphasic mixture was cooled to 0 °C. Sodium bicarbonate (290 mg, 3.48 mmol) was added in one portion, before adding sodium periodate (1.49 g, 6.96 mmol) in six equal portions over a 5 min span. The mixture was now cloudy white with a faint brown hue. The cold bath was removed, and the mixture was stirred vigorously for 5 hrs at room temp. Salts aggregated over time, reducing the mixing efficiency, likely inhibiting transfer of material between phases. Solids were removed via filtration, rinsing with 25 mL ether. Reaction was then diluted with 25 mL sat. Na₂S₂O₃, adding ~500 μL 50% NaOH to get pH to ~14. Phases were separated, and the aqueous phase was extracted with 25 mL portions of ether three times. Combined organics were washed with 25 mL brine, dried over anhydrous sodium sulfate, filtered to remove solids, and carefully concentrated *in vacuo*. Obtained 429 mg of an orange liquid. Crude ¹H NMR revealed the desired product as a mixture in toluene (~55 wt%) with only minor byproducts present (impurity peaks suggest some diol remains). This mixture correlates to ~300 mg of aldehyde, which was moved forward without purification.

¹H NMR (CDCl₃, 500 MHz): δ = 9.77 (t, 1H, *J* = 2.0 Hz, CHO), 3.63-3.58 (m, 4H, morph.), 2.53-2.49 (m, 4H, morph.), 2.44 (dt, 2H, *J* = 7.1, 2.0 Hz, C3), 1.82 (t, 2H, *J* = 7.2 Hz, C2), 0.70-0.67 (m, 2H, CP), 0.38-0.35 (m, 2H, CP) ppm

$R_f = 0.15$ (40% EtOAc in hexanes), one yellow spot, KMnO_4

In a dry flask under inert atmosphere, trimethyl phosphonoacetate (660 μL , 4.09 mmol) was dissolved in 20 mL dry THF then cooled to 0 °C. NaHMDS (2.0 M in THF, 2.25 mL, 4.50 mmol) was added dropwise via syringe over 1 min. White precipitate quickly forms, necessitating vigorous stirring. Stirred 1 hr at 0 °C. In a separate flask under inert atmosphere, the crude aldehyde (~150 mg [half of mixture detailed above], 0.82 mmol) was dissolved in 3 mL dry THF. This solution was then transferred into the ylid suspension via syringe, at which point the mixture clarifies to some extent and stirs more readily. Transfer was quantified with two washes, each of 1 mL dry THF. The reaction was stirred 1.5 hrs at 0 °C then 30 min at room temp. The reaction was quenched by pouring into 20 mL 1:1 sat. NaHCO_3 :water containing ~500 μL 50% NaOH (resultant aqueous phase pH ~14). The reaction was diluted with 20 mL ether, and the phases were separated. Aqueous phase was extracted with 20 mL portions of ether three times. The combined organics were washed with 20 mL brine, dried over anhydrous magnesium sulfate, filtered to remove solids, and concentrated *in vacuo*. The crude residue was purified by flash chromatography over silica (5 to 30% ethyl acetate:hexanes, increasing in 5% increments; loaded residue with PhMe). Collected 67.2 mg from center fractions and 48.1 mg of edge fractions. Both portions were mostly pure by ^1H NMR, with the only visible impurity being a minor amount of the *Z*-enoate ester. The middle fractions were exposed to another round of chromatography over silica (3 to 33% ethyl acetate:hexanes, increasing in 3% increments; residue was loaded with toluene). Obtained 36.7 mg of the *E*-enoate aminoCP **2.68** as a clear, colorless oil. When totaled with the fractions containing a minor amount (~5%) of the *Z*-enoate, the overall amount of product was 115 mg (~59% yield for olefination; 41.5% over 2 steps).

¹H NMR (CDCl₃, 700 MHz): δ = 6.95 (td, 1H, *J* = 15.7, 7.0 Hz, C4), 5.80 (d, 1H, *J* = 15.7 Hz, C7), 3.72 (s, 3H, CO₂Me), 3.63-3.57 (m, 4H, morph.), 2.64-2.59 (m, 4H, morph.), 2.22-2.17 (m, 2H, C3), 1.65 (*app.* t, 2H, *J* = 8.9 Hz, C2), 0.61-0.58 (m, 2H, CP), 0.42-0.39 (m, 2H, CP) ppm

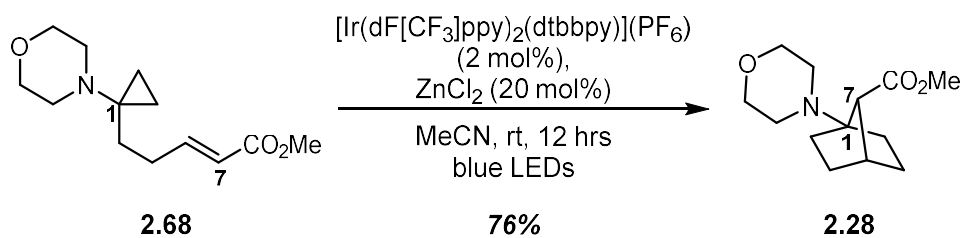
¹³C NMR (CDCl₃, 176 MHz): δ = 167.2, 149.5, 120.8, 67.8, 51.6, 49.8, 44.0, 30.2, 29.3, 12.6 ppm

IR (thin film): 2952, 2852, 1720, 1655, 1436, 1264, 1199, 1166, 1114, 1014, 984, 854 cm⁻¹

HRMS (ES⁺, *m/z*) calculated for C₁₃H₂₂NO₃⁺: 240.1594, Found: 240.1601

R_f (*E*-enoate) = 0.25 (30% EtOAc in hexanes), one yellow spot, KMnO₄, UV

R_f (*Z*-enoate) = 0.20 (30% EtOAc in hexanes), one yellow spot, KMnO₄, UV



In a dry vial under inert atmosphere, aminoCP **2.68** (35.2 mg, 147 μmol) was dissolved in 1.5 mL dry MeCN before adding $[\text{Ir}(\text{dF}[\text{CF}_3]\text{ppy})_2(\text{dtbbpy})](\text{PF}_6)$ (3.3 mg, 2.9 μmol) then ZnCl_2 (1.0 M in ether, 29 μL , 29 μmol) in one portion each. Reaction mixture was bright yellow. Reaction mixture was degassed with three freeze-pump-thaw cycles. The reaction was performed by stirring at room temp (as controlled with jacketed water bath, temp maintained between 18-23 $^\circ\text{C}$) while irradiating with two strips of 4.4 W blue LEDs for 12 hrs. Mixture appeared the same as it did prior to irradiation. A 25 μL aliquot was removed and diluted into 450 μL MeCN + 25 μL of a dodecane standard solution (5 mM in MeCN) both prior to degassing (total volume = MeCN volume) and after 12 hrs (5 mL total volume; reaction mixture diluted with ether in 5 mL vol. flask); these samples were run on the GCMS to measure starting material conversion. The diluted mixture was added to 10 mL 1:1 sat. NaHCO_3 :water containing 1 mL of 50% NaOH, then diluted further with 5 mL hexanes. Phases were separated, and the aqueous phase was extracted with 10 mL portions of 1:1 ether:hexanes three times. Combined organics were washed with 10 mL brine, dried over anhydrous MgSO_4 , filtered to remove solids, and concentrated *in vacuo*. The crude residue was purified via flash chromatography over silica (10 to 50% ethyl acetate:hexanes, increasing in 10% increments; residue loaded with PhMe).

- GCMS conversion: >99%
- Recovered starting material: none detected
- Product: 26.0 mg; slightly yellow oil; 75.5% yield

¹H NMR (CDCl₃, 500 MHz): δ = 3.71-3.62 (m, 4H, morph.), 3.66 (s, 3H, CO₂Me), 2.64-2.55 (m, 5H, morph., C7), 2.34 (tquart., 1H, *J* = 12.5, 3.9 Hz, C3-eq), 2.27 (t, 1H, *J* = 4.2 Hz, C4), 1.91 (tt, 1H, *J* = 12.0, 4.2 Hz, C2-eq), 1.81 (tt, 1H, *J* = 12.0, 4.2 Hz, C6-eq), 1.66 (tquart., 1H, *J* = 12.2, 3.7 Hz, C5-eq), 1.59 (td, 1H, *J* = 9.5, 3.7 Hz, C2-ax), 1.45-1.38 (m, 2H, C5-ax, C3-ax), 1.28-1.21 (m, 1H, C6-ax) ppm

¹³C NMR (CDCl₃, 126 MHz): δ = 173.1, 74.6, 67.6, 53.3, 51.3, 48.8, 38.9, 32.6, 30.1, 28.8, 25.0 ppm

IR (neat): 2951, 2870, 1732, 1450, 1434, 1375, 1327, 1278, 1202, 1178, 1153, 1116, 1069, 1036, 920, 896, 863 cm⁻¹

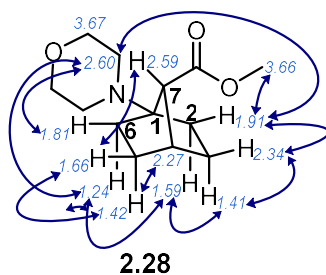
HRMS (ES⁺, *m/z*) calculated for C₁₃H₂₂NO₃⁺: 240.1594, Found: 240.1599

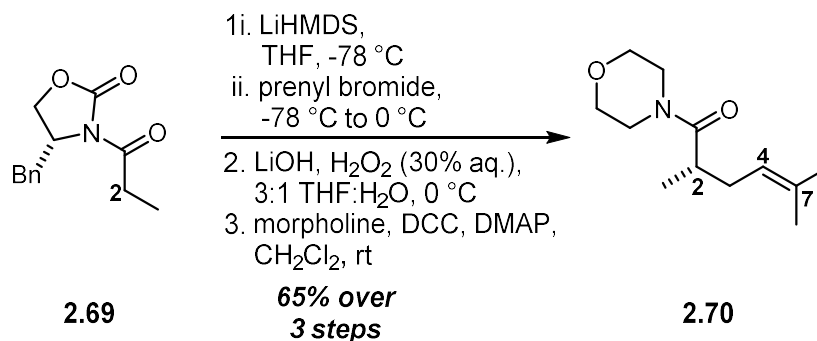
R_f = 0.15 (40% EtOAc in hexanes), one yellow spot, KMnO₄ + weak UV

2D NMR Data

- Structure determined via COSY, HSQC, and NOESY experiments; see key NOESY correlations

(blue arrows):





(4*R*)-Benzyl propanoyloxazolidinone **2.69** (204 mg, 0.875 mmol; purchased from Alfa Aesar) was dissolved in 2 mL dry THF in a dry flask under inert atmosphere before cooling to -78 °C. LiHMDS (1.0 M in THF, 920 μ L, 0.92 mmol) was added dropwise down the side of the vial via syringe over the course of 1 min. The reaction mixture was stirred at -78 °C for 1 hr. In a separate dry vial under N₂, prenyl bromide (152 μ L, 1.31 mmol) was dissolved in 1 mL dry THF. This solution was transferred into the enolate solution dropwise down the side of the vial over 2 min via syringe. The transfer was quantified with two 400 μ L washes with dry THF. The resultant reaction mixture was stirred at -78 °C for 1 hr followed by 30 min at 0 °C. The reaction was quenched by pouring into 10 mL sat. NaHCO₃, then diluted with 10 mL ethyl acetate. The phases were separated, and the aqueous phase was further extracted with 10 mL portions of ethyl acetate three times. The combined organics were washed with 10 mL brine, dried over anhydrous sodium sulfate, filtered to remove solids, and concentrated *in vacuo*. The resultant crude, colorless oil was moved on without further purification. ¹H NMR line-listings for this intermediate are provided below.

¹H NMR (CDCl₃, 500 MHz): δ = 7.35-7.31 (m, 2H, Ph), 7.30-7.27 (m, 1H, Ph), 7.23-7.20 (m, 2H, Ph), 5.17 (t, 1H, *J* = 7.6 Hz, C4), 4.72-4.65 (m, 1H, oxazolidinone-C4), 4.21-4.13 (m, 2H, benzyl-CH₂), 3.80 (quart., 1H, *J* = 6.9 Hz, C2), 3.24 (dd, 1H, *J* = 13.9, 2.9 Hz, oxazolidinone-C3), 2.71 (dd, 1H, *J* = 13.2, 10.0 Hz, oxazolidinone-C3), 2.44 (td, 1H, *J* = 14.4, 7.1 Hz, C3), 2.20 (td, 1H, *J*

= 13.9, 7.3 Hz, C3), 1.70 (s, 3H, C7-Me), 1.65 (s, 3H, C7-Me), 1.17 (d, 3H, $J = 6.8$ Hz, C2-Me) ppm

$R_f = 0.90$ (70% EtOAc in hexanes), one yellow spot, KMnO_4

Alkylated product from above (assumed 0.875 mmol) was dissolved in 12 mL THF before adding 4.0 mL HPLC-grade water; this mixture was cooled to 0 °C (ice/water) under inert atmosphere. H_2O_2 (30% in water, 715 μL , 7.0 mmol) was added dropwise over 15 sec, followed by bolus addition of LiOH (73 mg, 1.75 mmol). The reaction mixture was stirred at 0 °C for 3 hrs and then quenched by pouring into 10 mL of sat. $\text{Na}_2\text{S}_2\text{O}_3$. This mixture was diluted with 10 mL ethyl acetate and 10 mL 1 M HCl (resultant aq. phase pH ~ 2). Phases were separated, and the aqueous phase was further extracted with 10 mL portions of ethyl acetate three times. The combined organics were washed with 10 mL brine, dried over anhydrous sodium sulfate, filtered to remove solids, and concentrated *in vacuo*. The crude residue was purified by flash chromatography over silica (20 to 60% ethyl acetate:hexanes + 1% AcOH, 10% increments; residue was loaded with PhMe). The resultant oil was taken up in a few mL of PhMe and re-concentrated two times to remove residual AcOH. The clear, colorless oil was moved on without further purification. ^1H NMR line-listings for this intermediate are provided below.

^1H NMR (CDCl_3 , 500 MHz): $\delta = 11.08$ (br s, 1H, CO_2H), 2.48 (tq, 1H, $J = 7.1, 6.8$ Hz, C2), 2.37 (td, 1H, $J = 14.4, 6.6$ Hz, C3), 2.17 (td, 1H, $J = 14.4, 7.6$ Hz, C3), 1.71 (s, 3H, C7-Me), 1.62 (s, 3H, C7-Me), 1.17 (d, 3H, $J = 7.1$ Hz, C2-Me) ppm

$R_f = 0.60$ (60% EtOAc in hexanes), one yellow spot, KMnO_4

The acid generated above (assumed 875 μmol) was dissolved in dry CH_2Cl_2 in dry a flask under nitrogen. Morpholine (92 μL , 1.05 mmol), DMAP (160 mg, 1.31 mmol), and DCC (217 mg, 1.05 mmol) were added respectively, in one portion each. The reaction mixture was stirred 20 hrs at room temp before filtering through a plug of celite to remove some of the dicyclohexyl urea byproduct; 10 mL ether was used to fully elute product. The crude residue was purified via flash chromatography over silica (15 to 75% ethyl acetate:hexanes, increasing in 15% increments; crude residue loaded with PhMe). The desired morphamide **2.70** was obtained as a slightly yellow oil (120 mg, 64.9% over 3 steps).

$^1\text{H NMR}$ (CDCl_3 , 700 MHz): δ = 5.07 (t, 1H, J = 7.2 Hz, C4), 3.70-3.62 (m, 4H, morph.), 3.62-3.56 (m, 2H, morph.), 3.53-3.45 (m, 2H, morph.), 2.65 (*app.* sextet, 1H, J = 6.9 Hz, C2), 2.29 (dt, 1H, J = 14.2, 6.9 Hz, C3), 2.12 (dt, 1H, J = 14.6, 7.4 Hz, C3), 1.69 (s, 3H, C7-Me), 1.61 (s, 3H, C7-Me), 1.11 (d, 3H, J = 6.8 Hz, C2-Me) ppm

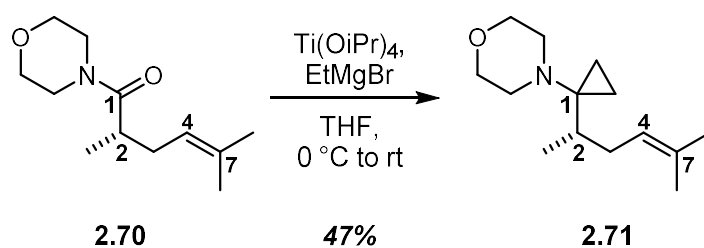
$^{13}\text{C NMR}$ (CDCl_3 , 176 MHz): δ = 175.2, 133.8, 121.8, 67.2, 67.0, 46.3, 42.2, 35.7, 32.8, 26.0, 18.0, 17.4 ppm

IR (thin film): 2965, 2917, 2854, 1639, 1430, 1376, 1265, 1224, 1114, 1068, 1028, 847 cm^{-1}

HRMS (ES^+ , m/z) calculated for $\text{C}_{12}\text{H}_{22}\text{NO}_2^+$: 212.1645, Found: 212.1647

$[\alpha]_{\text{D}}^{26.1^\circ\text{C}} = +12.6 \pm 0.1^\circ$ (c = 1.2, CH_2Cl_2)

R_f = 0.45 (60% EtOAc in hexanes), one yellow spot, KMnO_4



Morphamide **2.70** (115 mg, 544 μmol) was dissolved in 9 mL dry THF before adding titanium isopropoxide (177 μL , 0.60 mmol). The reaction mixture was cooled to 0 $^\circ\text{C}$. Ethylmagnesium bromide (1.0 M in THF, 1.9 mL, 1.9 mmol) was added dropwise via syringe over the course of 5 min. A vent line was added to account for gas evolution. The reaction mixture (clear, colorless at outset of addition) undergoes a series of color changes, first turning a bright yellow with initial drops, then transitioning to orange and red hues, and ultimately turning a dark red-brown (almost black) upon complete addition of EtMgBr. Vent line was removed, and the reaction mixture was stirred 1.5 hr while coming to room temp in cold bath (still slightly cold to touch at 1.5 hrs), at which point starting material had been consumed as revealed by TLC analysis. The reaction was quenched with 10 mL sat. Rochelle salt and stirred vigorously for 30 min at room temp. The mixture was diluted with 5 mL sat. Rochelle salt, 5 mL brine, and 10 mL ether. Phases were separated, then the aqueous phase was extracted with 10 mL portions of ether three times. The combined organics were then washed with 10 mL brine, dried over anhydrous sodium sulfate, filtered to remove solids, and concentrated *in vacuo*. The crude residue was purified via flash chromatography over silica (2.5 to 20% ethyl acetate:hexanes, increasing in 2.5% increments; residue was loaded with PhMe). Collected 46.2 mg of a clear, colorless oil from the center fractions and 11.0 mg of a slightly yellow oil from the edge fractions. Both residues were clean by $^1\text{H NMR}$, thus the total yield was 57.2 mg of the desired aminoCP **2.71** (47.1% yield).

$^1\text{H NMR}$ (CDCl_3 , 700 MHz): δ = 5.13 (t, 1H, J = 7.0 Hz, C4), 3.65-3.60 (m, 4H, morph.), 2.56-2.50 (m, 4H, morph.), 2.12-2.06 (m, 1H, C3), 1.89-1.81 (m, 1H, C3), 1.69 (s, 3H, C7-Me), 1.59

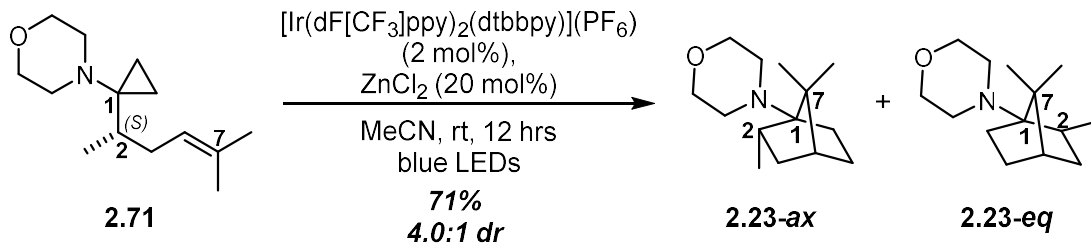
(s, 3H, C7-Me), 1.25-1.19 (m, 1H, C2), 0.87 (d, 3H, $J = 6.8$ Hz, C2-Me), 0.67-0.62 (m, 2H, CP),
0.44-0.33 (m, 2H, CP) ppm

^{13}C NMR (CDCl₃, 176 MHz): $\delta = 131.7, 124.1, 68.0, 51.2, 48.9, 39.4, 33.4, 26.0, 18.0, 17.9, 11.2,$
10.9 ppm

IR (thin film): 2957, 2850, 1450, 1374, 1266, 1118, 1014, 983, 855 cm⁻¹

HRMS (ES⁺, m/z) calculated for C₁₄H₂₆NO⁺: 224.2009, Found: 224.2012

$R_f = 0.45$ (20% EtOAc in hexanes), one yellow spot, KMnO₄



In a dry vial under nitrogen, aminoCP **2.71** (42.7 mg, 191 μmol) was dissolved in 2.0 mL dry MeCN before adding $[\text{Ir}(\text{dF}[\text{CF}_3]\text{ppy})_2(\text{dtbbpy})](\text{PF}_6)$ (4.3 mg, 3.8 μmol) then ZnCl_2 (1.0 M in ether, 38 μL , 38 μmol) in one portion each. Reaction mixture was bright yellow, but slightly cloudy from the Zn salt. Reaction mixture was degassed with three freeze-pump-thaw cycles. The reaction was performed by stirring at room temp (as controlled with jacketed water bath, temp maintained between 18-23 $^\circ\text{C}$) while irradiating with two strips of 4.4 W blue LEDs for 12 hrs. Mixture appeared somewhat cloudier than it did prior to irradiation and perhaps slightly darker yellow. A 25 μL aliquot was removed and diluted into 450 μL MeCN + 25 μL of a dodecane standard solution (5 mM in MeCN) both prior to degassing (total volume = MeCN volume) and after 12 hrs (5 mL total volume; reaction mixture diluted with ether in 5 mL vol. flask); these samples were run on the GCMS to measure starting material conversion. The diluted mixture was added to 10 mL 1:1 sat. NaHCO_3 :water containing 1 mL of 50% NaOH to ensure aq phase pH ~ 14 , then diluted further with 5 mL hexanes. Phases were separated, and the aqueous phase was extracted with 10 mL portions of 1:1 ether:hexanes three times. Combined organics were washed with 10 mL brine, dried over anhydrous magnesium sulfate, filtered to remove solids, and concentrated *in vacuo*. The crude residue was purified via flash chromatography over silica (4 to 20% ethyl acetate:hexanes, increasing in 4% increments; residue loaded with PhMe). Starting material and both products are entirely inseparable by any solvent system tested, and were thus collected together (33.7 mg; clear, colorless oil; 6.0:1.5:1 mix of ax-C2-Me:eq-C2-Me:recovered

starting material); characterization data was collected on the mixture but is presented separately for clarity.

- GCMS conversion: 94%

- Recovered starting material: 4.0 mg; clear, colorless oil; 9.5% recovery

- Product mixture: 29.7 mg; clear, colorless oil; 70.8% yield, 4.0:1 dr; 78.2% BORSM

IR (thin film): 2954, 2874, 1449, 1378, 1267, 1159, 1120, 1025, 900, 870 cm^{-1}

HRMS (ES+, m/z) calculated for $\text{C}_{14}\text{H}_{26}\text{NO}^+$: 224.2009, Found: 224.2013

$R_f = 0.45$ (20% EtOAc in hexanes), one yellow spot, KMnO_4

NMR Data for **2.23-ax**

^1H NMR (CDCl_3 , 700 MHz): $\delta = 3.64\text{-}3.59$ (m, 4H, morph.), 2.82 (dt, 2H, $J = 11.6, 4.3$ Hz, morph.), 2.73 (dt, 2H, $J = 11.6, 4.4$ Hz, morph.), 2.55-2.52 (m, 1H, C2), 2.07 (tdd, 1H, $J = 11.2, 4.8, 3.2$ Hz, C3-eq), 1.75-1.67 (m, 3H, C5-eq, C6-ax, C6-eq), 1.32 (*app.* t, 1H, $J = 4.6$ Hz, C4), 1.13-1.09 (m, 1H, C5-ax), 1.07 (s, 3H, C7-Me), 1.03 (d, 3H, $J = 6.8$ Hz, C3-Me), 1.00 (s, 3H, C7-Me), 0.70 (dd, 1H, $J = 12.3, 4.6$ Hz, C3-ax) ppm

^{13}C NMR (CDCl_3 , 176 MHz): $\delta = 71.2$ (C1), 68.6 (morph.), 49.7 (morph.), 48.9 (C7), 45.7 (C4), 37.7 (C3), 30.2 (C2), 27.6 (C5), 25.6 (C6), 22.1 (C7-Me), 21.0 (C7-Me), 17.3 (C2-Me) ppm

NMR Data for **2.23-eq**

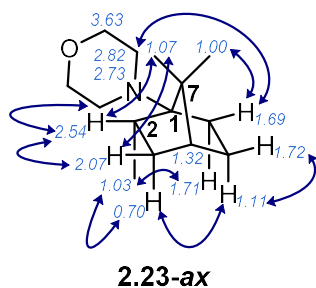
^1H NMR (CDCl_3 , 700 MHz): $\delta = 3.68$ (*app.* t, 4H, $J = 4.6$ Hz, morph.), 2.59-2.51 (m, 4H, morph.), 1.94-1.87 (m, 1H, C2), 1.89-1.86 (m, 1H, C6), 1.79-1.76 (m, 1H, C5), 1.60 (dd, 1H, $J = 12.6, 9.9$ Hz, C3-ax), 1.55-1.51 (m, 1H, C3-eq), 1.44 (*app.* t, 1H, C4), 1.20 (ddd, 1H, $J = 12.4, 9.7, 4.4$ Hz,

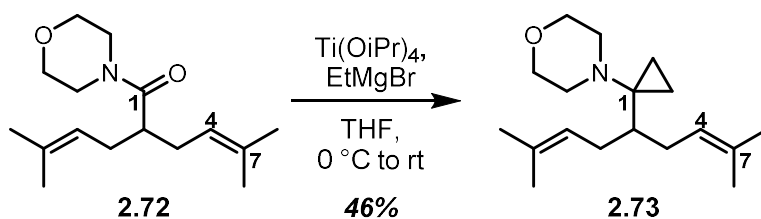
C5), 1.16-1.12 (m, 1H, C6), 1.07 (s, 3H, C7-Me), 1.06 (s, 3H, C7-Me), 1.05 (d, 3H, $J = 7.6$ Hz, C2-Me) ppm

^{13}C NMR (CDCl_3 , 176 MHz): $\delta = 71.4$ (C1), 67.8 (morph.), 48.8 (morph.), 47.4 (C4), 47.0 (C7), 40.8 (C2), 38.0 (C3), 26.9 (C6), 26.6 (C5), 25.2 (C7-Me), 20.9 (C2-Me), 20.0 (C7-Me) ppm

2D NMR Data

- COSY, HSQC, and NOESY experiments were employed to assign the various resonances to the two isomers and confirm the structure of the desired products. Key NOESY correlations (denoted by blue arrows) for the major isomer are provided below:





Bis-Prenylated amide **2.72** (byproduct obtained *en route* to aminoCP **2.14**; 357 mg, 1.35 mmol) was dissolved in 22 mL dry THF before adding titanium isopropoxide (440 μL , 1.48 mmol). The reaction mixture was cooled to 0 °C. Ethylmagnesium bromide (1.0 M in THF, 4.7 mL, 4.7 mmol) was added dropwise via syringe over the course of 5 min. A vent line was added to account for gas evolution. Reaction mixture (clear, colorless at outset of addition) undergoes a series of color changes, first turning a bright yellow with initial drops, then transitioning to orange and red hues, and ultimately turning a dark red-brown (almost black) upon complete addition of EtMgBr . Vent line was removed, and the reaction mixture was stirred 1.5 hrs while coming to room temp in cold bath (still slightly cold to touch at 1.5 hrs), at which point starting material had been consumed as revealed by TLC analysis. The reaction was quenched with 20 mL sat. Rochelle salt and stirred vigorously for 30 min at room temp. The mixture was further diluted with 10 mL sat. Rochelle salt, 10 mL brine, and 20 mL ether. Phases were separated, and the aqueous phase was extracted with 20 mL portions of ether three times. The combined organics were then washed with 100 mL brine, dried over anhydrous sodium sulfate, filtered to remove solids, and concentrated *in vacuo*. The crude residue was purified via flash chromatography over silica (3 to 15% ethyl acetate:hexanes, increasing in 5% increments; residue was loaded with PhMe). A slightly yellow oil was obtained, mostly pure by ^1H NMR. Two more rounds of chromatography still did not afford a sufficiently pure sample. Only one impurity remained (~10-20% of mix), suspected to be ethyl ketone byproduct. Material was exposed to NaBH_4 in methanol to attempt to reduce this impurity, though this had no effect on product distribution upon re-isolating material.

A final round of chromatography was employed (1 to 8% ethyl acetate:hexanes, increasing in 1% increments). Obtained 96.8 mg of material still mixed with a small percentage of impurity (barely above noise) along with 76.7 mg of a clear, colorless oil that was sufficiently pure for characterization of aminoCP **2.73**. Total amount isolated was thus 173 mg (46.4% yield).

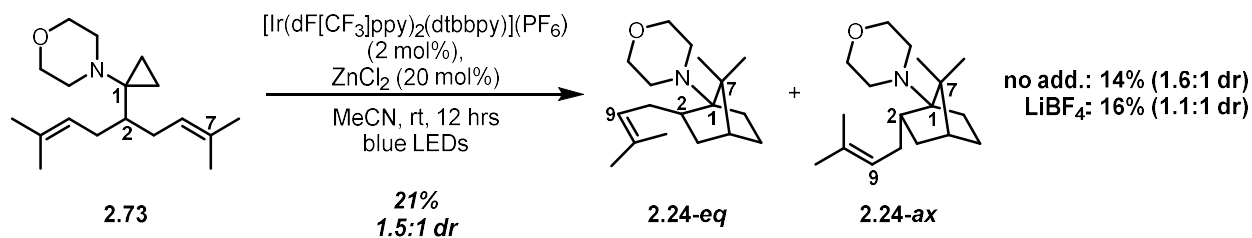
¹H NMR (CDCl₃, 700 MHz): δ = 5.18-5.14 (m, 2H, vinyl CH's), 3.66-3.60 (m, 4H, morph.), 2.52-2.46 (m, 4H, morph.), 2.04-1.93 (m, 4H, allyl CH₂'s), 1.68 (s, 6H, Me, Me), 1.58 (s, 6H, Me, Me), 1.15-1.07 (m, 1H, C2), 0.68-0.64 (m, 2H, CP), 0.42-0.37 (m, 2H, CP) ppm

¹³C NMR (CDCl₃, 176 MHz): δ = 131.5, 124.5, 68.0, 51.1, 47.4, 31.5, 26.0, 18.0, 11.2 ppm

IR (thin film): 2960, 2916, 2852, 1450, 1375, 1266, 1118, 1017, 983, 856 cm⁻¹

HRMS (ES⁺, *m/z*) calculated for C₁₈H₃₂NO⁺: 278.2478, Found: 278.2481

R_f = 0.55 (20% EtOAc in hexanes), one yellow spot, KMnO₄ or one blue-green spot, *p*-anisaldehyde



In a dry vial under nitrogen, aminoCP **2.73** (67.4 mg, 243 μmol) was dissolved in 2.5 mL dry MeCN before adding $[\text{Ir}(\text{dF}[\text{CF}_3]\text{ppy})_2(\text{dtbbpy})](\text{PF}_6)$ (5.5 mg, 4.9 μmol) then ZnCl_2 (1.0 M in ether, 49 μL , 49 μmol) in one portion each. Reaction mixture is bright yellow, but slightly cloudy from the Zn salt. Reaction mixture was degassed with three freeze-pump-thaw cycles. The reaction was performed by stirring at room temp (as controlled with jacketed water bath, temp maintained between 18-23 $^\circ\text{C}$) while irradiating with two strips of 4.4 W blue LEDs for 12 hrs. Mixture now has a grey precipitate; solution is still yellow. A 25 μL aliquot was removed and diluted into 450 μL MeCN + 25 μL of a dodecane standard solution (5 mM in MeCN) both prior to degassing (total volume = MeCN volume) and after 12 hrs (5 mL total volume; reaction mixture diluted with ether in 5 mL vol. flask); these samples were run on the GCMS to measure starting material conversion. The diluted mixture was added to 10 mL 1:1 sat. NaHCO_3 :water containing 1 mL of 50% NaOH to ensure aq phase pH \sim 14, then diluted further with 5 mL hexanes. Phases were separated, and the aqueous phase was extracted with 10 mL portions of 1:1 ether:hexanes three times. Combined organics were washed with 10 mL brine, dried over anhydrous magnesium sulfate, filtered to remove solids, and concentrated *in vacuo*. The crude residue was purified via flash chromatography over silica (1 to 2 to 3 to 4 to 6 to 8% ethyl acetate:hexanes; residue loaded with PhMe).

- GCMS conversion: 79%

- Recovered starting material: 20.0 mg; clear, colorless oil; ^1H NMR revealed predominantly starting material, but appears to be contaminated with some of the product isomers

- Product: 13.7 mg; clear, colorless oil; 20.6% yield, collected as a 1.5:1 mix of the eq:ax diastereomers (characterization data was collected on the mixture; NMR data below is listed separately for clarity)

IR (thin film): 2952, 1456, 1374, 1266, 1161, 1120, 1024, 896, 733 cm^{-1}

HRMS (ES⁺, *m/z*) calculated for C₁₈H₃₂NO⁺: 278.2478, Found: 278.2486

R_f = 0.25 (20% EtOAc in hexanes), one yellow spot, KMnO₄

NMR Data for **2.24-eq**

¹H NMR (CDCl₃, 700 MHz): δ = 5.00 (*app.* t, 1H, *J* = 7.6 Hz, C9), 3.68 (*app.* t, 4H, *J* = 4.8 Hz, morph.), 2.59-2.51 (m, 4H, morph.), 2.42 (br d, 1H, *J* = 14.0 Hz, C8), 1.97-1.92 (m, 1H, C8), 1.94-1.90 (m, 1H, C6-eq), 1.80-1.75 (m, 1H, C5-eq), 1.77-1.71 (m, 1H, C2), 1.68 (s, 3H, C10-Me), 1.61 (s, 3H, C10-Me), 1.57-1.53 (m, 1H, C3-eq), 1.53-1.49 (m, 1H, C3-ax), 1.45 (*app.* t, 1H, *J* = 4.3 Hz, C4), 1.21-1.15 (m, 1H, C5-ax), 1.19-1.13 (m, 1H, C6-ax), 1.08 (s, 3H, C7-Me), 1.07 (s, 3H, C7-Me) ppm

¹³C NMR (CDCl₃, 176 MHz): δ = 131.1 (C10), 125.0 (C9), 71.6 (C1), 67.8 (morph.), 48.8 (morph.), 47.4 (C4), 47.3 (C2), 46.8 (C7), 35.7 (C3), 32.5 (C8), 27.0 (C6), 26.6 (C5), 26.0 (C10-Me), 25.2 (C7-Me), 21.1 (C7-Me), 18.3 (C10-Me) ppm

NMR Data for **2.24-ax**

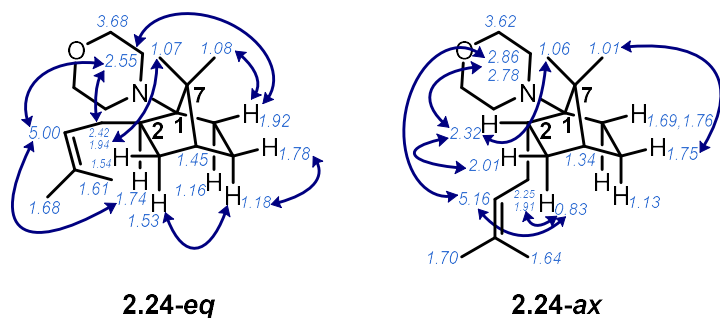
¹H NMR (CDCl₃, 700 MHz): δ = 5.16 (*app.* t, 1H, *J* = 6.8 Hz, C9), 3.62 (*app.* quint., 4H, *J* = 3.1 Hz, morph.), 2.86 (dt, 2H, *J* = 11.7, 4.5 Hz, morph.), 2.78 (dt, 2H, *J* = 11.7, 4.5 Hz, morph.), 2.34-2.29 (m, 1H, C2), 2.25 (dd, 1H, *J* = 13.2, 7.6 Hz, C8), 2.00 (ddt, 1H, *J* = 12.1, 4.6, 3.2 Hz, C3-eq), 1.93-1.88 (m, 1H, C8), 1.78-1.72 (m, 2H, C5-eq, C6), 1.70 (s, 3H, C10-Me), 1.72-1.67 (m, 1H,

C6), 1.64 (s, 3H, C10-Me), 1.34 (*app.* t, 1H, $J = 4.5$ Hz, C4), 1.16-1.10 (m, 1H, C5-ax), 1.06 (s, 3H, C7-Me), 1.01 (s, 3H, C7-Me), 0.83 (dd, 1H, $J = 12.5, 4.7$ Hz, C3-ax) ppm

^{13}C NMR (CDCl_3 , 176 MHz): $\delta = 131.3$ (C10), 124.2 (C9), 71.4 (C1), 68.7 (morph.), 49.7 (morph.), 49.5 (C7), 45.4 (C4), 37.1 (C2), 35.3 (C3), 30.8 (C8), 27.5 (C5), 26.0 (C6), 26.0 (C10-Me), 22.0 (C7-Me), 21.0 (C7-Me), 18.2 (C10-Me) ppm

2D NMR Data

- COSY, HSQC, HMBC, and NOESY experiments were employed to assign the various resonances to the two isomers and confirm the structure of the desired products. Key NOESY correlations (denoted by blue arrows) are provided for both 1-aminoNBs **2.24-eq** and **2.24-ax**.



Additional Trials with Varied Additives

No Additive

Following the general procedure outlined above, 80.5 mg of aminoCP **2.73** (290 μmol) were dissolved in 2.9 mL dry MeCN along with 6.5 mg of $[\text{Ir}(\text{dF}[\text{CF}_3]\text{ppy})_2(\text{dtbbpy})](\text{PF}_6)$ (5.8 μmol) prior to irradiation. Isolation provided the following:

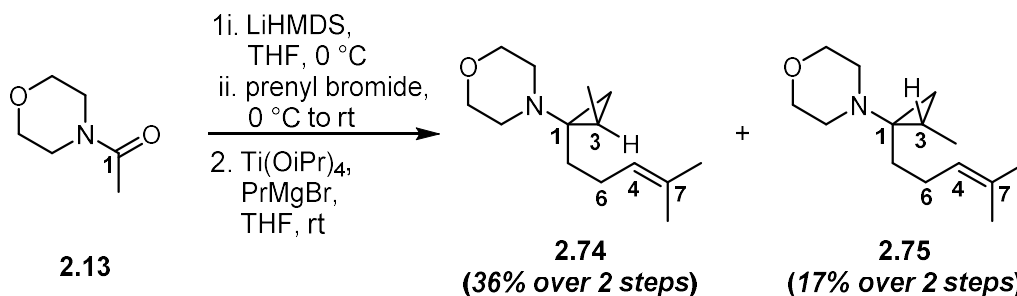
- GCMS conversion: *[data was of insufficient quality to include]*
- Recovered starting material: 35.0 mg; clear, colorless oil; 44.1% recovery

- Product: 11.2 mg; clear, colorless oil; 14.1% yield, 25.2% BORSM, collected as a 1.1:1 mix of the eq:ax diastereomers
- Byproduct: also collected 13 mg of a side product of this reaction, suspected to be a 1-morpholino-2-vinyl [5.1.0]bicyclooctane arising from *7-endo-trig* cyclization and a subsequent C-H abstraction.

LiBF₄

Following the general procedure outlined above, 79.3 mg of aminoCP **2.73** (286 μmol) were dissolved in 2.7 mL dry MeCN along with 6.8 mg of $[\text{Ir}(\text{dF}[\text{CF}_3]\text{ppy})_2(\text{dtbbpy})](\text{PF}_6)$ (61 μmol) and 5.8 mg of LiBF_4 (62 μmol) prior to irradiation. Isolation provided the following:

- GCMS conversion: 73%
- Recovered starting material: 25.0 mg; clear, colorless oil; 32.0% recovery
- Product: 12.5 mg; slightly yellow oil; 16.0% yield, 23.5% BORSM, collected as a 1.6:1 mix of the eq:ax diastereomers



N-Acetyl morpholine (**2.13**, 179 μ L, 1.55 mmol) was dissolved in 5 mL dry THF in a dry flask under N_2 , before cooling to 0 $^{\circ}$ C (ice/water). LiHMDS (1.0 M in THF, 1.6 mL, 1.6 mmol) was added dropwise down the side of the vial over 2 min, then the reaction mixture was allowed to stir at 0 $^{\circ}$ C for 1 hr. In a separate dry flask kept under inert atmosphere, prenyl bromide (240 μ L, 2.1 mmol) was dissolved in 2 mL dry THF. The enolate solution was then cannulated into the bromide solution slowly down the side of the vial over the course of 2 hrs. Transfer was quantified with two rinses of 1 mL dry THF. The mixture was stirred at room temp for 30 min before quenching with 20 mL 1:1 sat. $NaHCO_3$:sat. $Na_2S_2O_3$. Mixture was diluted with 20 mL ether, and the phases were separated. The aqueous phase was then extracted with 20 mL portions of ether three times. Combined organics were washed with 100 mL brine, dried over anhydrous magnesium sulfate, filtered to remove solids, and concentrated *in vacuo* to afford a slightly yellow oil. This crude residue was purified by flash chromatography over silica (20 to 60% ethyl acetate:hexanes, increasing in 10% increments; residue was loaded with PhMe). The desired mono-alkylated intermediate was collected as a clear, colorless oil (229 mg, 75.0% yield). 1H NMR line-listings for this product (same as was prepared en route to aminoCP **2.14**) are again provided below.

1H NMR ($CDCl_3$, 500 MHz): δ = 5.15-5.10 (m, 1H, C4), 3.68-3.64 (m, 4H, morph.), 3.64-3.60 (m, 2H, morph.), 3.46 (*app.* t, 2H, J = 4.6 Hz, morph.), 2.33 (*app.* d, 4H, J = 2.9 Hz, C2, C3), 1.69 (s, 3H, C7-Me), 1.63 (s, 3H, C7-Me) ppm

R_f = 0.20 (60% EtOAc in hexanes), one yellow spot, $KMnO_4$

The mono-prenylated amide from above (1.16 mmol) was dissolved in 23 mL dry THF under inert atmosphere, followed by addition of titanium isopropoxide (0.38 mL, 1.27 mmol). The reaction vessel was submerged in a water bath at ambient temp to serve as a heat sink. Propylmagnesium bromide (2.0 M in THF, 2.0 mL, 4.0 mmol) was added dropwise via syringe over the course of 4 min. A vent line was added to account for gas evolution (note: gas evolution can be quite vigorous along with substantial heat generation if addition is too rapid). Reaction mixture (clear, colorless at outset of addition) undergoes a series of color changes, first turning a bright yellow with initial drops, then transitioning to orange and red hues, and ultimately turning a dark red-brown (almost black) upon complete addition of PrMgBr. Vent line was removed, and the reaction mixture was stirred at room temp for 1 hr, at which point starting material had been consumed as revealed by TLC analysis. Reaction was quenched with 25 mL sat. Rochelle salt and stirred vigorously for 30 min. The mixture was then diluted with 20 mL sat. Rochelle salt, 20 mL brine, and 50 mL ether. Phases were separated. The aqueous phase was extracted with 50 mL portions of ether three times. The combined organics were then washed with 50 mL brine, dried over anhydrous sodium sulfate, filtered to remove solids, and concentrated *in vacuo*. Two major products were present based on crude TLC analysis. The crude residue was purified via flash chromatography over silica (1 to 2 to 3 to 4 to 6 to 8 to 10 to 20% ethyl acetate:hexanes; residue was loaded with PhMe). Both products were obtained cleanly as clear, colorless oils. The *syn*-aminoCP **2.74** eluted first (124 mg, 48.0%, 35.6% yield over two steps), followed by the *anti*-aminoCP **2.75** (59.0 mg, 22.9%, 17.0% yield over two steps).

Characterization Data for **2.74**

¹H NMR (CDCl₃, 700 MHz): δ = 5.04 (br s, 1H, C4), 3.65-3.57 (m, 4H, morph.), 2.74-2.62 (m, 4H, morph.), 1.96-1.87 (m, 2H, C6), 1.67 (s, 3H, C7-Me), 1.66-1.59 (m, 1H, C5), 1.59 (s, 3H, C7-Me), 1.40-1.32 (m, 1H, C5), 1.14 (d, 3H, J = 5.3 Hz, C3-Me), 0.80-0.74 (m, 1H, C3), 0.58-0.52 (m, 1H, C2-□), 0.08-0.02 (m, 1H, C2-□) ppm

¹³C NMR (CDCl₃, 176 MHz): δ = 131.3, 124.8, 68.0, 50.4, 47.3, 31.2, 26.2, 25.8, 20.2, 19.5, 17.8, 13.1 ppm

IR (thin film): 2912, 2850, 1450, 1374, 1264, 1205, 1116, 1028, 995, 857 cm⁻¹

HRMS (ES⁺, m/z) calculated for C₁₄H₂₆NO⁺: 224.2009, Found: 224.2012

R_f = 0.70 (20% EtOAc in hexanes), one yellow spot, KMnO₄

Characterization Data for **2.75**

¹H NMR (CDCl₃, 700 MHz): δ = 5.11 (t, 1H, J = 7.1 Hz, C4), 3.62-3.55 (m, 4H, morph.), 2.68-2.64 (m, 2H, morph.), 2.64-2.60 (m, 4H, morph.), 2.13-2.00 (m, 2H, C6), 1.68 (s, 3H, C7-Me), 1.61 (s, 3H, C7-Me), 1.55 (ddd, 1H, J = 14.3, 11.9, 5.5 Hz, C5), 1.38 (ddd, 1H, 14.8, 12.3, 5.5 Hz, C5), 1.04 (d, 3H, J = 6.5 Hz, C3-Me), 0.92-0.86 (m, 1H, C3), 0.66 (dd, 1H, J = 9.5, 4.3 Hz, C2-□), 0.00 (*app.* t, 1H, J = 5.2 Hz, C2-□) ppm

¹³C NMR (CDCl₃, 176 MHz): δ = 131.4, 124.9, 68.0, 49.9, 47.6, 27.6, 27.2, 25.8, 20.4, 20.1, 17.8, 14.7 ppm

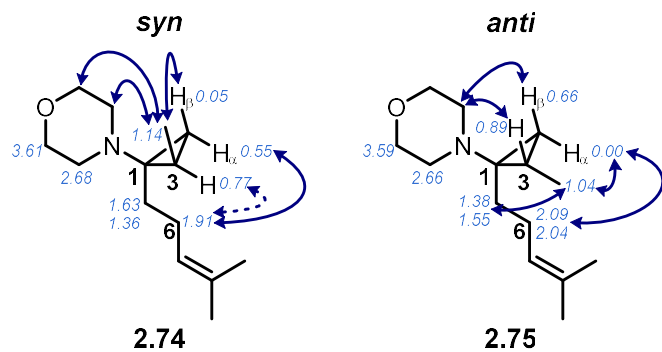
IR (thin film): 2927, 2852, 1450, 1374, 1264, 1116, 1069, 855 cm⁻¹

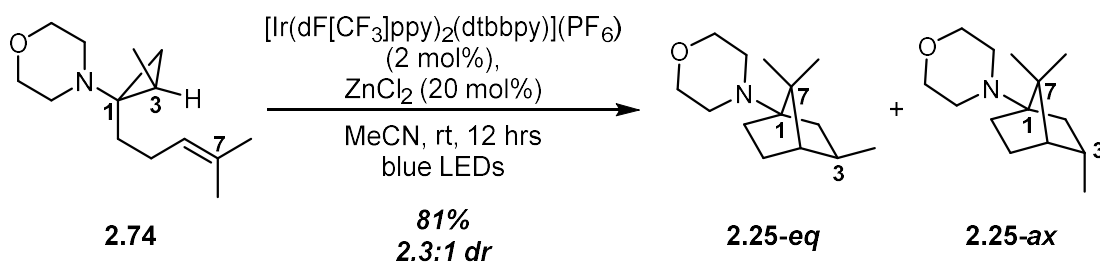
HRMS (ES⁺, m/z) calculated for C₁₄H₂₆NO⁺: 224.2009, Found: 224.2011

R_f = 0.40 (20% EtOAc in hexanes), one yellow spot, KMnO₄

2D NMR Data

- key NOESY correlations (denoted by blue arrows) used for the assignment of the two isomers are provided below





In a dry vial under nitrogen, aminoCP **2.74** (56.5 mg, 253 μmol) was dissolved in 2.6 mL dry MeCN before adding $[\text{Ir}(\text{dF}[\text{CF}_3]\text{ppy})_2(\text{dtbbpy})](\text{PF}_6)$ (5.7 mg, 5.1 μmol) then ZnCl_2 (1.0 M in ether, 51 μL , 51 μmol) in one portion each. Reaction mixture is bright yellow, but slightly cloudy from the Zn salt. Reaction mixture was degassed with three freeze-pump-thaw cycles. The reaction was performed by stirring at room temp (as controlled with jacketed water bath, temp maintained between 18-23 $^\circ\text{C}$) while irradiating with two strips of 4.4 W blue LEDs for 12 hrs. Mixture appears somewhat cloudier than it did prior to irradiation and perhaps slightly darker yellow. A 25 μL aliquot was removed and diluted into 450 μL MeCN + 25 μL of a dodecane standard solution (5 mM in MeCN) both prior to degassing (total volume = MeCN volume) and after 12 hrs (5 mL total volume; reaction mixture diluted with ether in 5 mL vol. flask); these samples were run on the GCMS to measure starting material conversion. The diluted mixture was added to 10 mL 1:1 sat. NaHCO_3 :water containing 1 mL of 50% NaOH to ensure aq phase pH \sim 14, then diluted further with 5 mL hexanes. Phases were separated, and the aqueous phase was extracted with 10 mL portions of 1:1 ether:hexanes three times. Combined organics were washed with 10 mL brine, dried over anhydrous magnesium sulfate, filtered to remove solids, and concentrated *in vacuo*. The crude residue was purified via flash chromatography over silica (3 to 21% ethyl acetate:hexanes, increasing in 3% increments; residue loaded with PhMe).

- GCMS conversion: >99%

- Recovered starting material: none detected

- Product: 44.8 mg; clear, colorless oil; 80.5% yield, product obtained as a 2.3:1 mixture of eq:ax diastereomers (characterization data was collected on the mixture; NMR data below is listed separately for clarity)

IR (thin film): 2951, 2875, 1449, 1386, 1317, 1273, 1150, 1120, 1029, 881 cm^{-1}

HRMS (ES⁺, *m/z*) calculated for C₁₄H₂₆NO⁺: 224.2009, Found: 224.2013

R_f = 0.15 (20% EtOAc in hexanes), one yellow spot, KMnO₄

NMR Data for **2.25-eq**

¹H NMR (CDCl₃, 700 MHz): δ = 3.69-3.65 (m, 4H, morph.), 2.61-2.54 (m, 4H, morph.), 1.79-1.75 (m, 2H, C5-eq, C6-eq), 1.74 (*app.* t, 1H, *J* = 11.2 Hz, C2-ax), 1.65 (*app.* sextet, 1H, *J* = 7.8 Hz, C3-ax), 1.59-1.55 (m, 1H, C2-eq), 1.42-1.36 (m, 1H, C6-ax), 1.20 (s, 1H, C4), 1.15 (*app.* t, 1H, *J* = 11.2 Hz, C5-ax), 1.13 (s, 3H, C7-Me), 1.09 (d, 3H, *J* = 7.5 Hz, C3-Me), 1.00 (s, 3H, C7-Me) ppm

¹³C NMR (CDCl₃, 176 MHz): δ = 71.2 (C1), 67.8 (morph.), 52.8 (C4), 49.0 (morph.), 47.2 (C7), 38.1 (C2), 36.2 (C3), 29.3 (C5), 28.5 (C6), 23.6 (C7-Me), 23.5 (C7-Me), 22.2 (C3-Me) ppm

NMR Data for **2.25-ax**

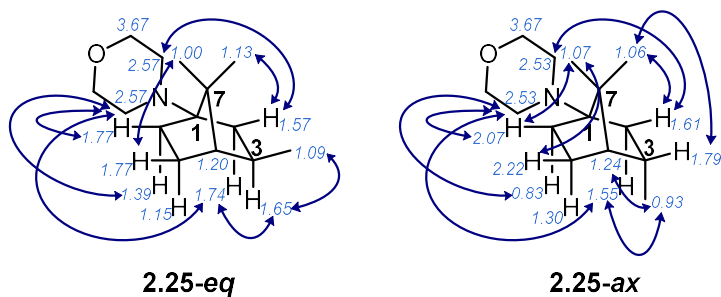
¹H NMR (CDCl₃, 700 MHz): δ = 3.69-3.65 (m, 4H, morph.), 2.55-2.50 (m, 4H, morph.), 2.25-2.19 (m, 1H, C5-eq), 2.07 (dt, 1H, *J* = 11.8, 3.8 Hz, C6-eq), 1.81-1.78 (m, 1H, C3-eq), 1.62-1.59 (m, 1H, C2-eq), 1.56-1.53 (m, 1H, C2-ax), 1.33-1.28 (m, 1H, C5-ax), 1.24 (br s, 1H, C4), 1.07 (s, 3H, C7-Me), 1.06 (s, 3H, C7-Me), 0.93 (d, 3H, *J* = 7.0 Hz, C3-Me), 0.83 (dd, 1H, *J* = 12.1, 4.6 Hz, C6-ax) ppm

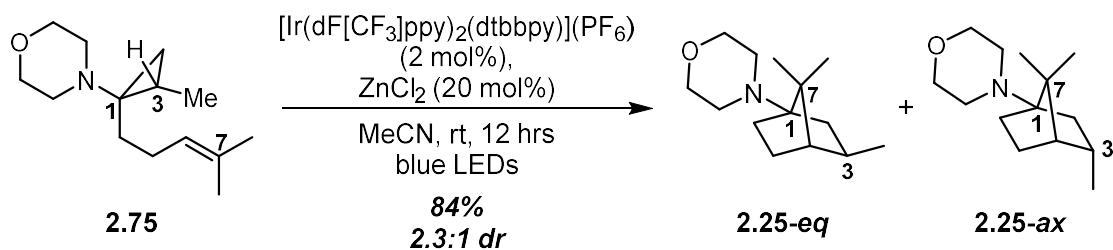
¹³C NMR (CDCl₃, 176 MHz): δ = 70.8 (C1), 67.8 (morph.), 51.8 (C4), 48.8 (morph.), 48.7 (C7),

38.3 (C6), 29.8 (C5), 29.7 (C3), 22.1 (C7-Me), 21.6 (C7-Me), 19.5 (C2), 18.3 (C3-Me) ppm

2D NMR Data

- COSY, HSQC, and NOESY experiments were employed to assign the various resonances to the two isomers and confirm the structure of the desired products. Key NOESY correlations (denoted by blue arrows) are provided for both 1-aminoNBs **2h-*eq*** and **2h-*ax***.



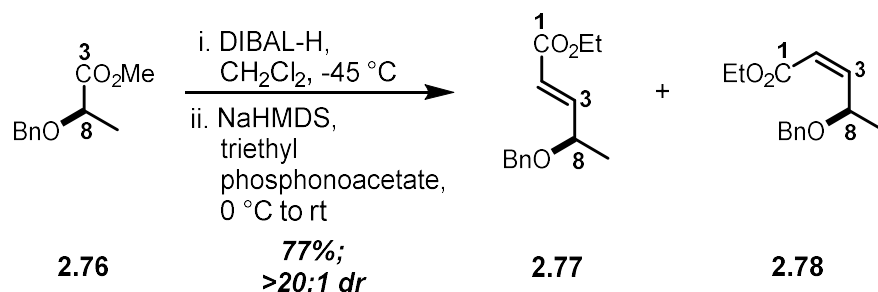


In a dry vial under nitrogen, aminoCP **2.75** (56.7 mg, 254 μmol) was dissolved in 2.6 mL dry MeCN before adding $[\text{Ir}(\text{dF}[\text{CF}_3]\text{ppy})_2(\text{dtbbpy})](\text{PF}_6)$ (5.7 mg, 5.1 μmol) then ZnCl_2 (1.0 M in ether, 51 μL , 51 μmol) in one portion each. Reaction mixture is bright yellow, but slightly cloudy from the Zn salt. Reaction mixture was degassed with three freeze-pump-thaw cycles. The reaction was performed by stirring at room temp (as controlled with jacketed water bath, temp maintained between 18-23 $^\circ\text{C}$) while irradiating with two strips of 4.4 W blue LEDs for 12 hrs. Mixture appears somewhat cloudier than it did prior to irradiation and perhaps slightly darker yellow. A 25 μL aliquot was removed and diluted into 450 μL MeCN + 25 μL of a dodecane standard solution (5 mM in MeCN) both prior to degassing (total volume = MeCN volume) and after 12 hrs (5 mL total volume; reaction mixture diluted with ether in 5 mL vol. flask); these samples were run on the GCMS to measure starting material conversion. The diluted mixture was added to 10 mL 1:1 sat. NaHCO_3 :water containing 1 mL of 50% NaOH to ensure aq phase pH \sim 14, then diluted further with 5 mL hexanes. Phases were separated, and the aqueous phase was extracted with 10 mL portions of 1:1 ether:hexanes three times. Combined organics were washed with 10 mL brine, dried over anhydrous magnesium sulfate, filtered to remove solids, and concentrated *in vacuo*. The crude residue was purified via flash chromatography over silica (3 to 21% ethyl acetate:hexanes, increasing in 3% increments; residue loaded with PhMe).

- GCMS conversion: >99%

- Recovered starting material: none detected

- Product: 46.8 mg; clear, colorless oil; 83.8% yield, product obtained as an 2.3:1 mixture of eq:ax diastereomers



Benzyl-protected methyl (*R*)-lactate⁷⁰ (**2.76**; 2.00 g, 10.3 mmol) was dissolved in 25 mL dry CH_2Cl_2 in a dry flask under nitrogen, then cooled to $-45\text{ }^\circ\text{C}$ (MeCN/ CO_2). DIBAL (1.0 M in hexanes, 10.8 mL, 10.8 mmol) was added dropwise down the side of the flask over 5 min via syringe. The mixture was stirred at $-45\text{ }^\circ\text{C}$ for 3.5 hrs. In a separate dry flask under inert atmosphere, triethyl phosphonoacetate (2.6 mL, 12.9 mmol) was dissolved in 50 mL dry THF then cooled to $0\text{ }^\circ\text{C}$. NaHMDS (2.0 M in THF, 6.4 mL, 12.9 mmol) was added dropwise down the side of the flask over 4 min, followed by 1 hr of stirring at $0\text{ }^\circ\text{C}$. The reduced starting material (still at $-45\text{ }^\circ\text{C}$) was cannulated into this ylid solution over the course of 12 min; transfer was quantified with two 2 mL rinses with dry THF. The reaction mixture was stirred for an additional 12 hrs while slowly coming to room temp. The mixture was then quenched with 100 mL of 1:1 sat. Rochelle salt:1 M NaOH; the resultant biphasic mixture was stirred vigorously for 10 min. The mixture was diluted with 200 mL ether then another 100 mL of the same aqueous quenching solution. The phases were separated, and the aqueous phase was extracted with 200 mL ether three times. The combined organics were washed with 200 mL brine, dried over anhydrous magnesium sulfate, filtered to remove solids, and concentrated *in vacuo*. The crude residue was purified by flash chromatography over silica (2.5 to 12.5% ethyl acetate:hexanes, increasing in 2.5% increments; residue loaded with PhMe). Obtained 1.86 g of a clear, colorless liquid; this material was revealed to be pure *E*-isomer **S11** by ^1H NMR (77.1% yield; >20:1 dr). Of note, additional

trials of this reaction did afford both the *E* and *Z* product isomers, which were separable by column chromatography, thus characterization data is provided for both isomers.

Characterization Data for **2.77**

¹H NMR (CDCl₃, 700 MHz): δ = 7.36-7.32 (m, 4H, Ph), 7.30-7.27 (m, 1H, Ph), 6.89 (dd, 1H, *J* = 16.2, 6.3 Hz, C3), 6.02 (d, 1H, *J* = 16.0 Hz, C2), 4.57 (d, 1H, *J* = 12.1 Hz, Bn), 4.44 (d, 1H, *J* = 12.1 Hz, Bn), 4.22 (quart., 2H, *J* = 7.2 Hz, CO₂Et), 4.12 (*app.* quint., 1H, *J* = 6.6 Hz, C8), 1.33 (d, 3H, *J* = 6.5 Hz, C8-Me), 1.31 (t, 3H, *J* = 7.3 Hz, CO₂Et) ppm

¹³C NMR (CDCl₃, 176 MHz): δ = 166.5, 149.4, 138.3, 128.6, 127.8, 127.8, 121.5, 74.0, 70.9, 60.6, 20.8, 14.4 ppm

IR (neat): 1716, 1659, 1453, 1368, 1296, 1265, 1179, 1028, 980, 865, 734, 696 cm⁻¹

HRMS (ES⁺, *m/z*) calculated for C₁₄H₁₉O₃⁺: 235.1329, Found: 235.1326

[α]_D^{26.8°C} = +2.2 ± 0.2° (*c* = 0.2, CH₂Cl₂)

R_f = 0.60 (20% EtOAc in hexanes), one dark blue spot, *p*-anisaldehyde + UV

Characterization Data for **2.78**

¹H NMR (CDCl₃, 700 MHz): δ = 7.35-7.31 (m, 4H, Ph), 7.29-7.25 (m, 1H, Ph), 6.23 (dd, 1H, *J* = 11.6, 8.5 Hz, C3), 5.85 (d, 1H, *J* = 11.8 Hz, C2), 5.16 (*app.* quint., 1H, *J* = 6.9 Hz, C8), 4.52 (d, 1H, *J* = 12.1 Hz, Bn), 4.44 (d, 1H, *J* = 12.1 Hz, Bn), 4.17 (quart., 2H, *J* = 7.0 Hz, CO₂Et), 1.33 (d, 3H, *J* = 6.5 Hz, C8-Me), 1.28 (t, 3H, *J* = 7.2 Hz, CO₂Et) ppm

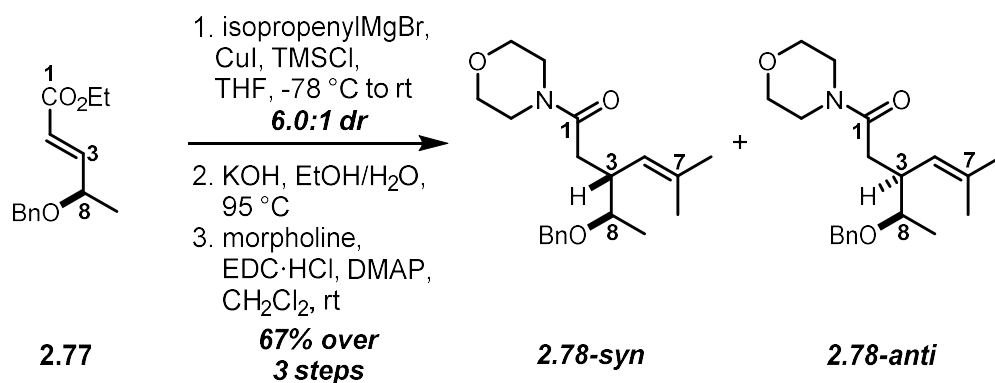
¹³C NMR (CDCl₃, 176 MHz): δ = 166.0, 152.4, 138.6, 128.5, 127.9, 127.7, 120.5, 71.7, 71.2, 60.4, 20.6, 14.3 ppm

IR (neat): 1716, 1652, 1386, 1188, 1073, 1027, 823, 734, 696 cm⁻¹

HRMS (ES⁺, *m/z*) calculated for C₁₄H₁₉O₃⁺: 235.1329, Found: 235.1326

$[\alpha]_{\text{D}}^{26.8^{\circ}\text{C}} = -4.5 \pm 0.3^{\circ}$ (*c* = 0.3, CH₂Cl₂)

R_f = 0.50 (20% EtOAc in hexanes), one dark blue spot, *p*-anisaldehyde + UV



Anhydrous CuI (1.02 g, 5.33 mmol) was loaded into a dry flask under Ar; this flask was evacuated and purged three times with nitrogen. The salt was then suspended in 35 mL dry THF before cooling to -78 °C. Isopropenylmagnesium bromide (0.5 M in THF, 21.3 mL, 10.7 mmol; purchased from Acros) was added dropwise via syringe over 5 min. This mixture was stirred 45 min at -78 °C, resulting in a cloudy suspension with a faint orange-yellow color. TMSCl (0.81 mL, 6.4 mmol) was added in one portion via syringe. In a separate dry vial, the enoate ester **S11** (999 mg, 4.26 mmol) was dissolved in 5 mL dry THF, then transferred into the cuprate suspension solution via syringe down the side of the vial over 5 min; the transfer was quantified with three 1 mL with dry THF. The reaction mixture was stirred while coming to room temp for 4.5 hrs. At the 2.5 hr mark, the bath temperature was approximately -20 °C, at which point the reaction mixture darkened, then transitioned to red and ultimately dark green (about 10 min elapsed for full color change). At the 3 hr mark, the cold bath was exchanged for an ice bath. The suspension had only darkened slightly after 3 hrs, but quickly transitioned to red and then a dark green upon removing the cold bath. The reaction was quenched with 100 mL of a 1:1 sat Rochelle salt:2 M NaOH mix. This biphasic mixture was stirred vigorously for 15 min at room temp, then diluted with an additional 50 mL of the same aqueous mix and 150 mL ether. The phases were separated, and the aqueous phase was extracted with three 150 mL portions of ether. The combined organics were washed with 100 mL brine, then dried over anhydrous magnesium sulfate, filtered to remove

solids, and concentrated under vacuum. The crude residue was purified by flash chromatography over silica (2 to 10% ethyl acetate:hexanes, increasing in 2% increments; residue loaded with PhMe). Obtained 888 mg of a clear, colorless oil that proved to be a 6.0:1 ratio of product isomers (71.7% combined yield). Based on subsequent manipulations, it was determined that the *syn* isomer is favored. The products proved to be inseparable and were thus moved forward as the mixture.

The ethyl ester (still 6.0:1 *syn:anti*; 886 mg, 3.05 mmol) was dissolved in 6.0 mL 200 proof EtOH under Ar. In separate flask, KOH (1.59 g, 30.5 mmol) was dissolved in 24 mL HPLC-grade water, then poured into the ethanolic solution slowly (swirling to mix) over the course of 1 min. A reflux condenser was attached, and the system was flushed with Ar before heating to 95 °C for 4 hrs. After cooling back to room temp., the reaction mixture was quenched by pouring slowly into 50 mL 1 M HCl. The mixture was diluted with 50 mL CH₂Cl₂, and the phases were separated. The aqueous phase pH was determined to be between 1 and 2. The aqueous phase was further extracted with three portions of CH₂Cl₂, each totaling 50 mL. The combined organic phases were dried over anhydrous magnesium sulfate, filtered to remove solids, and concentrated *in vacuo*, affording 804 mg of a viscous, clear, colorless oil. ¹H NMR of the crude residue revealed clean conversion to the carboxylic acids, still a 6.0:1 mixture of diastereomers ($R_f = 0.45$ [70% EtOAc in hexanes], one bright blue spot, *p*-anisaldehyde + UV). This material was moved on without further purification.

The crude carboxylic acid from above (assumed 3.05 mmol) was dissolved in 15 mL dry CH₂Cl₂ in a dry flask under nitrogenous atmosphere. DMAP (560 mg, 4.57 mmol), morpholine (400 μL, 4.57 mmol), and EDC·HCl (0.88 g, 4.57 mmol) were each added in one portion each, respectively. This mixture was stirred at room temp for 12 hrs, then quenched by pouring into 50 mL 1 M HCl. The mixture was diluted with 50 mL CH₂Cl₂, and the phases were separated. The

aqueous phase was further extracted with three 50 mL portions of CH₂Cl₂. The combined organic phases were washed with 50 mL brine, dried over anhydrous magnesium sulfate, filtered to remove solids, and concentrated *in vacuo*. The crude residue was purified by flash chromatography over silica (20 to 30 to 45 to 60 to 75% ethyl acetate:hexanes; residue was loaded with PhMe). This afforded the desired C1-morphamides (still a 6:1 mix of *syn*-**2.78** to *anti*-**2.78**) as a slightly yellow oil (950 mg; 94.0% over final two steps, 67.4% over three steps). Characterization data was collected on a 4.0:1 mixture of products that was produced via the same protocol (starting from 5:1 mix of olefin isomers); NMR data below is listed separately for clarity.

IR (neat): 2967, 2919, 2857, 1636, 1426, 1374, 1271, 1214, 1114, 1068, 1027, 847, 755, 698 cm⁻¹

HRMS (ES⁺, *m/z*) calculated for C₂₀H₃₀NO₃⁺: 332.2220, Found: 332.2228

$[\alpha]_{\text{D}}^{26.9\text{ }^{\circ}\text{C}} = -9.1 \pm 0.3^{\circ}$ (*c* = 0.2, CH₂Cl₂)

R_f = 0.45 (70% EtOAc in hexanes), one bright blue spot, *p*-anisaldehyde + UV

NMR Data for **2.78-syn**

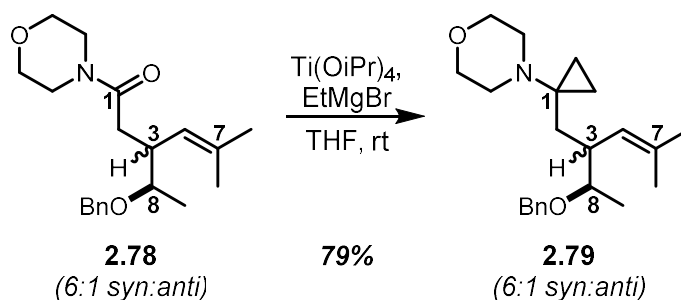
¹H NMR (CDCl₃, 500 MHz): δ = 7.36-7.30 (m, 4H, Ph), 7.30-7.26 (m, 1H, Ph), 4.98 (d, 1H, *J* = 10.0 Hz, C4), 4.62 (d, 1H, *J* = 11.5 Hz, benzyl CH₂), 4.40 (d, 1H, *J* = 11.5 Hz, benzyl CH₂), 3.65-3.55 (m, 5H, morph., C8), 3.54-3.47 (m, 2H, morph.), 3.46-3.37 (m, 2H, morph.), 2.93-2.85 (m, 1H, C3), 2.69 (dd, 1H, *J* = 14.2, 4.2 Hz, C2), 2.22 (dd, 1H, *J* = 14.2, 9.1 Hz, C2), 1.71 (s, 3H, C7-Me), 1.65 (s, 3H, C7-Me), 1.31 (d, 3H, *J* = 6.1 Hz, C8-Me) ppm

¹³C NMR (CDCl₃, 126 MHz): δ = 171.4, 139.0, 134.0, 128.5, 127.8, 127.6, 124.9, 78.2, 71.0, 67.1, 66.8, 46.5, 42.0, 42.0, 35.3, 26.2, 18.6, 17.4 ppm

NMR Data for **2.78-anti**

¹H NMR (CDCl₃, 500 MHz): δ = 7.36-7.30 (m, 4H, Ph), 7.30-7.26 (m, 1H, Ph), 5.08 (d, 1H, *J* = 10.5 Hz, C4), 4.60 (d, 1H, *J* = 11.5 Hz, benzyl CH₂), 4.40 (d, 1H, *J* = 11.5 Hz, benzyl CH₂), 3.65-3.55 (m, 5H, morph., C8), 3.46-3.37 (m, 4H, morph.), 3.06-3.00 (m, 1H, C3), 2.52 (dd, 1H, *J* = 14.6, 5.3 Hz, C2), 2.29 (dd, 1H, *J* = 14.4, 8.1 Hz, C2), 1.72 (s, 3H, C7-Me), 1.64 (s, 3H, C7-Me), 1.14 (d, 3H, *J* = 6.1 Hz, C8-Me) ppm

¹³C NMR (CDCl₃, 126 MHz): δ = 171.4, 139.0, 134.0, 128.5, 127.7, 127.6, 123.8, 77.1, 70.8, 67.1, 66.8, 46.4, 42.0, 40.3, 34.5, 62.2, 18.3, 16.8 ppm



The mixture of C3 morphamides (**2.78**, 6.0:1 mixture of *syn:anti*; 401 mg, 1.21 mmol) was dissolved in 24 mL dry THF under inert atmosphere, followed by addition of titanium isopropoxide (0.39 mL, 1.33 mmol). The reaction vessel was submerged in a water bath at ambient temp to serve as a heat sink. Ethylmagnesium bromide (1.0 M in THF; 4.2 mL, 4.2 mmol) was added dropwise via syringe over course of 10 min. A vent line was added to account for gas evolution (note: gas evolution can be quite vigorous along with substantial heat generation if addition is too rapid). Reaction mixture (clear, colorless at outset of addition) undergoes a series of color changes, first turning a bright yellow with initial drops, then transitioning to orange and red hues, and ultimately turning a dark red-brown (almost black) upon complete addition of EtMgBr. Vent line was removed, and the reaction mixture was stirred at room temp for 75 min. An aqueous solution of 3:1 sat. Rochelle's salt:1 M NaOH in brine was prepared. The reaction was quenched with 30 mL of this aqueous mixture, and stirred vigorously for 90 min. The mixture was then diluted with the remainder of the quenching solution and 50 mL ether. The phases were separated. The aqueous phase was extracted with 25 mL portions of ether three times. The combined organics were then washed with 25 mL brine, dried over anhydrous magnesium sulfate, filtered to remove solids, and concentrated under vacuum. The crude residue was purified via flash chromatography over silica (4 to 20% ethyl acetate:hexanes, increasing in 4% increments; the residue was loaded with PhMe). Collected aminoCP **2.79** as a clear, colorless liquid totaling 330 mg (79.4%) still as a 6.0:1 *syn:anti*

mixture. Characterization data was collected on a 4.0:1 mixture of products that was produced via the same protocol (starting from 4:1 mix of morphamide isomers); NMR data below is listed separately for clarity.

IR (neat): 2967, 2919, 2857, 1636, 1426, 1374, 1271, 1214, 1114, 1068, 1027, 847, 735, 698 cm^{-1}

1

HRMS (ES⁺, *m/z*) calculated for C₂₂H₃₄NO₂⁺: 344.2584, Found: 344.2593

$[\alpha]_{\text{D}}^{26.9\text{ }^{\circ}\text{C}} = -5.2 \pm 0.1^{\circ}$ (*c* = 0.8, CH₂Cl₂)

R_f = 0.25 (20% EtOAc in hexanes), one dark blue spot, *p*-anisaldehyde + UV

NMR Data for **2.79-syn**

¹H NMR (CDCl₃, 500 MHz): δ = 7.36-7.31 (m, 4H, Ph), 7.29-7.24 (m, 1H, Ph), 4.89 (d, 1H, *J* = 10.0 Hz, C4), 4.59 (d, 1H, *J* = 11.7 Hz, benzyl CH₂), 4.43 (d, 1H, *J* = 12.5 Hz, benzyl CH₂), 3.62-3.57 (m, 4H, morph.), 3.30 (*app.* quint., 1H, *J* = 6.3 Hz, C8), 2.61-2.49 (m, 5H, morph., C3), 2.13 (dd, 1H, *J* = 14.2, 2.9 Hz, C2), 1.70 (s, 3H, C7-Me), 1.64 (s, 3H, C7-Me), 1.12 (dd, 1H, *J* = 14.2, 9.5 Hz, C2), 1.11 (d, 1H, *J* = 6.4 Hz, C8-Me) ppm

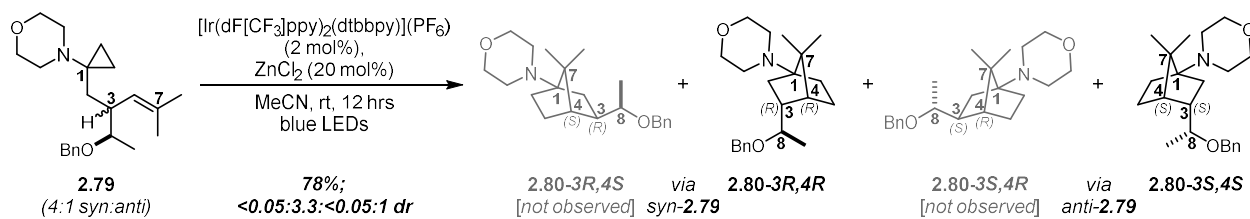
¹³C NMR (CDCl₃, 176 MHz): δ = 139.3, 132.1, 128.4, 127.7, 127.5, 79.0, 70.9, 67.9, 49.5, 43.2, 41.7, 33.1, 26.1, 18.8, 16.8, 11.9 ppm

NMR Data for **2.79-anti**

¹H NMR (CDCl₃, 500 MHz): δ = 7.36-7.31 (m, 4H, Ph), 7.29-7.24 (m, 1H, Ph), 4.97 (d, 1H, *J* = 9.5 Hz, C4), 4.57 (d, 1H, *J* = 11.7 Hz, benzyl CH₂), 4.48 (d, 1H, *J* = 11.7 Hz, benzyl CH₂), 3.62-3.57 (m, 4H, morph.), 3.49-3.44 (m, 1H, C8), 2.61-2.49 (m, 5H, morph., C3), 1.98 (dd, 1H, *J* =

14.2, 3.4 Hz, C2), 1.70 (s, 3H, C7-Me), 1.59 (s, 3H, C7-Me), 1.36 (dd, 1H, $J = 14.2, 9.5$ Hz, C2),
1.07 (d, 1H, $J = 6.4$ Hz, C8-Me) ppm

^{13}C NMR (CDCl_3 , 176 MHz): $\delta = 139.3, 132.1, 128.4, 78.1, 70.5, 67.9, 49.5, 43.2, 40.0, 31.7,$
26.1, 18.3, 16.4, 11.4 ppm



In dry vial under nitrogen, aminoCPs **2.79** (106 mg, 307 μmol ; 4:1 mix of *syn:anti* isomers) was dissolved in 3.1 mL dry MeCN before adding $[\text{Ir}(\text{dF}[\text{CF}_3]\text{ppy})_2(\text{dtbbpy})](\text{PF}_6)$ (6.9 mg, 6.2 μmol) then ZnCl_2 (1.0 M in ether, 62 μL , 62 μmol) in one portion each. Reaction mixture is bright yellow, but slightly cloudy from the Zn salt and what appears to be only modest solubility of the starting material. Reaction mixture was degassed with three freeze-pump-thaw cycles. The reaction was performed by stirring at room temp (as controlled with jacketed water bath, temp maintained between 18-23 $^\circ\text{C}$) while irradiating with two strips of 4.4 W blue LEDs for 12 hrs. Mixture still only slightly cloudy and has a darker yellow-green hue than pre-irradiation. The mixture was added to 10 mL 1:1 sat bicarb:water containing 500 μL of 50% NaOH to ensure aq phase pH \sim 14, then diluted further with 5 mL hexanes and 5 mL ether. Phases were separated, and the aqueous phase was extracted with 10 mL 1:1 ether:hexanes three times. Combined organics were washed with 10 mL brine, dried over anhydrous sodium sulfate, filtered to remove solids, and concentrated *in vacuo*. Three new spots were visible by TLC, with the product mixture ultimately proving to be the major spot. The crude residue was purified via flash chromatography (10 to 15 to 20 to 30 to 50 to 70 to 90% ethyl acetate:hexanes + 0.1% NEt_3 ; residue loaded with PhMe); the product mixture streaked through with starting material, thus a second round of chromatography was required (10 to 15 to 22.5 to 30 to 40 to 55 to 70% ethyl acetate:hexanes; loaded residue with PhMe), affording the following:

- Recovered starting material: 5.8 mg; yellow oil; ^1H NMR reveals a number of impurities

- Product: 83.1 mg; slightly yellow oil; ^1H NMR reveals 3.3:1 mixture of what proved to be the two C3-axial isomers of the four possible *anti* and *syn* products (no detectable C3-eq isomers); 78.4% combined yield (characterization data was collected on the mixture; NMR data below is listed separately for clarity)

IR (neat): 2957, 1451, 1372, 1315, 1272, 1118, 1094, 1028, 883, 733, 697 cm^{-1}

HRMS (ES⁺, *m/z*) calculated for $\text{C}_{22}\text{H}_{34}\text{NO}_2^+$: 344.2584, Found: 344.2590

$[\alpha]_{\text{D}}^{27.3\text{ }^\circ\text{C}} = -3.7 \pm 0.1^\circ$ ($c = 1.3$, CH_2Cl_2)

$R_f = 0.40$ (60% EtOAc in hexanes), one blue spot, Hanessian's stain

NMR Data for major isomer **2.80-3R,4R**:

^1H NMR (CDCl_3 , 700 MHz): $\delta = 7.36\text{-}7.31$ (m, 4H, Ph), 7.29-7.26 (m, 1H, Ph), 4.64 (d, 1H, $J = 11.9$ Hz, benzyl CH_2), 4.40 (d, 1H, $J = 11.9$ Hz, benzyl CH_2), 3.68-3.65 (m, 4H, morph.), 3.37-3.32 (m, 1H, C8), 2.55-2.51 (m, 4H, morph.), 2.14-2.05 (m, 2H, C2-eq, C3), 1.83-1.77 (m, 1H, C6-eq), 1.65-1.60 (m, 1H, C5-eq), 1.37 (t, 1H, $J = 4.1$ Hz, C4), 1.34-1.30 (m, 1H, C5-ax), 1.29-1.25 (m, 1H, C6-ax), 1.17 (dd, 1H, $J = 11.7, 4.0$ Hz, C2-ax), 1.12 (d, 3H, $J = 6.0$ Hz, C8-Me), 1.07 (s, 3H, C7-Me), 1.04 (s, 3H, C7-Me) ppm

^{13}C NMR (CDCl_3 , 176 MHz): $\delta = 139.1, 128.5, 128.0, 127.6, 79.5, 71.0, 70.2, 67.8, 48.8, 48.8, 48.3, 42.9, 35.4, 29.6, 21.7, 21.6, 20.3, 17.5$ ppm

NMR Data for minor isomer **2.80-3S,4S**:

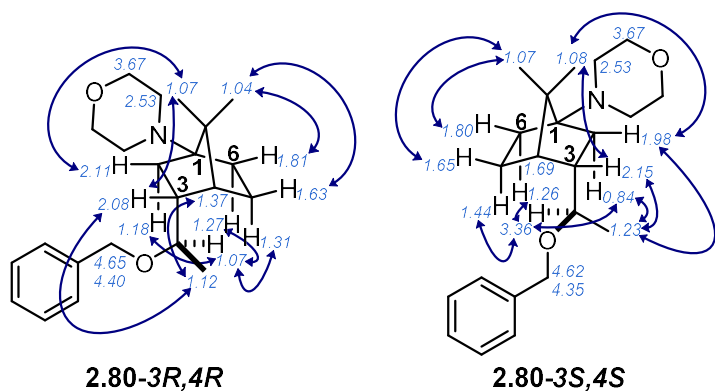
^1H NMR (CDCl_3 , 700 MHz): $\delta = 7.36\text{-}7.31$ (m, 4H, Ph), 7.29-7.26 (m, 1H, Ph), 4.62 (d, 1H, $J = 11.9$ Hz, benzyl CH_2), 4.35 (d, 1H, $J = 11.9$ Hz, benzyl CH_2), 3.68-3.65 (m, 4H, morph.), 3.38-3.33 (m, 1H, C8), 2.55-2.51 (m, 4H, morph.), 2.18-2.12 (m, 1H, C3), 1.98 (td, 1H, $J = 11.8, 4.1$

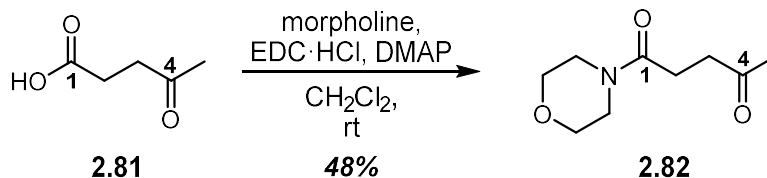
Hz, C2-eq), 1.83-1.77 (m, 1H, C6-eq), 1.69 (t, 1H, $J = 4.1$ Hz, C4), 1.67-1.64 (m, 1H, C5-eq), 1.46-1.41 (m, 1H, C5-ax), 1.28-1.24 (m, 1H, C6-ax), 1.22 (d, 3H, $J = 5.8$ Hz, C8-Me), 1.08 (s, 3H, C7-Me), 1.07 (s, 3H, C7-Me), 0.85 (dd, 1H, $J = 12.1, 5.5$ Hz, C2-ax) ppm

^{13}C NMR (CDCl_3 , 176 MHz): $\delta = 139.1, 128.4, 127.8, 127.6, 76.8, 71.0, 70.4, 67.8, 48.8, 48.4, 48.1, 43.3, 34.3, 29.8, 22.0, 21.5, 20.3, 18.3$ ppm

2D NMR Data

- COSY, HSQC, and NOESY experiments were employed to assign the various resonances to the two isomers and confirm the structure of the desired products. Key NOESY correlations (denoted by blue arrows) are provided for both 1-aminoNBs **2.80-3R,4R** and **2.80-3S,4S**. Of note, the COSY correlation between C4 and the C3-eq resonances is highly indicative of the axial configuration; the dihedral angles between C4 and the C3/C5-ax H's is close to orthogonality (making those correlations NMR silent), thus the presence of strong C4-C3 COSY correlations was central to the assignment. NOESY data provided clear support for this conclusion.





Levulinic acid (**2.81**; 0.88 mL, 8.61 mmol) was dissolved in 15 mL dry CH₂Cl₂ in a dry flask under inert atmosphere. DMAP (1.25 g, 10.2 mmol), EDC·HCl (2.15 g, 11.2 mmol), and morpholine (0.90 mL, 10.3 mmol) were added respectively in one portion each. The reaction was stirred for 22 hrs at room temp before quenching by pouring into 50 mL 1 M HCl. The mixture was further diluted with 50 mL CH₂Cl₂, and the phases were separated. The organic phase was further washed with 50 mL 1 M HCl, two 50 mL portions of 1:1 sat. NaHCO₃/water solution, and 50 mL brine, in that order. The organic phase was then dried over anhydrous magnesium sulfate, filtered to remove solids, and concentrated *in vacuo*. Obtained 757 mg of a white, free-flowing solid (47.5% yield).

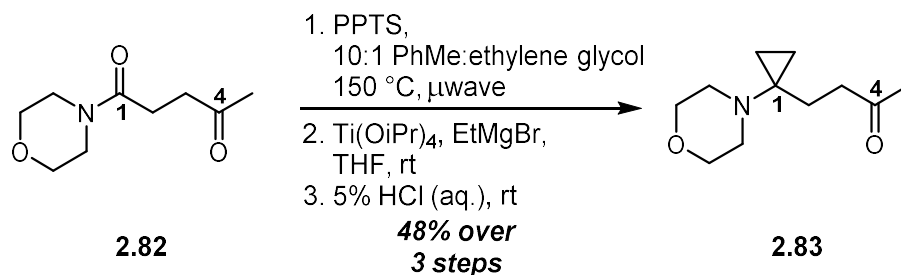
¹H NMR (CDCl₃, 500 MHz): δ = 3.70-3.63 (m, 4H, morph.), 3.60-3.56 (m, 2H, morph.), 3.54-3.47 (m, 2H, morph.), 2.79 (t, 2H, *J* = 6.4 Hz, C3), 2.57 (t, 2H, *J* = 6.4 Hz, C2), 2.21 (s, 3H, C4-Me) ppm

¹³C NMR (CDCl₃, 126 MHz): δ = 207.9, 170.3, 66.9, 66.6, 45.9, 42.2, 38.1, 30.3, 26.9 ppm

IR (neat): 2856, 1702, 1628, 1437, 1399, 1365, 1165, 1108, 1065, 1031, 852, 838 cm⁻¹

HRMS (ES⁺, *m/z*) calculated for C₉H₁₅NNaO₃⁺: 208.0944, Found: 208.0939

R_f = 0.40 (5% MeOH in ethyl acetate), one dark blue-green spot, *p*-anisaldehyde



Morphamide **2.82** (350 mg, 1.89 mmol) was dissolved in 10 mL dry toluene in a dry 20 mL microwave vial under inert atmosphere. PPTS (95 mg, 0.38 mmol) then ethylene glycol (2.11 mL, 37.8 mmol) were added in one portion each. The mixture was flushed with argon, capped, and irradiated in a Biotage Initiator+ microwave reactor for 3 hrs at 150 °C. The reaction was allowed to cool to room temp and quenched with 25 mL of a 1:1 sat. NaHCO₃/water solution. The phases were separated, and the aqueous phase was extracted with 25 mL portions of CH₂Cl₂ three times. The combined organic phases were washed with 25 mL of brine, dried over anhydrous magnesium sulfate, filtered to remove solids, and concentrated *in vacuo*. Remaining toluene was removed from the crude residue through a plug of silica (slurry made with 99% EtOAc + 1% NEt₃, eluted with 0-8% acetone/EtOAc, increasing in 2% increments; residue was loaded with PhMe). Obtained 415 mg of a 3:1 mixture of the desired C4-acetal:starting material by ¹H NMR (~76% yield, >99% BORSM).

¹H NMR (CDCl₃, 500 MHz): δ = 3.97-3.87 (m, 4H, acetal), 3.71-3.63 (m, 4H, morph.), 3.63-3.56 (m, 2H, morph.), 3.49-3.44 (m, 2H, morph.), 2.43-2.38 (m, 2H, C2), 2.05-2.00 (m, 2H, C3), 1.33 (s, 3H, C4-Me) ppm

R_f = 0.25 (100% EtOAc), two overlapping spots (dark green), *p*-anisaldehyde

The 3:1 mixture from above was subsequently dissolved in 25 mL dry THF under inert atmosphere, followed by the addition of titanium isopropoxide (0.53 mL, 1.77 mmol). The reaction

vessel was submerged in a water bath at ambient temperature to serve as a heat sink. Ethylmagnesium bromide (1.0 M in THF, 5.64 mL, 5.64 mmol) was added dropwise via syringe over 4.5 min. A vent line was added to account for gas evolution (note: gas evolution can be quite vigorous along with substantial heat generation if addition is too rapid). The reaction mixture (clear, colorless at the outset of addition) undergoes a series of color changes, first turning a bright yellow with initial drops, then transitioning to orange and red hues, and ultimately turning a dark red-brown (almost black) upon complete addition of EtMgBr. Vent line was removed, and the reaction mixture was stirred at room temp for 70 min. The reaction was quenched with an aqueous solution containing 45 mL Rochelle salt and 10 mL 2.0 M NaOH and stirred vigorously for 90 min. The mixture was then diluted with 25 mL ether. The phases were separated. The aqueous phase was extracted with 25 mL portions of ether three times. The combined organics were then washed with 100 mL brine, dried over anhydrous magnesium sulfate, filtered to remove solids, and concentrated *in vacuo* to afford 306 mg of crude residue.

¹H NMR (CDCl₃, 500 MHz): δ = 3.97-3.87 (m, 4H, acetal), 3.63-3.58 (m, 4H, morph.), 2.68-2.62 (m, 4H, morph.), 1.87-1.83 (m, 2H, C3), 1.33-1.28 (m, 2H, C2), 1.29 (s, 3H, C4-Me), 0.56-0.52 (m, 2H, CP), 0.43-0.39 (m, 2H, CP) ppm

R_f = 0.30 (20% EtOAc in hexanes), purple spot, *p*-anisaldehyde

The crude C4-acetal-protected aminoCP was dissolved in 6 mL of 5% aqueous HCl solution under inert atmosphere. The reaction mixture was stirred for 10 min at room temp before quenching with an aqueous solution containing 10 mL sat. NaHCO₃ and 6 mL 2.0 M NaOH. The mixture was further diluted with 12 mL ether. The phases were separated. The aqueous phase (pH ~14) was extracted with 12 mL portions of ether three times. The combined organic phases were

washed with 12 mL brine, dried over anhydrous magnesium sulfate, filtered to remove solids, and concentrated *in vacuo*. The crude residue was purified via flash chromatography over silica (6 to 48% ethyl acetate:hexanes, increasing in 6% increments; the residue was loaded with PhMe). Obtained 177 mg of a tan, waxy solid (47.5% over three steps).

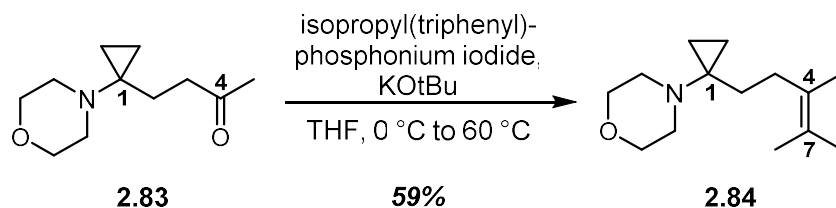
¹H NMR (CDCl₃, 500 MHz): δ = 3.63-3.57 (m, 4H, morph.), 2.59-2.55 (m, 4H, morph.), 2.45 (t, 2H, *J* = 7.7 Hz, C3), 2.15 (s, 3H, C4-Me), 1.78 (t, 2H, *J* = 7.7 Hz, C2), 0.64-0.59 (m, 2H, CP), 0.38-0.33 (m, 2H, CP) ppm

¹³C NMR (CDCl₃, 126 MHz): δ = 208.7, 67.7, 49.8, 44.1, 41.7, 30.2, 25.7, 12.1 ppm

IR (neat): 2925, 2813, 1710, 1448, 1270, 1241, 1109, 1013, 983, 853, 733, 713 cm⁻¹

HRMS (ES⁺, *m/z*) calculated for C₁₁H₂₀NO₂⁺: 198.1489, Found: 198.1487

R_f = 0.20 (50% EtOAc in hexanes), one yellow spot, KMnO₄



Isopropyltriphenylphosphonium iodide (723 mg, 1.67 mmol) was dissolved in 4.0 mL dry THF in a dry flask under inert atmosphere. The mixture was cooled to 0 °C. Potassium *tert*-butoxide (1.0 M in THF, 1.52 mL, 1.52 mmol) was added dropwise over 1 min, resulting in a dark red solution that was stirred at 0 °C for 30 min. Ketone **2.83** (144 mg, 0.730 mmol) was then added dropwise over 30 s as a solution in 0.50 mL dry THF. The reaction mixture was warmed to room temperature, then heated to 60 °C for 20 hrs. The resulting light-orange reaction mixture was cooled to room temp and quenched with 10 mL sat. ammonium chloride. The phases were separated. The aqueous phase was extracted with 10 mL portions of ether three times. The combined organic phases were washed with 10 mL brine, dried over anhydrous magnesium sulfate, filtered to remove solids, and concentrated *in vacuo*. The crude residue was purified by flash chromatography over silica (1 to 2 to 3 to 4 to 5 to 6 to 8 to 20% ethyl acetate:hexanes; residue was loaded with PhMe). Obtained 97 mg of a clear, colorless oil (59.4% yield).

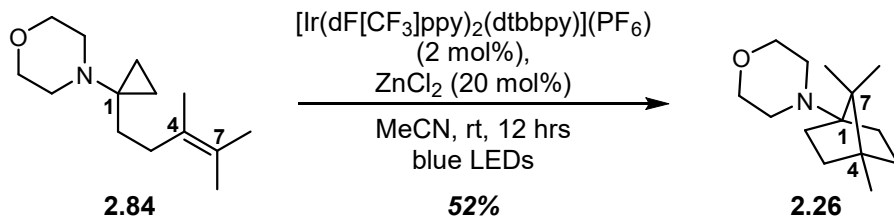
¹H NMR (CDCl₃, 500 MHz): δ = 3.65-3.59 (m, 4H, morph.), 2.72-2.66 (m, 4H, morph.), 2.00-1.94 (m, 2H, C2), 1.56-1.52 (m, 2H, C3), 1.64 (s, 3H, Me), 1.63 (s, 3H, Me), 1.62 (s, 3H, Me), 0.57-0.53 (m, 2H, CP), 0.47-0.42 (m, 2H, CP) ppm

¹³C NMR (CDCl₃, 126 MHz): δ = 127.8, 123.9, 67.9, 50.0, 44.5, 32.5, 28.7, 20.7, 20.2, 18.6, 13.1 ppm

IR (neat): 2913, 2850, 1448, 1372, 1262, 1115, 1011, 985, 857, 732 cm⁻¹

HRMS (ES⁺, *m/z*) calculated for C₁₄H₂₆NO⁺: 224.2009, Found: 224.2010

R_f = 0.50 (10% EtOAc in hexanes), one blue spot, *p*-anisaldehyde



In a dry vial under nitrogen, aminoCP **2.84** (58.2 mg, 261 μmol) was dissolved in 2.6 mL dry MeCN before adding $[\text{Ir(dF[CF}_3\text{]ppy)}_2\text{(dtbbpy)](PF}_6\text{)}$ (5.9 mg, 5.2 μmol) then ZnCl_2 (1.0 M in ether, 52 μL , 52 μmol) in one portion each. Reaction mixture was bright yellow, but slightly cloudy from the Zn salt. Reaction mixture was degassed with three freeze-pump-thaw cycles. The reaction was performed by stirring at room temp (as controlled with jacketed water bath, temp maintained between 18-23 $^\circ\text{C}$) while irradiating with two strips of 4.4 W blue LEDs for 12 hrs. Reaction mixture was still slightly cloudy but had turned bright orange. Mixture was quenched with 10 mL 1:1 sat. NaHCO_3 :1 M NaOH to ensure aq phase pH \sim 14, then diluted further with 10 mL 1:1 ether:hexanes. Phases were separated, and the aqueous phase was extracted with 10 mL portions of 1:1 ether:hexanes three times. Combined organics were washed with 10 mL brine, dried over anhydrous magnesium sulfate, filtered to remove solids, and concentrated *in vacuo*. The crude residue was purified via flash chromatography over silica (5 to 35% ethyl acetate:hexanes, increasing in 5% increments; residue loaded with PhMe).

- Recovered starting material: 5.9 mg; clear, colorless oil, but $^1\text{H NMR}$ reveals a number of minor impurities; <10% recovery

- Product: 30.5 mg; slightly yellow oil; 52.4% yield

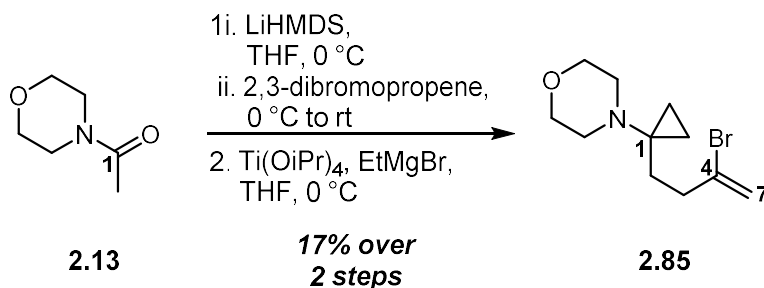
$^1\text{H NMR}$ (CDCl_3 , 500 MHz): δ = 3.68 (*app.* t, 4H, J = 4.4 Hz, morph.), 2.63-2.60 (m, 4H, morph.), 1.79-1.71 (m, 2H, NB-core), 1.50-1.43 (m, 2H, NB-core), 1.42-1.36 (m, 2H, NB-core), 1.28-1.22 (m, 2H, NB-core), 0.86 (s, 6H, C7-Me, C7-Me), 0.78 (s, 3H, C4-Me) ppm

$^{13}\text{C NMR}$ (CDCl_3 , 126 MHz): δ = 72.1, 67.9, 49.1, 48.2, 45.6, 34.7, 28.6, 19.0, 16.7 ppm

IR (neat): 2951, 2870, 1448, 1387, 1281, 1150, 1119, 910, 897, 870, 733, 688 cm^{-1}

HRMS (ES+, m/z) calculated for $\text{C}_{14}\text{H}_{26}\text{NO}^+$: 224.2009, Found: 224.2009

R_f = 0.20 (20% EtOAc in hexanes), one yellow spot, KMnO_4



N-Acetyl morpholine (**2.13**, 720 μ L, 6.2 mmol) was dissolved in 15 mL dry THF in a dry flask under N₂ before cooling to 0 °C (ice/water). LiHMDS (1.0 M in THF, 6.5 mL, 6.5 mmol) was added dropwise down the side of the vial over 2 min, then the reaction mixture was allowed to stir at 0 °C for 1 hr. In a separate dry flask kept under inert atmosphere, 2,3-dibromo-1-propene (1.0 mL, 8.4 mmol) was dissolved in 10 mL dry THF. The enolate solution was then cannulated into the bromide solution slowly down the side of the vial over the course of 2 hrs. Transfer was quantified with two rinses of 1 mL dry THF. The reaction mixture was stirred at room temp for 30 min before quenching with 40 mL 1:1 sat. NaHCO₃:sat. Na₂S₂O₃. The mixture was diluted with 40 mL ether, and the phases were separated. The aqueous phase was then extracted with 100 mL portions of ether three times. Combined organics were washed with 40 mL brine, dried over anhydrous magnesium sulfate, filtered to remove solids, and concentrated *in vacuo* to afford a slightly yellow oil. This crude residue was purified by flash chromatography over silica (10 to 60% ethyl acetate:hexanes, increasing in 10% increments, residue was loaded with PhMe). Obtained 630 mg of the desired mono-alkylated species (41% yield), along with 45 mg of the bis-alkylated material. ¹H NMR line-listings for the desired intermediate are provided below.

¹H NMR (CDCl₃, 500 MHz): δ = 5.67 (s, 1H, C7), 5.43 (s, 1H, C7), 3.70-3.64 (m, 4H, morph.), 3.64-3.60 (m, 2H, morph.), 3.52-3.48 (m, 2H, morph.), 2.79 (t, 2H, *J* = 7.5 Hz, C2), 2.58 (t, 2H, *J* = 7.3 Hz, C3) ppm

R_f = 0.20 (60% EtOAc in hexanes), one yellow spot, KMnO₄

The mono-prenylated amide from above (520 mg, 2.1 mmol) was dissolved in 35 mL dry THF under inert atmosphere, followed by addition of titanium isopropoxide (0.69 mL, 2.3 mmol). The reaction was cooled to 0 °C. Ethylmagnesium bromide (1.0 M in THF, 7.3 mL, 7.3 mmol) was added dropwise via syringe over the course of 5 min. A vent line was added to account for gas evolution (note: gas evolution can be quite vigorous along with substantial heat generation if addition is too rapid). The reaction mixture (clear, colorless at the outset of addition) undergoes a series of color changes, first turning a bright yellow with initial drops, then transitioning to orange and red hues, and ultimately turning a dark red-brown (almost black) upon complete addition of EtMgBr. Vent line was removed, and the reaction mixture was stirred at 0 °C for 2 hrs before quenching with 50 mL sat. Rochelle salt and stirred vigorously for 10 min. The mixture was then diluted with 25 mL sat. Rochelle salt, 25 mL brine, and 100 mL ether. Phases were separated. The aqueous phase was extracted with 100 mL portions of ether three times. The combined organics were then washed with 100 mL brine, dried over anhydrous sodium sulfate, filtered to remove solids, and concentrated *in vacuo*. The crude residue was purified via flash chromatography over silica (4 to 28% ethyl acetate:hexanes, increasing in 4% increments; residue was loaded with PhMe). Obtained aminoCP **S18** as a slightly red oil (221 mg, 40.5%, 16.6% over two steps).

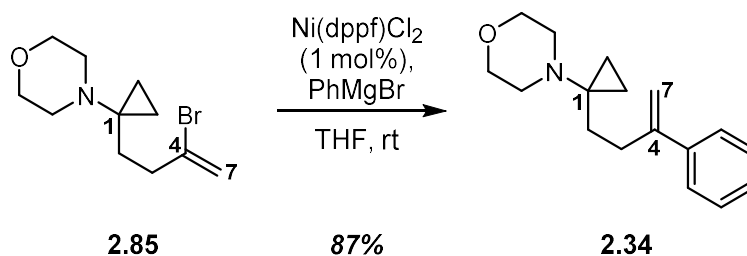
¹H NMR (CDCl₃, 500 MHz): δ = 5.55 (d, 1H, *J* = 1.2 Hz, C7), 5.36 (d, 1H, *J* = 1.5 Hz, C7), 3.64-3.59 (m, 4H, morph.), 2.65-2.61 (m, 4H, morph.), 2.47-2.43 (m, 2H, C3), 1.79-1.74 (m, 2H, C2), 0.62-0.59 (m, 2H, CP), 0.45-0.42 (m, 2H, CP) ppm

¹³C NMR (CDCl₃, 126 MHz): δ = 134.8, 116.3, 67.8, 49.9, 43.9, 39.7, 30.0, 12.7 ppm

IR (neat): 2933, 2852, 1629, 1264, 1114, 1013, 985, 884, 857 cm⁻¹

HRMS (ES⁺, *m/z*) calculated for C₁₁H₁₉BrNO⁺: 260.0645, Found: 260.0650

R_f = 0.25 (20% EtOAc in hexanes), one yellow spot, KMnO₄



Bromobenzene (0.17 mL, 1.6 mmol) was dissolved in 3 mL dry THF in a dry vial under inert atmosphere before adding magnesium turnings (42 mg, 1.7 mmol; purchased from Alfa Aesar, 99.8% metals basis) in one portion. This vial was flushed with Ar, capped, and heated to 70 °C for 30 min, revealing a somewhat grey-brown but still clear solution which contained only small traces of residual Mg turnings (~0.5 M phenylMgBr). In a separate dry vial under N₂, C4-bromo aminoCP **2.85** (148 mg, 0.57 mmol) was dissolved in 3 mL dry THF. Ni(dppf)Cl₂ (3.9 mg, 5.7 μmol; purchased from TCI America) was added to this solution in one portion before adding 2.8 mL of the Grignard solution (~1.4 mmol) dropwise via syringe over the course of one minute. The reaction mixture quickly turns a reddish-brown color upon addition. This mixture was stirred at room temp for 14 hrs, then quenched by pouring into 10 mL of a 1:1 mixture of sat. NaHCO₃:water. The quenched reaction was diluted with 10 mL ether, and the phases were separated. The aqueous phase was further extracted with 10 mL portions of ether three times. The combined organics were washed with 10 mL brine, dried over anhydrous magnesium sulfate, filtered to remove solids, and concentrated *in vacuo*. The crude residue was purified via flash chromatography over silica (4 to 24% ethyl acetate:hexanes; increasing in 4% increments; crude residue was loaded with PhMe). The desired aminoCP **2.34** was obtained as a slightly yellow liquid (127 mg, 86.7% yield).

¹H NMR (CDCl₃, 700 MHz): δ = 7.39 (d, 2H, *J* = 7.3 Hz, Ph), 7.33 (t, 2H, *J* = 7.5 Hz, Ph), 7.28 (d, 1H, *J* = 7.2 Hz, Ph), 5.25 (s, 1H, C7), 5.05 (s, 1H, C7), 3.66-3.57 (m, 4H, morph.), 2.69-2.62

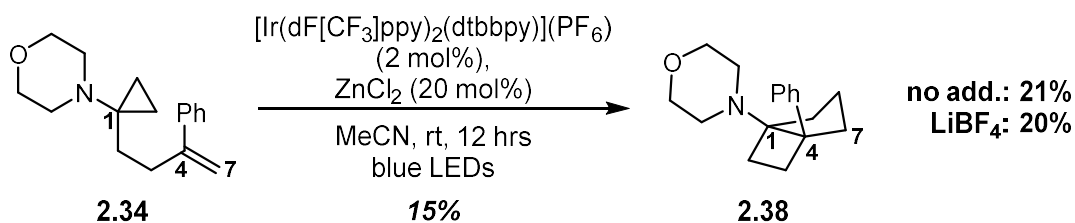
(m, 4H, morph.), 2.51 (*app.* t, 2H, $J = 8.7$ Hz, C3), 1.67 (*app.* t, 2H, $J = 8.6$ Hz, C2), 0.60-0.57 (m, 2H, CP), 0.46-0.43 (m, 2H, CP) ppm

^{13}C NMR (CDCl₃, 176 MHz): $\delta = 148.8, 141.3, 128.5, 127.5, 126.2, 112.1, 67.9, 49.9, 44.3, 33.2, 29.8, 12.9$ ppm

IR (neat): 2930, 2851, 1626, 1494, 1450, 1264, 1114, 1069, 1012, 984, 892, 857, 778, 703 cm⁻¹

HRMS (ES⁺, m/z) calculated for C₁₇H₂₄NO⁺: 258.1852, Found: 258.1857

$R_f = 0.30$ (20% EtOAc in hexanes), one yellow spot, KMnO₄ + UV



In a dry vial under nitrogen, aminoCP **2.34** (56.9 mg, 221 μmol) was dissolved in 2.2 mL dry MeCN before adding $[\text{Ir}(\text{dF}[\text{CF}_3]\text{ppy})_2(\text{dtbbpy})](\text{PF}_6)$ (5.0 mg, 4.4 μmol) then ZnCl_2 (1.0 M in ether, 44 μL , 44 μmol) in one portion each. Reaction mixture is bright yellow, but slightly cloudy from the Zn salt. Reaction mixture was degassed with three freeze-pump-thaw cycles. The reaction was performed by stirring at room temp (as controlled with jacketed water bath, temp maintained between 18-23 $^\circ\text{C}$) while irradiating with two strips of 4.4 W blue LEDs for 12 hrs. The mixture appears substantially cloudier than prior to irradiation, with some grey precipitate adhering to the walls of the vial. The diluted mixture was added to 10 mL 1:1 NaHCO_3 :water containing 1 mL of 50% NaOH to ensure aq phase pH \sim 14, then diluted further with 5 mL hexanes. Phases were separated, and the aqueous phase was extracted with 10 mL portions of 1:1 ether:hexanes three times. Combined organics were washed with 10 mL brine, dried over anhydrous magnesium sulfate, filtered to remove solids, and concentrated *in vacuo*. The crude residue was purified via flash chromatography over silica (4 to 28% ethyl acetate:hexanes, increasing in 4% increments; residue loaded with PhMe).

- Recovered starting material: 28.2 mg; clear, colorless oil; 50.4% recovery

- Product: 8.2 mg; clear, colorless oil; 14.7% yield, 29.5% BORSM

$^1\text{H NMR}$ (C_6D_6 , 500 MHz): δ = 7.52-7.49 (m, 2H, Ph), 7.25-7.21 (m, 2H, Ph), 7.11 (tt, 1H, J = 7.3, 1.2 Hz, Ph), 3.43 (*app.* t, 4H, J = 4.4 Hz, morph.), 2.13-2.05 (m, 3H, morph. [2H], C2), 1.98 (td, 1H, J = 12.5, 5.1 Hz, C3), 1.84-1.70 (m, 5H, morph. [2H], C7, C5, C5), 1.69-1.57 (m, 3H, C3, C7, C6), 1.50 (ddd, 1H, J = 11.9, 10.0, 5.3 Hz, C2), 1.28-1.23 (m, 1H, C6) ppm

^{13}C NMR (C_6D_6 , 126 MHz): δ = 146.7 (Ph), 127.7 (Ph), 127.3 (Ph), 125.9 (Ph), 72.7 (C1), 67.4 (morph.), 52.6 (C4), 47.0 (morph.), 39.0 (C7), 31.4 (C6), 29.5 (C3), 27.6 (C2), 23.4 (C5) ppm

IR (thin film): 2949, 2850, 1496, 1449, 1311, 1273, 1206, 1114, 1031, 928, 892, 863, 756, 695 cm^{-1}

HRMS (ES+, m/z) calculated for $\text{C}_{17}\text{H}_{24}\text{NO}^+$: 258.1852, Found: 258.1852

R_f = 0.35 (10% EtOAc in hexanes), one yellow spot, KMnO_4 + UV

Additional Trials with Varied Additives

No Additive

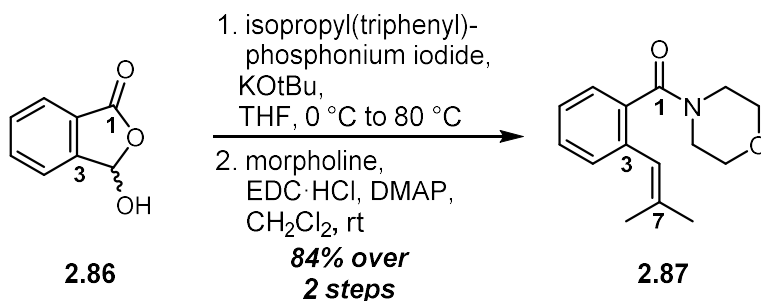
Following the general procedure outlined above, 76.7 mg of aminoCP **1ab** (298 μmol) were dissolved in 3.0 mL dry MeCN along with 6.7 mg of $[\text{Ir}(\text{dF}[\text{CF}_3]\text{ppy})_2(\text{dtbbpy})](\text{PF}_6)$ (6.0 μmol) prior to irradiation. Isolation provided the following:

- Recovered starting material: 31.4 mg; clear, colorless oil; 41.5% recovery
- Product: 16.2 mg; clear, colorless oil; 21.4% yield, 36.6% BORSM

LiBF₄

Following the general procedure outlined above, 71.6 mg of aminoCP **1ab** (278 μmol) were dissolved in 3.0 mL dry MeCN along with 6.3 mg of $[\text{Ir}(\text{dF}[\text{CF}_3]\text{ppy})_2(\text{dtbbpy})](\text{PF}_6)$ (5.6 μmol) and 5.3 mg of LiBF_4 (57 μmol) prior to irradiation. Isolation provided the following:

- Recovered starting material: 21.4 mg; clear, colorless oil; 30.4% recovery
- Product: 14.2 mg; slightly yellow oil; 20.2% yield, 29.0% BORSM



Isopropyl(triphenyl)phosphonium iodide (3.46 g, 8.00 mmol) was dissolved in 15 mL dry THF in a dry flask under nitrogen then cooled to 0 °C (ice/water). Potassium *tert*-butoxide (1.0 M in THF; 12 mL, 12.0 mmol) was added via syringe dropwise down the side of the vial over the course of 90 s, quickly turning the mixture bright red. The ice bath was removed and the mixture was stirred at room temp for 30 min. 2-Formylbenzoic acid (**S19**; 600 mg, 4.00 mmol) was added in one portion, then the flask was fitted with a reflux condenser. The mixture was heated to 70 °C for 21 hrs under a balloon of Ar. Upon cooling to room temp, the reaction was quenched by pouring into 20 mL sat. NH₄Cl, then diluting with 20 mL ethyl acetate. The phases were separated, and the organic phase was extracted with six 20 mL portions of 2 M NaOH. The combined aqueous phases were acidified to pH ~1 with concentrated HCl, then extracted with six 40 mL portions of ethyl acetate. The combined organics were dried over anhydrous sodium sulfate, filtered to remove solids, and concentrated *in vacuo*. The crude residue was purified via flash chromatography over silica (4 to 20% ethyl acetate:hexanes, increasing in 4% increments; loaded residue with PhMe). Obtained 655 mg of a white solid (93.0% yield).

¹H NMR (CDCl₃, 500 MHz): δ = 8.05 (d, 1H, *J* = 7.8 Hz, Ar), 7.51 (t, 1H, *J* = 7.6 Hz, Ar), 7.33-7.26 (m, 2H, Ar), 6.71 (br s, 1H, C4), 1.95 (s, 3H, C7-Me), 1.74 (s, 3H, C7-Me) ppm

R_f = 0.25 (20% EtOAc in hexanes), one yellow spot, KMnO₄ + UV

The resultant carboxylic acid (602 mg, 3.42 mmol) was dissolved in 13 mL dry CH₂Cl₂ in a flame-dried flask under inert atmosphere. To this solution, DMAP (1.00 g, 8.20 mmol), EDC·HCl (852 mg, 4.44 mmol), and morpholine (0.36 mL, 4.10 mmol) were added respectively, in one portion each. The reaction was flushed with Ar and stirred at room temp for 22 hrs. The mixture was then quenched by pouring into 25 mL 2 M HCl and diluted with 25 mL ether. The phases were separated, and the organic phase was washed with two additional 25 mL portions of 2 M HCl. The combined aqueous washes were extracted with three 25 mL portions of ethyl acetate. The combined organic phases were then washed with 25 mL brine, dried over anhydrous magnesium sulfate, filtered to remove solids, and concentrated *in vacuo*. The crude residue was purified with flash chromatography over silica (20 to 60% ethyl acetate:hexanes, increasing in 10% increments; loaded residue with PhMe). Obtained 760 mg of morphamide **2.87** as a viscous, slightly yellow oil; 90.6% yield, 84.3% over two steps.

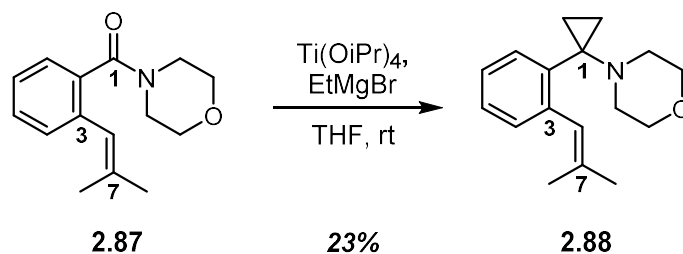
¹H NMR (CDCl₃, 500 MHz): δ = 7.36-7.32 (m, 1H, Ar), 7.27-7.21 (m, 3H, Ar), 6.23 (br s, 1H, C4), 3.90-3.80 (m, 1H, morph.), 3.81-3.66 (m, 3H, morph.), 3.57-3.44 (m, 2H, morph.), 3.13 (*app.* quart., 2H, *J* = 4.5 Hz, morph.), 1.90 (s, 3H, C7-Me), 1.78 (s, 3H, C7-Me) ppm

¹³C NMR (CDCl₃, 126 MHz): δ = 170.1, 137.6, 135.6, 135.3, 129.9, 128.8, 126.8, 126.3, 122.5, 67.1, 66.9, 47.3, 42.1, 26.6, 19.6 ppm

IR (neat): 2916, 2851, 1635, 1446, 1424, 1299, 1274, 1255, 1154, 1113, 1019, 1012, 841, 775, 748 cm⁻¹

HRMS (ES⁺, *m/z*) calculated for C₁₅H₂₀NO₂⁺: 246.1489, Found: 246.1489

R_f = 0.30 (60% EtOAc in hexanes), one yellow spot, KMnO₄ + UV



Morphamide **2.87** (250 mg, 1.02 mmol) was dissolved in 16 mL dry THF under inert atmosphere, followed by addition of titanium isopropoxide (0.33 mL, 1.12 mmol). The reaction vessel was submerged in a water bath at ambient temp to serve as a heat sink. Ethylmagnesium bromide (1.0 M in THF, 3.6 mL, 3.6 mmol) was added dropwise via syringe over the course of 10 min. A vent line was added to account for gas evolution (note: gas evolution can be quite vigorous along with substantial heat generation if addition is too rapid). Reaction mixture (clear, colorless at outset of addition) undergoes a series of color changes, first turning a bright yellow with initial drops, then transitioning to orange and red hues, and ultimately turning a dark red-brown (almost black) upon complete addition of EtMgBr. Vent line was removed, and the reaction mixture was stirred at room temp for 1 hr. An aqueous solution containing 30 mL sat. Rochelle salt, 10 mL brine, and 2 mL of 50% NaOH was prepared. The reaction was quenched with 10 mL of this aqueous mixture and stirred vigorously for 15 min. The mixture was then diluted with the remainder of the quenching solution and 40 mL ether. The phases were separated. The aqueous phase was extracted with 40 mL portions of ether three times. The combined organics were then washed with 40 mL brine, dried over anhydrous magnesium sulfate, filtered to remove solids, and concentrated *in vacuo*. TLC revealed a complicated mixture of byproducts, most of which have similar polarity relative to the desired product. The crude residue was purified via flash chromatography over silica (2 to 4 to 6 to 10 to 14 to 20 to 28 to 40% ethyl acetate:hexanes; the residue was loaded with PhMe). The desired aminoCP **2.88** was isolated from this mixture as a

yellow oil; ^1H NMR revealed a few minor impurities, but it would ultimately take multiple rounds of chromatography to fully remove these (as discovered on a second sample). This material was moved on as it was initially isolated, 61.3 mg (23.4%).

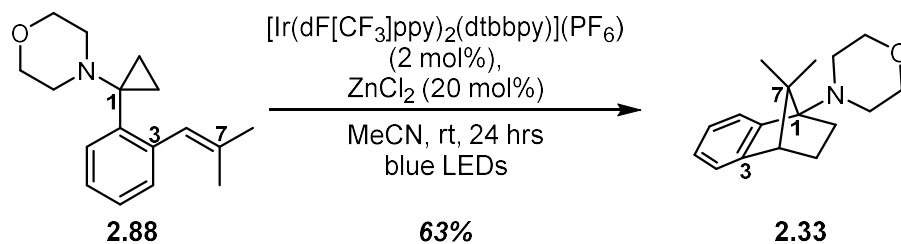
^1H NMR (CDCl_3 , 500 MHz): δ = 7.26-7.14 (m, 4H, Ar), 6.60 (br s, 1H, C4), 3.60-3.56 (m, 4H, morph.), 2.53-2.48 (m, 4H, morph.), 1.90 (s, 3H, C7-Me), 1.73 (s, 3H, C7-Me), 0.99 (*app.* dd, 2H, J = 4.4, 2.2 Hz, CP), 0.81 (*app.* dd, 2H, J = 4.2, 2.2 Hz, CP) ppm

^{13}C NMR (CDCl_3 , 126 MHz): δ = 140.0, 135.2, 134.4, 133.0, 130.7, 126.9, 125.7, 125.6, 67.7, 50.4, 47.3, 26.6, 19.6, 15.7 ppm

IR (neat): 2929, 2849, 1448, 1373, 1296, 1263, 1234, 1116, 1017, 982, 916, 852, 760, 733 cm^{-1}

HRMS (ES^+ , m/z) calculated for $\text{C}_{17}\text{H}_{24}\text{NO}^+$: 258.1852, Found: 258.1855

R_f = 0.60 (30% EtOAc in hexanes), one yellow spot, KMnO_4 + strong UV



In a dry vial under nitrogen, aminoCP **1i** (51.6 mg, 200 μmol) was dissolved in 2.0 mL dry MeCN before adding $[\text{Ir}(\text{dF}[\text{CF}_3]\text{ppy})_2(\text{dtbbpy})](\text{PF}_6)$ (4.5 mg, 4.0 μmol) then ZnCl_2 (1.0 M in ether, 40 μL , 40 μmol) in one portion each. Reaction mixture was bright yellow and slightly cloudy. Reaction mixture was degassed with three freeze-pump-thaw cycles. The reaction was performed by stirring at room temp (as controlled with jacketed water bath, temp maintained between 18-23 $^\circ\text{C}$) while irradiating with two strips of 4.4 W blue LEDs for 24 hrs. Mixture was somewhat orange and a little cloudier than pre-irradiation. The mixture was added to 10 mL 1:1 sat NaHCO_3 :water containing 0.5 mL of 50% NaOH to ensure aq phase pH \sim 14, then diluted further with 10 mL ether. Phases were separated, and the aqueous phase was extracted with 10 mL portions of ether three times. Combined organics were washed with 10 mL brine, dried over anhydrous magnesium sulfate, filtered to remove solids, and concentrated *in vacuo*. The crude residue was purified via flash chromatography over silica (3 to 5 to 7 to 10 to 15 to 21 to 28% ethyl acetate:hexanes; residue loaded with PhMe; silica was pre-neutralized with 3% ethyl acetate:hexanes + 1% NEt_3). Collected the following:

- Recovered starting material: 3.5 mg; slightly yellow oil; contaminated with several impurities based on ^1H NMR

- Product: 32.5 mg; white solid; 63.0% yield

^1H NMR (C_6D_6 , 500 MHz): δ = 7.31 (*app.* d, 1H, J = 7.3 Hz, Ar), 7.15-7.08 (m, 2H, Ar), 7.07-7.04 (m, 1H, Ar), 3.70-3.62 (m, 4H, morph.), 2.93-2.83 (m, 4H, morph.), 2.31 (d, 1H, J = 4.2 Hz,

C4), 2.11 (td, 1H, $J = 10.9, 3.8$ Hz, C6), 1.86 (ddt, 1H, $J = 11.7, 10.5, 3.9$ Hz, C5), 1.07 (ddd, 1H, $J = 11.5, 5.9, 3.9$ Hz, C5), 1.00 (s, 3H, C7-Me), 1.01-0.96 (m, 1H, C6), 0.79 (s, 3H, C7-Me) ppm
 ^{13}C NMR (C_6D_6 , 126 MHz): $\delta = 147.4, 147.2, 126.0, 125.7, 122.2, 121.9, 77.2, 68.4, 59.3, 54.0, 49.8, 29.6, 26.0, 24.0, 21.3$ ppm

IR (neat): 2951, 2839, 1455, 1299, 1265, 1111, 1019, 886, 755 cm^{-1}

HRMS (ES⁺, m/z) calculated for $\text{C}_{17}\text{H}_{24}\text{NO}^+$: 258.1852, Found: 258.1855

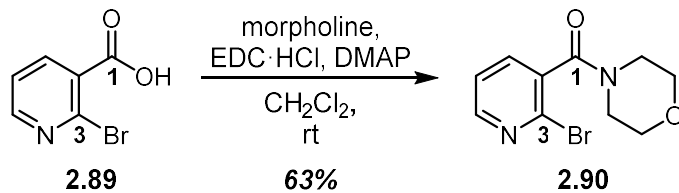
$R_f = 0.45$ (20% EtOAc in hexanes), one yellow spot, $\text{KMnO}_4 + \text{UV}$

Additional Trials

12-hr irradiation trial

Following the general procedure outlined above, 48.1 mg of aminoCP **2.88** (187 μmol) were dissolved in 1.9 mL dry MeCN along with 4.2 mg of $[\text{Ir}(\text{dF}[\text{CF}_3]\text{ppy})_2(\text{dtbbpy})](\text{PF}_6)$ (3.7 μmol) and 37 μL ZnCl_2 (1.0 M in ether; 37 μmol) prior to irradiating for 12 hrs. Isolation provided the following:

- Recovered starting material: 11.9 mg (obtained 12.9 mg as a 92.0 wt% mix with water); slightly yellow oil; 27.4% recovery
- Product: 27.6 mg (obtained 28.9 mg as a 95.5 wt% mix with water); clear, colorless oil which upon slow concentration from pentane, solidified to an amorphous, white solid; 57.4% yield



2-Bromonicotinic acid (**2.89**; 1.60 g, 7.92 mmol) was dissolved in 30 mL dry CH₂Cl₂ in a dry flask under nitrogen. DMAP (194 mg, 1.58 mmol), EDC·HCl (1.97 g, 10.3 mmol), and morpholine (0.83 mL, 9.50 mmol) were added respectively, in one portion each. The flask was flushed with Ar, and the reaction was stirred at room temp for 48 hrs. The reaction mixture was poured into 200 mL water, diluted with 100 mL CH₂Cl₂, and the phases were separated. The aqueous phase was extracted with 200 mL portions of CH₂Cl₂ three times. The combined organics were washed with 100 mL brine, dried over anhydrous magnesium sulfate, filtered to remove solids, and concentrated *in vacuo*. The crude residue was purified via flash chromatography over silica (60 to 100% ethyl acetate:hexanes + 0.1% NEt₃, increasing in 10% increments; residue was loaded with PhMe). Obtained a viscous oil that solidifies upon prolonged storage under vacuum. Final product is a white powder. Collected 1.35 g of morphamide **2.90** (4.98 mmol, 62.9% yield).

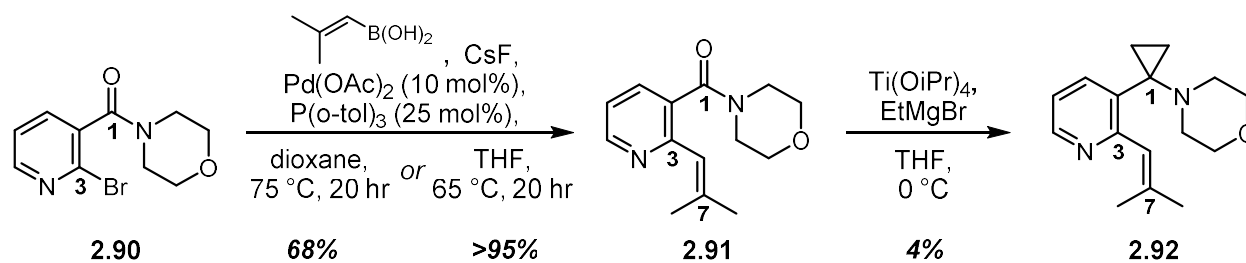
¹H NMR (CDCl₃, 700 MHz): δ = 8.42-8.41 (m, 1H, Ar), 7.59-7.57 (m, 1H, Ar), 7.36-7.34 (m, 1H, Ar), 3.90-3.85 (m, 1H, morph.), 3.84-3.80 (m, 1H, morph.), 3.79-3.72 (m, 3H, morph.), 3.62-3.58 (m, 1H, morph.), 3.33 (ddd, 1H, *J* = 13.4, 6.2, 3.1, morph.), 3.21 (ddd, 1H, *J* = 13.4, 6.2, 3.1, morph.) ppm

¹³C NMR (CDCl₃, 176 MHz): δ = 167.0, 150.7, 138.7, 136.5, 134.9, 123.1, 66.7, 66.6, 47.3, 42.3 ppm

IR (neat): 2855, 1633, 1577, 1555, 1465, 1429, 1389, 1281, 1165, 1110, 1063, 1009, 935, 892, 842, 811, 755, 731, 671, 607 cm⁻¹

HRMS (ES⁺, *m/z*) calculated for C₁₀H₁₂BrN₂O₂⁺: 271.0077, Found: 271.0078

$R_f = 0.30$ (90% EtOAc in hexanes), one yellow spot, KMnO_4 + weak UV



A stock solution of the active palladium catalyst was generated in a dry vial under inert atmosphere; $\text{Pd}(\text{OAc})_2$ (75 mg, 0.33 mmol) and $\text{P}(\text{o-tol})_3$ (255 mg, 0.84 mmol) were dissolved in 5.0 mL dry, degassed dioxane (sparged with Ar for 15 min), then stirred 30 min at room temp to produce a clear, orange catalyst stock. Oven-dried CsF (2.03 g, 13.4 mmol) was loaded into a separate dry flask under inert atmosphere before evacuating and purging with nitrogen three times and suspending in 3.0 mL dry, degassed dioxane. In a separate dry flask under inert atmosphere, brominated nicotinic acid derivative **2.90** (726 mg, 2.68 mmol) and (2,2-dimethyl)vinylboronic acid (535 mg, 5.36 mmol; purchased from Synthonyx) were dissolved in 10 mL dry, degassed dioxane, then cannulated into CsF suspension; the transfer was quantified with three rinses with dry, degassed dioxane (5.0 mL then 2.5 mL twice). The palladium catalyst stock solution (4.0 mL, corresponding to 0.27 mmol Pd and 0.67 mmol ligand) was then added dropwise via syringe over 1 min, generating a cloudy orange reaction mixture in which the CsF does not appear to be fully soluble. The reaction vessel was flushed with Ar, capped, and heated to 75 °C for 20 hrs, affording a nearly black reaction mixture with minor amounts of CsF still insoluble. The reaction mixture was quenched with 100 mL sat. NaHCO_3 then diluted with 100 mL 2 M NaOH and 100 mL ether. The phases were separated. The aqueous phase was then extracted with 100 mL portions of ether three times. The combined organic phases were washed with 100 mL brine, dried over anhydrous magnesium sulfate, filtered to remove solids, and concentrated *in vacuo*. The resultant residue was purified via flash chromatography over silica (2.5 to 5 to 10 to 15 to 25% acetone: CH_2Cl_2 ; the

silica was pre-neutralized with 2.5% acetone:CH₂Cl₂ + 1% NEt₃; residue was loaded with PhMe). The desired Suzuki product **2.91** (450 mg, 68.2% yield) was collected as a slightly orange oil; this material was sufficiently pure by ¹H NMR, but a small amount was exposed to a second round of chromatography to obtain the characterization data below (collected as a clear, colorless oil).

A second portion of starting material **2.90** (630 mg, 2.32 mmol) was exposed to analogous conditions using THF as the solvent and heating to 65 °C for 20 hrs (final reaction mixture was dark orange with brown precipitate). The extraction was performed with CH₂Cl₂ rather than ether before employing the same conditions to purify the crude residue. This trial afforded 590 mg of the desired morphamide **2.91** as a slightly orange oil, though this material was mixed with a small amount of a ligand-derived impurity as determined by ¹H NMR (approximate yield > 95%). Both batches were exposed to identical Kulinkovich cyclopropanation conditions without further purification.

¹H NMR (CDCl₃, 500 MHz): δ = 8.62 (dd, 1H, *J* = 4.9, 1.7 Hz, Ar), 7.54 (dd, 1H, *J* = 7.8, 1.7 Hz, Ar), 7.15 (dd, 1H, *J* = 7.6, 4.9 Hz, Ar), 6.25 (br s, 1H, C4), 3.93-3.84 (m, 1H, morph.), 3.83-3.69 (m, 3H, morph.), 3.56 (*app.* t, 2H, *J* = 4.3 Hz, morph.), 3.19-3.15 (m, 2H, morph.), 2.09 (s, 3H, C7-Me), 1.96 (s, 3H, C7-Me) ppm

¹³C NMR (CDCl₃, 126 MHz): δ = 168.5, 153.4, 149.6, 144.1, 134.5, 130.9, 121.2, 120.8, 67.0, 66.8, 47.4, 42.2, 27.6, 20.1 ppm

IR (neat): 2832, 1631, 1579, 1556, 1418, 1275, 1258, 1111, 1066, 1012, 844, 811, 767, 658 cm⁻¹

HRMS (ES⁺, *m/z*) calculated for C₁₄H₁₉N₂O₂⁺: 247.1441, Found: 247.1443

R_f = 0.35 (20% dichloromethane in acetone), one yellow spot, KMnO₄ + UV

Morphamide **2.91** (450 mg, 1.83 mmol) was dissolved in 30 mL dry THF in a dry flask under nitrogen. Titanium isopropoxide (0.60 mL, 2.01 mmol) was added in one portion, and the flask was submerged in a water bath for temperature control. Ethylmagnesium bromide (1.0 M in THF; 6.4 mL, 6.4 mmol) was added dropwise via syringe over the course of 5 min. A vent line was added to account for gas evolution (note: gas evolution can be quite vigorous along with substantial heat generation if addition is too rapid). Reaction mixture (clear, colorless at outset of addition) undergoes a series of color changes, first turning a bright yellow with initial drops, then transitioning to orange and red hues, and ultimately turning a dark red-brown (almost black) upon complete addition of EtMgBr. The vent line was removed after 2 min, and the reaction mixture was stirred at room temp for 1 hr. A quenching solution was prepared from 150 mL sat. Rochelle salt, 50 mL brine, and 5 mL 6 M NaOH. The reaction was quenched with 100 mL of this solution, before stirring vigorously for 20 min. The biphasic mixture was diluted with the remaining quenching solution and 100 mL ether. The phases were separated, and the aqueous phase was further extracted with 100 mL portions of ether three times. The combined organic phases were washed with 100 mL brine, dried over anhydrous magnesium sulfate, filtered to remove solids, and concentrated *in vacuo*. The initial attempt to purify the crude residue relied upon flash chromatography over silica (2.5 to 5 to 10 to 15 to 25% acetone:CH₂Cl₂; the silica was pre-neutralized with 2.5% acetone:CH₂Cl₂ + 1% NEt₃; residue was loaded with PhMe).

As mentioned above, the product of the THF-based Suzuki coupling trial (assumed 2.32 mmol starting material) was exposed to the same Kulinkovich cyclopropanation conditions as the product of the dioxane-based trial. The residues obtained after column chromatography from both trials were combined and all further purification efforts were attempted on the combined product. Ultimately, three additional rounds of chromatography (as detailed above) were employed to

remove the minor impurities of the cyclopropanation from the desired aminoCP **2.92**. At this point, the phosphine ligand-derived byproduct from the THF-based Suzuki coupling was the only major impurity. Trituration from 25% ether:pentane and filtration through celite removed a portion of this impurity, but pure material was not obtained until exposing to two additional rounds of flash chromatography over silica (40 to 50 to 70 to 80 to 90% ethyl acetate:hexanes; the silica was pre-neutralized with 40% ethyl acetate:hexanes + 1% NEt₃). The desired aminoCP **2.92** was finally obtained in sufficiently pure form as a yellow oil (45.5 mg; 4.2% yield of combined trials), along with 120 mg of a red oil mixed with various impurities.

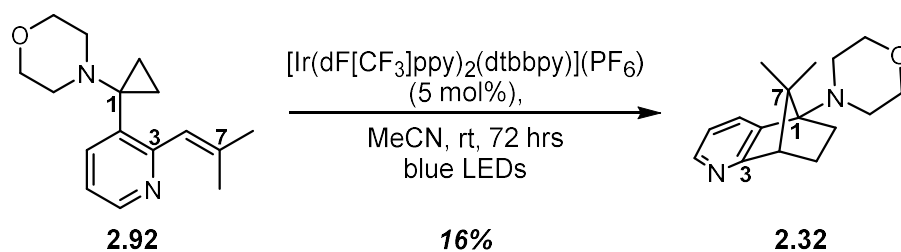
¹H NMR (CDCl₃, 500 MHz): δ = 8.51 (dd, 1H, *J* = 4.6, 1.7 Hz, Ar), 7.52 (dd, 1H, *J* = 7.6, 1.7 Hz, Ar), 7.08 (dd, 1H, *J* = 7.7, 4.8 Hz, Ar), 6.74 (br s, 1H, C4), 3.59 (*app.* t, 4H, *J* = 4.5 Hz, morph.), 2.51 (br s, 4H, morph.), 1.99 (s, 3H, C7-Me), 1.95 (s, 3H, C7-Me), 1.09-1.06 (m, 2H, CP), 0.84-0.81 (m, 2H, CP) ppm

¹³C NMR (CDCl₃, 176 MHz): δ = 157.9, 147.7, 140.4, 140.3, 130.6, 123.8, 120.3, 67.6, 50.3, 46.4, 27.5, 19.9, 15.8 ppm

IR (neat): 2956, 2849, 1578, 1556, 1443, 1418, 1264, 1236, 1117, 1020, 985, 918, 853, 808, 773, 730 cm⁻¹

HRMS (ES⁺, *m/z*) calculated for C₁₈H₂₃N₂O⁺: 259.1805, Found: 259.1807

R_f = 0.40 (80% EtOAc in hexanes), one yellow spot, KMnO₄ + UV



In dry vial under nitrogen, aminoCP **2.92** (30.0 mg, 116 μmol) was dissolved in 1.2 mL dry MeCN before adding $[\text{Ir}(\text{dF}[\text{CF}_3]\text{ppy})_2(\text{dtbbpy})](\text{PF}_6)$ (5.5 mg, 5.8 μmol) in one portion. Reaction mixture was a clear, yellow solution. Reaction mixture was degassed with three freeze-pump-thaw cycles. The reaction was performed by stirring at room temp (as controlled with jacketed water bath, temp maintained between 18-23 $^{\circ}\text{C}$) while irradiating with two strips of 4.4 W blue LEDs for 72 hrs. Mixture was still clear but had taken on an orange hue. The reaction mixture was quenched with 20 mL 1:1 sat. NaHCO_3 :1 M NaOH to ensure aq phase pH \sim 14, then diluted further with 10 mL CH_2Cl_2 . Phases were separated, and the aqueous phase was extracted with 10 mL portions of CH_2Cl_2 three times. Combined organics were dried over anhydrous magnesium sulfate, filtered to remove solids, and concentrated *in vacuo*. The crude residue was purified via flash chromatography over silica (20 to 30 to 40 to 50 to 70 to 90% ethyl acetate:hexanes; silica was pre-neutralized with 20% ethyl acetate:hexanes + 1% NEt_3 ; residue loaded with PhMe).

- Recovered starting material: 10.0 mg; slightly yellow oil, 33.3% recovery

- Product: 4.8 mg; white solid; 16.0% yield, 24.0% BORSM

$^1\text{H NMR}$ (CDCl_3 , 500 MHz): δ = 8.23 (dd, 1H, J = 5.3, 1.3 Hz, Ar), 7.50 (dd, 1H, J = 7.3, 1.0 Hz, Ar), 7.03 (dd, 1H, J = 7.5, 5.3 Hz, Ar), 3.75 (*app.* t, 4H, J = 4.5 Hz, morph.), 3.10-3.01 (m, 4H, morph.), 2.67 (d, 1H, J = 4.4 Hz, C4), 2.42 (td, 1H, J = 11.7, 3.4 Hz, C6), 2.18-2.11 (m, 1H, C5), 1.21 (s, 3H, C7-Me), 1.23-1.13 (m, 2H, C5, C6), 0.87 (s, 3H, C7-Me) ppm

^{13}C NMR (CDCl_3 , 176 MHz): $\delta = 167.6, 146.2, 140.3, 129.1, 120.7, 76.6, 68.3, 58.9, 55.6, 49.5, 29.5, 24.0, 23.6, 21.0$ ppm

IR (neat): 2959, 1725, 1669, 1575, 1450, 1407, 1268, 1167, 1117, 1011, 919, 886, 789, 728 cm^{-1}

HRMS (ES^+ , m/z) calculated for $\text{C}_{18}\text{H}_{23}\text{N}_2\text{O}^+$: 259.1805, Found: 259.1807

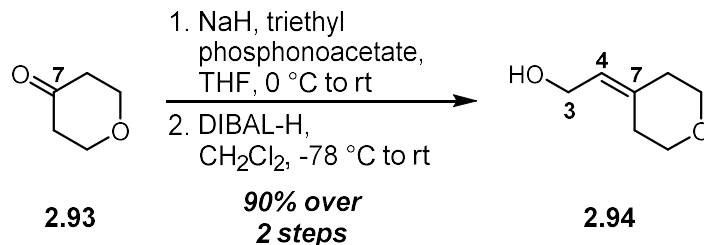
$R_f = 0.15$ (80% EtOAc in hexanes), one yellow spot, $\text{KMnO}_4 + \text{UV}$

Additional Trial

2 mol% photocatalyst, 24 hrs

Following the general procedure outlined above, 45.5 mg of aminoCP **2.92** (176 μmol) were dissolved in 1.8 mL dry MeCN along with 4.0 mg of $[\text{Ir}(\text{dF}[\text{CF}_3]\text{ppy})_2(\text{dtbbpy})](\text{PF}_6)$ (3.5 μmol) prior to irradiation for 24 hrs. Isolation provided the following:

- Recovered starting material: 30.0 mg; slightly yellow oil; 65.9% recovery
- Product: 3.6 mg; white solid; 7.9% yield, 23.2% BORSM



In a dry flask under inert atmosphere, NaH (60% dispersion in mineral oil; 0.46 g, 12.0 mmol) was washed with 2 mL pentane to remove mineral oil. The flask was flushed with nitrogen to dryness, then the NaH was suspended in 17 mL dry THF. The suspension was cooled to 0 °C (ice/water) before adding triethyl phosphonoacetate (2.2 mL, 11.0 mmol) down the side of the vial over 4 min; vent line was added during the duration of the addition to compensate for gas evolution. The mixture was stirred vigorously for 30 min at 0 °C (ylide suspension becomes foamy). Tetrahydropyranone **2.93** (1.00 g, 9.99 mmol) was then added down the side of the vial over the course of 3 min. The reaction was allowed to stir while coming to room temp for 16 hrs; the reaction thickens initially upon addition of pyranone, but eventually transitions to a nearly homogeneous brown solution. The reaction mixture was quenched by pouring into 100 mL sat. NH₄Cl, diluted with 100 mL ether, and the phases were separated. The aqueous phase was extracted with 100 mL portions of ether three times, then the combined organics were washed with 100 mL brine, dried over anhydrous MgSO₄, and concentrated. The crude yellow oil was moved on without further purification.

¹H NMR (CDCl₃, 500 MHz): δ = 5.68 (s, 1H, C4), 4.15 (quart., 2H, *J* = 7.1 Hz, CO₂Et), 3.77 (t, 2H, *J* = 5.4 Hz, THP), 3.74 (t, 2H, *J* = 5.4 Hz, THP), 3.01 (t, 2H, *J* = 5.4 Hz, THP), 2.33 (t, 2H, *J* = 5.3 Hz, THP), 1.28 (t, 2H, *J* = 7.1 Hz, CO₂Et) ppm

R_f = 0.60 (20% EtOAc in hexanes), one yellow spot, KMnO₄ + UV

A portion of the ethyl enoate ester obtained above (ca. 3.4 mmol) was dissolved in 10 mL dry CH₂Cl₂ in a dry flask under nitrogen then cooled to -78 °C. DIBAL-H (1.0 M in hexanes; 7.4 mL, 7.4 mmol) was added down the side of the vial over the course of 7 min. The reaction was allowed to slowly warm to room temp over the next 12 hrs before quenching with 30 mL of 1:1 sat. Rochelle salt:2 M NaOH. The biphasic mixture was stirred vigorously for 10 min, then diluted with 20 mL CH₂Cl₂. The phases were separated, and the aqueous phase was extracted with 20 mL portions of CH₂Cl₂ three times. The combined organic phases were washed with 20 mL brine, dried over anhydrous magnesium sulfate, and concentrated *in vacuo*. The crude residue was purified via flash chromatography over silica (30 to 80% ethyl acetate:hexanes, increasing in 10% increments; loaded residue with PhMe). Obtained 393 mg of the desired alcohol as a faintly yellow oil (solid below 0 °C) with trace amounts of an unidentified byproduct that could not be removed even upon multiple rounds of chromatography. 393 mg corresponds to 90.0% yield over 2 steps.

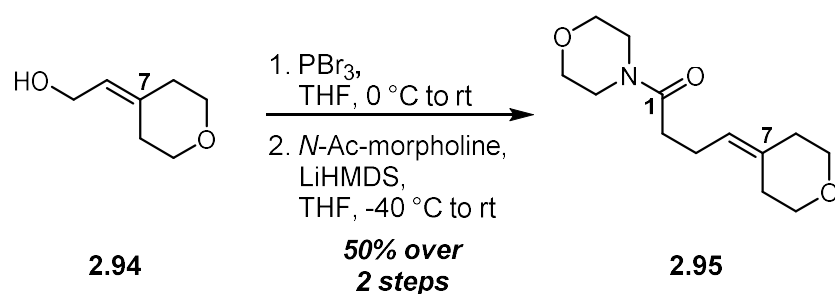
¹H NMR (CDCl₃, 700 MHz): δ = 5.47 (t, 1H, *J* = 7.1 Hz, C4), 4.16 (d, 2H, *J* = 7.0 Hz, C3), 3.70 (t, 2H, *J* = 5.5 Hz, THP), 3.67 (t, 2H, *J* = 5.6 Hz, THP), 2.33 (t, 2H, *J* = 5.5 Hz, THP), 2.25 (t, 2H, *J* = 5.3 Hz, THP), 1.26 (br s, 1H, C3-OH) ppm

¹³C NMR (CDCl₃, 176 MHz): δ = 139.0, 122.3, 69.5, 68.8, 58.4, 36.9, 30.0 ppm

IR (neat): 3386, 2958, 2850, 1422, 1384, 1234, 1168, 1095, 1000, 838, 667 cm⁻¹

HRMS (EI, *m/z*) calculated for C₇H₁₂O₂⁺: 128.0837, Found: 128.0843

R_f = 0.25 (80% EtOAc in hexanes), one yellow spot, KMnO₄



Allylic alcohol **2.94** (304 mg, 2.37 mmol) was dissolved in 15 mL dry THF in a dry flask under inert atmosphere, then cooled to 0 °C (ice/water). Phosphorous tribromide (90 μ L, 0.95 mmol) was added dropwise down the side of the flask over 20 s. The reaction was allowed to slowly warm to rt over 100 min before quenching by pouring into 20 mL sat. Na₂CO₃. Phases were separated, and the aqueous phase was extracted with 20 mL portions of ether three times. Organic phases were combined and washed with 10 mL brine, dried with anhydrous magnesium sulfate, filtered to remove solids, and concentrated *in vacuo*. The crude yellow oil was moved forward without further purification.⁷¹

N-Acetyl morpholine (**2.13**; 0.41 mL, 3.56 mmol) was dissolved in 15 mL dry THF in a dry flask under N₂ before cooling to -40 °C (MeCN/CO₂). LiHMDS (1.0 M in THF, 3.7 mL, 3.7 mmol) was added dropwise down the side of the vial over 3 min, then the reaction mixture was allowed to stir at -40 °C for 1.5 hr. Freshly prepared allylic bromide from above (assumed 2.37 mmol) was dissolved in 1.0 mL dry THF in a separate vial under nitrogen. The bromide solution was transferred into the enolate solution via syringe down the side of the flask over 15 s; the transfer was quantified with two 1.0 mL portions of dry THF. The reaction was allowed to slowly warm to room temp over the course of 4.5 hrs. The reaction was quenched by pouring into 40 mL of 1:1 sat. NaHCO₃:sat. Na₂S₂O₃, then was diluted with 40 mL ether. The phases were separated, and the aqueous phase was extracted with 40 mL portions of ether three times. The combined organics were washed with 20 mL brine, dried over magnesium sulfate, filtered to remove solids,

and concentrated *in vacuo*. The crude residue was purified via flash chromatography over silica (30 to 100% ethyl acetate:hexanes, increasing in 10% increments; loaded residue with PhMe).

Obtained 281 mg of morphamide **2.95** as a white solid (49.5% over two steps)

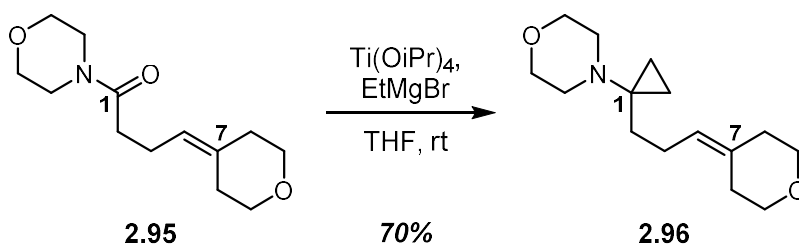
¹H NMR (CDCl₃, 500 MHz): δ = 5.22-5.18 (m, 1H, C4), 3.69-3.60 (m, 10H, morph. [6H], THP [4H]), 3.48-3.44 (m, 2H, morph.), 2.39-2.32 (m, 4H, THP), 2.29 (t, 2H, *J* = 5.5 Hz, C2), 2.20 (t, 2H, *J* = 5.4 Hz, C3) ppm

¹³C NMR (CDCl₃, 176 MHz): δ = 171.3, 135.8, 121.7, 69.7, 68.9, 67.1, 66.8, 46.1, 42.1, 37.0, 33.3, 29.9, 22.8 ppm

IR (neat): 2956, 2848, 1639, 1429, 1271, 1227, 1113, 1097, 1069, 1021, 845, 665 cm⁻¹

HRMS (ES⁺, *m/z*) calculated for C₁₃H₂₂NO₃⁺: 240.1594, Found: 240.1596

R_f = 0.15 (80% EtOAc in hexanes), one yellow spot, KMnO₄



The C1 morphamide **2.95** (305 mg, 1.27 mmol) was dissolved in 20 mL dry THF under inert atmosphere, followed by addition of titanium isopropoxide (0.42 mL, 1.40 mmol). The reaction vessel was submerged in a water bath at ambient temp to serve as a heat sink. Ethylmagnesium bromide (1.0 M in THF, 4.5 mL, 4.5 mmol) was added dropwise via syringe over the course of 5 min. A vent line was added to account for gas evolution (note: gas evolution can be quite vigorous along with substantial heat generation if addition is too rapid). Reaction mixture (clear, colorless at outset of addition) undergoes a series of color changes, first turning a bright yellow with initial drops, then transitioning to orange and red hues, and ultimately turning a dark red-brown (almost black) upon complete addition of EtMgBr. Vent line was removed, and the reaction mixture was stirred at room temp for 50 min. An aqueous solution containing 75 mL sat. Rochelle salt, 25 mL brine, and 2 mL of 50% NaOH was prepared. The reaction was quenched with 50 mL of this aqueous mixture, and stirred vigorously for 30 min. The mixture was then diluted with the remainder of the quenching solution and 100 mL ether. The phases were separated. The aqueous phase was extracted with 100 mL portions of ether three times. The combined organics were then washed with 100 mL brine, dried over anhydrous magnesium sulfate, filtered to remove solids, and concentrated *in vacuo*. The crude residue was purified via flash chromatography over silica (15 to 25 to 40 to 60% ethyl acetate:hexanes; the residue was loaded with PhMe). Collected aminoCP **2.96** in two portions. The central fractions afforded 74.2 mg as clear, colorless oil, while the shoulder fractions totaled 184 mg of a yellow liquid. The latter was exposed to a second round of chromatography (20 to 35 to 50 to 60% ethyl acetate:hexanes; the

residue was loaded with PhMe), ultimately yielding 150.5 mg of pure material. Total yield of aminoCP **2.96**: 223 mg (69.9% yield).

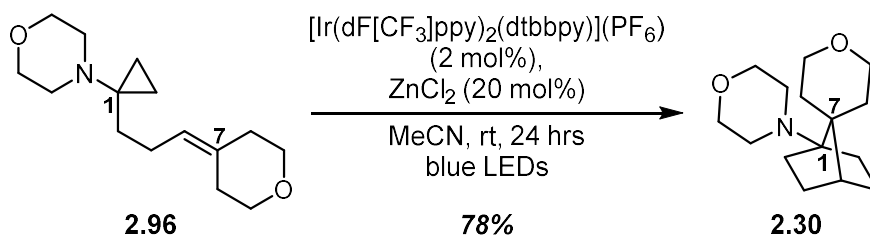
¹H NMR (CDCl₃, 500 MHz): δ = 5.14 (t, 1H, J = 7.1 Hz, C4), 3.68-3.63 (m, 4H, THP), 3.63-3.59 (m, 4H, morph.), 2.67-2.64 (m, 4H, morph.), 2.25 (t, 2H, J = 5.4 Hz, C3), 2.18 (t, 2H, J = 5.4 Hz, C2), 1.99-1.93 (m, 2H, THP), 1.57-1.53 (m, 2H, THP), 0.56-0.53 (m, 2H, CP), 0.45-0.42 (m, 2H, CP) ppm

¹³C NMR (CDCl₃, 126 MHz): δ = 134.2, 123.4, 69.8, 68.9, 67.9, 49.9, 44.2, 37.0, 30.5, 29.9, 24.9, 12.9 ppm

IR (neat): 2950, 2846, 1450, 1371, 1264, 1227, 1115, 1099, 1010, 985, 854, 662 cm⁻¹.

HRMS (ES⁺, m/z) calculated for C₁₅H₂₆NO₂⁺: 252.1958, Found: 252.1962

R_f = 0.55 (80% EtOAc in hexanes), one yellow spot, KMnO₄



In a dry vial under nitrogen, aminoCP **2.96** (75.0 mg, 298 μmol) was dissolved in 3.0 mL dry MeCN before adding $[\text{Ir}(\text{dF}[\text{CF}_3]\text{ppy})_2(\text{dtbbpy})](\text{PF}_6)$ (6.7 mg, 6.0 μmol) then ZnCl_2 (1.0 M in ether, 60 μL , 60 μmol) in one portion each. Reaction mixture was bright yellow and slightly cloudy. Reaction mixture was degassed with three freeze-pump-thaw cycles. The reaction was performed by stirring at room temp (as controlled with jacketed water bath, temp maintained between 18-23 $^\circ\text{C}$) while irradiating with two strips of 4.4 W blue LEDs for 24 hrs. Mixture was somewhat orange and still only slightly cloudy. The mixture was added to 10 mL 1:1 sat. NaHCO_3 :water containing 0.5 mL of 50% NaOH to ensure aq phase pH \sim 14, then diluted further with 10 mL ether. Phases were separated, and the aqueous phase was extracted with 10 mL portions of ether three times. Combined organics were washed with 10 mL brine, dried over anhydrous magnesium sulfate, filtered to remove solids, and concentrated *in vacuo*. The crude residue was purified via flash chromatography over silica (20 to 30 to 40 to 60 to 80 to 100(5x)% ethyl acetate:hexanes; residue loaded with PhMe); product eluted very slowly, thus another solvent system may be more optimal; product required trituration from 50% ether:hexanes and filtration through plug of celite to remove co-eluted catalyst-derived degradation products. Collected the following:

- Recovered starting material: 9.1 mg; clear, colorless oil; 12.1% recovery
- Product: 58.2 mg; off-white solid; 77.6% yield, 88.3% BORSM; of note, product can be recrystallized from 50% ether:pentane to afford white, needle-like crystals

¹H NMR (C₆D₆, 700 MHz): δ = 3.86 (dd, 2H, *J* = 11.2, 4.2 Hz, THP), 3.62-3.59 (m, 4H, morph.), 3.38 (t, 2H, *J* = 11.9 Hz, THP), 2.40-2.37 (m, 4H, morph.), 1.97 (t, 1H, *J* = 4.5 Hz, C4), 1.72 (td, 2H, *J* = 13.0, 4.4 Hz, THP), 1.62-1.55 (m, 2H, C3, C5), 1.49-1.42 (m, 2H, C2, C6), 1.16-1.12 (m, 2H, C2, C6), 1.15-1.11 (m, 2H, THP), 1.06-1.01 (m, 2H, C3, C5) ppm

¹³C NMR (C₆D₆, 176 MHz): δ = 70.7, 68.0, 66.1, 50.9, 50.6, 36.8, 30.3, 28.4, 27.0 ppm

IR (neat): 2959, 2845, 2228, 2049, 1453, 1277, 1143, 1116, 1068, 942, 882, 833, 695 cm⁻¹

HRMS (ES⁺, *m/z*) calculated for C₁₅H₂₆NO₂⁺: 252.1958, Found: 252.1962

R_f = 0.55 (60% EtOAc in hexanes), one yellow spot, KMnO₄

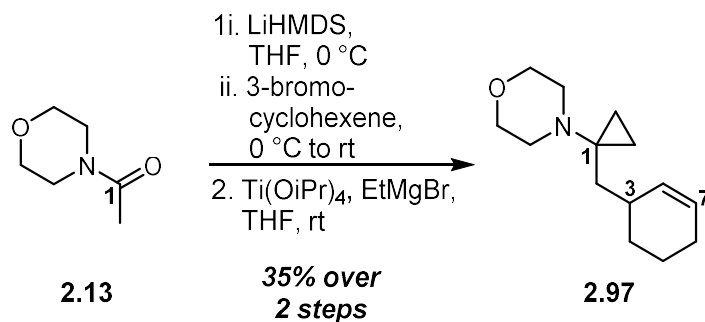
Additional Trials

12-hr irradiation trial

Following the general procedure outlined above, 63.4 mg of aminoCP **1p** (252 μmol) were dissolved in 2.5 mL dry MeCN along with 5.7 mg of [Ir(dF[CF₃]ppy)₂(dtbbpy)](PF₆) (5.0 μmol) and 50 μL ZnCl₂ (1.0 M in ether; 50 μmol) prior to irradiating for 12 hrs. Isolation provided the following:

- Recovered starting material: 16.8 mg; slightly yellow oil; 26.5% recovery
- Product: 39.2 mg; white solid that was recrystallized to white needles; 61.8% yield, 84.1%

BORSM



N-Acetyl morpholine (**2.13**; 250 mg, 1.94 mmol) was dissolved in 5.0 mL dry THF in a dry flask under N₂ before cooling to 0 °C (ice/water). LiHMDS (1.0 M in THF, 2.0 mL, 2.0 mmol) was added dropwise down the side of the vial over 2 min, then the reaction mixture was allowed to stir at 0 °C for 75 min. In a separate dry flask kept under inert atmosphere, 3-bromocyclohexene (0.30 mL, 2.61 mmol) was dissolved in 2 mL dry THF. The enolate solution was then cannulated into the bromide solution slowly down the side of the vial over the course of 105 min. Transfer was quantified with two rinses of 0.5 mL dry THF. The mixture was stirred at room temp for 30 min before quenching with 15 mL 1:1 sat. NaHCO₃:sat. Na₂S₂O₃. Mixture was diluted with 15 mL ether, and the phases were separated. The aqueous phase was then extracted with 15 mL portions of ether three times. Combined organics were washed with 15 mL brine, dried over anhydrous magnesium sulfate, filtered, and concentrated *in vacuo* to afford a slightly yellow oil. This crude residue was purified by flash chromatography over silica (10 to 60% ethyl acetate:hexanes, increasing in 10% increments; residue was loaded with PhMe). The desired mono-alkylated product was afforded as a white solid (190 mg, 46.9% yield).

¹H NMR (CDCl₃, 500 MHz): δ = 5.75-5.69 (m, 1H, vinyl-H), 5.60-5.54 (m, 1H, vinyl-H), 3.71-3.58 (m, 6H, morph.), 3.52-3.45 (m, 2H, morph.), 2.70-2.68 (m, 1H, C3), 2.34-2.24 (m, 2H, C2), 2.01-1.95 (m, 2H, bridge), 1.90-1.83 (m, 1H, bridge), 1.74-1.66 (m, 1H, bridge), 1.63-1.53 (m, 1H, bridge), 1.32-1.23 (m, 1H, bridge) ppm

R_f = 0.50 (60% EtOAc in hexanes), one yellow spot, KMnO₄

The amide from above (125 mg, 0.60 mmol) was dissolved in 10 mL dry THF under inert atmosphere, followed by addition of titanium isopropoxide (0.20 mL, 0.66 mmol). The reaction vessel was submerged in a water bath at ambient temp to serve as a heat sink. Ethylmagnesium bromide (1.0 M in THF, 2.1 mL, 2.1 mmol) was added dropwise via syringe over the course of 4 min. A vent line was added to account for gas evolution (note: gas evolution can be quite vigorous along with substantial heat generation if addition is too rapid). Reaction mixture (clear, colorless at outset of addition) undergoes a series of color changes, first turning a bright yellow with initial drops, then transitioning to orange and red hues, and ultimately turning a dark red-brown (almost black) upon complete addition of EtMgBr. Vent line was removed, and the reaction mixture was stirred at room temp for 1 hr. An aqueous quench was prepared from 30 mL sat. Rochelle salt, 10 mL brine, and 2 mL 50% NaOH. The reaction was quenched with 10 mL of this solution and stirred vigorously for 15 min. The mixture was then diluted with the remaining quenching solution and 20 mL ether. Phases were separated. The aqueous phase was extracted with 20 mL portions of ether three times. The combined organics were then washed with 20 mL brine, dried over anhydrous magnesium sulfate, filtered to remove solids, and concentrated *in vacuo*. The crude residue was purified via flash chromatography over silica (5 to 25% ethyl acetate, increasing in 5% increments, residue was loaded with PhMe). Collected the aminoCP **2.97** in two portions; the center fractions afforded 58.1 mg of a clear, colorless oil, and the shoulder fractions yielded 41.2 mg of a slightly yellow oil. Both fractions were clean by ¹H NMR, bringing the total yield of aminoCP **2.97** to 99.3 mg (75.1%; 35.2% over 2 steps).

¹H NMR (CDCl₃, 500 MHz): δ = 5.65-5.62 (m, 2H, C4, C7), 3.63-3.59 (m, 4H, morph.), 2.66-2.62 (m, 4H, morph.), 2.20-2.13 (m, 1H, C3), 1.99-1.93 (m, 2H, bridge), 1.84-1.77 (m, 1H, C2),

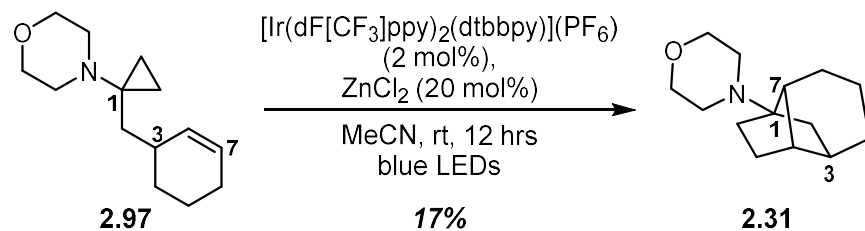
1.72-1.65 (m, 1H, C2), 1.56-1.43 (m, 3H, bridge), 1.27-1.19 (m, 1H, bridge), 0.64-0.57 (m, 2H, CP), 0.44-0.36 (m, 2H, CP) ppm

¹³C NMR (CDCl₃, 176 MHz): δ = 132.4, 126.9, 67.9, 49.5, 42.3, 38.3, 33.2, 30.2, 25.5, 21.5, 12.9, 12.8 ppm

IR (neat): 2919, 2850, 1448, 1264, 1116, 1012, 987, 857, 720, 675 cm⁻¹

HRMS (ES⁺, *m/z*) calculated for C₁₄H₂₄NO⁺: 222.1852, Found: 222.1855

R_f = 0.45 (30% EtOAc in hexanes), one yellow spot, KMnO₄



In a dry vial under nitrogen, aminoCP **2.97** (57.5 mg, 260 μmol) was dissolved in 2.6 mL dry MeCN before adding $[\text{Ir}(\text{dF}[\text{CF}_3]\text{ppy})_2(\text{dtbbpy})](\text{PF}_6)$ (5.8 mg, 5.2 μmol) then ZnCl_2 (1.0 M in ether, 52 μL , 52 μmol) in one portion each. Reaction mixture was bright yellow and slightly cloudy. Reaction mixture was degassed with three freeze-pump-thaw cycles. The reaction was performed by stirring at room temp (as controlled with jacketed water bath, temp maintained between 18-23 $^\circ\text{C}$) while irradiating with two strips of 4.4 W blue LEDs for 12 hrs. Mixture was clear, dark yellow-green with dark grey precipitate. The mixture was added to 10 mL 1:1 sat. NaHCO_3 :water containing 0.5 mL of 50% NaOH to ensure aq phase pH \sim 14, then diluted further with 10 mL ether. Phases were separated, and the aqueous phase was extracted with 10 mL portions of ether three times. Combined organics were washed with 10 mL brine, dried over anhydrous magnesium sulfate, filtered to remove solids, and concentrated *in vacuo*. The crude residue was purified via flash chromatography over silica (3 to 6 to 9 to 12 to 16 to 20 to 25 to 40% ethyl acetate:hexanes; residue loaded with PhMe). Collected the following:

- Recovered starting material: obtained 30.6 mg of an \sim 4:1 mix of the starting material with what is expected to be the C1 ethyl ketone byproduct; \sim 26 mg recovered, \sim 45% recovery
- Product: 9.5 mg; slightly yellow oil; 16.5% yield

$^1\text{H NMR}$ (C_6D_6 , 700 MHz): δ = 3.67 (*app.* t, 4H, J = 4.5 Hz, morph.), 2.38 (dt, 2H, J = 11.2, 4.4 Hz, morph.), 2.27 (dt, 2H, J = 11.4, 4.6 Hz, morph.), 1.87 (br s, 1H, C3), 1.76-1.68 (m, 1H, C9), 1.67-1.62 (m, 1H, C10), 1.56-1.50 (m, 1H, C5-eq), 1.48 (d, 1H, J = 5.1 Hz, C4), 1.45 (br s, 1H, C7), 1.44-1.40 (m, 3H, C8, C8, C10), 1.40-1.33 (m, 3H, C6-eq, C9, C2), 1.27 (dd, 1H, J = 11.8,

8.0 Hz, C2), 1.12 (ddd, 1H, $J = 12.1, 9.5, 5.6$ Hz, C5-ax), 0.97 (td, 1H, $J = 10.4, 2.6$ Hz, C6-ax) ppm

^{13}C NMR (C_6D_6 , 176 MHz): $\delta = 71.9$ (C1), 67.8 (morph.), 49.0 (morph.), 44.8 (C7), 43.4 (C4), 39.9 (C3), 37.4 (C2), 30.7 (C8), 26.5 (C5), 25.3 (C6), 23.4 (C10), 17.9 (C9) ppm

IR (neat): 2929, 2847, 1449, 1329, 1278, 1249, 1152, 1117, 1037, 910, 888 cm^{-1}

HRMS (ES⁺, m/z) calculated for $\text{C}_{14}\text{H}_{24}\text{NO}^+$: 222.1852, Found: 222.1853

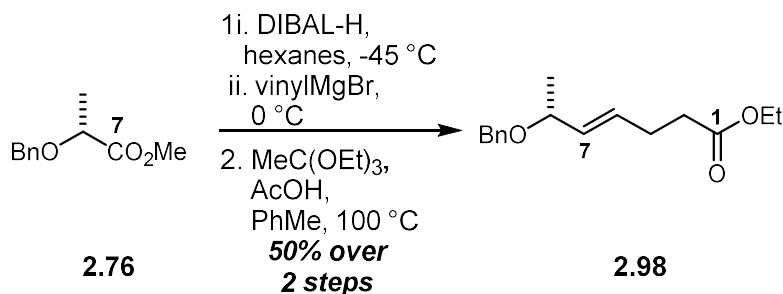
$R_f = 0.20$ (20% EtOAc in hexanes), one yellow spot, KMnO_4

Additional Trials

24-hr extended irradiation trial

Following the general procedure outlined above, 65.4 mg of aminoCP **1k** (295 μmol) were dissolved in 2.8 mL dry MeCN along with 6.6 mg of $[\text{Ir}(\text{dF}[\text{CF}_3]\text{ppy})_2(\text{dtbbpy})](\text{PF}_6)$ (5.9 μmol) and 59 μL ZnCl_2 (1.0 M in ether; 59 μmol) prior to irradiating for 24 hrs. Isolation provided the following:

- Recovered starting material: obtained 24.2 mg of starting material mixed with an unknown byproduct (estimated 4:3 molar ratio if the materials are isomeric)
- Product: 11.2 mg; clear, colorless oil; 17.1% yield



Benzyl-protected methyl (*R*)-lactate (**2.76**; 3.1 g, 16.0 mmol) was dissolved in 25 mL dry hexanes in a dry flask under nitrogen, then cooled to -45 °C (MeCN/CO₂). DIBAL (1.0 M in CH₂Cl₂, 17.6 mL, 17.6 mmol) was added dropwise down the side of the flask over 3 min via syringe. The mixture was stirred at -45 °C for 3 hrs before warming to 0 °C. Vinylmagnesium bromide (1.0 M in THF, 20.0 mL, 20.0 mmol) was added dropwise down the side of the flask over 3 min, followed by stirring for an additional 30 min at 0 °C then 1.5 hrs at room temp. The reaction mixture was then quenched with 100 mL of 3:1 sat. Rochelle salt with water + 5 mL 50% NaOH; the resultant biphasic mixture was stirred vigorously for 15 min. The mixture was diluted with 200 mL ether then another 100 mL of the same aqueous quenching solution. The phases were separated, and the aqueous phase was extracted with 200 mL portions of ether three times. The combined organics were washed with 150 mL brine, dried over anhydrous sodium sulfate, filtered to remove solids, and concentrated *in vacuo*. The crude residue was purified by flash chromatography over silica (6 to 30% ethyl acetate:hexanes, increasing in 6% increments; residue loaded with PhMe). Obtained 1.76 g of a slightly yellow liquid, determined to be a 4:1 mix of epimers by ¹H NMR (57.2% combined yield). As both isomers proceed to the same product in the subsequent Johnson-Claisen rearrangement, this mixture was moved forward without separating the diastereomers. The ¹H NMR line-listings are provided below (isomers are listed separately for clarity).

¹H NMR - major (CDCl₃, 500 MHz): δ = 7.38-7.32 (m, 4H, Ph), 7.32-7.29 (m, 1H, Ph), 5.86-5.81 (m, 1H, C4), 5.37 (d, 1H, *J* = 17.4 Hz, C3), 5.23 (d, 1H, *J* = 11.1 Hz, C3), 4.68 (d, 1H, *J* = 11.9 Hz, benzyl CH₂), 4.48 (d, 1H, *J* = 11.9 Hz, benzyl CH₂), 3.97-3.94 (m, 1H, C7), 3.44 (dquart., 1H, *J* = 13.3, 6.8 Hz, C8), 2.74 (d, 1H, *J* = 3.1 Hz, C4-OH), 1.20 (d, 1H, *J* = 5.8 Hz, C8-Me) ppm

¹H NMR - minor (CDCl₃, 500 MHz): δ = 7.38-7.32 (m, 4H, Ph), 7.32-7.29 (m, 1H, Ph), 5.89-5.84 (m, 1H, C4), 5.32 (d, 1H, *J* = 18.2 Hz, C3), 5.21 (d, 1H, *J* = 11.1 Hz, C3), 4.64 (d, 1H, *J* = 11.9 Hz, benzyl CH₂), 4.54 (d, 1H, *J* = 11.9 Hz, benzyl CH₂), 4.27-4.23 (m, 1H, C7), 3.62 (dquart., 1H, *J* = 13.1, 3.6 Hz, C8), 2.20 (d, 1H, *J* = 4.6 Hz, C4-OH), 1.16 (d, 1H, *J* = 6.3 Hz, C8-Me) ppm

R_f = 0.25 (20% EtOAc in hexanes), one grey-purple spot, *p*-anisaldehyde + UV

The mixture of allylic alcohols from above (1.76 g, 9.15 mmol) were dissolved in 9 mL dry PhMe while transferring to a microwave vial flushed with Ar. Triethyl orthoacetate (4.2 mL, 22.9 mmol) and glacial acetic acid (0.26 mL, 4.58 mmol) were each added in one portion, respectively. The vial was flushed with Ar, capped, and then irradiated in a Biotage Initiator+ microwave reactor for 2 hrs at 150 °C. TLC analysis revealed complete consumption of the starting material. The reaction mixture was quenched by pouring into 200 mL sat. NaHCO₃, then diluted with 200 mL ether; the phases were separated. The aqueous phase was extracted with 100 mL portions of ether three times. The combined organics were washed with 100 mL brine, dried over anhydrous magnesium sulfate, filtered to remove solids, and concentrated *in vacuo*. The crude residue was purified by flash chromatography over silica (2.5 to 12.5% ethyl acetate:hexanes, increasing in 2.5% increments; residue was loaded with PhMe). Obtained 2.11 g of C1 ethyl ester **2.98** as a slightly yellow liquid (87.9%, 50.3% over two steps).

¹H NMR (CDCl₃, 700 MHz): δ = 7.35-7.31 (m, 4H, Ph), 7.27-7.24 (m, 1H, Ph), 5.83 (dt, 1H, *J* = 15.7, 6.5 Hz, C4), 5.45 (dd, 1H, *J* = 15.3, 8.0 Hz, C7), 4.53 (d, 1H, *J* = 11.8 Hz, benzyl CH₂), 4.35 (d, 1H, *J* = 11.9 Hz, benzyl CH₂), 4.13 (quart., 2H, *J* = 7.1 Hz, CO₂Et), 3.88 (dq, 1H, *J* = 7.2, 6.1 Hz, C8), 2.43-2.37 (m, 4H, C2, C3), 1.26 (d, 3H, *J* = 6.3 Hz, C8-Me), 1.25 (t, 3H, *J* = 7.0 Hz, CO₂Et) ppm

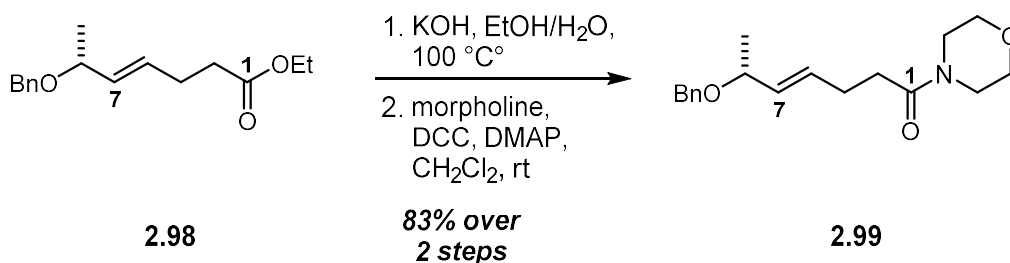
¹³C NMR (CDCl₃, 176 MHz): δ = 173.1, 139.0, 133.3, 130.9, 128.5, 127.8, 127.5, 75.7, 69.9, 60.5, 34.1, 27.6, 21.8, 14.4 ppm

IR (neat): 2979, 1732, 1453, 1370, 1244, 1168, 1145, 1089, 1071, 1028, 970, 734, 697 cm⁻¹

HRMS (ES⁺, *m/z*) calculated for C₁₆H₂₆NO₃⁺ (ammonium adduct): 280.1907, Found: 280.1915

[α]_D^{26.2 °C} = +6.0 ± 0.3° (*c* = 0.3, CH₂Cl₂)

R_f = 0.45 (20% EtOAc in hexanes), one blue-green spot, *p*-anisaldehyde + UV



C1 ethyl ester **2.98** (2.09 g, 7.97 mmol) was dissolved in 15 mL 200 proof EtOH under Ar. In a separate flask, KOH (4.15 g, 79.7 mmol) was dissolved in 60 mL HPLC-grade water, then poured into the ethanolic solution slowly (swirling to mix) over the course of 2 min. A reflux condenser was attached, and the system was flushed with Ar before heating to 95 °C for 4 hrs. After cooling back to room temp., the reaction mixture was quenched by pouring slowly into 100 mL 1 M HCl. The mixture was diluted with 100 mL CH₂Cl₂, and the phases were separated. The aqueous phase pH was determined to be between 1 and 2. The aqueous phase was further extracted with 100 mL portions of CH₂Cl₂ three times. The combined organic phases were washed with 100 mL brine, dried over anhydrous magnesium sulfate, filtered to remove solids, and concentrated *in vacuo*. ¹H NMR of the crude residue revealed nearly pure carboxylic acid, the line-listings for which are provided below. This material was moved on without further purification.

¹H NMR (CDCl₃, 500 MHz): δ = 7.35-7.31 (m, 4H, Ph), 7.29-7.24 (m, 1H, Ph), 5.64 (dt, 1H, *J* = 15.4, 6.4 Hz, C4), 5.48 (dd, 1H, *J* = 15.7, 7.6 Hz, C7), 4.53 (d, 1H, *J* = 12.2 Hz, benzyl CH₂), 4.36 (d, 1H, *J* = 12.2 Hz, benzyl CH₂), 3.89 (*app.* quint., 1H, *J* = 6.4 Hz, C8), 2.48-2.36 (m, 4H, C3, C2), 1.26 (d, 3H, *J* = 6.4 Hz, C8-Me) ppm

R_f = 0.05 (20% EtOAc in hexanes), one bright blue spot, *p*-anisaldehyde + UV

The crude carboxylic acid from above (~7.9 mmol) was dissolved in 40 mL dry CH₂Cl₂ in a dry flask under inert atmosphere. DMAP (1.22 g, 10. mmol), morpholine (0.87 mL, 10. mmol),

and DCC (2.06 g, 10. mmol) were each added in one portion each, respectively. This mixture was stirred at room temp for 12 hrs, at which point the original clear solution had become cloudy with a white precipitate. The reaction mixture was concentrated to approximately half the volume under a stream of nitrogen before diluting with 20 mL 10% ether in hexanes. This mixture was filtered through a pad of celite to remove the bulk of the dicyclohexyl urea byproduct, eluting the desired product with 100 mL 10% ether in hexanes. This was concentrated to a crude residue which was purified by flash chromatography over silica (30 to 40 to 50 to 65 to 80% ethyl acetate:hexanes; residue was loaded with PhMe). This afforded the C1 morphamide **2.99** as a clear, colorless oil (2.00 g; 82.7% over two steps).

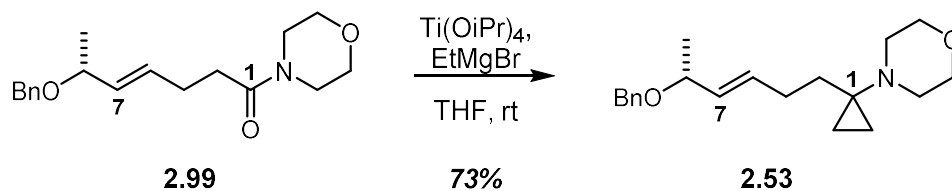
¹H NMR (CDCl₃, 700 MHz): δ = 7.34-7.30 (m, 4H, Ph), 7.27-7.24 (m, 1H, Ph), 5.71-5.65 (m, 1H, C4), 5.45 (dd, 1H, J = 15.4, 7.8 Hz, C7), 4.53 (d, 1H, J = 11.9 Hz, benzyl CH₂), 4.37 (d, 1H, J = 11.9 Hz, benzyl CH₂), 3.89 (*app.* quint., 1H, J = 6.6 Hz, C8), 3.68-3.64 (m, 4H, morph.), 3.63-3.60 (m, 2H, morph.), 3.48-3.44 (m, 2H, morph.), 2.43-2.37 (m, 4H, C2, C3), 1.26 (d, 3H, J = 6.3 Hz, C8-Me) ppm

¹³C NMR (CDCl₃, 176 MHz): δ = 171.0, 139.1, 133.1, 131.3, 128.5, 127.8, 127.5, 75.7, 69.9, 67.1, 66.8, 46.1, 42.1, 32.8, 27.8, 21.7 ppm

IR (neat): 2855, 1645, 1433, 1271, 1115, 1070, 971, 740, 698 cm⁻¹

HRMS (ES⁺, m/z) calculated for C₁₈H₂₅NNaO₃⁺: 326.1727, Found: 326.1729

R_f = 0.20 (60% EtOAc in hexanes), one bright blue spot, *p*-anisaldehyde + UV



The C1 morphamide **2.99** (1.99 g, 6.56 mmol) was dissolved in 130 mL dry THF under inert atmosphere, followed by addition of titanium isopropoxide (2.1 mL, 7.2 mmol). The reaction vessel was submerged in a water bath at ambient temp to serve as a heat sink. Ethylmagnesium bromide (1.0 M in THF, 23.0 mL, 23.0 mmol) was added dropwise via syringe over the course of 10 min. A vent line was added to account for gas evolution (note: gas evolution can be quite vigorous along with substantial heat generation if addition is too rapid). Reaction mixture (clear, colorless at outset of addition) undergoes a series of color changes, first turning a bright yellow with initial drops, then transitioning to orange and red hues, and ultimately turning a dark red-brown (almost black) upon complete addition of EtMgBr. Vent line was removed, and the reaction mixture was stirred at room temp for 50 min. An aqueous solution containing 150 mL sat. Rochelle salt, 50 mL brine, and 10 mL of 50% NaOH was prepared. The reaction was quenched with 100 mL of this aqueous mixture, and stirred vigorously for 15 min. The mixture was then diluted with the remainder of the quenching solution and 200 mL ether. The phases were separated. The aqueous phase was extracted with 200 mL portions of ether three times. The combined organics were then washed with 100 mL brine, dried over anhydrous magnesium sulfate, filtered to remove solids, and concentrated *in vacuo*. The crude residue was purified via flash chromatography over silica (2 to 4 to 8 to 12 to 18 to 24% ethyl acetate:hexanes; the residue was loaded with PhMe). Collected aminoCP **1s** in two portions. The central fractions afforded 513 mg as clear, colorless liquid, while the shoulder fractions totaled 992 mg of a faintly yellow liquid. Both portions were pure by ^1H NMR, bringing the total yield of aminoCP **2.100** to 1.51 g (72.7% yield).

¹H NMR (CDCl₃, 500 MHz): δ = 7.34-7.31 (m, 4H, Ph), 7.29-7.24 (m, 1H, Ph), 5.59 (dt, 1H, *J* = 15.2, 6.6 Hz, C4), 5.38 (dd, 1H, *J* = 15.5, 7.8 Hz, C7), 4.54 (d, 1H, *J* = 12.2 Hz, benzyl CH₂), 4.37 (d, 1H, *J* = 12.0 Hz, benzyl CH₂), 3.87 (*app.* quint., 1H, *J* = 6.7 Hz, C8), 3.61 (*app.* t, 4H, *J* = 4.2 Hz, morph.), 2.66 (*app.* t, 4H, *J* = 4.9 Hz, morph.), 2.06-1.99 (m, 2H, C3), 1.62 (*app.* t, 2H, *J* = 8.6 Hz, C2), 1.26 (d, 3H, *J* = 6.4 Hz, C8-Me), 0.57-0.54 (m, 2H, CP), 0.46-0.42 (m, 2H, CP) ppm

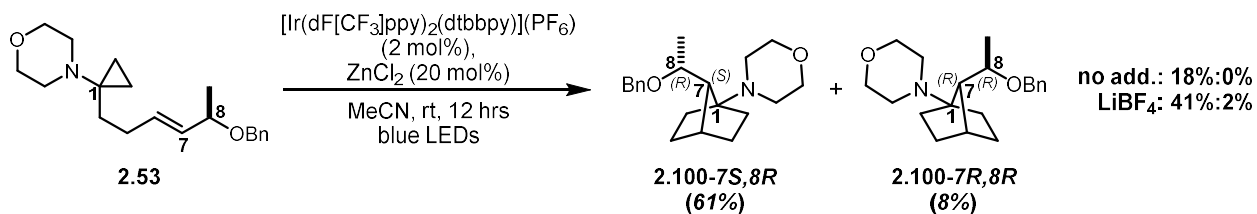
¹³C NMR (CDCl₃, 126 MHz): δ = 139.1, 133.0, 132.0, 128.5, 127.8, 127.5, 75.9, 69.8, 67.9, 49.8, 44.0, 30.1, 29.8, 21.8, 12.9, 12.9 ppm

IR (neat): 2928, 2851, 1671, 1451, 1371, 1264, 1115, 1089, 1069, 969, 856, 733, 696 cm⁻¹

HRMS (ES⁺, *m/z*) calculated for C₂₀H₃₀NO₂⁺: 316.2271, Found: 316.2283

$[\alpha]_{\text{D}}^{26.4\text{ }^{\circ}\text{C}} = 8.6 \pm 0.1^{\circ}$ (*c* = 0.5, CH₂Cl₂)

R_f = 0.30 (20% EtOAc in hexanes), one bright blue spot, *p*-anisaldehyde + UV



In dry vial under nitrogen, aminoCP **2.53** (80.2 mg, 254 μmol) was dissolved in 2.5 mL dry MeCN before adding $[\text{Ir}(\text{dF}[\text{CF}_3]\text{ppy})_2(\text{dtbbpy})](\text{PF}_6)$ (5.7 mg, 5.1 μmol) then ZnCl_2 (1.0 M in ether, 51 μL , 51 μmol) in one portion each. Reaction mixture is bright yellow, but slightly cloudy from the Zn salt. Reaction mixture was degassed with three freeze-pump-thaw cycles. The reaction was performed by stirring at room temp (as controlled with jacketed water bath, temp maintained between 18-23 $^\circ\text{C}$) while irradiating with two strips of 4.4 W blue LEDs for 12 hrs. Mixture appears the same as it did prior to irradiation. The mixture was added to 10 mL 1:1 sat bicarb:water containing 1 mL of 50% NaOH to ensure aq phase pH \sim 14, then diluted further with 5 mL hexanes and 5 mL ether. Phases were separated, and the aqueous phase was extracted with 10 mL 1:1 ether:hexanes three times. Combined organics were washed with 10 mL brine, dried over anhydrous sodium sulfate, filtered to remove solids, and concentrated *in vacuo*. The crude residue was purified via flash chromatography (10 to 15 to 20 to 30 to 50 to 70 to 90% ethyl acetate:hexanes + 0.1% NEt_3 ; residue loaded with PhMe), providing the minor isomer cleanly. A number of fraction had overlapped starting material and major isomer, and these were exposed to a second round of chromatography (10 to 20 to 30 to 40 to 60 to 90% ethyl acetate:hexanes + 0.1% NEt_3 ; residue loaded with PhMe), though this still did not remove all of the major isomer from the starting material.

- GCMS conversion: *[data not collected]*

- Recovered starting material: 19.9 mg; clear, colorless oil; ^1H NMR revealed a 4:1 mix with the major isomer **2.100-7S,8R**, \sim 20% recovery

- *7S,8R*-Isomer (**2.100-7S,8R**): 48.8 mg; yellow oil; 60.8% yield

- *7R,8R*-Isomer (**2.100-7R,8R**): 6.1 mg; clear, colorless oil; 7.6% yield

Characterization Data for **2.100-7S,8R**

¹H NMR (CDCl₃, 700 MHz): δ = 7.38 (d, 2H, *J* = 7.5 Hz, Ph), 7.31 (t, 2H, *J* = 7.7 Hz, Ph), 7.24 (t, 1H, *J* = 7.5 Hz, Ph), 4.65 (d, 1H, *J* = 11.8 Hz, benzyl CH₂), 4.63 (d, 1H, *J* = 11.8 Hz, benzyl CH₂), 3.58-3.49 (m, 5H, morph., C8), 2.75 (br s, 2H, morph.), 2.55-2.49 (m, 2H, morph.), 1.91 (br s, 1H, C4), 1.87 (d, 1H, *J* = 8.5 Hz, C7), 1.80 (*app.* t, 1H, *J* = 13.3 Hz, C6-*eq*), 1.66-1.60 (m, 4H, C3-*eq*, C2-*ax*, C5-*eq*, C2-*eq*), 1.37-1.33 (m, 1H, C3-*ax*), 1.30 (ddd, 1H, *J* = 12.1, 9.9, 4.3 Hz, C5-*ax*), 1.20 (ddd, 1H, *J* = 11.4, 10.0, 4.4 Hz, C6-*ax*), 1.16 (d, 3H, *J* = 6.1 Hz, C8-Me) ppm

¹³C NMR (CDCl₃, 126 MHz): δ = 139.7 (Ph), 128.3 (Ph), 127.5 (Ph), 127.2 (Ph), 73.6 (C8), 72.0 (C1), 71.5 (benzyl CH₂), 67.8 (morph.), 55.3 (C7), 49.0 (morph.), 37.3 (C4), 33.4 (C2), 28.9 (C5), 28.1 (C3), 23.5 (C6), 19.0 (C8-Me) ppm

IR (thin film): 2953, 2871, 1450, 1372, 1328, 1277, 1448, 1241, 1182, 1116, 1068, 1028, 897, 861, 734, 696 cm⁻¹

HRMS (ES⁺, *m/z*) calculated for C₂₀H₃₀NO₂⁺: 316.2271, Found: 316.2285

R_f = 0.05 (70% EtOAc in hexanes), one blue spot, Hanessian's stain

Characterization Data for **2.100-7R,8R**

¹H NMR (CDCl₃, 700 MHz): δ = 7.36-7.31 (m, 4H, Ph), 7.28-7.25 (m, 1H, Ph), 4.64 (d, 1H, *J* = 11.4 Hz, benzyl CH₂), 4.37 (d, 1H, *J* = 11.4 Hz, benzyl CH₂), 3.70-3.64 (m, 4H, morph.), 3.48-3.43 (m, 1H, C8), 2.58-2.54 (m, 2H, morph.), 2.53-2.48 (m, 2H, morph.), 2.33 (t, 1H, *J* = 4.6 Hz, C4), 1.81 (*app.* t, 1H, *J* = 12.6 Hz, C6-*eq*), 1.77 (d, 1H, *J* = 10.0 Hz, C7), 1.75-1.70 (m, 1H, C3-

eq), 1.60-1.55 (m, 1H, C5-eq), 1.55-1.52 (m, 2H, C2-eq, C2-ax), 1.38 (d, 3H, $J = 6.1$ Hz, C8-Me), 1.34-1.29 (m, 2H, C3-ax, C5-ax), 1.19 (ddd, 1H, $J = 11.8, 9.7, 4.9$ Hz, C6-ax) ppm

^{13}C NMR (CDCl_3 , 176 MHz): $\delta = 139.2, 128.5, 128.0, 127.6, 74.0, 71.4, 70.6, 67.6, 54.8, 49.2, 37.1, 33.3, 28.4, 28.0, 24.1, 18.4$ ppm

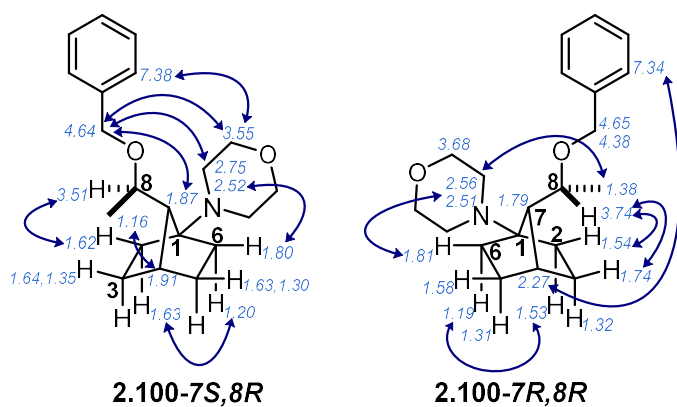
IR (thin film): 2955, 2870, 1453, 1371, 1329, 1276, 1164, 1117, 1062, 1041, 1027, 895, 735, 697 cm^{-1}

HRMS (ES^+ , m/z) calculated for $\text{C}_{20}\text{H}_{30}\text{NO}_2^+$: 316.2271, Found: 316.2278

$R_f = 0.55$ (30% EtOAc in hexanes), one blue spot, Hanessian's stain

2D NMR Data

- COSY, HSQC, and NOESY experiments were employed to assign the various resonances to the two isomers and confirm the structure of the desired products. Key NOESY correlations (denoted by blue arrows) are provided for both 1-morpholinonorbornanes **2.100-7S,8R** and **2.100-7R,8R**.



Additional Trials with Varied Additives

No Additive

Following the general procedure outlined above, 87.7 mg of aminoCP **2.53** (278 μmol) were dissolved in 2.8 mL dry MeCN along with 6.2 mg of $[\text{Ir}(\text{dF}[\text{CF}_3]\text{ppy})_2(\text{dtbbpy})](\text{PF}_6)$ (5.6 μmol) prior to irradiation. Crude residue was isolated through altered chromatographic gradient over silica (7.5 to 15 to 22.5 to 30 to 50 to 75 to 100% ethyl acetate:hexanes, adding 0.1% NEt_3 upon reaching 100% ethyl acetate to elute the major isomer, needed multiple column volumes to fully elute; residue was loaded with PhMe). This procedure flushed the major product along with some red solid, suspected to be catalyst degradation byproducts. This could be triturated out in 10% ether:hexanes, then removed via filtration through a plug of celite, eluting with the same solvent mix. Isolation provided the following:

- GCMS conversion: *[data not collected]*
- Recovered starting material: 56.2 mg; slightly red-orange oil; 64.1% recovery
- *7S,8R*-Isomer (**2.100-7S,8R**): 15.9 mg (20.2 mg pre-trituration); slightly yellow oil; 18.1% yield
- *7R,8R*-Isomer (**2.100-7R,8R**): not detected

LiBF₄

Following the general procedure outlined above, 89.1 mg of aminoCP **2.53** (282 μmol) were dissolved in 2.8 mL dry MeCN along with 6.3 mg of $[\text{Ir}(\text{dF}[\text{CF}_3]\text{ppy})_2(\text{dtbbpy})](\text{PF}_6)$ (5.7 μmol) and 5.3 mg of LiBF_4 (57 μmol) prior to irradiation. Crude residue was isolated through altered chromatographic gradient over silica (7.5 to 15 to 22.5 to 30 to 50 to 75 to 100% ethyl acetate:hexanes, adding 0.1% NEt_3 upon reaching 30% ethyl acetate to elute the major isomer, needed multiple column volumes at 100% ethyl acetate + 0.1% NEt_3 to fully elute; residue was

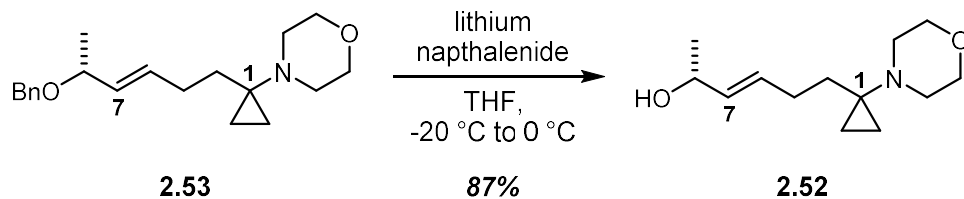
loaded with PhMe). The same trituration procedure was used for the major isomer. Isolation provided the following:

- GCMS conversion: *[data not collected]*

- Recovered starting material: 40.0 mg; slightly red-orange oil; 44.9% recovery

- *7S,8R*-Isomer (**2.100-7S,8R**): 36.7 mg (39.0 mg pre-trituration); slightly yellow oil; 41.2% yield, 74.7% BORSM

- *7R,8R*-Isomer (**2.100-7R,8R**): 2.0 mg; clear, colorless film; 2.2% yield, 4.1% BORSM



C8-benzyloxy aminoCP **2.53** (162 mg, 0.51 mmol) was dissolved in 7.5 mL dry THF in dry flask under Ar before cooling to $-20\text{ }^\circ\text{C}$ (brine/ice). Lithium naphthalenide⁷² (1.0 M in THF, 2.6 mL, 2.6 mmol) was added via syringe dropwise down the side of the flask over the course of 2 min. Initial drops turn reaction mixture red which quickly fades back to clear colorless; as addition proceeds, red color briefly persists before reaction mixture takes on the dark green color of the lithium naphthalenide solution. Stirred reaction for 1.5 hrs while slowly coming to $0\text{ }^\circ\text{C}$. Quenched reaction by pouring into 20 mL sat. NaHCO_3 then diluted with 20 mL ether. The phases were separated, and the aqueous phase was further extracted with 20 mL portions of ether three times. The combined organics were washed with 20 mL brine, dried over anhydrous magnesium sulfate, filtered to remove solids, and concentrated *in vacuo*. The crude residue was purified via flash chromatography over silica (10 to 20 to 30 to 40 to 55 to 70 to 90% ethyl acetate:hexanes, residue loaded with PhMe). Obtained 101 mg of aminoCP **2.52** as a clear, slightly yellow oil (87.3% yield).

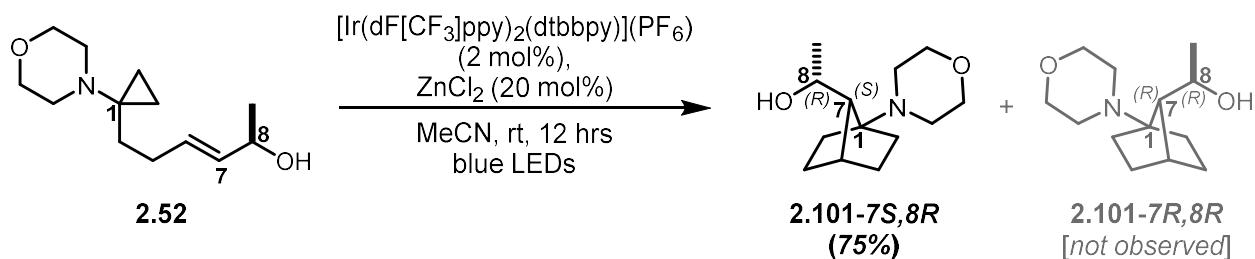
$^1\text{H NMR}$ (CDCl_3 , 700 MHz): $\delta = 5.61$ (dt, 1H, $J = 15.3, 6.6$ Hz, C4), 5.50 (dd, 1H, $J = 15.3, 6.5$ Hz, C7), $4.28\text{-}4.22$ (m, 1H, C8), $3.64\text{-}3.57$ (m, 4H, morph.), $2.67\text{-}2.61$ (m, 4H, morph.), $2.01\text{-}1.96$ (m, 2H, C3), $1.62\text{-}1.57$ (m, 2H, C2), 1.39 (d, 1H, $J = 3.6$ Hz, C8-OH), 1.25 (d, 3H, $J = 6.3$ Hz, C8-Me), $0.56\text{-}0.53$ (m, 2H, CP), $0.44\text{-}0.41$ (m, 2H, CP) ppm

$^{13}\text{C NMR}$ (CDCl_3 , 176 MHz): $\delta = 134.2, 130.9, 69.0, 67.9, 49.8, 44.1, 30.0, 29.7, 23.6, 12.9$ ppm

IR (neat): $3388, 2926, 2851, 1449, 1367, 1263, 1115, 1068, 1013, 968, 856\text{ cm}^{-1}$

HRMS (ES^+ , m/z) calculated for $\text{C}_{13}\text{H}_{24}\text{NO}_2^+$: 226.1802, Found: 226.1803

R_f = 0.25 (70% EtOAc in hexanes), one yellow spot, KMnO_4



In dry vial under nitrogen, aminoCP **2.52** (59.2 mg, 263 μmol) was dissolved in 2.6 mL dry MeCN before adding $[\text{Ir}(\text{dF}[\text{CF}_3]\text{ppy})_2(\text{dtbbpy})](\text{PF}_6)$ (5.9 mg, 5.3 μmol) then ZnCl_2 (1.0 M in ether, 53 μL , 53 μmol) in one portion each. Reaction mixture was bright yellow and slightly cloudy, even after sonication. Reaction mixture was degassed with three freeze-pump-thaw cycles. The reaction was performed by stirring at room temp (as controlled with jacketed water bath, temp maintained between 18-23 $^\circ\text{C}$) while irradiating with two strips of 4.4 W blue LEDs for 12 hrs. Mixture was yellow-green but had become extremely cloudy with a light grey precipitate, to the point of being opaque. The mixture was added to 10 mL 1:1 sat bicarb:water containing 1 mL of 50% NaOH to ensure aq phase pH \sim 14, then diluted further with 10 mL ether. Phases were separated, and the aqueous phase was extracted with 10 mL ether three times. Combined organics were washed with 10 mL brine, dried over anhydrous sodium sulfate, filtered to remove solids, and concentrated *in vacuo*. The crude residue was purified via flash chromatography (3 to 5 to 7 to 10 to 15 to 20 to 30 to 40 to 50% acetone: CH_2Cl_2 + 0.1% NEt_3 ; residue loaded with PhMe). No detectable starting material or *7R,8R*-isomer (**2.101-7R,8R**). Collected the following:

- Recovered starting material: not detected
- *7S,8R*-Isomer (**2.101-7S,8R**): 44.5 mg (obtained 44.8 mg as a 99.4 wt% mix with acetone); slightly yellow oil; 75.2% yield
- *7R,8R*-Isomer (**2.101-7R,8R**): not detected

Characterization Data for **2.101-7S,8R**

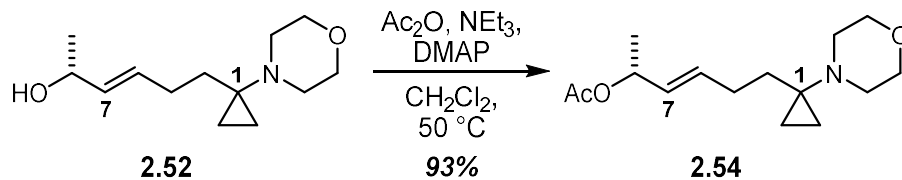
¹H NMR (CDCl₃, 700 MHz @ 43 °C): δ = 6.01 (br s, 1H, C8-OH), 3.97 (dq, 1H, *J* = 10.1, 6.1 Hz, C8), 3.69 (br s, 4H, morph.), 2.68-2.61 (m, 4H, morph.), 1.87 (s, 1H, C7), 1.90-1.80 (m, 3H, C3-eq, C6-eq, C2-eq), 1.65 (d, 1H, *J* = 9.9 Hz, C7), 1.65-1.59 (m, 2H, C5-eq, C2-ax), 1.40-1.35 (m, 2H, C3-ax, C5-ax), 1.26-1.20 (m, 1H, C6-ax), 1.16 (d, 3H, *J* = 6.0 Hz, C8-Me) ppm

¹³C NMR (CDCl₃, 176 MHz @ 43 °C): δ = 73.0 (C1), 67.6 (morph.), 67.4 (C8), 54.5 (C7), 49.3 (morph.), 36.5 (C4), 32.4 (C2), 29.6 (C5), 28.2 (C3), 23.7 (C6), 22.5 (C8-Me) ppm

IR (neat): 3302, 2955, 2851, 1451, 1328, 1275, 1249, 1180, 1116, 1071, 1038, 1004, 964, 896, 880, 862 cm⁻¹

HRMS (ES⁺, *m/z*) calculated for C₁₃H₂₄NO₂⁺: 226.1802, Found: 226.1804

R_f = 0.30 (90% EtOAc in hexanes), one green spot, ninhydrin (only effective stain)



C8-OH aminoCP **2.52** (80.6 mg, 0.36 mmol) was dissolved in 1.2 mL dry CH_2Cl_2 in a dry vial under inert atmosphere. Triethylamine (125 μL , 0.89 mmol), DMAP (22 mg, 0.18 mmol), and acetic anhydride (51 μL , 0.54 mmol) were all added respectively in one portion each. The vial was flushed with argon before heating to 50 $^\circ\text{C}$ for 18 hrs. The reaction was quenched by pouring into 10 mL sat. NaHCO_3 then diluting with 10 mL ether. The phases were separated, and the aqueous phase was further extracted with 10 mL portions of ether three times. The combined organics were washed with 10 mL brine, dried over anhydrous magnesium sulfate, filtered to remove solids, and concentrated *in vacuo*. The crude residue was purified via flash chromatography over silica (5 to 35% ethyl acetate:hexanes, increasing in 5% increments, residue loaded with PhMe). Obtained 89.0 mg of aminoCP **2.54** as a clear, colorless oil (93.1% yield).

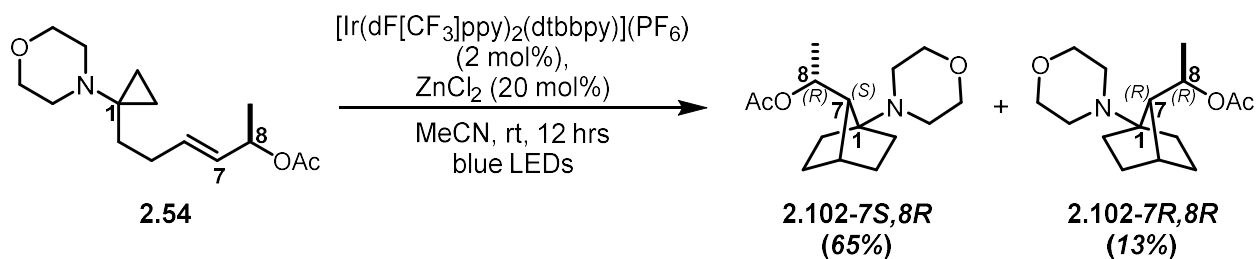
$^1\text{H NMR}$ (CDCl_3 , 700 MHz): δ = 5.67 (dt, 1H, J = 15.5, 6.5 Hz, C4), 5.44 (dd, 1H, J = 15.5, 6.6 Hz, C7), 5.29 (*app.* pent., 1H, J = 6.5 Hz, C8), 3.63-3.57 (m, 4H, morph.), 2.66-2.61 (m, 4H, morph.), 2.03 (s, 3H, -OAc), 2.01-1.97 (m, 2H, C3), 1.62-1.57 (m, 2H, C2), 1.28 (d, 3H, J = 6.5 Hz, C8-Me), 0.57-0.52 (m, 2H, CP), 0.43-0.38 (m, 2H, CP) ppm

$^{13}\text{C NMR}$ (CDCl_3 , 176 MHz): δ = 170.5, 133.2, 129.5, 71.2, 67.8, 49.8, 44.0, 30.1, 29.6, 21.6, 20.5, 12.8 ppm

IR (neat): 2931, 2849, 1730, 1450, 1370, 1235, 1112, 1041, 966, 949, 854, 616 cm^{-1}

HRMS (ES^+ , m/z) calculated for $\text{C}_{15}\text{H}_{26}\text{NO}_3^+$: 268.1907, Found: 268.1910

R_f = 0.55 (50% EtOAc in hexanes), one yellow spot, KMnO_4



In dry vial under nitrogen, aminoCP **2.54** (68.4 mg, 256 μmol) was dissolved in 2.6 mL dry MeCN before adding $[\text{Ir}(\text{dF}[\text{CF}_3]\text{ppy})_2(\text{dtbbpy})](\text{PF}_6)$ (5.7 mg, 5.1 μmol) then ZnCl_2 (1.0 M in ether, 51 μL , 51 μmol) in one portion each. Reaction mixture was clear and bright yellow. Reaction mixture was degassed with three freeze-pump-thaw cycles. The reaction was performed by stirring at room temp (as controlled with jacketed water bath, temp maintained between 18-23 $^\circ\text{C}$) while irradiating with two strips of 4.4 W blue LEDs for 12 hrs. Mixture was still clear but had taken on a slightly darker yellow-green hue. The mixture was added to 10 mL 1:1 sat bicarb:water containing 1 mL of 50% NaOH to ensure aq phase pH \sim 14, then diluted further with 5 mL hexanes. Phases were separated, and the aqueous phase was extracted with 10 mL 1:1 ether:hexanes three times. Combined organics were washed with 10 mL brine, dried over anhydrous sodium sulfate, filtered to remove solids, and concentrated *in vacuo*. The crude residue was purified via flash chromatography (5 to 10 to 15 to 25 to 35 to 50 to 70% ethyl acetate:hexanes; residue loaded with PhMe). The product needed to be triturated from 25% ether:hexanes and filtered through a plug of celite to remove minor catalyst-derived byproducts. Collected the following:

- Recovered starting material: 7.2 mg; clear, colorless oil; 10.5% recovery
- 7S,8R-Isomer (**2.102-7S,8R**): 44.3 mg (obtained 46.2 mg as a 95.8 wt% mix with water); slightly yellow oil; 64.8% yield, 72.4% BORSM
- 7R,8R-Isomer (**2.102-7R,8R**): 9.1 mg; clear, colorless oil; 13.3% yield, 14.9% BORSM

Characterization Data for **2.102-7S,8R**

¹H NMR (CDCl₃, 700 MHz): δ = 5.02 (dq_uart., 1H, J = 9.5, 6.1 Hz, C8), 3.66-3.58 (m, 4H, morph.), 2.61-2.55 (m, 2H, morph.), 2.54-2.50 (m, 2H, morph.), 2.01 (s, 3H, C8-OAc), 1.93 (t, 1H, J = 4.1 Hz, C4), 1.89 (d, 1H, J = 9.5 Hz, C7), 1.81 (tt, 1H, J = 12.1, 3.9 Hz, C6-eq), 1.77-1.71 (m, 1H, C3-eq), 1.72-1.66 (m, 1H, C2-eq), 1.67-1.61 (m, 1H, C5-eq), 1.57 (ddd, 1H, J = 11.2, 9.5, 3.6 Hz, C2-ax), 1.39-1.31 (m, 2H, C3-ax, C5-ax), 1.22 (ddd, 1H, J = 11.6, 9.9, 4.8 Hz, C6-ax), 1.18 (d, 3H, J = 6.3 Hz, C8-Me) ppm

¹³C NMR (CDCl₃, 176 MHz): δ = 170.4, 72.1, 69.3, 67.8, 52.8, 48.9, 37.4, 32.8, 28.8, 27.8, 23.7, 21.9, 20.1 ppm

IR (neat): 2954, 2873, 1724, 1448, 1366, 1324, 1242, 1113, 1066, 1030, 892, 847, 603 cm⁻¹

HRMS (ES⁺, m/z) calculated for C₁₅H₂₆NO₃⁺: 268.1907, Found: 268.1909

R_f = 0.40 (50% EtOAc in hexanes), one yellow spot, KMnO₄

Characterization Data for **2.102-7R,8R**

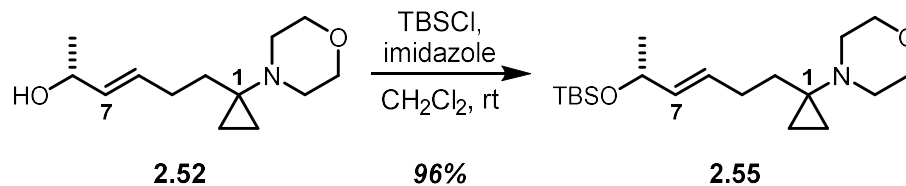
¹H NMR (C₆D₆, 500 MHz): δ 5.20 (dq_uart., 1H, J = 10.3, 6.4 Hz, C8), 3.54 (t, 4H, J = 4.5 Hz, morph.), 2.22 (td, 2H, J = 11.5, 4.6 Hz, morph.), 2.15 (td, 2H, J = 11.5, 4.4 Hz, morph.), 2.04 (t, 1H, J = 4.2 Hz, C4), 1.98-1.91 (m, 1H, C3), 1.74 (s, 3H, C8-OAc), 1.65 (d, 1H, J = 10.3 Hz, C7), 1.55 (tt, 1H, J = 12.2, 3.7 Hz, C6), 1.48-1.40 (m, 2H, C2, C5), 1.39 (d, 3H, J = 6.1 Hz, C8-Me), 1.24-1.13 (m, 3H, C3, C2, C6), 0.91 (ddd, 1H, J = 11.5, 10.0, 4.9 Hz, C5) ppm

¹³C NMR (CDCl₃, 176 MHz): δ = 170.6, 71.7, 70.6, 67.5, 53.3, 49.1, 37.3, 33.0, 28.4, 27.8, 24.0, 21.5, 19.9 ppm

IR (neat): 2956, 2873, 1731, 1368, 1246, 1118, 1075, 1019, 895 cm⁻¹

HRMS (ES⁺, *m/z*) calculated for C₁₅H₂₆NO₃⁺: 268.1907, Found: 268.1909

R_f = 0.75 (50% EtOAc in hexanes), one yellow spot, KMnO₄



C8-OH aminoCP **2.52** (72.2 mg, 0.32 mmol) was dissolved in 1.6 mL dry CH_2Cl_2 in dry vial under inert atmosphere. Imidazole (87 mg, 1.3 mmol) and TBSCl (purchased from Oakwood Chemical, 72 mg, 0.48 mmol) were added respectively, in one portion each. The reaction mixture was stirred for 1 hr at room temp before pouring into 10 mL sat. NaHCO_3 to quench the reaction. Upon diluting with 10 mL ether, the phases were separated, and the aqueous phase was further extracted with 10 mL portions of ether three times. The combined organics were washed with 10 mL brine, dried over anhydrous magnesium sulfate, filtered to remove solids, and concentrated *in vacuo*. The crude residue was purified via flash chromatography over silica (5 to 10 to 20% ethyl acetate:hexanes; residue loaded with PhMe). Obtained 104.1 mg of aminoCP **2.55** as a clear, colorless oil (95.7% yield).

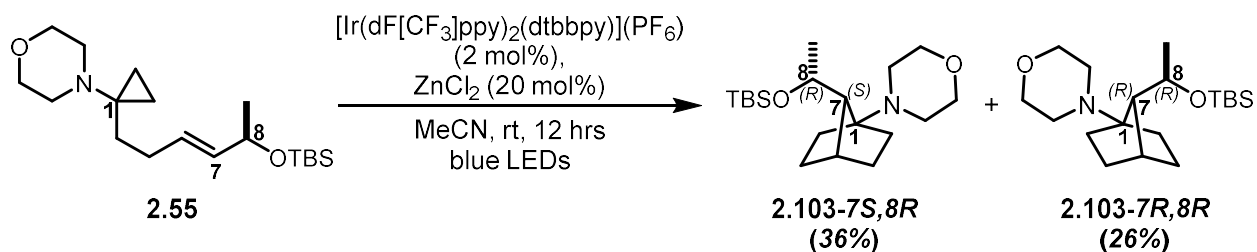
$^1\text{H NMR}$ (CDCl_3 , 500 MHz): $\delta = 5.50$ (dt, 1H, $J = 15.4, 6.4$ Hz, C4), 5.42 (dd, 1H, $J = 15.4, 6.4$ Hz, C7), 4.23 (*app.* pent., 1H, $J = 5.9$ Hz, C8), 3.63-3.58 (m, 4H, morph.), 2.68-2.64 (m, 4H, morph.), 1.98-1.91 (m, 2H, C3), 1.62-1.56 (m, 2H, C2), 1.18 (d, 3H, $J = 6.4$ Hz, C8-Me), 0.89 (s, 9H, TBS), 0.55-0.51 (m, 2H, CP), 0.45-0.31 (m, 2H, CP), 0.05 (s, 3H, TBS), 0.04 (s, 3H, TBS) ppm

$^{13}\text{C NMR}$ (CDCl_3 , 126 MHz): $\delta = 134.8, 128.9, 69.4, 67.9, 49.8, 44.0, 29.9, 29.5, 26.1, 24.7, 18.5, 12.9, -4.3, -4.5$ ppm

IR (neat): 2929, 2853, 1471, 1455, 1359, 1252, 1115, 1075, 965, 831, 774 cm^{-1}

HRMS (ES^+ , m/z) calculated for $\text{C}_{19}\text{H}_{38}\text{NO}_2\text{Si}^+$: 340.2666, Found: 340.2670

R_f = 0.45 (20% EtOAc in hexanes), one yellow spot, KMnO_4



In dry vial under nitrogen, aminoCP **2.55** (84.1 mg, 248 μmol) was dissolved in 2.5 mL dry MeCN before adding $[\text{Ir}(\text{dF}[\text{CF}_3]\text{ppy})_2(\text{dtbbpy})](\text{PF}_6)$ (5.6 mg, 5.0 μmol) then ZnCl_2 (1.0 M in ether, 50 μL , 50 μmol) in one portion each. Reaction mixture was clear and bright yellow. Reaction mixture was degassed with three freeze-pump-thaw cycles. The reaction was performed by stirring at room temp (as controlled with jacketed water bath, temp maintained between 18-23 $^\circ\text{C}$) while irradiating with two strips of 4.4 W blue LEDs for 12 hrs. Mixture was still clear but had taken on a slightly darker yellow-green hue. The mixture was added to 10 mL 1:1 sat bicarb:water containing 1 mL of 50% NaOH to ensure aq phase pH \sim 14, then diluted further with 5 mL hexanes. Phases were separated, and the aqueous phase was extracted with 10 mL 1:1 ether:hexanes three times. Combined organics were washed with 10 mL brine, dried over anhydrous sodium sulfate, filtered to remove solids, and concentrated *in vacuo*. The crude residue was purified via flash chromatography (2 to 3 to 4 to 6 to 9 to 15 to 30 to 60 to 90% ethyl acetate:hexanes; residue loaded with PhMe). Collected high polarity elution fractions to search for deprotected products, starting material, or byproducts; none detected. The starting material and major isomer eluted as an inseparable mixture (44.3 mg of 2.2:1 **2.103-7S,8R:1q**; clear, colorless oil); data presented separately below for clarity:

- Recovered starting material: 13.8 mg; clear, colorless oil; 16.4% recovery
- 7S,8R-Isomer (**2.103-7S,8R**): 30.5 mg; clear, colorless oil; 36.3% yield, 43.4% BORSM
- 7R,8R-Isomer (**2.103-7R,8R**): 21.8 mg (obtained 22.9 mg as a 95.4 wt% mix with water); clear, colorless oil; 25.9% yield, 31.0% BORSM

Characterization Data for **2.103-7S,8R**

¹H NMR (CDCl₃, 700 MHz): δ = 3.92-3.87 (m, 1H, C8), 3.73-3.69 (m, 2H, morph.), 3.66-3.62 (m, 2H, morph.), 2.74-2.67 (m, 2H, morph.), 2.56-2.52 (m, 2H, morph.), 1.90 (t, 1H, *J* = 4.4 Hz, C4), 1.84 (tt, 1H, *J* = 12.1, 3.8 Hz, C6-eq), 1.75 (d, 1H, *J* = 7.8 Hz, C7), 1.73-1.67 (m, 1H, C5-eq), 1.65-1.55 (m, 3H, C5-ax, C3-eq, C2), 1.34-1.29 (m, 1H, C3-ax), 1.28-1.24 (m, 1H, C6-ax), 1.22-1.17 (m, 1H, C2), 1.16 (d, 3H, *J* = 6.1 Hz, C8-Me), 0.90 (s, 9H, TBS), 0.15 (s, 3H, TBS), 0.09 (s, 3H, TBS) ppm

¹³C NMR (CDCl₃, 176 MHz): δ = 71.9, 67.5, 67.1, 56.9, 48.6, 38.0, 33.1, 28.9, 28.0, 26.4, 24.1, 23.6, 18.5, -2.6, -3.6 ppm

IR (neat): 2952, 2854, 1457, 1248, 1118, 1074, 1046, 988, 893, 831, 774 cm⁻¹

HRMS (ES⁺, *m/z*) calculated for C₁₉H₃₈NO₂Si⁺: 340.2666, Found: 340.2667

R_f = 0.45 (20% EtOAc in hexanes), one yellow spot, KMnO₄

Characterization Data for **2.103-7R,8R**

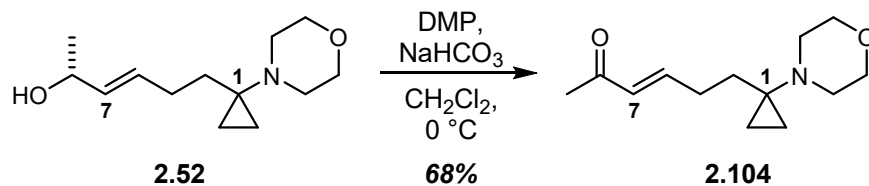
¹H NMR (C₆D₆, 700 MHz): δ = 3.78 (dqart., 1H, *J* = 9.0, 6.1 Hz, C8), 3.60 (t, 4H, *J* = 4.4 Hz, morph.), 2.33 (t, 1H, *J* = 4.4 Hz, C4), 2.30 (dt, 2H, *J* = 11.4, 4.4 Hz, morph.), 2.26 (dt, 2H, *J* = 11.4, 4.4 Hz, morph.), 1.97-1.91 (m, 1H, C3-eq), 1.61 (tt, 1H, *J* = 12.3, 4.3 Hz, C6-eq), 1.58 (d, 1H, *J* = 9.0 Hz, C7), 1.51-1.45 (m, 2H, C5, C2), 1.35 (d, 3H, *J* = 6.1 Hz, C8-Me), 1.33-1.24 (m, 2H, C3-eq, C2), 1.24-1.19 (m, 1H, C6-ax), 1.03 (s, 9H, TBS), 1.00-0.95 (m, 1H, C5), 0.12 (s, 3H, TBS), 0.11 (s, 3H, TBS) ppm

¹³C NMR (CDCl₃, 176 MHz): δ = 70.9, 67.9, 67.8, 56.4, 49.2, 37.1, 33.1, 28.4, 27.9, 26.1, 24.2, 23.4, 18.3, -3.5, -4.6 ppm

IR (neat): 2955, 2854, 1462, 1275, 1248, 1118, 1097, 1038, 952, 905, 835, 772, 478 cm⁻¹

HRMS (ES⁺, *m/z*) calculated for C₁₉H₃₈NO₂Si⁺: 340.2666, Found: 340.2670

R_f = 0.65 (20% EtOAc in hexanes), one yellow spot, KMnO₄



C8-OH aminoCP **2.52** (118 mg, 0.52 mmol) was dissolved in 5.0 mL dry CH_2Cl_2 in a dry vial under inert atmosphere before cooling to 0 °C. Sodium bicarbonate (110 mg, 1.3 mmol) and Dess-Martin periodinane (purchased from Ark Pharm Inc., 333 mg, 0.79 mmol) were added respectively, in one portion each. After 30 min stirring at 0 °C, it appeared that some starting material remained based on TLC analysis (difficult to tell, SM and product nearly co-spot on TLC). Reaction was stirred an additional 30 min at 0 °C to achieve full conversion, though this additional time enabled the formation of a number of other byproducts based on TLC. The reaction mixture was quenched by pouring into 10 mL of 1:1 sat. NaHCO_3 :sat. $\text{Na}_2\text{S}_2\text{O}_3$. Upon diluting with 10 mL ether, the phases were separated, and the aqueous phase was further extracted with 10 mL portions of ether three times. The combined organics were washed with 10 mL brine, dried over anhydrous magnesium sulfate, filtered to remove solids, and concentrated *in vacuo*. The crude residue was purified via flash chromatography over silica (20 to 30 to 40 to 50 to 60 to 75 to 90% ethyl acetate:hexanes, residue loaded with PhMe). Collected product in two fractions: 53.4 mg of a clear, colorless oil from the central fractions and 25.8 mg of a yellow oil from the shoulder fractions. Both samples were clean by ^1H NMR, thus the total yield for the reaction was 79.2 mg (67.7% yield).

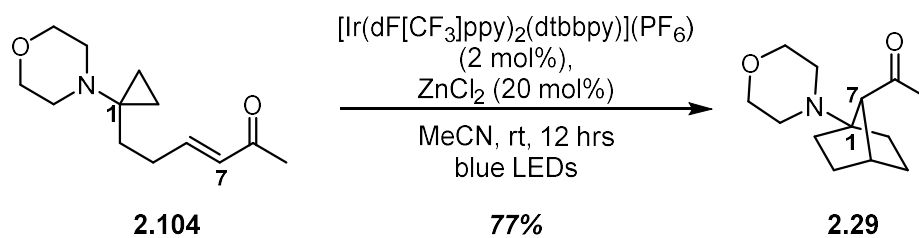
^1H NMR (C_6D_6 , 700 MHz): δ = 6.42 (dt, 1H, J = 16.0, 6.6 Hz, C4), 5.93 (d, 1H, J = 16.0 Hz, C7), 3.54-3.49 (m, 4H, morph.), 2.35-2.31 (m, 4H, morph.), 1.91 (s, 3H, C9), 1.81-1.76 (m, 2H, C3), 1.29-1.25 (m, 2H, C2), 0.51-0.48 (m, 2H, CP), 0.18-0.14 (m, 2H, CP) ppm

^{13}C NMR (C_6D_6 , 176 MHz): δ = 196.4, 146.8, 131.3, 67.8, 50.0, 44.0, 30.3, 29.6, 26.9, 12.7 ppm

IR (neat): 2924, 2854, 1694, 1672, 1453, 1360, 1263, 1114, 1070, 1012, 976, 856, 807, 619 cm^{-1}

HRMS (ES+, m/z) calculated for $\text{C}_{13}\text{H}_{22}\text{NO}_2^+$: 224.1645, Found: 224.1647

R_f = 0.55 (80% EtOAc in hexanes), one yellow spot, KMnO_4 + UV



In a dry vial under nitrogen, aminoCP **2.104** (52.6 mg, 236 μmol) was dissolved in 2.5 mL dry MeCN before adding $[\text{Ir}(\text{dF}[\text{CF}_3]\text{ppy})_2(\text{dtbbpy})](\text{PF}_6)$ (5.3 mg, 4.7 μmol) then ZnCl_2 (1.0 M in ether, 47 μL , 47 μmol) in one portion each. Reaction mixture was bright yellow. Reaction mixture was degassed with three freeze-pump-thaw cycles. The reaction was performed by stirring at room temp (as controlled with jacketed water bath, temp maintained between 18-23 $^\circ\text{C}$) while irradiating with two strips of 4.4 W blue LEDs for 12 hrs. Mixture had turned red-orange but was still clear. The mixture was added to 10 mL 1:1 sat. NaHCO_3 :water containing 1 mL of 50% NaOH to ensure aq phase pH \sim 14, then diluted further with 10 mL ether. Phases were separated, and the aqueous phase was extracted with 10 mL portions of ether three times. Combined organics were washed with 10 mL brine, dried over anhydrous sodium sulfate, filtered to remove solids, and concentrated *in vacuo*. The crude residue was purified via flash chromatography over silica (30 to 90% ethyl acetate:hexanes, increasing in 15% increments; residue loaded with PhMe). Collected a yellow oil at first which contained some catalyst-derived byproducts; trituration from 50% ether:hexanes followed by filtration through a plug of celite (eluting with 10 mL 50% ether:hexanes) afforded clean product.

- Recovered starting material: none detected

- Product: 40.3 mg (obtained 41.3 mg which was 97.5 wt% mixed with water); slightly yellow oil; 76.6% yield

$^1\text{H NMR}$ (CDCl_3 , 700 MHz): δ = 3.75-3.66 (m, 4H, morph.), 2.67 (br s, 1H, C7), 2.67-2.63 (m, 2H, morph), 2.59-2.54 (m, 2H, morph.), 2.30 (br s, 1H, C4), 2.23 (s, 3H, C9), 2.14-2.08 (m, 1H,

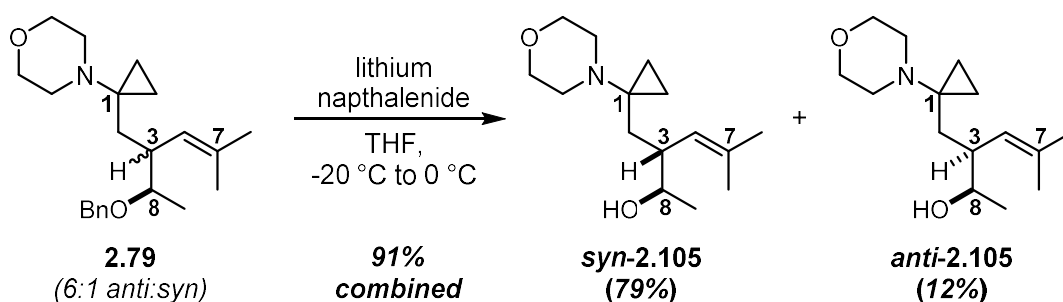
C5), 1.91-1.83 (m, 1H, C2), 1.77-1.70 (m, 1H, C6), 1.66-1.60 (m, 1H, C3), 1.60-1.54 (m, 1H, C5),
1.44-1.34 (m, 2H, C2, C6), 1.30-1.24 (m, 1H, C3) ppm

¹³C NMR (CDCl₃, 176 MHz): δ = 209.4, 74.0, 67.5, 60.5, 49.2, 38.6, 32.3, 31.6, 29.3, 28.5, 25.5
ppm

IR (neat): 2929, 2855, 1709, 1423, 1360, 1274, 1232, 1192, 1158, 1116 cm⁻¹

HRMS (ES⁺, *m/z*) calculated for C₁₃H₂₂NO₂⁺: 224.1645, Found: 224.1647

R_f = 0.25 (80% EtOAc in hexanes), one yellow spot, KMnO₄



The mixture of C8-OBn aminoCPs (**2.79**; 6.0:1 mix of *syn:anti*; 330 mg, 0.96 mmol) in 15 mL dry THF in a dry flask. Flushed with a full balloon of argon; remainder of reaction was carried out under Ar balloon(s). Cooled reaction mixture to -20 °C (ice/salt). Lithium naphthalenide (1.0 M in THF, 4.8 mL, 4.8 mmol) was added via syringe dropwise down the side of the flask over the course of 2 min. Initial drops turn reaction mixture red which quickly fades back to clear colorless; as addition proceeds, red color briefly persists before reaction mixture takes on the dark green color of the lithium naphthalenide solution. Stirred reaction for 2 hrs while slowly coming to 0 °C. Quenched reaction by pouring into 50 mL sat. NaHCO₃ then diluted with 50 mL ethyl acetate. The phases were separated, and the aqueous phase was further extracted with three portions of ethyl acetate, 50 mL each. The combined organics were washed with 50 mL brine, dried over anhydrous magnesium sulfate, filtered to remove solids, and concentrated *in vacuo*. The crude residue was purified via flash chromatography over silica (20 to 25 to 30 to 35 to 40 to 50 to 65% ethyl acetate:hexanes, residue loaded with PhMe). Collected a total 121.4 mg of the *syn* isomer (*syn*-**S31**) and 100 mg of a mixture of the two isomers (79:21 ratio *syn:anti*). Additional rounds of analogous chromatography procedures separated this mixture, leading to a combined yield of 90.8% (78.9% *syn*-**2.105**; 11.9% *anti*-**2.105**).

Characterization Data for *syn*-**2.105**

¹H NMR (CDCl₃, 500 MHz): δ = 6.19 (br s, 1H, C8-OH), 4.91 (d, 1H, *J* = 10.5 Hz, C4), 3.74-3.69 (m, 4H, morph.), 3.59-3.53 (m, 1H, C8), 2.55-2.47 (m, 2H, morph.), 2.44-2.36 (m, 3H, morph., C3), 2.09 (*app.* ddd, 1H, *J* = 15.0, 7.2, 2.0 Hz, C2), 1.68 (s, 3H, C7-Me), 1.62 (s, 3H, C7-Me), 1.09 (d, 3H, *J* = 6.1 Hz, C8-Me), 0.99-0.89 (m, 2H, C2, CP), 0.72-0.66 (m, 1H, CP), 0.45-0.40 (m, 1H, CP), 0.35-0.30 (m, 1H, CP) ppm

¹³C NMR (CDCl₃, 126 MHz): δ = 130.7, 127.6, 71.9, 67.0, 49.0, 46.5, 45.2, 41.6, 26.0, 21.8, 18.5, 9.7, 8.6 ppm

IR (neat): 3415, 2962, 2911, 2853, 1449, 1373, 1293, 1263, 1116, 1069, 1014, 984, 855 cm⁻¹

HRMS (ES⁺, *m/z*) calculated for C₁₅H₂₈NO₂⁺: 254.2115, Found: 254.2114

R_f = 0.20 (70% EtOAc in hexanes), one yellow spot, KMnO₄

Characterization Data for *anti*-**2.105**

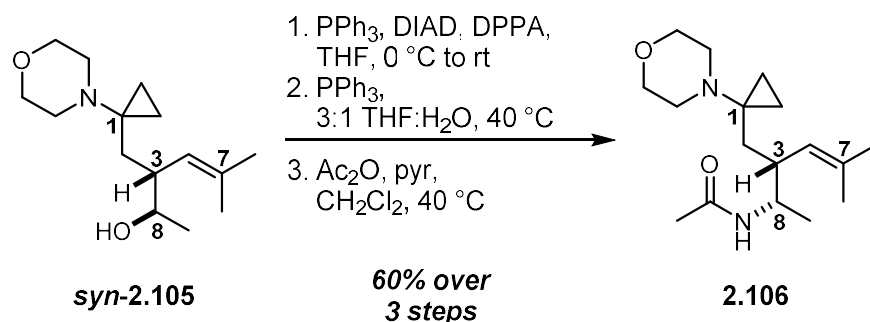
¹H NMR (CDCl₃, 500 MHz): δ = 5.05 (d, 1H, *J* = 10.0 Hz, C4), 4.77 (br s, 1H, C8-OH), 3.77-3.72 (m, 1H, C8), 3.72-3.65 (m, 4H, morph.), 2.54-2.43 (m, 4H, morph.), 2.46-2.41 (m, 1H, C3), 1.95 (ddd, 1H, *J* = 14.9, 7.3 Hz, C2), 1.72 (s, 3H, C7-Me), 1.61 (s, 3H, C7-Me), 1.14 (dd, 1H, *J* = 14.9, 5.4 Hz, C2), 1.11 (d, 3H, *J* = 6.4 Hz, C8-Me), 0.83-0.77 (m, 1H, CP), 0.72-0.67 (m, 1H, CP), 0.43-0.37 (m, 1H, CP), 0.37-0.32 (m, 1H, CP) ppm

¹³C NMR (CDCl₃, 126 MHz): δ = 132.7, 125.7, 69.5, 67.2, 49.2, 44.1, 43.9, 37.3, 26.1, 20.1, 18.3, 9.5, 9.3 ppm

IR (neat): 3443, 2963, 2925, 2853, 1450, 1374, 1293, 1263, 1116, 1069, 1014, 984, 856 cm⁻¹

HRMS (ES⁺, *m/z*) calculated for C₁₅H₂₈NO₂⁺: 254.2115, Found: 254.2113

R_f = 0.25 (70% EtOAc in hexanes), one yellow spot, KMnO₄



The C8-OH aminoCP **syn-2.105** (60.7 mg, 0.24 mmol) was dissolved in 2.4 mL dry THF in a dry flask under inert atmosphere. Triphenylphosphine (75 mg, 0.29 mmol) was added in one portion before cooling to 0 °C. DIAD (61 μL , 0.31 mmol) was added dropwise over 15 sec, and the reaction mixture was stirred 20 min at 0 °C while covered in foil. DPPA (67 μL , 0.31 mmol) was then added dropwise over 15 sec. Upon complete addition, the ice bath was removed, and the reaction mixture was stirred at room temp. for 24 hrs while wrapped in foil. The reaction was quenched with 10 mL 1:1 sat. NaHCO_3 :1 M NaOH then diluted with 10 mL ether. The phases were separated. The aqueous phase was extracted with 10 mL portions of ether three times. The combined organics were then washed with 10 mL brine, dried over anhydrous magnesium sulfate, filtered to remove solids, and concentrated under vacuum. The crude residue was purified via flash chromatography over silica (5 to 25% ethyl acetate:hexanes, increasing in 5% increments; the residue was loaded with PhMe), affording 59.2 mg of a clear, colorless oil that proved to be the desired *anti*-C8-azide (88.8% yield).

$^1\text{H NMR}$ (CDCl_3 , 700 MHz): δ = 4.91 (d, 1H, J = 10.7 Hz, C4), 3.62 (*app.* t, 1H, J = 4.4 Hz, morph.), 3.62-3.58 (m, 1H, C8), 2.58-2.50 (m, 5H, morph., C3), 1.77 (dd, 1H, J = 14.2, 4.9 Hz, C2), 1.73 (s, 3H, C7-Me), 1.63 (s, 3H, C7-Me), 1.37 (dd, 1H, J = 14.4, 8.6 Hz, C2), 1.18 (d, 3H, J = 6.6 Hz, C8-Me), 0.62-0.55 (m, 2H, CP), 0.40-0.34 (m, 2H, CP) ppm

R_f = 0.25 (20% EtOAc in hexanes), one yellow spot, KMnO_4

The *anti*-C8-azide (59.2 mg, 0.21 mmol) was suspended in 1.8 mL THF and 0.6 mL HPLC-grade water. Triphenylphosphine (84 mg, 0.32 mmol) was added to the biphasic mixture in one portion, after which the vial was flushed with Ar, capped and sealed, then heated to 40 °C with vigorous stirring for 12 hrs. Upon cooling to room temp., the reaction was quenched by pouring into 3 mL 1 M HCl and diluting with 3 mL ether. The phases were separated, and the aqueous phase was washed with three 1 mL portions of ether. After basifying the aqueous phase with 2 mL 6 M NaOH (added dropwise with stirring; reaction mixture becomes slightly cloudy with a white precipitate), the suspension was diluted with 1 mL water and 2 mL ethyl acetate. The phases were separated, and the aqueous phase was extracted with 2 mL portions of ethyl acetate three times. The combined organics were then washed with 2 mL brine, dried over anhydrous magnesium sulfate, filtered to remove solids, and concentrated under vacuum. This material was moved forward without any further purification.

¹H NMR (CDCl₃, 500 MHz): δ = 4.89 (d, 1H, *J* = 10.0 Hz, C4), 3.62 (*app.* t, 1H, *J* = 4.6 Hz, morph.), 2.79 (*app.* quint., 1H, *J* = 6.1 Hz, C8), 2.61-2.51 (m, 4H, morph.), 2.29-2.22 (m, 1H, C3), 1.93 (dd, 1H, *J* = 14.4, 3.7 Hz, C2), 1.73 (s, 3H, C7-Me), 1.63 (s, 3H, C7-Me), 1.20 (dd, 1H, *J* = 14.2, 9.5 Hz, C2), 1.03 (d, 1H, *J* = 6.4 Hz, C2), 0.62-0.57 (m, 1H, CP), 0.52-0.47 (m, 1H, CP), 0.47-0.42 (m, 1H, CP), 0.35-0.30 (m, 1H, CP) ppm

The crude residue from the Staudinger reduction detailed above (assumed 0.21 mmol) was dissolved in 2.1 mL dry CH₂Cl₂ under inert atmosphere. Added pyridine (86 μL, 1.06 mmol) then acetic anhydride (50 μL, 0.53 mmol) in one portion each. The vial was flushed with argon, capped and sealed, then heated to 40 °C for 2 hrs. The reaction was quenched with 4 mL 1:1 sat.

NaHCO₃:1 M NaOH then diluted with 2 mL ethyl acetate. The phases were separated. The aqueous phase was extracted with 2 mL portions of ethyl acetate three times. The combined organics were then dried over anhydrous magnesium sulfate, filtered to remove solids, and concentrated under vacuum. The crude residue was purified via flash chromatography over silica (10 to 50% acetone:CH₂Cl₂, increasing in 10% increments; the silica was pre-neutralized with 10% acetone:CH₂Cl₂ + 1% triethylamine). The product was collected in two portions, a shoulder fraction consisting of 34.3 mg and center fractions totaling 8.0 mg. Both were clear, colorless oils and were pure by ¹H NMR, bringing the total to 42.3 mg of aminoCP **2.106** (67.4% over two steps, or 59.9% over three steps).

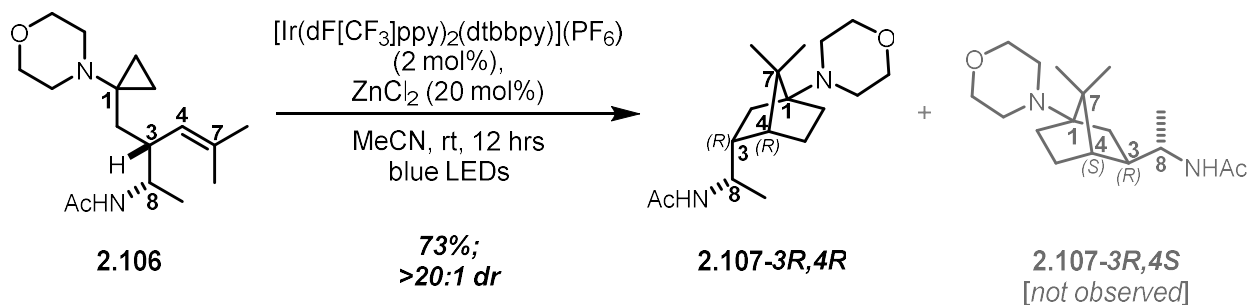
¹H NMR (CDCl₃, 700 MHz): δ = 5.33 (d, 1H, *J* = 9.2 Hz, C8-NHAc), 4.83 (d, 1H, *J* = 9.9 Hz, C4), 4.06-4.00 (m, 1H, C8), 3.63-3.59 (m, 4H, morph.), 2.57-2.48 (m, 5H, morph., C3), 1.96 (s, 3H, Ac), 1.84 (dd, 1H, *J* = 14.3, 3.8 Hz, C2), 1.73 (s, 3H, C7-Me), 1.66 (s, 3H, C7-Me), 1.22 (dd, 1H, *J* = 14.1, 9.0 Hz, C2), 1.03 (d, 3H, *J* = 6.8 Hz, C8-Me), 0.61-0.57 (m, 1H, CP), 0.54-0.50 (m, 1H, CP), 0.40-0.36 (m, 1H, CP), 0.34-0.30 (m, 1H, CP) ppm

¹³C NMR (CDCl₃, 176 MHz): δ = 169.4, 134.2, 125.7, 67.8, 49.5, 49.4, 43.0, 40.4, 34.5, 26.2, 23.8, 19.0, 18.8, 11.8, 11.2 ppm

IR (neat): 3290, 2965, 2929, 2853, 2812, 1642, 1543, 1449, 1372, 1292, 1264, 1115, 985, 860, 739 cm⁻¹

HRMS (ES⁺, *m/z*) calculated for C₁₇H₃₁N₂O₂⁺: 295.2380, Found: 295.2384

R_f = 0.30 (50% acetone in CH₂Cl₂), one yellow spot, KMnO₄



In dry vial under nitrogen, aminoCP **2.106** (46.7 mg, 159 μmol) was dissolved in 1.6 mL dry MeCN before adding $[\text{Ir}(\text{dF}[\text{CF}_3]\text{ppy})_2(\text{dtbbpy})](\text{PF}_6)$ (3.6 mg, 3.2 μmol) then ZnCl_2 (1.0 M in ether, 32 μL , 32 μmol) in one portion each. Reaction mixture was bright yellow and slightly cloudy, even after sonication. Reaction mixture was degassed with three freeze-pump-thaw cycles. The reaction was performed by stirring at room temp (as controlled with jacketed water bath, temp maintained between 18-23 $^\circ\text{C}$) while irradiating with two strips of 4.4 W blue LEDs for 12 hrs. Mixture became slightly orange and cloudier. The mixture was added to 10 mL 1:1 sat bicarb:water containing 1 mL of 50% NaOH to ensure aq phase pH \sim 14, then diluted further with 10 mL ether. Phases were separated, and the aqueous phase was extracted with 10 mL ether three times. Combined organics were washed with 10 mL brine, dried over anhydrous magnesium sulfate, filtered to remove solids, and concentrated *in vacuo*. The crude residue was purified via flash chromatography over silica (10 to 90% acetone: CH_2Cl_2 + 0.1% NEt_3 , increasing in 10% increments; residue loaded with PhMe; pre-neutralized silica with 10% acetone: CH_2Cl_2 + 1% triethylamine. The center fractions of this attempt were not sufficiently pure and were purified via a subsequent round of pipet chromatography over silica (30 to 50 to 80% acetone: CH_2Cl_2 + 0.1% NEt_3 ; pre-neutralized silica with 30% acetone: CH_2Cl_2 + 1% triethylamine), which afforded 4.5 mg of pure material. The shoulder fractions from both rounds of chromatography were subjected to an additional purification over silica (20 to 30 to 40 to 60 to 80% acetone: CH_2Cl_2 + 0.1% NEt_3 ; pre-neutralized silica with 20% acetone: CH_2Cl_2 + 1% triethylamine), yielding 29.7 mg of a white

solid (collected 31.3 mg that proved to be 94.9 wt% with pentane based on ^1H NMR). 2D NMR studies demonstrated that the isolated material was the *3R,4R* isomer, totaling 34.2 mg (73.2% yield). Of note, the first chromatography provided 6.2 mg of mixed material that was predominantly starting material, but also appeared to contain the *3R,4S*-isomer in minor amounts; if this assertion is correct, it would likely be well under the ~ 1.5 mg needed to alter to dr from $>20:1$. Collected the following:

- Recovered starting material: 6.2 mg of material of insufficient purity for a calculation of a BORSM yield
- *1R,3R,4R,8R*-Isomer (**2.107-3R,4R**): 34.2 mg; white solid; 73.2% yield
- *1S,3R,4S,8R* -Isomer (**2.107-3R,4S**): none isolated

Characterization Data for **2.107-3R,4R**:

^1H NMR (CDCl_3 , 700 MHz): δ = 5.10 (d, 1H, J = 8.7 Hz, C8-NHAc), 3.88-3.81 (m, 1H, C8), 3.66 (*app.* t, 4H, J = 4.2 Hz, morph.), 2.56-2.50 (m, 4H, morph.), 2.03 (td, 1H, J = 12.1, 3.6 Hz, C2-eq), 1.93 (s, 3H, Ac), 1.96-1.91 (m, 1H, C3-eq), 1.84-1.78 (m, 1H, C6-eq), 1.65-1.55 (m, 2H, C5-eq, C5-ax), 1.37 (*app.* t, 1H, J = 4.1 Hz, C4), 1.36-1.32 (m, 1H, C6-ax), 1.14 (d, 3H, J = 6.3 Hz, C8-Me), 1.07 (s, 3H, C7-Me), 1.07 (s, 3H, C7-Me), 0.98 (dd, 1H, J = 12.4, 5.2 Hz, C2-ax) ppm

^{13}C NMR (CDCl_3 , 176 MHz): δ = 169.6 (Ac), 70.3 (C1), 67.7 (morph.), 48.8 (morph.), 48.8 (C4), 48.3 (C7), 47.5 (C8), 42.9 (C3), 35.3 (C2), 29.6 (C6), 23.7 (Ac), 22.0 (C7-Me), 21.6 (C7-Me), 20.9 (C8-Me), 20.0 (C5) ppm

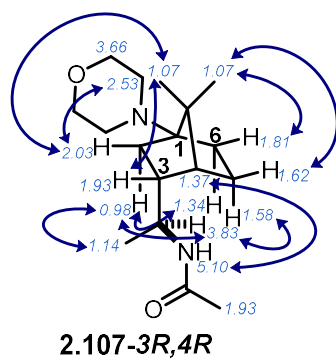
IR (neat): 3286, 2960, 2875, 2853, 2810, 1639, 1549, 1449, 1370, 1303, 1273, 1136, 1118, 885, 735 cm^{-1}

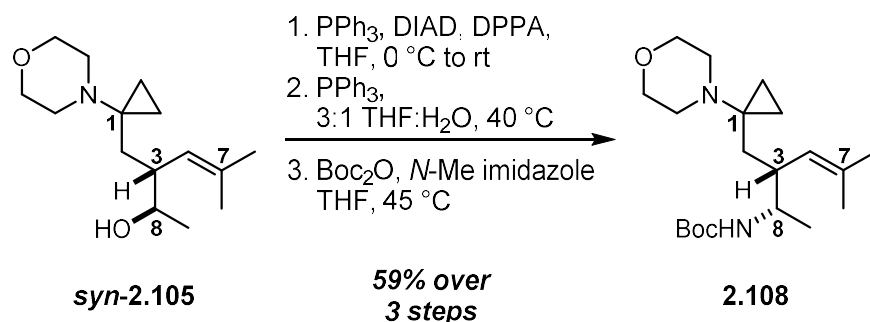
HRMS (ES^+ , m/z) calculated for $\text{C}_{17}\text{H}_{31}\text{N}_2\text{O}_2^+$: 295.2380, Found: 295.2381

$R_f = 0.20$ (50% acetone in CH_2Cl_2), one yellow spot, KMnO_4

2D NMR Data

- COSY, HSQC, and NOESY experiments were employed to assign the relative configuration of the isomer obtained. Key NOESY correlations (denoted by blue arrows) are provided below:





The C8-OH aminoCP **syn-2.105** (199 mg, 0.79 mmol) was dissolved in 8.0 mL dry THF in a dry flask under inert atmosphere. Triphenylphosphine (247 mg, 0.94 mmol) was added in one portion before cooling to 0 °C. DIAD (0.20 mL, 1.02 mmol) was added dropwise over 15 sec, and the reaction mixture was stirred 20 min at 0 °C while covered in foil. DPPA (0.22 mL, 1.02 mmol) was then added dropwise over 15 sec. Upon complete addition, the ice bath was removed, and the reaction mixture was stirred at room temp. for 20 hrs while wrapped in foil. The reaction was quenched with 25 mL 1:1 sat. NaHCO₃:1 M NaOH then diluted with 25 mL ether. The phases were separated. The aqueous phase was extracted with 25 mL portions of ether three times. The combined organics were then washed with 10 mL brine, dried over anhydrous magnesium sulfate, filtered to remove solids, and concentrated under vacuum. The crude residue was purified via flash chromatography over silica (5 to 25% ethyl acetate:hexanes, increasing in 5% increments; the residue was loaded with PhMe). Obtained 178 mg of a clear, colorless oil that was moved on without further purification. This *anti*-C8-azide is the same that was detailed en route toward aminoCP **anti-1y** (pg. S183); partial characterization for the *anti*-C8-azide and subsequent *anti*-C8-amine can be found in that procedure.

The *anti*-C8-azide (ca. 0.64 mmol) was suspended in 4.5 mL THF and 1.5 mL HPLC-grade water. Triphenylphosphine (252 mg, 0.96 mmol) was added to the biphasic mixture in one portion, after which the vial was flushed with Ar, capped and sealed, then heated to 40 °C with vigorous stirring for 14 hrs. Upon cooling to room temp., the reaction was quenched by pouring into 20 mL

1 M HCl and diluting with 20 mL ether. The phases were separated, and the aqueous phase was washed with three 10 mL portions of ether. After adding a handful of ice, the aqueous phase was basified with slow addition of 12 mL 6 M NaOH (swirling occasionally; reaction mixture becomes slightly cloudy with a white precipitate). The suspension was diluted 20 mL ethyl acetate, and the phases were separated. The aqueous phase was extracted with 10 mL portions of ethyl acetate three times. The combined organics were then dried over anhydrous magnesium sulfate, filtered to remove solids, and concentrated under vacuum. This revealed 135 mg of a slightly yellow oil that was confirmed to be the desired *anti*-C8-amine.

A portion of the *anti*-C8-amine from above (57.5 mg, 0.23 mmol) was dissolved in 2.5 mL dry THF in a dry vial under inert atmosphere. *N*-methylimidazole (1.8 μ L, 23 μ mol) was added in one portion, followed by bolus addition of Boc anhydride (79 μ L, 0.34 mmol). The vial was flushed with argon, capped and sealed, then heated to 45 °C for 20 hrs. The reaction was quenched with 20 mL 1:1 sat. NaHCO₃:1 M NaOH then diluted with 10 mL ether. The phases were separated. The aqueous phase was extracted with 10 mL portions of ether three times. The combined organics were then washed with 10 mL brine, dried over anhydrous magnesium sulfate, filtered to remove solids, and concentrated under vacuum. The crude residue was purified via flash chromatography over silica (7 to 35% ethyl acetate:hexanes, increasing in 7% increments; the residue was loaded with PhMe; the silica was pre-neutralized with 7% ethyl acetate:hexanes + 1% triethylamine). Collected product in two portions. The shoulder fractions totaled 58.6 mg of a slightly yellow oil that proved to be 97.2 wt% aminoCP **1v** with pentane (57.0 mg desired product). The center fractions yielded 13.0 mg of a clear, colorless oil, thus the total yield of aminoCP **1v** was 70.0 mg (59.4% over three steps).

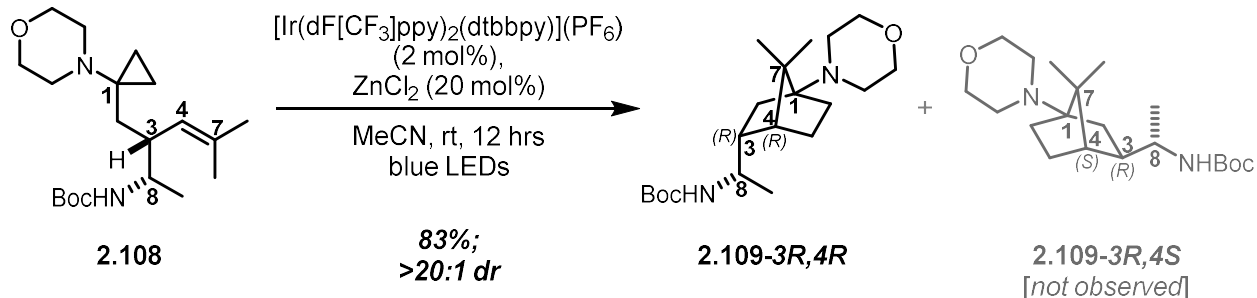
¹H NMR (CDCl₃, 700 MHz @ 40 °C): δ = 4.85 (d, 1H, *J* = 9.9 Hz, C4), 4.70 (br s, 1H, C8-NHBoc), 3.67 (br s, 1H, C8), 3.62 (*app.* t, 4H, *J* = 4.4 Hz, morph.), 2.57-2.49 (m, 5H, morph., C3), 1.86 (dd, 1H, *J* = 14.7, 3.9 Hz, C2), 1.71 (s, 3H, C7-Me), 1.65 (s, 3H, C7-Me), 1.45 (s, 9H, Boc), 1.21 (dd, 1H, *J* = 14.1, 8.3 Hz, C2), 1.01 (d, 3H, *J* = 6.8 Hz, C8-Me), 0.63-0.58 (m, 1H, CP), 0.56-0.51 (m, 1H, CP), 0.41-0.37 (m, 1H, CP), 0.35-0.31 (m, 1H, CP) ppm

¹³C NMR (CDCl₃, 176 MHz @ 40 °C): δ = 155.7, 133.4, 126.3, 79.0, 67.8, 50.6, 49.6, 43.3, 40.7, 34.3, 28.7, 26.1, 18.7, 11.6, 11.1 ppm

IR (neat): 3343, 2968, 2929, 2854, 2815, 1699, 1499, 1451, 1388, 1364, 1263, 1245, 1167, 1116, 1052, 1014, 985, 856 cm⁻¹

HRMS (ES⁺, *m/z*) calculated for C₂₀H₃₇N₂O₃⁺: 353.2799, Found: 353.2801

R_f = 0.45 (40% acetone in CH₂Cl₂), one yellow spot, KMnO₄



In dry vial under nitrogen, aminoCP **2.108** (73.9 mg, 210 μmol) was dissolved in 2.1 mL dry MeCN before adding $[\text{Ir}(\text{dF}[\text{CF}_3]\text{ppy})_2(\text{dtbbpy})](\text{PF}_6)$ (4.7 mg, 4.2 μmol) then ZnCl_2 (1.0 M in ether, 42 μL , 42 μmol) in one portion each. Reaction mixture was clear and bright yellow. Reaction mixture was degassed with three freeze-pump-thaw cycles. The reaction was performed by stirring at room temp (as controlled with jacketed water bath, temp maintained between 18-23 $^\circ\text{C}$) while irradiating with two strips of 4.4 W blue LEDs for 12 hrs. Mixture was orange, but still clear. The mixture was added to 20 mL 1:1 sat bicarb:1 M NaOH to ensure aq phase pH \sim 14, then diluted further with 10 mL ether. Phases were separated, and the aqueous phase was extracted with 10 mL ether three times. Combined organics were washed with 10 mL brine, dried over anhydrous sodium sulfate, filtered to remove solids, and concentrated *in vacuo*. The crude residue was purified via flash chromatography over silica (20 to 80% acetone: CH_2Cl_2 , increasing in 10% increments; residue loaded with PhMe; pre-neutralized with 20% acetone: CH_2Cl_2 + 1% NEt_3). No detectable starting material (perhaps a faint spot by TLC) or *3R,4S*-isomer (**2.109-3R,4S**). Collected the following:

- Recovered starting material: not detected
- *1R,3R,4R,8R*-Isomer (**2.109-3R,4R**): 61.0 mg; white solid; 82.5% yield
- *1S,3R,4S,8R* -Isomer (**2.109-3R,4S**): not detected

Characterization Data for **2.109-3R,4R**

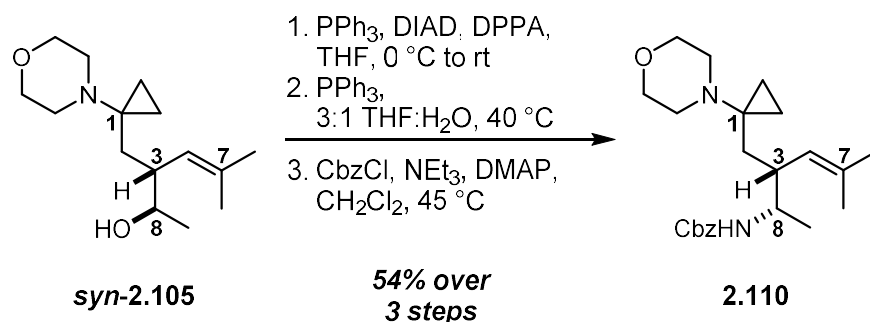
¹H NMR (CDCl₃, 500 MHz): δ = 4.20 (br s, 1H, C8-NHBoc), 3.69-3.63 (m, 4H, morph.), 3.48 (br s, 1H, C8), 2.57-2.50 (m, 4H, morph.), 2.01 (td, 1H, *J* = 11.5, 4.4 Hz, C2-eq), 1.92-1.84 (m, 1H, C3-eq), 1.84-1.77 (m, 1H, C6-eq), 1.69-1.59 (m, 2H, C5-eq, C5-ax), 1.45 (br s, 1H, C4), 1.43 (s, 9H, Boc), 1.37-1.30 (m, 1H, C6-ax), 1.13 (d, 3H, *J* = 6.3 Hz, C8-Me), 1.07 (s, 3H, C7-Me), 1.06 (s, 3H, C7-Me), 0.95 (dd, 1H, *J* = 12.0, 5.1 Hz, C2-ax) ppm

¹³C NMR (CDCl₃, 176 MHz @ 40 °C): δ = 155 (Boc), 79.2 (Boc), 70.5 (C1), 67.8 (morph.), 48.9 (morph.), 48.9 (C8), 48.8 (C7), 48.3 (C4), 43.3 (C3), 35.4 (C2), 29.7 (C6), 28.6 (Boc), 22.0 (C7-Me), 21.6 (C7-Me), 21.2 (C8-Me), 20.1 (C5) ppm

IR (neat): 3337, 2963, 2877, 2854, 2809, 1708, 1523, 1449, 1389, 1365, 1295, 1243, 1170, 1119, 1061, 1040, 887 cm⁻¹

HRMS (ES⁺, *m/z*) calculated for C₂₀H₃₇N₂O₃⁺: 353.2799, Found: 353.2801

R_f = 0.35 (60% acetone in CH₂Cl₂), one yellow spot, KMnO₄



The C8-OH aminoCP **syn-2.105** (199 mg, 0.79 mmol) was dissolved in 8.0 mL dry THF in a dry flask under inert atmosphere. Triphenylphosphine (247 mg, 0.94 mmol) was added in one portion before cooling to 0 °C. DIAD (0.20 mL, 1.02 mmol) was added dropwise over 15 sec, and the reaction mixture was stirred 20 min at 0 °C while covered in foil. DPPA (0.22 mL, 1.02 mmol) was then added dropwise over 15 sec. Upon complete addition, the ice bath was removed, and the reaction mixture was stirred at room temp. for 20 hrs while wrapped in foil. The reaction was quenched with 25 mL 1:1 sat. NaHCO₃:1 M NaOH then diluted with 25 mL ether. The phases were separated. The aqueous phase was extracted with 25 mL portions of ether three times. The combined organics were then washed with 10 mL brine, dried over anhydrous magnesium sulfate, filtered to remove solids, and concentrated under vacuum. The crude residue was purified via flash chromatography over silica (5 to 25% ethyl acetate:hexanes, increasing in 5% increments; the residue was loaded with PhMe). Obtained 178 mg of a clear, colorless oil that was moved on without further purification. This *anti*-C8-azide is the same that was detailed en route toward aminoCP **anti-1y** (pg. S183); partial characterization for the *anti*-C8-azide and subsequent *anti*-C8-amine can be found in that procedure.

The *anti*-C8-azide (ca. 0.64 mmol) was suspended in 4.5 mL THF and 1.5 mL HPLC-grade water. Triphenylphosphine (252 mg, 0.96 mmol) was added to the biphasic mixture in one portion, after which the vial was flushed with Ar, capped and sealed, then heated to 40 °C with vigorous stirring for 14 hrs. Upon cooling to room temp., the reaction was quenched by pouring into 20 mL

1 M HCl and diluting with 20 mL ether. The phases were separated, and the aqueous phase was washed with three 10 mL portions of ether. After adding a handful of ice, the aqueous phase was basified with slow addition of 12 mL 6 M NaOH (swirling occasionally; reaction mixture becomes slightly cloudy with a white precipitate). The suspension was diluted 20 mL ethyl acetate, and the phases were separated. The aqueous phase was extracted with 10 mL portions of ethyl acetate three times. The combined organics were then dried over anhydrous magnesium sulfate, filtered to remove solids, and concentrated under vacuum. This revealed 135 mg of a slightly yellow oil that was confirmed to be the desired *anti*-C8-amine.

A portion of the *anti*-C8-amine from above (57.5 mg, 0.23 mmol) was dissolved in 2.5 mL dry CH₂Cl₂ in a dry vial under inert atmosphere. Triethylamine (64 μ L, 0.46 mmol) and DMAP (5.6 mg, 46 μ mol) were added in one portion before cooling to 0 °C and then adding CbzCl (51 μ L, 0.34 mmol) dropwise over 1 min. The vial was removed from ice bath, flushed with Ar capped and sealed, and heated to 45 °C for 21 hrs. The reaction was quenched with 20 mL 1:1 sat. NaHCO₃:1 M NaOH then diluted with 10 mL ether. The phases were separated. The aqueous phase was extracted with 10 mL portions of ether three times. The combined organics were then washed with 10 mL brine, dried over anhydrous magnesium sulfate, filtered to remove solids, and concentrated under vacuum. The crude residue was purified via flash chromatography over silica (7 to 49% ethyl acetate:hexanes, increasing in 7% increments; the residue was loaded with PhMe; the silica was pre-neutralized with 7% ethyl acetate:hexanes + 1% triethylamine). Collected product in two portions. The shoulder fractions totaled 61.8 mg of a slightly yellow oil that proved to be 99.0 wt% aminoCP **2.110** with pentane (61.2 mg desired product). The center fractions yielded 8.8 mg of a clear, colorless oil, thus the total yield of aminoCP **2.110** was 70.0 mg (54.0% over three steps).

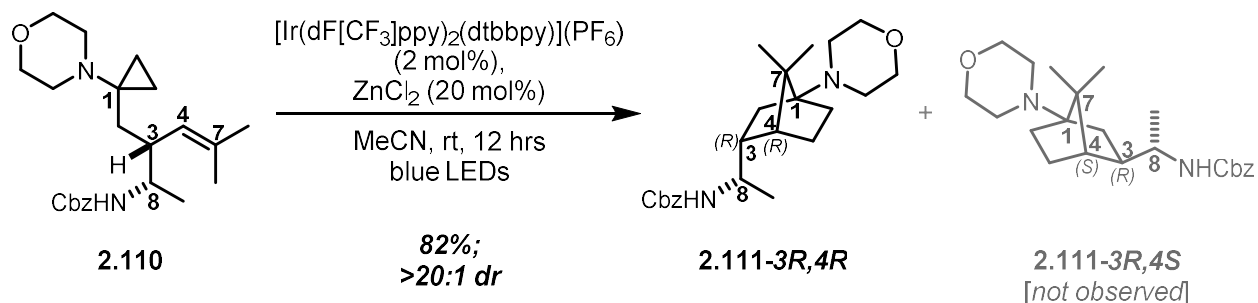
¹H NMR (CDCl₃, 700 MHz @ 40 °C): δ = 7.37-7.34 (m, 4H, Ph), 7.33-7.29 (m, 1H, Ph), 5.10 (s, 2H, CH₂Ph), 5.00 (br s, 1H, C8-NHCbz), 4.84 (d, 1H, *J* = 9.9 Hz, C4), 3.76 (br s, 1H, C8), 3.63-3.58 (m, 4H, morph.), 2.56 (br s, 1H, C3), 2.54-2.45 (m, 4H, morph.), 1.87 (dd, 1H, *J* = 13.8, 3.4 Hz, C2), 1.71 (s, 3H, C7-Me), 1.66 (br s, 3H, C7-Me), 1.19 (dd, 1H, *J* = 14.4, 8.3 Hz, C2), 1.05 (d, 3H, *J* = 6.8 Hz, C8-Me), 0.63-0.59 (m, 1H, CP), 0.56-0.51 (m, 1H, CP), 0.39-0.35 (m, 1H, CP), 0.33-0.29 (m, 1H, CP) ppm

¹³C NMR (CDCl₃, 176 MHz @ 40 °C): δ = 156.1, 137.0, 133.8, 128.7, 128.3, 128.2, 126.0, 67.7, 66.7, 51.3, 49.5, 43.3, 40.7, 34.7, 26.1, 18.7, 18.6, 11.4, 10.9 ppm

IR (neat): 3330, 2964, 2929, 2853, 2813, 1702, 1525, 1452, 1375, 1334, 1234, 1114, 1053, 1014, 984, 854, 735, 697 cm⁻¹

HRMS (ES⁺, *m/z*) calculated for C₂₃H₃₅N₂O₃⁺: 387.2642, Found: 387.2644

R_f = 0.45 (40% acetone in CH₂Cl₂), one yellow spot, KMnO₄



In dry vial under nitrogen, aminoCP **2.110** (72.6 mg, 188 μmol) was dissolved in 1.9 mL dry MeCN before adding $[\text{Ir}(\text{dF}[\text{CF}_3]\text{ppy})_2(\text{dtbbpy})](\text{PF}_6)$ (4.2 mg, 3.8 μmol) then ZnCl_2 (1.0 M in ether, 38 μL , 38 μmol) in one portion each. Reaction mixture was bright yellow and slightly cloudy, even after sonication. Reaction mixture was degassed with three freeze-pump-thaw cycles. The reaction was performed by stirring at room temp (as controlled with jacketed water bath, temp maintained between 18-23 $^\circ\text{C}$) while irradiating with two strips of 4.4 W blue LEDs for 12 hrs. No change in the appearance of the reaction mixture was observed. The mixture was added to 20 mL 1:1 sat bicarb:1 M NaOH to ensure aq phase pH \sim 14, then diluted further with 10 mL ether. Phases were separated, and the aqueous phase was extracted with 10 mL ether three times. Combined organics were washed with 10 mL brine, dried over anhydrous sodium sulfate, filtered to remove solids, and concentrated *in vacuo*. The crude residue was purified via flash chromatography over silica (10 to 90% acetone: CH_2Cl_2 , increasing in 10% increments; residue loaded with PhMe); the product partially co-eluted with some unidentified, colored catalyst decomposition product(s) (pre-neutralization of the silica would likely have prevented this). These byproduct(s) were removed through trituration from 60% ether:pentane followed by filtration through a plug of celite. No detectable starting material or 3R,4S-isomer (**2.111-3R,4S**). Collected the following:

- Recovered starting material: not detected
- 1R,3R,4R,8R-Isomer (**2.111-3R,4R**): 59.7 mg; white solid; 82.2% yield

- *1S,3R,4S,8R* -Isomer (**2.111-3R,4S**): not detected

Characterization Data for 2.111-3R,4R

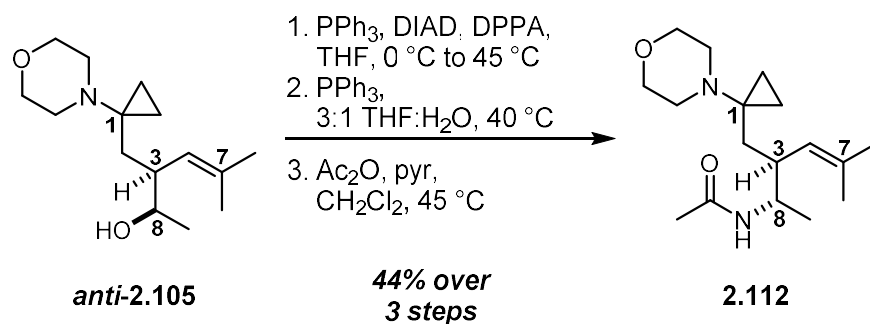
¹H NMR (CDCl₃, 700 MHz @ 40 °C): δ = 7.37-7.33 (m, 4H, Ph), 7.32-7.29 (m, 1H, Ph), 5.09 (s, 2H, Cbz), 4.41 (br s, 1H, C8-NHCbz), 3.68-3.64 (m, 4H, morph.), 3.58 (br s, 1H, C8), 2.57-2.50 (m, 4H, morph.), 2.03 (td, 1H, *J* = 11.9, 3.9 Hz, C2-eq), 1.95-1.89 (m, 1H, C3-eq), 1.83 (t, 1H, *J* = 11.9, 4.4 Hz, C6-eq), 1.68-1.57 (m, 2H, C5-eq, C5-ax), 1.42 (br s, 1H, C4), 1.37-1.31 (m, 1H, C6-ax), 1.17 (d, 3H, *J* = 6.1 Hz, C8-Me), 1.07 (s, 3H, C7-Me), 1.06 (s, 3H, C7-Me), 0.97 (dd, 1H, *J* = 12.2, 4.8 Hz, C2-ax) ppm

¹³C NMR (CDCl₃, 176 MHz @ 40 °C): δ = 155.7, 137.0, 128.7, 128.2, 128.1, 70.4, 67.8, 66.66, 49.5, 48.9, 48.7, 48.3, 43.2, 35.4, 29.6, 22.0, 21.5, 21.1, 20.1 ppm

IR (neat): 3320, 2955, 2876, 2810, 1697, 1529, 1450, 1286, 1231, 1213, 1117, 1085, 1062, 1040, 1028, 885, 736, 697 cm⁻¹

HRMS (ES⁺, *m/z*) calculated for C₂₃H₃₅N₂O₃⁺: 387.2642, Found: 387.2648

R_f = 0.35 (60% acetone in CH₂Cl₂), one yellow spot, KMnO₄



The C8-OH aminoCP **anti-2.105** (30.8 mg, 122 μmol) was dissolved in 1.2 mL dry THF in a dry flask under inert atmosphere. Triphenylphosphine (38 mg, 146 μmol) was added in one portion before cooling to 0 $^\circ\text{C}$. DIAD (31 μL , 158 μmol) was added dropwise over 15 sec, and the reaction mixture was stirred 20 min at 0 $^\circ\text{C}$ while covered in foil. DPPA (34 μL , 158 μmol) was then added dropwise over 15 sec. Upon complete addition, the ice bath was removed, and the reaction mixture was stirred at room temp for 20 hrs while wrapped in foil. The reaction was quenched with 2 mL 1:1 sat. NaHCO_3 :1 M NaOH then diluted with 2 mL ether. The phases were separated. The aqueous phase was extracted with 2 mL portions of ether three times. The combined organics were then dried over anhydrous magnesium sulfate, filtered to remove solids, and concentrated under vacuum. The crude residue was purified via flash chromatography over silica (5 to 25% ethyl acetate:hexanes, increasing in 5% increments, then 50 to 80 to 90% ethyl acetate:hexanes; the residue was loaded with PhMe). This provided 31.7 mg of the desired *syn*-C8-azide, along with 10.5 mg of starting material. The recovered starting material was exposed to essentially identical conditions, with the only adjustment being a 16 hr stir at 45 $^\circ\text{C}$ post-DPPA addition. Upon isolation of the product from this trial, a total of 42 mg of crude residue was obtained (in combination with the first exposure). This material was moved forward without further purification.

$^1\text{H NMR}$ (CDCl_3 , 500 MHz): δ = 4.85 (d, 1H, J = 10.0 Hz, C4), 3.62 (*app.* t, 4H, J = 4.6 Hz, morph.), 3.24 (*app.* quint., 1H, J = 6.8 Hz, C8), 2.58-2.47 (m, 5H, C3, morph.), 2.04 (dd, 1H, J =

14.4, 2.9 Hz, C2), 1.71 (s, 3H, C7-Me), 1.66 (s, 3H, C7-Me), 1.20 (d, 3H, $J = 6.6$ Hz, C8-Me), 1.10 (dd, 1H, $J = 14.4, 9.8$ Hz, C2), 0.64-0.59 (m, 1H, CP), 0.53-0.48 (m, 1H, CP), 0.45-0.40 (m, 1H, CP), 0.30-0.25 (m, 1H, CP) ppm

$R_f = 0.25$ (20% EtOAc in hexanes), one yellow spot, KMnO_4

The *syn*-C8-azide (assumed 0.12 mmol) was suspended in 1.2 mL THF and 0.4 mL HPLC-grade water. Triphenylphosphine (60 mg, 0.23 mmol) was added to the biphasic mixture in one portion, after which the vial was flushed with Ar, capped and sealed, then heated to 40 °C with vigorous stirring for 12 hrs. Upon cooling to room temp., the reaction was quenched by pouring into 3 mL 1 M HCl and diluting with 2 mL ether. The phases were separated, and the aqueous phase was washed with three 1 mL portions of ether. After basifying the aqueous phase with 1.5 mL 6 M NaOH (added dropwise with stirring; reaction mixture becomes slightly cloudy with a white precipitate), the suspension was diluted with 2 mL ethyl acetate. The phases were separated, and the aqueous phase was extracted with 2 mL portions of ethyl acetate three times. The combined organics were then dried over anhydrous magnesium sulfate, filtered to remove solids, and concentrated under vacuum. This material was moved forward without any further purification.

$^1\text{H NMR}$ (CDCl_3 , 500 MHz): $\delta = 4.89$ (d, 1H, $J = 10.0$ Hz, C4), 3.62 (*app.* t, 1H, $J = 4.6$ Hz, morph.), 2.81-2.76 (m, 1H, C8), 2.61-2.52 (m, 4H, morph.), 2.30-2.21 (m, 1H, C3), 1.93 (dd, 1H, $J = 14.4, 3.7$ Hz, C2), 1.73 (s, 3H, C7-Me), 1.63 (s, 3H, C7-Me), 1.20 (dd, 1H, $J = 14.2, 9.5$ Hz, C2), 1.03 (d, 1H, $J = 6.4$ Hz, C2), 0.62-0.57 (m, 1H, CP), 0.54-0.48 (m, 1H, CP), 0.48-0.43 (m, 1H, CP), 0.35-0.30 (m, 1H, CP) ppm

The crude residue from the Staudinger reduction detailed above (assumed 0.12 mmol) was dissolved in 800 μL dry CH_2Cl_2 under inert atmosphere. Added pyridine (61 μL , 0.76 mmol) then acetic anhydride (36 μL , 0.38 mmol) in one portion each. The vial was flushed with argon, capped and sealed, then heated to 45 $^\circ\text{C}$ for 4 hrs. The reaction was quenched with 2 mL 1:1 sat. NaHCO_3 :1 M NaOH then diluted with 2 mL ethyl acetate. The phases were separated. The aqueous phase was extracted with 2 mL portions of ethyl acetate three times. The combined organics were then dried over anhydrous magnesium sulfate, filtered to remove solids, and concentrated under vacuum. The crude residue was purified via flash chromatography over silica (10 to 60% acetone: CH_2Cl_2 , increasing in 10% increments; the silica was pre-neutralized with 10% acetone: CH_2Cl_2 + 1% triethylamine). This did not reveal pure material (18.4 mg total), thus the collected residue was exposed to a second round of chromatography over silica on pipet scale (10 to 30 to 50% acetone: CH_2Cl_2 ; the silica was pre-neutralized with 10% acetone: CH_2Cl_2 + 1% triethylamine). Obtained 15.6 mg of aminoCP ***syn*-2.112** as a clear, colorless oil (43.6% over three steps).

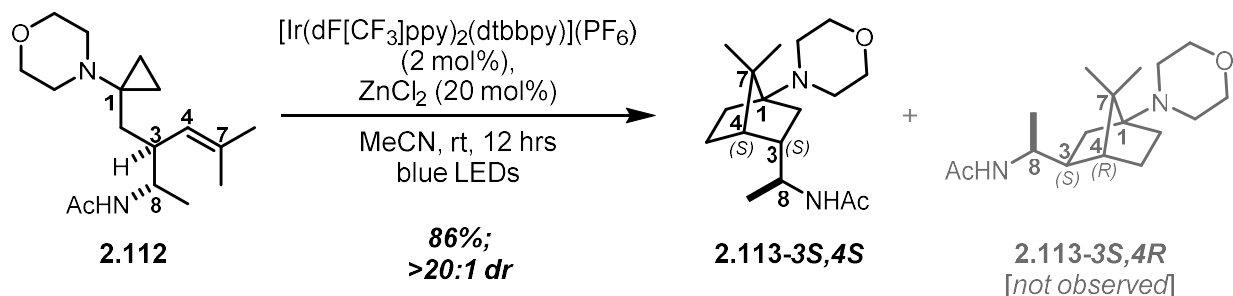
^1H NMR (CDCl_3 , 500 MHz): δ = 5.34 (d, 1H, J = 8.5 Hz, C8-NHAc), 4.92 (d, 1H, J = 10.5 Hz, C4), 4.03-3.95 (m, 1H, C8), 3.61 (*app.* t, 4H, J = 4.5 Hz, morph.), 2.60-2.48 (m, 5H, C3, morph.), 1.93 (s, 3H, Ac), 1.76 (dd, 1H, J = 13.9, 3.4 Hz, C2), 1.74 (s, 3H, C7-Me), 1.63 (s, 3H, C7-Me), 1.26 (dd, 1H, J = 14.2, 9.3 Hz, C2), 0.99 (d, 3H, J = 6.8 Hz, C8-Me), 0.60-0.55 (m, 1H, CP), 0.53-0.48 (m, 1H, CP), 0.46-0.41 (m, 1H, CP), 0.34-0.29 (m, 1H, CP) ppm

^{13}C NMR (CDCl_3 , 176 MHz): δ = 166.9, 134.1, 125.7, 67.8, 49.5, 48.8, 43.1, 39.8, 34.6, 26.2, 23.8, 18.6, 15.9, 11.8, 11.1 ppm

IR (neat): 3277, 3082, 2963, 2931, 2852, 2811, 1642, 1549, 1450, 1373, 1293, 1264, 1117 cm^{-1}

HRMS (ES^+ , m/z) calculated for $\text{C}_{17}\text{H}_{31}\text{N}_2\text{O}_2^+$: 295.2380, Found: 295.2382

$R_f = 0.30$ (50% acetone in CH_2Cl_2), one yellow spot, KMnO_4



In dry vial under nitrogen, aminoCP **2.112** (12.1 mg, 41 μmol) was dissolved in 450 μL dry MeCN before adding $[\text{Ir}(\text{dF}[\text{CF}_3]\text{ppy})_2(\text{dtbbpy})](\text{PF}_6)$ (0.9 mg, 0.8 μmol) then ZnCl_2 (1.0 M in ether, 8.2 μL , 8.2 μmol) in one portion each. Reaction mixture was bright yellow and slightly cloudy, even after sonication. Reaction mixture was degassed with three freeze-pump-thaw cycles. The reaction was performed by stirring at room temp (as controlled with jacketed water bath, temp maintained between 18-23 $^\circ\text{C}$) while irradiating with two strips of 4.4 W blue LEDs for 12 hrs. Mixture retained the yellow color but had become slightly cloudier. The mixture was added to 1 mL 1:1 sat bicarb:water containing 1 mL of 50% NaOH to ensure aq phase pH \sim 14, then diluted further with 1 mL ethyl acetate. Phases were separated, and the aqueous phase was extracted with 1 mL ethyl acetate three times. Combined organics were dried over anhydrous magnesium sulfate, filtered to remove solids, and concentrated *in vacuo*. The crude residue was purified via pipet chromatography over silica (50 to 70 to 90% acetone: CH_2Cl_2 ; pre-neutralized silica with 50% acetone: CH_2Cl_2 + 1% NEt_3). No detectable starting material or 3*S*,4*R*-isomer (**2.113-3*S*,4*R***). Collected the following:

- Recovered starting material: not detected
- 1*S*,3*S*,4*S*,8*R*-Isomer (**2.113-3*S*,4*S***): 10.4 mg; white solid; 86.0% yield
- 1*R*,3*S*,4*R*,8*R* -Isomer (**2.113-3*S*,4*R***): not detected

Characterization Data for **2.113-3S,4S**

¹H NMR (CDCl₃, 700 MHz): δ = 5.22 (d, 1H, *J* = 8.5 Hz, C8-NHAc), 3.93-3.86 (m, 1H, C8), 3.68-3.63 (m, 4H, morph.), 2.53-2.48 (m, 4H, morph.), 1.97 (s, 3H, Ac), 1.94 (td, 1H, *J* = 11.6, 3.8 Hz, C2-eq), 1.88-1.78 (m, 2H, C3-eq, C6-eq), 1.67 (tt, 1H, *J* = 12.9, 4.3 Hz, C5-eq), 1.52-1.47 (m, 1H, C5-ax), 1.45-1.40 (m, 1H, C6-ax), 1.40 (*app.* t, 1H, *J* = 4.6 Hz, C4), 1.16 (dd, 1H, *J* = 12.3, 4.6 Hz, C2-ax), 1.06 (s, 6H, C7-Me, C7-Me), 1.01 (d, 3H, *J* = 6.5 Hz, C8-Me) ppm

¹³C NMR (CDCl₃, 176 MHz): δ = 169.5 (Ac), 70.3 (C1), 67.7 (morph.), 48.9 (C8), 48.8 (C4), 48.8 (morph.), 48.4 (C7), 43.2 (C3), 35.0 (C2), 29.1 (C6), 23.8 (Ac), 21.9 (C7-Me), 21.5 (C7-Me), 19.9 (C5), 19.8 (C8-Me) ppm

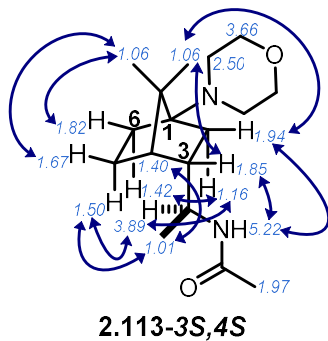
IR (neat): 3276, 2957, 2877, 2853, 2810, 1639, 1550, 1449, 1371, 1305, 1272, 1151, 1118, 920, 884, 730 cm⁻¹

HRMS (ES⁺, *m/z*) calculated for C₁₇H₃₁N₂O₂⁺: 295.2380, Found: 295.2383

R_f = 0.15 (70% acetone in CH₂Cl₂), one yellow spot, KMnO₄

2D NMR Data

- COSY, HSQC, and NOESY experiments were employed to assign the relative configuration of the isomer obtained. Key NOESY correlations (denoted by blue arrows) are provided below:



2.5 References

1. Lovering, F.; Bikker, J.; Humblet, C. "Escape from flatland: increasing saturation as an approach to improving clinical success." *J. Med. Chem.* **2009**, *52*, 6752-6756.
2. Lovering, F. "Escape from flatland 2: complexity and promiscuity." *Med. Chem. Commun.* **2013**, *4*, 515-519.
3. Meanwell, N. "Improving drug design: an update on recent applications of efficiency metrics, strategies for replacing problematic elements, and compounds in nontraditional drug space." *Chem. Res. Toxicol.* **2016**, *29*, 564-616.
4. Stockdale, T.; Williams, C. "Pharmaceuticals that contain polycyclic hydrocarbon scaffolds." *Chem. Soc. Rev.* **2015**, *44*, 7737-7763.
5. Ritchie, T.; Macdonald, S.; Young, R.; Pickett, S. "The impact of aromatic ring count on compound developability: further insights by examining carbo- and hetero-aromatic and -aliphatic ring types." *Drug Disc. Today* **2011**, *16*, 164-171.
6. Orr, S.; Ripp, S.; Ballard, E.; Henderson, J.; Scott, D.; Obach, S.; Sun, H.; Kalgutkar, A. "Mechanism-based inactivation (MBI) of cytochrome P450 enzymes: structure-activity relationships and discovery strategies to mitigate drug-drug interaction risks." *J. Med. Chem.* **2012**, *55*, 4896-4933.
7. Kalgutkar, A.; Dalvie, D. "Predicting toxicities of reactive metabolite-positive drug candidates." *Annu. Rev. Pharmacol. Toxicol.* **2015**, *55*, 35-54.
8. Thompson, R.; Isin, E.; Ogeese, M.; Mettetal, J.; Williams, D. "Reactive metabolites: current and emerging risk and hazard assessments." *Chem. Res. Toxicol.* **2016**, *29*, 505-533.
9. Brink, A.; Pahler, A.; Funk, C.; Schuler, F.; Schadt, S. "Minimizing the risk of chemically reactive metabolite formation of new drug candidates: implications for preclinical design." *Drug Disc. Today* **2017**, *22*, 751-756.
10. Iorga, A.; Dara, L.; Kaplowitz, N. "Drug-induced liver injury: cascade of events leading to cell death, apoptosis or necrosis." *Int. J. Mol. Sci.* **2017**, *18*, 1018.
11. Specific commentary can be found in Box 1 of: Scannell, J.; Blanckley, A.; Boldon, H.; Warrington, B. "Diagnosing the decline in pharmaceutical R&D efficiency." *Nat. Rev. Drug. Disc.* **2012**, *11*, 191-200.
12. Applequist, D.; Roberts, J. "Displacement reactions at bridgeheads of bridged polycarbocyclic systems." *Chem. Rev.* **1954**, *54*, 1065-1089.
13. Bartlett, P.; Knox, L. "Bicyclic structures prohibiting the Walden inversion. Replacement reactions in 1-substituted 1-apocamphanes." *J. Am. Chem. Soc.* **1939**, *61*, 3184-3192.

14. Walden, P. "Ueber die gegenseitige Umwandlung optischer Antipoden." *Ber. Dtsch. Chem. Ges.* **1896**, *29*, 133-138.
15. Kenyon, J.; Phillips, H. "Some recent developments in the study of the Walden inversion." *Trans. Faraday Soc.* **1930**, *26*, 451-458.
16. Olson, A.; Long, F. "The mechanism of substitution reactions." *J. Am. Chem. Soc.* **1934**, *56*, 1294-1299.
17. von Houben, J.; Pfankuch, E. "Über den ersatz von 2,6-umlagerungen in der campherreihe, die racemization optisch aktiver campherivate und den ubergang von D- in L-campherivate durch camphenumlagerungen zweiter art. (Über campher und terpene. VII)." *Justus Liebigs Ann. Chem.* **1931**, *489*, 193-223.
18. Wilt, J.; Parsons, C.; Schneider, C.; Schultenover, D.; Wagner, W. "The preparation and study of some 1-norbornenyl and norbornenyl-1-carbinyl derivatives." *J. Org. Chem.* **1968**, *33*, 694-708.
19. Nickon, A.; Nishida, T.; Lin, Y. "Bridgehead ketols." *J. Am. Chem. Soc.* **1969**, *91*, 6860-6861.
20. Beak, P.; Harris, B. "Reactions of apotricyclyl, apocamphor, and apobornenyl chloroformates with silver(I). Generation and aromatic substitution of a bridgehead radical and a bridgehead cation." *J. Am. Chem. Soc.* **1974**, *96*, 6363-6372.
21. Kropp, P.; Poindexter, G.; Pienta, N.; Hamilton, D. "Photochemistry of alkyl halides. 4. 1-Norbornyl, 1-norbornylmethyl, 1- and 1-adamantyl, and 1-octyl bromides and iodides." *J. Am. Chem. Soc.* **1976**, *98*, 8135-8144.
22. Martinez, A.; Vilar, E.; Fraile, A.; Cerero, S.; Herrero, M.; Ruiz, P.; Subramanian, L.; Gancedo, A. "Synthesis of substituted 1-norbornylamines with antiviral activity." *J. Med. Chem.* **1995**, *38*, 4474-4477.
23. Buser, S.; Vasella, A. "7-Oxanorbornane and norbornane mimics of a distorted β -D-mannopyranoside: synthesis and evaluation as β -mannosidase inhibitors." *Helv. Chim. Acta* **2005**, *88*, 3151-3173.
24. Dejmek, M.; Hrebabecky, H.; Sala, M.; Dracinsky, M.; Prochazkova, E.; Leyssen, P.; Neyts, J.; Balzarini, J.; Nencka, R. "From norbornane-based nucleotide analogs locked in south conformation to novel inhibitors of feline herpes virus." *Bioorg. Med. Chem.* **2014**, *22*, 2974-2983.
25. For a single example of a Rh(I)-catalyzed method from a (diallyl)vinylsulfonamide, see: Aïssa, C.; Ho, K.; Tetlow, D.; Pin-Nó, M. "Diastereoselective carbocyclization of 1,6-heptadienes triggered by rhodium-catalyzed activation of an olefinic C-H bond." *Angew. Chem. Int. Ed.* **2014**, *53*, 4209-4212.

26. Della, E.; Knill, A. "Synthesis of bridgehead-substituted bicyclo[2.2.1]heptanes. Radical cyclization of an oxime ether and an α,β -unsaturated ester." *Aust. J. Chem.* **1994**, *47*, 1833-1841.
27. DeLaive, P.; Lee, J.; Sprintschnik, H.; Abruna, H.; Meyer, T.; Whitten, D. "Photoinduced redox reactions of hydrophobic ruthenium(II) complexes." *J. Am. Chem. Soc.* **1977**, *99*, 7094-7097.
28. Hedstrand, D.; Kruizinga, W.; Kellogg, R. "Light induced and dye accelerated reductions of phenacyl onium salts by 1,4-dihydropyridines." *Tetrahedron Lett.* **1978**, *14*, 1255-1258.
29. Xu, W.; Jeon, Y.; Hasegawa, E.; Yoon, U.; Mariano, P. "Novel electron-transfer photocyclization reactions of α -silyl amine α,β -unsaturated ketone and ester systems." *J. Am. Chem. Soc.* **1989**, *111*, 406-408.
30. Douglas, J.; Nguyen, J.; Cole, K.; Stephenson, C.R.J. "Enabling novel photoredox reactivity via photocatalyst selection." *Aldrichim. Acta* **2014**, *47*, 15-25.
31. Shaw, M.; Twilton, J.; MacMillan, D. "Photoredox catalysis in organic chemistry." *J. Org. Chem.* **2016**, *81*, 6898-6926.
32. Douglas, J.; Sevrin, M.; Stephenson, C.R.J. "Visible light photocatalysis: applications and new disconnections in the synthesis of pharmaceutical agents." *Org. Process Res. Dev.* **2016**, *20*, 1134-1147.
33. Beatty, J.; Stephenson, C.R.J. "Amine functionalization via oxidative photoredox catalysis: methodology development and complex molecule synthesis." *Acc. Chem. Res.* **2015**, *48*, 1474-1484.
34. Staveness, D.; Bosque, I.; Stephenson, C.R.J. "Free radical chemistry enabled by visible light-induced electron transfer." *Acc. Chem. Res.* **2016**, *49*, 2295-2306.
35. Morris, S.; Wang, J.; Zheng, N. "The prowess of photogenerated amine radical cations in cascade reactions: from carbocycles to heterocycles." *Acc. Chem. Res.* **2016**, *49*, 1957-1968.
36. Condie, A.; Gonzalez-Gomez, J.; Stephenson, C.R.J. "Visible-light photoredox catalysis: aza-Henry reactions via C-H functionalization." *J. Am. Chem. Soc.* **2010**, *132*, 1464-1465.
37. Yoon, U.; Su, Z.; Mariano, P. (2004). The Dynamics and Photochemical Consequences of Aminium Radical Reactions. In *CRC Handbook of Organic Photochemistry and Photobiology*, 2nd Ed., W. Horspool and F. Lenci, eds. (CRC Press), ch., 101.
38. For the seminal proposal of homolytic amine radical cation decomposition pathways, see: DeLaive, P.; Foreman, T.; Giannotti, C.; Whitten, D. "Photoinduced electron transfer reactions of transition-metal complexes with amines. Mechanistic studies of alternate pathways to back electron transfer." *J. Am. Chem. Soc.* **1980**, *102*, 5627-5631.

39. For the seminal use of an oxidized aminoCP in synthesis, see: Itoh, T.; Kaneda, K.; Teranishi, S. "Novel oxygenolysis of cyclopropylamines to epoxy ketones." *Tetrahedron Lett.* **1975**, *32*, 2801-2804.
40. Beatty, J.; Stephenson, C.R.J. "Synthesis of (-)-pseudotabersonine, (-)-pseudovincadifformine, and (+)-coronaridine enabled by photoredox catalysis in flow." *J. Am. Chem. Soc.* **2014**, *136*, 10270-10273.
41. Takemoto, Y.; Yamagata, S.; Furuse, S.; Hayase, H.; Echigo, T.; Iwata, C. "CAN-mediated tandem 5-*exo*-cyclisation of tertiary aminocyclopropanes: novel accelerative effect of an *N*-benzyl group for oxidative ring-opening." *Chem. Commun.* **1998**, 651-652.
42. Lee, J.; Sun, J.; Blackstock, S.; Cha, J. "Facile ring opening of tertiary aminocyclopropanes." *J. Am. Chem. Soc.* **1997**, *119*, 10241-10242.
43. Maity, S.; Zhu, M.; Shinabery, R.; Zheng, N. "Intermolecular [3+2] cycloaddition of cyclopropylamines with olefins by visible-light photocatalysis." *Angew. Chem. Int. Ed.* **2012**, *51*, 222-224.
44. Wang, J.; Zheng, N. "The Cleavage of a C-C Bond in Cyclobutylanilines by Visible-Light Photoredox Catalysis: Development of a [4+2] Annulation Method." *Angew. Chem. Int. Ed.* **2015**, *54*, 11424-11427.
45. Wang, J.; Nguyen, T.H.; Zheng, N. "Photoredox-catalyzed [4 + 2] annulation of cyclobutylanilines with alkenes, alkynes, and diynes in continuous flow." *Sci. China: Chem.* **2016**, *59*, 180-183.
46. Nguyen, T.; Maity, S.; Zheng, N. "Visible light mediated intermolecular [3+2] annulation of cyclopropylamines with alkynes." *Beilstein J. Org. Chem.* **2014**, *10*, 975-980.
47. Nguyen, T.; Morris, S.; Zheng, N. "Intermolecular [3+2] annulation of cyclopropylanilines with alkynes, enynes, and diynes via visible light photocatalysis." *Adv. Synth. Catal.* **2014**, *356*, 2831-2837.
48. Cha, J.; Kulinkovich, O. (2012). The Kulinkovich cyclopropanation of carboxylic acid derivatives. In *Organic Reactions*, Vol. 77, S. Denmark, ed. (John Wiley & Sons, Inc.), pp. 1-160.
49. Lowry, M.; Goldsmith, J.; Slinker, J.; Rohl, R.; Pascal, R.; Malliaras, G.; Bernhard, S. "Single-layer electroluminescent devices and photoinduced hydrogen production from an ionic iridium(III) complex." *Chem. Mater.* **2005**, *17*, 5712-5719.
50. Brooks, A.; Basore, K.; Bernhard, S. "Photon-driven reduction of Zn²⁺ to Zn metal." *Inorg. Chem.* **2013**, *52*, 5794-5800.
51. Smith, J.; Masheder, D. "Amine Oxidation. Part IX." *J. Chem. Soc., Perkin Trans. 2* **1976**, 47-51.

52. Tajima, T.; Fuchigami, T. "An Electrolytic System That Uses Solid-Supported Bases for *In Situ* Generation of a Supporting Electrolyte from Acetic Acid Solvent." *Angew. Chem. Int. Ed.* **2005**, *44*, 4760-4763.
53. Douglas, J.; Cole, K.; Stephenson, C.R.J. "Photoredox catalysis in a complex pharmaceutical setting: toward the preparation of JAK2 inhibitor LY2784544." *J. Org. Chem.* **2014**, *79*, 11631-11643.
54. Musacchio, A.; Lainhart, B.; Zhang, X.; Naguib, S.; Sherwood, T.; Knowles, R. "Catalytic intermolecular hydroaminations of unactivated olefins with secondary alkyl amines." *Science* **2017**, *355*, 727-730.
55. Hancock, A.; Tanko, J. "Radical Cation/Anion and Neutral Radicals: A Comparison" in *Encyclopedia of Radicals in Chemistry, Biology and Materials* (John Wiley & Sons, Inc., 2012).
56. Wayner, D.; McPhee, D.; Griller, D. "Oxidation and reduction potentials of transient free radicals." *J. Am. Chem. Soc.* **1998**, *110*, 132-137.
57. Fu, Y.; Liu, L.; Yu, H.; Wang, Y.; Guo, Q. "Quantum-Chemical Predictions of Absolute Standard Redox Potentials of Diverse Organic Molecules and Free Radicals in Acetonitrile." *J. Am. Chem. Soc.* **2005**, *127*, 7227-7234.
58. Arias-Rotondo, D.; McCusker, J. "The photophysics of photoredox catalysis: a roadmap for catalyst design." *Chem. Soc. Rev.* **2016**, *45*, 5803-5820.
59. Cismesia, M.; Yoon, T. "Characterizing chain processes in visible light photoredox catalysis." *Chem. Sci.* **2015**, *6*, 5426-5434.
60. Cai, Y.; Wang, J.; Zhang, Y.; Li, Z.; Hu, D.; Zheng, N.; Chen, H. "Detection of fleeting amine radical cations and elucidation of chain processes in visible light-mediated [3+2] annulation by online mass spectrometric techniques." *J. Am. Chem. Soc.* **2017**, *139*, 12259-12266.
61. Staveness, D.; Collins, J.L. III.; McAtee, R.C.; Stephenson, C.R.J. "Exploiting Imine Photochemistry for Masked N-Centered Radical Reactivity." *Angew. Chem. Int. Ed.* **2019**, *58*, 19000-19006.
62. Alpers, D.; Gallhof, M.; Witt, J.; Hoffmann, F.; Brasholz, M. "Photoassisted oxidation of ruthenium(II)-photocatalysts Ru(bpy)₃²⁺ and Ru(bpz)₃²⁺ to RuO₄: orthogonal tandem photoredox and oxidation catalysis." *Chem. Commun.* **2017**, *52*, 1025-1028.
63. Beatty, J.; Douglas, J.; Cole, K.; Stephenson, C.R.J. "A scalable and operationally simple radical trifluoromethylation." *Nature Commun.* **2015**, *6*, 7919.

64. Devery, J.; Douglas, J.; Nguyen, J.; Cole, K.; Flowers, R.; Stephenson, C.R.J. "Ligand functionalization as a deactivation pathway in a *fac*-Ir(ppy)₃-mediated radical addition." *Chem. Sci.* **2015**, *6*, 537.
65. Lowry, M.; Goldsmith, J.; Slinker, J.; Rohl, R.; Pascal, R.; Malliaras, G.; Bernhard, S. "Single-Layer Electroluminescent Devices and Photoinduced Hydrogen Production from an Ionic Iridium(III) Complex." *Chem. Mater.* **2005**, *17*, 5712-5719.
66. Pangborn, A.; Giardello, M.; Grubbs, R.; Rosen, R.; Timmers, F. "Safe and Convenient Procedure for Solvent Purification." *Organometallics* **1996**, *15*, 1518-1520.
67. Beatty, J.; Douglas, J.; Miller, R.; McAtee, R.; Cole, K.; Stephenson, C.R.J. "Photochemical perfluoroalkylation with pyridine *N*-oxides: mechanistic insights and performance on a kilogram scale." *Chem* **2016**, *1*, 456-472.
68. Braddock, D.C.; Cansell, G.; Hermitage, S.A. "*Ortho*-substituted iodobenzene as novel organocatalysts for bromination of alkenes." *Chem. Commun.* **2006**, 2483-2485.
69. Kopka, K.; Faust, A.; Keul, P.; Wagner, S.; Breyholz, H-J.; Höltke, C.; Schober, O.; Schäfers, M.; Levkau, B. "5-Pyrrolidinylsulfonyl Isatins as a Potential Tool for the Molecular Imaging of Caspases in Apoptosis." *J. Med. Chem.* **2006**, *49*, 6704-6715.
70. Dubost, C.; Leroy, B.; Markó, I.E.; Tinant, B.; Declercq, J-P.; Bryans, J. "Stereoselective synthesis of functionalised triol units by SnCl₄ promoted allylation of α -benzyloxyaldehydes: crucial role of the stoichiometry of the Lewis acid." *Tetrahedron* **2004**, *60*, 7693-7704.
71. Koo, J.; Park, H-S.; Shin, S. "Selectivity control by silver catalysts in the cycloisomerization of 1,6-enynes derived from propiolamides." *Tet. Lett.* **2013**, *54*, 834-839.
72. Wender, P.A.; Schrier, A.J. "Total Synthesis of Bryostatin 9." *J. Am. Chem. Soc.* **2011**, *133*, 9228-9231.

Chapter 3

Examining Multiple Modes of Diastereoselectivity in the Synthesis of 1-Aminonorbornanes

The work presented in this chapter is in preparation for publication and has been completed in collaboration with Dr. Logan Combee (University of Michigan), Dr. Mark Raycroft (University of Ottawa), Alexander Levashkevich (University of Michigan), and Dr. Daryl Staveness (University of Michigan)

3.1 Introduction

Chemical transformations invoking radical intermediates have been established as powerful tools in the areas of complex molecule synthesis owing to high functional group tolerance and mild reaction conditions. The stereochemical outcome of many classes of radical reactions have been investigated rigorously over the last 30 years, with foundational contributions by Curran,¹ Porter,² and Beckwith,^{3,4} among others,⁵⁻⁸ and selectivity can commonly be attributed to arising from either catalyst or substrate control.

A resurgence of new methods to generate radical species employing photoredox catalysis⁹⁻¹¹ and electrochemical¹² protocols has emerged in the last decade, and the development of many enantioselective radical reactions have focused on stereochemical outcomes derived from catalyst control.¹³⁻¹⁸ While asymmetric catalysis has proven to be a transformative technology by expanding the breadth of readily-available chiral starting materials and allowing divergent access

to stereoisomeric products by changing the stereochemical configuration of the catalyst, these approaches have inherent limitations such as overcoming innate substrate control.¹⁹

Leveraging substrate control through stereochemical models for systems which are well studied offers a robust means of predicting and targeting desired stereochemistry without the need to design effective asymmetric catalysts. These examples commonly require the minimization of A_{1,3} strain or *syn*-pentane interactions,²⁰ which are reliably assessed through elementary structural analysis.

There exist, however, notable exceptions which rely on stereoelectronic effects. In 1978, Shono *et. al.* disclosed high diastereoselectivity in the synthesis of five-membered cyclic tertiary alcohols.²¹ Electrochemical reduction of nonconjugated olefinic ketones generated a ketyl radical which underwent stereoselective cyclization to yield the *cis*-disposed product (Figure 3.1A). The selectivity is driven by minimization of electrostatic repulsion in the transition state, in which the oxyanion and developing negative charge on the distal olefinic carbon are positioned in a *trans* configuration. Renaud reported the radical cyclization of bromoacetals into chiral tetrahydrofurans, with stereoinduction arising from an acetal center.²²⁻²⁵ Concurrent computational and experimental studies by Beckwith²⁶ highlighted the importance of the anomeric effect in stabilizing the axial conformer in the transition state of the 5-*exo-trig* cyclization (Figure 3.1B).²⁷ In another approach, Hanessian described 1,2-asymmetric induction via an intramolecular hydrogen-bonding interaction as the stereocontrolling element in the radical α -allylation of chiral amino acids.²⁸ Felkin-Ahn analysis of the pseudo six-membered transition state illustrates the origin of the observed *anti*-selectivity (Figure 3.1C).

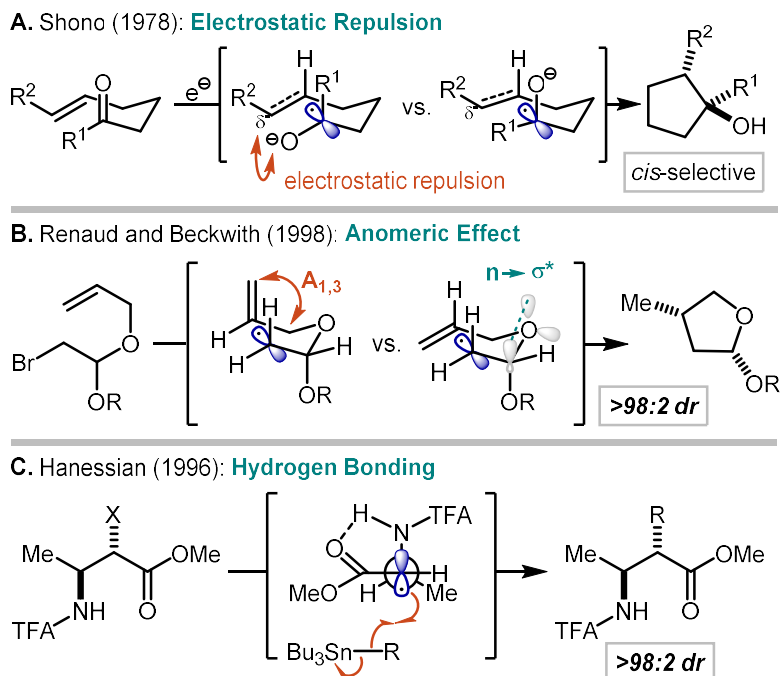


Figure 3.1. Stereochemical models for chiral induction via substrate control

Recently, our group disclosed an unusual trend in the diastereomeric outcome in the synthesis of 1-aminonorbornanes (aminoNBs) as a result of substrate control.²⁹ Our interest in employing aminoNBs as saturated aniline isosteres led us to design a robust method to synthesize differentially substituted aminoNBs with the overarching goal of providing efficient access to new, versatile chemical building blocks.³⁰ Toward that end, and given the multiple stereodefined sites present in aminoNBs, developing our understanding of stereochemical determinants would enable predictive design of aminoNBs and broaden the utility of such a scaffold in drug discovery and synthesis.

In the presence of the excited state of an iridium photocatalyst, aminocyclopropanes (aminoCPs; **3.1**) undergo single electron oxidation to the amine radical cation (**3.2**) (Figure 3.2). Rapid strain-driven homolysis yields β -iminium radical **3.3**, which is poised to undergo serial 6-*exo-trig* and 5-*exo-trig* cyclizations to construct the norbornane core. Subsequent reduction of **3.5** closes the catalytic cycle and releases the final aminoNB product (**3.6**). Both cyclization steps can

result in diastereomeric products. The initial *6-exo-trig* cyclization sets the stereochemical configuration of the C2 and C3 positions (**3.3** to **3.4**), while the subsequent *5-exo-trig* (**3.4** to **3.5**) determines the configuration of C7. For C2 and C3 substituents, we hypothesized that canonical steric models would sufficiently describe the observed outcomes. Simple steric models, however, were insufficient in describing the outcome observed for the C7 position following the *5-exo-trig* cyclization. We thus endeavored to evaluate the effects governing C3 and C7 independently.

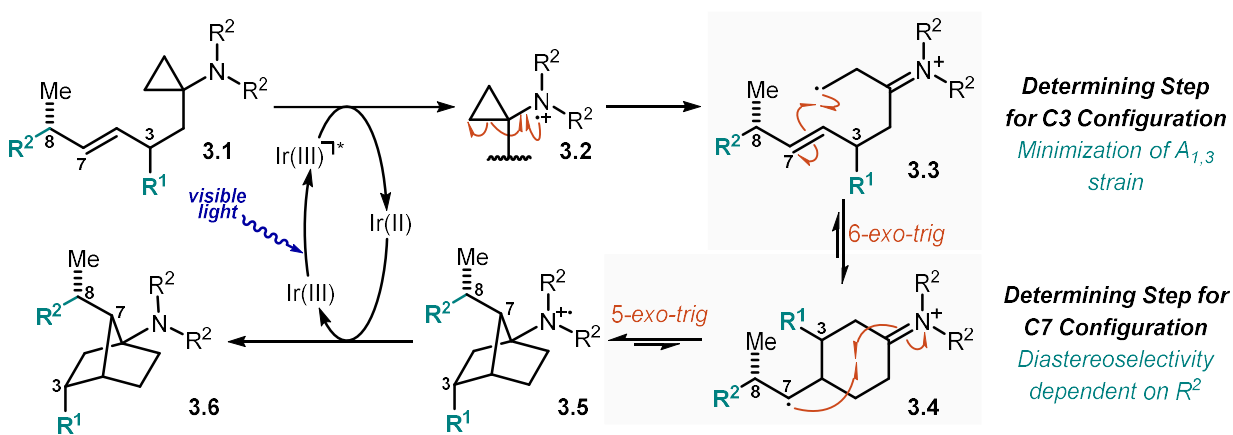


Figure 3.2. Mechanism of [3+2] photochemical cyclization of aminoCPs to aminoNBs

3.2 Results and Discussion

3.2.1 C3 Diastereoselectivity

As hypothesized, the C3 stereochemical outcome is readily rationalized via minimization of $A_{1,3}$ strain through a chair-like transition state. This results in selectivity for axial positioning of substituents at C3 in >20:1 dr. This strong preference for axial positioning of substituents in the final product has been evaluated computationally with a clear energetic benefit for this outcome. Upon generation of β -iminium radical **3.8**, 5.4 kcal/mol energy difference separates the favorably positioned equatorial methyl group (**TS-Me_{eq}**) from the more highly strained **TS-Me_{ax}** in the transition state of the *6-exo-trig* cyclization (Figure 3.3). The calculated transition state structures

exhibit obvious $A_{1,3}$ relationships as the reaction proceeds – the minimization of which accounts for a $>10^4$ preference for equatorial positioning in **3.9-eq**. Subsequent conformational change of the six-membered ring from a chair to a boat prior to the *5-exo-trig* cyclization results in the final axially-substituted norbornane.

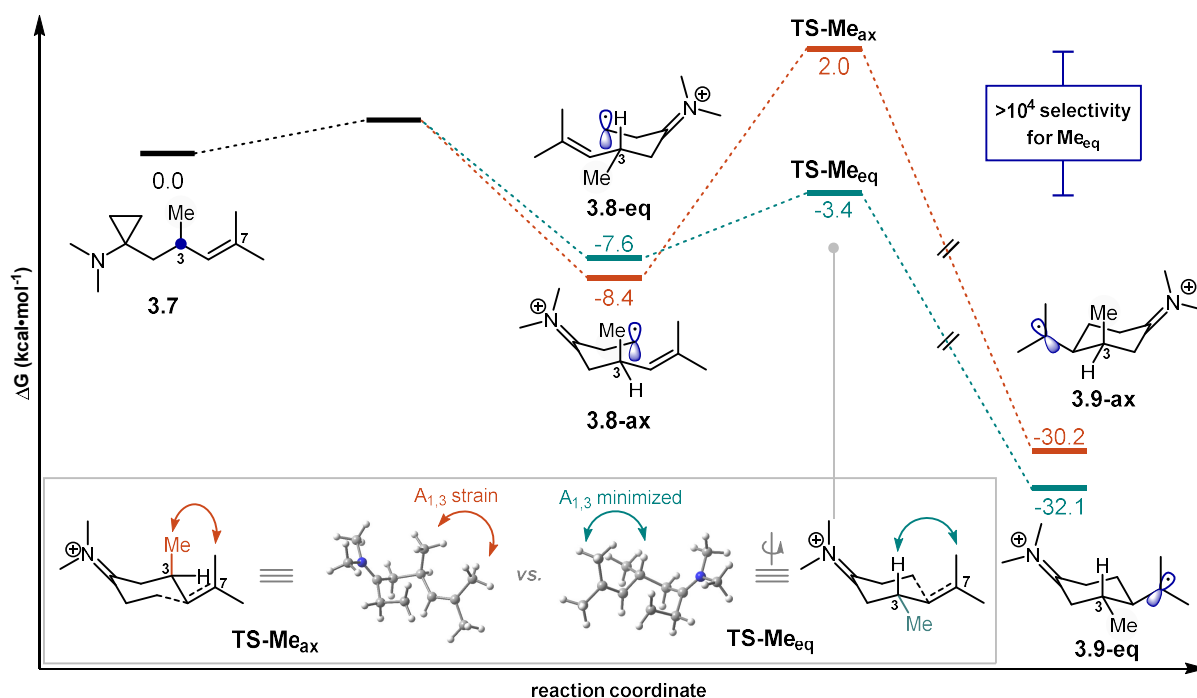


Figure 3.3. Computational evaluation of C3 diastereoselectivity (CBS-QB3)

3.2.2 C7 Diastereoselectivity

When evaluating mono-C7 substituted aminoCPs with a chiral center at C8 in this transformation (**3.10**; Figure 3.4A), it was determined that the identity of the C8 functionality influenced the distribution of the expected diastereomeric products. Based on these initial observations, a kinetic model was developed to explain the observed outcomes in which the non-bonding lone pairs on the oxygen engage in an electrostatic interaction with the π^* orbital of the iminium ion early in the transition state of the *5-exo-trig* cyclization (Figure 3.4B). In the transition state towards the observed minor diastereomer (*7R,8R*), the electrostatic interaction is obstructed

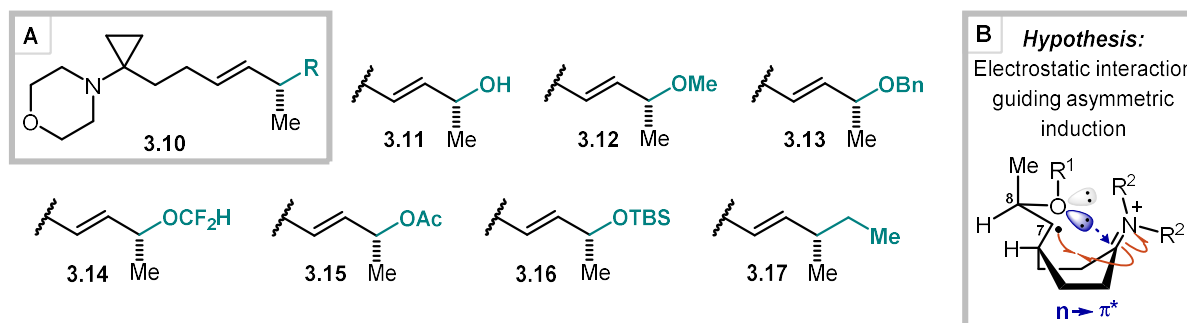


Figure 3.4. (A) AminoCPs evaluated to probe diastereomeric outcomes; (B) Proposed transition state model for observed diastereoselectivity

by an energetically unfavorable gauche interaction between the C8-methyl and the norbornyl backbone (Figure 3.5). In order to interrogate this model, we synthesized a representative set of C7-substituted aminoCPs (**3.11-3.17**) displaying a range of oxygen lone pair availability based on differing steric and electronic properties. We hypothesized that if an electrostatic interaction was primarily dictating the stereochemical outcome, this array of substrates should present distinct trends in diastereoselectivity upon cyclization.

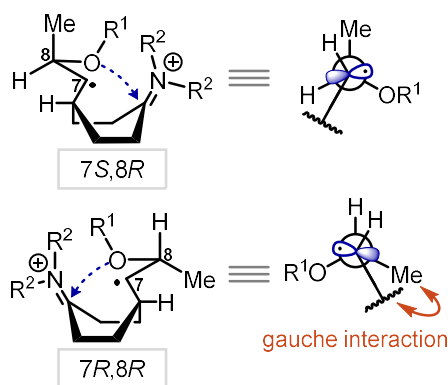


Figure 3.5. Unfavorable gauche interaction towards $7R,8R$ product hinders electrostatic interaction

Alcohol **3.11** produces the $7S,8R$ diastereomer (**3.18**) as the sole product of the reaction (Figure 3.6). Methyl ether **3.12** also proceeds in excellent selectivity (**3.19**, >20:1 *dr*) in 48% yield, but when appending the sterically equivalent but electron-withdrawing difluoromethyl ether **3.14**, the *dr* is significantly eroded to 7:1 (**3.21**). Moderately increasing the steric contribution with

benzyl ether **3.13** decreases the selectivity to 8:1 (**3.20**), and the electron-withdrawing acetate **3.15** diminishes the selectivity to 5:1 (**3.22**). When the ability for the oxygen lone pairs are further blocked by the sterically demanding TBS group as in **3.16**, poor selectivity is observed (**3.23**, 2.4:1 *dr*). Completely removing the ability for the electrostatic interaction to occur by replacing the oxygen atom with an ethyl group (for direct steric comparison to R = OMe, **3.12**), aminoCP **3.17** yielded little to no diastereoselectivity (**3.24**, 1.1:1 *dr*). These results align with the proposed kinetic model, suggesting that as the electron density in the n-orbital decreases (R = CHF₂, Ac) or is sterically less accessible (R = TBS), there is no longer a conformational preference in the 5-*exo-trig* transition state.

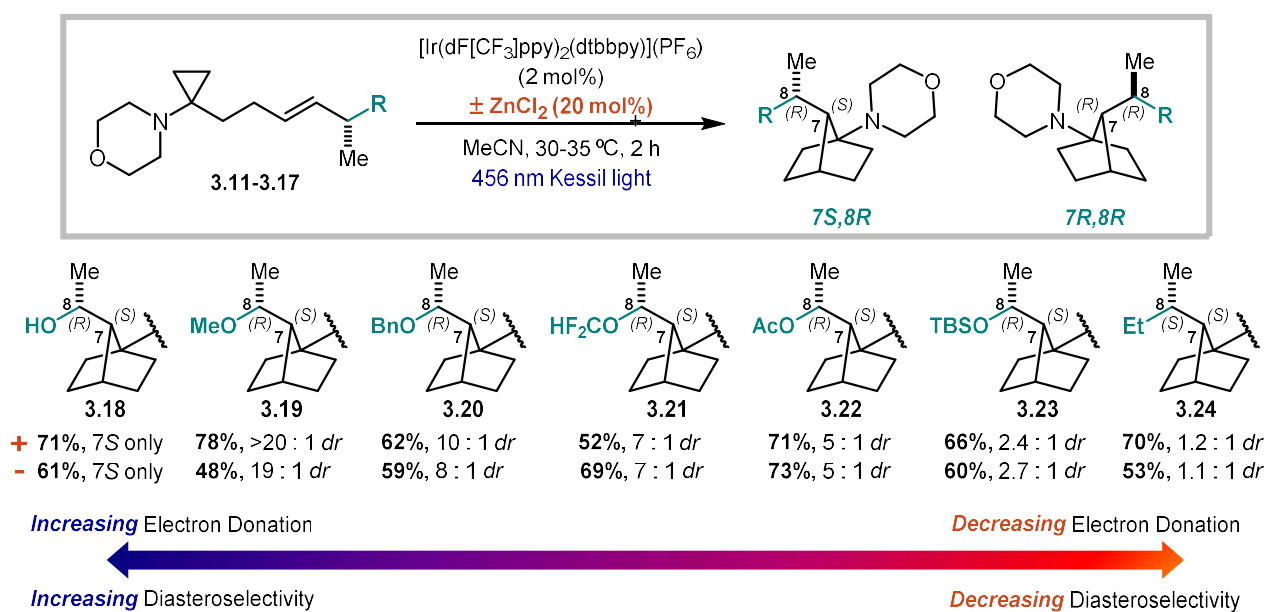


Figure 3.6. Relationship between electron donating ability of the C8 substituent and diastereomeric ratio of aminoNB products

Previous optimization (see Section 3.4.2) of this method found that the addition of Lewis acidic salts such as ZnCl₂ or LiBF₄ enhanced yields in most cases. As both Lewis and Brønsted acids have been implicated in controlling the stereochemical outcome of radical reactions,^{13,31,32} we wanted to exclude the possibility of ZnCl₂ influencing the observed diastereoselectivities. As

such, each substrate was subjected to the reaction conditions in both the presence and absence of 20 mol% ZnCl₂. While there was generally a decrease in product yield in the absence of ZnCl₂, the overall selectivity trend was unchanged. Thus, the role of Lewis acids in the reaction can be excluded as a variable influencing the stereochemical outcome.

Efforts were also made to characterize the observed selectivity through computational analysis of the 5-*exo-trig* step using **3.25**, a structural congener of aminoCP **3.11** which leads to a single diastereomer. The computed energy surface for the penultimate 5-*exo-trig* cyclization is characterized by various minima likely contributing to the relevant transition states. Figure 3.7 depicts two sets of transition state conformers, which in part demonstrate the complexity of structures leading to selectivity. **TS-3.26-R** and related **TS-3.26-S** exhibit dominance of steric effects, positioning the pendant heteroatom in a transannular position over the forming norbornyl core (Figure 3.7A). These structures are separated by merely 0.2 kcal/mol of energy and offer little

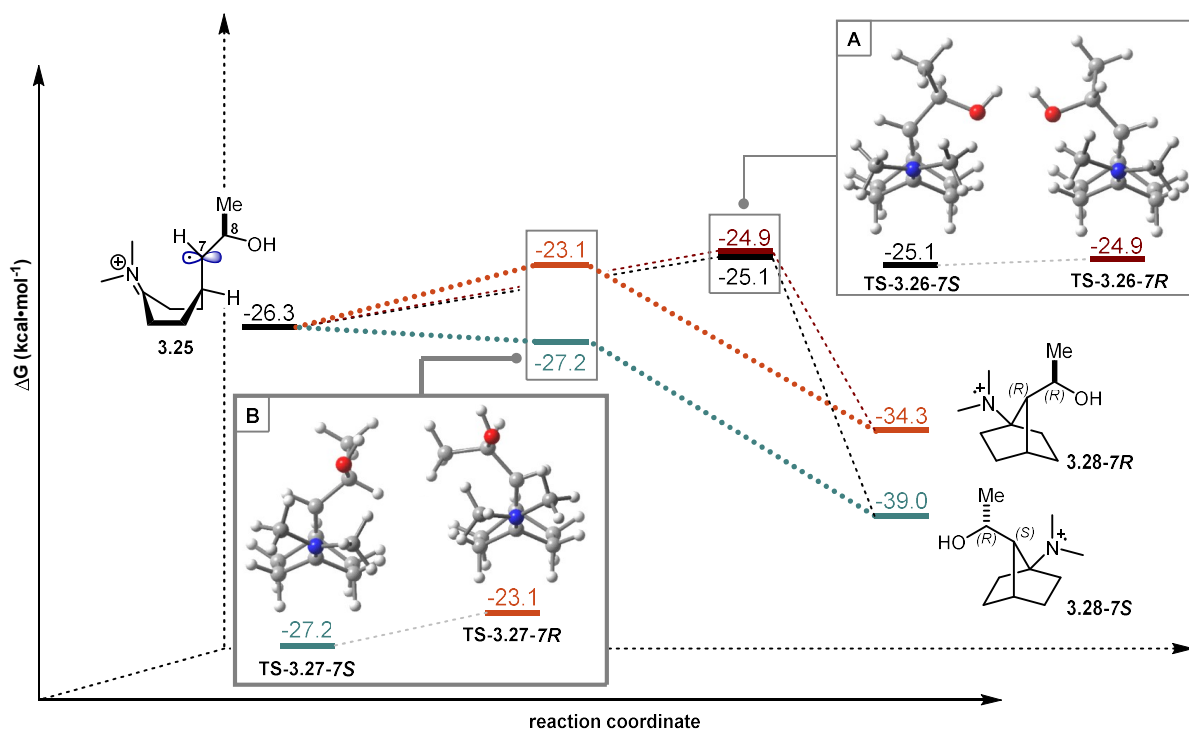


Figure 3.7. Energy coordinate diagram with two transition state models

to no insight into the observed experimental selectivity. Given the presence of multiple minima on the energy surface as **3.25** proceeds to product, we looked for other structures which might correlate to our hypothesized electrostatic interaction. In this way, **TS-3.27-R** and **TS-3.27-S** were identified as alternative transition state structures (Figure 3.7B). These are characterized by the positioning of the oxygen over the intermediate iminium as C7 approaches C1. Interestingly, **TS-3.27-R** and **TS-3.27-S** are separated by 4.1 kcal/mol of energy, and the reaction of **TS-3.27-S** represents a barrierless process within this context. As such, these transition states approximating the presence of an electrostatic interaction are in better agreement with observed experimental outcomes.

Having now identified two sets of transition states, we evaluated each aminoCP substrate computationally and compiled the data for both the sterically-controlled transition states (e.g. **TS-26**) and the electronically-controlled transition states (e.g. **TS-27**) in the *5-exo-trig* cyclization (Table 3.1). For all substrates, no trend could be observed by analysis of the steric-dominant transition states. Energy differences in these systems were nominal and did not correspond to the experimental diastereoselectivities. In contrast, the alternate transition states positioning the oxygen functionality over the iminium resulted in greater consistency with the experimental trend.

Additionally, the calculated reaction pathway through either type of transition state suggested reversibility of the *5-exo-trig* step based on the relatively low energy barriers. This turned our attention to evaluating thermodynamic factors that may also contribute to the observed selectivities. To probe the reversibility of the reaction, free alcohol aminoNB **3.18-7R** was independently prepared via protodesilylation of **3.23-7R** (Figure 3.8A). Subjecting **3.23-7R** to the standard reaction conditions in the absence of ZnCl₂, the production of **3.23-7S** was monitored

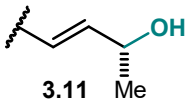
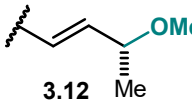
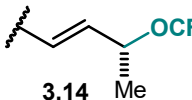
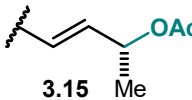
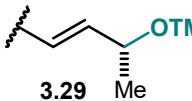
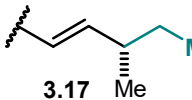
Substrate	$\Delta\Delta G^\ddagger$, kcal·mol ⁻¹		Experimental <i>dr</i> (7 <i>S</i> /7 <i>R</i>) ^b
	Steric	Electronic	
 3.11	0.1 ^a 0.2	-4.3 ^a -4.2	7 <i>S</i> only
 3.12	-0.6	-3.2	>20.0 : 1
 3.14	-0.9	-2.5	7 : 1
 3.15	-2.4	-1.4	5 : 1
 3.29	-0.9	-2.2	2.4 : 1.0 ^c
 3.17	-0.4	--	1.2 : 1.0

Table 3.1. Summary of $\Delta\Delta G^\ddagger$ for identified transition states: (a) Solvent corrected data; (b) These values are for the morpholine-containing compounds. Calculated structures were truncated to the *N,N*-dimethylamine to ease computational burden; (c) Value corresponds to -OTBS substrate **3.16** while the computational structure was truncated to -OTMS (**3.29**).

over time by ¹H NMR. After 3 h, **3.23-7*R*** had converted to **3.23-7*S*** in a 5.5:1 ratio. Despite observing complete selectivity for the **3.23-7*S*** isomer in the forward reaction, complete conversion of **3.23-7*R*** to **3.23-7*S*** did not occur. Several factors influence this outcome, including the decrease in thermodynamic driving force for the initial electron-transfer step (aminoCP $E_p \sim +1.02$ V vs. SCE; aminoNB $E_p \sim +1.18$ V vs. SCE)²⁹ and the exclusion of ZnCl₂.³³

In contrast to **3.11**, which proceeds with complete selectivity to the 7*S* isomer, acetate-protected aminoCP **3.15** proceeds in a modest 5:1 *dr*. To probe whether the acetate aminoNBs were operating under a dynamic equilibrium, minor diastereomer **3.22-7*R*** alone was subjected to

the reaction conditions (Figure 3.8B). No conversion to the major diastereomer **3.22-7S** was detected. Instead, a small amount of oxidative decomposition was detected in the form of morpholine oxidation. Exposing the 5:1 diastereomeric mixture of **3.22** to the reaction conditions resulted in no change in the ratio over 3 hours, further demonstrating that these radical intermediates do not interconvert.³⁶ Additionally, the reaction of aminoCP **3.15** was monitored by ¹H NMR in order to assess whether the diastereomeric ratio was constant throughout the reaction. No evidence of shifting diastereomeric ratios was observed, but rather the 5:1 ratio appeared constant. Taken together, the results from the reversibility studies for -OH aminoNBs **3.18** and -OAc aminoNBs **3.22** suggest that thermodynamics may play a more significant role in product distribution for substrates that are able to undergo interconversion of the radical cation aminoNB intermediates.

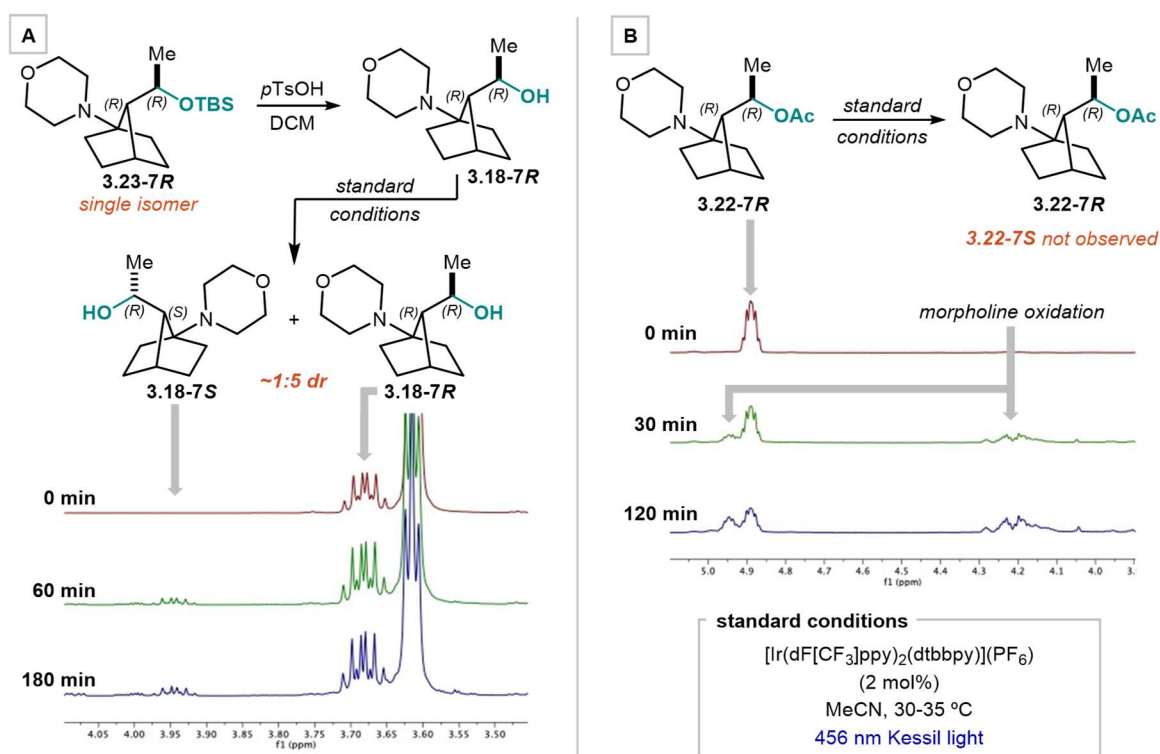


Figure 3.8. (A) ¹H NMR observation of reversibility between **3.18-7R** and **3.18-7S**; (B) Attempted reversibility between **3.22-7R** and **3.22-7S**.

3.3 Conclusion

We have investigated two different modes of diastereocontrol in the synthesis of aminoNBs. Substitution at the C3 position is controlled by minimization of A_{1,3} strain in the 6-*exo-trig* cyclization as supported by experimental and computational studies. For C7 substituents, we identified a unique mode of 1,2-asymmetric induction via a transient electrostatic interaction. The model proposed invokes the lone pair donation of distal heteroatom functionality into the π^* orbital of the reacting iminium during the transition state of the 5-*exo-trig* cyclization. When this donation is attenuated by electron-withdrawing substituents or an increase in steric encumbrance, the diastereoselectivity decreases. While kinetic effects predominately predict the stereochemical outcome, thermodynamics may also influence the diastereoselectivity of individual substrates. The conversion of aminoNB **3.18-7R** to aminoNB **3.18-7S** was experimentally measured, while aminoNB **3.22-7R** was shown to be irreversible likely due to a prohibitive energy barrier. This new stereochemical model allows for the predictable and modular synthesis of C7 mono-substituted aminoNBs and further enhances the utility of this scaffold as a new building block for aniline isosterism and complex molecule synthesis.

3.4 Experimental Procedures and Characterization of Compounds

3.4.1 General Methods

Unless otherwise noted, all reactions were run under a nitrogen atmosphere in flame-dried glassware. Reactions were stirred with Teflon-coated magnetic stir bars. Reactions were monitored by thin layer chromatography (TLC) using glass-backed plates pre-coated with 230-400 mesh silica gel (250 μm thickness) with fluorescent indicator F254 (MilliporeSigma Cat. No. 1.05715.0001). Plates were visualized with dual short wave/long wave UV light or by treatment with acidic *p*-anisaldehyde stain, KMnO_4 stain, or aqueous ceric ammonium molybdate (Hanessian's stain) with gentle heating. Products were purified by manual or automated flash column chromatography over 230-400 mesh silica (SiliCycle Cat No. R12030B) unless otherwise noted using the solvent systems indicated.

All chemicals were used as received unless otherwise noted and stored as recommended by the supplier. Organic solvents (acetonitrile, dichloromethane, diethyl ether, dimethylformamide, dimethyl sulfoxide, methanol, tetrahydrofuran, toluene) and amine bases (triethylamine, pyridine, *N,N*-diisopropylethylamine, and diisopropylamine) were purified prior to use by the method of Grubbs using a Phoenix Solvent Drying System (available from JC-Meyer Solvent Systems) or PureSolv Micro Amine Drying Column (available from Innovative Technology/Inert) under positive argon pressure.

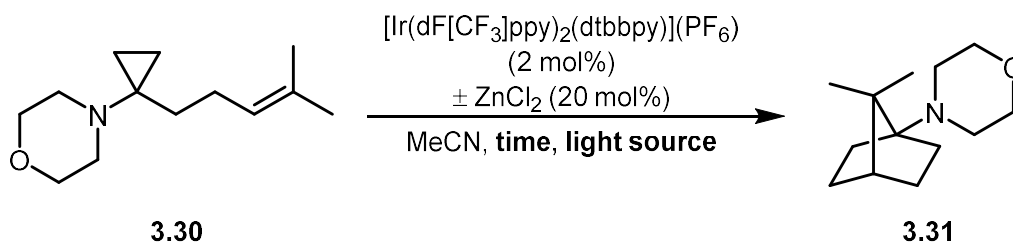
Reactions conducted with microwave irradiation were performed in a Biotage Initiator+ Microwave Synthesizer. GC/MS data was collected using a Shimadzu GCMS-QP2010 SE. NMR spectra were measured on Varian MR400, Varian Inova 500, Varian VNMRS 500, or Varian VNMRS 700 magnetic resonance spectrometers. Deuterated solvents were obtained from Cambridge Isotopes, Inc. Chemical shifts for ^1H NMR were reported as δ , parts per million,

relative to the signal of CHCl₃ at 7.26 ppm, C₆H₆ at 7.16 ppm, or CH₃CN at 1.94 ppm. Chemical shifts for ¹³C NMR were reported as δ, parts per million, relative to the center line signal of the CHCl₃ triplet at 77.16 ppm or of the C₆H₆ triplet at 128.06 ppm. Chemical shifts for ¹⁹F NMR were uncorrected and reported as δ, parts per million. Abbreviations for chemical shifts are as follows: singlet (s), broad singlet (br s), doublet (d), triplet (t), quartet (q), quintet (quint.), septet (sept.), multiplet (m). Infrared spectra were recorded on a Thermo-Nicolet IS-50 spectrophotometer and ATR accessory with diamond crystal and are reported in wavenumbers (cm⁻¹). High resolution mass spectra were obtained using an Agilent Q-TOF HPLC-MS using electrospray ionization (ESI) positive ion mode or electron impact (EI). We thank Dr. James Windak and Dr. Paul Lennon at the University of Michigan Department of Chemistry for conducting these experiments.

Reactions were irradiated using Kessil Model PR160 456 nm LED light at 100% intensity. The temperature was maintained below 35 °C by a Westpointe 4" High Velocity Fan. As protective measures, reactions were shielded with 3 layers of UV Process Amber UV Filter Film (F007-011NA) and Uvex Skyper Blue Light Blocking Computer Glasses with SCT-Orange Lens (S1933X, purchased from [Amazon.com](https://www.amazon.com) ASIN B000USRG90) were used.

3.4.2 Reaction Optimization

The previously reported method²⁹ employed 2x 4.4 W blue LED strips as the lighting source for the reaction (Creative Lighting Solutions, Product Code: [CL-FRS5050-12WP-12V](#)). Several groups have now reported that photochemical reaction efficiency can be directly correlated to the photon flux of the light source.^{34,35} High-powered Kessil lights have become a common source of irradiation in the photochemistry community, and to standardize our methodologies against a single light source, the photochemical cyclization was optimized against these light sources.



Entry	Light Source	Time	Additive (20 mol%)	Yield ^a
1	LED strips	12 h	ZnCl ₂	84%
2	LED strips	8 h	ZnCl ₂	90% ^b
3	1x 456 nm Kessil	8 h	ZnCl ₂	>99% ^b
4	1x 456 nm Kessil	2 h	ZnCl ₂	86%
5	1x 456 nm Kessil	8 h	--	69% ^b
6	1x 456 nm Kessil	2 h	--	57% ^c
7	2x 456 nm Kessil	2 h	--	62% ^d

^aisolated yields; ^bNMR yield using (Me)₃SiPh as an internal standard; ^c22% RSM; ^d17% RSM; isolated yields 250 μmol scale, NMR yields 100 μmol scale

Table 3.2. Results of reaction optimization

To determine an optimal time for reactions performed both in the presence and in the absence of 20 mol% of ZnCl₂, conversion was monitored over time by NMR (Table 3.2, Entries 2, 3, and 5).

To a flame-dried 2 dram vial was added aminoCP **3.30** (100 μmol), 0.5 mL MeCN-d₃, photocatalyst (2 μmol), and if required, ZnCl₂ as a 1.0 M solution in diethyl ether (20 μmol). Separately, a 0.25 M solution of (Me)₂SiPh was prepared in MeCN-d₃, and 0.5 mL (125 μmol) of the internal standard was added to the reaction mixture. The reaction was carefully degassed by 3x freeze-pump-thaw cycles and transferred via syringe to an oven-dried, screw-cap NMR tube that had been evacuated and refilled 3x with N₂ (g). The NMR tube was then irradiated either with blue LED strips in accordance with reference 29 or a PR160 456 nm Kessil light as outlined in General Procedure A/B (Section 3.4.4). Conversion was determined by ¹H NMR analysis (Figure 3.9).

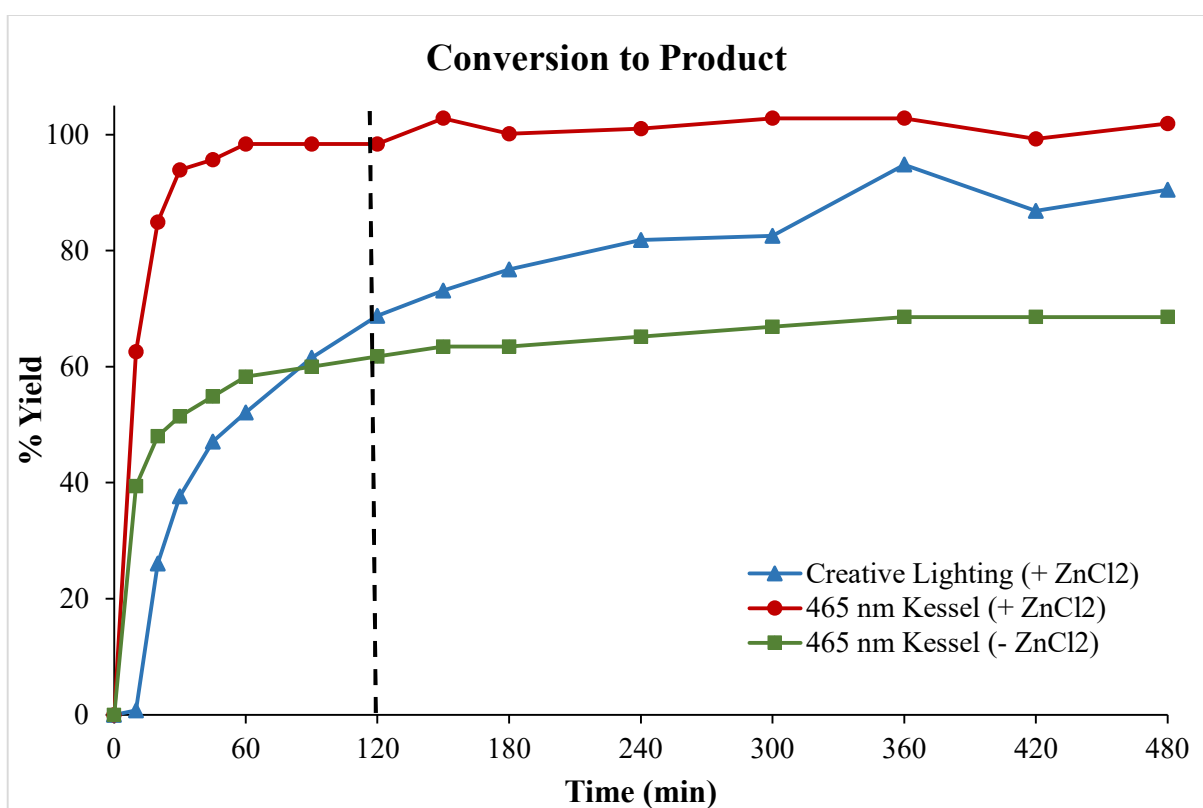


Figure 3.9. Plot of percent yield of aminoNB **3.31** over time as determined by ¹H NMR

The reactions employing Kessil lights in the presence and absence of ZnCl₂ plateaued after approximately 2 h, so this was chosen as the optimized reaction time. The observed increase in rate of the reactions employing the Kessil lights is consistent with the reports that demonstrate the

position correlation between reaction efficiency and photon flux. Increasing the photon flux further by irradiating with two Kessil lights (Entry 7) did not significantly enhance the yield of the reaction. Also of note is that product degradation is not observed over the course of irradiation under any conditions.

The contrast in conversion between the Kessil +[ZnCl₂] trial (Entry 3) and the Kessil – [ZnCl₂] (Entry 5) is stark. One hypothesis for this outcome is that ZnCl₂ increases the efficiency of the reaction such that small quantities of off-cycle products that may lead to covalent deactivation of the photocatalyst are not formed. The additive may also function to stabilize intermediates and/or accelerate processes, completely preventing deleterious off-cycle reactivity. Monitoring the concentration of active photocatalyst over time in the reaction shows rapid decomposition of the photocatalyst under no ZnCl₂ conditions (not shown), providing experimental support for this hypothesis. In the absence of ZnCl₂, the desired reaction is less efficient and does not occur at a rate fast enough to out-compete photocatalyst decomposition. In the case of the blue LED strips (Entry 2), the desired forward reaction occurs at a slower rate, and consequently, decomposition is also slower, extending the lifetime of the photocatalyst.

Other roles of ZnCl₂ may also be operative. Based on ¹H NMR spectra, ZnCl₂ appears to associate more strongly to the aminoNB than to the aminoCP by significant broadening of individual resonances. Based on this observation, the ZnCl₂ may be sequestering the product, driving the equilibrium of the reaction forward via Le Chatlier's Principle. Another consequence of ZnCl₂ coordination to the product appears to be a protective effect against further oxidative transformations. In the case of aminoCP **3.11**, the reaction proceeds in high yield to **3.18-7S** as a single diastereomer in the presence of ZnCl₂. In the absence of ZnCl₂, **3.11** converts to two major products: the desired product **3.18-7S** and fused tetracyclic hemiaminal **3.32**. This product is

likewise produced as a single diastereomer and is presumed to derive from oxidative α -functionalization of the morpholine (Figure 3.10).

While the discussion above describes several possibilities as to the mechanistic role of ZnCl_2 , the contributions of ZnCl_2 and some other Lewis acid additives to the enhancement of the reaction efficiency as measured by conversion and yield have yet to be fully validated. However, it is important to note that the presence of ZnCl_2 has been ruled out as a variable controlling the stereochemical outcomes investigated in this work.

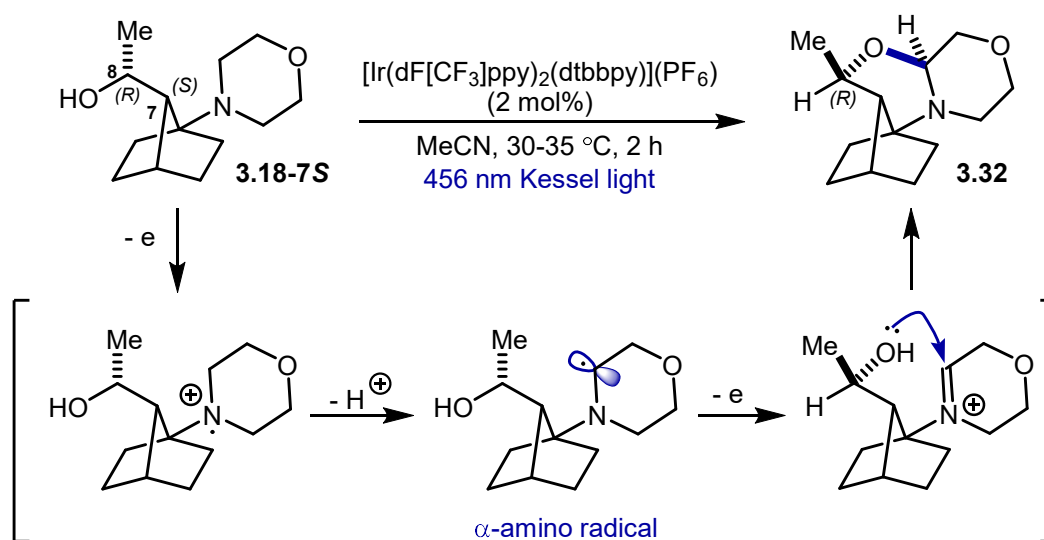


Figure 3.10. Proposed pathway for the formation of tetracycle **3.32**

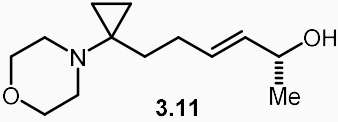
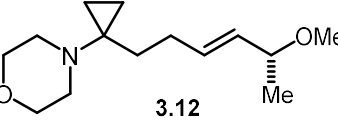
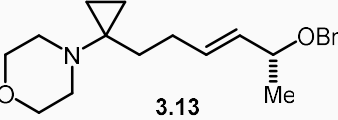
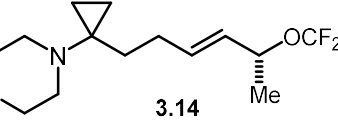
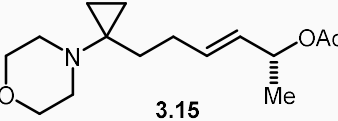
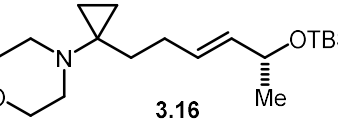
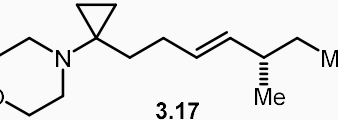
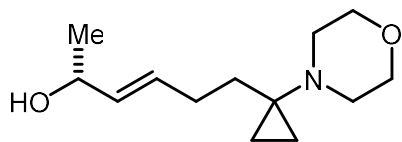
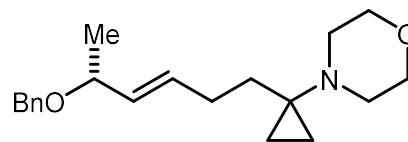
Substrate	<i>dr</i> (7 <i>S</i> ,8 <i>R</i> : 7 <i>R</i> ,8 <i>R</i>)		
	GC	¹ H NMR	
 3.11	- ZnCl ₂	7 <i>S</i> , 8 <i>R</i> only	n/a
	+ ZnCl ₂	7 <i>S</i> , 8 <i>R</i> only	n/a
 3.12	- ZnCl ₂	19:1	19:1
	+ ZnCl ₂	>20:1	17:1
 3.13	- ZnCl ₂	8:1	10:1
	+ ZnCl ₂	10:1	10:1
 3.14	- ZnCl ₂	7:1	8:1
	+ ZnCl ₂	7:1	8:1
 3.15	- ZnCl ₂	n/a	5:1
	+ ZnCl ₂	n/a	5:1
 3.16	- ZnCl ₂	n/a	2.7:1.0
	+ ZnCl ₂	n/a	2.4:1.0
 3.17	- ZnCl ₂	n/a	1.1:1.0
	+ ZnCl ₂	n/a	1.2:1.0

Table 3.3. Summary of stereochemical outcomes

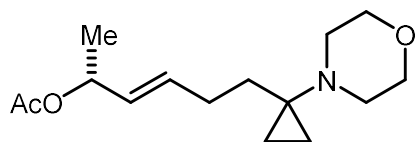
3.4.3 Preparation of AminoCPs



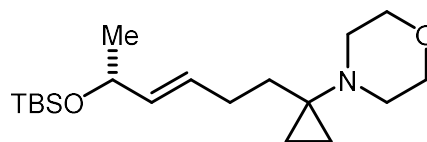
3.11



3.13

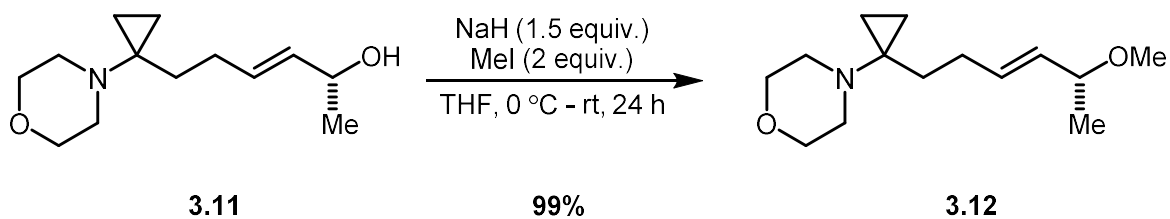


3.15



3.16

Substrates **3.11**, **3.13**, **3.15**, and **3.16** were synthesized as previously reported.²⁹



(*R,E*)-4-(1-(5-methoxyhex-3-en-1-yl)cyclopropyl)morpholine (3.12)

AminoCP **3.11** (65 mg, 288 μmol , 1 equiv.) was dissolved in 2 mL dry THF. After cooling to 0°C, NaH (17 mg, 60% dispersion in mineral oil, 433 μmol , 1.5 equiv.) was added in a single portion and the reaction stirred 10 minutes. Iodomethane (36 μL , 577 μmol , 2 equiv.) was added via syringe, and the reaction was allowed to warm to room temperature overnight. The reaction was quenched with saturated aqueous NaHCO_3 , then extracted with Et_2O (3 x 40 mL). The combined organic layers were washed with brine, dried over anhydrous Na_2SO_4 , filtered, and concentrated *in vacuo*. The crude residue was purified by flash column chromatography over silica (10-40% EtOAc /hexanes, 10% increments), providing methyl ether **3.12** as 68.0 mg of a clear oil (284 μmol , 99% yield).

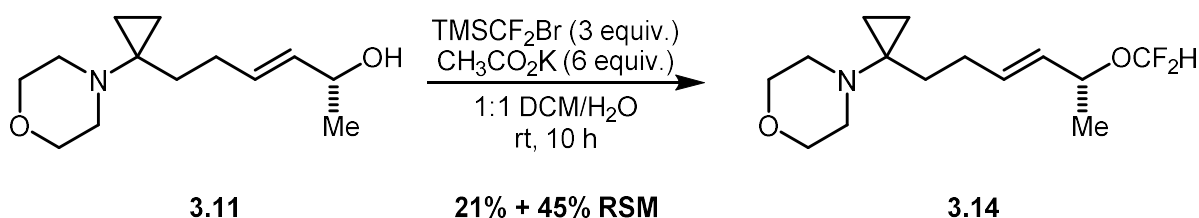
$R_f = 0.60$ (50% EtOAc /hexanes)

$^1\text{H NMR}$ (500 MHz, CDCl_3) δ 5.51 – 5.43 (m, 1H), 5.20 (ddd, $J = 15.4, 7.7, 0.9$ Hz, 1H), 3.58 – 3.52 (m, $J = 13.5, 6.7$ Hz, 1H), 3.52 – 3.47 (m, 4H), 3.14 (s, 3H), 1.95 – 1.85 (m, 2H), 1.54 – 1.47 (m, 2H), 1.10 (d, $J = 6.3$ Hz, 3H), 0.44 (t, $J = 5.1$ Hz, 2H), 0.33 (q, $J = 4.5$ Hz, 2H) ppm

$^{13}\text{C NMR}$ (126 MHz, CDCl_3) δ 132.95, 131.75, 78.10, 67.84, 55.81, 49.82, 44.03, 30.02, 29.74, 21.48, 12.88, 12.85 ppm

IR (neat): 3971, 2930, 2850, 2815, 1449, 1264, 1114, 1092, 968, 856 cm^{-1}

HRMS (ESI+, m/z) calculated for $\text{C}_{14}\text{H}_{26}\text{NO}_2^+$ 240.1958; found 240.1969



(R,E)-4-(1-(5-(difluoromethoxy)hex-3-en-1-yl)cyclopropyl)morpholine (3.14)

Preparation of **3.14** was adapted from a procedure previously reported for the difluoromethylation of aliphatic alcohols.³⁶ To a 15 mL plastic tube with a cap was added alcohol **3.11** (124 mg, 548 μmol , 1 equiv.) and potassium acetate (323 mg, 3.3 mmol, 6 equiv.). Next, 0.34 mL DCM and 0.34 mL HPLC-grade H_2O were added. The reaction mixture was stirred until the solids had dissolved, then TMSCF_2Br (0.26 mL, 1.6 mmol, 3 equiv.) was added dropwise over 1 min. After stirring at room temperature for 10 h, the reaction mixture was diluted with 5 mL DCM and 10 mL water. The layers were separated, and the aqueous layer was extracted with DCM (3 x 10 mL). The combined organic layers were washed with brine, dried over anhydrous Na_2SO_4 , filtered, and concentrated *in vacuo*. The crude residue was purified by flash column chromatography over silica (10-50% EtOAc/hexanes + 0.2% NEt_3 , 10% increments) and aminoCP. **3.14** was isolated as 31.1 mg of a clear oil (113 μmol , 21% yield). Additionally, 90 mg (45%) of starting material was recovered.

$R_f = 0.70$ (50% EtOAc/hexanes)

$^1\text{H NMR}$ (500 MHz, C_6D_6) δ 5.89 (dd, $J = 77.7, 74.4$ Hz, 1H), 5.44 – 5.33 (m, 1H), 5.26 (dd, $J = 15.5, 7.0$ Hz, 1H), 4.41 – 4.30 (m, 1H), 3.60 – 3.47 (m, 4H), 2.47 – 2.34 (m, 4H), 1.83 – 1.73 (m, 2H), 1.43 – 1.33 (m, 2H), 1.14 (d, $J = 6.4$ Hz, 3H), 0.52 (t, $J = 4.9$ Hz, 2H), 0.24 (t, $J = 5.0$ Hz, 2H) ppm

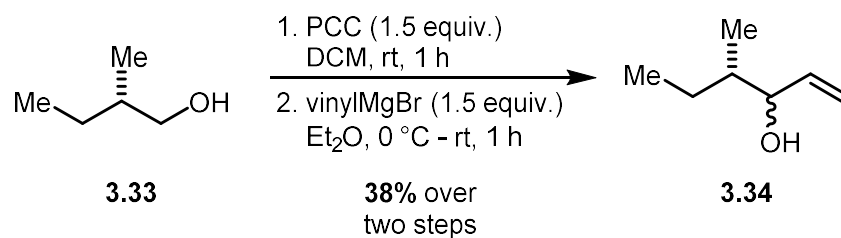
$^{13}\text{C NMR}$ (126 MHz, C_6D_6) δ 133.59, 130.06, 117.02 (dd, $J = 257.8, 254.3$ Hz), 73.53 (t, $J = 3.8$ Hz), 67.80, 50.07, 44.00, 30.07, 29.99, 21.74, 12.86 ppm

^{19}F NMR (377 MHz, CDCl_3) δ -80.97 (dd, $J = 164.1, 78.3$ Hz), -82.63 (dd, $J = 163.9, 74.0$ Hz)

ppm

IR (neat): 3088, 2934, 2854, 1728, 1672, 1451, 1187, 1115, 1011, 856 cm^{-1}

HRMS (ESI+, m/z) calculated for $\text{C}_{14}\text{H}_{24}\text{F}_2\text{NO}_2^+$ 276.1775; found 276.1780



(4S)-4-methylhex-1-en-3-ol (3.34)

(2S)-2-methylbutan-1-ol **3.33** (2.04 mL, 19 mmol, 1 equiv.) was dissolved in 22 mL dry DCM. Separately, pyridinium chlorochromate (6.14 g, 28.5 mmol, 1.5 equiv.) was mixed with 6 g Celite. The PCC/Celite mixture was added portion-wise to the alcohol solution over 10 minutes, stirring vigorously at room temperature. The mixture quickly turned from yellow to orange to black. After 1 hour, the mixture was filtered through a pad of silica and eluted with Et₂O. The solvent was removed *in vacuo* to afford the aldehyde as 1.21 g of a volatile yellow oil that was used without further purification (14 mmol, 74% yield). The spectroscopic data matched that previously reported in the literature.³⁷

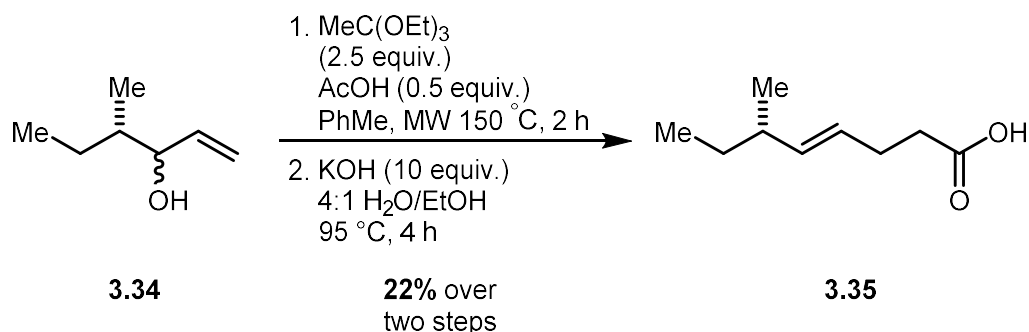
R_f = 0.50 (10% EtOAc/hexanes)

A solution of crude (2S)-2-methylbutanal (1.21 g, 14 mmol, 1 equiv.) in anhydrous Et₂O was cooled to 0 °C. Vinylmagnesium bromide (21 mL, 1 M in THF, 21 mmol, 1.5 equiv.) was added dropwise via syringe and the mixture was stirred 15 minutes at 0 °C before warming to room temperature. After a total reaction time of 1 hour, the reaction was quenched by slow addition of 50 mL saturated aqueous NH₄Cl. The aqueous mixture was then extracted with Et₂O (2 x 50 mL). The combined organic layers were washed with brine, dried over anhydrous Na₂SO₄, filtered, and concentrated *in vacuo*. The crude yellow oil was purified by flash column chromatography over silica (eluting with 2-10% EtOAc/hexanes, 2% increments) and the allylic alcohol diastereomers **3.34** were collected as 823 mg (7.2 mmol, 52% yield) of a clear, colorless oil in 1:1.4 *dr*.

R_f = 0.27 (10% EtOAc/hexanes)

¹H NMR (500 MHz, CDCl₃) δ 5.90 – 5.83 (m, 1H), 5.24 (d, *J* = 1.3 Hz, 1H), 5.19 – 5.16 (m, 1H), 4.02-3.99 (m, 1H), 1.61 – 1.46 (m, 2H), 1.15 (tt, *J* = 12.3, 6.4 Hz, 1H), 0.94-0.86 (m, 8H).

¹³C NMR (126 MHz, CDCl₃) δ 140.10, 139.37, 115.88, 115.30, 40.41, 25.50, 25.11, 14.59, 14.02, 11.91, 11.68 ppm



(S,E)-6-methyloct-4-enoic acid (3.35)

Allylic alcohol **3.34** (278 mg, 2.43 mmol, 1 equiv.) was dissolved in 1 mL dry toluene in a microwave vial. Triethyl orthoacetate (987 mg, 6.09 mmol, 2.5 equiv.) and glacial acetic acid (70 μ L, 1.22 mmol, 0.5 equiv.) were added, and the vial was flushed with nitrogen and capped. The mixture was irradiated in a microwave reactor at 150 °C for 2 hours. Upon cooling, the reaction was poured into 50 mL saturated aqueous NaHCO₃, then extracted with diethyl ether (3 x 20 mL). The combined organic layers were washed with brine, dried over anhydrous Na₂SO₄, filtered, and concentrated *in vacuo* to provide 566 mg of a pale yellow oil (3.1 mmol, 23% yield). The crude ethyl ester was used without further purification in the subsequent step.

R_f = 0.71 (20% EtOAc/hexanes)

¹H NMR (401 MHz, CDCl₃) δ 5.40 – 5.26 (m, 1H), 4.12 (q, *J* = 7.1 Hz, 1H), 2.40 – 2.25 (m, 2H), 1.95 (sept., 6.7 Hz, 1H), 1.34 – 1.20 (m, 3H), 1.25 (t, *J* = 7.1 Hz, 2H), 0.93 (d, *J* = 6.7 Hz, 2H), 0.82 (t, *J* = 7.4 Hz, 2H) ppm

The crude ethyl ester (500 mg, 2.7 mmol, 1 equiv.) was dissolved in 4.5 mL 200 proof ethanol. Potassium hydroxide (1.52 g, 27 mmol, 10 equiv.) was dissolved in 17 mL HPLC-grade water, then added slowly to the ethanol solution, stirring at room temperature. A reflux condenser was attached, and the mixture was heated to 95 °C for 4 hours. The reaction was then cooled to room temperature and slowly poured into 25 mL 1 M HCl. The solution was extracted with DCM

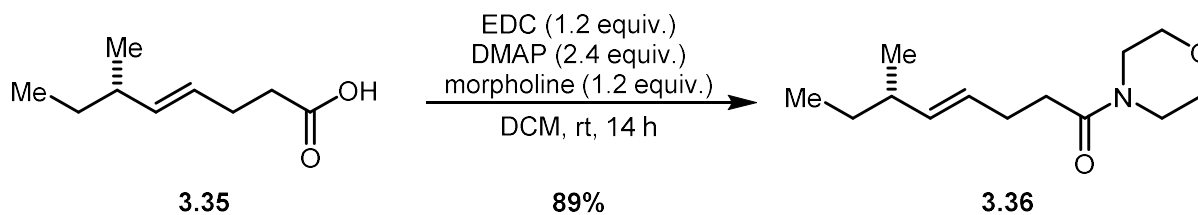
(3 x 25 mL). The combined organic layers were washed with 25 mL brine, dried over anhydrous MgSO₄, filtered, and concentrated *in vacuo*, yielding 410 mg (2.6 mmol, 97% yield) of the desired carboxylic acid **3.35**.

¹H NMR (401 MHz, CDCl₃) δ 5.38 – 5.33 (m, 2H), 2.42 (dd, *J* = 11.0, 4.2 Hz, 2H), 2.36 – 2.28 (m, 2H), 1.97 (sept., *J* = 6.6, 1H), 1.33 – 1.20 (m, 2H), 0.94 (d, *J* = 6.7 Hz, 3H), 0.83 (t, *J* = 7.4 Hz, 3H) ppm

¹³C NMR (176 MHz, CDCl₃) δ 179.18, 138.05, 126.01, 38.46, 34.34, 29.83, 27.80, 20.41, 11.83 ppm

IR (neat): 3073, 2961, 2927, 2875, 1708, 1454, 1412, 1282, 1209, 968, 920, 773 cm⁻¹

HRMS (ESI+, *m/z*): calculated for C₉H₁₄O₂⁻ 155.1072; found 155.1075



(*S,E*)-6-methyl-1-morpholinooct-4-en-1-one (3.36)

Carboxylic acid **3.35** (140 mg, 896 μmol , 1 equiv.) was dissolved in 4 mL dry DCM. Next, DMAP (263 mg, 2.15 mmol, 2.4 equiv.) and EDC·HCl (223 mg, 1.17 mmol, 1.3 equiv.) were added each as one portion. After all the solids had dissolved, morpholine (94 μL , 1.08 mmol, 1.2 equiv.) was added and the reaction was stirred 24 hours at room temperature. The mixture was then diluted with 10 mL Et₂O and the organic layer was washed with 2 M HCl (2 x 10 mL) to remove DMAP. The aqueous layer was then extracted with Et₂O (3 x 10 mL). The combined organic layers were washed with 10 mL brine, dried over anhydrous MgSO₄, filtered, and concentrated *in vacuo*. Purification by flash column chromatography over silica (10-50% EtOAc/hexanes + 0.1% Et₃N, 10% increments) provided 180 mg the desired morphamide **3.36** as a colorless oil (799 μmol , 89% yield).

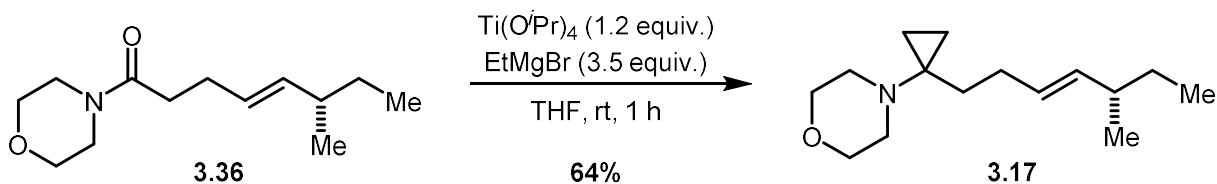
$R_f = 0.25$ (50% EtOAc/hexanes)

¹H NMR (700 MHz, CDCl₃) δ 5.39 (dt, $J = 15.3, 6.2$ Hz, 1H), 5.33 (dd, $J = 15.4, 7.3$ Hz, 1H), 3.70 – 3.65 (m, 4H), 3.62 (br s, 2H), 3.47 (br s, 2H), 2.39 – 2.35 (m, 2H), 2.35 – 2.30 (m, 2H), 1.96 (sept., $J = 6.6$ Hz, 1H), 1.32 – 1.22 (m, 2H), 0.94 (d, $J = 6.7$ Hz, 3H), 0.83 (t, $J = 7.4$ Hz, 3H) ppm

¹³C NMR (176 MHz, CDCl₃) δ 171.45, 137.60, 126.86, 67.09, 66.89, 46.21, 42.09, 38.43, 33.42, 29.88, 28.48, 20.41, 11.90 ppm

IR (neat): 2959, 2922, 2854, 1642, 1431, 1271, 1233, 1115, 1069, 1025, 970 cm⁻¹

HRMS (ESI⁺, m/z): calculated for C₁₃H₂₄NO₂⁺ 226.1802; found 226.1811



(*S,E*)-4-(1-(5-methylhept-3-en-1-yl)cyclopropyl)morpholine (3.17)

Morphamide **3.36** (87.3 mg, 387 μmol , 1 equiv.) was dissolved in 8 mL dry THF. The flask was submerged in a water bath to act as a heat sink. $\text{Ti}(\text{O}^i\text{Pr})_4$ (138 μL , 465 μmol , 1.2 equiv.) was added in one portion via syringe, then ethylmagnesium bromide (452 μL , 3 M in THF, 1.36 mmol, 3.5 equiv.) was added dropwise via syringe over 2 minutes. The clear solution turned yellow, then brown/orange, before turning black upon complete addition of EtMgBr . After 1 hour, the reaction was quenched with 25 mL of a solution containing 75% saturated aqueous Rochelle salt, 20% brine, and 5% 6 M NaOH. The layers were separated, and the aqueous layer was extracted Et_2O (3 x 50 mL). The combined organic layers were washed with brine, dried over anhydrous Na_2SO_4 , filtered, and concentrated *in vacuo*. The crude residue was purified by flash column chromatography over silica (10-40% EtOAc /hexanes, 10% increments) and the aminoCP **3.17** was collected as 58.3 mg of a clear oil (246 μmol , 64% yield).

$R_f = 0.60$ (50% EtOAc /hexanes)

$^1\text{H NMR}$ (500 MHz, CDCl_3) δ 5.32 (dt, $J = 15.3, 6.2$ Hz, 1H), 5.24 (dd, $J = 15.4, 7.3$ Hz, 1H), 3.63 – 3.57 (m, 4H), 2.70 – 2.61 (m, 4H), 1.98 – 1.89 (m, 3H), 1.62 – 1.56 (m, 3H), 1.33 – 1.20 (m, 2H), 0.94 (d, $J = 6.7$ Hz, 3H), 0.84 (t, $J = 7.4$ Hz, 3H), 0.54 – 0.50 (m, 2H), 0.43 (q, $J = 4.2$ Hz, 2H) ppm

$^{13}\text{C NMR}$ (100 MHz, C_6D_6) δ 136.22, 129.06, 67.85, 50.13, 44.16, 38.90, 30.79, 30.50, 30.26, 20.77, 13.05, 12.11 ppm

IR (neat): 2957, 2930, 2873, 2852, 2813, 1451, 1264, 1117, 1012, 985, 857 cm^{-1}

HRMS (ESI+, m/z): calculated for $\text{C}_{15}\text{H}_{28}\text{NO}^+$ 238.2165; found 238.2176

3.4.4 Photochemical Conversion of AminoCPs to AminoNBs

General Procedure A for the Photochemical Cyclization (without ZnCl₂)

In a dry 2 dram vial under nitrogen, the aminocyclopropane (200 μmol) was dissolved in dry MeCN (0.1 M) before adding [Ir(dF[CF₃]ppy)₂(dtbbpy)](PF₆) (2 mol%). The reaction mixture was bright yellow-green unless otherwise noted. The reaction was degassed with 3 freeze-pump-thaw cycles. The vial was then centered 5 cm away from a Kessil Model PR160 456 nm LED light at 100% intensity and irradiated for 2 hours. The temperature was maintained at 35 °C with a fan placed 5 cm away from the vial for the duration of the reaction. The reaction mixture was added to 10 mL of a solution containing 5 mL saturated aqueous NaHCO₃, 5 mL water, and 1 mL 6 M NaOH. The aqueous mixture was further diluted with 10 mL ether/hexanes (1:1) and the phases were separated. The aqueous layer was extracted with 1:1 diethyl ether/hexanes (3 x 10 mL). The combined organic layers were washed with 10 mL brine, dried over anhydrous MgSO₄, filtered, and concentrated *in vacuo*. The crude residue was purified by flash column chromatography over silica using the solvent system indicated.

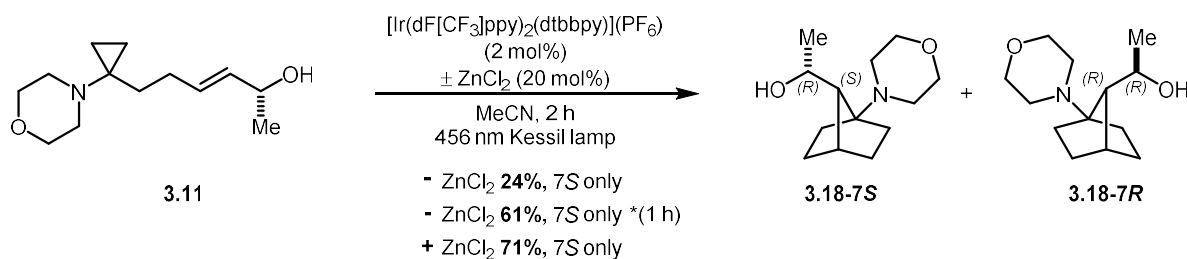
General Procedure B for the Photochemical Cyclization (with 20 mol% ZnCl₂)

In a dry 2 dram vial under nitrogen, the aminocyclopropane (200 μmol) was dissolved in dry MeCN (0.1 M) before adding [Ir(dF[CF₃]ppy)₂(dtbbpy)](PF₆) (2 mol%), then ZnCl₂ (1.0 M in ether, 20 mol%) in one portion each. The reaction mixture was bright yellow-green unless otherwise noted. The reaction was degassed with 3 freeze-pump-thaw cycles. The vial was then centered 5 cm away from a Kessil Model PR160 456 nm LED light at 100% intensity and irradiated for 2 hours. The temperature was maintained at 35 °C with a fan placed 5 cm away from the vial for the duration of the reaction. The reaction mixture was added to 10 mL of a solution containing

5 mL saturated aqueous NaHCO₃, 5 mL water, and 1 mL 6 M NaOH. The aqueous mixture was further diluted with 10 mL ether/hexanes (1:1) and the phases were separated. The aqueous layer was extracted with 1:1 diethyl ether/hexanes (3 x 10 mL). The combined organic layers were washed with 10 mL brine, dried over anhydrous MgSO₄, filtered, and concentrated *in vacuo*. The crude residue was purified by flash column chromatography over silica using the solvent system indicated.



Figure 3.11. (A) Structure of photocatalyst; (B) Side and top view of reaction set up



(R)-1-((1S,4S,7S)-1-morpholinobicyclo[2.2.1]heptan-7-yl)ethan-1-ol (3.18-7S)

Following **General Procedure A**, aminoCP **3.11** (45.1 mg, 200 μmol , 1 equiv.) and $[\text{Ir}(\text{dF}[\text{CF}_3]\text{ppy})_2(\text{dtbbpy})](\text{PF}_6)$ (4.5 mg, 4 μmol , 2 mol%) were combined in 2.4 mL MeCN. The crude residue was purified by flash column chromatography over silica (5, 10, 15, 20, 25, 30, 40, 50, 60% EtOAc/hexanes + 0.1% NEt_3) and aminoNB **3.18-7S** was collected as 10.9 mg of a clear oil (24% yield, single 7S,8R diastereomer as determined by GC/MS analysis). Over-oxidation byproduct **3.32** was isolated as 8.9 mg (20%) of a clear oil.

Following **General Procedure A**, aminoCP **3.11** (45.1 mg, 200 μmol , 1 equiv.) and $[\text{Ir}(\text{dF}[\text{CF}_3]\text{ppy})_2(\text{dtbbpy})](\text{PF}_6)$ (4.5 mg, 4 μmol , 2 mol%) were combined in 2.4 mL MeCN. *The reaction was irradiated for 1 h.* The crude residue was purified by flash column chromatography over silica (5, 10, 20, 30, 40, 50% acetone/DCM) and aminoNB **3.18-7S** was collected as 27.5 mg of a clear oil (61% yield, single 7S, 8R diastereomer as determined by GC/MS analysis). Additionally, 4.6 mg (10%) of starting material was recovered. Less than 10% of the over-oxidation byproduct **3.32** was observed.

Following **General Procedure B**, aminoCP **3.11** (46.2 mg, 205 μmol , 1 equiv.), $[\text{Ir}(\text{dF}[\text{CF}_3]\text{ppy})_2(\text{dtbbpy})](\text{PF}_6)$ (4.6 mg, 4 μmol , 2 mol%), and ZnCl_2 (41 μL , 1.0 M in ether, 41 μmol , 20 mol%) were combined in 2 mL MeCN. The crude residue was purified by flash column chromatography over silica (10-40% acetone/DCM + 0.1% NEt_3 , 10% increments) and aminoNB

3.18-7S was collected as 32.7 mg of a clear, dark red oil (71% yield, single *7S*, *8R* diastereomer as determined by GC/MS analysis).

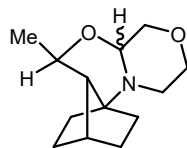
The spectroscopic data matched that previously reported in the literature.²⁹

R_f = 0.30 (30% acetone/DCM + 1% NEt_3), 0.30 (90% EtOAc/hexanes)

$^1\text{H NMR}$ (700 MHz, CDCl_3 , 43 °C): δ 6.01 (br s, 1H), 3.97 (dq, J = 10.1, 6.1 Hz, 1H), 3.69 (br s, 4H), 2.68-2.61 (m, 4H), 1.87 (s, 1H), 1.90-1.80 (m, 3H), 1.65 (d, J = 9.9 Hz, 1H), 1.65-1.59 (m, 2H), 1.40-1.35 (m, 2H), 1.26-1.20 (m, 1H), 1.16 (d, J = 6.0 Hz, 3H) ppm

$^1\text{H NMR}$ (500 MHz, C_6D_6 , 25 °C) δ 5.59 (br s, 1H), 3.98 (dq, J = 12.1, 6.1 Hz, 1H), 3.58 – 3.51 (m, 2H), 3.49 (br s, 2H), 2.39 (br s, 2H), 2.26 – 2.18 (m, 2H), 1.65 (ddd, J = 13.0, 8.5, 4.7 Hz, 1H), 1.61 (t, J = 4.5 Hz, 1H), 1.58 – 1.49 (m, 2H), 1.47 (d, J = 9.6 Hz, 1H), 1.35 (tdd, J = 12.2, 8.0, 4.3 Hz, 1H), 1.26 (d, J = 6.1 Hz, 3H), 1.23 – 1.16 (m, 1H), 1.13 – 1.05 (m, 2H), 0.83 (ddd, J = 11.2, 10.0, 4.9 Hz, 1H) ppm

Additional thermodynamic factors have been considered in contributing to the diastereoselectivity observed for alcohol aminoCP **3.11**. Comparison of $^1\text{H NMR}$ data in C_6D_6 of **3.18-7S** and **3.18-7R** show a dramatic shift in the location of the -OH resonance. For **3.18-7S**, the resonance is shifted significantly downfield at 5.59 ppm, whereas this same resonance appears at 0.51 ppm in **3.18-7R**. This observation suggested that **3.18-7S** adopts a conformation in which the alcohol could engage in an intramolecular hydrogen bonding interaction with the morpholine nitrogen. Computational modeling of the ground state of aminoNB **3.18-7S** supports this conclusion. The energy stabilization imparted by this interaction and the observed reversibility of **3.18-7R** to **3.18-7S** suggests that thermodynamics may play of a role in the superior diastereoselectivity reported for aminoCP **3.11**.



3.32

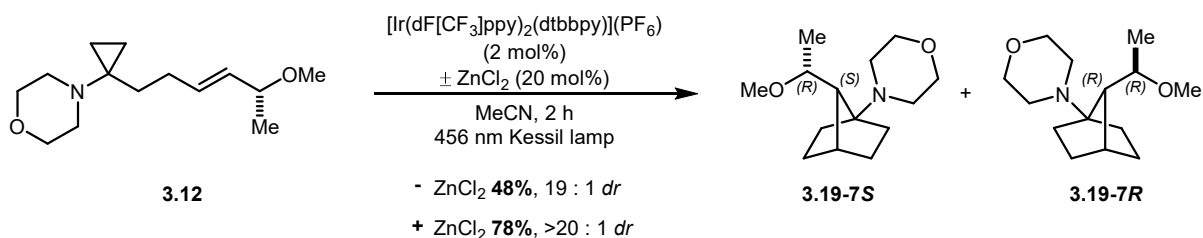
(6R,6aS,7S,9aS)-6-methyloctahydro-6H-7,9a-ethanocyclopenta[d][1,4]oxazino[3,4-b][1,3]oxazine (3.32)

R_f = 0.55 (60% EtOAc/hexanes)

¹H NMR (500 MHz, C₆D₆) δ 4.06 (dd, *J* = 10.3, 3.3 Hz, 1H), 3.92 (dd, *J* = 8.3, 3.3 Hz, 1H), 3.61 (dd, *J* = 10.3, 8.3 Hz, 1H), 3.59 – 3.51 (m, 2H), 3.32 (dq, *J* = 12.1, 6.1 Hz, 1H), 2.35 (dt, *J* = 11.6, 2.4 Hz, 1H), 2.25 (ddd, *J* = 11.5, 9.8, 4.1 Hz, 1H), 1.79 (tt, *J* = 12.4, 3.8 Hz, 1H), 1.65 (t, *J* = 4.3 Hz, 1H), 1.50 (ddd, *J* = 18.2, 9.3, 3.9 Hz, 1H), 1.41 (dtd, *J* = 19.8, 10.7, 9.7, 4.2 Hz, 2H), 1.31 (d, *J* = 10.4 Hz, 1H), 1.20 (ddd, *J* = 12.9, 9.7, 3.7 Hz, 1H), 1.12 (d, *J* = 6.1 Hz, 4H), 0.79 (ddd, *J* = 12.5, 9.5, 5.5 Hz, 1H) ppm

¹³C NMR (126 MHz, C₆D₆) δ 83.03, 72.13, 70.01, 67.50, 65.66, 55.47, 46.68, 35.64, 35.20, 30.07, 28.12, 20.91, 20.49 ppm

IR (neat): 2952, 2871, 2818, 1322, 1205, 1131, 1105, 1075, 996, 908, 689, 652 cm⁻¹



4-((1*S*,4*S*,7*S*)-7-((*R*)-1-methoxyethyl)bicyclo[2.2.1]heptan-1-yl)morpholine (3.19-7*S*) and 4-((7*R*)-7-((*R*)-1-methoxyethyl)bicyclo[2.2.1]heptan-1-yl)morpholine (3.19-7*R*)

Following **General Procedure A**, aminoCP **3.12** (47.9 mg, 200 μmol , 1 equiv.) and $[\text{Ir}(\text{dF}[\text{CF}_3]\text{ppy})_2(\text{dtbbpy})](\text{PF}_6)$ (4.5 mg, 4 μmol , 2 mol%) were combined in 2.3 mL MeCN. The crude residue was purified by flash column chromatography over silica (10, 15, 20, 30, 40, 55, 75% EtOAc/hexanes + 0.1 NEt_3) and aminoNBs **3.19-7*S*** and **3.19-7*R*** were collected as 21.6 mg (45.1%) and ~2 mg (impure), respectively, as clear oils (48% combined yield, 19:1 *dr* as determined by GC/MS analysis). Additionally, 11.9 mg (24.9%) of starting material was recovered.

Following **General Procedure B**, aminoCP **3.12** (47.9 mg, 200 μmol , 1 equiv.), $[\text{Ir}(\text{dF}[\text{CF}_3]\text{ppy})_2(\text{dtbbpy})](\text{PF}_6)$ (4.5 mg, 4 μmol , 2 mol%), and ZnCl_2 (40 μL , 1.0 M in ether, 40 μmol , 20 mol%) were combined in 2.4 mL MeCN. The crude residue was purified by flash column chromatography over silica (10, 15, 20, 30, 40, 55, 75% EtOAc/hexanes + 0.1 NEt_3) and aminoNBs **3.19-7*S*** and **3.19-7*R*** were collected as 37.1 mg (78%) and ~1 mg (impure), respectively, as clear oils (78% combined yield, >20:1 *dr* as determined by GC/MS analysis).

R_f (50% EtOAc/hexanes) = Major diastereomer 0.15; Minor diastereomer 0.55

¹H NMR

Major diastereomer: (700 MHz, C_6D_6) δ 3.74 (dt, $J = 7.5, 3.7$ Hz, 4H), 3.23 (s, 3H), 3.05 (dq, $J = 8.6, 6.3$ Hz, 1H), 2.75 (s, 2H), 2.38 (dt, $J = 10.2, 4.5$ Hz, 2H), 1.72 – 1.67 (m, 2H), 1.63 (ddd, $J =$

16.0, 11.9, 4.0 Hz, 1H), 1.49 – 1.42 (m, 3H), 1.38 – 1.34 (m, 1H), 1.18 – 1.10 (m, 2H), 1.02 (d, $J = 6.3$ Hz, 3H), 1.01 – 0.98 (m, 1H) ppm

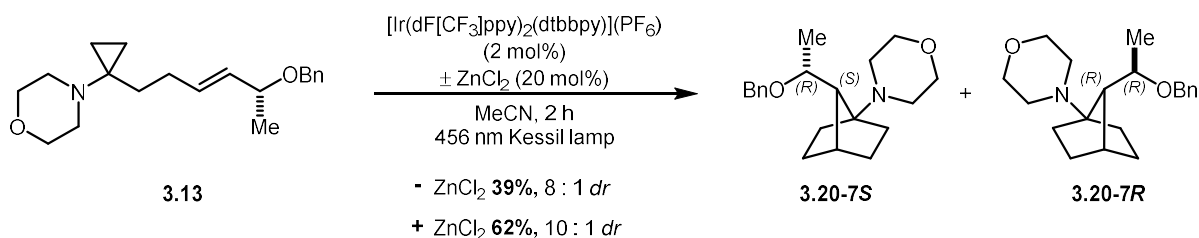
Minor diastereomer: (700 MHz, C_6D_6) δ 3.60 (t, $J = 4.4$ Hz, 4H), 3.17 (s, 3H), 2.30 (dt, $J = 9.3, 4.5$ Hz, 2H), 2.27 – 2.21 (m, 2H), 1.90 (dq, $J = 12.2, 4.5, 3.8$ Hz, 1H), 1.64 – 1.56 (m, 2H), 1.49 (ddt, $J = 17.5, 9.4, 4.4$ Hz, 1H), 1.33 – 1.27 (m, 2H), 1.27 (d, $J = 6.1$ Hz, 3H), 1.22 (tt, $J = 9.8, 4.3$ Hz, 1H), 0.98 (ddd, $J = 11.4, 9.8, 4.8$ Hz, 1H), 0.93 (ddd, $J = 10.3, 6.6, 3.0$ Hz, 1H) ppm

^{13}C NMR

Major diastereomer: (176 MHz, C_6D_6) δ 75.51, 71.84, 67.99, 57.11, 55.53, 49.46, 37.10, 33.61, 29.09, 28.29, 23.50, 18.22 ppm

IR (neat): 2953, 2872, 2810, 1734, 1449, 1369, 1332, 1276, 1184, 1116, 896, 850 cm^{-1}

HRMS (ESI+, m/z): calculated for $C_{14}H_{16}NO_2^+$ 240.1964; found 240.1969



4-((1S,4S,7S)-7-((R)-1-(benzyloxy)ethyl)bicyclo[2.2.1]heptan-1-yl)morpholine (3.20-7S) and 4-((7R)-7-((R)-1-(benzyloxy)ethyl)bicyclo[2.2.1]heptan-1-yl)morpholine (3.20-7R)

Following **General Procedure A**, aminoCP **3.13** (65.0 mg, 206 μmol , 1 equiv.) and $[\text{Ir}(\text{dF}[\text{CF}_3]\text{ppy})_2(\text{dtbbpy})](\text{PF}_6)$ (4.6 mg, 4 μmol , 2 mol%) were combined in 2.1 mL MeCN. The crude residue was purified by flash column chromatography over silica (10%, 15%, 20%, 30%, 40%, 60%, 90% EtOAc/hexanes + 0.1% NEt_3) and aminoNB **3.20-7S** was collected as 22.2 mg (34%), and 34.6 mg (53%) of starting material mixed with ~3.5 mg (5%) of **3.20-7R** was recovered, each as colored oils (39% combined yield, 8:1 *dr* as determined by GC/MS analysis, 10:1 *dr* as determined by crude ^1H NMR).

Following **General Procedure B**, aminoCP **3.13** (50.0 mg, 159 μmol , 1 equiv.), $[\text{Ir}(\text{dF}[\text{CF}_3]\text{ppy})_2(\text{dtbbpy})](\text{PF}_6)$ (3.6 mg, 3.2 μmol , 2 mol%), and ZnCl_2 (32 μL , 1.0 M in ether, 32 μmol , 20 mol%) were combined in 1.6 mL MeCN. The crude residue was purified by flash column chromatography over silica (4-36% EtOAc/hexanes + 0.1% NEt_3 , 4% increments) and aminoNBs **3.20-7S** and **3.20-7R** were collected as 28.2 mg (56.4%) and 2.9 mg (5.8%), respectively, as clear oils (62% combined yield, 10:1 *dr* as determined by GC/MS analysis, 10:1 *dr* as determined by crude ^1H NMR). Additionally, 16.3 mg (32.6%) of starting material was recovered.

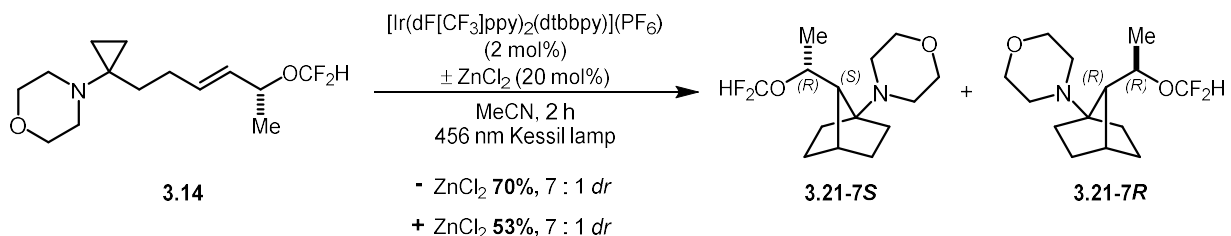
The spectroscopic data matched that previously reported in the literature.²⁹

R_f (50% EtOAc/hexanes) = Major diastereomer 0.50; Minor diastereomer 0.85

¹H NMR

Major diastereomer *7S,8R*: (700 MHz, CDCl₃): δ 7.38 (d, J = 7.5 Hz, 2H), 7.31 (t, J = 7.7 Hz, 2H), 7.24 (t, J = 7.5 Hz, 1H), 4.65 (d, J = 11.8 Hz, 1H), 4.63 (d, J = 11.8 Hz, 1H), 3.58-3.49 (m, 5H), 2.75 (br s, 2H), 2.55-2.49 (m, 2H), 1.91 (br s, 1H), 1.87 (d, J = 8.5 Hz, 1H), 1.80 (t, J = 13.3 Hz, 1H), 1.66-1.60 (m, 4H), 1.37-1.33 (m, 1H), 1.30 (ddd, J = 12.1, 9.9, 4.3 Hz, 1H), 1.20 (ddd, J = 11.4, 10.0, 4.4 Hz, 1H), 1.16 (d, J = 6.1 Hz, 3H) ppm

Minor diastereomer *7R,8R*: (700 MHz, CDCl₃): δ 7.36-7.31 (m, 4H), 7.28-7.25 (m, 1H), 4.64 (d, J = 11.4 Hz, 1H), 4.37 (d, J = 11.4 Hz, 1H), 3.70-3.64 (m, 4H), 3.48-3.43 (m, 1H), 2.58-2.54 (m, 2H), 2.53-2.48 (m, 2H), 2.33 (t, J = 4.6 Hz, 1H), 1.81 (t, J = 12.6 Hz, 1H), 1.77 (d, J = 10.0 Hz, 1H), 1.75-1.70 (m, 1H), 1.60-1.55 (m, 1H), 1.55-1.52 (m, 2H), 1.38 (d, J = 6.1 Hz, 3H), 1.34-1.29 (m, 2H), 1.19 (ddd, J = 11.8, 9.7, 4.9 Hz, 1H) ppm



4-((1S,4S,7S)-7-((R)-1-(difluoromethoxy)ethyl)bicyclo[2.2.1]heptan-1-yl)morpholine (3.17-7S) and 4-((7R)-7-((R)-1-(difluoromethoxy)ethyl)bicyclo[2.2.1]heptan-1-yl)morpholine (3.17-7R)

Following **General Procedure A**, aminoCP **3.14** (49.4 mg, 179 μmol , 1 equiv.) and $[\text{Ir}(\text{dF}[\text{CF}_3]\text{ppy})_2(\text{dtbbpy})](\text{PF}_6)$ (4.0 mg, 3.6 μmol , 2 mol%) were combined in 2.2 mL MeCN. The crude residue was purified by flash column chromatography over silica (5-40% EtOAc/hexanes + 0.2% NEt_3 , 5% increments) and aminoNBs **3.21-7S** and **3.21-7R** were collected as 29.4 mg (60%) and 4.8 mg (10%), respectively, as clear oils (70% combined yield, 7:1 *dr* as determined by GC/MS analysis).

Following **General Procedure B**, aminoCP **3.14** (22.8 mg, 82.8 μmol , 1 equiv.), $[\text{Ir}(\text{dF}[\text{CF}_3]\text{ppy})_2(\text{dtbbpy})](\text{PF}_6)$ (1.9 mg, 1.7 μmol , 2 mol%), and ZnCl_2 (17 μL , 1.0 M in ether, 16.6 μmol , 20 mol%) were combined in 1 mL MeCN. The crude residue was purified by flash column chromatography over silica (loading with toluene, 5-40% EtOAc/hexanes, 5% increments with 0.1% Et_3N) and aminoNBs **3.21-7S** and **3.21-7R** were collected as 10.2 mg (45%) and 1.8 mg (8%), respectively, as clear oils (53% combined yield, 7:1 *dr* as determined by GC analysis).

R_f (50% EtOAc/hexanes) = Major diastereomer 0.55; Minor diastereomer 0.65

^1H NMR

Major diastereomer *7S,8R*: (500 MHz, C_6D_6) δ 6.37 (dd, $J = 89.3, 71.7$ Hz, 1H), 3.73 – 3.63 (m, 3H), 3.59 (br s, 2H), 2.42 (br s, 2H), 2.27 – 2.19 (m, 2H), 1.59 (d, $J = 9.1$ Hz, 1H), 1.52 (tt, $J =$

12.2, 3.8 Hz, 1H), 1.48 (t, $J = 4.3$ Hz, 1H), 1.38 – 1.25 (m, 2H), 1.25 – 1.15 (m, 2H), 1.08 (d, $J = 6.3$ Hz, 3H), 1.05 – 0.96 (m, 2H), 0.92 – 0.82 (m, 1H) ppm

Minor diastereomer *7R,8R*: (700 MHz, C_6D_6) δ 5.86 (t, $J = 76.4$ Hz, 1H), 4.00 – 3.93 (m, 1H), 3.51 (s, 4H), 2.22 – 2.16 (m, 2H), 2.12 – 2.05 (m, 2H), 1.88 (t, $J = 11.7$ Hz, 1H), 1.51 (t, $J = 14.4$ Hz, 2H), 1.43 – 1.36 (m, 1H), 1.33 (d, $J = 6.0$ Hz, 4H), 1.29 – 1.10 (m, 4H), 0.92 – 0.82 (m, 1H) ppm

^{13}C NMR

Major diastereomer *7S,8R*: (126 MHz, C_6D_6) δ 118.39 (dd, $J = 262.5, 246.9$ Hz), 72.33 (d, $J = 3.2$ Hz), 71.88, 67.38, 54.14, 49.09, 37.22, 33.01, 28.69, 27.63, 22.90, 20.87 ppm

Minor diastereomer *7R,8R*: (176 MHz, C_6D_6) δ 116.77 (t, $J = 256.6$ Hz), 72.57 (t, $J = 2.8$ Hz), 70.64, 66.90, 53.38, 48.85, 36.86, 32.39, 28.06, 27.12, 23.46, 20.24 ppm

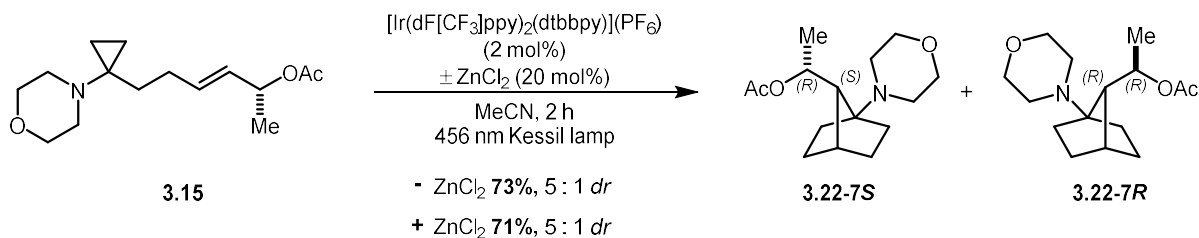
^{19}F NMR

Major diastereomer *7S,8R*: (377 MHz, C_6D_6) δ -78.24 (dd, $J = 165.6, 89.3$ Hz), -81.54 (dd, $J = 165.6, 71.8$ Hz) ppm

Minor diastereomer *7R,8R*: (377 MHz, C_6D_6) δ -78.34 (dd, $J = 162.3, 76.9$ Hz), -79.48 (dd, $J = 162.2, 76.0$ Hz) ppm

IR (neat): 2960, 2875, 2821, 1721, 1452, 1376, 1277, 1213, 1181, 1151, 992, 896, 863 cm^{-1}

HRMS (ESI+, m/z): calculated for $C_{14}H_{24}F_2NO_2^+$ 276.1775; found 276.1773



(R)-1-((1S,4S,7S)-1-morpholinobicyclo[2.2.1]heptan-7-yl)ethyl acetate (3.22-7S) and (1R)-1-((7R)-1-morpholinobicyclo[2.2.1]heptan-7-yl)ethyl acetate (3.22-7R)

Following **General Procedure A**, aminoCP **3.15** (53.5 mg, 200 μmol , 1 equiv.) and $[\text{Ir}(\text{dF}[\text{CF}_3]\text{ppy})_2(\text{dtbbpy})](\text{PF}_6)$ (4.5 mg, 4.5 μmol , 2 mol%) were combined in 2.4 mL MeCN. The crude residue was purified by flash column chromatography over silica (4-36% EtOAc/hexanes + 0.1% NEt_3 , 4% increments) and aminoNBs **3.22-7S** and **3.22-7R** were collected as 31.8 mg (60%) and 7.0 mg (13%), respectively, as clear oils (73% combined yield, 5:1 *dr* as determined by crude NMR analysis; diastereomers were not resolved by GC/MS).

Following **General Procedure B**, aminoCP **3.15** (45.0 mg, 168 μmol , 1 equiv.), $[\text{Ir}(\text{dF}[\text{CF}_3]\text{ppy})_2(\text{dtbbpy})](\text{PF}_6)$ (3.8 mg, 3.4 μmol , 2 mol%), and ZnCl_2 (34 μL , 1.0 M in ether, 34 μmol , 20 mol%) were combined in 2.1 mL MeCN. The crude residue was purified by flash column chromatography over silica (5, 10, 15, 25, 35, 45, 75% EtOAc/hexanes) and aminoNBs **3.22-7S** and **3.22-7R** were collected as 26.6 mg (59%) and 5.3 mg (12%), respectively, as clear oils (71% combined yield, 5:1 *dr* as determined by crude NMR analysis; diastereomers were not resolved by GC/MS).

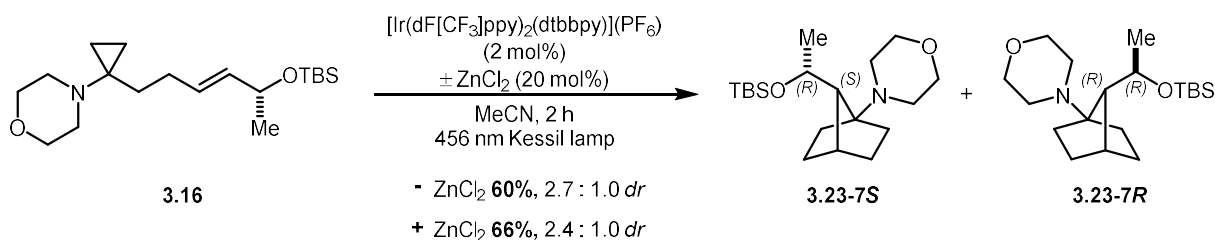
The spectroscopic data matched that previously reported in the literature.²⁹

R_f (50% EtOAc/hexanes) = Major diastereomer 0.45; Minor diastereomer 0.60

¹H NMR

Major diastereomer *7S,8R*: (700 MHz, CDCl₃): δ = 5.02 (dq_uart., J = 9.5, 6.1 Hz, 1H), 3.66-3.58 (m, 4H), 2.61-2.55 (m, 2H), 2.54-2.50 (m, 2H), 2.01 (s, 3H), 1.93 (t, J = 4.1 Hz, 1H), 1.89 (d, J = 9.5 Hz, 1H), 1.81 (tt, J = 12.1, 3.9 Hz, 1H), 1.77-1.71 (m, 1H), 1.72-1.66 (m, 1H), 1.67-1.61 (m, 1H), 1.57 (ddd, J = 11.2, 9.5, 3.6 Hz, 1H), 1.39-1.31 (m, 2H), 1.22 (ddd, J = 11.6, 9.9, 4.8 Hz, 1H), 1.18 (d, J = 6.3 Hz, 3H) ppm

Minor diastereomer *7R,8R*: (500 MHz, C₆D₆): δ 5.20 (dq_uart., J = 10.3, 6.4 Hz, 1H), 3.54 (t, J = 4.5 Hz, 4H), 2.22 (td, J = 11.5, 4.6 Hz, 2H), 2.15 (td, J = 11.5, 4.4 Hz, 2H), 2.04 (t, J = 4.2 Hz, 1H), 1.98-1.91 (m, 1H), 1.74 (s, 3H), 1.65 (d, J = 10.3 Hz, 1H), 1.55 (tt, J = 12.2, 3.7 Hz, 1H), 1.48-1.40 (m, 2H), 1.39 (d, J = 6.1 Hz, 3H), 1.24-1.13 (m, 3H), 0.91 (ddd, J = 11.5, 10.0, 4.9 Hz, 1H) ppm



4-((1S,4S,7S)-7-((R)-1-((tert-butyldimethylsilyl)oxy)ethyl)bicyclo[2.2.1]heptan-1-yl)morpholine (3.23-7S) and 4-((7R)-7-((R)-1-((tertbutyldimethylsilyl)oxy)ethyl)bicyclo[2.2.1]heptan-1-yl)morpholine (3.23-7R)

Following **General Procedure A**, aminoCP **3.16** (70.1 mg, 206 μmol , 1 equiv.) and $[\text{Ir}(\text{dF}[\text{CF}_3]\text{ppy})_2(\text{dtbbpy})](\text{PF}_6)$ (4.6 mg, 4.1 μmol , 2 mol%) were combined in 2.1 mL MeCN. The crude residue was purified by flash column chromatography over silica (loading with toluene, 2, 3, 4, 6, 9, 15% EtOAc/hexanes) and aminoNBs **3.23-7S** and **3.23-7R** were collected as 26.3 mg (38%; mixed with 9.2 mg recovered starting material, 13%) and 15.4 mg (22%), respectively, as clear oils (60% combined yield, 2.7:1.0 *dr* as determined by crude NMR analysis; diastereomers were not resolved by GC/MS).

Following **General Procedure B**, aminoCP **3.16** (71.3 mg, 210 μmol , 1 equiv.), $[\text{Ir}(\text{dF}[\text{CF}_3]\text{ppy})_2(\text{dtbbpy})](\text{PF}_6)$ (4.7 mg, 4.2 μmol , 2 mol%), and ZnCl_2 (42 μL , 1.0 M in ether, 42 μmol , 20 mol%) were combined in 2.1 mL MeCN. The crude residue was purified by flash column chromatography over silica (loading with toluene, 2, 3, 4, 6, 9, 15% EtOAc/hexanes) and aminoNBs **3.23-7S** and **3.23-7R** were collected as 24.3 mg (34%) and 23.0 mg (32%), respectively, as clear oils (66% combined yield, 2.4:1.0 *dr* as determined by crude NMR analysis; diastereomers were not resolved by GC/MS). Upon sitting, the 7S, 8R isomer crystallized as a white solid.

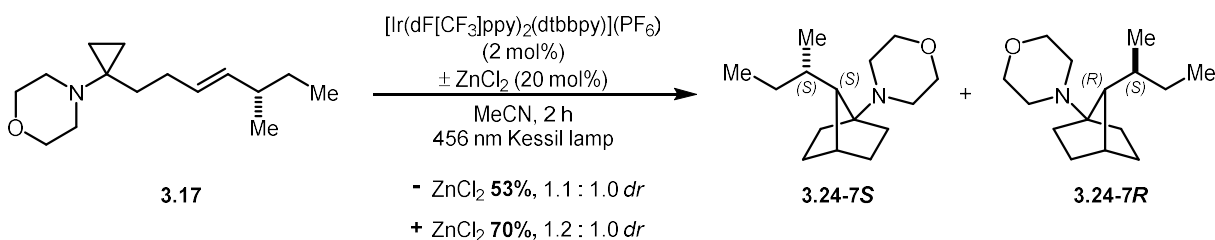
The spectroscopic data matched that previously reported in the literature.²⁹

R_f (10% EtOAc/hexanes) = Major diastereomer 0.40; Minor diastereomer 0.50

¹H NMR

Major diastereomer *7S,8R*: (700 MHz, CDCl₃): δ 3.92-3.87 (m, 1H), 3.73-3.69 (m, 2H), 3.66-3.62 (m, 2H), 2.74- 2.67 (m, 2H), 2.56-2.52 (m, 2H), 1.90 (t, J = 4.4 Hz, 1H), 1.84 (tt, J = 12.1, 3.8 Hz, 1H), 1.75 (d, J = 7.8 Hz, 1H), 1.73-1.67 (m, 1H), 1.65-1.55 (m, 3H), 1.34-1.29 (m, 1H), 1.28-1.24 (m, 1H), 1.22-1.17 (m, 1H), 1.16 (d, J = 6.1 Hz, 3H), 0.90 (s, 9H), 0.15 (s, 3H), 0.09 (s, 3H) ppm

Minor diastereomer *7R,8R*: (700 MHz, C₆D₆): δ = 3.78 (dquart., J = 9.0, 6.1 Hz, 1H), 3.60 (t, J = 4.4 Hz, 4H), 2.33 (t, J = 4.4 Hz, 1H), 2.30 (dt, J = 11.4, 4.4 Hz, 2H), 2.26 (dt, J = 11.4, 4.4 Hz, 2H), 1.97-1.91 (m, 1H), 1.61 (tt, J = 12.3, 4.3 Hz, 1H), 1.58 (d, J = 9.0 Hz, 1H), 1.51-1.45 (m, 2H), 1.35 (d, J = 6.1 Hz, 3H), 1.33-1.24 (m, 2H), 1.24-1.19 (m, 1H), 1.03 (s, 9H), 1.00-0.95 (m, 1H), 0.12 (s, 3H), 0.11 (s, 3H) ppm



4-((1S,4S,7S)-7-((S)-sec-butyl)bicyclo[2.2.1]heptan-1-yl)morpholine (3.24-7S) and 4-((7R)-7-((S)-sec-butyl)bicyclo[2.2.1]heptan-1-yl)morpholine (3.24-7R)

Following **General Procedure A**, aminoCP **3.17** (47.5 mg, 200 μmol , 1 equiv.) and $[\text{Ir}(\text{dF}[\text{CF}_3]\text{ppy})_2(\text{dtbbpy})](\text{PF}_6)$ (4.5 mg, 4 μmol , 2 mol%) were combined in 2.4 mL MeCN. The crude residue was purified by flash column chromatography over silica (2, 5, 10, 15, 25, 30% EtOAc/hexanes + 0.1% NEt_3) and aminoNBs **3.24-7S** and **3.24-7R** were collected together as 25.0 mg of a clear oil (53% yield, 1.1:1.0 *dr* as determined by GC/MS analysis). Additionally, 6.6 mg (13.9%) of starting material were recovered.

Following **General Procedure B**, aminoCP **3.17** (47.5 mg, 200 μmol , 1 equiv.), $[\text{Ir}(\text{dF}[\text{CF}_3]\text{ppy})_2(\text{dtbbpy})](\text{PF}_6)$ (4.5 mg, 4 μmol , 2 mol%), and ZnCl_2 (40 μL , 1.0 M in ether, 40 μmol , 20 mol%) were combined in 2.4 mL MeCN. The crude residue was purified by flash column chromatography over silica (loading with toluene, 10-30% EtOAc/hexanes, 4% increments + 0.1% Et_3N) and aminoNBs **3.24-7S** and **3.24-7R** were collected together as 33.3 mg of a clear oil (70% yield, 1.2:1.0 *dr* as determined by GC/MS analysis). Additionally, 4.3 mg (9%) of starting material were recovered.

$R_f = 0.75$ (50% EtOAc/hexanes)

$^1\text{H NMR}$ (500 MHz, CDCl_3) δ 3.67 (t, $J = 4.5$ Hz, 4H), 2.60 – 2.53 (m, 2H), 2.53 – 2.47 (m, 2H), 2.15 – 2.05 (m, 1H), 2.01 – 1.94 (m, 1H), 1.84 – 1.70 (m, 2H), 1.67 – 1.61 (m, 1H), 1.60 (s, 1H),

1.57 – 1.46 (m, 2H), 1.46 – 1.35 (m, 3H), 1.32 – 1.22 (m, 2H), 1.22 – 1.10 (m, 2H), 1.09 – 0.96 (m, 2H), 0.85 (dt, $J = 7.5, 4.8$ Hz, 4H) ppm

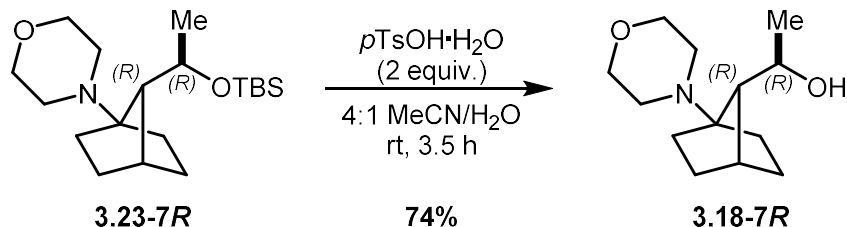
^{13}C NMR (126 MHz, CDCl_3) Major diastereomer δ 71.82, 67.46, 53.04, 49.16, 36.96, 32.83, 31.30, 28.36, 28.23, 27.70, 23.54, 16.99, 10.21 ppm; Minor diastereomer δ 71.93, 67.48, 53.02, 49.22, 37.28, 32.83, 32.09, 28.28, 27.61, 26.37, 23.72, 17.79, 11.50 ppm

IR (neat): 2954, 2871, 2852, 2814, 1743, 1452, 1372, 1276, 1166, 1118, 1040, 894 cm^{-1}

HRMS (ESI+, m/z): calculated for $\text{C}_{15}\text{H}_{28}\text{NO}^+$ 238.2165; found 238.2175

3.4.5 Mechanistic Studies

A. Experimental determination of reaction reversibility



(1R)-1-((7R)-1-morpholinobicyclo[2.2.1]heptan-7-yl)ethan-1-ol (**3.18-7R**)

AminoNB **3.23-7R** (38.2 mg, 122 μmol , 1 equiv.) was dissolved in 1 mL dry MeCN and the reaction mixture became heterogeneous upon the addition of 250 μL of HPLC-grade water. *Para*-toluenesulfonic acid monohydrate (42.8 mg, 225 μmol , 2 equiv.) was added as one portion, and the reaction mixture instantly became homogeneous. The reaction was flushed with nitrogen, capped, and vigorously stirred at room temperature for 3.5 h. The reaction was neutralized with 2 mL saturated aqueous NaHCO_3 solution and further diluted with 1 mL ethyl acetate. The layers were separated and the aqueous layer was extracted with ethyl acetate (3 x 1 mL). The combined organic layers were washed with 1 mL brine, dried over anhydrous MgSO_4 , filtered, and concentrated *in vacuo*. The crude residue was purified by flash column chromatography over silica (eluting with 10-30% acetone/DCM, 10% increments) and the product **3.18-7R** was collected as 18.8 mg (74% yield) of a white solid.

$R_f = 0.35$ (30% acetone/DCM), no UV, stains in KMnO_4

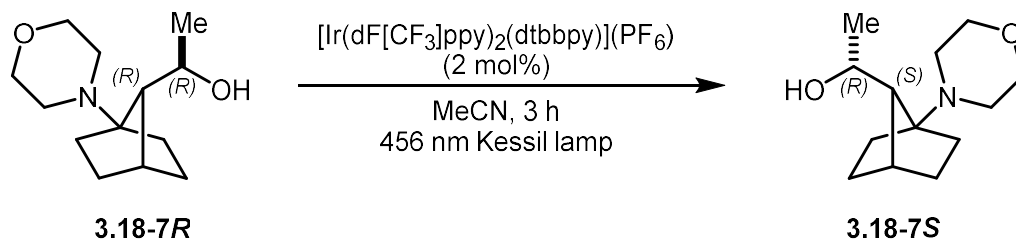
$^1\text{H NMR}$ (700 MHz, C_6D_6) δ 3.64 (dq, $J = 12.5, 6.2$ Hz, 1H), 3.56 (s, 4H), 2.31 – 2.24 (m, 2H), 2.24 – 2.18 (m, 2H), 2.16 (d, $J = 4.1$ Hz, 1H), 1.92 (ddd, $J = 11.7, 7.3, 3.5$ Hz, 1H), 1.55 (tt, $J = 12.2, 4.1$ Hz, 1H), 1.52 – 1.46 (m, 1H), 1.44 (ddd, $J = 15.9, 8.4, 3.8$ Hz, 1H), 1.37 (d, $J = 8.8$ Hz,

1H), 1.29-1.22 (m, 2H), 1.25 (d, $J = 6.3$ Hz, 3H), 1.21 – 1.16 (m, 1H), 0.97 – 0.91 (m, 1H), 0.51 (br s, 1H) ppm

^{13}C NMR (176 MHz, C_6D_6) δ 71.40, 67.46, 66.30, 55.73, 49.40, 36.86, 33.64, 28.78, 28.44, 24.11, 22.85 ppm

IR (neat): 3405, 2953, 2871, 2815, 1450, 1276, 1165, 1115, 1025, 980, 894, 692 cm^{-1}

HRMS (ESI+, m/z): calculated for $\text{C}_{13}\text{H}_{24}\text{NO}_2^+$ 226.1802; found 226.1808



To a flame-dried 2 dram vial containing aminoNB **3.18-7R** (17.1 mg, 75.9 μmol , 1 equiv.) was added $[\text{Ir}(\text{dF}[\text{CF}_3]\text{ppy})_2(\text{dtbbpy})](\text{PF}_6)$ (1.7 mg, 1.5 μmol , 2 mol%) and 760 μL of MeCN- d_3 (stored over 4 \AA molecular sieves). The reaction mixture was degassed with 3 freeze-pump-thaw cycles and transferred into a screw-cap NMR tube that had been dried overnight in a 150 $^\circ\text{C}$ oven and purged with argon for 10 min. The NMR tube was capped and placed 5 cm away from a 456 nm Kessil light and irradiated at 100% intensity. The temperature was maintained at 35 $^\circ\text{C}$ with a fan placed 5 cm away from the NMR tube during irradiation. ^1H NMR spectra were obtained at 0 h, 1 h, and 3 h timepoints.

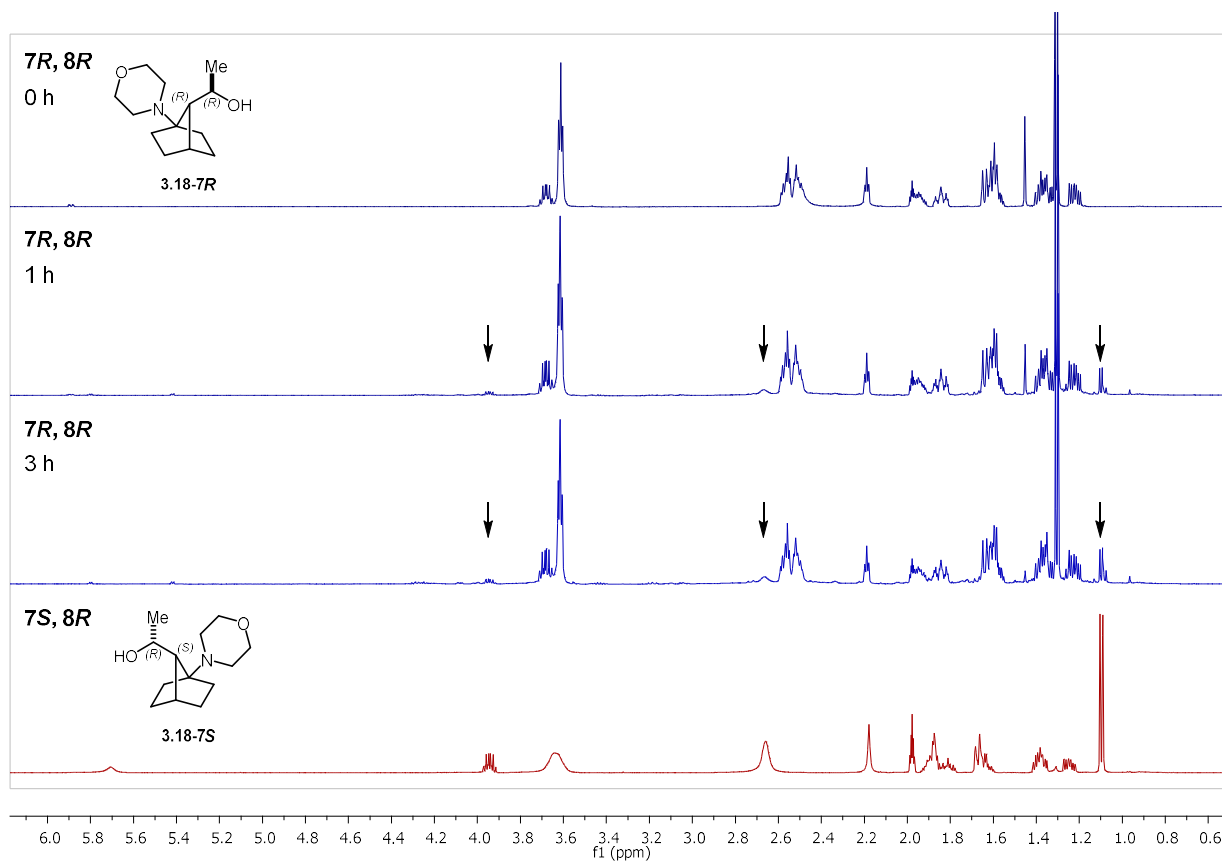
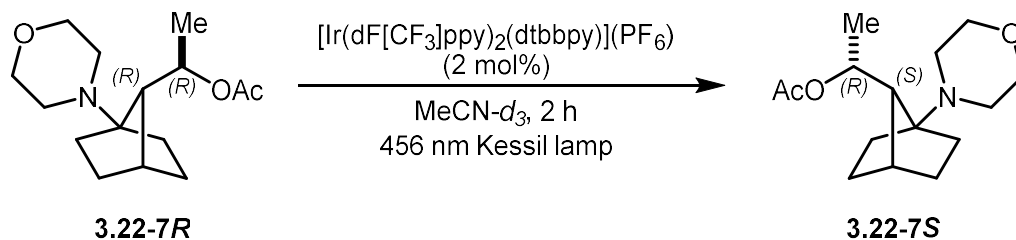


Figure 3.12. ^1H NMR spectra monitoring reversibility of photochemical cyclization of aminoNB **3.18-7R** over 3 h



To a flame-dried 2 dram vial containing aminoNB **3.22-7R** (17.1 mg, 75.9 μmol , 1 equiv.) was added $[\text{Ir}(\text{dF}[\text{CF}_3]\text{ppy})_2(\text{dtbbpy})](\text{PF}_6)$ (1.7 mg, 1.5 μmol , 2 mol%) and 760 μL of $\text{MeCN-}d_3$ (stored over 4 \AA molecular sieves). The reaction mixture was degassed with 3 freeze-pump-thaw cycles and transferred into a screw-cap NMR tube that had been dried overnight in a 150 $^\circ\text{C}$ oven and purged with argon for 10 min. The NMR tube was capped and placed 5 cm away from a 456 nm Kessil light and irradiated at 100% intensity. The temperature was maintained at 35 $^\circ\text{C}$ with a fan placed 5 cm away from the NMR tube during irradiation. ^1H NMR spectra were obtained at 15 min timepoints for 2 hours of total irradiation.

No conversion to the aminoNB **3.22-7S** was observed. As shown in Figure 3.13, the only observed product was a byproduct likely derived from oxidation of the morpholine ring. This byproduct is only observed in trace (<5%) conversion in the standard [3+2] reaction at 2 hours of irradiation.

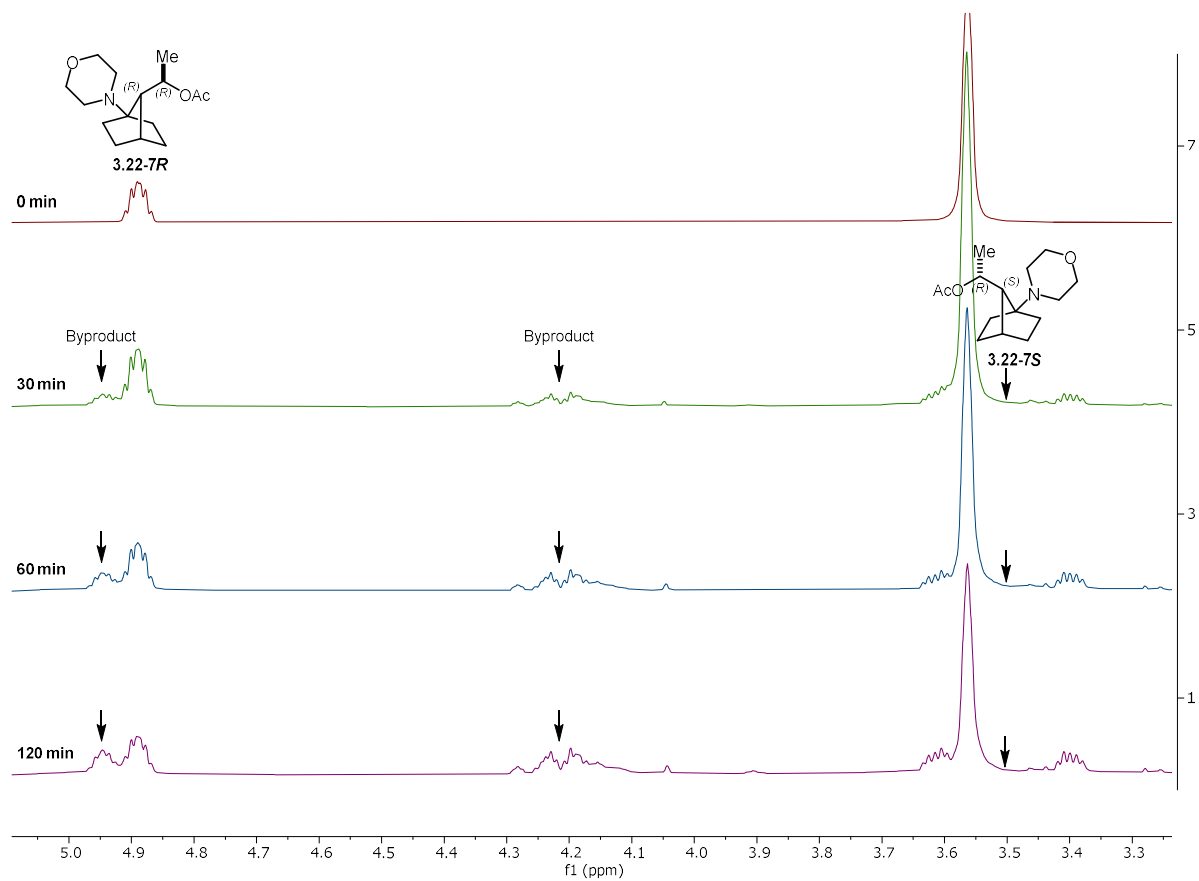


Figure 3.13. ^1H NMR spectra monitoring reversibility of photochemical cyclization for aminoNB **3.22-7R** over 2 h

3.5 References

1. Curran, D.P.; Abraham, A.C.; Liu, H. "Radical Translocation Reactions of *o*-Iodoanilides: The Use of Carbon-Hydrogen Bonds as Precursors of Radicals Adjacent to Carbonyl Groups." *J. Org. Chem.* **1991**, *56*, 4335-4337.
2. Porter, N. A.; Lacher, B.; Chang, V. H.; Magnin, D. R. "Regioselectivity and diastereoselectivity in free-radical macrocyclization." *J. Am. Chem. Soc.* **1989**, *111*, 8309.
3. Beckwith, A.L.J.; Schiesser, C.H. "Regio- and Stereo-Selectivity of Alkenyl Radical Ring Closure: A Theoretical Study." *Tetrahedron*, **1985**, *41*, 3925-3941.
4. Beckwith, A. L. J. "Regio-Selectivity and Stereo-Selectivity in Radical Reactions." *Tetrahedron*, **1981**, *37*, 3073-3100.
5. Hart, D.J.; Krishnamurthy, R. "Investigation of a Model for 1,2-Asymmetric Induction in Reactions of α -Carbalkoxy Radicals: A Stereochemical Comparison of Reactions of α -Carbalkoxy Radicals and Ester Enolates." *J. Org. Chem.* **1992**, *57*, 4457-5570.
6. Porter, N.A.; Giese, B.; Curran, D.P. "Acyclic Stereochemical Control in Free-Radical Cyclizations." *Acc. Chem. Res.* **1991**, *24*, 296-304 and references therein.
7. RajanBabu, T.V. "Stereochemistry of Intramolecular Free-Radical Cyclization Reactions." *Acc. Chem. Res.* **1991**, *24*, 139-145.
8. Molander, G.A.; Kenny, C. "Intramolecular Reductive Coupling Reactions Promoted by Samarium Diiodide." *J. Am. Chem. Soc.* **1989**, *111*, 8236-8246.
9. McAtee, R.C.; McClain, E.J.; Stephenson, C.R.J. "Illuminating Photoredox Catalysis." *Trends Chem.* **2019**, *1*, 111-125.
10. Romero, N.A.; Nicewicz, D.A. "Organic Photoredox Catalysis." *Chem. Rev.* **2016**, *116*, 10075-10166.
11. Prier, C.K.; Rankic, D.A.; MacMillan, D.W.C. "Visible Light Photoredox Catalysis with Transition Metal Complexes: Applications in Organic Synthesis." *Chem. Rev.* **2013**, *113*, 5322-5363.
12. Yan, M.; Kawamata, Y.; Baran, P.S. "Synthetic Organic Electrochemical Methods Since 2000: On the Verge of a Renaissance." *Chem. Rev.* **2017**, *117*, 13230-13319.
13. Rono, L.J.; Yayla, H.G.; Wang, D.Y.; Armstrong, M.F.; Knowles, R.R. "Enantioselective Photoredox Catalysis Enabled by Proton-Coupled Electron Transfer: Development of an Asymmetric Aza-Pinacol Cyclization." *J. Am. Chem. Soc.* **2013**, *135*, 17735-17738.

14. Amador, A. G. Yoon, T.P. "A Chiral Metal Photocatalyst Architecture for Highly Enantioselective Photoreactions." *Angew. Chem. Int. Ed.* **2016**, *55*, 2304-2306.
15. Yoon, T.P. "Photochemical Stereocontrol Using Tandem Photoredox-Chiral Lewis Acid Catalysis." *Acc. Chem. Res.* **2016**, *49*, 2307-2315 and references therein.
16. Nicewicz, D.A.; MacMillan, D.W.C. "Merging Photoredox Catalysis with Organocatalysis: The Direction Asymmetric Alkylation of Aldehydes." *Science* **2008**, *322*, 77-80.
17. Zuo, Z.; Cong, H. Li, W.; Choi, J.; Fu, G.C.; MacMillan, D.W.C. "Enantioselective Decarboxylative Arylation of α -Amino Acids via the Merger of Photoredox and Nickel Catalysis." *J. Am. Chem. Soc.* **2016**, *138*, 1832-1835.
18. Huang, X.; Meggers, E. "Asymmetric Photocatalysis with Bis-Cyclometalated Rhodium Complexes." *Acc. Chem. Res.* **2019**, *52*, 833-847.
19. Taylor, M.S.; Jacobsen, E.N. "Asymmetric catalysis in complex target synthesis." *Proc. Natl. Acad. Sci.* **2004**, *101*, 5368-5373.
20. Hart, D.J.; Huang, H-C.; Krishnamurthy, R.; Schwartz, T. "Free-Radical Cyclizations: Application to the Total Synthesis of dl-Pleurotin and dl-Dihydropleurotin Acid." *J. Am. Chem. Soc.* **1989**, *111*, 7507-7519.
21. Shono, T.; Nishiguchi, I.; Ohmizu, H.; Mitani, M. "Electroorganic Chemistry. 31. Reductive Cyclization of Nonconjugated Olefinic Ketones to Cyclic Tertiary Alcohols." *J. Am. Chem. Soc.* **1978**, *100*, 545-550.
22. Villar, F.; Andrey, O.; Renaud, P. "Diastereoselective Radical Cyclization of Bromoacetals: Efficient Synthesis of (-)-Botryodiplodin." *Tetrahedron Lett.* **1999**, *40*, 3375-3378.
23. Villar, F.; Renaud, P. "Diastereoselective Radical Cyclization of Bromoacetals (Ueno-Stork Reaction) Controlled by the Acetal Center." *Tetrahedron Lett.* **1998**, *39*, 8655-8658.
24. Stork, G.; Mook, R. Jr.; Biller, S.A.; Rychnovsky, S.D. "Free-Radical Cyclization of Bromoacetals. Use in the Construction of Bicyclic Acetals and Lactones." *J. Am. Chem. Soc.* **1983**, *105*, 3741-3742.
25. Villar, F.; Kolly-Kovac, T.; Equey, O.; Renaud, P. "Highly Stereoselective Radical Cyclization of Haloacetals Controlled by the Acetal Center." *Chem. Eur. J.* **2003**, *9*, 1566-1577.
26. Beckwith, A.L.J.; Page, D.M. "Formation of Some Oxygen-Containing Heterocycles by Radical Cyclization: The Stereochemical Influence of Anomeric Effects" *J. Org. Chem.* **1998**, *63*, 5144-5153.
27. Corminboeuf, O.; Renaud, P.; Schiesser, C.H. "A Computational Study of Radical Haloacetal Cyclizations Controlled by the Acetal Center." *Chem. Eur. J.* **2003**, *9*, 1578-1584.

28. Hanessian, S.; Yang, H.; Schaum, R. "Hydrogen-Bonding as a Stereocontrolling Element in Free-Radical C-Allylation Reactions: Vicinal, Proximal, and Remote Asymmetric Induction in the Amino Acid Series." *J. Am. Chem. Soc.* **1996**, *118*, 2507-2508.
29. Staveness, D.; Sodano, T.M.; Li, Kangjun, Burnham, E.A.; Jackson, K.D.; Stephenson, C.R.J. "Providing a New Aniline Bioisostere Through the Photochemical Production of 1-Aminonorbornanes." *Chem*, **2019**, *5*, 215-226.
30. Sodano, T.M.; Combee, L.A.; Stephenson, C.R.J. "Recent Advances and Outlook for the Isosteric Replacement of Anilines." *ACS Med. Chem. Lett.* **2020**, DOI:10.1021/acsmchemlett.9b00687.
31. Guidon, Y.; Lavallée, J-F.; Llinas-Brunet, M.; Horner, G.; Rancourt, J. "Stereoselective Chelation-Controlled Reduction of α -Iodo- β -alkoxy Esters under Radical Conditions." *J. Am. Chem. Soc.* **1991**, *113*, 9701-9702.
32. Guidon, Y.; Guérin, B.; Chabot, C.; Mackintosh, N.; Ogilvie, W.W. "Stereoselective Radical Allylations of α -Iodo- β -Alkoxy Esters: Reversal of Facial Selectivity by Lewis Acid Complexation." *Synlett*, **1995**, *5*, 449-451.
33. ZnCl₂ was excluded from these experiments in order to maintain reliable peak shape and multiplicity. The presence of ZnCl₂ causes unpredictable broadening of peaks in the ¹H NMR spectra and detracts or completely prevents interpretation (i.e. peak picking, integration).
34. Harper, K.C.; Moschetta, E.G.; Bordawekar, S.V.; Wittenberger, S.J. "A Laser Driven Flow Chemistry Platform for Scaling Photochemical Reactions with Visible Light." *ACS Cent. Sci.* **2019**, *5*, 109-115.
35. Le, C.; Wismer, M.K.; Shi, Z-C.; Zhang, R.; Conway, D.V.; Li, G.; Vachal, P.; Davies, I.W.; MacMillan, D.W.C. "A General Small-Scale Reactor To Enable Standardization and Acceleration of Photocatalytic Reactions." *ACS Cent. Sci.* **2017**, *3*, 647-653.
36. Xie, Q.; Ni, C.; Zhang, R.; Li, L.; Rong, J.; Hu, J. "Efficient Difluoromethylation of Alcohols Using TMSCF₂Br as a Unique and Practical Difluorocarbene Reagent under Mild Conditions." *Angew. Chem. Int. Ed.* **2017**, *56*, 3206-3210.
37. Pouységu, L.; Marguerit, M.; Gagnepain, J.; Lyvinec, G.; Eatherton, A.J.; Quideau, S. "Total Synthesis of Wasabidienones B₁ and B₀ via SIBX-Mediated Hydroxylative Phenol Dearomatization." *Org. Lett.* **2008**, *10*, 5211-5214.

Chapter 4

Re-Engineering the Acrylamide S1 Scaffold by Substitution of 1-Aminonorbornanes in Metabolic Hotspot

The work presented in this chapter is unpublished and has been completed in collaboration with Dr. Daryl Staveness, Dr. Logan Combee, Alexander Levashkevich, and Alyiah Chmiel at the University of Michigan.

4.1 Introduction

To provide proof-of-concept for the 1-aminonorbornanes (aminoNBs) as metabolically innocuous aniline isostere hypothesis, two goals needed to be met: the aminoNB scaffold must (1) impart a degree of metabolic inertness and/or prevent the formation of reactive metabolite species

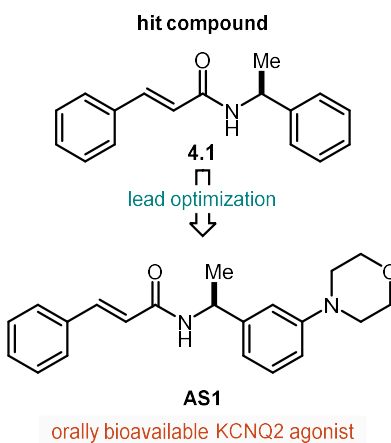


Figure 4.1. Discovery of acrylamide S1 (AS1)

to avert toxicity; and (2) the biological activity of the parent compound must be recapitulated. For

these purposes, a scaffold with known toxicity due to aniline functionality needed to be selected for re-engineering, employing the photochemical methodology described in Chapter 2. After a survey of the literature, acrylamide S1 (**AS1**) was chosen as the target. In 2003, Bristol-Myers Squibb reported **4.1** as a hit in a high-throughput screening effort from its in-house compound library employing a thallium flux assay (Figure 4.1).¹ Subsequent lead optimization identified **AS1** as an orally bioavailable KCNQ2 agonist with activity in a cortical spreading depression (CSD) model of migraine with 10 mg/kg dosing. While **AS1** has promising potency and efficacy, it has also been shown to be a time-dependent inhibitor of CYP3A4, the predominant P450 enzyme in the liver responsible for phase I metabolism.² This type of activity is a strong indicator for the formation of reactive metabolites. Perhaps unsurprisingly, the functionality responsible for this liability was found to be the morpholinoaniline motif (further discussion in Chapter 5), providing an ideal opportunity to test the metabolic stability of aminoNBs in direct comparison to an aniline.

The synthetic route towards **AS1** begins with an amide bond coupling between cinnamic

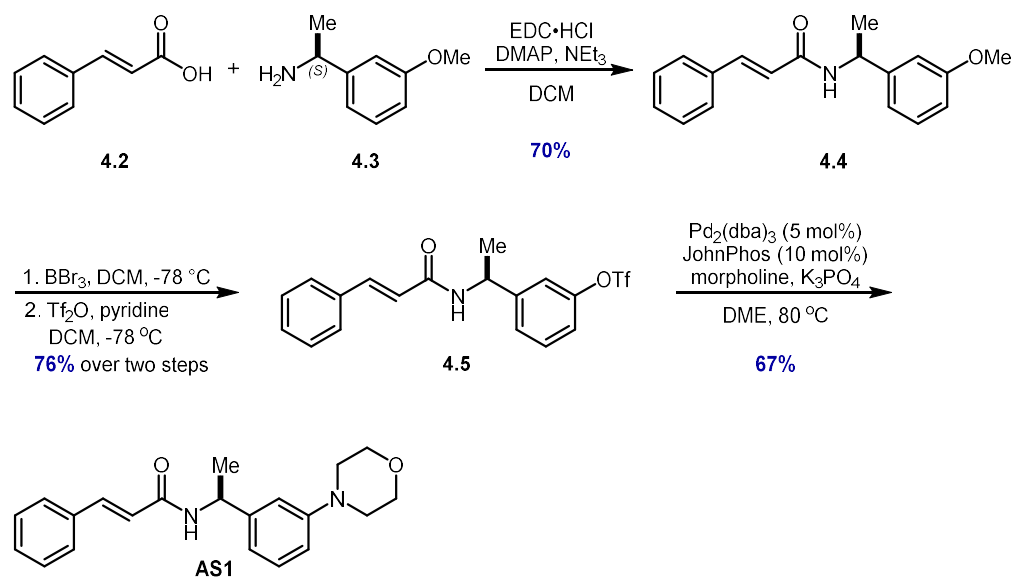


Figure 4.2. Synthesis of **AS1**

acid (**4.2**) and chiral amine **4.3** (Figure 4.2). Next, demethylation using BBr_3 at low temperature

revealed the free phenol and ensuing triflation provided a handle for a metal-mediated cross coupling in 76% yield over two steps. Buchwald-Hartwig cross-coupling between **4.5** and morpholine was accomplished in 67% yield to provide **AS1**. This approach is succinct and versatile, with the cross-coupling allowing for broad diversification in the final step.

To identify the active pharmacophore in **AS1**, a study on the structure-activity relationship (SAR) was performed (Figure 4.3).³ **AS1** was shown to be 163% more efficacious at agonizing mKCNQ2 than the vehicle control. However, when inverting the stereocenter from *S* to *R*, the activity was completely lost (**4.6**, 98% control). When the amide carbonyl was reduced to the methylene (**4.7**), or the styrenyl olefin reduced to the alkane (**4.8**), complete loss of activity was also observed (110% and 105% control, respectively). Interestingly, when the secondary amide was methylated (**4.9**), moderate inhibition of mKCNQ2 was reported (72% control). These studies demonstrated the importance of the acrylamide functionality and configuration of the methyl stereocenter in the activation of KCNQ2, as well as offer some insight into potential interactions of the N-H within the binding pocket. This analysis also showed that modulation of the amine had an overall negative impact on activity (not shown), but subsequent studies have demonstrated that the eastern half of the molecule is amenable to diversification without loss of function.^{4,5}

With the deleterious metabolic processing attributed to the aniline and promising reports of successful substitution of this motif, **AS1** is an ideal candidate to investigate the metabolic stability and biological activity of aminoNBs. As an additional area of investigation, the aniline within **AS1** is meta-substituted, a pattern not readily mimicked by other benzene ring isosteres, such as bicyclo[1.1.1]pentane and cubane. However, aminoNBs have multiple sites for substitution

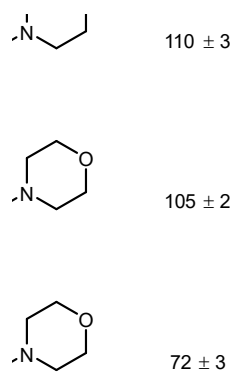


Figure 4.3. SAR study of **AS1** active pharmacophore

with unique spatial vectors, all of which are accessible with the photochemical methodology.

Preliminary *in silico* analysis demonstrated that several of these isomers orient the key acrylamide pharmacophore at a “meta-like” angle. For example, the energy-minimized structures of both **AS1** and C3-axial substituted aminoNB **4.12** show promising shape complimentary when

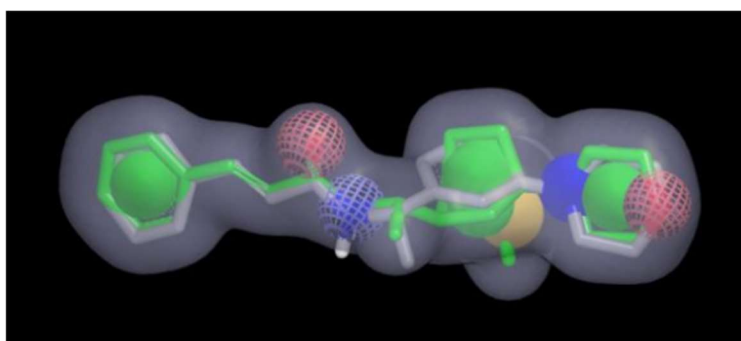


Figure 4.4. Overlay of energy minimized structure of **AS1** (grey skeleton) and C3 aminoNB **4.12** (green skeleton)

superimposed (Figure 4.4), with the key carbonyl and N-H bond closely aligned. The **AS1** scaffold is a non-selective agonist across the KCNQ family of ion channels, but the overall breadth of chemical space available with aminoNBs may facilitate stronger interactions within the protein binding pocket and impart selectivity between KCNQ isoforms. However, only synthesis and biological evaluation will reveal the most clinically-relevant substitution pattern, so all available sites are being targeted through the synthesis of C7 (**4.10** and **4.11**), C3-axial (**4.12**, **4.13**, **4.14**, and **4.15**), C3-equatorial (**4.16** and **4.17**), C4 (**4.18**), and C2 (**4.19**, **4.20**, **4.21**, and **4.22**) aminoNB analogs (Figure 4.5). The 2-fluoroacrylamide motif was selected over the unsubstituted acrylamide present within **AS1** due to enhanced activity in preliminary studies. This chapter describes these synthetic efforts, while subsequent evaluation of KCNQ agonism activity and metabolic profiling of the first-generation library of analogs are reported in Chapter 5.

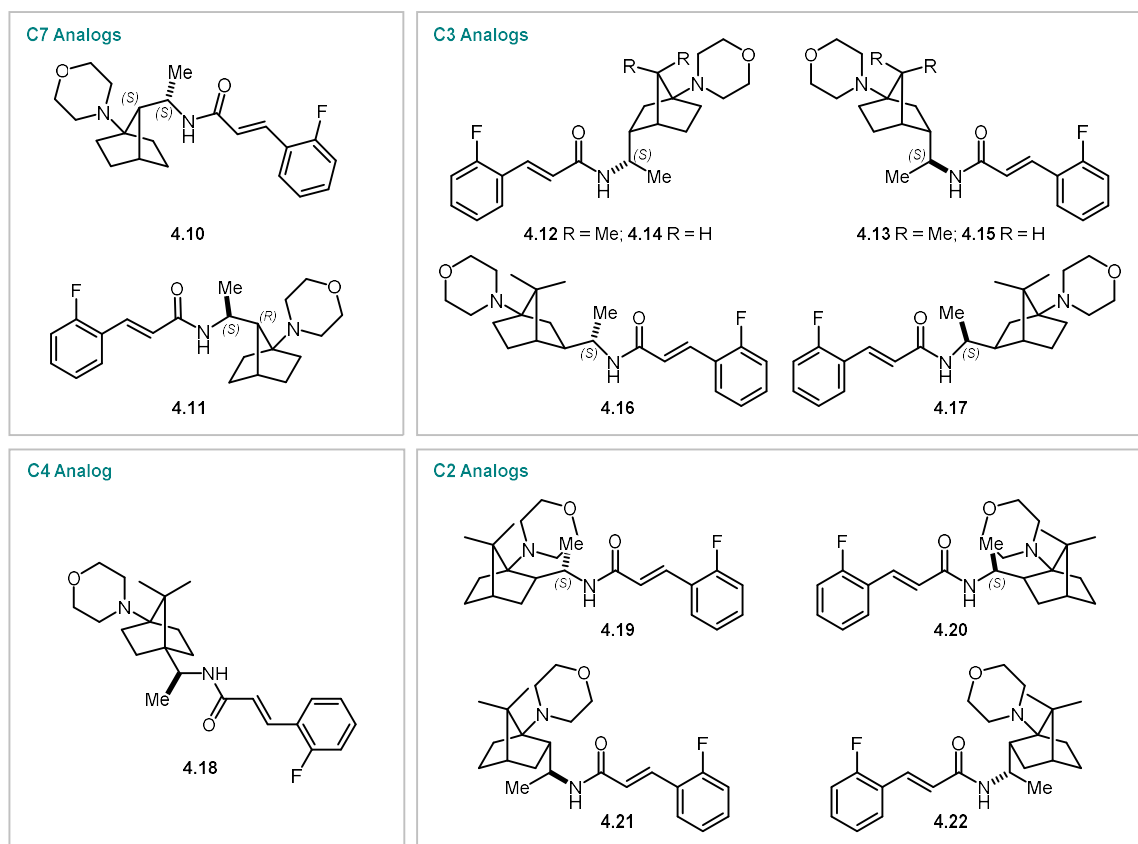


Figure 4.5. First-generation library of **AS1** aminoNB analogs

4.2 Synthesis of C7 Analogs 4.10 and 4.11

4.2.1 First-Generation Synthesis

Synthesis of the C7 analogs **4.10** and **4.11** were envisioned to arise from a common aminocyclopropane (aminoCP) intermediate that would diverge into the requisite 7*S*, 8*S* and 7*R*, 8*S* diastereomers in the photochemical cyclization. Beginning with (*R*)-methyl lactate (**4.23**), protection of the alcohol through benzylation furnished **4.24** (Figure 4.6). Generation of the corresponding aldehyde from ester **4.24** *in situ* by 1 equiv. of DIBAL-H and treatment with vinyl Grignard provided an inconsequential mixture of allylic alcohol diastereomers **4.25** in 75% yield. Conversion of **4.25** to linear ester **4.26** proceeded in high yield (91%) through a Johnson-Claisen reaction mediated by microwave heating. Saponification and subsequent amide bond coupling

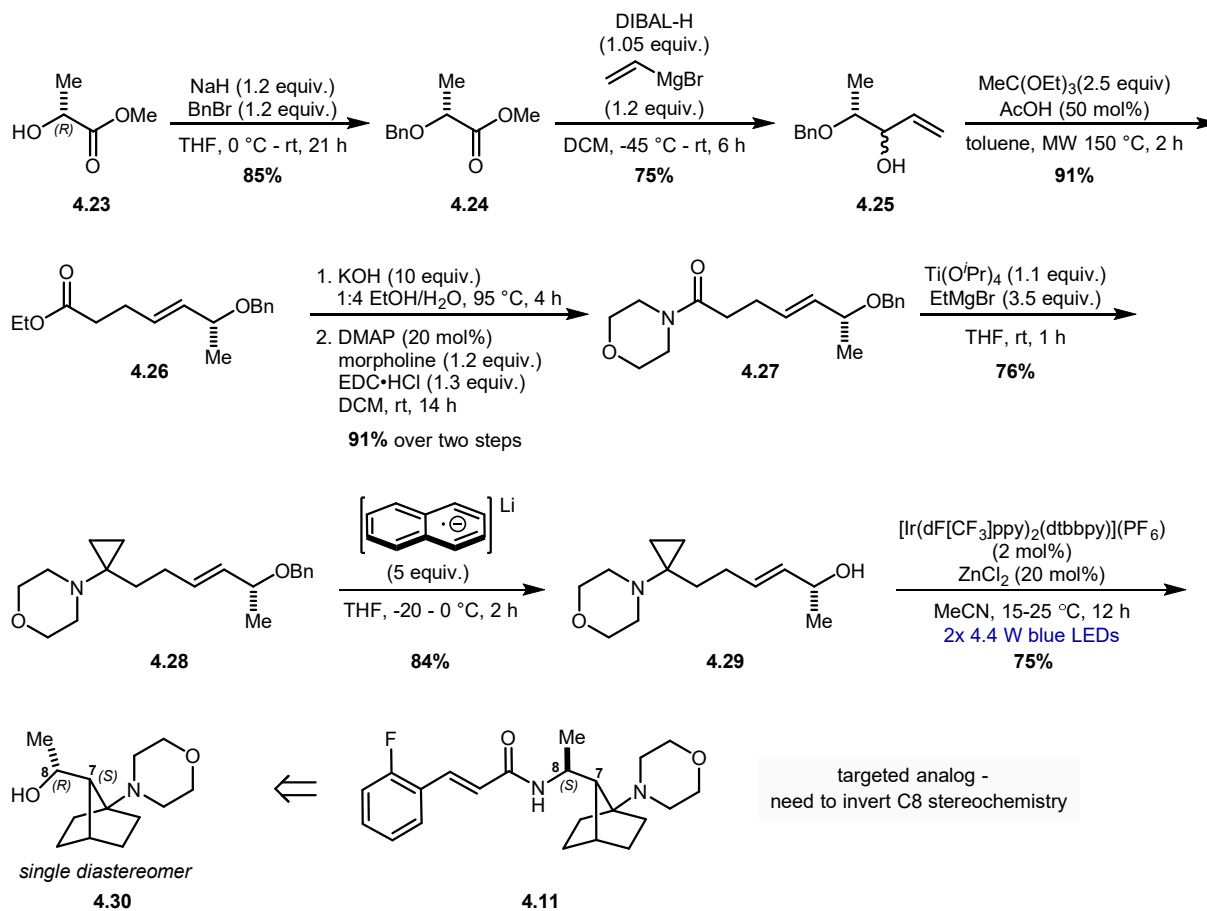


Figure 4.6. Synthesis of 7*S*, 8*R* aminoNB **4.30**

provided **4.27** in 91% yield over two steps. Subjection of amide **4.27** to $\text{Ti}(\text{O}^i\text{Pr})_4$ and EtMgBr under standard Kulinkovich cyclopropanation conditions yielded aminoCP **4.28**. Debenzylation employing lithium naphthalenide preserved the olefin to give alcohol **4.29**, which was subjected to the photochemical cyclization protocol, resulting in aminoNB **4.30** as a single diastereomer in 75% yield.

As described in Chapter 3, the exquisite control over diastereoselectivity was unexpected at this time. However, attempts were made to convert the *7S*, *8R* diastereomer to the final analog. It was envisioned that the stereocenter at the C8 position would be inverted from *R* to the required *S* configuration through an $\text{S}_{\text{N}}2$ reaction with an amine nucleophile. A number of different conditions were evaluated to enact this transformation, but none of the attempts led to the desired reactivity. Under Mitsunobu conditions, several different nitrogenous nucleophiles were employed, such as phthalimide, *N*-Boc cinnamimide, and azide, but in all cases, only SM or phosphate adducts (e.g. **4.31**) were recovered (Figure 4.7). To investigate why even small

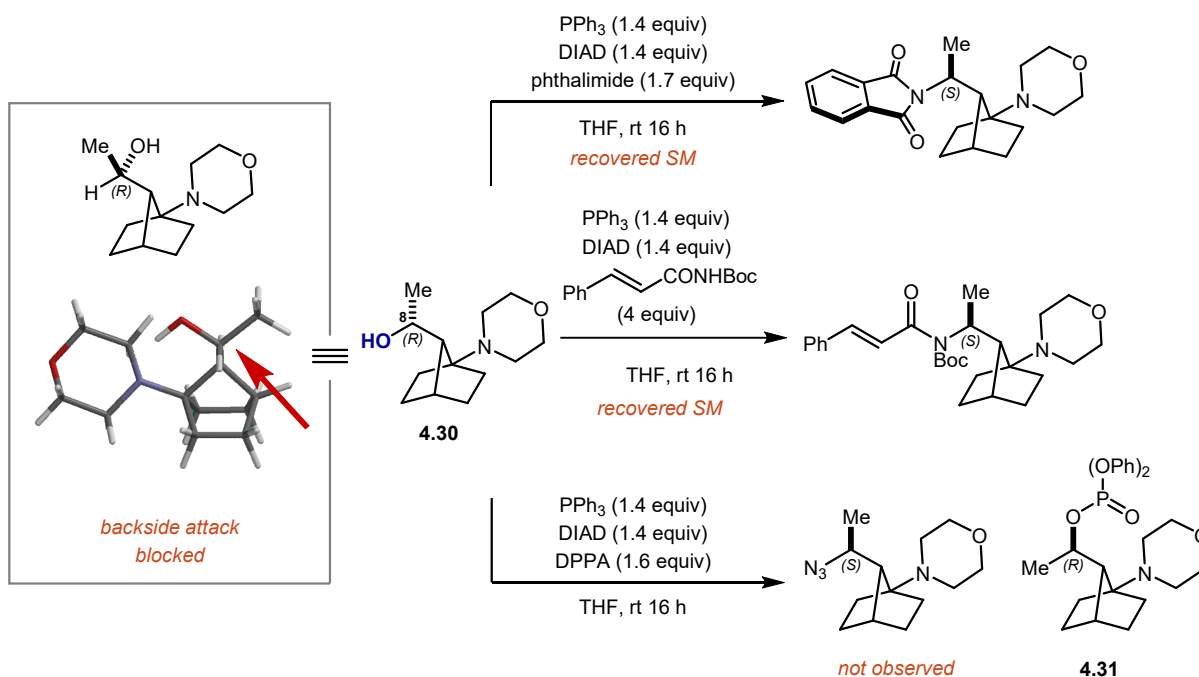


Figure 4.7. Alcohol **4.30** is resistant to substitution due to blocked backside approach

nucleophiles, such as azide, were resisting substitution even at elevated temperatures, we turned to *in silico* modeling to better understand the structure of aminoNB **4.30**. The low energy conformation of aminoNB **4.30** positions the alcohol proximal to the morpholine at an orientation suggesting an intramolecular hydrogen bonding interaction. Due to this, the trajectory for backside attack at the C8 position is blocked by the norbornane core, prohibiting nucleophilic displacement.

With this limitation in mind, the synthetic route was revised to incorporate the amine functionality before the photochemical cyclization. This also proved to be challenging, and after extensive optimization, alcohol **4.29** was converted to azide **4.32** by treatment with PPh₃, DIAD, and DPPA (Figure 4.8). However, branched azide **4.33** was also generated in a 1:1 ratio with the desired **4.32**, the reaction was overall low yielding (63% yield combined), and **4.32** and **4.33** were inseparable by flash column chromatography. Other nucleophiles, such as phthalimide, also led to mixtures of S_N2 and S_N2' products (not shown). However, in the case of the allylic azides, we were not able to definitively differentiate between an S_N2' mechanism or interconversion of **4.32** and **4.33** via an allylic azide rearrangement. The mixture of **4.32** and **4.33** were further elaborated to carbamate **4.34** plus the branched isomer via Staudinger reduction and Boc-protection in 83% yield over two steps. Photochemical cyclization provided aminoNB **4.35** as a single diastereomer in

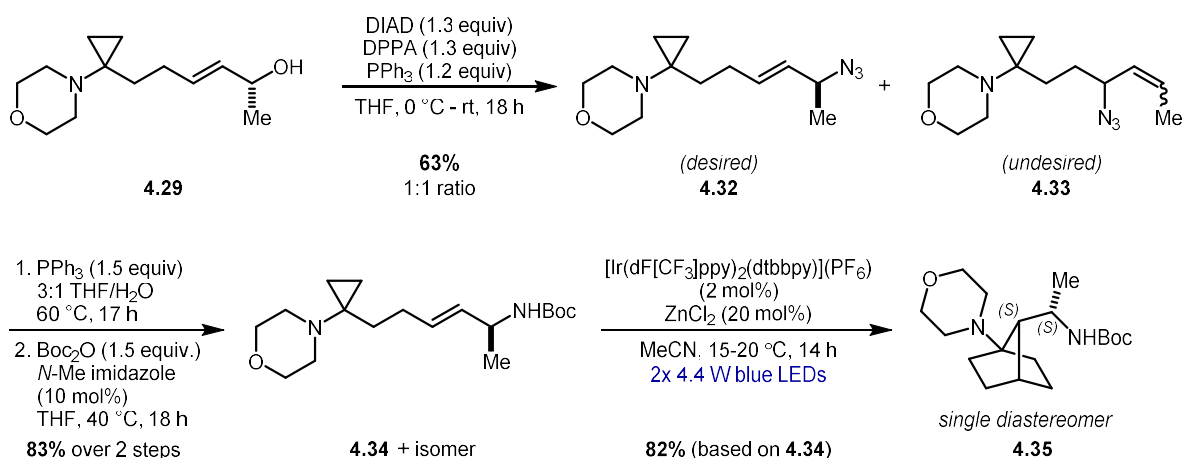


Figure 4.8. Incorporation of amine functionality prior to photochemical cyclization

82% yield based on the desired linear aminoCP **4.34**. Removal of the Boc group was achieved under acidic conditions and elevated temperatures. The resultant free amine was treated with cinnamoyl chloride in the presence of NEt₃ and DMAP to provide analog **4.36** in 40% yield over two steps or subjected to amide bond coupling conditions to produce 2-fluoro analog **4.10** in 62% yield over two steps (Figure 4.9).

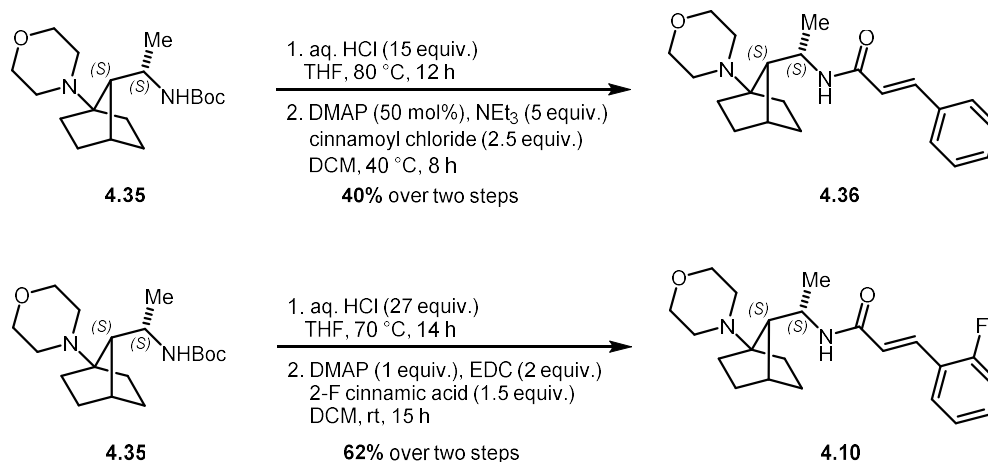


Figure 4.9. Completion of analogs **4.36** and **4.10**

While this route proved viable for the synthesis of the 7*S*, 8*S* diastereomer, the 7*R*, 8*S* diastereomer proved to be elusive. The mechanistic study detailed in Chapter 2 established a model for the stereocontrol at the C7 position based on 1,2-asymmetric induction via a transition state electrostatic interaction between the C8 heteroatom and the iminium. Based on this kinetic model, aminoCP **4.34** would fall somewhere on the less selective side of the spectrum, similar in electronics to the acetate (5:1 *dr*) but more sterically demanding. However, this does not account for any thermodynamic effects that may contribute to the selectivity, and we sought to understand the factors contributing to this outcome.

The first observation that suggested a thermodynamic preference for the 7*R*, 8*S* diastereomer was apparent in a comparison of the ¹H NMR spectra of **AS1** and **4.36** (Figure 4.10). In **AS1**, the amide proton has a chemical shift of 5.77 ppm. However, this same resonance is

considerably shifted downfield in the aminoNB analog **4.36** to 9.48 ppm. The dramatic shift suggests that this proton resides in a different chemical environment than that of **AS1**, so computational modeling was used to probe the three-dimensional structure of **4.36**. A search for

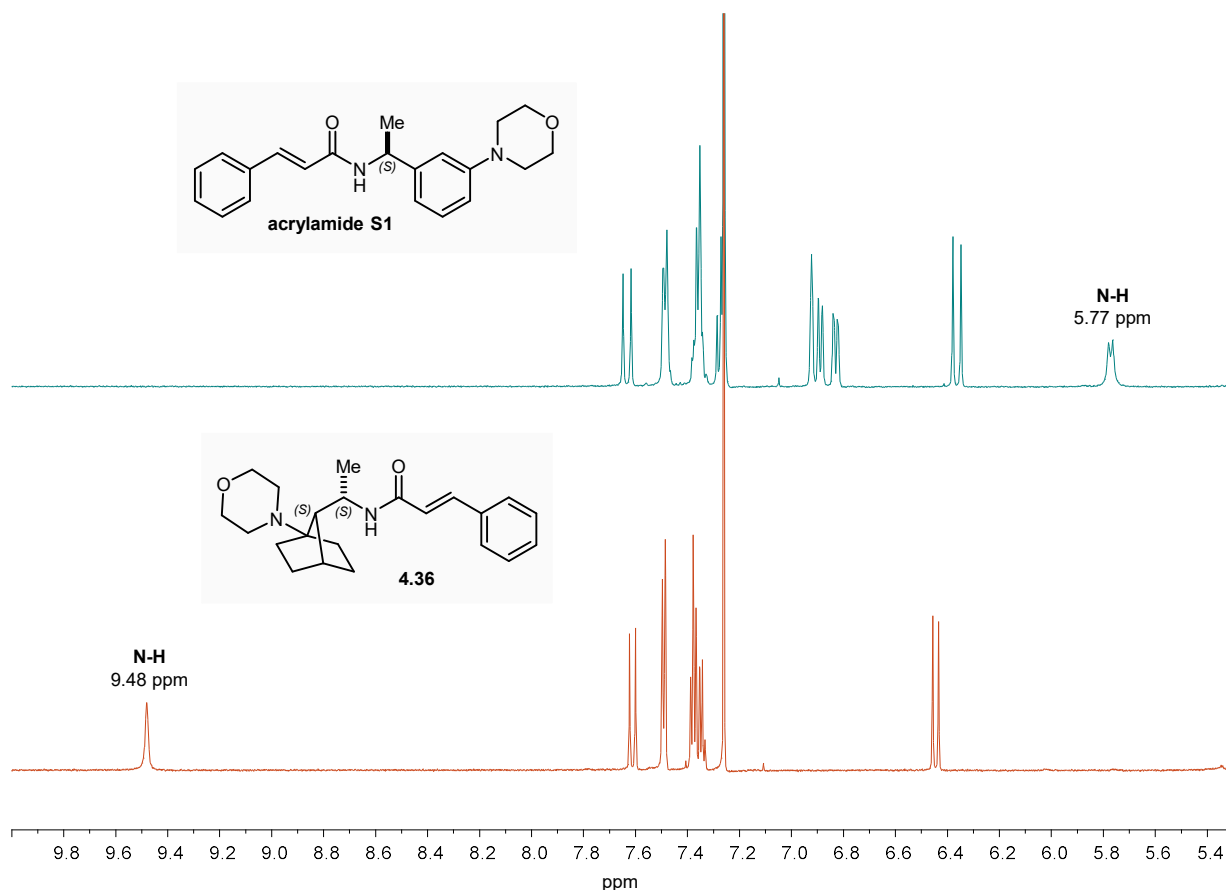


Figure 4.10. Comparison of ¹H NMR spectra of **AS1** and **4.36**

low energy conformers of **4.36** showed a significant energy minimum corresponding to a structure in which the amide is oriented such that the N-H bond is engaging in an intramolecular hydrogen bonding interaction with the morpholine (Figure 4.11). This bond distance was estimated to be 1.99 Å, corresponding to approximately 5 kcal/mol of stabilization energy. To ensure that the 7*R*, 8*S* isomer is not able to engage in a similar interaction and benefit energetically, analog **4.37** was subjected to the same *in silico* analysis. As depicted in Figure 4.11, the low energy conformer of **4.37** positions the acrylamide in the opposite direction of the morpholine, preventing a hydrogen-

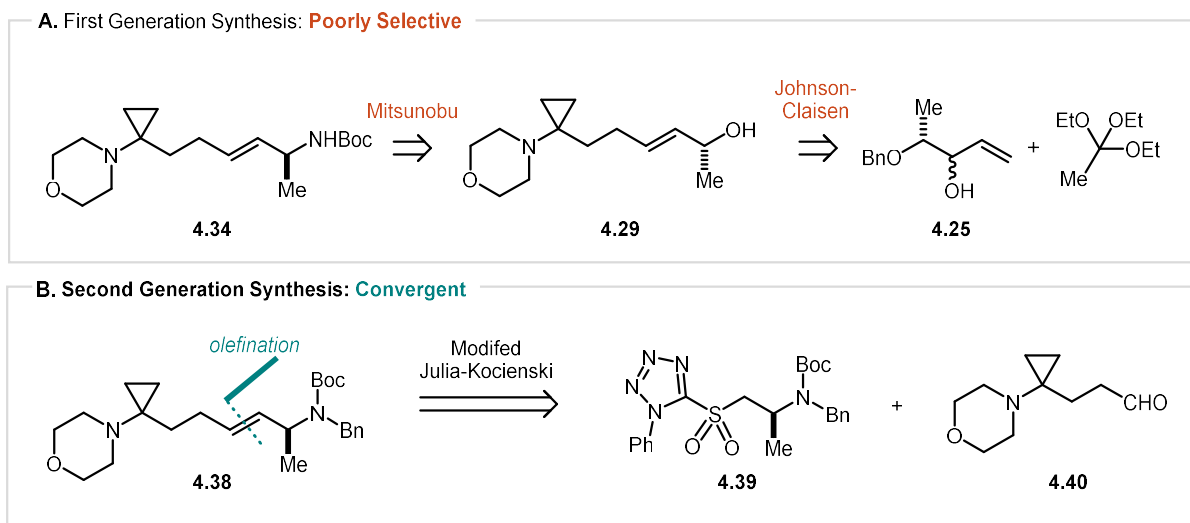


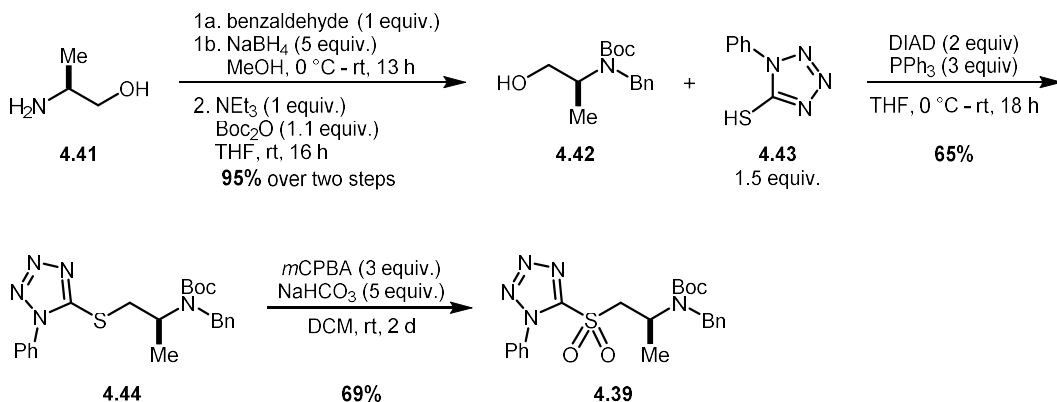
Figure 4.12. (A) Retrosynthetic analysis of first-generation approach; (B) Proposed disconnection for second-generation synthesis

neither desirable nor efficient to attempt a second protection of the isomers of advanced intermediate **4.34** and continue forward. Instead, a new synthetic disconnection was targeted in which the aminoCP could be constructed by a modified Julia-Kocienski olefination between phenyl tetrazole sulfone (PTS) **4.39** and aldehyde **4.40** (Figure 4.12B).

The PTS **4.39** was synthesized from L-alaninol (**4.41**), which was transformed in a known sequence via reductive amination with benzaldehyde followed by treatment with Boc_2O to alcohol **4.42**. A Mitsunobu reaction employing sulfide **4.43** as the nucleophile provided intermediate **4.44** in 65% yield (Figure 13A). Oxidation of the sulfide to the sulfone was achieved with *m*CPBA in 69% yield, completing the PTS fragment **4.39** in 4 steps in 40% overall yield.

Synthesis of aldehyde **4.40** was also prepared expediently, beginning by refluxing γ -butyrolactone (**4.44**) neat in morpholine. After cooling to room temperature, TBSCl and imidazole were added directly, yielding silyl ether **4.46** in 95% yield in a two-step, one-pot process (Figure 13B). Subsequent Kulinkovich cyclopropanation provided aminoCP **4.47**. Protodesilylation under acidic conditions proceeded in 95% yield to alcohol **4.48**, which was oxidized to aldehyde **4.40**

A. Synthesis of Phenyl Tetrazole Sulfone



B. Synthesis of -N(Boc)(Bn) AminoCP

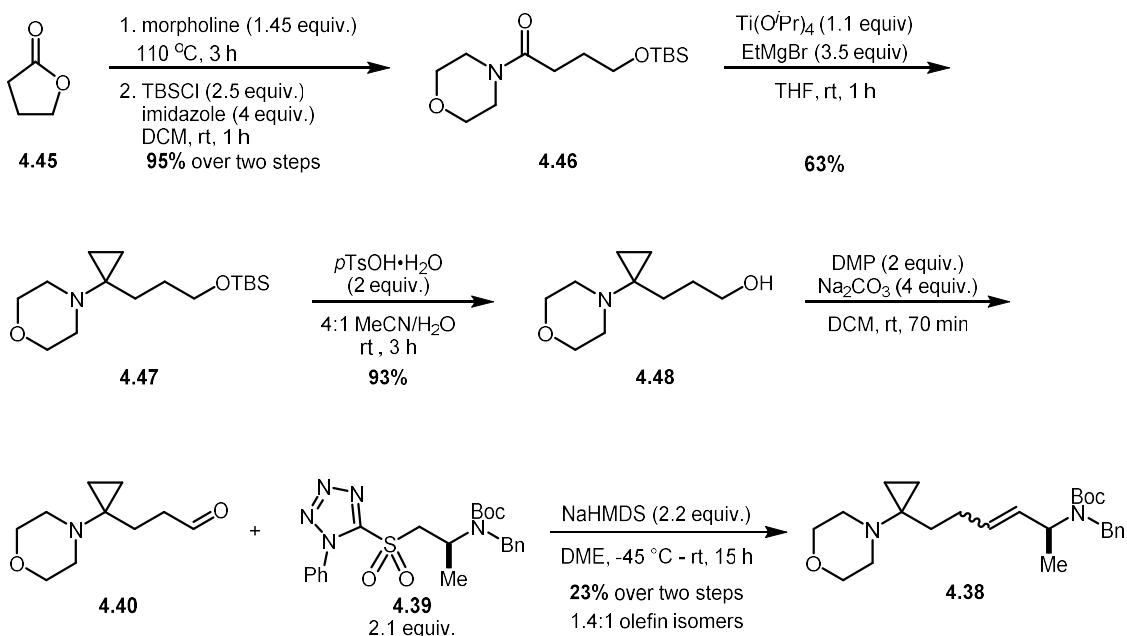


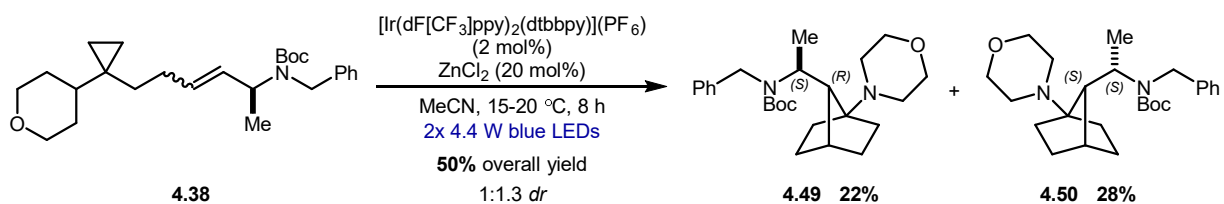
Figure 4.13. (A) Synthesis of PTS **4.39**; (B) Synthesis of aldehyde **4.40** and results of the modified Julia-Kocienski olefination

employing NaHCO₃-buffered DMP. Aldehyde **4.40** proved to be relatively unstable to chromatography, and due to additional concerns of volatility, it was used without further purification in the modified Julia-Kocienski olefination with **4.39**. Desired aminoCP **4.38** was generated in 23% yield over two steps under unoptimized conditions.

With aminoCP **4.38** in hand, the photochemical cyclization proceeded smoothly, and 7*R*, 8*S* isomer **4.49** was isolated in 22% yield while the 7*S*,8*S* isomer **4.50** was isolated in 28% yield, for a combined yield of 50% and 1:1.3 *dr*. Unfortunately, both **4.49** and **4.50** proved resistant to debenzoylation under standard hydrogenolysis conditions (stoichiometric 10% Pd/C, 30% Pd/C, or 20% Pd(OH)₂; EtOH, H₂, rt; data not shown). Hypothesizing that the steric contribution of the Boc group may be inhibiting reactivity, Boc deprotection of **4.50** under acidic conditions at 100 °C yielded aminoNB **4.51** (Figure 4.14). No longer contending with Boc rotomers, **4.51** was subjected to lithium naphthalenide to remove the benzyl group, but no reaction occurred.

At this stage, further manipulation of **4.49** and **4.50** would have necessitated extensive optimization. One of the drawbacks of this approach was the use of two distinct protecting groups, requiring a total of four protection/deprotection steps. While this second-generation route succeeded in demonstrating that the removal of the hydrogen-bonding interaction overcame the thermodynamic bias and both *C*7 diastereomers were produced in the photochemical cyclization, a more efficient route was required to complete the analog synthesis.

A. Photochemical Cyclization



B. Successful -Boc Removal

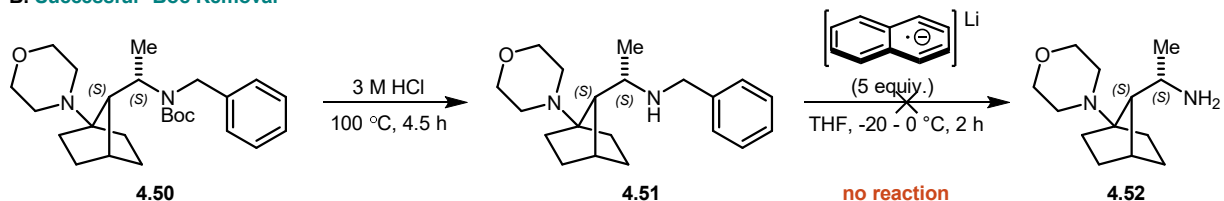


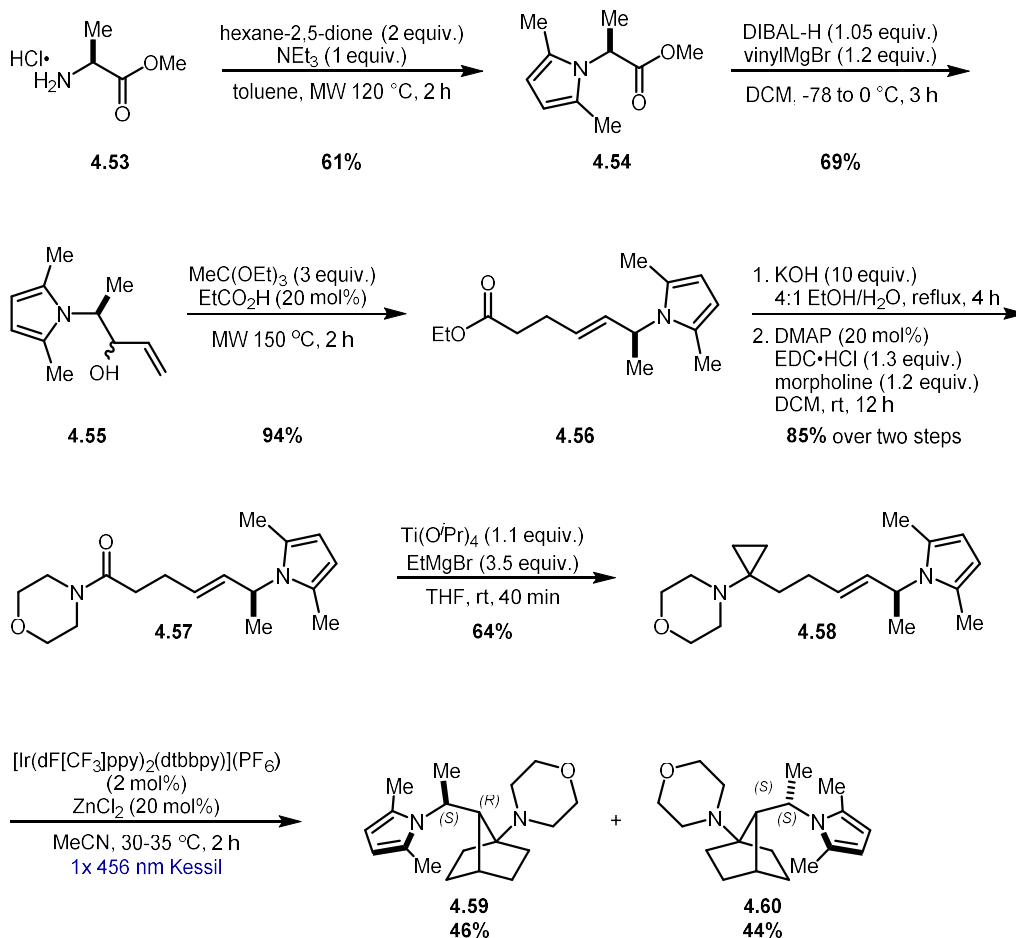
Figure 4.14. (A) Photochemical cyclization generates both *C*7 diastereomers; (B) Removal of Boc group and failed attempts at debenzoylation

4.2.3 Third-Generation Synthesis

The ideal nitrogen protecting group for the third-generation synthesis would require only one protection and one deprotection step, prevent the formation of the intramolecular hydrogen bond after cyclization to the aminoNB, and be tolerated in the Kulinkovich cyclopropanation. 2,5-dimethylpyrrole fit this description, and L-alanine methyl ester (**4.53**) was subjected to Paal-Knorr pyrrole synthesis conditions employing hexane-2,5-dione and microwave heating (Figure 4.15A). After accessing **4.54** in 61% yield, the remainder of the route closely mimicked the first-generation synthesis. The one-pot DIBAL-H reduction/vinylation sequence provided allylic alcohols **4.55**, which were taken forward in a Johnson-Claisen rearrangement, yielding linear ether ester **4.56** in 94%. Saponification and EDC coupling of the resultant carboxylic acid with morpholine gave **4.57** in high yield over two steps, and the cyclopropanation proceeded smoothly in 64% yield. AminoCP **4.58** was subjected to the photochemical conditions in batch, employing 2 mol% $[\text{Ir}(\text{dF}[\text{CF}_3]\text{ppy})_2(\text{dtbbpy})](\text{PF}_6)$, 20 mol% ZnCl_2 , and irradiating with one 456 nm Kessil LED for 2 h. Both *7R*, *8S* (**4.59**) and *7S*, *8R* (**4.60**) aminoNBs were isolated in a 1:1 ratio and 90% overall yield. Deprotection of the pyrrole on the *7R* isomer **4.59** was achieved by treatment with concentrated HCl and microwave heating under unoptimized conditions, and the crude amine was coupled to 2-fluorocinnamic acid to provide the *7R*, *8S* analog **4.11**.

Due to the synthetic challenges presented from having to overcome inherent diastereoselectivity in order to access both targeted C7 analogs, we sought to obtain physical evidence of the proposed intramolecular hydrogen bonding interaction. Both *7S*-NHBoc aminoNB **4.35** and *7S* dimethylpyrrole aminoNB **4.60** were crystalline (while the corresponding *7R* isomer is an oil) and were analyzed by single crystal x-ray diffraction (Figure 4.16). For aminoNB **4.35**, an intramolecular hydrogen bond is not apparent as the amide proton is not directed towards the

A. Third-Generation Synthesis



B. Elaboration of 7S, 8S Isomer to Final Analog

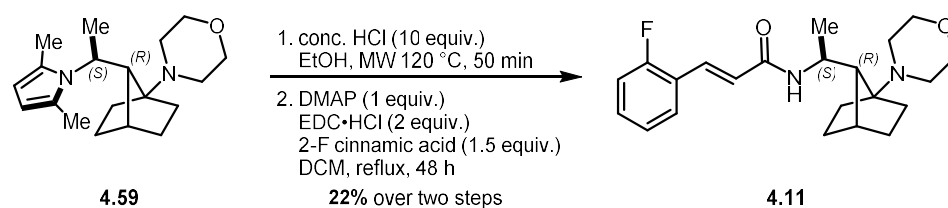


Figure 4.15. (A) Third-generation synthesis employing 2,5-dimethylpyrrole as a nitrogen protecting group; (B) Pyrrole deprotection and completion of **4.11** synthesis

morpholine nitrogen. However, the N-H bond and the carbonyl are coplanar and facing opposite directions, and the unit cell suggests *intermolecular* hydrogen bonding between these H-bond donor and H-bond acceptor functionalities (not shown). As the crystallographic analysis isn't necessarily representative of solution-phase conformations, and with the strong evidence provided

by the ^1H NMR spectrum and computational modeling, the diastereoselectivity is likely controlled by the thermodynamics of an intramolecular hydrogen bond. Further studies seek to identify and understand any contributions of asymmetric induction and the role of the C8 configuration on selectivity.

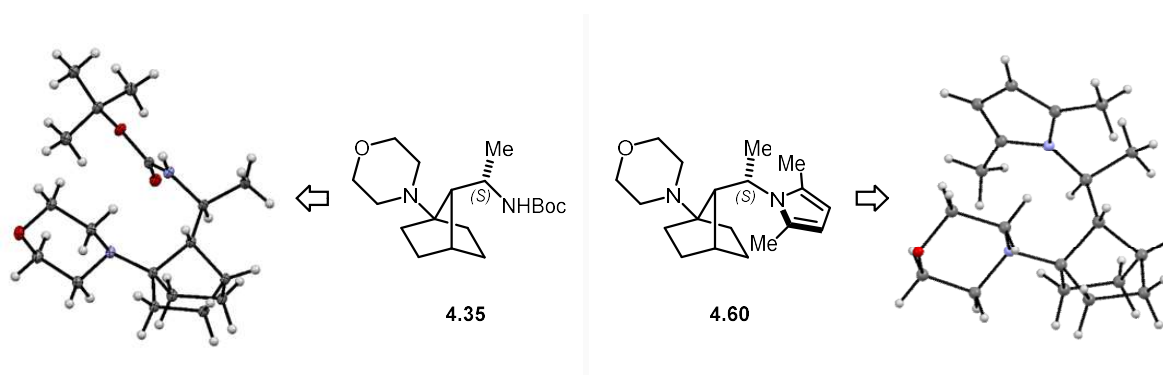


Figure 4.16. Comparison of x-ray crystal structures of **4.35** and **4.60**

4.3 Synthesis of C3-Axial Analogs **4.12** and **4.13**

Substitution off the C3 position on the aminoNB core can arise from aminoCPs with cyclopropane substitution or allylic substitution (Chapter 2). Preparing the appropriate olefin required in a ligand-exchange Kulinkovich reaction to give the desired substitution pattern on the cyclopropane was attempted, but branched alkenes were unreactive (Figure 4.17).

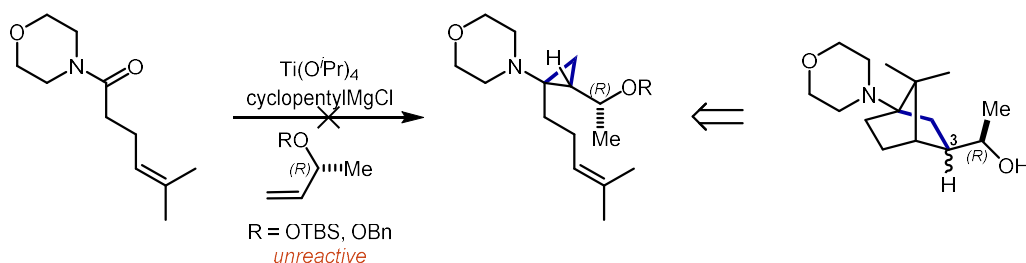


Figure 4.17. Branched olefins will not undergo ligand exchange to form substituted aminoCPs

An aminoCP with allylic substitution was deemed more prudent for analog synthesis, and a route was designed that closely resembled the first-generation synthesis of C7 analogs. (*R*-

methyl lactate (**4.23**) was once again employed as a chiral pool source, and benzylation of the alcohol provided **4.24** (Figure 4.18). Next, the aldehyde was generated *in situ* by treatment of **4.24** with 1 equiv. of DIBAL-H, and subsequent Horner-Wadsworth-Emmons olefination produced enoate ester **4.61** in 75% yield. Next, conjugate addition yielded branched ester **4.62** in 1:5 *dr*. The diastereomers were inseparable and subjected to saponification and amide bond coupling conditions as a mixture to give **4.63** in 94% yield over two steps. Reacting amide **4.63** with $\text{Ti}(\text{O}^i\text{Pr})_4$ and EtMgBr generated aminoCP **4.64** in 79% yield, and after debenzoylation with lithium naphthalenide, alcohols **4.65** and **4.66** were separable by flash column chromatography and isolated in 79% yield and 12% yield, respectively.

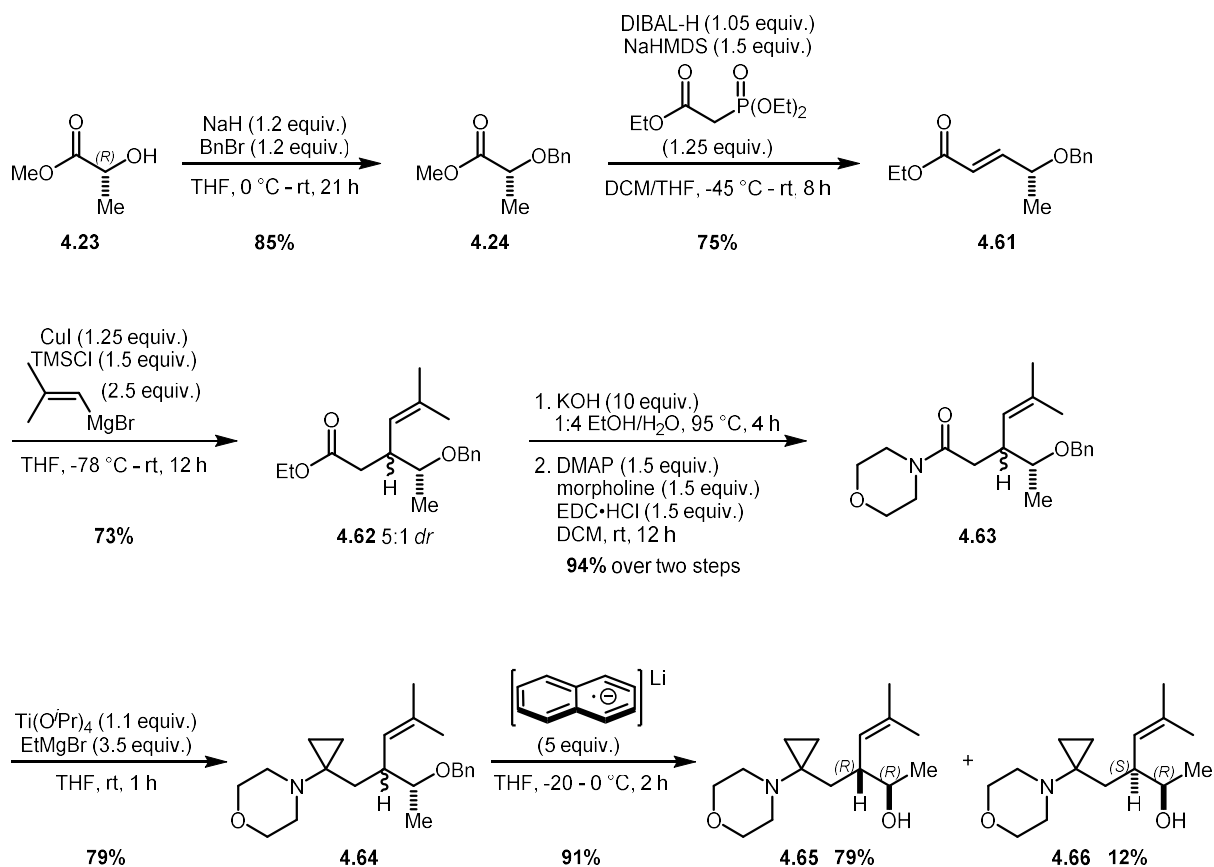
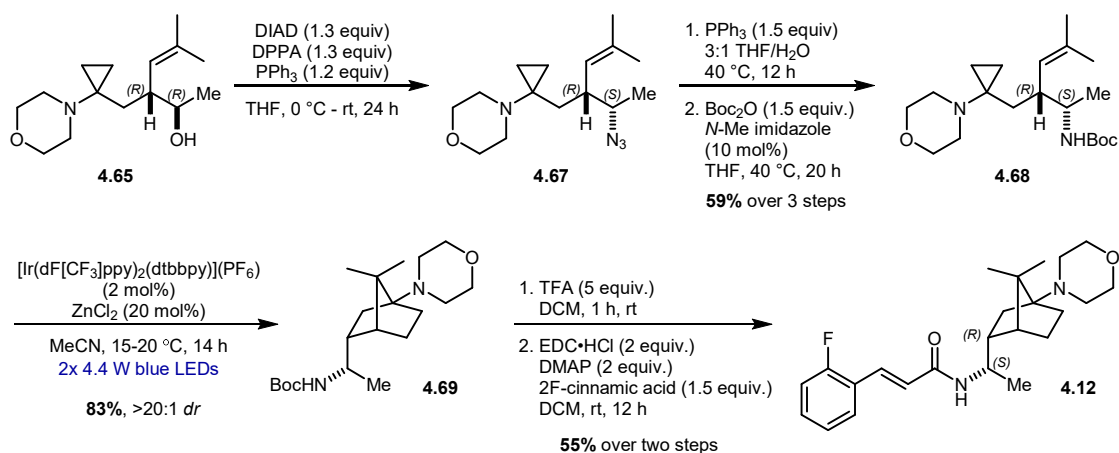


Figure 4.18. Synthesis of aminoCPs **4.65** and **4.66** for C3-axial aminoNBs

Major alcohol **4.65** was smoothly converted to azide **4.67** via a Mitsunobu reaction, and a Staudinger reduction/Boc-protection sequence provided aminoCP **4.68** in 59% yield over three

steps (Figure 4.19A). Photochemical cyclization resulted in the formation of the axial aminoNB **4.69** in 83% yield and >20:1 *dr*. The Boc group was removed upon treatment with TFA at room temperature, and amide bond coupling of the crude amine with 2-fluorocinnamic acid yielded analog **4.12** in 55% yield over two steps.

A. Completion of axial 3*R* analog **4.12**



B. Completion of axial 3*S* analog **4.13**

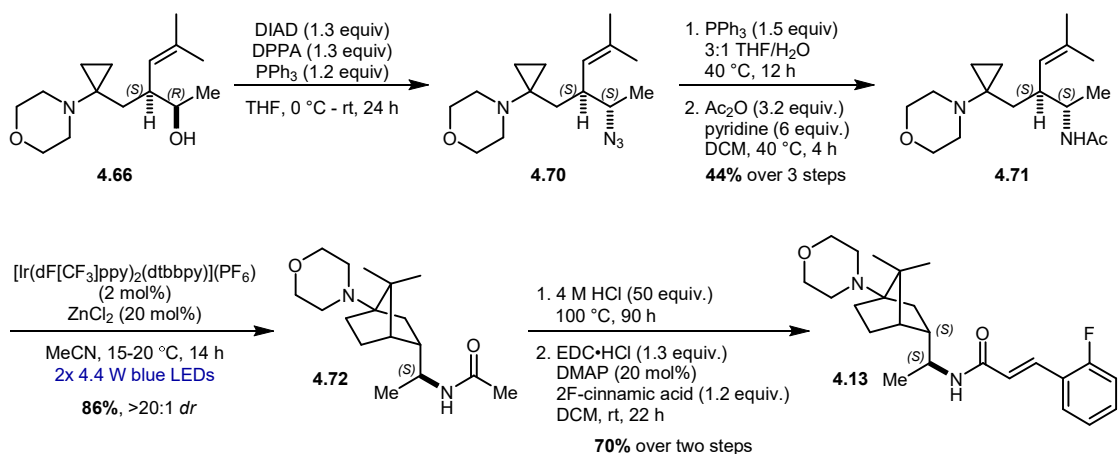


Figure 4.19. Second half of C3-axial analog syntheses (A) 3*R* **4.12** and (B) 3*S* **4.13**

The minor alcohol **4.66** was similarly treated; Mitsunobu reaction with DPPA as the azide source, reduction, and acetylation resulted in aminoCP **4.71** in 44% yield over three steps (Figure 19B). The photochemical cyclization proceeded in high yield and >20:1 axial selectivity. Direct conversion of aminoNB **4.72** to final analog **4.13** was pursued through aldol condensation with

benzaldehyde, but no reaction occurred (not shown).⁶ Instead, acetyl deprotection was necessary, but proved challenging. Several reported protocols were tested (lithium naphthalenide,⁷ Tf₂O/2-fluoropyridine/EtMgBr,⁸ pyridine/oxalyl chloride/propylene glycol,⁹ conc. H₂SO₄ at 100 °C) but **4.72** was unreactive in all cases. Only after treatment with 4 M aqueous HCl at 100 °C for 90 h was the desired amine obtained. Shorter reaction times resulted in incomplete conversion. The crude amine was subjected to the standard amide bond coupling conditions and C3 axial analog **4.13** was isolated in 70% yield over two steps.

4.4 Efforts Towards the Synthesis of C3-Equatorial Analogs **4.16** and **4.17**

While C3-equatorial substitution has been observed with aminoCPs with functionality appended to the cyclopropane, these substrates are difficult to prepare due to limitations of the Kulinkovich reaction (Figure 4.17). Theoretically, the allylic substitution employed in the previous section could also provide C3 equatorial substitution, but the stereoselectivity is controlled by minimization of A_{1,3} strain in the *6-exo-trig* cyclization and only C3-axial aminoNBs are produced (Chapter 3). Therefore, an alternative strategy was required to synthesize this class of aminoNB analogs. Retrosynthetically, we envisioned that thermodynamic deprotonation of axial ketone **4.73** would generate an intermediary enolate (**4.74**) that could then undergo kinetic protonation from the less hindered bottom face to yield equatorial ketone **4.75** (Figure 4.20).¹⁰

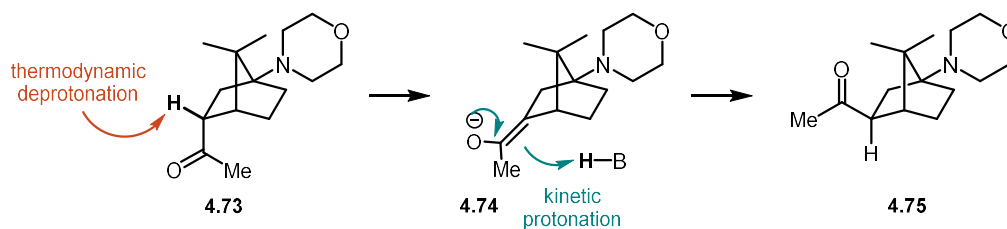
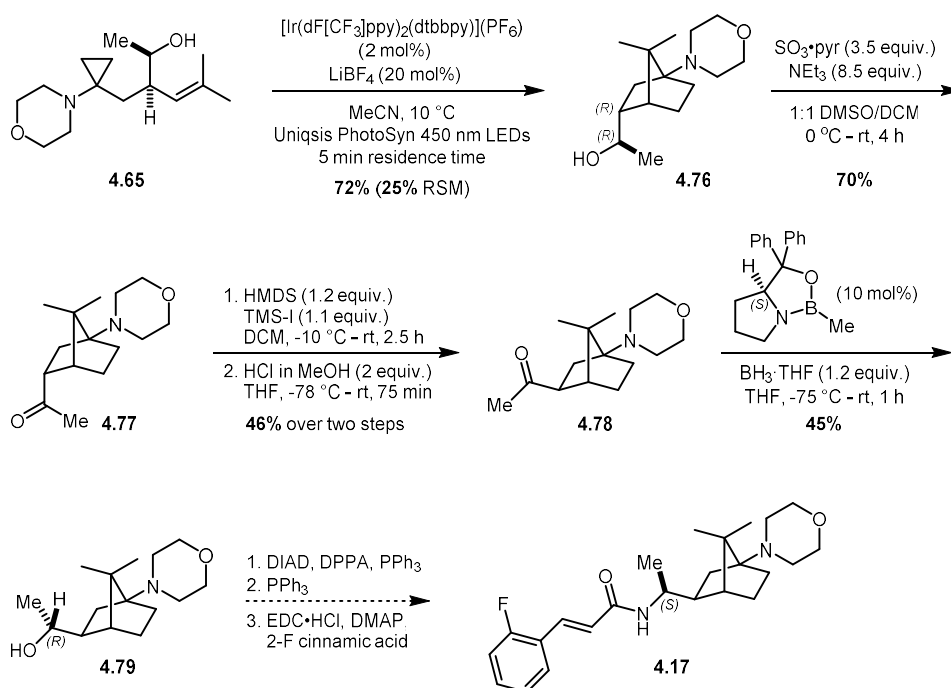


Figure 4.20. Epimerization strategy to access C3-equatorial substitution

Employing intermediates from the C3-axial analog syntheses, alcohol **4.65** was converted to aminoNB **4.76** under the photochemical conditions (Figure 4.21). In this case, the scale of the reaction (~400 mg) warranted continuous flow processing, and a commercial reactor (Uniqsis PhotoSyn) equipped with 450 nm LEDs and variable temperature control was employed. Using 2 mol% photocatalyst, 20 mol% LiBF₄, and a 5 min residence time, the reaction proceeded in 72% yield with 25% of aminoCP **4.65** recovered. The overall mass recovery in this reaction (97%) was higher than normally observed, and we are tentatively attributing this result to the lower temperature (10 °C Uniqsis vs. 20-25 °C Creative Lighting vs. 30-35 °C Kessil) controlling off-cycle reactivity and/or photocatalyst decomposition. With the temperature control capabilities of the Uniqsis Polar Bear Plus Flow add-on (-40 °C to +150 °C), further studies on the affect of lower temperatures on this reaction and other photochemical reactions can be carried out.

Parikh-Doering oxidation of **4.76** provided axial ketone **4.77**, and attempts were made to epimerize the C3 position by thermodynamic deprotonation followed by kinetic protonation. Enolization with KO^tBu and quenching with sterically hindered bases such as ^tBuOH or lutidine·HCl at -10 °C led to small amounts of equatorial ketone formation (~1:5 equatorial to axial), but the two isomers were inseparable by chromatography (not shown). To better control the selectivity for both the thermodynamic deprotonation and the kinetic protonation, each step was performed separately. Reacting **4.77** with HMDS in the presence of TMS-I produced the silyl enol ether (mixture of *E:Z* isomers) which was stable to purification by flash column chromatography. Protonation was carried out by addition of HCl in MeOH at -78 °C and slowly warming to room temperature. Equatorial ketone **4.78** was isolated in 46% yield over two steps in an unoptimized process.

A. Approach to C3-Equatorial Analogs



B. Probing Inherent Facial Bias

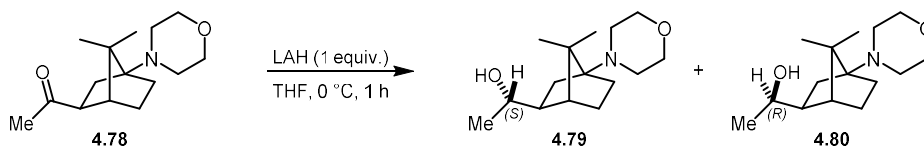


Figure 4.21. (A) Preliminary studies towards C3-equatorial analogs; (B) Selectivity in the reduction of **4.78** is partially controlled by substrate

Next, stereoselective reduction of the ketone to the alcohol was required. To control the facial approach of the hydride, (*S*)-CBS catalyst was employed in the presence of $\text{BH}_3 \cdot \text{THF}$ at -75 °C, and a single alcohol diastereomer (**4.79**) was isolated. However, it was unknown if the observed selectivity was a result of CBS coordination to the ketone or if the steric environment of the norbornane provided inherent stereocontrol in the reduction. To probe this, **4.78** was reduced with LAH, and two C3-equatorial aminoNB products were isolated in 6:1 ratio, with the major product being **4.79**. While this experiment demonstrates that there is partial substrate control for the

stereochemical outcome of the reduction, the addition of the CBS catalyst is synergist with the inherent bias.

Elaboration of alcohol **4.79** would proceed as reported for the C3-axial analogs. Conversion of the alcohol to the azide through a Mitsunobu reaction would invert the stereocenter and install the requisite nitrogen atom. Reduction to the amine and amide bond coupling would yield analog **4.17**. This same route can be applied to aminoCP **4.66** to access analog **4.16**.

4.5 Efforts Towards the Synthesis of C7-Methylene, C3-Axial Analogs 4.14 and 4.15

As discussed in Chapter 2, aminoNBs without substitution at the C7 position cannot be prepared from terminal olefin aminoCPs. Due to this limitation, the first-generation library of aminoNB analogs (with the exception of C7 analogs **4.10** and **4.11**) all bear gem-dimethyl substitution at the C7 position. These two carbons not only increase the spatial occupancy of aminoNBs compared to anilines, but also dramatically increase the lipophilicity. To examine the affect that the gem-dimethyl motif may have on the biological activity, selectivity, and metabolic profile of the analogs in this application, a C7 methylene analog needed to be synthesized. The C3-axial analogs were chosen as the first scaffold to modify due to the promising computational modeling (Figure 4.4) and preliminary biological activity (Chapter 5).

As terminal olefin aminoCPs will not undergo radical cyclization to produce the desired aminoNB, a functional handle at the C7 position will need to be in place for the photochemical cyclization but able to be removed afterwards. Our group has previously used this approach in the synthesis of C7 methylene aminoNBs in which a C7 carboxylic acid was removed via radical decarboxylation (Figure 4.22A).¹¹

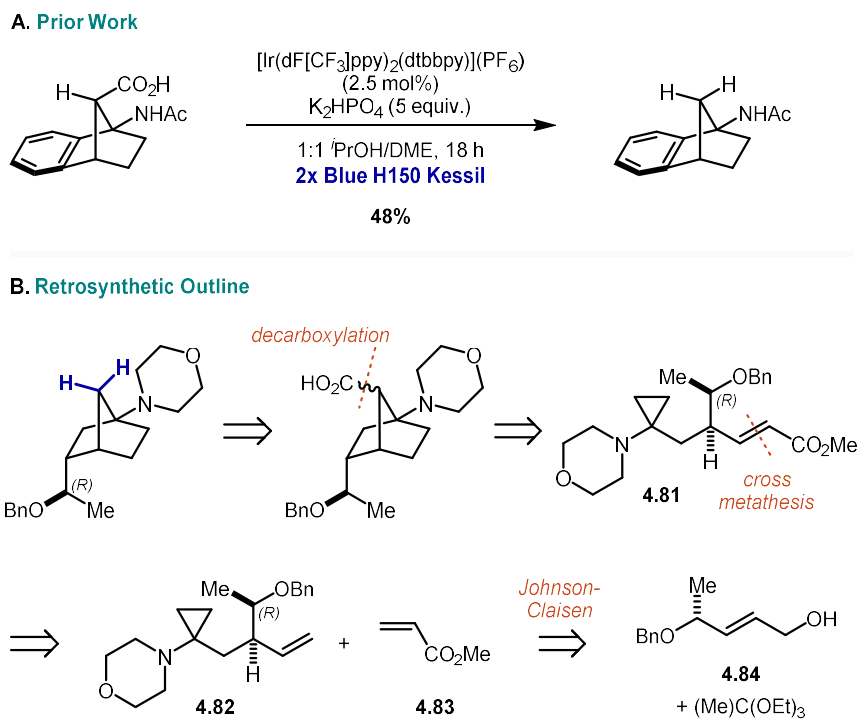


Figure 4.22. (A) Example of C7 decarboxylation to access C7 methylene aminoNB; (B) Retrosynthetic analysis for synthesis of C3-axial, C7-methylene aminoNB analog

AminoCP of type **4.81** was targeted, but several considerations needed to be may when designing the synthetic route. The chosen C7 functional handled ($-\text{CO}_2\text{Me}$ shown as one example in Figure 4.22B) would need to be tolerated in the cyclopropanation step. As most carbonyls react under the Kulinkovich conditions, enone **4.81** would need to be installed after cyclopropanation. The strategy that we ultimately pursued relied on cross metathesis between terminal olefin **4.82** and methyl acrylate (**4.83**) (Figure 4.22B).

As a starting point, allylic alcohol **4.84** was prepared by [1,2]-reduction of **4.61**. Ethyl ester **4.85** was then prepared in 60% yield and 1:1.3 *dr* by a Johnson-Claisen rearrangement with triethyl orthoacetate and substoichiometric propionic acid. Saponification and amide bond coupling with morpholine yielded termination alkene **4.86** (Figure 4.23). At this stage, **4.86** was subjected to Kulinkovich cyclopropanation conditions to generate the proposed metathesis precursor **4.82**. However, the reaction profile was complex, and the desired aminoCP was not produced in any

appreciable quantity likely due to competing coordination of the terminal olefin to titanium(IV) (not shown).

With this result, we adapted the strategy to perform the cross metathesis prior to the cyclopropanation, but needed to select a cross metathesis partner that would survive treatment by $\text{Ti}(\text{O}^i\text{Pr})_4/\text{EtMgBr}$. Vinyl silanes (e.g. dimethylphenylvinyl silane) were initially considered as cross metathesis partners as they are unreactive under Kulinkovich cyclopropanation conditions (not shown), and the resultant vinyl silane aminoCP would generate C7 silane aminoNBs. Unactivated $\text{Csp}^3\text{-Si}$ bonds have been reported to undergo efficient protodesilylation under mild conditions.^{12,13} However, it is well-documented that these electron-rich vinyl silanes do not undergo cross metathesis,^{14,15} and this synthetic direction was abandoned.

Two other options were identified that would tolerate cyclopropanation conditions and contained oxygenation that could be converted to C7 carboxylates; allyl-OTBS (**4.90**) and acrolein diethyl acetal (**4.91**).¹⁶ A small screen of cross metathesis conditions was carried out, investigating

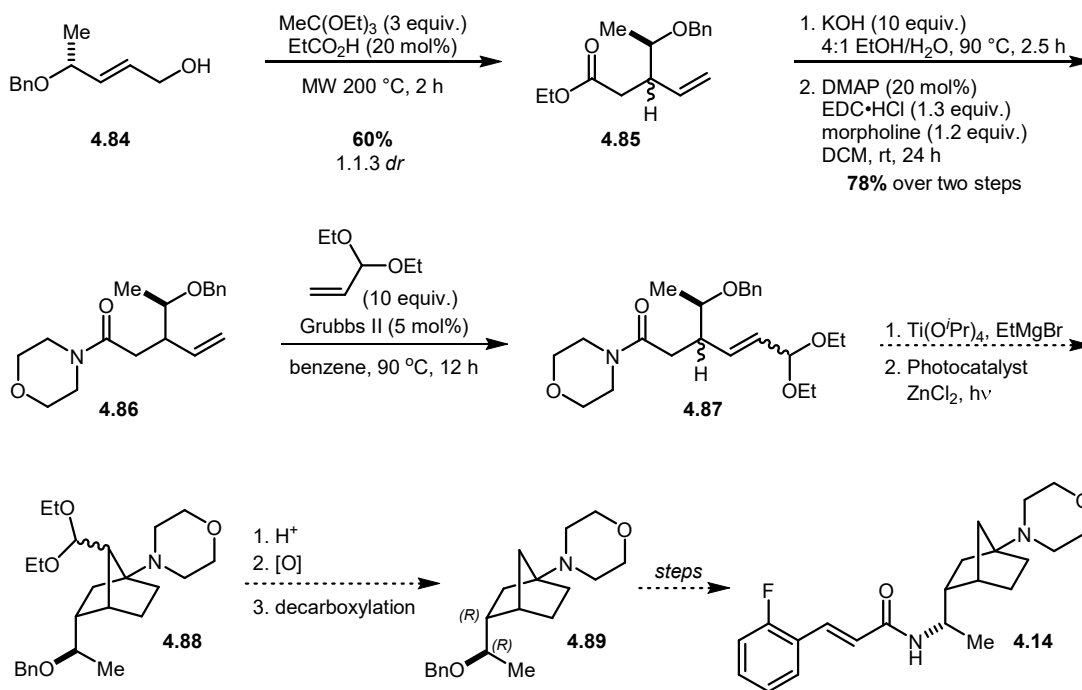


Figure 4.23. Preliminary studies towards C3-axial, C7-methylene analogs

time, temperature, catalyst, and olefin coupling partner (Table 4.1). Allyl-OTBS (**4.90**) and **4.86** were unreactive under all conditions tested, including under conventional and microwave heating with either Grubbs II (GII) and Hoyveda-Grubbs II (HGII) (Entries 1-4). However, acrolein diethyl acetal (**4.91**) and **4.86** underwent cross metathesis in the presence of GII and HGII at 80 °C over

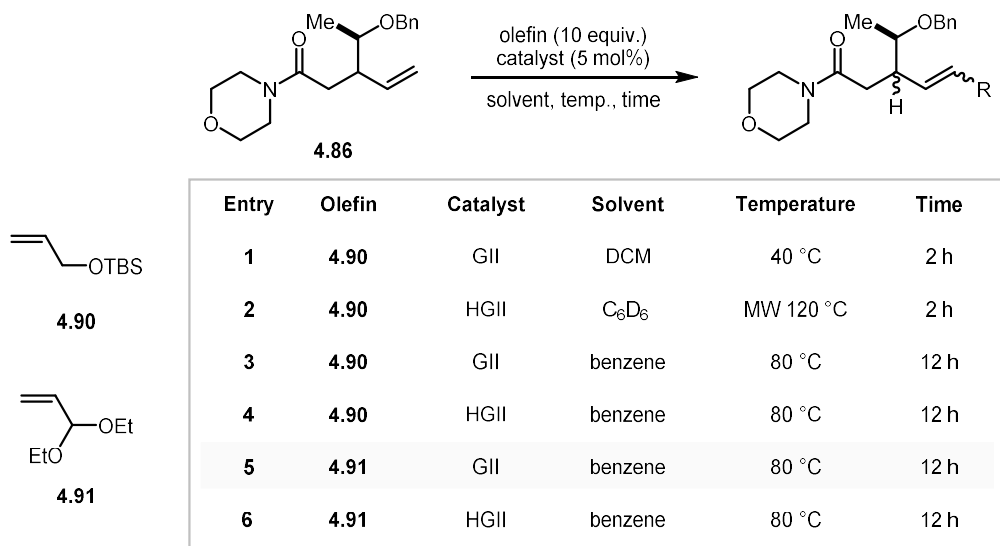


Table 4.1. Screen of cross metathesis conditions

12 h (Entries 5-6).¹⁷ Based on UPLC/MS analysis, GII outperformed HGII in terms of conversion, but the desired products **4.87** were detected by HRMS for both reactions. While **4.87** was formed as an intractable mixture of 4 diastereomers (syn/anti + cis/trans), this initial screen demonstrated the viability of this route, and further reaction development will seek to enhance cis/trans selectivity through exploration of additional catalysts and solvents.

After addressing this challenge, the route to accessing **4.14** is modular. One pathway could proceed via Kulinkovich cyclopropanation followed by photochemical cyclization with the acetal intact to yield aminoNB **4.88**. Acidic hydrolysis to the aldehyde and oxidation to the carboxylic acid would give the precursor to the decarboxylation. While our prior work employed a photochemical methodology for the C7 carboxylation, traditional conditions such as Barton-McCombie can be evaluated. With **4.89** in hand (only *R,R* diastereomer drawn for clarity),

elaboration to the final analog will proceed via the Mitsunobu sequence described for the other C3 syntheses.

4.6 Synthesis of C4 Analog 4.18

Unlike the C7 and C3 analog syntheses which employed chiral pool building blocks, the key (*S*)-methyl stereocenter was envisioned to arise from a late-stage asymmetric transformation for the C4 analog. Towards this end, achiral benzyl ether **4.92** was prepared through a known Morita-Bayliss-Hillman-etherification reaction between methyl vinyl ketone, formaldehyde, and benzyl alcohol¹⁸ (Figure 4.24). Addition of MeMgBr produced tertiary alcohol **4.93**, which was subjected to our standard microwave-assisted Johnson-Claisen procedure to give ethyl ester **4.94** in 34% yield. Saponification and amide bond coupling produced intermediate **4.95** in 53% yield over two steps, and subsequent Kulinkovich cyclopropanation yielded aminoCP **4.96**. The photochemical cyclization required 14 h of irradiation with a 456 nm Kessil LED source, resulting in 53% yield of aminoNB **4.97**. Debenzylation proceeded smoothly in 86% to give alcohol **4.98**. Oxidation to aldehyde **4.99** was achieved using NaHCO₃-buffered DMP. The amine was then introduced by condensation of Ellman's (*R*)-sulfinamide in the presence of Ti(O^{*i*}Pr)₄. The chiral auxiliary then directed methyl Grignard addition into **4.100**. The addition proceeded sluggishly at 0 °C, requiring 10 equiv. MeMgBr and extended reaction times (65 h) to furnish **4.101** as a single diastereomer in 46% yield. The sulfinamide was removed by treatment of HCl in MeOH at room temperature, and amide bond coupling with 2-fluorocinnamic acid provided C4 analog **4.18** in 64% yield over two steps.

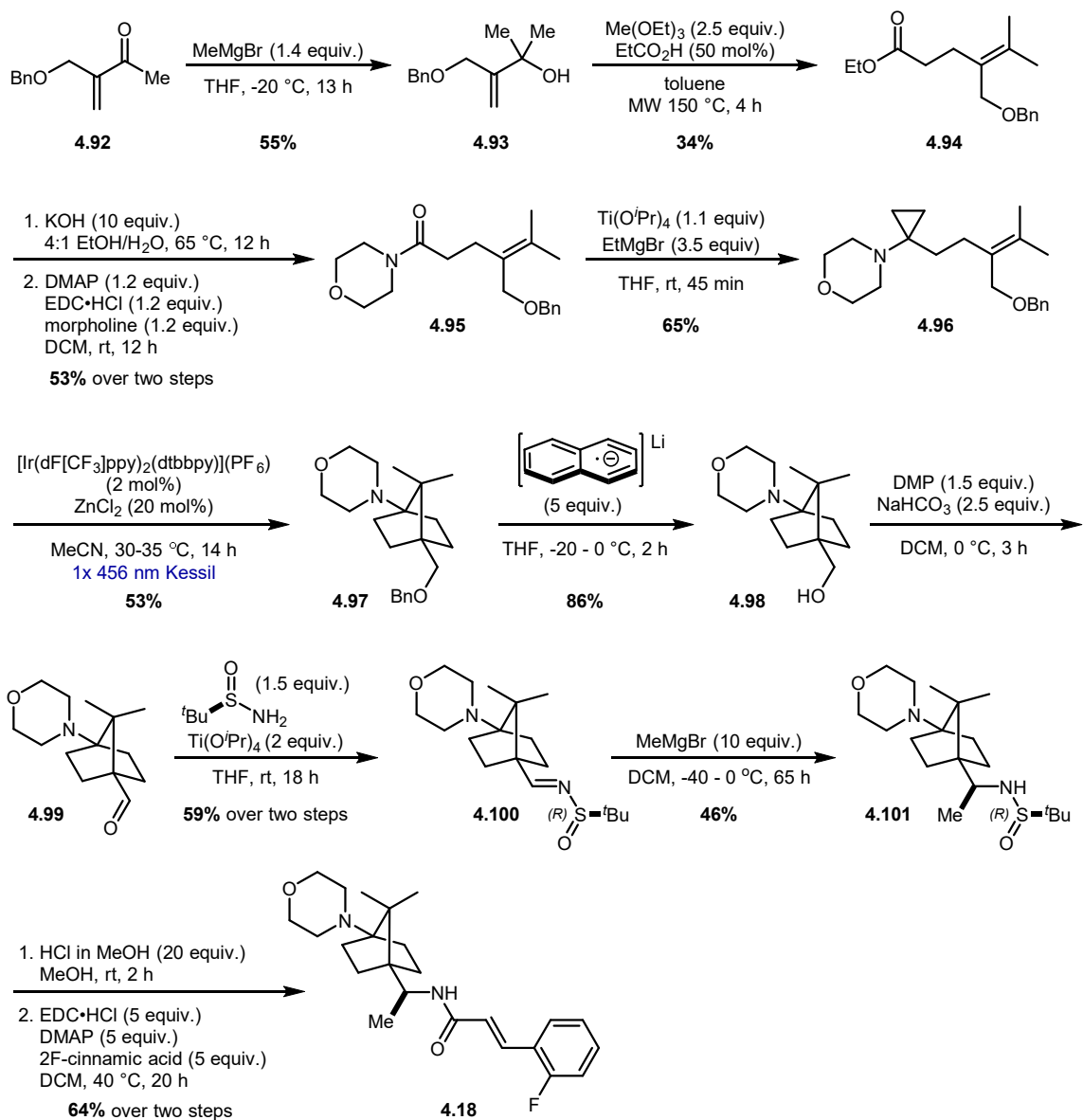


Figure 4.24. Synthesis of C4 analog **4.18**

4.7 Efforts Towards the Synthesis of C2 Analogs **4.19**, **4.20**, **4.21**, and **4.22**

Efforts towards the synthesis of C2 analogs **4.19-4.22** are in the preliminary stages. Methyl ester **4.103** was prepared as a single diastereomer by alkylation of the lithium enolate of methyl (*R*)-3-hydroxybutyrate (**4.102**) with prenyl bromide (Figure 4.25). Alcohol **4.103** was benzylated

in 63% yield with minimal erosion of *dr*. The saponification of **4.104** was carried out using 10 equiv. LiOH and microwave heating to 120 °C for 1 h, and amide bonding coupling of the resultant carboxylic acid with morpholine provided **4.105** in 57% yield over two steps. The Kulinkovich cyclopropanation was low yielding, producing only 39% of aminoCP **4.106**. When TBS was used as the protecting group in place of benzyl, the Kulinkovich cyclopropanation did not proceed to any extent, and only starting amide was recovered (data not shown). These results suggest that

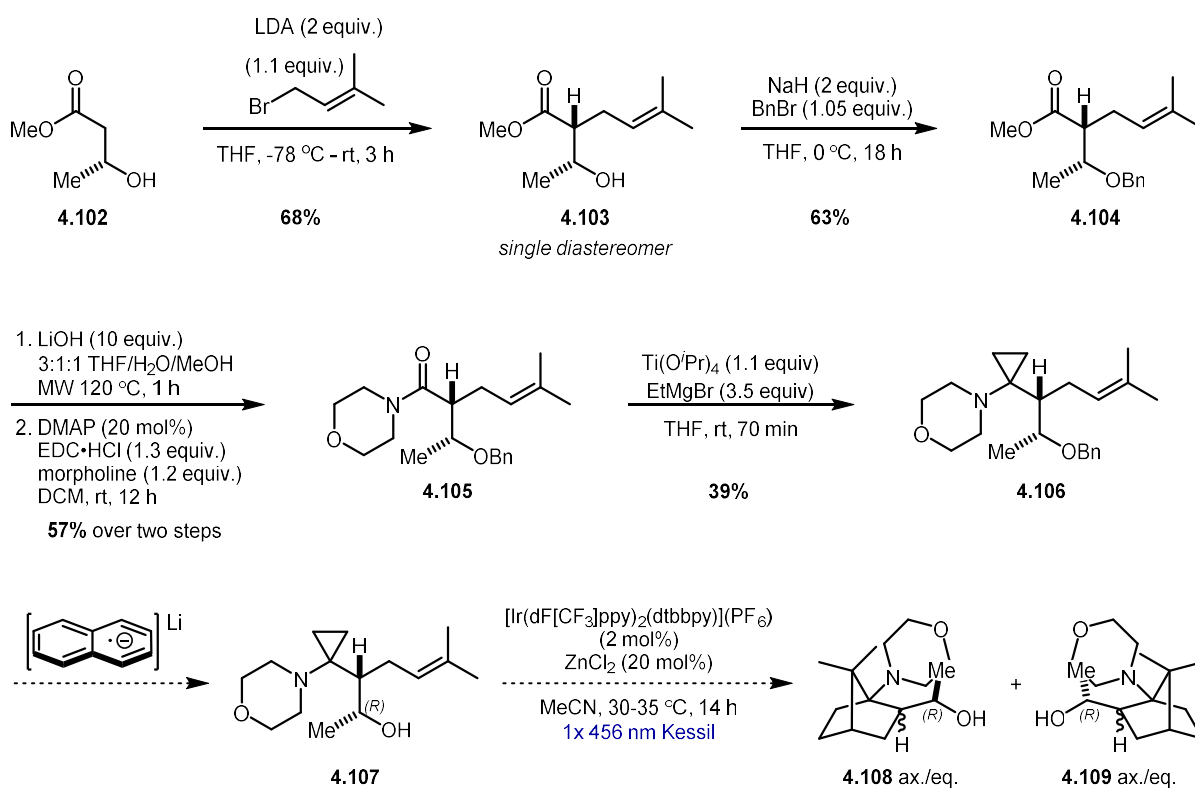


Figure 4.25. Studies toward the synthesis of C2 analogs

amide **4.105** and aminoCP **4.106** are significantly hindered, and the sterics at the C2 position appear to affect the efficiency of the photochemical cyclization. In exploratory studies, subjecting **4.106** to 2 mol% iridium photocatalyst, 20 mol% ZnCl₂, and 456 nm Kessil LED irradiation for 1.5 h led to low conversion and a complex reaction profile. As cyclization of aminoCP **4.106** can potentially yield all four C2 diastereomers **4.19-4.22**, future work will focus on removal of the benzyl group before the photochemical cyclization to reduce steric affects.

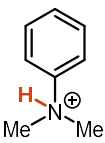
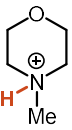
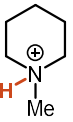
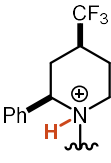
4.8 Future Directions: Developing a Second-Generation Library

The first-generation library of KCNQ analogs depicted in Figure 4.5 was designed to probe the SAR of the different substitution patterns on the aminoNB core. Once the best substitution pattern is identified in terms of KCNQ agonistic activity, the metabolic profile of the lead analog will be evaluated through CYP450 isoform selectivity, microsomal stability assays, metabolite identification, and TDI studies in collaboration with Prof. Klarissa Jackson. While a demonstration of biological activity comparable to **AS1** and improved metabolic stability would validate the aminoNB as aniline isostere hypothesis, our long-term goals are to develop new, safer KCNQ agonists as therapies for epilepsy and other hyperexcitability disorders. The second phase of this project would seek to improve the potency and selectivity of the aminoNB lead compound through targeted SAR analysis. This optimization may involve modification of the acrylamide to increase the negative surface potential of the carbonyl,¹⁹ but one critical physiochemical parameter that was not examined in the first-generation library was protonation-state of the amine functionality.

The **AS1** morpholinoaniline is unlikely to be protonated at physiological pH (7.4). The pK_a of protonated *N,N*-dimethylaniline (**4.110**) is 5.1,²⁰ giving it a percent ionization of only 0.5% at pH = 7.4 (Figure 4.26A). Conversely, the pK_a of protonated *N*-methyl morpholine (**4.111**) is 7.41,²¹ corresponding to 50.6% ionization under physiological conditions, although the pK_a of the bridgehead morpholine of the analog compounds is likely lower than **4.111** due to the steric crowding imparted by the aminoNB scaffold.²² As **AS1** binds to a cytoplasmic residue of KCNQ, necessitating transport across the lipophilic cell membrane, these differences in percent ionization could significantly influence distribution. Additionally, the implications of ionization within the charged environment of the protein is unknown. To address these questions, modulation of the aminoNB tertiary amine is required.

One of the most common ways medicinal chemists decrease the basicity of alkyl amines is by appending inductively withdrawing functionality. In 2001, Nelson *et. al.* conducted a study on the influence of fluorination on the pK_a of propranolol (**4.114**).²³ The pK_a of the propranolol secondary amine was measured to be 9.53 (Figure 4.26B). When the *N*-isopropyl substituent was sequentially modified with fluorine atoms, the pK_a decreased overall by over 5 orders of magnitude, with each addition of fluorine decreasing the pK_a by 1.72 units on average (**4.115**, -CH₂F, 7.69; **4.116**, -CHF₂, 6.13; **4.117**, -CF₃, 4.37). At pH = 7.4, the change in percent ionization of the compounds with lower pK_a manifests as a larger logD value (increased partitioning in the organic phase).

A. pK_a and %ionization of tertiary amines at physiological pH (7.4)

				
4.110	4.111	4.112	4.113	
pK_a	5.1	7.41	10.08	5.50
%ionization	0.5%	50.6%	99.8%	1.2%

B. pK_a and logD of fluorinated propranolol derivatives

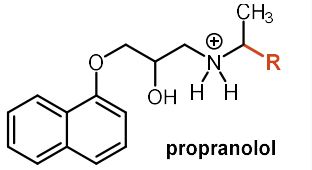
	propranolol	R	pK_a	logD
4.114	-CH ₃	9.53	1.35	
4.115	-CH ₂ F	7.69	2.26	
4.116	-CHF ₂	6.13	4.03	
4.117	-CF ₃	4.37	3.66	

Figure 4.26. (A) pK_a values of protonated tertiary amines and their corresponding %ionization at pH = 7.4; (B) Experimental determination of pK_a and logD (at pH = 7.4) for propranolol derivatives with electron-withdrawing groups

In the case of cyclic amines, Genentech recently reported a Nav1.7 inhibitor scaffold containing a substituted trialkyl piperidine.²⁴ Unsubstituted *N*-methyl piperidine (**4.112**) is nearly completely protonated at physiological pH with a %ionization of 99.8%, and this had a negative impact on potency within this ion channel program. However, γ -CF₃ substitution (**4.113**) decreased

the pK_a to 5.50, dramatically altering the %ionization to only 1.2% and improving potency 5-fold (not shown). We envision that similar structural modifications on the morpholine, or substitution of the morpholine for other cyclic amines with electron withdrawing groups, will result in a favorable decrease in pK_a to better align with the parent aniline functionality. These investigations will take priority in the design of a second-generation library and inform future use of aminoNBs are aniline isosteres in other applications.

4.9 Experimental Procedures and Characterization of Compounds

4.9.1 General Methods

Unless otherwise noted, all reactions were run under a nitrogen or argon atmosphere in flame-dried or oven-dried (150 °C, 24 h) glassware. Reactions were stirred with Teflon-coated magnetic stir bars. Reactions were monitored by thin layer chromatography (TLC) using glass-backed plates pre-coated with 230-400 mesh silica gel (250 μm thickness) with fluorescent indicator F254 (MilliporeSigma Cat. No. 1.05715.0001). Plates were visualized with dual short wave/long wave UV light and/or by treatment with acidic *p*-anisaldehyde stain, KMnO₄ stain, aqueous ceric ammonium molybdate (Hanesian's stain), or phosphomolybdic acid (PMA) stain with gentle heating. Products were purified by manual or automated flash column chromatography over 230-400 mesh silica (SiliCycle Cat No. R12030B) unless otherwise noted using the solvent systems indicated.

All chemicals were used as received unless otherwise noted and stored as recommended by the supplier. Organic solvents (acetonitrile, dichloromethane, diethyl ether, dimethylformamide, dimethyl sulfoxide, methanol, tetrahydrofuran, toluene) and amine bases (triethylamine, pyridine, N,N-diisopropylethylamine, and diisopropylamine) were purified prior to use by the method of Grubbs using a Phoenix Solvent Drying System (available from JC-Meyer Solvent Systems) or PureSolv Micro Amine Drying Column (available from Innovative Technology/Inert) under positive argon pressure. Morpholine and Ti(O^{*i*}Pr)₄ were distilled periodically as needed if reagents discolored.

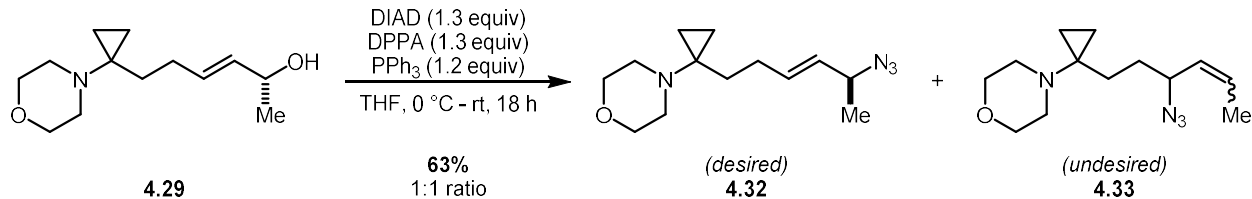
Reactions conducted with microwave irradiation were performed in a Biotage Initiator+ Microwave Synthesizer. NMR spectra were measured on Varian MR400, Varian Inova 500, Varian VNMRS 500, or Varian VNMRS 700 magnetic resonance spectrometers. Deuterated

solvents were obtained from Cambridge Isotopes, Inc. Chemical shifts for ^1H NMR were reported as δ , parts per million, relative to the signal of CHCl_3 at 7.26 ppm or C_6H_6 at 7.16 ppm. Chemical shifts for ^{13}C NMR were reported as δ , parts per million, relative to the center line signal of the CHCl_3 triplet at 77.16 ppm or of the C_6H_6 triplet at 128.06 ppm. Chemical shifts for ^{19}F NMR were uncorrected and reported as δ , parts per million. Abbreviations for chemical shifts are as follows: singlet (s), broad singlet (br s), doublet (d), triplet (t), quartet (q), quintet (quint.), septet (sept.), multiplet (m), apparent (app.). Infrared spectra were recorded on a Thermo-Nicolet IS-50 spectrophotometer and ATR accessory with diamond crystal and are reported in wavenumbers (cm^{-1}). High resolution mass spectra were obtained using an Agilent Q-TOF HPLC-MS using electrospray ionization (ESI) positive or negative ion mode or electron impact (EI). We thank Dr. James Windak and Dr. Paul Lennon at the University of Michigan Department of Chemistry for assisting with these experiments. UPLC/MS data were collected on a Agilent 1290 Infinity II with 6230B TOF LC/MS. Analytical and semi-preparative HPLC/MS were analysis were performed on an Agilent 1260 Infinity II with 6120B Single Quadrapole MS (ESI) equipped with a fraction collector. Preparative HPLC was conducted on an Agilent Preparatory 1290 Infinity II with 6120B Single Quadrapole MS (ESI) equipped with a fraction collector. Dr. Jeff Kampf at the University of Michigan performed single crystal x-ray diffraction experiments and solved the corresponding crystal structures; his assistance and expertise are gratefully acknowledged. Computational analysis and molecular modeling were performed using either Spartan or OpenEye software.

Photochemical reactions were irradiated using 2x 4.4 W blue LED strips (Creative Lighting Solutions, Product Code: [CL-FRS5050-12WP-12V](#)), Kessil Model PR160 456 nm LED light at 100% intensity, or in continuous flow employing a [Uniqsis PhotoSyn Reactor](#) outfitted with 450 nm LEDs. Temperatures were maintained between 20-25 $^\circ\text{C}$ by submerging the reaction in a

jacketed water bath with continuously flowing cold water or at 35 °C by a Westpointe 4" High Velocity Fan.

4.9.2 Synthesis of C7 Analogs and Intermediates

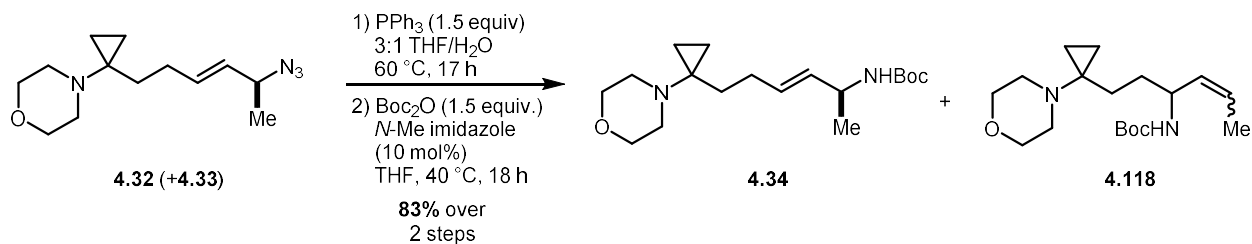


(S,E)-4-(1-(5-azidohex-3-en-1-yl)cyclopropyl)morpholine (**4.32**)

Alcohol **4.29**²⁵ (24.2 mg, 107 μ mol, 1 equiv.) was dissolved in 2.2 mL dry THF and PPh₃ (33.8 mg, 129 μ mol, 1.2 equiv.) was added in one portion. The reaction was cooled to 0 °C in an ice/water bath, and DIAD (28 μ L, 140 μ mol, 1.3 equiv.) was added dropwise down the side of the vial over 15 s. The mixture was stirred at 0 °C for 20 min before DPPA (30 μ L, 140 μ mol, 1.3 equiv.) was added over 15 s. The reaction mixture was warmed to room temperature, wrapped in foil to protect from light, and stirred for 18 h. The reaction was judged complete by TLC analysis and quenched with 1 mL sat. sodium bicarbonate, 1 mL 1 M NaOH, and further diluted with 2 mL diethyl ether. The layers were separated, and the aqueous layer was extracted with 3x 2 mL diethyl ether. The combined organic layers were dried over anhydrous MgSO₄, filtered, and concentrated *in vacuo*. The crude material was purified by flash column chromatography over silica (4-28% EtOAc/hexanes, 4% increments) and the product was concentrated to 17.0 mg (68 μ mol, 63% yield) of a clear, colorless oil that is a 1:1 ratio of desired **4.32** and undesired **4.33** products.

R_f = 0.20 (20% EtOAc/hexanes)

¹H NMR (500 MHz, CDCl₃) δ 5.70 (m, 1H), 5.43 – 5.34 (m, 1H), 3.94 (p, J = 7.0 Hz, 1H), 3.72 (dd, J = 14.2, 7.3 Hz, 1H), 3.61 (dd, J = 9.0, 4.3 Hz, 5H), 2.68 – 2.59 (m, 5H), 2.08 – 2.00 (m, 1H), 1.76 (dd, J = 6.5, 1.6 Hz, 2H), 1.71 (dd, J = 7.0, 1.8 Hz, 1H), 1.65 – 1.59 (m, 1H), 1.59 – 1.55 (m, 1H), 1.54 – 1.44 (m, 2H), 1.24 (d, J = 6.7 Hz, 2H), 0.56 (t, J = 4.9 Hz, 2H), 0.43 (q, J = 4.3 Hz, 1H), 0.41 – 0.37 (m, 1H) ppm



tert-butyl (S,E)-(6-(1-morpholinocyclopropyl)hex-3-en-2-yl)carbamate (4.34)

Allylic azides **4.32** + **4.33** (298 mg, 1.19 mmol, 1 equiv.) was dissolved in 9 mL dry THF and 3 mL HPLC-grade water, and PPh₃ (468 mg, 1.78 mmol, 1.5 equiv.) was added in one portion. The reaction was heated to 60 °C and stirred for 17 h. The reaction mixture was cooled to room temperature, poured into 15 mL 1 M HCl, and further diluted with 15 mL diethyl ether. The layers were separated and the aqueous layer (pH = 1) was basified with 8 mL 6 M NaOH. The aqueous layer (pH = 14) was extracted with 3x 15 mL ethyl acetate, and the combined organic layers were washed with 30 mL brine, dried over anhydrous MgSO₄, filtered, and concentrated *in vacuo*. The crude amine was used without further purification.

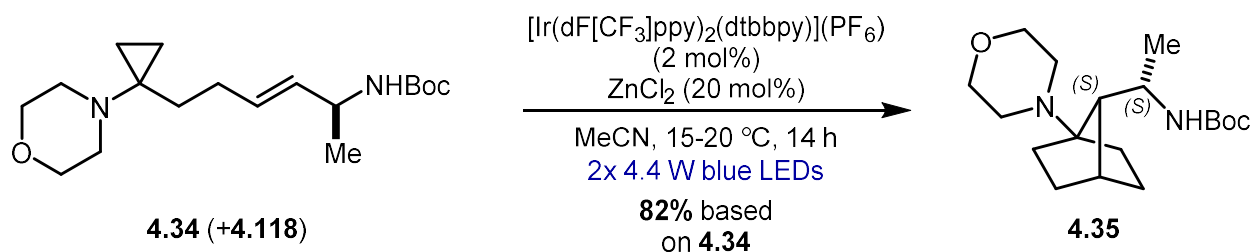
¹H NMR (500 MHz, CDCl₃) δ 5.56 – 5.37 (m, 3H), 5.33 (dd, *J* = 15.2, 7.3 Hz, 1H), 3.62 – 3.57 (m, 8H), 3.47 (q, *J* = 7.0 Hz, 1H), 3.42 (p, *J* = 6.3 Hz, 1H), 3.14 (q, *J* = 6.9 Hz, 1H), 2.66 – 2.62 (m, 8H), 1.98 – 1.92 (m, 2H), 1.67 (d, *J* = 6.4 Hz, 2.5H), 1.64 (dd, *J* = 6.9, 1.1 Hz, 0.5H), 1.62 – 1.56 (m, 2H), 1.55 – 1.50 (m, 2H), 1.37 – 1.30 (m, 2H), 1.12 (d, *J* = 6.4 Hz, 3H), 0.53 (q, *J* = 4.2 Hz, 4H), 0.45 – 0.37 (m, 4H) ppm

The mixture of crude amines (267 mg, 1.19 mmol, 1 equiv.) was dissolved in 10 mL dry THF. *N*-methyl imidazole (9.5 μL, 119 μmol, 10 mol%) and Boc₂O (0.41 mL, 1.79 mmol, 1.5 equiv.) were each added as one portion and the reaction was heated to 40 °C for 18 h. The reaction was cooled to room temperature and 25 mL sat. sodium bicarbonate and 25 mL diethyl ether were added. The layers were separated, and the aqueous layer was extracted with 3x 25 mL diethyl ether. The

combined organic layers were washed with 25 mL brine, dried over anhydrous MgSO₄, filtered, and concentrated *in vacuo*. The crude material was purified by flash column chromatography over silica (20-50% EtOAc/hexanes, 10% increments), and **4.34** and **4.118** were collected as an inseparable mixture and concentrated to 319.3 mg (984 μmol, 83% yield over two steps) of a clear, pale yellow oil.

R_f = 0.50 (50% EtOAc/hexanes)

¹H NMR (500 MHz, CDCl₃) δ 5.62 – 5.49 (m, 2H), 5.35 (ddd, *J* = 21.5, 14.9, 5.9 Hz, 2H), 4.60 (s, 1H), 4.40 (s, 1H), 4.14 (s, 1H), 3.95 (s, 1H), 3.61 (dd, *J* = 8.5, 4.0 Hz, 8H), 2.67 – 2.59 (m, 8H), 1.97 (dd, *J* = 15.8, 7.0 Hz, 2H), 1.71 – 1.66 (m, 2H), 1.61 – 1.54 (m, 2H), 1.44 (s, 18H), 1.18 (d, *J* = 6.7 Hz, 3H), 0.57 – 0.55 (m, 2H), 0.55 – 0.52 (m, 2H), 0.42 (q, *J* = 4.3 Hz, 2H), 0.40 – 0.37 (m, 2H) ppm

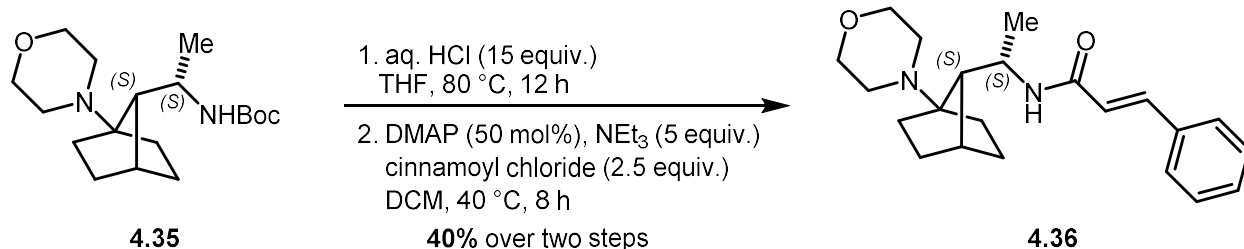


tert-butyl ((1S)-1-((7S)-1-morpholinobicyclo[2.2.1]heptan-7-yl)ethyl)carbamate (4.35)

Two reactions were prepared in parallel on the same scale according to the following procedure: In a dry 2 dram vial under nitrogen, aminoCPs **4.34** + **4.118** (87 mg, 268 μmol , 1 equiv.) were dissolved in 2.75 mL dry MeCN before adding $[\text{Ir}(\text{dF}[\text{CF}_3]\text{ppy})_2(\text{dtbbpy})](\text{PF}_6)$ (6.0 mg, 5.36 μmol , 2 mol%), then ZnCl_2 (54 μL , 1.0 M in ether, 53.4 μmol , 20 mol%) in one portion each. The reaction was degassed with 3x freeze-pump-thaw cycles. The reaction mixture was placed in a jacketed water bath with continuously flowing cold water and irradiated with 2x 4.4 W blue LED strips for 14 h. The two reactions were combined, poured into 13 mL sat. sodium bicarbonate and 2 mL 6 M NaOH, and further diluted with 15 mL diethyl ether. The layers were separated, and the aqueous layer was extracted with 3x 15 mL diethyl ether. The combined organic layers were washed with 15 mL brine, dried over anhydrous MgSO_4 , filtered, and concentrated *in vacuo*. The crude material was purified by flash column chromatography over silica (4-28% EtOAc/hexanes, 4% increments), and aminoNB **4.35** was collected as 71.7 mg (219 μmol , 82% yield based off **4.34**) of a white, crystalline solid. The 7*R*,8*S* diastereomer was not observed.

R_f = 0.40 (30% EtOAc/hexanes)

$^1\text{H NMR}$ (500 MHz, CDCl_3) δ 7.93 (s, 1H), 3.82 – 3.63 (m, 4H), 3.51 – 3.40 (m, 1H), 2.69 – 2.62 (m, 2H), 2.58 (m, 2H), 2.00 – 1.91 (m, 2H), 1.84 (tt, J = 12.4, 3.8 Hz, 1H), 1.67 (ddd, J = 15.0, 11.3, 4.0 Hz, 1H), 1.57 (m, 2H), 1.45 (s, 9H), 1.41 – 1.32 (m, 2H), 1.27 (d, J = 6.1 Hz, 34H), 1.25 – 1.14 (m, 2H) ppm



N-((1S)-1-((7S)-1-morpholinobicyclo[2.2.1]heptan-7-yl)ethyl)cinnamide (4.36)

AminoNB **4.35** (62.4 mg, 192 μ mol, 1 equiv.) was dissolved in 1 mL THF and 0.75 mL water. Concentrated aqueous HCl (0.25 mL, 2.91 mmol, 15 equiv.) was then added dropwise to the reaction mixture over 15 s. The reaction was capped and heated to 80 °C for 12 h. After cooling to room temperature, the mixture was diluted with 2 mL water and 3 mL diethyl ether. The layers were separated, and the aqueous layer washed with 3x 1 mL diethyl ether. The aqueous layer was basified with 2 mL 6 M NaOH, further diluted with 1 mL water, and extracted with 4x 2 mL ethyl acetate. The combined organic layers were dried over anhydrous MgSO₄, filtered, and concentrated *in vacuo*. The crude product was used without further purification.

The crude amine (43.1 mg, 192 μ mol, 1 equiv.) was dissolved in 2 mL dry DCM and NEt₃ (0.13 mL, 960 μ mol, 5 equiv.), DMAP (11.7 mg, 96 μ mol, 50 mol%), and cinnamoyl chloride (80 mg, 480 μ mol, 2.5 equiv.) were each added as one portion. The reaction was then heated to 40 °C and stirred for 8 h. The reaction was quenched with 2 mL sat. sodium bicarbonate and 2 mL 1 M NaOH and further diluted with 2 mL ethyl acetate. The layers were separated, and the aqueous layer was extracted with 3x 2 mL ethyl acetate. The combined organic layers were dried over anhydrous MgSO₄, filtered, and concentrated *in vacuo*. The crude material was purified by flash column chromatography over silica pre-neutralized with 1% NEt₃ (6-36% acetone/DCM%, 6% increments), and final analog **4.36** was collected as 27.3 mg (77.0 μ mol, 40% yield over two steps).

To prepare stock solutions used in biological evaluation, further purification by HPLC (10%

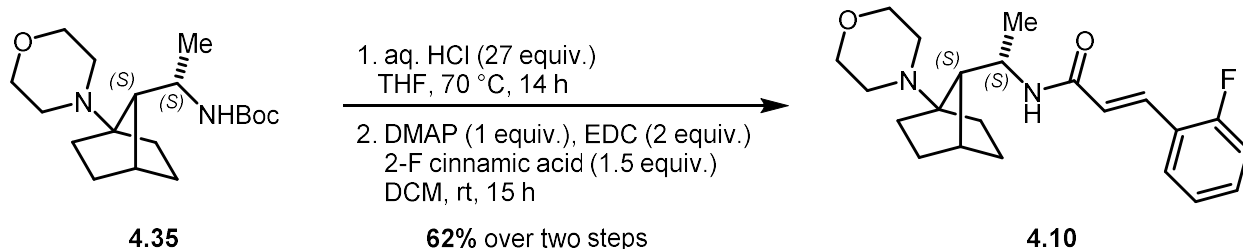
MeCN/water + 0.1% TFA for 5 min, then 10-100% MeCN/water + 0.1% TFA over 30 min) yielded a white powder.

$R_f = 0.20$ (20% acetone/DCM)

$^1\text{H NMR}$ (700 MHz, CDCl_3) δ 9.48 (br s, 1H), 7.61 (d, $J = 15.6$ Hz, 1H), 7.49 (d, $J = 7.4$ Hz, 2H), 7.38 (t, $J = 7.3$ Hz, 2H), 7.34 (t, $J = 7.3$ Hz, 1H), 6.44 (d, $J = 15.6$ Hz, 1H), 3.90 – 3.85 (m, 1H), 3.83 (br s, 4H), 2.79 – 2.73 (m, 2H), 2.67 (br s, 2H), 2.07 – 2.02 (m, 1H), 2.02 – 1.99 (m, 1H), 1.91 (tt, $J = 11.9, 3.7$ Hz, 1H), 1.68 (d, $J = 8.5$ Hz, 1H), 1.67 – 1.58 (m, 3H), 1.46 – 1.39 (m, 2H), 1.36 (d, $J = 6.2$ Hz, 3H), 1.28 – 1.22 (m, 2H) ppm

$^{13}\text{C NMR}$ (176 MHz, CDCl_3) δ 166.72, 139.80, 135.28, 129.57, 129.02, 127.72, 121.89, 73.02, 67.81, 51.46, 48.72, 47.23, 38.26, 32.04, 28.86, 28.59, 24.40, 22.37 ppm

HRMS (ESI+, m/z) calculated for $\text{C}_{22}\text{H}_{31}\text{N}_2\text{O}_2^+$ 355.2380; found 355.2384



(E)-3-(2-fluorophenyl)-N-((1S)-1-((7S)-1-morpholinobicyclo[2.2.1]heptan-7-yl)ethyl)acrylamide (4.10)

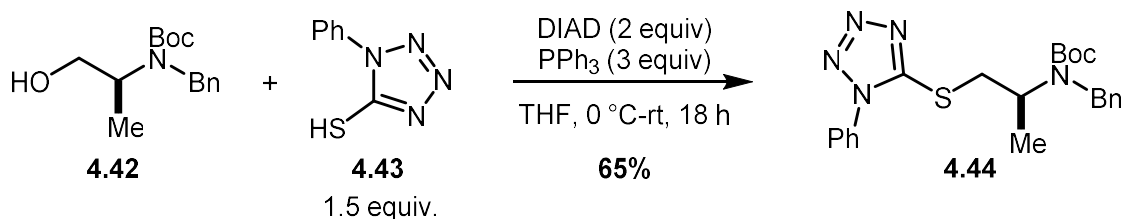
AminoNB **4.35** (71.7 mg, 221 μmol , 1 equiv.) was dissolved in 2 mL THF and 2 mL aqueous 3 M HCl (6 mmol, 27 equiv.). The reaction was capped and heated to 70 °C for 14 h, during which time the reaction significantly darkened in color. After cooling to room temperature, the mixture was diluted with 1 mL water and 5 mL diethyl ether. The layers were separated, and the aqueous layer was basified with 5 mL sat. sodium bicarbonate and 2 mL 6 M NaOH. The aqueous layer (pH ~ 14) was extracted with 3x 5 mL ethyl acetate. The combined organic layers were washed with 5 mL brine, dried over anhydrous MgSO_4 , filtered, and concentrated *in vacuo* to 41.1 mg (183 μmol , 83% yield) of a white powder mixed with a brown oil. The crude product was used without further purification.

The crude amine (10.9 mg, 48.6 μmol , 1 equiv.) was dissolved in 1 mL dry DCM and DMAP (1.2 mg, 9.72 μmol , 20 mol%), 2-fluorocinnamic acid (12.1 mg, 72.9 μmol , 1.5 equiv.), and EDC·HCl (18.6 mg, 97.2 μmol , 2 equiv.) were each added as one portion. The reaction was then stirred at room temperature for 15 h, darkening over time. The reaction was quenched with 2 mL sat. sodium bicarbonate and further diluted with 2 mL ethyl acetate. The layers were separated, and the aqueous layer was extracted with 3x 1 mL ethyl acetate. The combined organic layers were washed with 2 mL brine, dried over anhydrous MgSO_4 , filtered, and concentrated *in vacuo* to a yellow oil. The crude material was purified in combination with a reaction run concurrently on the same scale by

flash column chromatography over silica (25%, then 50% EtOAc/pentane), and final analog **4.10** was collected as 24.8 mg (66.6 μmol , 75% yield, 62% yield over two steps) of a yellow oil that solidified over time.

$R_f = 0.50$ (50% EtOAc/hexanes + 1% NH_4OH)

$^1\text{H NMR}$ (700 MHz, CDCl_3) δ 9.63 (br s, 1H), 7.63 (d, $J = 15.8$ Hz, 1H), 7.46 (t, $J = 7.5$ Hz, 1H), 7.30 (dd, $J = 13.8, 6.8$ Hz, 1H), 7.15 (t, $J = 7.5$ Hz, 1H), 7.09 (dd, $J = 10.9, 8.4$ Hz, 1H), 6.65 (d, $J = 15.9$ Hz, 1H), 3.90 – 3.84 (m, 1H), 3.81 (br s, 4H), 2.80 – 2.71 (m, 2H), 2.66 (br s, 2H), 2.07 – 2.02 (m, 1H), 2.01 (d, $J = 3.3$ Hz, 1H), 1.91 (tt, $J = 12.3, 3.8$ Hz, 1H), 1.67 (d, $J = 8.6$ Hz, 1H), 1.66 – 1.57 (m, 3H), 1.47 – 1.40 (m, 2H), 1.36 (d, $J = 6.2$ Hz, 3H), 1.25 (td, $J = 11.8, 5.4$ Hz, 2H)
ppm



tert-butyl (S)-benzyl(1-((1-phenyl-1H-tetrazol-5-yl)thio)propan-2-yl)carbamate (4.44)

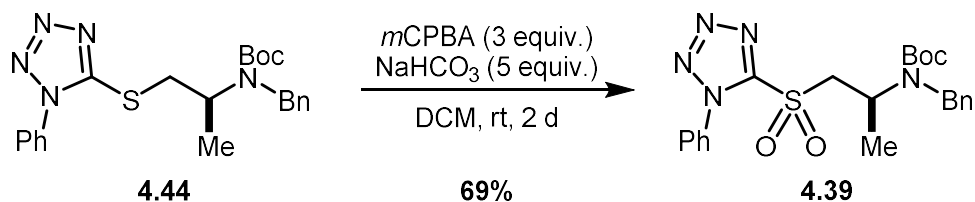
Alcohol²⁶ **4.42** (2.00 g, 7.54 mmol, 1 equiv.) was dissolved in 150 mL dry THF, and tetrazole **4.43** (2.02 g, 11.3 mmol, 1.5 equiv.) and PPh₃ (5.93 g, 22.6 mmol, 3 equiv.) were each added as one portion. The reaction was cooled to 0 °C in an ice/water bath, and DIAD (3.0 mL, 15.1 mmol, 2 equiv.) was added dropwise down the side of the flask over 2.5 min. After the addition was complete, the reaction mixture became heterogeneous (opaque white). The reaction was warmed to room temperature and stirred for 18 h. The reaction was quenched with 75 mL sat. sodium bicarbonate, 75 mL 1 M NaOH, and further diluted with 150 mL diethyl ether. The layers were separated, and the aqueous layer was extracted 3x 150 mL diethyl ether. The combined organic layers were washed with 150 mL brine, dried over anhydrous MgSO₄, filtered, and concentrated *in vacuo* to a light yellow oil. The crude material was purified by flash column chromatography over silica (loading on Celite, eluting with 4-24% EtOAc/hexanes, 4% increments), and **4.44** was collected as 2.32 g (4.92 mmol, 65% yield) of a cloudy, light yellow oil.

$R_f = 0.75$ (40% EtOAc/hexanes)

¹H NMR (500 MHz, C₆D₆, 50 °C) δ 7.24 (d, $J = 7.4$ Hz, 4H), 7.08 (t, $J = 7.5$ Hz, 2H), 7.03 – 6.90 (m, 4H), 4.37 (app. s, 1H), 4.33 – 4.23 (br m, 2H), 3.49 (br m, 2H), 1.36 (s, 9H), 1.07 (br s, 3H) ppm

IR 2974, 2932, 1685, 1597, 1499, 1365, 1240, 1160, 1091, 1013, 760, 731, 694 cm⁻¹

HRMS (ESI+, m/z) calculated for C₂₂H₂₇N₅NaO₂S⁺ 448.1778; found 448.1813



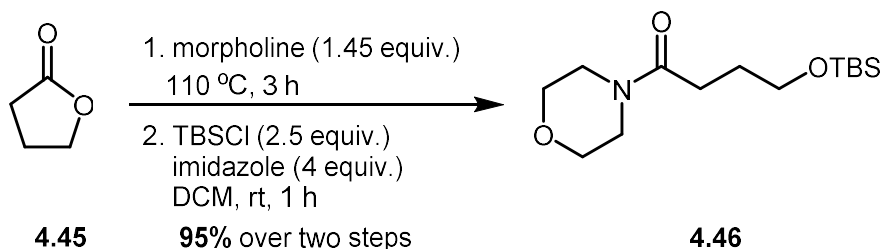
tert-butyl (S)-benzyl(1-((1-phenyl-1H-tetrazol-5-yl)sulfonyl)propan-2-yl)carbamate (4.39)

Sulfide **4.44** (251 mg, 589 μmol , 1 equiv.) was dissolved in 3.8 mL dry DCM, and NaHCO_3 (247 mg, 2.95 mmol, 5 equiv.) and *m*CPBA (436 mg, 1.77 mmol, 3 equiv.) were each added in one portion. The reaction was stirred vigorously at room temperature under an atmosphere of argon. Due to solvent evaporation, at 1 h, an additional 4 mL DCM were added to the heterogeneous mixture. The reaction was stirred 53 h and formed a white gel. The mixture was quenched with 10 mL sat. sodium thiosulfate and 10 mL sat. sodium bicarbonate, and further diluted with 20 mL DCM. The layers were separated, and the aqueous layer was extracted 1x 20 mL DCM. The combined organic layers were washed with 20 mL brine, dried over anhydrous MgSO_4 , filtered, and concentrated *in vacuo*. The crude material was purified by flash column chromatography over silica (eluting with 8-40% EtOAc/hexanes, 8% increments), and sulfone **4.39** was collected as 185.1 mg (405 μmol , 69% yield) of a colorless sticky foam.

$R_f = 0.35$ (20% EtOAc/hexanes)

$^1\text{H NMR}$ (500 MHz, C_6D_6 , 70 $^\circ\text{C}$) δ 7.34 (m, 2H), 7.12 – 6.91 (m, 8H), 4.54 (d, $J = 13.8$ Hz, 1H), 4.30 (br s, 2H), 4.16 (d, $J = 15.6$ Hz, 1H), 3.57 (d, $J = 9.8$ Hz, 1H), 1.36 (s, 9H), 1.06 (d, $J = 6.5$ Hz, 3H) ppm

HRMS (ESI+, m/z) calculated for $\text{C}_{22}\text{H}_{27}\text{N}_5\text{NaO}_4\text{S}^+$ 480.1676; found 480.1673



4-((tert-butyldimethylsilyloxy)-1-morpholinobutan-1-one (4.46)

To a dry flask was added γ -butyrolactone (**4.45**) (0.89 mL, 11.6 mmol, 1 equiv.) and morpholine (1.46 mL, 16.9 mmol, 1.45 equiv.). The flask was fitted with a reflux condenser, and the reaction was heated 100 °C for 3 h.²⁷ After cooling to room temperature, the reaction mixture was diluted with 35 mL dry DCM. Next, imidazole (3.16 g, 46.5 mmol, 4 equiv.) was added, followed by TBSCl (4.38 g, 29.0 mmol, 2.5 equiv.). The flask was capped and stirred at room temperature for 1 h, after which the reaction was judged complete by TLC analysis. The reaction mixture was poured into 100 mL sat. sodium bicarbonate and further diluted with 100 mL DCM. The layers were separated, and the aqueous layer was extracted 3x 100 mL DCM. The combined organic layers were washed with 100 mL brine, dried over anhydrous MgSO_4 , filtered, and concentrated *in vacuo* to a clear, yellow oil. The crude material was purified by flash column chromatography over silica (eluting with 10, 20, 40, 50, 60% EtOAc/hexanes), and silyl ether **4.46** was collected as 3.17 g (3.18 g, 11.0 mmol, 95% yield over two steps) of a clear, light yellow oil.

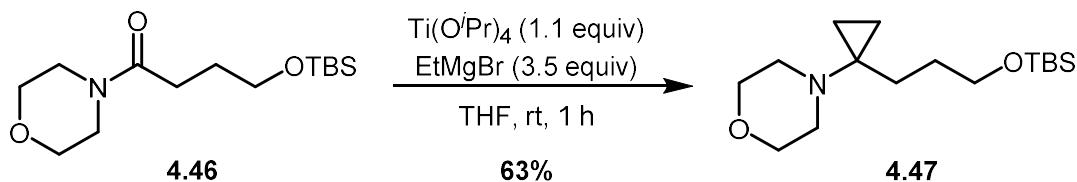
$R_f = 0.45$ (60% EtOAc/hexanes)

$^1\text{H NMR}$ (700 MHz, C_6D_6) δ 3.70 – 3.63 (m, 6H), 3.63 – 3.58 (m, 2H), 3.50 – 3.43 (m, 2H), 2.40 (t, $J = 7.5$ Hz, 2H), 1.87 – 1.81 (m, 2H), 0.88 (s, 9H), 0.04 (d, $J = 1.7$ Hz, 6H) ppm

$^{13}\text{C NMR}$ (176 MHz, CDCl_3) δ 171.78, 67.09, 66.81, 62.25, 46.09, 42.00, 29.35, 28.43, 26.06, 18.43, -5.18 ppm

IR 2954, 2928, 2855, 1645, 1461, 1431, 1253, 1102, 1071, 1033, 959, 834, 774 cm^{-1}

HRMS (ESI+, m/z) calculated for $\text{C}_{14}\text{H}_{29}\text{NNaO}_3\text{Si}^+$ 310.1809; found 310.1809



4-(1-(3-((tert-butyldimethylsilyl)oxy)propyl)cyclopropyl)morpholine (4.47)

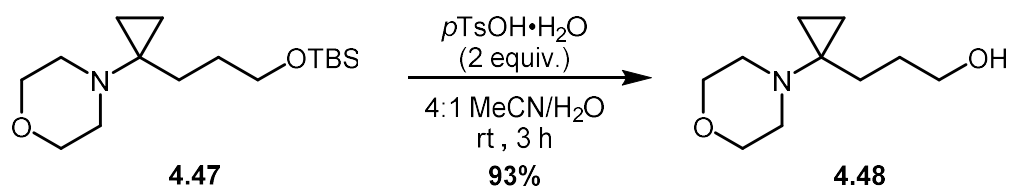
Silyl ether **4.46** (1.03 g, 3.37 mmol, 1 equiv.) was dissolved in 60 mL dry THF, and the flask was submerged in a water bath to serve as a heat sink. $\text{Ti(O}^i\text{Pr)}_4$ (1.10 mL, 3.70 mmol, 1.1 equiv.) was added as one portion, then a vent needle was put in place. EtMgBr (3.9 mL, 3 M in diethyl ether, 11.8 mmol, 3.5 equiv.) was added dropwise down the side of the flask over 3 min, and the vent line was removed. During the addition, the reaction underwent the standard color changes (yellow - yellow/green/brown - brown/red - red black). The reaction was stirred in the water bath for 55 min, after which an aqueous mixture containing 60 mL Rochelle salt, 60 mL sat. sodium bicarbonate, and 10 mL 6 M NaOH was added, and the reaction was stirred vigorously for 10 min. The mixture was further diluted with 60 mL diethyl ether, and the layers were separated. The aqueous layer was extracted 3x 60 mL diethyl ether. The combined organic layers were washed with 60 mL brine, dried over anhydrous MgSO_4 , filtered, and concentrated *in vacuo*. The crude material was purified by flash column chromatography over silica (eluting with 2-10% EtOAc/hexanes, 2% increments), and aminoCP **4.47** was collected as 638.9 mg (2.13 mmol, 63% yield) of a clear, colorless oil.

$R_f = 0.40$ (10% EtOAc/hexanes)

$^1\text{H NMR}$ (500 MHz, CDCl_3) δ 3.64 – 3.59 (m, 4H), 3.56 (t, $J = 6.4$ Hz, 2H), 2.70 – 2.62 (m, 4H), 1.59 – 1.53 (m, 2H), 1.50 – 1.41 (m, 2H), 0.89 (s, 9H), 0.53 (q, $J = 4.1$ Hz, 2H), 0.42 (q, $J = 4.1$ Hz, 2H), 0.04 (s, 6H) ppm

IR 2953, 2929, 2854, 1472, 1462, 1450, 1254, 1116, 1099, 987, 833, 812, 773 cm^{-1}

HRMS (ESI+, m/z) calculated for $\text{C}_{16}\text{H}_{34}\text{NO}_2\text{Si}^+$ 300.2353; found 300.2498



3-(1-morpholinocyclopropyl)propan-1-ol (4.48)

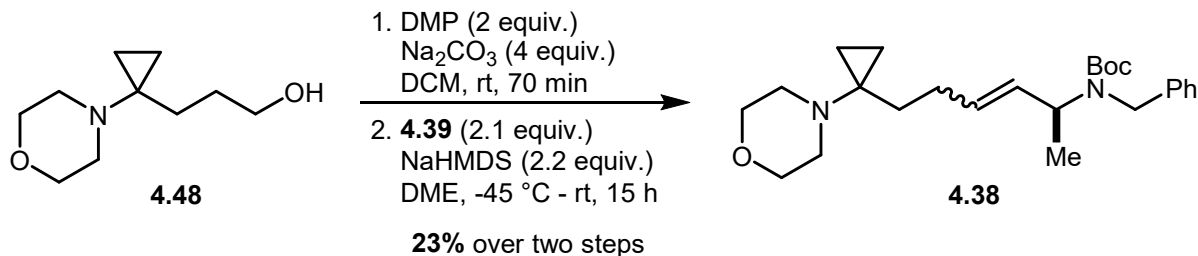
AminoCP **4.47** (1.10 g, 3.67 mmol, 1 equiv.) was dissolved in 28 mL MeCN and 7 mL HPLC-grade water. Next, *p*TsOH·H₂O (1.40 g, 7.34 mmol, 2 equiv.) was added in one portion. The reaction was stirred rapidly at room temperature for 3 h, at which point the reaction was judged complete by TLC analysis. The reaction mixture was poured into 70 mL sat. sodium bicarbonate and further diluted with 70 mL ethyl acetate. The aqueous layer was further basified with 6 M NaOH until pH = 14. The layers were separated, and the aqueous layer was extracted 3x 70 mL ethyl acetate. The combined organic layers were washed with 70 mL brine, dried over anhydrous MgSO₄, filtered, and concentrated *in vacuo*. The crude material was purified by flash column chromatography over silica (eluting isocratic 40% acetone/DCM), and alcohol **4.48** was collected as 630.2 mg (3.40 mmol, 93% yield) of a clear, yellow oil.

R_f = 0.30 (40% acetone/DCM)

¹H NMR (500 MHz, C₆D₆) δ 3.60 – 3.49 (m, 4H), 3.42 (m, 2H), 2.50 (br s, 1H), 2.39 – 2.20 (m, 4H), 1.36 m, 4H), 0.51 (q, *J* = 4.6 Hz, 2H), 0.27 – 0.13 (m, 2H) ppm

IR 3397, 2937, 2854, 1712, 1450, 1264, 1114, 1066, 984, 854, 734 cm⁻¹

HRMS (ESI+, *m/z*) calculated for C₁₀H₂₀NO₂⁺ 186.1489; found 186.1489



tert-butyl (S)-benzyl(6-(1-morpholinocyclopropyl)hex-3-en-2-yl)carbamate (4.38)

Alcohol **4.48** (150 mg, 777 μ mol, 1 equiv.) was dissolved in 6 mL dry DCM. Next, anhydrous Na₂CO₃ (330 mg, 3.11 mmol, 4 equiv.) was added, followed by Dess-Martin periodinane (659 mg, 1.55 mmol, 2 equiv.), each as one portion. The reaction mixture was stirred at room temperature for 70 min, at which point the reaction was heterogeneous and light orange in color. The reaction was quenched with 6 mL sat. sodium thiosulfate and 6 mL 6 M NaOH, and further diluted with 10 mL DCM. The layers were separated, and the aqueous layer was extracted 3x 10 mL DCM. The combined organic layers were washed with 10 mL brine, dried over anhydrous MgSO₄, filtered, and concentrated *in vacuo* to an orange oil with some solids. The crude material was filtered through a plug of Celite, eluting with pentane. The crude aldehyde **4.40** was carefully concentrated to 68.2 mg (372 μ mol, 48% yield) of a clear, orange oil that was used without further purification.

¹H NMR (500 MHz, CDCl₃) δ 9.77 (s, 1H), 3.60 (app s, 4H), 2.51 (m, 4H), 2.44 (t, *J* = 7.1 Hz, 2H), 1.82 (t, *J* = 7.2 Hz, 3H), 0.68 (app s, 2H), 0.37 (app s, 2H) ppm

Sulfone **4.39** (350 mg, 764 μ mol, 2.1 equiv.) was dissolved in 14.5 mL dry DME, and the solution was cooled to -45 °C in a dry ice/MeCN bath. Next, NaHMDS (0.82 mL, 1 M in DME, 820 μ mol, 2.2 equiv.) was added dropwise over 1 min, resulting in a yellow-orange reaction mixture. The reaction was stirred at -45 °C for 1 h. In a separate vial was added aldehyde **4.40** (68.2 mg, 372 μ mol, 1 equiv.) and 0.5 mL dry DME. This room temperature aldehyde solution was transferred

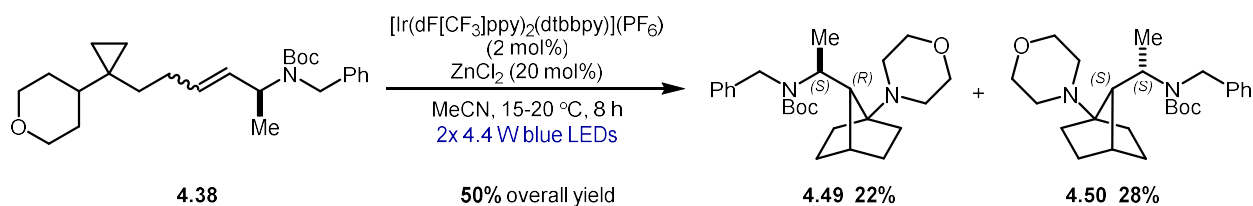
to the ylide. To quantify the transfer, the aldehyde vial was rinsed 3x 0.5 mL dry DME. The reaction was allowed to stir at -45 °C for 5 min, at which point the dry ice/MeCN bath was removed, and the reaction was allowed to warm to room temperature overnight. After 15 h, the reaction was opaque and yellow in color. The reaction was quenched with 10 mL water and 10 mL sat. sodium bicarbonate, and further diluted with 20 mL diethyl ether. The layers were separated, and the aqueous layer was extracted 3x 20 mL diethyl ether. The combined organic layers were washed with 20 mL brine, dried over anhydrous MgSO₄, filtered, and concentrated *in vacuo* to an orange oil. The crude material was purified by flash column chromatography over silica (eluting with 5-30% EtOAc/hexanes), and aminoCP **4.38** was collected as 72.9 mg (176 μmol, 47% yield, 23% over two steps, 1.4:1 olefin isomers) of a clear, colorless semi-solid.

R_f = 0.35 (25% EtOAc/hexanes)

¹H NMR The *cis* and *trans* olefin isomers were collected as a mixture, but the line listings below are reported separately for clarity

Major (700 MHz, C₆D₆, 70 °C) δ 7.27 (d, *J* = 7.3 Hz, 2H), 7.18 (m, *J* = 7.7 Hz, 2H), 7.07 (t, *J* = 7.4 Hz, 1H), 5.53 – 5.39 (m, 1H), 5.37 – 5.30 (m, 1H), 5.08 (br s, 1H), 4.40 – 4.32 (br m, 2H), 3.58 – 3.53 (m, 4H) 2.52 – 2.47 (m, 4H), 2.10 (dd, *J* = 15.6, 7.5 Hz, 2H), 1.53 – 1.46 (m, 2H), 1.41 (s, 9H), 1.15 (d, *J* = 6.9 Hz, 3H), 0.56 (s, 2H), 0.42 – 0.36 (m, 2H) ppm

Minor (700 MHz, C₆D₆, 70 °C) δ 7.27 (d, *J* = 7.3 Hz, 2H), 7.18 (d, *J* = 7.7 Hz, 2H), 7.07 (t, *J* = 7.4 Hz, 1H), 5.53 – 5.39 (m, 2H), 4.81 (br s, 1H), 4.40 – 4.32 (br m, 2H), 3.53 – 3.48 (m, 4H), 2.45 – 2.41 (m, 4H), 1.86 (dd, *J* = 16.1, 6.8 Hz, 2H), 1.43 (s, 9H), 1.41-1.37 (m, 2H), 1.18 (d, *J* = 6.9 Hz, 3H), 0.53 – 0.50 (m, 2H), 0.27 (q, *J* = 4.4 Hz, 2H) ppm



tert-butyl benzyl((S)-1-((1R,4R,7R)-1-morpholinobicyclo[2.2.1]heptan-7yl)ethyl)carbamate (4.49) and tert-butyl benzyl((1S)-1-((7S)-1-morpholinobicyclo[2.2.1]heptan-7yl)ethyl)carbamate (4.50)

In a dry 2 dram vial under nitrogen, aminoCP **4.38** (66.5 mg, 160 μmol , 1 equiv.) was dissolved in 1.5 mL dry MeCN before adding $[\text{Ir}(\text{dF}[\text{CF}_3]\text{ppy})_2(\text{dtbbpy})](\text{PF}_6)$ (3.6 mg, 3.2 μmol , 2 mol%), then ZnCl_2 (32 μL , 1 M in diethyl ether, 32. μmol , 20 mol%) in one portion each. The reaction was degassed with 3x freeze-pump-thaw cycles. The reaction mixture was placed in a jacketed water bath with continuously flowing cold water and irradiated with 2x 4.4 W blue LED strips for 8 h. The reaction was poured into 2 mL sat. sodium bicarbonate and 1 mL 6 M NaOH, and further diluted with 5 mL diethyl ether. The layers were separated, and the aqueous layer was extracted with 3x 5 mL diethyl ether. The combined organic layers were washed with 5 mL brine, dried over anhydrous MgSO_4 , filtered, and concentrated *in vacuo*. The crude material was purified by flash column chromatography over silica (3-15% EtOAc/hexanes, 3% increments). AminoNB **7S-4.50** was collected as 18.5 mg (44.6 μmol , 28% yield) of a colorless, crystalline solid, and aminoNB **7R-4.49** was collected as 14.8 mg (35.7 μmol , 22% yield) of a clear, colorless oil (50% overall yield). Stereochemical assignments were made based on subsequent NMR analysis and by analogy.

$R_f =$

7S, 8S **4.50** 0.40 (15% EtOAc/hexanes)

7R, 8S **4.49** 0.35 (15% EtOAc/hexanes)

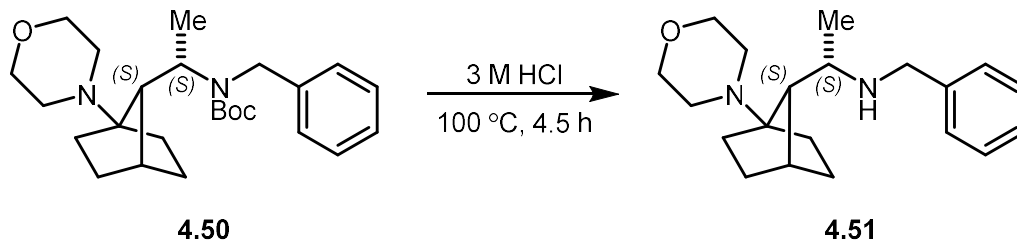
$^1\text{H NMR}$ Not reported due to unresolved rotomers even at elevated temperatures (70 °C in C_6D_6)

¹³C NMR Not reported due to unresolved rotomers even at elevated temperatures (70 °C in C₆D₆)

HRMS

7*S*, 8*S* **4.50** (ESI+, *m/z*) calculated for C₂₅H₃₉N₂O₃⁺ 415.2955; found 415.2960

7*R*, 8*S* **4.49** (ESI+, *m/z*) calculated for C₂₅H₃₉N₂O₃⁺ 415.2955; found 415.2966

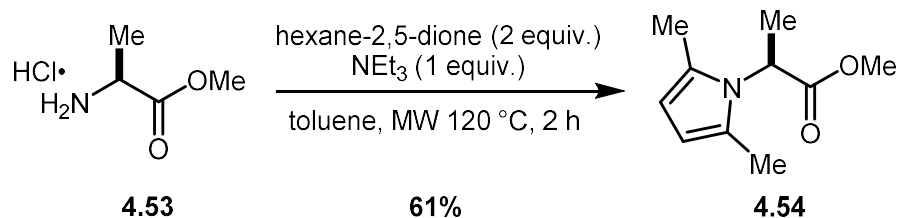


(1S)-N-benzyl-1-((7S)-1-morpholinobicyclo[2.2.1]heptan-7-yl)ethan-1-amine (4.51)

To a vial was added aminoNB **4.50** and aqueous 3 M HCl (150 μ L, 450 mmL). The vial was capped and heated to 100 °C for 4.5 h. After cooling to room temperature, the mixture was carefully basified with 0.15 mL sat. sodium bicarbonate, 0.15 mL 6 M NaOH, and further diluted with 1 mL ethyl acetate. The layers were separated, and the aqueous layer (pH = 14) was extracted 3x 1 mL ethyl acetate. The combined organic layers were washed with 1 mL brine, dried over anhydrous MgSO_4 , filtered, and concentrated *in vacuo* to a white film.

^1H NMR (500 MHz, C_6D_6) δ 7.39 (d, $J = 7.4$ Hz, 2H), 7.22 (t, $J = 7.5$ Hz, 2H), 7.12 (t, $J = 7.4$ Hz, 1H), 3.92 (d, $J = 12.4$ Hz, 1H), 3.49 (d, $J = 12.4$ Hz, 1H), 3.45 (br s, 2H), 3.39 (br s, 2H), 2.75 (dq, $J = 11.9, 6.0$ Hz, 1H), 2.49 (br s, 2H), 2.29 – 2.22 (m, 2H), 1.77 (t, $J = 4.2$ Hz, 1H), 1.72 – 1.63 (m, 1H), 1.58 (m, 2H), 1.38 (m, 2H), 1.27 – 1.21 (m, 1H), 1.15-1.07 (m, 2H), 1.11 (d, $J = 6.0$ Hz, 3H), 0.99 – 0.85 (m, 1H) ppm

^{13}C NMR (176 MHz, C_6D_6) δ 129.07, 128.51, 128.35, 127.13, 72.14, 67.64 – 66.34 (br m), 53.71, 52.99, 52.77, 49.29, 37.26, 32.55, 29.10, 28.28, 23.56, 19.54 ppm

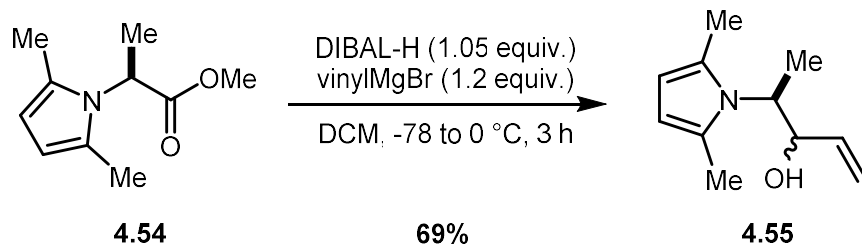


methyl (S)-2-(2,5-dimethyl-1H-pyrrol-1-yl)propanoate (4.54)

L-alanine methyl ester hydrochloride **4.53** (698 mg, 5 mmol, 1 equiv.) was added to a 10-20 mL microwave vial and 20 mL dry toluene was added. Next, NEt₃ (0.70 mL, 5 mmol, 1 equiv.) and hexane-2,5-dione (1.17 mL, 10 mmol, 2 equiv.) were each added as one portion. The reaction mixture was briefly sonicated to dissolve the solids as much as possible, and the vial was capped and the heterogeneous mixture was irradiated in a Biotage Initiator+ microwave reactor for 2 h at 120 °C. After cooling to room temperature, the mixture was a dark red/brown solution with some solids at the bottom of the vial. The mixture was poured into 20 mL sat. sodium bicarbonate and further diluted with diethyl ether. The layers were separated, and the aqueous layer was extracted with 3x 40 mL diethyl ether. The combined organic layers were washed with brine, dried over anhydrous Na₂SO₄, filtered, and concentrated *in vacuo*. The crude material was purified by flash column chromatography over silica (2-20% EtOAc/hexanes), and **4.54** was collected as 555 mg (3.06 mmol, 61% yield) of a light yellow oil. The spectroscopic properties match those reported in the literature.²⁸

R_f = 0.50 (20% EtOAc/hexanes)

¹H NMR (401 MHz, CDCl₃) δ 5.79 (br s, 1H), 4.85 (q, *J* = 7.3 Hz, 1H), 3.75 (s, 3H), 2.18 (s, 6H), 1.64 (d, *J* = 7.3 Hz, 3H) ppm



(4S)-4-(2,5-dimethyl-1H-pyrrol-1-yl)pent-1-en-3-ol (4.55)

Ester **4.54** (428 mg, 2.36 mmol, 1 equiv.) was added to flame-dried flask under dry nitrogen atmosphere, then evacuated and backfilled with dry nitrogen 3x. Next, 20 mL dry DCM was added, and the solution was cooled to -45 °C in a MeCN/dry ice bath. DIBAL-H (2.48 mL, 1 M in hexanes, 2.48 mmol, 1.05 equiv.) was added dropwise down the side of the flask over 5 min. The reaction was stirred at -45 °C for 3 h, then the reaction mixture was warmed to 0 °C in an ice/water bath over 10 min. Vinylmagnesium bromide (4.05 mL, 0.7 M in THF, 1.2 equiv.) was added dropwise down the side of the flask over 2 min, and the resultant yellow solution was warmed to room temperature and stirred overnight. The reaction was quenched slowly with 30 mL sat. ammonium chloride solution and 20 mL sat. Rochelle salt solution. The layers were separated, and the aqueous layer was extracted 2x 100 mL diethyl ether. The combined organic layers were washed with brine, dried over anhydrous Na₂SO₄, filtered, and concentrated *in vacuo*. The crude material was purified by flash column chromatography over silica (4-20% EtOAc/hexanes), affording **4.55** as 291.5 mg (1.63 mmol, 69% yield, 4.2:1 *dr*) of a clear, colorless oil.

R_f=

Major diastereomer 0.22 (20% EtOAc/hexanes)

Minor diastereomer 0.29 (20% EtOAc/hexanes)

¹H NMR

Major diastereomer:

(500 MHz, CDCl₃) δ 5.74 (s, 1H), 5.60 (ddd, J = 16.4, 10.5, 5.6 Hz, 1H), 5.26 (d, J = 17.2 Hz, 1H), 5.09 (d, J = 10.6 Hz, 1H), 4.47 (dt, J = 9.1, 5.0 Hz, 1H), 4.09 (p, J = 7.2 Hz, 1H), 2.26 (s, 3H), 1.75 (d, J = 4.4 Hz, 1H), 1.60 (d, J = 7.1 Hz, 2H) ppm

Minor diastereomer:

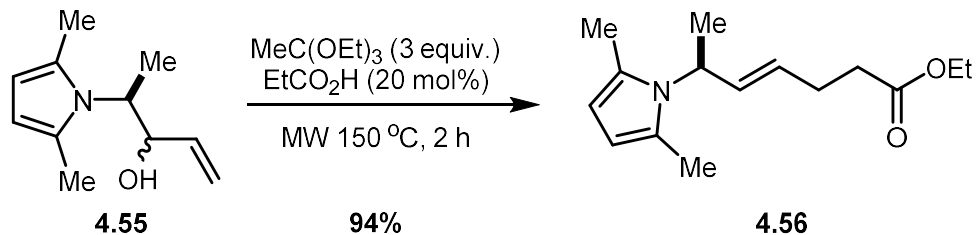
(500 MHz, CDCl₃) δ 5.87 (ddd, J = 17.2, 10.4, 6.9 Hz, 1H), 5.79 (s, 2H), 5.45 (d, J = 17.1 Hz, 1H), 5.31 (d, J = 10.4 Hz, 1H), 4.43 – 4.37 (m, 1H), 4.07 (dq, J = 9.6, 7.2 Hz, 1H), 2.30 (s, 6H), 1.75 (s, 1H), 1.43 (d, J = 7.2 Hz, 3H) ppm

¹³C NMR

Major diastereomer:

(126 MHz, CDCl₃) δ 138.22, 128.25 (br s), 116.07, 106.75 (br s), 75.21, 56.43, 17.12, 14.65 ppm

HRMS (ESI+, *m/z*) calculated for C₁₁H₁₈NO⁺ 180.1383; found 180.1379



ethyl (S,E)-6-(2,5-dimethyl-1H-pyrrol-1-yl)hept-4-enoate (4.56)

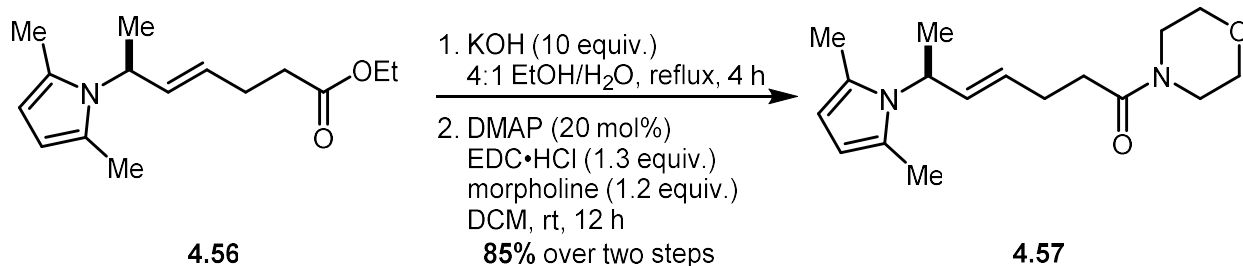
To a 2-5 mL microwave vial under a stream of dry nitrogen was added **4.55** (612 mg, 3.41 mmol, 1 equiv.), triethyl orthoacetate (1.88 mL, 10.2 mmol, 3 equiv.), and propionic acid (51 μL , 683 μmol , 20 mol%), each as one portion. The vial was capped, stirred vigorously for several minutes, then irradiated in a Biotage Initiator+ microwave reactor for 2 h at 150 $^\circ\text{C}$. The reaction mixture was poured into 100 mL sat. sodium bicarbonate solution and further diluted with 100 mL diethyl ether. The layers were separated, and the aqueous layer was extracted 3x 100 mL diethyl ether. The combined organic layers were washed with 100 mL brine, dried over anhydrous MgSO_4 , filtered, and concentrated *in vacuo* to an orange oil. The crude material was purified by automated flash column chromatography over silica (100 g column, eluting 5-10% EtOAc/hexanes over 7 CVs), and **4.56** was collected as 803 mg (3.22 mmol, 94% yield) of a clear, colorless oil.

$R_f = 0.75$ (20% EtOAc/hexanes)

$^1\text{H NMR}$ (500 MHz, CDCl_3) δ 5.76 – 5.68 (m, 3H), 5.43 – 5.33 (m, 1H), 4.82 – 4.74 (m, 1H), 4.12 (q, $J = 7.1$ Hz, 2H), 2.37 (d, $J = 2.8$ Hz, 4H), 2.21 (s, 6H), 1.52 (d, $J = 7.2$ Hz, 3H), 1.25 (t, $J = 7.1$ Hz, 3H) ppm

$^{13}\text{C NMR}$ (126 MHz, CDCl_3) δ 173.06, 132.48, 128.85, 128.00, 106.08, 60.50, 51.68, 33.97, 27.65, 19.72, 14.38, 14.06 ppm

HRMS (ESI+, m/z) calculated for $\text{C}_{15}\text{H}_{24}\text{NO}_2^+$ 250.1802; found 250.1801



(S,E)-6-(2,5-dimethyl-1H-pyrrol-1-yl)-1-morpholinohept-4-en-1-one (4.57)

Ethyl ester **4.56** (803 mg, 3.22 mmol, 1 equiv.) was dissolved in 32 mL EtOH and 8 mL HPLC-grade water, then KOH (1.81 g, 32.2 mmol, 10 equiv.) was added directly as one portion. The flask was fitted with a reflux condenser, and the reaction was heated to 90 °C for 3.5 h. After cooling to room temperature, the mixture was carefully acidified with 50 mL 1 M HCl, at which point the clear, colorless mixture turned pink and continued to darken over time. The aqueous layer (pH = 1) was extracted 4x 50 mL DCM, and the combined organic layers were washed with 50 mL brine, dried over anhydrous Na₂SO₄, filtered, and concentrated *in vacuo* to a dark red oil. The crude carboxylic acid was used without further purification.

R_f = 0.30 (streaky) (60% EtOAc/hexanes)

¹H NMR (700 MHz, CDCl₃) δ 5.75 (m, 3H), 5.39 (dt, J = 14.8, 6.5 Hz, 1H), 4.80 (m, 1H), 2.44 (t, J = 7.3 Hz, 2H), 2.38 (q, J = 6.8 Hz, 2H), 2.21 (s, 6H), 1.53 (d, J = 7.0 Hz, 3H) ppm

The crude acid (713 mg, 3.22 mmol, 1 equiv.) was dissolved in 32 mL dry DCM, then DMAP (78.7 mg, 644 μmol, 20 mol%), morpholine (0.34 mL, 3.87 mmol, 1.2 equiv.), and EDC·HCl (803 mg, 4.19 mmol, 1.3 equiv.) were added sequentially as one portion. The clear, red reaction mixture was stirred at room temperature for 16 h. The reaction was then poured into 50 mL sat. sodium bicarbonate and further diluted with 50 mL DCM. The layers were separated, and the aqueous layer was extracted 3x 50 mL DCM. The combined organic layers were washed with 50 mL brine,

dried over anhydrous MgSO₄, filtered, and concentrated *in vacuo*. The crude material was purified by automated flash column chromatography over silica (100 g column, eluting 4-20% acetone/DCM over 14 CVs), and the product was collected as 793.9 mg (2.73 mmol, 85% yield over two steps) of **4.57** as a clear, slightly yellow oil.

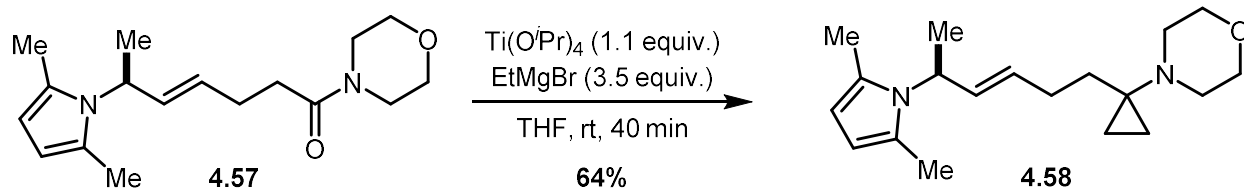
R_f = 0.15 (60% EtOAc/hexanes); 0.75 (30% acetone/DCM)

¹H NMR (500 MHz, CDCl₃) δ 5.73 (m, 3H), 5.44 (dd, J = 15.2, 6.8 Hz, 1H), 4.83 – 4.77 (m, 1H), 3.65 (m, 4H), 3.61 (m, 2H), 3.46 – 3.41 (m, 2H), 2.38 (m, 4H), 2.22 (s, 6H), 1.52 (d, J = 7.1 Hz, 3H) ppm

¹³C NMR (126 MHz, CDCl₃) δ 170.89, 132.28, 129.44, 127.97, 106.08, 67.06, 66.75, 51.73, 46.06, 42.07, 32.56, 27.84, 19.74, 14.09 ppm

IR 2970, 2922, 2855, 1643, 1518, 1431, 1395, 1114, 1020, 968, 747 cm⁻¹

HRMS (ESI+, *m/z*) calculated for C₁₇H₂₇N₂O₂⁺ 291.2067; found 291.2069



(S,E)-4-(1-(5-(2,5-dimethyl-1H-pyrrol-1-yl)hex-3-en-1-yl)cyclopropyl)morpholine (4.58)

Amide **4.57** (205 mg, 706 μ mol, 1 equiv.) was added to a flame-dried flask, and the flask was purged and refilled 3x with dry nitrogen. Next, 12.5 mL dry THF was added, and the flask was submerged in a water bath to serve as a heat sink. Ti(OⁱPr)₄ (0.23 mL, 777 μ mol, 1.1 equiv.) was added as one portion, then a vent needle was put in place. EtMgBr (0.82 mL, 3 M in diethyl ether, 2.47 mmol, 3.5 equiv.) was added dropwise down the side of the flask over 90 s and the vent line was removed. During the addition, the reaction underwent the standard color changes (yellow - yellow/green/brown - brown/red - red black). The reaction was stirred in the water bath for 40 min, after which point a mixture containing 5 mL Rochelle salt, 5 mL sat. sodium bicarbonate, and 5 mL 6 M NaOH was added, and the reaction was stirred vigorously for 5 min. The mixture was further diluted with 15 mL diethyl ether and the layers were separated. The aqueous layer was extracted 3x 15 mL diethyl ether. The combined organic layers were washed with 15 mL brine, dried over anhydrous MgSO₄, filtered, and concentrated *in vacuo*. The crude material was purified by automated flash column chromatography over silica (25 g column, eluting with 5-30% EtOAc/hexanes over 14 CVs), and aminoCP **4.58** was collected as 137.4 mg (454 μ mol, 64% yield) of a clear, colorless oil.

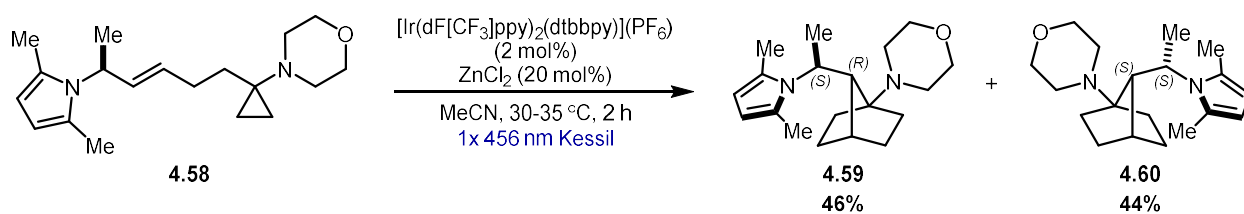
R_f = 0.30 (20% EtOAc/hexanes)

¹H NMR (400 MHz, CDCl₃) δ 5.74 (s, 2H), 5.65 (dd, J = 15.5, 4.3 Hz, 1H), 5.35 (dtd, J = 8.5, 6.7, 1.9 Hz, 1H), 4.92 – 4.70 (m, 1H), 3.68 – 3.52 (m, 4H), 2.71 – 2.50 (m, 4H), 2.22 (s, 6H), 2.00 (dt,

$J = 11.4, 6.8$ Hz, 2H), 1.65 – 1.55 (m, 2H), 1.52 (d, $J = 7.2$ Hz, 3H), 0.54 (q, $J = 4.3$ Hz, 2H), 0.40 (q, $J = 4.3$ Hz, 2H) ppm

$^{13}\text{C NMR}$ (100 MHz, CDCl_3) δ 131.07, 130.80, 128.03, 105.99, 67.84, 51.78, 49.82, 44.04, 30.14, 29.73, 19.80, 14.12, 12.88, 12.84 ppm

HRMS (ESI+, m/z) calculated for $\text{C}_{19}\text{H}_{31}\text{N}_2\text{O}^+$ 303.2431; found 303.2434



4-((7R)-7-((S)-1-(2,5-dimethyl-1H-pyrrol-1-yl)ethyl)bicyclo[2.2.1]heptan-1-yl)morpholine (4.59) and 4-((7S)-7-((S)-1-(2,5-dimethyl-1H-pyrrol-1-yl)ethyl)bicyclo[2.2.1]heptan-1-yl)morpholine (4.60)

In a dry 2 dram vial under nitrogen, aminoCP **4.58** (70.8 mg, 234 μmol , 1 equiv.) was dissolved in 2.8 mL dry MeCN before adding $[\text{Ir}(\text{dF}[\text{CF}_3]\text{ppy})_2(\text{dtbbpy})](\text{PF}_6)$ (5.3 mg, 4.68 μmol , 2 mol%), then ZnCl_2 (47 μL , 1.0 M in ether, 46.8 μmol , 20 mol%) in one portion each. The reaction was degassed with 3 freeze-pump-thaw cycles. The vial was then centered 5 cm away from a Kessil Model PR160 456 nm LED light at 100% intensity and irradiated for 2 hours. The temperature was maintained at 35 °C with a fan placed 5 cm away from the vial for the duration of the reaction. The reaction mixture was added to 20 mL of a solution containing 10 mL sat. sodium bicarbonate, 10 mL water, and 2 mL 6 M NaOH. The aqueous mixture was further diluted with 20 mL ether/hexanes (1:1) and the phases were separated. The aqueous layer was extracted 3x 20 mL with 1:1 diethyl ether/hexanes. The combined organic layers were washed with brine, dried over anhydrous Na_2SO_4 , filtered, and concentrated *in vacuo* to an orange oil. The crude material was purified by flash column chromatography over silica (eluting with 5-70% EtOAc/hexanes). AminoNB **7R-4.59** was collected as 32.7 mg (108 μmol , 46% yield) of a clear, colorless oil, and aminoNB **7S-4.60** was collected as 31.0 mg (102 μmol , 44% yield) of a colorless, crystalline solid (90% overall yield).

R_f =

7S, 8S **4.60** 0.80 (50% EtOAc/hexanes)

7R, 8S **4.59** 0.67 (50% EtOAc/hexanes)

¹H NMR

7R, 8S **4.59** (500 MHz, C₆D₆) δ 6.07 (d, *J* = 3.1 Hz, 1H), 6.00 (d, *J* = 3.2 Hz, 1H), 3.99 (dq, *J* = 10.0, 6.9 Hz, 1H), 3.65 – 3.54 (m, 4H), 2.31 (dt, *J* = 9.2, 4.5 Hz, 2H), 2.27 (s, 3H), 2.26 – 2.21 (m, 2H), 2.11 (s, 3H), 2.05 (d, *J* = 10.0 Hz, 1H), 1.65 (t, *J* = 4.2 Hz), 1.58 (m, 3H), 1.37 (m, 1H), 1.32 (d, *J* = 6.9 Hz, 3H), 1.28 (dd, *J* = 10.9, 3.3 Hz, 1H), 1.11 – 1.02 (m, 2H), 0.98 (td, *J* = 10.5, 9.7, 4.7 Hz, 1H) ppm

7S, 8S **4.60** (500 MHz, C₆D₆) δ 5.95 (d, *J* = 3.1 Hz, 1H), 5.88 (d, *J* = 3.1 Hz, 1H), 3.99 (dt, *J* = 14.9, 7.4 Hz, 1H), 3.48 (s, 4H), 2.34 (s, 3H), 2.24 (s, 3H), 2.21 (m, 4H), 1.82 (br s, 1H), 1.76 (s, 1H), 1.62 – 1.27 (m, 6H), 1.15 (d, *J* = 7.3 Hz, 3H), 1.14 (m, 2H), 0.96 (dt, *J* = 10.5, 5.3 Hz, 1H) ppm

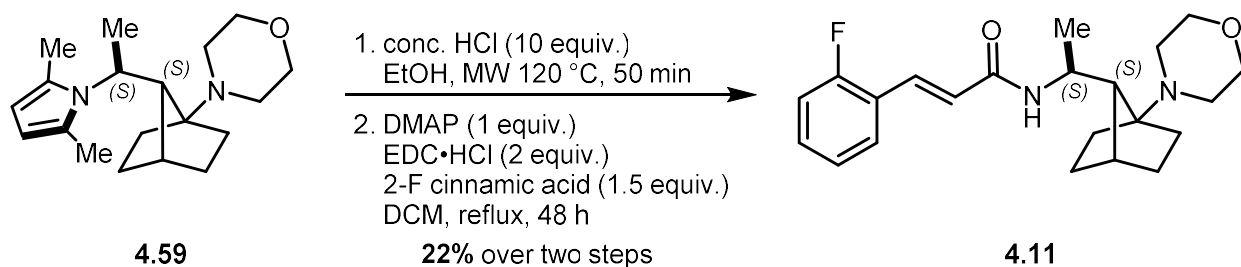
¹³C NMR

7R, 8S **4.59** (126 MHz, C₆D₆) δ 127.60, 126.89, 108.25, 106.08, 71.96, 67.43, 53.58, 50.04, 49.56, 38.21, 33.27, 28.43, 27.84, 23.83, 21.25, 15.63, 13.22 ppm

7S, 8S **4.60** (176 MHz, C₆D₆) δ 129.13, 125.61, 108.65, 105.89, 72.51, 67.43, 52.71, 49.13, 48.24, 37.52, 33.18, 28.64, 28.07, 23.08, 20.13, 15.62, 14.51 ppm

HRMS

7R, 8S **4.59** (ESI+, *m/z*) calculated for C₁₉H₃₁N₂O⁺ 303.2431; found 303.2444



(E)-3-(2-fluorophenyl)-N-((1S)-1-((7S)-1-morpholinobicyclo[2.2.1]heptan-7-yl)ethyl)acrylamide (4.11)

AminoNB **4.59** (20 mg, 66.1 μmol , 1 equiv.) was added to a 0.2-0.5 mL microwave vial and dissolved in 0.9 mL 200 proof EtOH. Next, concentrated HCl (60 μL , 699 μmol , 11 equiv.) was added directly, and the colorless solution immediately turned yellow in color and some white precipitate formed. The vial was capped and irradiated in a Biotage Initiator+ microwave reactor for 50 min at 120 °C. After irradiation, the reaction was bright red and two layers had formed. The reaction mixture was poured into 10 mL 3 M NaOH and 10 mL DCM. The layers were separated, and the aqueous layer (pH = 14) was extracted 3x 10 mL DCM. The combined organic layers were washed with 10 mL brine, dried over anhydrous MgSO_4 , filtered, and concentrated *in vacuo* to a dark magenta oil. The crude amine was used without further purification.

To the crude amine was added 1 mL dry DCM, DMAP (8.1 mg, 66 μmol , 1 equiv.), 2-fluorocinnamic acid (16.4 mg, 99 μmol , 1.5 equiv.), and EDC·HCl (25.3 mg, 132 μmol , 2 equiv.), each as one portion. After the addition of EDC.HCl, the reaction mixture was very dark brown/red in color. The reaction was then heated to 40 °C for 52 h. The reaction mixture was poured into 10 mL sat. sodium bicarbonate and further diluted with 10 mL DCM. The layers were separated, and the aqueous layer was extracted 3x 10 mL DCM. The combined organic layers were washed with 10 mL brine, dried over anhydrous MgSO_4 , filtered, and concentrated *in vacuo* to a dark brown oil. The crude material was purified by automated flash column chromatography over silica pre-

neutralized with 1% NH₄OH (25 g column, eluting with 10-100% EtOAc/hexanes). Final analog **4.11** was collected as 5.5 mg (14.8 μmol, 22% yield over two steps) of a dark brown oil.

R_f = 0.20 (50% EtOAc/hexanes)

¹H NMR (500 MHz, CDCl₃) δ 7.67 (d, *J* = 15.8 Hz, 1H), 7.47 (td, *J* = 7.6, 1.4 Hz, 1H), 7.31 (td, *J* = 7.3, 1.6 Hz, 1H), 7.14 (t, *J* = 7.5 Hz, 1H), 7.08 (dd, *J* = 10.9, 8.4 Hz, 1H), 6.50 (d, *J* = 15.8 Hz, 1H), 5.51 (d, *J* = 9.1 Hz, 1H), 4.26 – 4.14 (m, 1H), 3.68 (t, *J* = 4.3 Hz, 4H), 2.65 – 2.56 (m, 2H), 2.55 – 2.47 (m, 2H), 2.05 (ddd, *J* = 11.9, 8.2, 4.4 Hz, 1H), 2.00 (t, *J* = 4.2 Hz, 1H), 1.85 (tt, *J* = 12.3, 4.0 Hz, 1H), 1.75 (tt, *J* = 12.1, 4.2 Hz, 1H), 1.67 (d, *J* = 10.4 Hz, 1H), 1.62 – 1.50 (m, 1H), 1.39 (d, *J* = 6.5 Hz, 3H), 1.33 (m, 2H), 1.25 (m, 2H) ppm

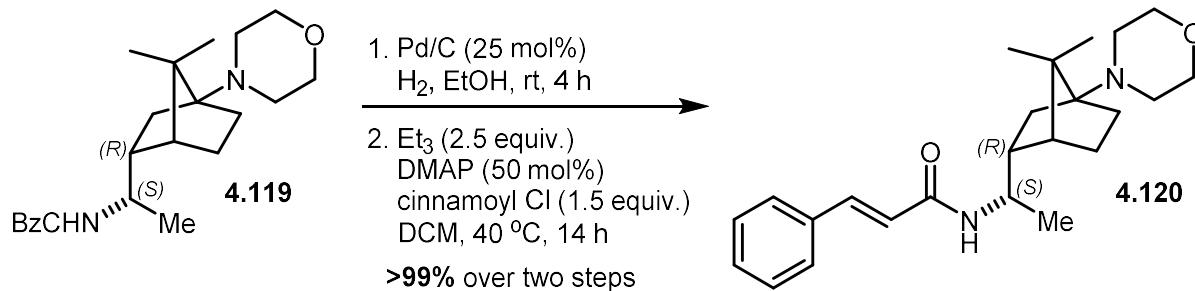
¹³C NMR (176 MHz, CDCl₃) δ 164.50, 161.50 (d, *J* = 252.9 Hz), 134.13, 130.93 (d, *J* = 8.7 Hz), 129.98 (d, *J* = 2.9 Hz), 124.51 (d, *J* = 3.4 Hz), 124.31 (d, *J* = 7.9 Hz), 123.08 (d, *J* = 11.6 Hz), 116.27 (d, *J* = 21.8 Hz), 72.00, 67.51, 54.25, 49.20, 44.70, 37.90, 32.75, 28.27, 27.91, 24.07, 20.84 ppm

¹⁹F NMR (377 MHz, CDCl₃) δ -113.98 – -114.12 (m) ppm

IR 3272.2, 2956.8, 2873.8, 2853.0, 2817.3, 1655.4, 1617.9, 1554.4, 1486.6, 1456.4, 1230.5, 1117.4, 757.8 cm⁻¹

HRMS (ESI+, *m/z*) calculated for C₂₂H₃₀FN₂O₂⁺ 373.2286; found 373.2324

4.9.3 Synthesis of C3-Axial Analogs and Intermediates



N-((S)-1-((1R,2R,4R)-7,7-dimethyl-4-morpholinobicyclo[2.2.1]heptan-2-yl)ethyl)cinnamamide (4.120)

AminoNB **4.119**²⁵ (14.4 mg, 37.3 μ mol, 1 equiv.) was dissolved in 0.76 mL 200-proof EtOH. Pd/C (3.3 mg, 30 wt%, 9.3 μ mol, 25 mol%) was added, and the reaction mixture was sparged with argon for 20 min, before sparging with H₂ (g) for 30 min. The reaction was then stirred under an atmosphere of H₂ (g) at room temperature for 4 h. The mixture was filtered through a plug of Celite, eluting with 5 mL ethyl acetate, and concentrated *in vacuo*. The crude amine was used without further purification.

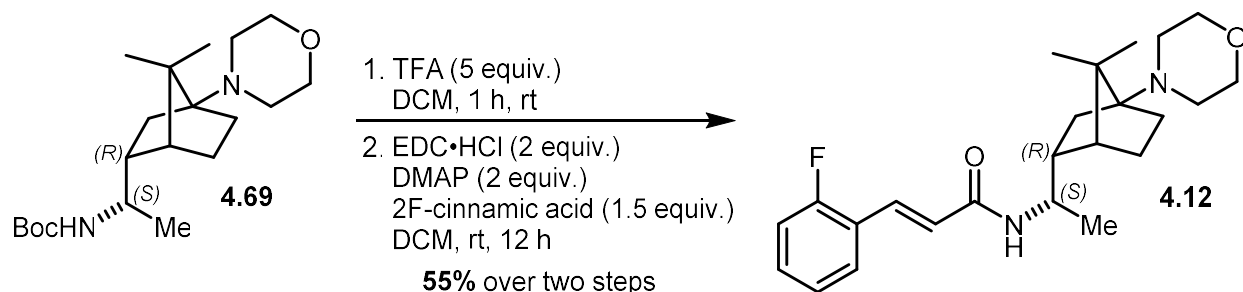
The crude amine (9.4 mg, 37.3 μ mol, 1 equiv.) was dissolved in 0.76 mL dry DCM. Next, NEt₃ (13 μ L, 93.1 μ mol, 2.5 equiv.), DMAP (2.3 mg, 18.6 μ mol, 50 mol%), and cinnamoyl chloride (9.3 mg, 55.9 μ mol, 1.5 equiv.) were each added as on portion. The reaction was heated to 40 °C for 14 h. The reaction was quenched with 4 mL 1:1 sat. sodium bicarbonate/1 M NaOH and further diluted with 2 mL ethyl acetate. The layers were separated, and the aqueous layer was extracted 3x 2 mL ethyl acetate. The combined organic layers were dried over anhydrous MgSO₄, filtered, and concentrated *in vacuo*. The crude material was purified by flash column chromatography over silica pre-neutralized with 1% NEt₃ (eluting 5, 10, 15, 25, 40% acetone/DCM), and final analog **4.120** was collected as 14.3 mg (37.3 μ mol, >99% yield over two steps) of an off-white solid.

R_f = 0.30 (50% acetone/DCM); 0.30 (20% acetone/DCM + 0.2% NEt₃)

¹H NMR (700 MHz, CDCl₃) δ 7.60 (d, *J* = 15.6 Hz, 1H), 7.49 (d, *J* = 6.7 Hz, 2H), 7.39 – 7.32 (m, 3H), 6.33 (d, *J* = 15.6 Hz, 1H), 5.28 (d, *J* = 8.8 Hz, 1H), 4.06 – 3.94 (m, 1H), 3.67 (t, *J* = 4.5 Hz, 4H), 2.55 (d, *J* = 2.5 Hz, 4H), 2.10 – 1.99 (m, 2H), 1.83 (ddd, *J* = 15.8, 10.3, 4.1 Hz, 1H), 1.64 (t, *J* = 6.8 Hz, 2H), 1.42 (s, 1H), 1.38 (dt, *J* = 12.0, 7.3 Hz, 1H), 1.22 (d, *J* = 6.3 Hz, 3H), 1.09 (s, 3H), 1.07 (s, 3H), 1.04 (dd, *J* = 11.6, 4.5 Hz, 1H) ppm

¹³C NMR (176 MHz, CDCl₃) δ 164.88, 141.03, 135.01, 129.74, 128.94, 127.87, 121.03, 70.40, 67.73, 48.81, 48.79, 48.34, 47.68, 43.12, 35.35, 29.55, 22.05, 21.61, 20.99, 20.09 ppm

HRMS (ESI⁺, *m/z*) calculated for C₂₄H₃₅N₂O₂⁺ 383.2693; found 383.2694



(E)-N-((S)-1-((1R,2R,4R)-7,7-dimethyl-4-morpholinobicyclo[2.2.1]heptan-2-yl)ethyl)-3-(2-fluorophenyl)acrylamide (4.12)

AminoNB **4.69**²⁵ (13.4 mg, 38.0 μ mol, 1 equiv.) was dissolved in 0.76 mL dry DCM. TFA (15 μ L, 190 μ mol, 5 equiv.) was added dropwise over 15 s and the reaction was stirred at room temperature for 1 h. Crude ¹H NMR analysis showed incomplete conversion (1:1 **4.69** to amine), and the mixture was resubjected to the above reaction conditions. After stirring for 6 h at room temperature, the reaction was basified with 2 mL 2 M NaOH and further diluted with 2 mL ethyl acetate. The layers were separated, and the aqueous layer was extracted 3x 1 mL ethyl acetate. The combined organic layers were dried over anhydrous MgSO₄, filtered, and concentrated *in vacuo*. The crude amine was used without further purification.

¹H NMR (500 MHz, CDCl₃) δ 3.71 – 3.58 (m, 4H), 2.83 (dq, *J* = 12.1, 6.1 Hz, 1H), 2.59 – 2.46 (m, 4H), 2.01 (td, *J* = 11.8, 3.6 Hz, 1H), 1.87 (m, 2H), 1.71 (t, *J* = 12.6 Hz, 1H), 1.50 (m, 2H), 1.35 – 1.27 (m, 1H), 1.14 (d, *J* = 6.1 Hz, 3H), 1.08 (s, 3H), 1.07 (s, 3H), 0.90 (dd, *J* = 12.0, 4.9 Hz, 1H) ppm

The crude amine (9.6 mg, 38 μ mol, 1 equiv.) was dissolved in 0.76 mL dry DCM. Next, DMAP (9.3 mg, 76 μ mol, 2 equiv.), 2-fluorocinnamic acid (9.5, 76 μ mol, 2 equiv.), and EDC·HCl (14.6 mg, 76 μ mol, 2 equiv.) were added, each as one portion. The reaction was stirred at room temperature for 12 h, then poured into 2 mL 1:1 sat. sodium bicarbonate/1 M NaOH and further

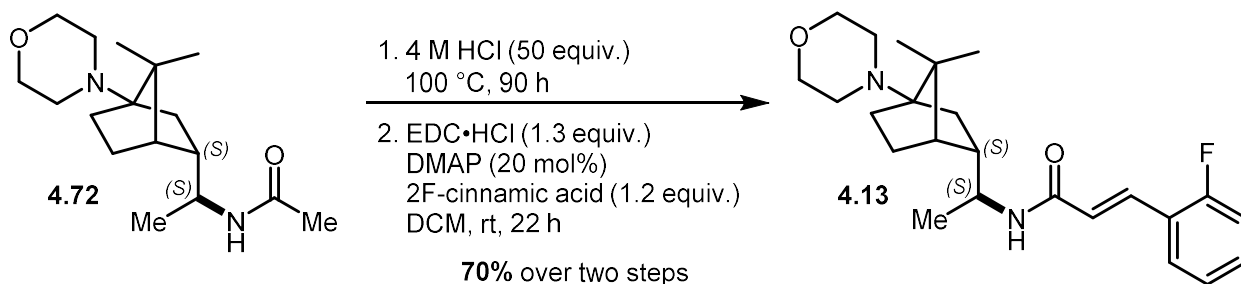
diluted with 2 mL ethyl acetate. The layers were separated, and the aqueous layer was extracted 3x 2 mL ethyl acetate. The combined organic layers were dried over anhydrous MgSO₄, filtered, and concentrated *in vacuo*. The crude material was purified by flash column chromatography over silica pre-neutralized with 1% NEt₃ (20-60% acetone/DCM), and final analog **4.12** was collected as 8.4 mg (21.0 μmol, 55% yield over two steps) of a white solid.

R_f = 0.40 (50% acetone/DCM)

¹H NMR (700 MHz, CDCl₃) δ 7.66 (d, *J* = 15.8 Hz, 1H), 7.47 (td, *J* = 7.6, 1.2 Hz, 1H), 7.31 (dd, *J* = 13.3, 5.9 Hz, 1H), 7.14 (t, *J* = 7.5 Hz, 1H), 7.08 (dd, *J* = 10.7, 8.5 Hz, 1H), 6.48 (d, *J* = 15.8 Hz, 1H), 5.30 (d, *J* = 8.7 Hz, 1H), 4.09 – 3.93 (m, 1H), 3.67 (t, *J* = 4.6 Hz, 4H), 2.55 (d, *J* = 2.6 Hz, 4H), 2.07 (td, *J* = 11.6, 3.8 Hz, 1H), 2.05 – 2.00 (m, 1H), 1.82 (dt, *J* = 11.6, 7.6 Hz, 1H), 1.64 (t, *J* = 7.7 Hz, 2H), 1.43 (s, 1H), 1.38 (dt, *J* = 12.0, 7.7 Hz, 1H), 1.22 (d, *J* = 6.3 Hz, 3H), 1.09 (s, 3H), 1.07 (s, 3H), 1.04 (dd, *J* = 11.6, 4.5 Hz, 1H) ppm

¹³C NMR (176 MHz, CDCl₃) δ 164.80, 161.51 (d, *J* = 253.3 Hz), 134.23, 130.99 (d, *J* = 8.6 Hz), 130.03 (d, *J* = 3.4 Hz), 124.52 (d, *J* = 3.5 Hz), 124.08 (d, *J* = 8.0 Hz), 123.02 (d, *J* = 11.8 Hz), 116.28 (d, *J* = 22.0 Hz), 70.40, 67.73, 48.79, 48.35, 47.74, 43.09, 35.34, 29.56, 28.57, 22.05, 21.61, 20.97, 20.10 ppm

HRMS (ESI+, *m/z*) calculated for C₂₄H₃₄FN₂O₂⁺ 401.2599; found 401.2606



(E)-N-((1S)-1-((1S,2S)-7,7-dimethyl-4-morpholinobicyclo[2.2.1]heptan-2-yl)ethyl)-3-(2-fluorophenyl)acrylamide (4.13)

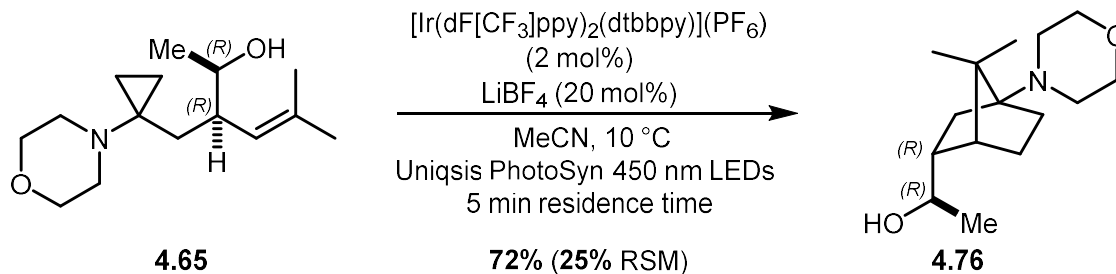
To aminoNB **4.72**²⁵ (9.3 mg, 31.6 μmol , 1 equiv.) was added aqueous 4 M HCl (0.40 mL, 1.60 mmol, 50 equiv.). The reaction was heated to 100 °C for 90 h. After cooling to room temperature, the mixture was diluted with 1 mL water. The aqueous layer was extracted 3x 1 mL ethyl acetate. The combined organic layers were washed with 1 mL brine, dried over anhydrous MgSO_4 , filtered, and concentrated *in vacuo* to a white solid. The crude amine was used without further purification.

The crude amine (6.4 mg, 25.4 μmol , 1 equiv.) was dissolved in 0.5 mL dry DCM. Next, DMAP (0.6 mg, 5.1 μmol , 20 mol%), 2-fluorocinnamic acid (5.1 mg, 30.4 μmol , 1.2 equiv.), and EDC·HCl (6.3 mg, 33.0 μmol , 1.3 equiv.) were added, each as one portion. The reaction was stirred at room temperature for 22 h, then poured into 1 mL sat. sodium bicarbonate and further diluted with 1 mL ethyl acetate. The layers were separated, and the aqueous layer was extracted 3x 1 mL ethyl acetate. The combined organic layers were dried over anhydrous MgSO_4 , filtered, and concentrated *in vacuo*. The crude material was purified by flash column chromatography over silica (20-50% acetone/DCM), and final analog **4.13** was collected as 8.9 mg (22.2 μmol , 88% yield, 70% yield over two steps) of a white solid.

^1H NMR (700 MHz, CDCl_3) δ 7.68 (d, $J = 15.8$ Hz, 1H), 7.48 (t, $J = 7.5$ Hz, 1H), 7.31 (dd, $J = 12.6, 6.6$ Hz, 1H), 7.14 (t, $J = 7.5$ Hz, 1H), 7.09 (dd, $J = 10.3, 8.9$ Hz, 1H), 6.52 (d, $J = 15.8$ Hz, 1H), 5.48 (d, $J = 8.2$ Hz, 1H), 4.15 – 4.01 (m, 1H), 3.64 (s, 4H), 2.51 (s, 4H), 2.01 – 1.90 (m, 2H),

1.83 (t, $J = 12.1$ Hz, 1H), 1.70 (t, $J = 12.8$ Hz, 1H), 1.61 – 1.51 (m, 1H), 1.49 – 1.40 (m, 2H), 1.24 – 1.19 (m, 1H), 1.09 (d, $J = 6.4$ Hz, 3H), 1.08 (s, 6H) ppm

4.9.4 Synthesis of C3-Equatorial Analog Intermediates



(R)-1-((1R,2R,4R)-7,7-dimethyl-4-morpholinobicyclo[2.2.1]heptan-2-yl)ethan-1-ol (4.76)

AminoCP **4.65** (406 mg, 1.6 mmol, 1 equiv.) was transferred using dry MeCN (4 x 5 mL) to a flame-dried 50 mL RBF, cooled under N₂ (g). Next, [Ir(dF[CF₃]ppy)₂(dtbbpy)](PF₆) (36 mg, 32 μmol, 2 mol%) and LiBF₄ (30 mg, 320 μmol, 20 mol%) were added each as one portion. The reaction was degassed with 3x freeze-pump-thaw cycles and kept under inert atmosphere. Using a peristaltic pump, the mixture was irradiated by flowing at 2 mL/min through a 10 mL Uniqsis PhotoSyn photoreactor with 450 nm LEDs. The irradiated reaction loop was cooled to approx. 10 °C. [The reactor loop had previously been purged with 10 mL degassed, dry MeCN under argon atmosphere.] Both reactant flask and the receiving flask were fitted with septa and an argon balloon to maintain inert atmosphere and prevent backpressure.

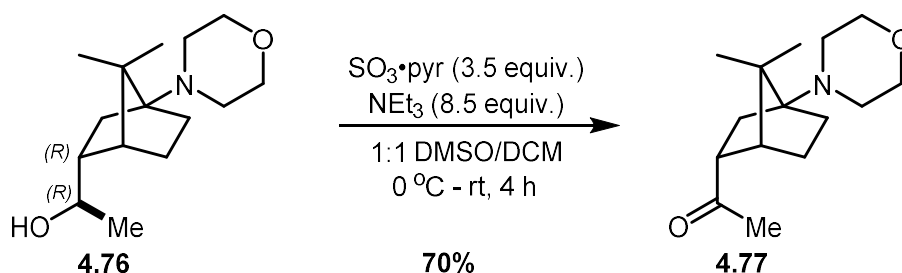
t_R = 5 min; **total time** = 25 min

After the reaction was complete, the reactant flask was rinsed with 5 mL MeCN and flowed through the reactor (no irradiation). The final reaction mixture was quenched with a solution containing 10 mL sat. sodium bicarbonate, 10 mL water, and 1 mL 6 M NaOH. The mixture was further diluted with 40 mL DCM. The layers were separated, and the aqueous layer was extracted 3x 20 mL DCM. The combined organic layers were washed with 20 mL brine, dried over anhydrous MgSO₄, filtered, and concentrated *in vacuo* to a dark red oil. The crude material was purified by flash column chromatography over silica pre-neutralized with 1% NEt₃ (eluting with

20-90% acetone/DCM), and aminoNB **4.76** was collected as 290 mg (1.14 mmol, 72% yield) of a thick, red oil. In addition, 100 mg (395 μ mol, 25%) of aminoCP **4.65** was recovered.

$R_f = 0.50$ (90% acetone/DCM)

$^1\text{H NMR}$ (401 MHz, C_6D_6) δ 3.68 – 3.59 (m, 4H), 3.37 (dq, $J = 9.4, 6.1$ Hz, 1H), 2.40 – 2.34 (m, 3H), 1.96 (td, $J = 11.8, 4.1$ Hz, 1H), 1.77 (ddt, $J = 8.7, 4.3, 1.9$ Hz, 1H), 1.68 (tt, $J = 11.6, 3.6$ Hz, 1H), 1.44 (ttd, $J = 11.8, 4.4, 1.9$ Hz, 1H), 1.25 – 1.05 (m, 4H), 0.98 (d, $J = 6.3$ Hz, 6H), 0.94 (s, 3H) ppm



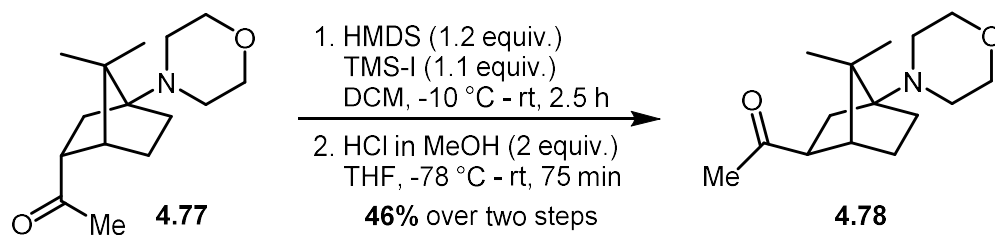
1-((1R,2R,4R)-7,7-dimethyl-4-morpholinobicyclo[2.2.1]heptan-2-yl)ethan-1-one (4.77)

A flame-dried 25 mL flask was charged with norbornyl alcohol **4.76** (290 mg, 1.14 mmol, 1 equiv.), then flushed and sealed under an argon atmosphere. To this flask was added 5 mL dry DCM, followed by NEt_3 (1.4 mL, 9.7 mmol, 8.5 equiv.). This solution was then cooled to 0 °C in an ice/water bath. In a separate flame-dried vial, $\text{Pyr} \cdot \text{SO}_3$ (638 mg, 4.0 mmol, 3.5 equiv.) was dissolved in 5 mL DMSO under an argon atmosphere. This mixture was stirred 15 min at room temperature before being transferred via syringe to the cooled 25 mL flask containing alcohol **4.76**. After addition, the reaction was stirred 30 min at 0 °C, then 3 h at room temp. The reaction was quenched with 20 mL of 10% aqueous sodium thiosulfate. The mixture was extracted with 3x 50 mL ethyl acetate, and the combined organic layers were washed with 3x 100 mL brine, dried over anhydrous MgSO_4 , and concentrated *in vacuo*. The crude residue was purified by flash column chromatography over silica (20-100% EtOAc/hexanes +0.2% NEt_3 , 10% increments) to provide 200 mg (796 μmol , 70%) of ketone **4.77** as a viscous oil.

R_f = 0.30 (50% EtOAc in hexanes)

$^1\text{H NMR}$ (700 MHz, C_6D_6) δ 3.60 (t, J = 4.6 Hz, 4H), 2.56 (dp, J = 11.5, 4.4, 3.7 Hz, 1H), 2.35 (tq, J = 11.3, 6.5, 5.6 Hz, 4H), 2.23 (dd, J = 12.4, 4.8 Hz, 1H), 1.67 (s, 3H), 1.59 (tt, J = 11.3, 2.6 Hz, 1H), 1.52 (td, J = 11.9, 4.1 Hz, 1H), 1.43 – 1.37 (m, 2H), 1.33 (ddd, J = 11.6, 9.6, 4.6 Hz, 1H), 1.02 – 0.97 (m, 1H), 0.91 (s, 3H), 0.89 (s, 3H) ppm

^{13}C NMR (176 MHz, C_6D_6) δ 207.38, 70.40, 67.68, 51.50, 49.81, 49.17, 49.15, 29.50, 28.14, 28.07, 22.13, 21.46, 21.29 ppm



1-((1R,2S,4R)-7,7-dimethyl-4-morpholinobicyclo[2.2.1]heptan-2-yl)ethan-1-one (4.78)

Norbornyl ketone **4.77** (87 mg, 346 μmol , 1 equiv.) was dissolved in 1.5 mL dry DCM. To this, HMDS (87 μL , 415 μmol , 1.2 equiv.) was added in a single portion at room temperature, and the mixture was then cooled to -10 °C. At this temperature, TMS-I (54 μL , 381 μmol , 1.1 equiv.) was added in a single portion via syringe. After stirring 20 minutes at -10 °C, the reaction was warmed to room temperature and stirred 2 hours before diluting with 5 mL diethyl ether and 10 mL water. The layers were separated, and the aqueous layer was extracted 3x 25 mL diethyl ether. The combined organic layers were washed with sat. sodium bicarbonate, brine, and dried over anhydrous Na_2SO_4 . After concentration *in vacuo*, the crude red oil was purified by flash column chromatography over silica (eluting with 20-70% EtOAc/hexanes, 10% increments) to provide 75 mg (232 μmol , mixture of *E:Z* regioisomers, 67% yield) of silyl enol ether as a clear oil.

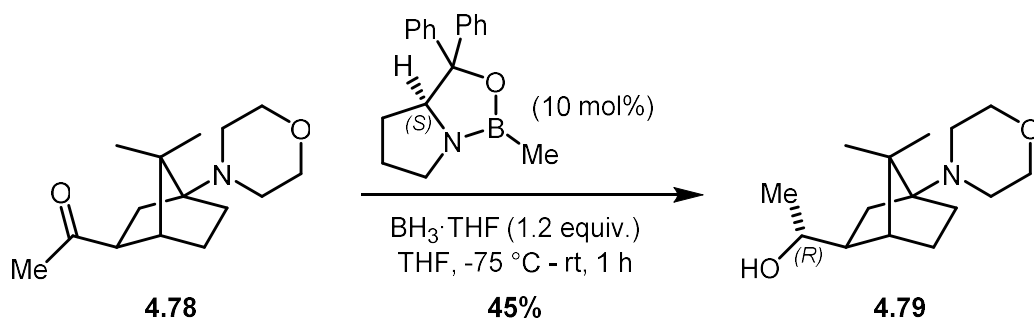
$R_f = 0.6$ (50% EtOAc/hexanes)

The silyl enol ether (75.0 mg, 232 μmol , 1 equiv.) was dissolved in 3.5 mL dry THF. The solution was cooled to -78 °C in a dry ice/acetone bath, and HCl in MeOH (0.93 mL, 0.5 M in MeOH, 464 μmol , 2 equiv.) was added as a single portion. The mixture was stirred at -78 °C for 1 h before warming to -45 °C (dry ice/MeCN) and stirring for 15 min. Full consumption of the silyl ether was determined by TLC analysis, and the reaction was quenched at -45 °C with 2 mL water and 5 mL sat. sodium bicarbonate. The mixture was warmed to room temperature, and 20 mL diethyl ether was added. The layers were separated, and the aqueous layer was extracted 2x 20 mL diethyl ether.

The combined organic layers were washed with brine, dried over anhydrous Na₂SO₄, filtered, and concentrated *in vacuo*. The crude material was purified by flash column chromatography over silica (eluting 5, 10, 20, 30, 40% EtOAc/hexanes), and ketone **4.78** was collected as 40 mg (159 μmol, 69% yield) of a clear oil.

¹H NMR (500 MHz, C₆D₆) δ 3.68 – 3.49 (m, 4H), 2.37 (dd, *J* = 5.7, 3.5 Hz, 4H), 2.35 – 2.32 (m, 1H), 1.81 (d, *J* = 3.9 Hz, 1H), 1.77 (s, 3H), 1.74 (dd, *J* = 9.8, 6.2 Hz, 1H), 1.66 – 1.60 (m, 2H), 1.28 (dd, *J* = 12.2, 10.0 Hz, 1H), 1.11 (dd, *J* = 6.3, 2.9 Hz, 1H), 0.93 (m, 1H), 0.48 (s, 1H), 0.79 (s, 1H) ppm

HRMS (ESI⁺, *m/z*) calculated for C₁₅H₂₆NO₂⁺ 252.1958; found 252.1967



(R)-1-((1R,2S,4R)-7,7-dimethyl-4-morpholinobicyclo[2.2.1]heptan-2-yl)ethan-1-ol (4.79)

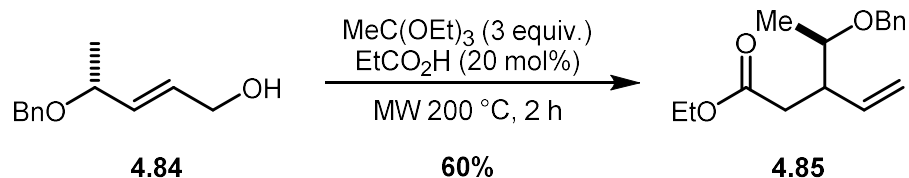
In a flame-dried vial, (*S*)-2-methyl-CBS-oxazaborolidine (1.1 mg, 4.0 μmol , 10 mol%) was dissolved in 1 mL dry THF. $\text{BH}_3 \cdot \text{THF}$ (48 μL , 1.0 M solution in THF, 47.7 μmol , 1.2 equiv.) was added, and the mixture was stirred for 15 min at room temperature. The solution was then cooled to $-78\text{ }^\circ\text{C}$, and a solution of norbornyl ketone **4.78** (10 mg, 39.8 μmol , 1.0 equiv.) in 1 mL dry THF was slowly added dropwise. After the addition was complete, the mixture was warmed to room temperature. After 1 hour of stirring at room temperature, the reaction was quenched by slow addition of 1 mL MeOH, followed by 10 mL sat. sodium bicarbonate. This mixture was then extracted 3x 10 mL ethyl acetate. The combined organic layers were washed with brine, dried over anhydrous MgSO_4 , and concentrated *in vacuo*. The crude material was purified by flash column chromatography on silica (1-10% of [10% NH_4OH in MeOH] in DCM) to provide **4.79** as 4.5 mg (17.8 μmol , 45% yield) of a single diastereomer.

$R_f = 0.11$ (50% EtOAc in hexanes)

$^1\text{H NMR}$ (700 MHz, C_6D_6) δ 3.63 (t, $J = 4.6$ Hz, 4H), 3.54 (dq, $J = 11.7, 6.0, 5.4$ Hz, 1H), 2.35 (td, $J = 4.2, 1.9$ Hz, 4H), 1.78 – 1.71 (m, 1H), 1.69 – 1.61 (m, 2H), 1.33 – 1.28 (m, 2H), 1.24 (td, $J = 9.9, 6.6$ Hz, 1H), 1.18 (ddd, $J = 12.1, 9.6, 4.9$ Hz, 1H), 1.05 (ddd, $J = 12.5, 9.5, 3.3$ Hz, 1H), 0.96 (d, $J = 6.0$ Hz, 3H), 0.95 (s, 3H), 0.94 (s, 3H) ppm

$^{13}\text{C NMR}$ (176 MHz, C_6D_6) δ 71.19, 70.60, 67.80, 52.06, 49.34, 47.70, 47.03, 33.03, 29.61, 28.81, 23.28, 23.07, 22.33 ppm

4.9.5 Synthesis of C3-Axial, C7-Methylene Analog Intermediates

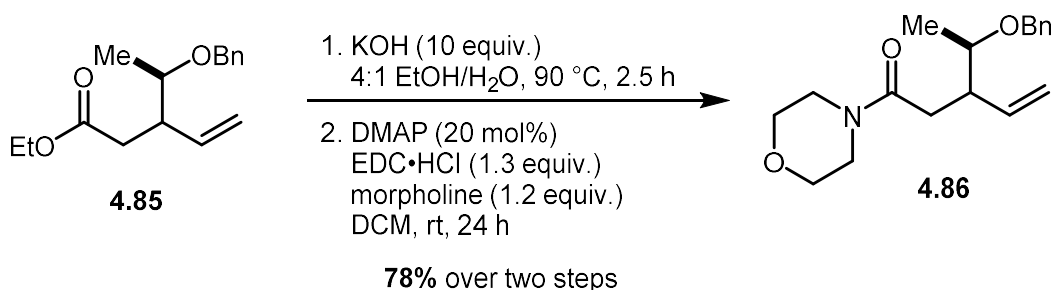


ethyl 3-((R)-1-(benzyloxy)ethyl)pent-4-enoate (4.85)

Alcohol **4.84**²⁹ (422 mg, 2.19 mmol, 1 equiv.) was transferred to a 0.5-2 mL microwave vial. Next, triethyl orthoacetate (1.2 mL, 6.58 mmol, 3 equiv.) was added, followed by propionic acid (33 μ L, 439 μ mol, 20 mol%). The microwave vial was flushed with dry N₂ (g), capped, and stirred vigorously for several minutes. The reaction was then irradiated in a Biotage Initiator+ microwave reactor for 2 h at 200 °C. The reaction mixture was poured into 20 mL sat. aqueous sodium bicarbonate and further diluted with 20 mL diethyl ether. The layers were separated, and the aqueous layer was extracted 3x 20 mL diethyl ether. The combined organic layers were washed with 25 mL brine, dried over anhydrous MgSO₄, filtered, and concentrated *in vacuo*. The crude material was purified by automated flash column chromatography over silica (eluting with 1-15% EtOAc/hexanes over 12 CVs). The product was collected as 303.3 mg (1.29 mmol, 59% yield, 1:1.3 *dr*) of a clear, colorless oil.

R_f = 0.40 (10% EtOAc/hexanes)

¹H NMR (500 MHz, CDCl₃) δ 7.33 (m, 8H), 7.31 – 7.26 (m, 2H), 5.84 – 5.59 (m, 2H), 5.10 (dd, J = 17.4, 8.4 Hz, 4H), 4.57 (d, J = 12.2 Hz, 2H), 4.46 (d, J = 10.6 Hz, 2H), 4.16 – 4.01 (m, 4H), 3.64 – 3.55 (m, 1H), 3.44 (p, J = 6.3 Hz, 1H), 2.85 – 2.77 (m, 1H), 2.74 (dd, J = 14.2, 7.2 Hz, 1H), 2.64 (dd, J = 15.0, 5.0 Hz, 1H), 2.58 (dd, J = 15.2, 5.1 Hz, 1H), 2.40 (dd, J = 15.7, 8.7 Hz, 1H), 2.32 (dd, J = 15.0, 8.8 Hz, 1H), 1.27 – 1.08 (m, 12H) ppm



3-((R)-1-(benzyloxy)ethyl)-1-morpholinopent-4-en-1-one (4.86)

Ethyl ester **4.85** (120 mg, 457 μ mol, 1 equiv.) was dissolved in 6 mL EtOH, then 1.5 mL HPLC-grade water was added. KOH (257 mg, 4.57 mmol, 10 equiv.) was added as one portion, and the flask was fitted with a reflux condenser. The reaction was heated to 90 °C for 2.5 h. After cooling to room temperature, the reaction mixture was poured into 10 mL 1 M HCl. The aqueous layer (pH = 1) was extracted 3x 10 mL DCM. The combined organic layers were washed with 10 mL brine, dried over anhydrous Na₂SO₄, filtered, and concentrated *in vacuo* to a clear, yellow oil. The crude carboxylic acid was used without further purification.

¹H NMR (500 MHz, CDCl₃) δ 10.63 (br s, 2H), 7.37 – 7.31 (m, 8H), 7.31 – 7.26 (m, 2H), 5.84 – 5.63 (m, 2H), 5.21 – 5.07 (m, 4H), 4.62 (d, *J* = 11.6 Hz, 1H), 4.58 (d, *J* = 11.8 Hz, 1H), 4.47 (d, *J* = 11.8 Hz, 1H), 4.44 (d, *J* = 11.6 Hz, 1H), 3.63 (qd, *J* = 6.3, 3.6 Hz, 1H), 3.45 (p, *J* = 6.3 Hz, 1H), 2.86 – 2.76 (m, 1H), 2.75 – 2.68 (m, 1H), 2.69 (dd, *J* = 10.8, 4.2 Hz, 1H), 2.67 (d, *J* = 5.6 Hz, 1H), 2.64 (d, *J* = 5.7 Hz, 1H), 2.44 (dd, *J* = 15.6, 8.5 Hz, 1H), 2.42 – 2.34 (m, 1H), 1.19 (d, *J* = 6.1 Hz, 3H), 1.14 (d, *J* = 6.3 Hz, 3H) ppm

HRMS (ESI-, *m/z*) calculated for C₁₄H₁₇O₃⁻ 233.1183; found 233.1180

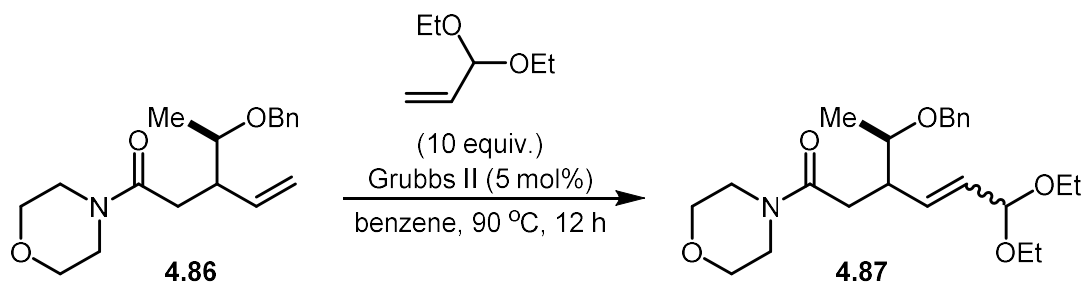
The crude carboxylic acid (107 mg, 457 μ mol, 1 equiv.) was dissolved in 4 mL dry DCM, then DMAP (11.2 mg, 91.3 μ L, 20 mol%), morpholine (48 μ L, 548 μ mol, 1.2 equiv.), and EDC·HCl (114 mg, 594 μ mol, 1.3 equiv.) were each added as one portion. The vial was flushed with argon

and stirred at room temperature for 24 h. The reaction was poured into 10 mL sat. sodium bicarbonate and further diluted with 10 mL DCM. The layers were separated, and the aqueous layer was extracted 3x 10 mL DCM. The combined organic layers were washed with 10 mL brine, dried over anhydrous MgSO₄, filtered, and concentrated *in vacuo*. The crude material was purified by automated flash column chromatography over silica (50 g column, eluting 40-80% EtOAc/hexanes), and amide **4.86** was collected as 354.8 mg (356 μmol, 78% yield over two steps, 1:1.3 *dr*) of a clear, light yellow oil.

R_f = 0.30 (60% EtOAc/hexanes)

¹H NMR (500 MHz, CDCl₃) δ 7.36 – 7.30 (m, 8H), 7.30 – 7.27 (m, 2H), 5.78 (ddd, *J* = 25.0, 14.3, 8.4 Hz, 2H), 5.18 – 5.03 (m, 4H), 4.61 (dd, *J* = 11.8, 7.0 Hz, 2H), 4.42 (t, *J* = 11.6 Hz, 2H), 3.69 – 3.48 (m, 14H), 3.43 (dt, *J* = 10.1, 5.0 Hz, 4H), 2.83 (dt, *J* = 11.5, 8.5 Hz, 1H), 2.76 – 2.68 (m, 1H), 2.65 (dd, *J* = 14.8, 4.5 Hz, 1H), 2.56 (dd, *J* = 15.2, 5.7 Hz, 1H), 2.36 (ddd, *J* = 14.6, 12.8, 8.5 Hz, 2H), 1.19 (d, *J* = 6.2 Hz, 3H), 1.16 (d, *J* = 6.3 Hz, 3H) ppm

HRMS (ESI+, *m/z*) calculated for C₁₈H₂₅NNaO₃⁺ 326.1727; found 326.1727

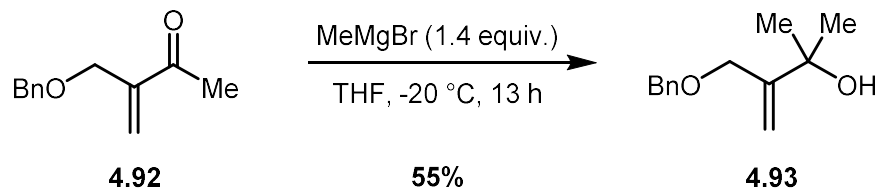


3-((R)-1-(benzyloxy)ethyl)-6,6-diethoxy-1-morpholinohex-4-en-1-one (4.87)

An oven-dried 1 dram vial with a stir bar was cooled under a stream of dry N₂ (g). Amide **4.86** (12 mg, 39.6 μmol, 1 equiv.) was added, followed by acrolein diethyl acetal (60 μL, 396 μmol, 10 equiv.). Next, 160 μL of benzene, then Grubbs II catalyst (1.6 mg, 2 μmol, 5 mol%) were added, resulting in a light pink mixture. The vial was flushed with argon, capped, and heated to 90 °C for 18 h. After cooling to room temperature, the reaction was black in color. A 10 mL aliquot was removed for UPLC/MS analysis. The remaining reaction mixture was concentrated *in vacuo*, and the crude material was purified by flash column chromatography over silica pre-neutralized with 0.1% NH₄OH (eluting with 5, 10, 15, 20% acetone/DCM) and the product was collected as a clear, light brown oil.

HRMS (ESI⁺, *m/z*) calculated for C₂₃H₃₅NNaO₅⁺ 428.2407; found 428.2413

4.9.6 Synthesis of C4 Analog and Intermediates



3-((benzyloxy)methyl)-2-methylbut-3-en-2-ol (4.93)

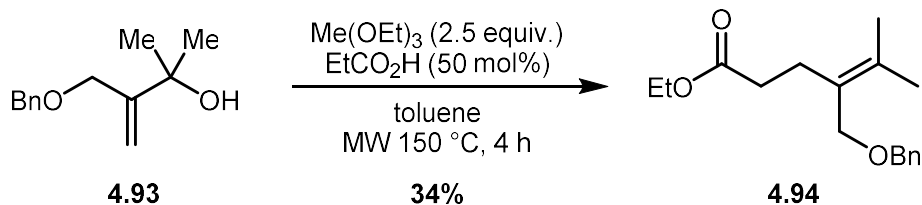
Ketone **4.92**¹⁸ (3.04 g, 16 mmol, 1 equiv.) was dissolved in 2 mL dry THF and concentrated to dryness under a stream of nitrogen three times to remove any residual water. Next, 9.6 mL dry THF was added, and the reaction mixture was cooled to -20 °C. MeMgBr (7.3 mL, 3 M in diethyl ether, 21.8 mmol, 1.4 equiv.) was added dropwise down the side of the flask over 9 min. The reaction was slowly allowed to warm to room temperature and stirred for 13 h. The reaction was quenched with 200 mL 1:1 Rochelle salt/sat. sodium bicarbonate and further diluted with 200 mL diethyl ether. The layers were separated, and the aqueous layer was extracted 3x 200 mL diethyl ether. The combined organic layers were dried over anhydrous Na₂SO₄, filtered, and concentrated *in vacuo*. The crude material was purified by flash column chromatography over silica pre-neutralized with 1% NEt₃ (eluting isocratic 25% EtOAc/hexanes), and alcohol **4.93** was collected as 1.78 g (8.63 mmol, 55% yield) of a clear, colorless liquid.

$R_f = 0.45$ (30% EtOAc/hexanes)

¹H NMR (400 MHz, CDCl₃) δ 7.39 – 7.32 (m, 4H), 7.30 (m, 1H), 5.20 (s, 1H), 5.11 (s, 1H), 4.55 (s, 2H), 4.19 (s, 2H), 1.39 (s, 6H) ppm

¹³C NMR (126 MHz, CDCl₃) δ 151.14, 137.90, 128.61, 127.96, 127.94, 112.29, 72.71, 72.59, 72.18, 29.79 ppm

IR 3423, 2975, 2858, 1496, 1453, 1367, 1161, 1087, 1071, 1027, 911, 868, 734, 696 cm⁻¹

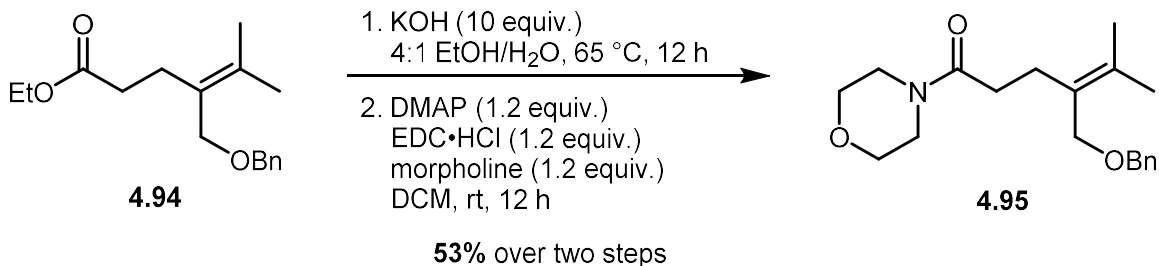


ethyl 4-((benzyloxy)methyl)-5-methylhex-4-enoate (4.94)

In an oven-dried microwave vial, allylic alcohol **4.93** (890 mg, 4.3 mmol, 1 equiv.) was dissolved in 2.2 mL dry toluene. Triethyl orthoacetate (2.0 mL, 10.8 mmol, 2.5 equiv.) and propionic acid (161 μL , 2.2 mmol, 50 mol%) were each added as one portion. The vial was then flushed with argon, capped, and irradiated in a Biotage Initiator+ microwave reactor for 4 h at 150 °C. The reaction mixture was poured into 100 mL sat. sodium bicarbonate, then diluted with 75 mL diethyl ether. The layers were separated, and the aqueous layer was extracted 3x 75 mL diethyl ether. The combined organic layers were dried over anhydrous Na_2SO_4 , filtered, and concentrated *in vacuo*. The crude material was purified by flash chromatography over silica pre-neutralized with 1% NEt_3 (eluting 2-14% diethyl ether/hexanes), and ethyl ester **4.94** was isolated as 401 mg (1.45 mmol, 34% yield) of a clear, colorless oil.

R_f = 0.30 (10% diethyl ether/hexanes)

$^1\text{H NMR}$ (500 MHz, CDCl_3) δ 7.40 – 7.31 (m, 4H), 7.29 (m, 1H), 4.47 (s, 2H), 4.11 (q, J = 7.1 Hz, 2H), 4.00 (s, 2H), 2.56 – 2.43 (m, 2H), 2.43 – 2.34 (m, 2H), 1.73 (s, 3H), 1.70 (s, 3H), 1.25 (t, J = 7.1 Hz, 3H) ppm



4-((benzyloxy)methyl)-5-methyl-1-morpholinohex-4-en-1-one (4.95)

Ethyl ester **4.94** (374 mg, 1.35 mmol, 1 equiv.) was dissolved in 5.4 mL 200 proof EtOH. In a separate flask was added KOH (759 mg, 13.5 mmol, 10 equiv.) and 1.4 mL HPLC-grade water. The KOH solution was added in one portion to the reaction flask containing the ester. The flask was fitted with a reflux condenser, and the reaction was heated to 65 °C overnight. After cooling to room temperature, the reaction was diluted with 30 mL water and 20 mL diethyl ether. The layers were separated, and the aqueous layer was extracted 3x 20 mL diethyl ether. The aqueous layer was then acidified to pH = 2 by adding 7.5 mL of 2 M HCl. The acidic aqueous layer was then extracted 4x 20 mL diethyl ether. The combined organic layers were dried over anhydrous Na₂SO₄, filtered, and concentrated *in vacuo* to 210 mg (846 μmol, 63% yield) of a slightly yellow oil. The crude carboxylic acid was used without further purification.

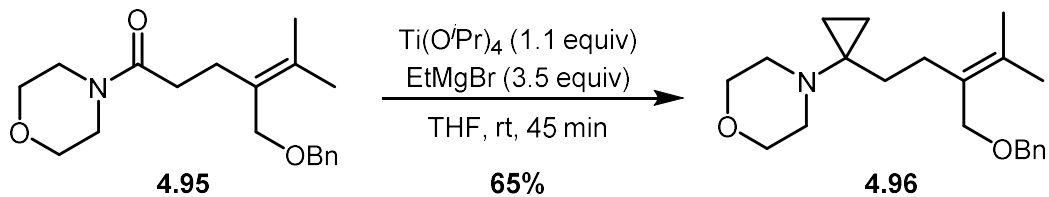
¹H NMR (500 MHz, CDCl₃) δ 7.34 (m, 4H), 7.29 (dt, *J* = 8.5, 4.1 Hz, 1H), 4.49 (s, 2H), 4.01 (s, 2H), 2.56 – 2.47 (m, 2H), 2.47 – 2.41 (m, 2H), 1.74 (s, 3H), 1.71 (s, 3H) ppm

The crude carboxylic acid (210 mg, 847 μmol, 1 equiv.) was added to a vial, and the vial was evacuated and refilled with dry nitrogen three times. Next, 4.2 mL of dry DCM were added, followed by morpholine (93 μL, 1.06 mmol, 1.2 equiv.), DMAP (130 mg, 1.06 mmol, 1.2 equiv.), and EDC·HCl (203 mg, 1.06 mmol, 1.2 equiv.) sequentially, each as one portion. The reaction was stirred overnight at room temperature. The reaction mixture was quenched with 10 mL water and

further diluted with 10 mL ethyl acetate. The layers were separated, and the aqueous layer was extracted 3x 10 mL ethyl acetate. The combined organic layers were dried over anhydrous Na₂SO₄, filtered, and concentrated *in vacuo*. The crude material was purified by flash column chromatography over silica (eluting isocratic 70% EtOAc/hexanes), and amide **4.95** was isolated as 224 mg (706 μmol, 84% yield, 53% over two steps) of a clear, colorless oil.

R_f = 0.40 (70% EtOAc/hexanes)

¹H NMR (500 MHz, CDCl₃) δ 7.38 – 7.31 (m, 4H), 7.31 – 7.27 (m, 1H), 4.46 (s, 2H), 4.04 (s, 2H), 3.62 (br s, 2H), 3.58 (br s, 2H), 3.50 (br s, 2H), 3.36 (br s, 2H), 2.50 – 2.43 (m, 2H), 2.43 – 2.35 (m, 2H), 1.74 (s, 3H), 1.72 (s, 3H) ppm

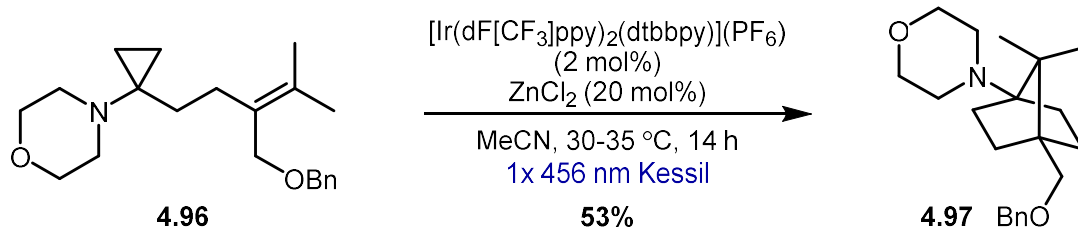


4-(1-(3-((benzyloxy)methyl)-4-methylpent-3-en-1-yl)cyclopropyl)morpholine (**4.96**)

Amide **4.95** (224 mg, 706 μmol , 1 equiv.) was dissolved in 14 mL dry THF, and the flask was submerged in a water bath to serve as a heat sink. $\text{Ti}(\text{O}^i\text{Pr})_4$ (230 μL , 777 μmol , 1.1 equiv.) was added as one portion, then a vent needle was put in place. EtMgBr (0.82 mL, 3 M in diethyl ether, 2.47 mmol, 3.5 equiv.) was added dropwise down the side of the flask over 7 min, and the vent line was removed. During the addition, the reaction underwent the standard color changes (yellow - yellow/green/brown - brown/red - red black). The reaction was stirred in the water bath for 45 min, after which an aqueous mixture containing 20 mL Rochelle salt, 5 mL brine, and 1.5 mL 6 M NaOH was added, and the reaction was stirred vigorously for 20 min. The mixture was further diluted with 10 mL diethyl ether, and the layers were separated. The aqueous layer was extracted 3x 15 mL diethyl ether. The combined organic layers were washed with 20 mL brine, dried over anhydrous Na_2SO_4 , filtered, and concentrated *in vacuo*. The crude material was purified by flash column chromatography over silica (eluting with 3-33% EtOAc/hexanes, 5% increments) and aminoCP **4.96** was collected as 150 mg (455 μmol , 65% yield) of a clear, colorless oil.

$R_f = 0.60$ (30% EtOAc/hexanes)

$^1\text{H NMR}$ (400 MHz, CDCl_3) δ 7.35 (m, 4H), 7.29 (m, 1H), 4.47 (s, 2H), 3.95 (s, 2H), 3.60 (s, 4H), 2.66 (s, 4H), 2.16 – 2.05 (m, 2H), 1.70 (s, 6H), 1.59 – 1.49 (m, 2H), 0.53 (s, 2H), 0.42 (s, 2 H)
ppm

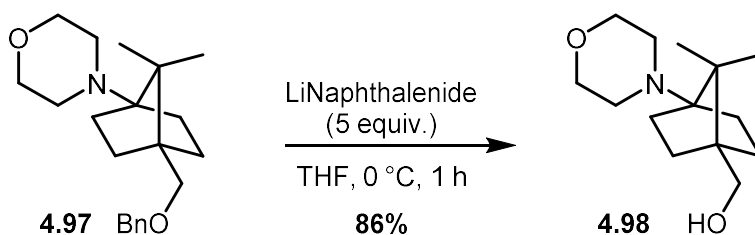


4-(4-((benzyloxy)methyl)-7,7-dimethylbicyclo[2.2.1]heptan-1-yl)morpholine (4.97)

In a dry 2 dram vial under argon was added $[\text{Ir}(\text{dF}[\text{CF}_3]\text{ppy})_2(\text{dtbbpy})](\text{PF}_6)$ (5.1 mg, 4.56 μmol , 2 mol%). The vial was purged and backfilled with dry N_2 (g) three times. Next, 1 mL dry MeCN was added. A separate 2 dram vial containing aminoCP **4.96** (75 mg, 228 μmol , 1 equiv.) was purged and backfilled with N_2 (g) three times, and then the solution of photocatalyst was added. The vial that had contained the photocatalyst was rinsed with an additional 1.3 mL dry MeCN. ZnCl_2 (46 μL , 1 M in diethyl ether, 45.6 μmol , 20 mol%) was then added, and the reaction was degassed 3x freeze-pump-thaw cycles. The vial was centered away from a Kessil Model PR160 456 nm LED at 100% intensity and irradiated for 14 h. The temperature was maintained at 35 °C with a fan placed above the vial for the duration of the reaction. The reaction mixture was added to a solution containing 5 mL sat. sodium bicarbonate and 5 mL 1 M NaOH. The aqueous mixture was further diluted with 10 mL diethyl ether, and the layers were separated. The aqueous layer was extracted 3x 20 mL diethyl ether. The combined organic layers were dried over anhydrous Na_2SO_4 , filtered, and concentrated *in vacuo*. The crude material was purified by flash column chromatography over silica (eluting with 10-40% EtOAc/hexanes, 5% increments). AminoNB **4.97** was collected as 39.7 mg (120 μmol , 53% yield) of a clear, colorless oil.

R_f = 0.40 (30% EtOAc/hexanes)

$^1\text{H NMR}$ (500 MHz, CDCl_3) δ 7.36 – 7.27 (m, 5H), 4.49 (s, 2H), 3.67 (s, 4H), 3.36 (s, 2H), 2.61 (s, 4H), 1.80 (t, J = 10.4 Hz, 2H), 1.68 (t, J = 11.2 Hz, 2H), 1.48 – 1.34 (m, 4H), 0.95 (s, 6H) ppm

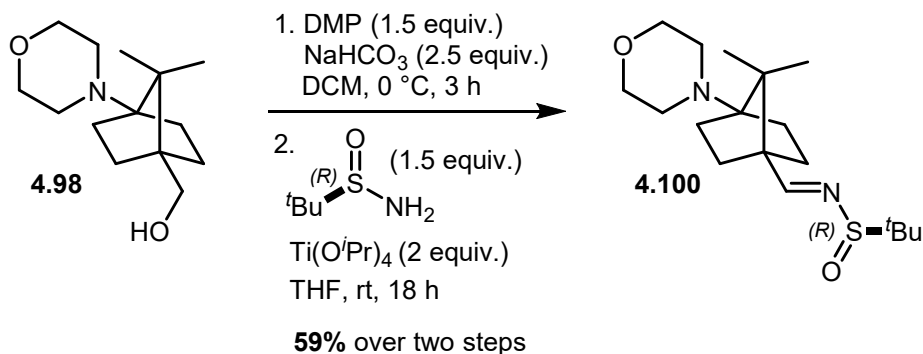


(7,7-dimethyl-4-morpholinobicyclo[2.2.1]heptan-1-yl)methanol (4.98)

A vial containing aminoNB **4.97** (74 mg, 225 μmol , 1 equiv.) was thoroughly purged with argon, then 2.3 mL dry THF was added. The reaction mixture was cooled to 0 $^\circ\text{C}$ in an ice/water bath, and lithium naphthalenide (1.12 mL, 1 M in THF, 1.13 mmol, 5 equiv.) was added dropwise down the side of the vial. The reaction was stirred for 1 h at 0 $^\circ\text{C}$, then warmed to room temperature and quenched with a solution containing 5 mL sat. sodium bicarbonate and 5 mL 1 M NaOH. The mixture was further diluted with 10 mL ethyl acetate, and the layers were separated. The aqueous layer was extracted 3x 10 mL ethyl acetate, and the combined organic layers were dried over anhydrous Na_2SO_4 , filtered, and concentrated *in vacuo*. The crude material was purified by flash column chromatography over silica pre-neutralized with 1% NEt_3 (35-65% EtOAc/hexanes, 5% increments). Alcohol **4.98** was isolated as 45.1 mg (188 μmol , 86% yield) of a clear, colorless oil.

R_f = 0.50 (70% EtOAc/hexanes + 1% NH_4OH)

$^1\text{H NMR}$ (500 MHz, CDCl_3) δ 3.72 – 3.63 (m, 4H), 3.58 (d, J = 5.6 Hz, 2H), 2.68 – 2.56 (m, 4H), 1.86 – 1.79 (m, 2H), 1.68 – 1.61 (m, 2H), 1.48 – 1.42 (m, 2H), 1.40 – 1.33 (m, 2H), 0.96 (s, 6H)
ppm



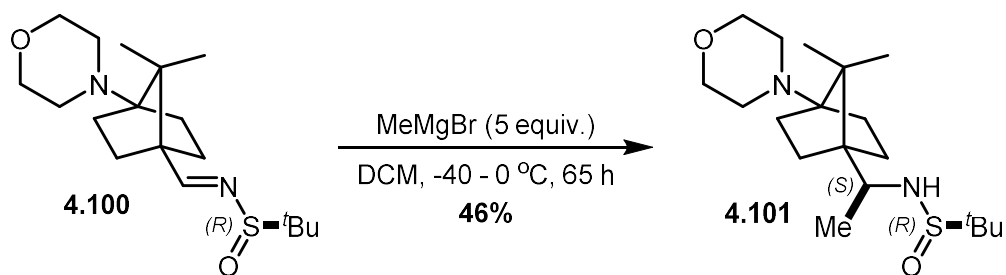
(R)-N-((E)-(7,7-dimethyl-4-morpholinobicyclo[2.2.1]heptan-1-yl)methylene)-2-methylpropane-2-sulfonamide (4.100)

To alcohol **4.98** (45 mg, 188 μmol, 1 equiv.) was added 1.9 mL dry DCM. The solution was cooled to 0 °C in an ice/water bath, then NaHCO₃ (39.5 mg, 470 μmol, 2.5 equiv.) and DMP (120 mg, 282 μmol, 1.5 equiv.) were added, each as one portion. The reaction was stirred for 3 h at 0 °C, then quenched with 5 mL 0.5 M NaOH and further diluted with 4 mL ethyl acetate. The layers were separated, and the aqueous layer was extracted 3x 4 mL ethyl acetate. The combined organic layers were dried over anhydrous Na₂SO₄, filtered, and concentrated *in vacuo* to 40 mg (169 μmol, 90% yield) of a clear, light yellow oil. The crude aldehyde **4.99** was used without further purification.

To **4.99** (40 mg, 169 μmol, 1 equiv.) was added (*R*)-Ellman's sulfonamide (31 mg, 254 μmol, 1.5 equiv.). Next, 1.7 mL dry THF was added, followed by Ti(O^{*i*}Pr)₄ (100 μL, 338 μmol, 2 equiv.). The reaction was stirred at room temperature for 16 h, then quenched with 10 mL sat. sodium bicarbonate and further diluted with 10 mL ethyl acetate. The layers were separated, and the aqueous layer was extracted 3x 10 mL ethyl acetate. The combined organic layers were dried over anhydrous Na₂SO₄, filtered, and concentrated *in vacuo*. The crude material was purified by flash column chromatography over silica (30 to 60 to 80% EtOAc/hexanes + 0.2% NEt₃) and sulfinimine

4.100 was collected as 37.3 mg (110 μmol , 65% yield, 59% yield over two steps) of a white crystalline solid.

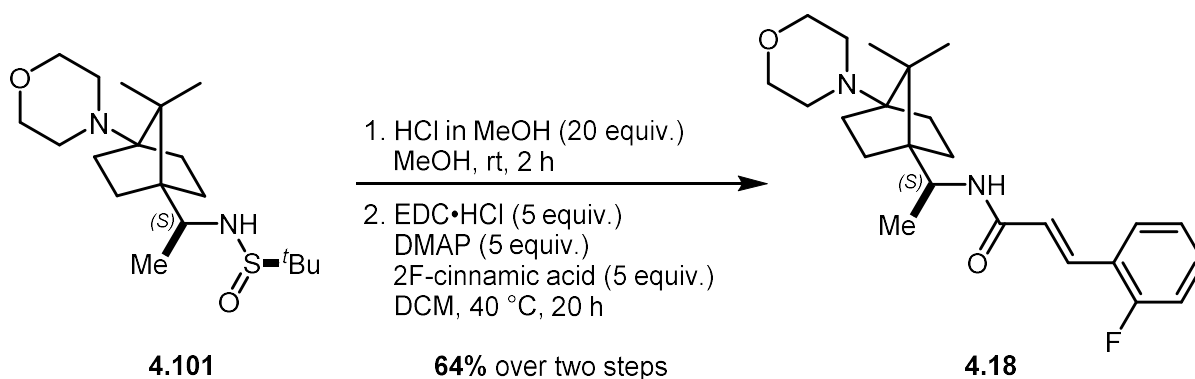
$R_f = 0.40$ (70% EtOAc/hexanes + 0.2% NEt_3)



(R)-N-((1S)-1-(7,7-dimethyl-4-morpholinobicyclo[2.2.1]heptan-1-yl)ethyl)-2-methylpropane-2-sulfinamide (4.101)

To sulfinimine **4.100** (37.3 mg, 110 μ mol, 1 equiv.) was added 0.55 mL dry DCM, and the solution was cooled to -40 $^{\circ}$ C. Next, MeMgBr (183 μ L, 3 M in diethyl ether, 550 μ mol, 5 equiv.) was added dropwise over 45 s. The mixture was warmed to 0 $^{\circ}$ C over 4 h, then the entire reaction mixture was placed in a refrigerator set to 0 $^{\circ}$ C for 40 h. The reaction was quenched with 5 mL sat. Rochelle salt and 5 mL 1 M NaOH. The mixture was further diluted with 10 mL ethyl acetate, and the layers were separated. The aqueous layer was extracted 3x 10 mL ethyl acetate, and the combined organic layers were dried over anhydrous Na_2SO_4 , filtered, and concentrated *in vacuo*. Crude ^1H NMR analysis revealed incomplete conversion, and the reaction was resubjected to the above conditions for 20 h at 0 $^{\circ}$ C. The crude material was purified by flash column chromatography over silica (15 to 30 to 45 to 60 to 75 to 90 to 100% EtOAc/hexanes + 0.2% NEt_3), and sulfinamide **4.101** was isolated as 18 mg (50.5 μ mol, 46% yield) of an oil.

$R_f = 0.20$ (70% EtOAc/hexanes + 0.2% NEt_3)



(E)-N-((1S)-1-(7,7-dimethyl-4-morpholinobicyclo[2.2.1]heptan-1-yl)ethyl)-3-(2-fluorophenyl)acrylamide (4.18)

Sulfonamide **4.101** (9.0 mg, 25.2 μmol , 1 equiv.) was dissolved in 0.5 mL of a 1.0 M HCl solution in dry MeOH (freshly prepared from the addition of acetyl chloride to dry MeOH). The reaction mixture was stirred for 2 h at room temperature. The mixture was diluted with 4 mL water and 2 mL diethyl ether. The layers were separated, and the aqueous layer ($\text{pH} < 2$) was washed 2x 2 mL diethyl ether. The aqueous layer was then basified with 0.5 mL 6 M NaOH and diluted with 2 mL ethyl acetate. The layers were separated, and the aqueous layer ($\text{pH} = 14$) was extracted 3x 2 mL ethyl acetate. The combined organic layers were dried over anhydrous MgSO_4 , filtered, and concentrated under a stream of dry N_2 (g). The free amine was collected as 5.3 mg (21.0 μmol , 83% yield) of a white, crystalline solid that was used without further purification.

$^1\text{H NMR}$ (500 MHz, C_6D_6): δ 3.64 (*app.* t, $J = 4.6$ Hz, 4H), 2.80 (q, $J = 6.5$ Hz, 1H), 2.44-2.40 (m, 4H), 1.72 (*app.* tt, $J = 12.0, 4.0$ Hz, 1H), 1.67-1.61 (m, 1H), 1.57 (*app.* tt, $J = 12.2, 4.2$ Hz, 1H), 1.29-1.19 (m, 2H), 1.15-1.03 (m, 3H), 1.01 (s, 3H), 0.84 (d, $J = 6.6$ Hz, 3H), 0.83 (s, 3H), 0.58 (br s, 2H) ppm

Crude amine (5.3 mg, 21.0 μmol , 1 equiv.) was dissolved in 0.75 mL dry DCM, then 2-fluorocinnamic acid (5.5 mg; 105 μmol , 5 equiv.), DMAP (4.2 mg, 105 μmol , 5 equiv.), and

EDC·HCl (6.4 mg, 105 μ mol, 5 equiv.) were each added in one portion. The reaction was flushed with argon, capped, and heated to 40 °C for 20 h. After cooling to room temperature, the reaction mixture was diluted with 2 mL 1:1 sat. sodium bicarbonate:1 M NaOH and 2 mL ethyl acetate. The layers were separated, and the aqueous layer was extracted 3x 2 mL ethyl acetate. The combined organic layers were dried over anhydrous MgSO₄, filtered, and concentrated under a stream of dry N₂ (g). The crude material was purified by flash column chromatography over silica pre-neutralized with 1% NEt₃ (eluting with 50, 70, 100% EtOAc/pentane), and final analog **4.18** was collected as 6.5 mg (16.2 μ mol, 78% yield, 64% yield over two steps) of a white solid.

R_f = 0.15 (80% EtOAc/hexanes + 1% NH₄OH)

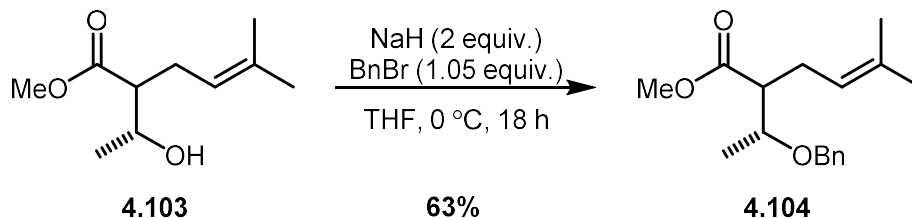
¹H NMR (700 MHz, C₆D₆): δ 8.08 (d, J = 15.7 Hz, 1H), 7.05 (td, J = 7.7, 1.4 Hz, 1H), 6.79-6.75 (m, 1H), 6.75-6.71 (m, 1H), 6.67 (td, J = 7.5, 1.2 Hz, 1H), 6.44 (d, J = 15.7 Hz, 1H), 4.94 (d, J = 9.7 Hz, 1H), 4.56 (dq, J = 9.6, 6.8 Hz, 1H), 3.60 (*app.* t, J = 4.6 Hz, 4H), 2.39 (*app.* ddt, J = 11.5, 10.8, 4.6 Hz, 4H), 1.63 (*app.* tt, J = 11.6, 4.0 Hz, 1H), 1.56 (*app.* tt, J = 12.2, 4.2 Hz, 1H), 1.33-1.26 (m, 2H), 1.23-1.19 (m, 1H), 1.07-1.03 (m, 1H), 1.02 (s, 3H), 1.03-0.97 (m, 2H), 0.93 (s, 3H), 0.88 (d, J = 6.8 Hz, 3H) ppm

¹³C NMR (176 MHz, C₆D₆): δ 163.9, 161.8 (d, J = 252.3 Hz), 134.4, 130.7, 130.7 (d, J = 10.9 Hz), 125.4 (d, J = 8.3 Hz), 124.5 (d, J = 3.5 Hz), 123.7 (d, J = 11.4 Hz), 116.2 (d, J = 22.0 Hz), 71.7, 67.9, 51.6, 49.6, 49.3, 45.8, 31.6, 30.6, 27.0, 25.0, 20.0, 19.2, 18.1 ppm

¹⁹F NMR (376 MHz, C₆D₆): δ -114.1 to -114.2 (m) ppm

HRMS (ESI+, m/z) calculated for C₂₄H₃₄FN₂O₂⁺ 401.2599; found: 401.2592

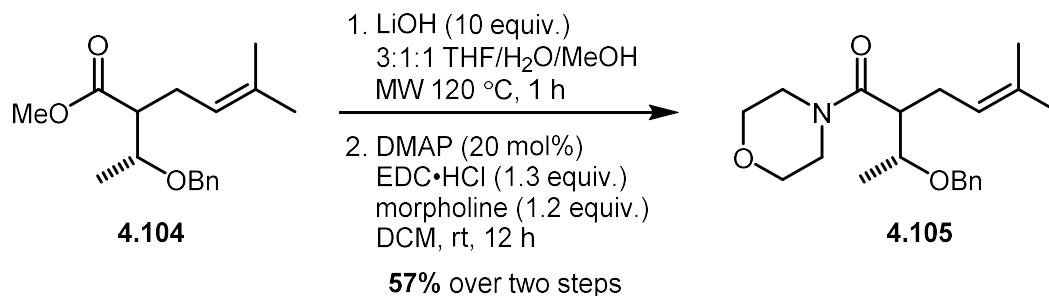
4.9.7 Synthesis of C2 Analog Intermediates



methyl 2-((R)-1-(benzyloxy)ethyl)-5-methylhex-4-enoate (4.104)

Hydroxy ester **4.103**³⁰ (75 mg, 403 μmol , 1 equiv.) was dissolved in 3 mL dry DMF. The solution was cooled to 0 °C in an ice/water bath, then NaH (17 mg, 60% dispersion in mineral oil, 443 μmol , 1.1 equiv.) was added in one portion. The suspension was stirred for 30 min at 0 °C, then benzyl bromide (72 μL , 604 μmol , 1.5 equiv.) was added. The reaction mixture was allowed to slowly warm to room temperature over 4 h. The reaction was poured into 10 mL sat. aqueous ammonium chloride and further diluted with 10 mL ethyl acetate. The layers were separated, and the aqueous layer was extracted 2x 10 mL ethyl acetate. The combined organic layers were washed with 10 mL brine, dried over anhydrous Na_2SO_4 , filtered, and concentrated *in vacuo*. The crude material was purified by automated flash column chromatography over silica (eluting with 0-35% EtOAc/hexanes), and benzyl ether **4.104** was collected as 70 mg (253 μmol , 63% yield) of a clear, colorless oil.

R_f = 0.35 (70% EtOAc/hexanes)



2-((R)-1-(benzyloxy)ethyl)-5-methyl-1-morpholinohex-4-en-1-one (4.105)

Methyl ester **4.104** (69.5 mg, 251 μ mol, 1 equiv.) was transferred to a 0.5-2.0 mL microwave vial with 3x 0.5 mL portions of THF. Next, 0.5 mL HPLC-grade water and 0.5 mL MeOH were added. Solid LiOH·H₂O (106 mg, 2.51 mmol, 10 equiv.) was added directly. The vial was flushed with argon, capped, and heated in the microwave for 1 h at 120 °C. The reaction mixture was poured into 2 mL 2 M HCl and further diluted with 2 mL ethyl acetate. The layers were separated, and the aqueous layer was extracted 3x 2 mL ethyl acetate. The combined organic layers were washed with 2 mL brine, dried over anhydrous MgSO₄, filtered, and concentrated *in vacuo* to a clear, yellow oil.

¹H NMR (500 MHz, C₆D₆) δ 7.28 (d, J = 7.7 Hz, 2H), 7.18 (d, J = 7.6 Hz, 2H), 7.08 (t, J = 7.3 Hz, 1H), 5.20 (t, J = 6.7 Hz, 1H), 4.35 (d, J = 11.8 Hz, 1H), 4.26 (d, J = 11.8 Hz, 1H), 3.68 (p, J = 6.3 Hz, 1H), 2.73 – 2.61 (m, 1H), 2.47 – 2.32 (m, 1H), 2.23 (dd, J = 13.2, 6.5 Hz, 1H), 1.59 (s, 3H), 1.52 (s, 3H), 1.03 (d, J = 6.2 Hz, 3H) ppm

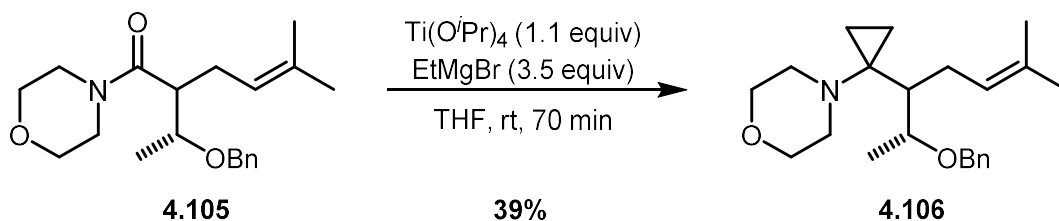
The crude carboxylic acid (70 mg, 267 μ mol, 1 equiv.) was dissolved in 2.5 mL dry DCM, then DMAP (6.5 mg, 53.4 μ mol, 20 mol%), morpholine (28 μ L, 320 μ mol, 1.2 equiv.), and EDC·HCl (66.5 mg, 347 μ mol, 1.3 equiv.) were each added as one portion. The reaction was flushed with dry N₂ (g), capped, and stirred at room temperature for 25 h. The reaction was quenched by adding 5 mL 1 M HCl and further diluted with 5 mL DCM. The layers were separated, and the aqueous

layer was extracted 3x 5 mL DCM. The combined organic layers were washed with 5 mL brine, dried over anhydrous MgSO₄, filtered, and concentrated *in vacuo* to a clear oil. The crude material was purified by automated flash column chromatography over silica (eluting with 30-70% EtOAc/hexanes), and amide **4.105** was collected as 50 mg (151 μmol, 57% yield over two steps) of a clear, colorless oil.

R_f = 0.40 (70% EtOAc/hexanes)

¹H NMR (500 MHz, CDCl₃) δ 7.34 – 7.29 (m, 5H), 5.02 (t, *J* = 7.2 Hz, 1H), 4.54 (d, *J* = 11.1 Hz, 1H), 4.38 (d, *J* = 11.1 Hz, 1H), 3.81 (dq, *J* = 12.4, 6.2 Hz, 1H), 3.64 (m, 2H), 3.58 (m, 2H), 3.46 (m, 4H), 2.75 (td, *J* = 10.6, 3.9 Hz, 1H), 2.35 (dd, *J* = 19.8, 12.1 Hz, 1H), 2.19 – 2.06 (m, 1H), 1.67 (s, 3H), 1.61 (s, 3H), 1.26 (d, *J* = 6.1 Hz, 3H) ppm

¹³C NMR (126 MHz, CDCl₃) δ 173.31, 138.87, 133.72, 128.39, 127.96, 127.69, 121.24, 77.91, 71.91, 67.19, 66.98, 48.17, 46.56, 27.93, 25.97, 17.91, 17.63 ppm



2-((R)-1-(benzyloxy)ethyl)-5-methyl-1-morpholinohex-4-en-1-one (4.106)

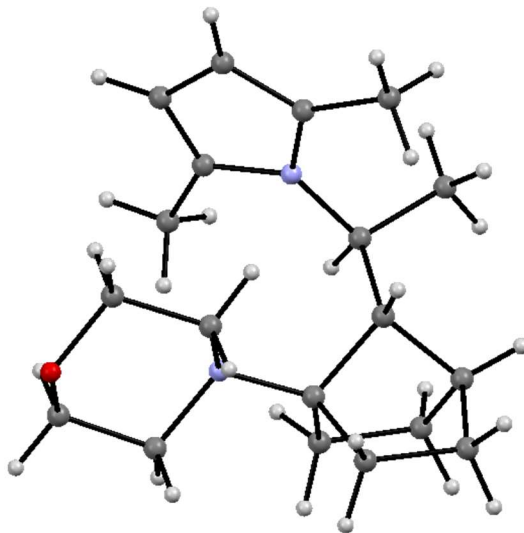
Amide **4.105** (50 mg, 151 μmol , 1 equiv.) was dissolved in 2 mL dry THF, and the flask was submerged in a water bath to serve as a heat sink. $\text{Ti(O}^i\text{Pr)}_4$ (49 μL , 166 μmol , 1.1 equiv.) was added as one portion, then a vent needle was put in place. EtMgBr (0.18 mL, 3 M in diethyl ether, 528 μmol , 3.5 equiv.) was added dropwise down the side of the flask over 30 s, and the vent line was removed. During the addition, the reaction underwent the standard color changes (yellow - yellow/green/brown - brown/red - red black). The reaction was stirred in the water bath for 70 min, after which an aqueous mixture containing 1 mL Rochelle salt, 1 mL sat. sodium bicarbonate, and 0.5 mL 6 M NaOH was added, and the reaction was stirred vigorously for 5 min. The mixture was further diluted with 1 mL diethyl ether, and the layers were separated. The aqueous layer was extracted 3x 1 mL diethyl ether. The combined organic layers were washed with 1 mL brine, dried over anhydrous MgSO_4 , filtered, and concentrated *in vacuo*. The crude material was purified by automated flash column chromatography over silica (eluting with 4-20% EtOAc/hexanes over 12 CVs), and aminoCP **4.106** was collected as 20.2 mg (58.8 μmol , 39% yield) of a clear, colorless oil.

R_f = 0.50 (20% EtOAc/hexanes)

$^1\text{H NMR}$ (500 MHz, C_6D_6) δ 7.32 (d, J = 7.6 Hz, 2H), 7.20 (t, J = 7.6 Hz, 2H), 7.10 (t, J = 7.3 Hz, 1H), 5.30 (t, J = 6.5 Hz, 1H), 4.43 (d, J = 11.9 Hz, 1H), 4.18 (d, J = 11.9 Hz, 1H), 3.59 (td, J = 10.2, 6.4 Hz, 1H), 3.54 (t, J = 4.3 Hz, 4H), 2.44 (dt, J = 15.4, 7.8 Hz, 1H), 2.34 (d, J = 4.1 Hz,

4H), 2.14 – 2.02 (m, 1H), 1.71 (s, 3H), 1.58 (s, 3H), 1.53 (s, 1H), 1.20 (d, $J = 6.3$ Hz, 3H), 0.96 (s, 1H), 0.73 – 0.60 (m, 2H), 0.60 – 0.52 (m, 1H) ppm

4.9.8 X-Ray Crystallographic Data



Structure Determination of 4.60

Colorless blocks of **4.60** were grown from a pentane solution of the compound at 25 deg. C. A crystal of dimensions 0.22 x 0.22 x 0.20 mm was mounted on a Rigaku AFC10K Saturn 944+ CCD-based X-ray diffractometer equipped with a low temperature device and Micromax-007HF Cu-target micro-focus rotating anode ($\lambda = 1.54187 \text{ \AA}$) operated at 1.2 kW power (40 kV, 30 mA). The X-ray intensities were measured at 85(1) K with the detector placed at a distance 42.00 mm from the crystal. A total of 2028 images were collected with an oscillation width of 1.0° in ω . The exposure times were 1 sec. for the low angle images, 4 sec. for high angle. Rigaku d*trek images were exported to CrysAlisPro for processing and corrected for absorption. The integration of the data yielded a total of 25540 reflections to a maximum 2θ value of 138.90° of which 3137 were independent and 3122 were greater than $2s(I)$. The final cell constants (Table 1) were based on the xyz centroids of 22446 reflections above $10s(I)$. Analysis of the data showed negligible decay during data collection. The structure was solved and refined with the Bruker SHELXTL (version 2018/3) software package, using the space group $P2(1)2(1)2(1)$ with $Z = 4$ for

the formula C₁₉H₃₀N₂O. All non-hydrogen atoms were refined anisotropically with the hydrogen atoms placed in idealized positions. Full matrix least-squares refinement based on F² converged at R₁ = 0.0375 and wR₂ = 0.0896 [based on I > 2σ(I)], R₁ = 0.0377 and wR₂ = 0.0900 for all data. Additional details are presented in Table 1 and are given as Supporting Information in a CIF file. Acknowledgement is made for funding from NSF grant CHE-0840456 for X-ray instrumentation.

G.M. Sheldrick (2015) "Crystal structure refinement with SHELXL", *Acta Cryst.*, C71, 3-8 (Open Access).

CrystalClear Expert 2.0 r16, Rigaku Americas and Rigaku Corporation (2014), Rigaku Americas, 9009, TX, USA 77381-5209, Rigaku Tokyo, 196-8666, Japan.

CrysAlisPro 1.171.38.41 (Rigaku Oxford Diffraction, 2015).

Identification code	4.60
Empirical formula	C ₁₉ H ₃₀ N ₂ O
Formula weight	302.45
Temperature	85(2) K
Wavelength	1.54184 Å
Crystal system, space group	Orthorhombic, P2(1)2(1)2(1)
Unit cell dimensions	a = 6.83800(10) Å α = 90 deg. b = 15.47210(10) Å β = 90 deg. c = 15.9616(2) Å γ = 90 deg.
Volume	1688.71(3) Å ³
Z, Calculated density	4, 1.190 Mg/m ³
Absorption coefficient	0.563 mm ⁻¹
F(000)	664
Crystal size	0.220 x 0.220 x 0.200 mm
Theta range for data collection	3.979 to 69.451 deg.
Limiting indices	-8 ≤ h ≤ 7, -18 ≤ k ≤ 18, -19 ≤ l ≤ 19
Reflections collected / unique	25540 / 3137 [R(int) = 0.0607]
Completeness to theta =	67.684 99.9 %
Absorption correction	Semi-empirical from equivalents
Max. and min. transmission	1.00000 and 0.77024
Refinement method	Full-matrix least-squares on F ²
Data / restraints / parameters	3137 / 0 / 203
Goodness-of-fit on F ²	1.106
Final R indices [I > 2σ(I)]	R ₁ = 0.0375, wR ₂ = 0.0896
R indices (all data)	R ₁ = 0.0377, wR ₂ = 0.0900
Absolute structure parameter	-0.09(12)

Extinction coefficient 0.0173(12)
Largest diff. peak and hole 0.231 and -0.285 e.A⁻³

Atomic coordinates (x 10⁴) and equivalent isotropic displacement parameters (A² x 10³) for **4.60**.

U(eq) is defined as one third of the trace of the orthogonalized U_{ij} tensor.

	x	y	z	U(eq)
O(1)	7423(2)	3590(1)	6393(1)	28(1)
N(1)	5369(2)	4084(1)	4900(1)	18(1)
N(2)	5403(2)	6098(1)	4467(1)	18(1)
C(1)	5369(3)	3473(1)	6311(1)	27(1)
C(2)	4778(3)	3338(1)	5406(1)	23(1)
C(3)	7484(3)	4210(1)	4993(1)	22(1)
C(4)	8008(3)	4325(1)	5907(1)	27(1)
C(5)	4712(3)	4028(1)	4028(1)	18(1)
C(6)	2467(3)	3911(1)	3963(1)	21(1)
C(7)	1967(3)	4235(1)	3067(1)	24(1)
C(8)	3988(3)	4470(1)	2711(1)	22(1)
C(9)	5047(2)	4850(1)	3478(1)	18(1)
C(10)	5131(3)	3627(1)	2566(1)	26(1)
C(11)	5643(3)	3320(1)	3466(1)	23(1)
C(12)	4215(2)	5714(1)	3795(1)	17(1)
C(13)	3865(3)	6362(1)	3083(1)	21(1)
C(14)	7249(3)	6471(1)	4396(1)	21(1)
C(15)	7755(3)	6779(1)	5174(1)	23(1)
C(16)	6201(3)	6595(1)	5729(1)	23(1)
C(17)	4771(3)	6183(1)	5286(1)	20(1)
C(18)	8430(3)	6520(1)	3610(1)	27(1)
C(19)	2832(3)	5869(1)	5584(1)	24(1)

Bond lengths [A] and angles [deg] for **4.60**.

O(1)-C(1)	1.422(2)
O(1)-C(4)	1.433(2)
N(1)-C(5)	1.465(2)
N(1)-C(2)	1.466(2)
N(1)-C(3)	1.467(2)
N(2)-C(17)	1.384(2)
N(2)-C(14)	1.393(2)
N(2)-C(12)	1.470(2)

C(1)-C(2)	1.514(3)
C(1)-H(1A)	0.9900
C(1)-H(1B)	0.9900
C(2)-H(2A)	0.9900
C(2)-H(2B)	0.9900
C(3)-C(4)	1.513(3)
C(3)-H(3A)	0.9900
C(3)-H(3B)	0.9900
C(4)-H(4A)	0.9900
C(4)-H(4B)	0.9900
C(5)-C(6)	1.550(3)
C(5)-C(11)	1.552(2)
C(5)-C(9)	1.562(2)
C(6)-C(7)	1.555(2)
C(6)-H(6A)	0.9900
C(6)-H(6B)	0.9900
C(7)-C(8)	1.538(3)
C(7)-H(7A)	0.9900
C(7)-H(7B)	0.9900
C(8)-C(10)	1.538(2)
C(8)-C(9)	1.539(2)
C(8)-H(8)	1.0000
C(9)-C(12)	1.538(2)
C(9)-H(9)	1.0000
C(10)-C(11)	1.553(3)
C(10)-H(10A)	0.9900
C(10)-H(10B)	0.9900
C(11)-H(11A)	0.9900
C(11)-H(11B)	0.9900
C(12)-C(13)	1.534(2)
C(12)-H(12)	1.0000
C(13)-H(13A)	0.9800
C(13)-H(13B)	0.9800
C(13)-H(13C)	0.9800
C(14)-C(15)	1.374(3)
C(14)-C(18)	1.495(3)
C(15)-C(16)	1.413(3)
C(15)-H(15)	0.9500
C(16)-C(17)	1.365(3)
C(16)-H(16)	0.9500
C(17)-C(19)	1.490(3)
C(18)-H(18A)	0.9800
C(18)-H(18B)	0.9800
C(18)-H(18C)	0.9800
C(19)-H(19A)	0.9800
C(19)-H(19B)	0.9800

C(19)-H(19C)	0.9800
C(1)-O(1)-C(4)	109.12(14)
C(5)-N(1)-C(2)	113.12(13)
C(5)-N(1)-C(3)	113.97(15)
C(2)-N(1)-C(3)	108.68(14)
C(17)-N(2)-C(14)	108.67(15)
C(17)-N(2)-C(12)	123.73(14)
C(14)-N(2)-C(12)	127.53(15)
O(1)-C(1)-C(2)	111.61(16)
O(1)-C(1)-H(1A)	109.3
C(2)-C(1)-H(1A)	109.3
O(1)-C(1)-H(1B)	109.3
C(2)-C(1)-H(1B)	109.3
H(1A)-C(1)-H(1B)	108.0
N(1)-C(2)-C(1)	110.09(15)
N(1)-C(2)-H(2A)	109.6
C(1)-C(2)-H(2A)	109.6
N(1)-C(2)-H(2B)	109.6
C(1)-C(2)-H(2B)	109.6
H(2A)-C(2)-H(2B)	108.2
N(1)-C(3)-C(4)	110.28(16)
N(1)-C(3)-H(3A)	109.6
C(4)-C(3)-H(3A)	109.6
N(1)-C(3)-H(3B)	109.6
C(4)-C(3)-H(3B)	109.6
H(3A)-C(3)-H(3B)	108.1
O(1)-C(4)-C(3)	111.18(15)
O(1)-C(4)-H(4A)	109.4
C(3)-C(4)-H(4A)	109.4
O(1)-C(4)-H(4B)	109.4
C(3)-C(4)-H(4B)	109.4
H(4A)-C(4)-H(4B)	108.0
N(1)-C(5)-C(6)	111.98(14)
N(1)-C(5)-C(11)	117.71(14)
C(6)-C(5)-C(11)	106.55(15)
N(1)-C(5)-C(9)	116.13(13)
C(6)-C(5)-C(9)	101.71(13)
C(11)-C(5)-C(9)	100.97(13)
C(5)-C(6)-C(7)	103.99(14)
C(5)-C(6)-H(6A)	111.0
C(7)-C(6)-H(6A)	111.0
C(5)-C(6)-H(6B)	111.0
C(7)-C(6)-H(6B)	111.0
H(6A)-C(6)-H(6B)	109.0
C(8)-C(7)-C(6)	102.61(14)

C(8)-C(7)-H(7A)	111.2
C(6)-C(7)-H(7A)	111.2
C(8)-C(7)-H(7B)	111.2
C(6)-C(7)-H(7B)	111.2
H(7A)-C(7)-H(7B)	109.2
C(7)-C(8)-C(10)	108.17(15)
C(7)-C(8)-C(9)	102.66(14)
C(10)-C(8)-C(9)	101.83(14)
C(7)-C(8)-H(8)	114.3
C(10)-C(8)-H(8)	114.3
C(9)-C(8)-H(8)	114.3
C(12)-C(9)-C(8)	114.82(14)
C(12)-C(9)-C(5)	117.96(13)
C(8)-C(9)-C(5)	93.83(13)
C(12)-C(9)-H(9)	109.7
C(8)-C(9)-H(9)	109.7
C(5)-C(9)-H(9)	109.7
C(8)-C(10)-C(11)	103.59(14)
C(8)-C(10)-H(10A)	111.0
C(11)-C(10)-H(10A)	111.0
C(8)-C(10)-H(10B)	111.0
C(11)-C(10)-H(10B)	111.0
H(10A)-C(10)-H(10B)	109.0
C(5)-C(11)-C(10)	103.06(14)
C(5)-C(11)-H(11A)	111.2
C(10)-C(11)-H(11A)	111.2
C(5)-C(11)-H(11B)	111.2
C(10)-C(11)-H(11B)	111.2
H(11A)-C(11)-H(11B)	109.1
N(2)-C(12)-C(13)	111.22(13)
N(2)-C(12)-C(9)	112.76(13)
C(13)-C(12)-C(9)	112.48(14)
N(2)-C(12)-H(12)	106.6
C(13)-C(12)-H(12)	106.6
C(9)-C(12)-H(12)	106.6
C(12)-C(13)-H(13A)	109.5
C(12)-C(13)-H(13B)	109.5
H(13A)-C(13)-H(13B)	109.5
C(12)-C(13)-H(13C)	109.5
H(13A)-C(13)-H(13C)	109.5
H(13B)-C(13)-H(13C)	109.5
C(15)-C(14)-N(2)	107.41(16)
C(15)-C(14)-C(18)	127.24(17)
N(2)-C(14)-C(18)	125.36(16)
C(14)-C(15)-C(16)	107.90(17)
C(14)-C(15)-H(15)	126.0

C(16)-C(15)-H(15)	126.0
C(17)-C(16)-C(15)	107.95(16)
C(17)-C(16)-H(16)	126.0
C(15)-C(16)-H(16)	126.0
C(16)-C(17)-N(2)	108.07(16)
C(16)-C(17)-C(19)	128.71(16)
N(2)-C(17)-C(19)	123.22(16)
C(14)-C(18)-H(18A)	109.5
C(14)-C(18)-H(18B)	109.5
H(18A)-C(18)-H(18B)	109.5
C(14)-C(18)-H(18C)	109.5
H(18A)-C(18)-H(18C)	109.5
H(18B)-C(18)-H(18C)	109.5
C(17)-C(19)-H(19A)	109.5
C(17)-C(19)-H(19B)	109.5
H(19A)-C(19)-H(19B)	109.5
C(17)-C(19)-H(19C)	109.5
H(19A)-C(19)-H(19C)	109.5
H(19B)-C(19)-H(19C)	109.5

Symmetry transformations used to generate equivalent atoms:

Anisotropic displacement parameters ($\text{Å}^2 \times 10^3$) for **4.60**.

The anisotropic displacement factor exponent takes the form:

$$-2 \pi^2 [h^2 a^{*2} U_{11} + \dots + 2 h k a^* b^* U_{12}]$$

	U11	U22	U33	U23	U13	U12
O(1)	28(1)	27(1)	27(1)	4(1)	-6(1)	3(1)
N(1)	20(1)	16(1)	19(1)	3(1)	-1(1)	0(1)
N(2)	18(1)	16(1)	20(1)	-1(1)	1(1)	1(1)
C(1)	29(1)	28(1)	24(1)	6(1)	1(1)	3(1)
C(2)	23(1)	19(1)	26(1)	6(1)	0(1)	-1(1)
C(3)	19(1)	21(1)	27(1)	4(1)	-1(1)	-2(1)
C(4)	26(1)	24(1)	31(1)	2(1)	-7(1)	0(1)
C(5)	20(1)	15(1)	20(1)	1(1)	0(1)	-1(1)
C(6)	21(1)	19(1)	24(1)	3(1)	0(1)	-4(1)
C(7)	24(1)	22(1)	25(1)	0(1)	-5(1)	-4(1)
C(8)	28(1)	18(1)	20(1)	-1(1)	-1(1)	-1(1)
C(9)	18(1)	17(1)	18(1)	1(1)	3(1)	-1(1)
C(10)	35(1)	19(1)	24(1)	-4(1)	2(1)	1(1)

C(11)	26(1)	17(1)	27(1)	-2(1)	0(1)	0(1)
C(12)	17(1)	17(1)	18(1)	0(1)	-1(1)	-1(1)
C(13)	24(1)	18(1)	22(1)	2(1)	-1(1)	1(1)
C(14)	19(1)	15(1)	28(1)	0(1)	-1(1)	0(1)
C(15)	23(1)	18(1)	29(1)	-2(1)	-5(1)	2(1)
C(16)	29(1)	19(1)	22(1)	-4(1)	-4(1)	6(1)
C(17)	24(1)	16(1)	19(1)	0(1)	1(1)	5(1)
C(18)	22(1)	26(1)	33(1)	-3(1)	6(1)	-6(1)
C(19)	24(1)	27(1)	22(1)	0(1)	5(1)	3(1)

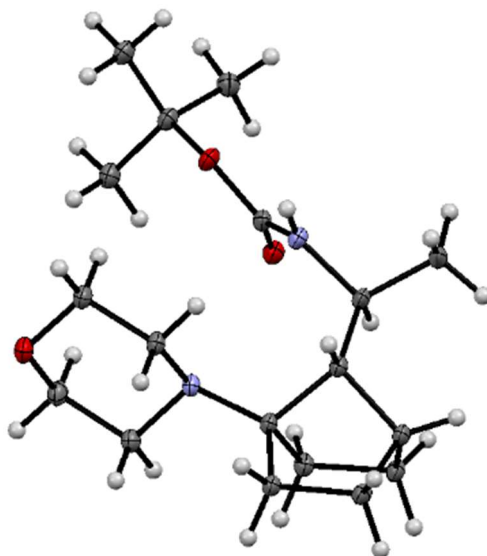
Hydrogen coordinates (x 10⁴) and isotropic displacement parameters (A² x 10³) for **4.60**.

	x	y	z	U(eq)
H(1A)	4686	3987	6536	33
H(1B)	4961	2966	6646	33
H(2A)	5409	2808	5187	27
H(2B)	3344	3261	5371	27
H(3A)	7897	4726	4673	27
H(3B)	8186	3702	4764	27
H(4A)	9438	4408	5961	32
H(4B)	7354	4849	6127	32
H(6A)	1783	4259	4393	25
H(6B)	2097	3296	4033	25
H(7A)	1334	3776	2731	28
H(7B)	1097	4747	3086	28
H(8)	3948	4864	2214	26
H(9)	6472	4916	3353	21
H(10A)	6330	3734	2234	31
H(10B)	4315	3194	2272	31
H(11A)	5067	2745	3584	28
H(11B)	7076	3290	3549	28
H(12)	2906	5583	4044	21
H(13A)	3592	6933	3321	32
H(13B)	2746	6173	2746	32
H(13C)	5032	6394	2729	32
H(15)	8941	7065	5313	28
H(16)	6159	6734	6309	28
H(18A)	7824	6933	3223	40
H(18B)	8480	5948	3346	40
H(18C)	9761	6711	3744	40
H(19A)	2789	5237	5548	36
H(19B)	1798	6115	5232	36

Torsion angles [deg] for **4.60**.

C(4)-O(1)-C(1)-C(2)	59.0(2)
C(5)-N(1)-C(2)-C(1)	-175.63(15)
C(3)-N(1)-C(2)-C(1)	56.73(19)
O(1)-C(1)-C(2)-N(1)	-59.1(2)
C(5)-N(1)-C(3)-C(4)	175.87(13)
C(2)-N(1)-C(3)-C(4)	-56.97(19)
C(1)-O(1)-C(4)-C(3)	-58.9(2)
N(1)-C(3)-C(4)-O(1)	59.0(2)
C(2)-N(1)-C(5)-C(6)	56.14(18)
C(3)-N(1)-C(5)-C(6)	-179.05(14)
C(2)-N(1)-C(5)-C(11)	-67.9(2)
C(3)-N(1)-C(5)-C(11)	57.0(2)
C(2)-N(1)-C(5)-C(9)	172.34(14)
C(3)-N(1)-C(5)-C(9)	-62.84(19)
N(1)-C(5)-C(6)-C(7)	157.65(13)
C(11)-C(5)-C(6)-C(7)	-72.33(16)
C(9)-C(5)-C(6)-C(7)	33.00(17)
C(5)-C(6)-C(7)-C(8)	1.95(17)
C(6)-C(7)-C(8)-C(10)	70.11(17)
C(6)-C(7)-C(8)-C(9)	-37.04(16)
C(7)-C(8)-C(9)-C(12)	-67.38(17)
C(10)-C(8)-C(9)-C(12)	-179.31(14)
C(7)-C(8)-C(9)-C(5)	55.90(15)
C(10)-C(8)-C(9)-C(5)	-56.04(15)
N(1)-C(5)-C(9)-C(12)	-54.8(2)
C(6)-C(5)-C(9)-C(12)	67.00(18)
C(11)-C(5)-C(9)-C(12)	176.67(15)
N(1)-C(5)-C(9)-C(8)	-175.60(15)
C(6)-C(5)-C(9)-C(8)	-53.78(15)
C(11)-C(5)-C(9)-C(8)	55.89(15)
C(7)-C(8)-C(10)-C(11)	-72.08(18)
C(9)-C(8)-C(10)-C(11)	35.64(18)
N(1)-C(5)-C(11)-C(10)	-162.97(15)
C(6)-C(5)-C(11)-C(10)	70.36(17)
C(9)-C(5)-C(11)-C(10)	-35.50(17)
C(8)-C(10)-C(11)-C(5)	0.34(19)
C(17)-N(2)-C(12)-C(13)	120.07(17)
C(14)-N(2)-C(12)-C(13)	-56.4(2)
C(17)-N(2)-C(12)-C(9)	-112.50(17)
C(14)-N(2)-C(12)-C(9)	71.0(2)

C(8)-C(9)-C(12)-N(2)	-173.62(13)
C(5)-C(9)-C(12)-N(2)	77.18(18)
C(8)-C(9)-C(12)-C(13)	-46.86(19)
C(5)-C(9)-C(12)-C(13)	-156.06(15)
C(17)-N(2)-C(14)-C(15)	0.38(18)
C(12)-N(2)-C(14)-C(15)	177.27(15)
C(17)-N(2)-C(14)-C(18)	-179.47(17)
C(12)-N(2)-C(14)-C(18)	-2.6(3)
N(2)-C(14)-C(15)-C(16)	-0.11(19)
C(18)-C(14)-C(15)-C(16)	179.73(17)
C(14)-C(15)-C(16)-C(17)	-0.2(2)
C(15)-C(16)-C(17)-N(2)	0.43(19)
C(15)-C(16)-C(17)-C(19)	-178.89(17)
C(14)-N(2)-C(17)-C(16)	-0.51(18)
C(12)-N(2)-C(17)-C(16)	-177.55(15)
C(14)-N(2)-C(17)-C(19)	178.86(16)
C(12)-N(2)-C(17)-C(19)	1.8(2)



Structure Determination of 4.35.

Colorless needles of **4.35** were grown from a pentane solution of the compound at -8 deg. C. A crystal of dimensions 0.11 x 0.02 x 0.02 mm was mounted on a Rigaku AFC10K Saturn 944+ CCD-based X-ray diffractometer equipped with a low temperature device and Micromax-007HF Cu-target micro-focus rotating anode ($\lambda = 1.54187 \text{ \AA}$) operated at 1.2 kW power (40 kV, 30 mA). The X-ray intensities were measured at 85(1) K with the detector placed at a distance 42.00 mm from the crystal. A total of 2028 images were collected with an oscillation width of 1.0° in ω . The exposure times were 5 sec. for the low angle images, 45 sec. for high angle. Rigaku d*trek images were exported to CrysAlisPro for processing and corrected for absorption. The integration of the data yielded a total of 55277 reflections to a maximum 2θ value of 138.71° of which 6701 were independent and 5664 were greater than $2s(I)$. The final cell constants (Table 1) were based on the xyz centroids of 10427 reflections above $10s(I)$. Analysis of the data showed negligible decay during data collection. The structure was solved and refined with the Bruker SHELXTL (version 2018/3) software package, using the space group $P2(1)2(1)2(1)$ with $Z = 8$ for the formula $C_{18}H_{32}N_2O_3$. All non-hydrogen atoms were refined anisotropically with the

hydrogen atoms placed in a combination of idealized and refined positions. Full matrix least-squares refinement based on F^2 converged at $R1 = 0.0434$ and $wR2 = 0.0973$ [based on $I > 2\sigma(I)$], $R1 = 0.0563$ and $wR2 = 0.1053$ for all data. Additional details are presented in Table 1 and are given as Supporting Information in a CIF file. Acknowledgement is made for funding from NSF grant CHE-0840456 for X-ray instrumentation.

G.M. Sheldrick (2015) "Crystal structure refinement with SHELXL", *Acta Cryst.*, C71, 3-8 (Open Access).

CrystalClear Expert 2.0 r16, Rigaku Americas and Rigaku Corporation (2014), Rigaku Americas, 9009, TX, USA 77381-5209, Rigaku Tokyo, 196-8666, Japan.

CrysAlisPro 1.171.38.41 (Rigaku Oxford Diffraction, 2015).

Crystal data and structure refinement for **4.35**.

Identification code	4.35
Empirical formula	C ₁₈ H ₃₂ N ₂ O ₃
Formula weight	324.45
Temperature	85(2) K
Wavelength	1.54184 Å
Crystal system, space group	Orthorhombic, P2(1)2(1)2(1)
Unit cell dimensions	a = 5.76700(17) Å alpha = 90 deg. b = 18.6859(3) Å beta = 90 deg. c = 33.6202(7) Å gamma = 90 deg.
Volume	3622.98(14) Å ³
Z, Calculated density	8, 1.190 Mg/m ³
Absorption coefficient	0.640 mm ⁻¹
F(000)	1424
Crystal size	0.110 x 0.020 x 0.020 mm
Theta range for data collection	2.629 to 69.354 deg.
Limiting indices	-6 ≤ h ≤ 6, -22 ≤ k ≤ 22, -40 ≤ l ≤ 40
Reflections collected / unique	55277 / 6701 [R(int) = 0.0930]
Completeness to theta = 67.684	100.0 %
Absorption correction	Semi-empirical from equivalents
Max. and min. transmission	1.00000 and 0.64664
Refinement method	Full-matrix least-squares on F^2
Data / restraints / parameters	6701 / 0 / 432
Goodness-of-fit on F^2	1.070
Final R indices [$I > 2\sigma(I)$]	R1 = 0.0434, wR2 = 0.0973

R indices (all data) R1 = 0.0563, wR2 = 0.1053
 Absolute structure parameter -0.06(12)
 Extinction coefficient 0.00075(13)
 Largest diff. peak and hole 0.159 and -0.174 e.A⁻³

Atomic coordinates (x 10⁴) and equivalent isotropic displacement parameters (A² x 10³) for **4.35**.

U(eq) is defined as one third of the trace of the orthogonalized Uij tensor.

	x	y	z	U(eq)
O(1)	6347(4)	4210(1)	4602(1)	39(1)
O(2)	9501(5)	4902(1)	4757(1)	48(1)
O(3)	4810(4)	3349(1)	5863(1)	39(1)
O(4)	8974(4)	8680(1)	6634(1)	40(1)
O(5)	6206(5)	7932(1)	6888(1)	43(1)
O(6)	10088(4)	9743(1)	7874(1)	43(1)
N(1)	5775(6)	5298(1)	4831(1)	42(1)
N(2)	6087(5)	4807(1)	5702(1)	32(1)
N(3)	10097(6)	7697(1)	6936(1)	37(1)
N(4)	9713(4)	8230(1)	7793(1)	31(1)
C(1)	7686(6)	3610(1)	4430(1)	35(1)
C(2)	9304(6)	3291(2)	4736(1)	42(1)
C(3)	5794(6)	3086(1)	4322(1)	40(1)
C(4)	8963(7)	3862(2)	4063(1)	47(1)
C(5)	7419(7)	4814(1)	4735(1)	39(1)
C(6)	6371(8)	5988(1)	5011(1)	45(1)
C(7)	5612(10)	6596(2)	4735(1)	69(1)
C(8)	5309(6)	6072(1)	5427(1)	36(1)
C(9)	6266(6)	5587(1)	5767(1)	32(1)
C(10)	5024(6)	5893(1)	6136(1)	36(1)
C(11)	4817(6)	6704(1)	6042(1)	40(1)
C(12)	6043(6)	6773(1)	5640(1)	38(1)
C(13)	8627(6)	6659(1)	5704(1)	41(1)
C(14)	8795(6)	5840(1)	5789(1)	38(1)
C(15)	3713(6)	4549(1)	5654(1)	35(1)
C(16)	3720(6)	3757(1)	5554(1)	37(1)
C(17)	7112(6)	3602(1)	5919(1)	39(1)
C(18)	7161(6)	4393(1)	6026(1)	34(1)
C(19)	7346(6)	9164(1)	6432(1)	40(1)
C(20)	5820(7)	9540(2)	6733(1)	45(1)
C(21)	9019(7)	9684(1)	6236(1)	44(1)
C(22)	5937(7)	8762(2)	6122(1)	48(1)

C(23)	8221(7)	8081(1)	6827(1)	38(1)
C(24)	9884(7)	7001(1)	7133(1)	39(1)
C(25)	10965(9)	6436(1)	6864(1)	57(1)
C(26)	11045(6)	6998(1)	7542(1)	32(1)
C(27)	9948(6)	7462(1)	7877(1)	31(1)
C(28)	11479(6)	7252(1)	8237(1)	34(1)
C(29)	11975(6)	6448(1)	8167(1)	34(1)
C(30)	10724(5)	6287(1)	7774(1)	33(1)
C(31)	8119(6)	6287(1)	7856(1)	36(1)
C(32)	7597(6)	7092(1)	7937(1)	35(1)
C(33)	8414(6)	8620(1)	8098(1)	35(1)
C(34)	7979(6)	9377(1)	7954(1)	40(1)
C(35)	11407(6)	9358(1)	7583(1)	39(1)
C(36)	11899(6)	8603(1)	7723(1)	34(1)

Bond lengths [Å] and angles [deg] for **4.35**.

O(1)-C(5)	1.362(4)
O(1)-C(1)	1.480(3)
O(2)-C(5)	1.215(4)
O(3)-C(17)	1.422(4)
O(3)-C(16)	1.434(4)
O(4)-C(23)	1.367(4)
O(4)-C(19)	1.469(4)
O(5)-C(23)	1.212(4)
O(6)-C(34)	1.422(4)
O(6)-C(35)	1.433(4)
N(1)-C(5)	1.349(4)
N(1)-C(6)	1.464(4)
N(1)-H(1N)	0.93(4)
N(2)-C(15)	1.461(4)
N(2)-C(18)	1.471(3)
N(2)-C(9)	1.477(3)
N(3)-C(23)	1.349(5)
N(3)-C(24)	1.464(3)
N(3)-H(3N)	0.90(4)
N(4)-C(36)	1.460(4)
N(4)-C(33)	1.465(4)
N(4)-C(27)	1.468(3)
C(1)-C(3)	1.511(4)
C(1)-C(4)	1.511(4)
C(1)-C(2)	1.512(4)
C(2)-H(2A)	0.9800
C(2)-H(2B)	0.9800

C(2)-H(2C)	0.9800
C(3)-H(3A)	0.9800
C(3)-H(3B)	0.9800
C(3)-H(3C)	0.9800
C(4)-H(4A)	0.9800
C(4)-H(4B)	0.9800
C(4)-H(4C)	0.9800
C(6)-C(7)	1.531(4)
C(6)-C(8)	1.536(4)
C(6)-H(6)	1.0000
C(7)-H(7A)	0.9800
C(7)-H(7B)	0.9800
C(7)-H(7C)	0.9800
C(8)-C(12)	1.553(4)
C(8)-C(9)	1.559(4)
C(8)-H(8)	1.0000
C(9)-C(14)	1.535(5)
C(9)-C(10)	1.542(4)
C(10)-C(11)	1.552(4)
C(10)-H(10A)	0.9900
C(10)-H(10B)	0.9900
C(11)-C(12)	1.531(4)
C(11)-H(11A)	0.9900
C(11)-H(11B)	0.9900
C(12)-C(13)	1.521(5)
C(12)-H(12)	1.0000
C(13)-C(14)	1.559(4)
C(13)-H(13A)	0.9900
C(13)-H(13B)	0.9900
C(14)-H(14A)	0.9900
C(14)-H(14B)	0.9900
C(15)-C(16)	1.518(3)
C(15)-H(15A)	0.9900
C(15)-H(15B)	0.9900
C(16)-H(16A)	0.9900
C(16)-H(16B)	0.9900
C(17)-C(18)	1.520(4)
C(17)-H(17A)	0.9900
C(17)-H(17B)	0.9900
C(18)-H(18A)	0.9900
C(18)-H(18B)	0.9900
C(19)-C(20)	1.514(4)
C(19)-C(21)	1.521(5)
C(19)-C(22)	1.521(4)
C(20)-H(20A)	0.9800
C(20)-H(20B)	0.9800

C(20)-H(20C)	0.9800
C(21)-H(21A)	0.9800
C(21)-H(21B)	0.9800
C(21)-H(21C)	0.9800
C(22)-H(22A)	0.9800
C(22)-H(22B)	0.9800
C(22)-H(22C)	0.9800
C(24)-C(25)	1.525(4)
C(24)-C(26)	1.527(4)
C(24)-H(24)	1.0000
C(25)-H(25A)	0.9800
C(25)-H(25B)	0.9800
C(25)-H(25C)	0.9800
C(26)-C(30)	1.553(3)
C(26)-C(27)	1.557(4)
C(26)-H(26)	1.0000
C(27)-C(32)	1.535(4)
C(27)-C(28)	1.547(4)
C(28)-C(29)	1.547(3)
C(28)-H(28A)	0.9900
C(28)-H(28B)	0.9900
C(29)-C(30)	1.536(4)
C(29)-H(29A)	0.9900
C(29)-H(29B)	0.9900
C(30)-C(31)	1.527(5)
C(30)-H(30)	1.0000
C(31)-C(32)	1.558(4)
C(31)-H(31A)	0.9900
C(31)-H(31B)	0.9900
C(32)-H(32A)	0.9900
C(32)-H(32B)	0.9900
C(33)-C(34)	1.516(4)
C(33)-H(33A)	0.9900
C(33)-H(33B)	0.9900
C(34)-H(34A)	0.9900
C(34)-H(34B)	0.9900
C(35)-C(36)	1.514(4)
C(35)-H(35A)	0.9900
C(35)-H(35B)	0.9900
C(36)-H(36A)	0.9900
C(36)-H(36B)	0.9900
C(5)-O(1)-C(1)	121.3(3)
C(17)-O(3)-C(16)	109.2(2)
C(23)-O(4)-C(19)	121.4(3)
C(34)-O(6)-C(35)	110.0(2)

C(5)-N(1)-C(6)	121.6(3)
C(5)-N(1)-H(1N)	119(2)
C(6)-N(1)-H(1N)	119(2)
C(15)-N(2)-C(18)	107.6(2)
C(15)-N(2)-C(9)	114.1(2)
C(18)-N(2)-C(9)	112.4(2)
C(23)-N(3)-C(24)	121.8(3)
C(23)-N(3)-H(3N)	120(2)
C(24)-N(3)-H(3N)	118(2)
C(36)-N(4)-C(33)	108.5(2)
C(36)-N(4)-C(27)	114.7(2)
C(33)-N(4)-C(27)	113.5(2)
O(1)-C(1)-C(3)	102.0(2)
O(1)-C(1)-C(4)	109.8(2)
C(3)-C(1)-C(4)	111.1(2)
O(1)-C(1)-C(2)	110.7(2)
C(3)-C(1)-C(2)	110.7(2)
C(4)-C(1)-C(2)	112.2(3)
C(1)-C(2)-H(2A)	109.5
C(1)-C(2)-H(2B)	109.5
H(2A)-C(2)-H(2B)	109.5
C(1)-C(2)-H(2C)	109.5
H(2A)-C(2)-H(2C)	109.5
H(2B)-C(2)-H(2C)	109.5
C(1)-C(3)-H(3A)	109.5
C(1)-C(3)-H(3B)	109.5
H(3A)-C(3)-H(3B)	109.5
C(1)-C(3)-H(3C)	109.5
H(3A)-C(3)-H(3C)	109.5
H(3B)-C(3)-H(3C)	109.5
C(1)-C(4)-H(4A)	109.5
C(1)-C(4)-H(4B)	109.5
H(4A)-C(4)-H(4B)	109.5
C(1)-C(4)-H(4C)	109.5
H(4A)-C(4)-H(4C)	109.5
H(4B)-C(4)-H(4C)	109.5
O(2)-C(5)-N(1)	126.1(3)
O(2)-C(5)-O(1)	125.5(3)
N(1)-C(5)-O(1)	108.4(3)
N(1)-C(6)-C(7)	109.7(3)
N(1)-C(6)-C(8)	111.8(3)
C(7)-C(6)-C(8)	111.2(3)
N(1)-C(6)-H(6)	108.0
C(7)-C(6)-H(6)	108.0
C(8)-C(6)-H(6)	108.0
C(6)-C(7)-H(7A)	109.5

C(6)-C(7)-H(7B)	109.5
H(7A)-C(7)-H(7B)	109.5
C(6)-C(7)-H(7C)	109.5
H(7A)-C(7)-H(7C)	109.5
H(7B)-C(7)-H(7C)	109.5
C(6)-C(8)-C(12)	113.5(2)
C(6)-C(8)-C(9)	117.8(2)
C(12)-C(8)-C(9)	93.2(2)
C(6)-C(8)-H(8)	110.4
C(12)-C(8)-H(8)	110.4
C(9)-C(8)-H(8)	110.4
N(2)-C(9)-C(14)	112.2(2)
N(2)-C(9)-C(10)	116.8(2)
C(14)-C(9)-C(10)	106.7(2)
N(2)-C(9)-C(8)	116.2(2)
C(14)-C(9)-C(8)	101.2(2)
C(10)-C(9)-C(8)	102.1(2)
C(9)-C(10)-C(11)	103.6(2)
C(9)-C(10)-H(10A)	111.0
C(11)-C(10)-H(10A)	111.0
C(9)-C(10)-H(10B)	111.0
C(11)-C(10)-H(10B)	111.0
H(10A)-C(10)-H(10B)	109.0
C(12)-C(11)-C(10)	103.0(2)
C(12)-C(11)-H(11A)	111.2
C(10)-C(11)-H(11A)	111.2
C(12)-C(11)-H(11B)	111.2
C(10)-C(11)-H(11B)	111.2
H(11A)-C(11)-H(11B)	109.1
C(13)-C(12)-C(11)	108.4(3)
C(13)-C(12)-C(8)	102.4(2)
C(11)-C(12)-C(8)	102.2(2)
C(13)-C(12)-H(12)	114.2
C(11)-C(12)-H(12)	114.2
C(8)-C(12)-H(12)	114.2
C(12)-C(13)-C(14)	103.0(3)
C(12)-C(13)-H(13A)	111.2
C(14)-C(13)-H(13A)	111.2
C(12)-C(13)-H(13B)	111.2
C(14)-C(13)-H(13B)	111.2
H(13A)-C(13)-H(13B)	109.1
C(9)-C(14)-C(13)	103.5(3)
C(9)-C(14)-H(14A)	111.1
C(13)-C(14)-H(14A)	111.1
C(9)-C(14)-H(14B)	111.1
C(13)-C(14)-H(14B)	111.1

H(14A)-C(14)-H(14B)	109.0
N(2)-C(15)-C(16)	110.1(3)
N(2)-C(15)-H(15A)	109.6
C(16)-C(15)-H(15A)	109.6
N(2)-C(15)-H(15B)	109.6
C(16)-C(15)-H(15B)	109.6
H(15A)-C(15)-H(15B)	108.2
O(3)-C(16)-C(15)	110.9(2)
O(3)-C(16)-H(16A)	109.5
C(15)-C(16)-H(16A)	109.5
O(3)-C(16)-H(16B)	109.5
C(15)-C(16)-H(16B)	109.5
H(16A)-C(16)-H(16B)	108.0
O(3)-C(17)-C(18)	111.8(3)
O(3)-C(17)-H(17A)	109.2
C(18)-C(17)-H(17A)	109.2
O(3)-C(17)-H(17B)	109.2
C(18)-C(17)-H(17B)	109.2
H(17A)-C(17)-H(17B)	107.9
N(2)-C(18)-C(17)	109.2(2)
N(2)-C(18)-H(18A)	109.8
C(17)-C(18)-H(18A)	109.8
N(2)-C(18)-H(18B)	109.8
C(17)-C(18)-H(18B)	109.8
H(18A)-C(18)-H(18B)	108.3
O(4)-C(19)-C(20)	110.4(2)
O(4)-C(19)-C(21)	100.9(3)
C(20)-C(19)-C(21)	111.3(2)
O(4)-C(19)-C(22)	110.7(2)
C(20)-C(19)-C(22)	112.2(3)
C(21)-C(19)-C(22)	110.9(3)
C(19)-C(20)-H(20A)	109.5
C(19)-C(20)-H(20B)	109.5
H(20A)-C(20)-H(20B)	109.5
C(19)-C(20)-H(20C)	109.5
H(20A)-C(20)-H(20C)	109.5
H(20B)-C(20)-H(20C)	109.5
C(19)-C(21)-H(21A)	109.5
C(19)-C(21)-H(21B)	109.5
H(21A)-C(21)-H(21B)	109.5
C(19)-C(21)-H(21C)	109.5
H(21A)-C(21)-H(21C)	109.5
H(21B)-C(21)-H(21C)	109.5
C(19)-C(22)-H(22A)	109.5
C(19)-C(22)-H(22B)	109.5
H(22A)-C(22)-H(22B)	109.5

C(19)-C(22)-H(22C)	109.5
H(22A)-C(22)-H(22C)	109.5
H(22B)-C(22)-H(22C)	109.5
O(5)-C(23)-N(3)	126.9(3)
O(5)-C(23)-O(4)	125.0(3)
N(3)-C(23)-O(4)	108.1(3)
N(3)-C(24)-C(25)	108.2(2)
N(3)-C(24)-C(26)	111.9(2)
C(25)-C(24)-C(26)	110.6(3)
N(3)-C(24)-H(24)	108.7
C(25)-C(24)-H(24)	108.7
C(26)-C(24)-H(24)	108.7
C(24)-C(25)-H(25A)	109.5
C(24)-C(25)-H(25B)	109.5
H(25A)-C(25)-H(25B)	109.5
C(24)-C(25)-H(25C)	109.5
H(25A)-C(25)-H(25C)	109.5
H(25B)-C(25)-H(25C)	109.5
C(24)-C(26)-C(30)	113.8(2)
C(24)-C(26)-C(27)	118.1(3)
C(30)-C(26)-C(27)	93.64(19)
C(24)-C(26)-H(26)	110.1
C(30)-C(26)-H(26)	110.1
C(27)-C(26)-H(26)	110.1
N(4)-C(27)-C(32)	112.6(2)
N(4)-C(27)-C(28)	116.8(2)
C(32)-C(27)-C(28)	106.7(2)
N(4)-C(27)-C(26)	116.2(2)
C(32)-C(27)-C(26)	101.7(2)
C(28)-C(27)-C(26)	101.2(2)
C(29)-C(28)-C(27)	103.5(2)
C(29)-C(28)-H(28A)	111.1
C(27)-C(28)-H(28A)	111.1
C(29)-C(28)-H(28B)	111.1
C(27)-C(28)-H(28B)	111.1
H(28A)-C(28)-H(28B)	109.0
C(30)-C(29)-C(28)	103.5(2)
C(30)-C(29)-H(29A)	111.1
C(28)-C(29)-H(29A)	111.1
C(30)-C(29)-H(29B)	111.1
C(28)-C(29)-H(29B)	111.1
H(29A)-C(29)-H(29B)	109.0
C(31)-C(30)-C(29)	107.9(2)
C(31)-C(30)-C(26)	101.9(2)
C(29)-C(30)-C(26)	102.0(2)
C(31)-C(30)-H(30)	114.5

C(29)-C(30)-H(30)	114.5
C(26)-C(30)-H(30)	114.5
C(30)-C(31)-C(32)	102.9(2)
C(30)-C(31)-H(31A)	111.2
C(32)-C(31)-H(31A)	111.2
C(30)-C(31)-H(31B)	111.2
C(32)-C(31)-H(31B)	111.2
H(31A)-C(31)-H(31B)	109.1
C(27)-C(32)-C(31)	103.9(2)
C(27)-C(32)-H(32A)	111.0
C(31)-C(32)-H(32A)	111.0
C(27)-C(32)-H(32B)	111.0
C(31)-C(32)-H(32B)	111.0
H(32A)-C(32)-H(32B)	109.0
N(4)-C(33)-C(34)	108.9(2)
N(4)-C(33)-H(33A)	109.9
C(34)-C(33)-H(33A)	109.9
N(4)-C(33)-H(33B)	109.9
C(34)-C(33)-H(33B)	109.9
H(33A)-C(33)-H(33B)	108.3
O(6)-C(34)-C(33)	111.6(3)
O(6)-C(34)-H(34A)	109.3
C(33)-C(34)-H(34A)	109.3
O(6)-C(34)-H(34B)	109.3
C(33)-C(34)-H(34B)	109.3
H(34A)-C(34)-H(34B)	108.0
O(6)-C(35)-C(36)	110.8(2)
O(6)-C(35)-H(35A)	109.5
C(36)-C(35)-H(35A)	109.5
O(6)-C(35)-H(35B)	109.5
C(36)-C(35)-H(35B)	109.5
H(35A)-C(35)-H(35B)	108.1
N(4)-C(36)-C(35)	109.5(3)
N(4)-C(36)-H(36A)	109.8
C(35)-C(36)-H(36A)	109.8
N(4)-C(36)-H(36B)	109.8
C(35)-C(36)-H(36B)	109.8
H(36A)-C(36)-H(36B)	108.2

Symmetry transformations used to generate equivalent atoms:

Anisotropic displacement parameters ($\text{\AA}^2 \times 10^3$) for **4.35**.

The anisotropic displacement factor exponent takes the form:

$$-2 \pi^2 [h^2 a^{*2} U_{11} + \dots + 2 h k a^* b^* U_{12}]$$

	U11	U22	U33	U23	U13	U12
O(1)	56(1)	23(1)	36(1)	-4(1)	2(1)	7(1)
O(2)	66(2)	30(1)	49(1)	-4(1)	4(1)	-2(1)
O(3)	50(1)	26(1)	42(1)	3(1)	-5(1)	-4(1)
O(4)	57(1)	23(1)	40(1)	7(1)	-1(1)	2(1)
O(5)	58(2)	30(1)	40(1)	2(1)	-2(1)	-3(1)
O(6)	56(1)	24(1)	48(1)	-4(1)	4(1)	2(1)
N(1)	64(2)	25(1)	36(1)	-3(1)	-4(1)	7(1)
N(2)	41(2)	21(1)	33(1)	1(1)	-2(1)	-1(1)
N(3)	57(2)	22(1)	34(1)	3(1)	1(1)	-3(1)
N(4)	42(2)	20(1)	33(1)	-2(1)	2(1)	2(1)
C(1)	52(2)	23(1)	30(1)	-3(1)	4(1)	6(1)
C(2)	56(2)	30(1)	39(1)	-2(1)	-3(2)	7(1)
C(3)	52(2)	29(1)	40(2)	-6(1)	-2(2)	2(1)
C(4)	68(2)	36(1)	37(2)	1(1)	10(2)	1(2)
C(5)	60(3)	24(1)	32(1)	1(1)	-1(2)	4(2)
C(6)	76(3)	21(1)	37(1)	0(1)	0(2)	5(2)
C(7)	143(4)	28(1)	37(2)	2(1)	-5(2)	17(2)
C(8)	47(2)	24(1)	36(1)	-1(1)	-4(1)	4(1)
C(9)	42(2)	20(1)	33(1)	-1(1)	-2(1)	2(1)
C(10)	45(2)	28(1)	35(1)	-4(1)	2(1)	0(1)
C(11)	49(2)	28(1)	43(2)	-8(1)	-2(2)	1(1)
C(12)	51(2)	20(1)	42(2)	-2(1)	-2(1)	3(1)
C(13)	49(2)	23(1)	50(2)	-1(1)	0(2)	-1(1)
C(14)	44(2)	25(1)	45(2)	0(1)	-1(1)	-1(1)
C(15)	42(2)	26(1)	38(1)	-1(1)	-2(1)	0(1)
C(16)	44(2)	28(1)	39(1)	-2(1)	-5(1)	-1(1)
C(17)	51(2)	28(1)	37(1)	5(1)	-4(1)	1(1)
C(18)	43(2)	28(1)	32(1)	2(1)	-4(1)	-1(1)
C(19)	57(2)	25(1)	37(1)	4(1)	-2(1)	4(1)
C(20)	59(2)	30(1)	45(2)	1(1)	3(2)	4(2)
C(21)	61(2)	28(1)	42(2)	7(1)	2(2)	6(2)
C(22)	67(2)	36(1)	39(2)	-1(1)	-4(2)	-1(2)
C(23)	61(2)	22(1)	30(1)	-2(1)	0(2)	-1(2)
C(24)	67(2)	19(1)	31(1)	2(1)	-3(2)	-2(1)
C(25)	117(3)	23(1)	31(1)	-2(1)	2(2)	5(2)
C(26)	45(2)	21(1)	30(1)	1(1)	2(1)	0(1)
C(27)	42(2)	19(1)	30(1)	0(1)	1(1)	0(1)
C(28)	47(2)	22(1)	31(1)	0(1)	0(1)	-1(1)
C(29)	46(2)	24(1)	34(1)	3(1)	-2(1)	0(1)
C(30)	50(2)	20(1)	31(1)	1(1)	0(1)	1(1)

C(31)	49(2)	22(1)	37(1)	2(1)	-3(1)	-5(1)
C(32)	42(2)	26(1)	36(1)	-1(1)	0(1)	-2(1)
C(33)	44(2)	26(1)	36(1)	-2(1)	3(1)	3(1)
C(34)	46(2)	27(1)	47(2)	-3(1)	4(2)	4(1)
C(35)	52(2)	24(1)	39(1)	1(1)	5(1)	2(1)
C(36)	43(2)	22(1)	38(1)	-1(1)	1(1)	-2(1)

Hydrogen coordinates (x 10⁴) and isotropic displacement parameters (A² x 10³) for **4.35**.

	x	y	z	U(eq)
H(1N)	4220(70)	5180(17)	4793(9)	36(9)
H(3N)	11520(70)	7844(18)	6864(10)	42(10)
H(2A)	10522	3638	4801	63
H(2B)	10012	2855	4628	63
H(2C)	8428	3174	4977	63
H(3A)	4983	2934	4564	60
H(3B)	6479	2667	4192	60
H(3C)	4691	3315	4141	60
H(4A)	7867	4092	3880	71
H(4B)	9686	3451	3931	71
H(4C)	10164	4207	4140	71
H(6)	8096	6010	5038	54
H(7A)	6280	6523	4470	104
H(7B)	6153	7054	4843	104
H(7C)	3916	6602	4716	104
H(8)	3580	6037	5413	43
H(10A)	5949	5811	6379	43
H(10B)	3475	5673	6170	43
H(11A)	3173	6853	6023	48
H(11B)	5600	6996	6248	48
H(12)	5651	7219	5491	45
H(13A)	9199	6942	5933	49
H(13B)	9523	6791	5464	49
H(14A)	9762	5597	5587	46
H(14B)	9459	5749	6056	46
H(15A)	2936	4819	5439	42
H(15B)	2835	4628	5904	42
H(16A)	2105	3589	5518	44
H(16B)	4561	3681	5300	44
H(17A)	8013	3525	5672	46

H(17B)	7861	3325	6135	46
H(18A)	6302	4473	6277	41
H(18B)	8783	4551	6065	41
H(20A)	4793	9191	6860	67
H(20B)	4886	9905	6598	67
H(20C)	6793	9768	6936	67
H(21A)	9968	9917	6440	66
H(21B)	8140	10048	6089	66
H(21C)	10026	9424	6051	66
H(22A)	6969	8455	5965	71
H(22B)	5166	9105	5946	71
H(22C)	4768	8466	6255	71
H(24)	8201	6889	7168	47
H(25A)	10277	6469	6598	85
H(25B)	10673	5959	6974	85
H(25C)	12641	6517	6846	85
H(26)	12732	7111	7515	38
H(28A)	12934	7533	8241	40
H(28B)	10643	7328	8491	40
H(29A)	13661	6358	8144	41
H(29B)	11344	6154	8387	41
H(30)	11303	5852	7632	40
H(31A)	7736	5988	8090	43
H(31B)	7240	6111	7622	43
H(32A)	6429	7278	7748	42
H(32B)	7023	7163	8212	42
H(33A)	9310	8631	8350	42
H(33B)	6919	8377	8150	42
H(34A)	7027	9361	7709	48
H(34B)	7096	9643	8159	48
H(35A)	12890	9610	7534	46
H(35B)	10535	9341	7329	46
H(36A)	12811	8345	7519	41
H(36B)	12819	8617	7971	41

Torsion angles [deg] for **4.35**.

C(5)-O(1)-C(1)-C(3)	-179.0(2)
C(5)-O(1)-C(1)-C(4)	-61.1(3)
C(5)-O(1)-C(1)-C(2)	63.3(3)
C(6)-N(1)-C(5)-O(2)	-5.4(5)
C(6)-N(1)-C(5)-O(1)	175.6(2)
C(1)-O(1)-C(5)-O(2)	-6.3(4)
C(1)-O(1)-C(5)-N(1)	172.7(2)

C(5)-N(1)-C(6)-C(7)	118.0(4)
C(5)-N(1)-C(6)-C(8)	-118.1(3)
N(1)-C(6)-C(8)-C(12)	175.9(3)
C(7)-C(6)-C(8)-C(12)	-61.1(4)
N(1)-C(6)-C(8)-C(9)	68.5(4)
C(7)-C(6)-C(8)-C(9)	-168.4(3)
C(15)-N(2)-C(9)-C(14)	-176.4(2)
C(18)-N(2)-C(9)-C(14)	60.7(3)
C(15)-N(2)-C(9)-C(10)	60.0(3)
C(18)-N(2)-C(9)-C(10)	-62.9(4)
C(15)-N(2)-C(9)-C(8)	-60.7(3)
C(18)-N(2)-C(9)-C(8)	176.4(3)
C(6)-C(8)-C(9)-N(2)	-58.7(4)
C(12)-C(8)-C(9)-N(2)	-177.4(3)
C(6)-C(8)-C(9)-C(14)	63.1(3)
C(12)-C(8)-C(9)-C(14)	-55.6(3)
C(6)-C(8)-C(9)-C(10)	173.1(3)
C(12)-C(8)-C(9)-C(10)	54.3(3)
N(2)-C(9)-C(10)-C(11)	-161.5(3)
C(14)-C(9)-C(10)-C(11)	72.1(3)
C(8)-C(9)-C(10)-C(11)	-33.6(3)
C(9)-C(10)-C(11)-C(12)	-2.1(3)
C(10)-C(11)-C(12)-C(13)	-70.3(3)
C(10)-C(11)-C(12)-C(8)	37.3(3)
C(6)-C(8)-C(12)-C(13)	-66.2(3)
C(9)-C(8)-C(12)-C(13)	56.1(3)
C(6)-C(8)-C(12)-C(11)	-178.4(3)
C(9)-C(8)-C(12)-C(11)	-56.1(3)
C(11)-C(12)-C(13)-C(14)	71.9(3)
C(8)-C(12)-C(13)-C(14)	-35.6(3)
N(2)-C(9)-C(14)-C(13)	160.5(2)
C(10)-C(9)-C(14)-C(13)	-70.4(3)
C(8)-C(9)-C(14)-C(13)	36.0(3)
C(12)-C(13)-C(14)-C(9)	-0.5(3)
C(18)-N(2)-C(15)-C(16)	-59.6(3)
C(9)-N(2)-C(15)-C(16)	175.0(2)
C(17)-O(3)-C(16)-C(15)	-57.9(3)
N(2)-C(15)-C(16)-O(3)	60.0(3)
C(16)-O(3)-C(17)-C(18)	58.4(3)
C(15)-N(2)-C(18)-C(17)	59.0(3)
C(9)-N(2)-C(18)-C(17)	-174.6(3)
O(3)-C(17)-C(18)-N(2)	-60.0(3)
C(23)-O(4)-C(19)-C(20)	67.7(3)
C(23)-O(4)-C(19)-C(21)	-174.6(2)
C(23)-O(4)-C(19)-C(22)	-57.1(3)
C(24)-N(3)-C(23)-O(5)	3.3(4)

C(24)-N(3)-C(23)-O(4)	-176.9(2)
C(19)-O(4)-C(23)-O(5)	-8.2(4)
C(19)-O(4)-C(23)-N(3)	172.0(2)
C(23)-N(3)-C(24)-C(25)	117.3(3)
C(23)-N(3)-C(24)-C(26)	-120.6(3)
N(3)-C(24)-C(26)-C(30)	176.2(3)
C(25)-C(24)-C(26)-C(30)	-63.1(4)
N(3)-C(24)-C(26)-C(27)	67.8(4)
C(25)-C(24)-C(26)-C(27)	-171.5(3)
C(36)-N(4)-C(27)-C(32)	-178.4(2)
C(33)-N(4)-C(27)-C(32)	56.1(3)
C(36)-N(4)-C(27)-C(28)	57.7(3)
C(33)-N(4)-C(27)-C(28)	-67.8(3)
C(36)-N(4)-C(27)-C(26)	-61.7(3)
C(33)-N(4)-C(27)-C(26)	172.8(3)
C(24)-C(26)-C(27)-N(4)	-57.4(4)
C(30)-C(26)-C(27)-N(4)	-177.0(3)
C(24)-C(26)-C(27)-C(32)	65.2(3)
C(30)-C(26)-C(27)-C(32)	-54.3(2)
C(24)-C(26)-C(27)-C(28)	175.1(2)
C(30)-C(26)-C(27)-C(28)	55.5(2)
N(4)-C(27)-C(28)-C(29)	-163.3(2)
C(32)-C(27)-C(28)-C(29)	69.9(3)
C(26)-C(27)-C(28)-C(29)	-36.1(3)
C(27)-C(28)-C(29)-C(30)	1.0(3)
C(28)-C(29)-C(30)-C(31)	-72.2(3)
C(28)-C(29)-C(30)-C(26)	34.7(3)
C(24)-C(26)-C(30)-C(31)	-66.7(3)
C(27)-C(26)-C(30)-C(31)	56.2(2)
C(24)-C(26)-C(30)-C(29)	-178.3(3)
C(27)-C(26)-C(30)-C(29)	-55.3(3)
C(29)-C(30)-C(31)-C(32)	69.8(2)
C(26)-C(30)-C(31)-C(32)	-37.2(3)
N(4)-C(27)-C(32)-C(31)	158.6(2)
C(28)-C(27)-C(32)-C(31)	-72.1(2)
C(26)-C(27)-C(32)-C(31)	33.5(3)
C(30)-C(31)-C(32)-C(27)	2.1(3)
C(36)-N(4)-C(33)-C(34)	59.3(3)
C(27)-N(4)-C(33)-C(34)	-171.9(3)
C(35)-O(6)-C(34)-C(33)	57.9(3)
N(4)-C(33)-C(34)-O(6)	-59.2(3)
C(34)-O(6)-C(35)-C(36)	-57.7(3)
C(33)-N(4)-C(36)-C(35)	-59.9(3)
C(27)-N(4)-C(36)-C(35)	172.0(2)
O(6)-C(35)-C(36)-N(4)	59.5(3)

4.10 References

1. Wu, Y-J.; Boissard, C.G.; Greco, C.; Gribkoff, V.K.; Harden, D.G.; He, H.; L'Heureux, A.; Kang, S.H.; Kinney, G.G.; Knox, R.J.; Natale, J.; Newton, A.E.; Lehtinen-Oboma, S.; Sinz, M.W.; Sivarao, D.V.; Starrett Jr., J.E.; Sun, L-Q.; Tertyshnikova, S.; Thompson, M.W.; Weaver, D.; Wong, H.S.; Zhang, L.; Dworetzky, S.I. "(S)-N-[1-(3-Morpholin-4-ylphenyl)ethyl]-3-phenylacrylamide: An Orally Bioavailable KCNQ2 Opener with Significant Activity in a Cortical Spreading Depression Model of Migraine." *J. Med. Chem.* **2003**, *46*, 3197-3200.
2. Wu, Y-J.; Davis, C.D.; Dworetzky, S.; Fitzpatrick, W.C.; Harden, D.; He, H.; Knox, R.J.; Newton, A.E.; Philip, T.; Polson, C.; Sivarao, D.V.; Sun, L-Q.; Tertyshnikova, S.; Weaver, D.; Yeola, S.; Zoeckler, M.; Sinz, M.W. "Fluorine Substitution Can Block CYP3A4 Metabolism-Dependent Inhibition: Identification of (S)-N-[1-(4-Fluoro-3-morpholin-4-ylphenyl)ethyl]-3-(4-fluorophenyl)acrylamide as an Orally Bioavailable KCNQ2 Opener Devoid of CYP3A4 Metabolism-Dependent Inhibition." *J. Med. Chem.* **2003**, *46*, 3778-3781.
3. Wu, Y-J.; He, H.; Sun, L-Q.; L'Heureux, A.; Chen, J.; Dextraze, P.; Starrett Jr., J.E.; Boissard, C.G.; Gribkoff, V.K.; Natale, J.; Dworetzky, S.I. "Synthesis and Structure-Activity Relationship of Acrylamides as KCNQ2 Potassium Channel Openers." *J. Med. Chem.* **2004**, *47*, 2887-2896.
4. Wu, Y-J.; Boissard, C.G.; Chen, J.; Fitzpatrick, W.; Gao, Q.; Gribkoff, V.K.; Harden, D.G.; He, H.; Know, R.J.; Natale, J.; Pieschl, R.L.; Starrett Jr.; J.E.; Sun, L-Q.; Thompson, M.; Weaver, D.; Wu, D.; Dworetzky, S.I. "(S)-N-[1-(4-Cyclopropylmethyl-3,4-dihydro-2H-benzo-1,4-oxazin-6-yl)-ethyl]-3-(2-fluoro-phenyl)-acrylamide is a potent and efficacious KCNQ2 opener which inhibits induced hyperexcitability of rat hippocampal neurons." *Bioorg. Med. Chem. Lett.* **2004**, *14*, 1991-1995.
5. Wu, Y-J.; Conway, C.M.; Sun, L-Q.; Machet, F.; Chen, J.; Chen, P.; He, H.; Bourin, C.; Calandra, V.; Polino, J.L.; Davis, C.D.; Heman, K.; Gribkoff, V.K.; Boissard, C.G.; Knox, R.J.; Thompson, M.W.; Fitzpatrick, W.; Weaver, D.; Harden, D.G.; Natale, J.; Dworetzky, S.I.; Starrett Jr.; J.E. "Discovery of (S,E)-3-(2-fluorophenyl)-N-(1-(3-(pyridine-3-yloxy)phenyl)ethyl)-acrylamide as a potent and efficacious KCNQ2 (Kv7.2) opener for the treatment of neuropathic pain." *Bioorg. Med. Chem. Lett.* **2013**, *23*, 6188-6191.
6. Bansal, E.; Srivastava, V.K.; Kumar, A. "Synthesis and anti-inflammatory activity of 1-acetyl-5-substitutedaryl-3-(β -aminonaphthyl)-2-pyrazolines and β -(substituted aminoethyl) amidonaphthalenes." *Eur. J. Med. Chem.* **2001**, *36*, 81-92.
7. Behloul, C.; Guijarro, D.; Yus, M. "Deacylation of Esters, Thioesters and Amides by a Naphthalene-Catalysed Lithiation." *Synthesis*, **2006**, *2*, 309-314.
8. Bechara, W.S.; Pelletier, G.; Charette, A.B. "Chemoselective synthesis of ketones and ketimines by addition of organometallic reagents to secondary amides." *Nat. Chem.* **2012**, *4*, 228-234.
9. Koenig, S.G.; Vandenbossche, C.P.; Zhao, H.; Mousaw, P.; Singh, S.P.; Bakale, R.P. "A Facile Deprotection of Secondary Acetamides." *Org. Lett.* **2009**, *11*, 433-436.

10. Zimmerman, H.E.; Wang, P. "Inter- and Intramolecular Stereoselective Protonation of Enols." *J. Org. Chem.* **2002**, *67*, 9216-9226.
11. Staveness, D.; Collins III, J.L.; McAtee, R.C.; Stephenson, C.R.J. "Exploiting Imine Photochemistry for Masked N-Centered Radical Reactivity." *Angew. Chem. Int. Ed.* **2019**, *58*, 19000-19006.
12. Heitzman, C.L.; Lambert, W.T.; Mertz, E.; Shotwell, J.B.; Tinsley, J.M.; Va, P.; Roush, W.R. "Efficient Protodesilylation of Unactivated C(sp³)-SiMe₂Ph Bonds Using Tetrabutylammonium Fluoride." *Org. Lett.* **2005**, *7*, 2405-2408.
13. Bian, Z.; Marvin, C.C.; Pettersson, M.; Martin, S.F. "Enantioselective Total Syntheses of Citrinadins A and B. Stereochemical Revision of Their Assigned Structures." *J. Am. Chem. Soc.* **2014**, *136*, 14184-14192.
14. Pietraszuk, C.; Marciniak, B.; Fischer, H. "Cross-metathesis of vinylsilanes carrying electron-withdrawing substituents with olefins in the presence of the second-generation Grubbs catalyst." *Tetrahedron Lett.* **2003**, *44*, 7121-7124.
15. Pietraszuk, C.; Fischer, H.; Rogalski, S.; Marciniak, B. "The effect of substituents at silicon on the cross-metathesis of trisubstituted vinylsilanes with olefins." *J. Organomet. Chem.* **2005**, *690*, 5912-5921.
16. Limbach, M.; Dalai, S.; de Meijere, A. "Cyclopropyl Building Blocks for Organic Synthesis, Part 11. Advanced Syntheses of Cyclopropylideneacetates – Versatile Multifunctional Building Blocks for Organic Synthesis." *Adv. Synth. Catal.* **2004**, *346*, 760-766.
17. O'Leary, D.J.; Blackwell, H.E.; Washenfelder, R.A.; Miura, K.; Grubbs, R.H. "Terminal Olefin Cross-Metathesis with Acrolein Acetals." *Tetrahedron Lett.* **1999**, *40*, 1091-1094.
18. Mantel, M.; Guder, M.; Pietruszka, J. "Simple organocatalysts in multi-step reactions: An efficient one-pot Morita-Baylis-Hillman-type α -hydroxymethylation of vinyl ketones followed by the convenient, temperature-controlled one-pot etherification using alcohols." *Tetrahedron*, **2018**, *74*, 5442-5450.
19. Kim, R.Y.; Yau, M.C.; Galpin, J.D.; Seebohm, G.; Ahern, C.A.; Pless, S.A.; Kurata, H.T. "Atomic basis for the therapeutic activation of neuronal potassium channels." *Nature Commun.* **2015**, *6*, 8116.
20. Kaljurand, I.; Lilleorg, R.; Murumaa, A.; Mishima, M.; Burk, P.; Koppel, I.; Koppel, I.A.; Leito, I. "The basicity of substituted *N,N*-dimethylanilines in solution and in the gas phase." *J. Phys. Org. Chem.* **2013**, *26*, 171-181.
21. Hall Jr., H.K. "Correlation of the Base Strengths of Amines." *J. Am. Chem. Soc.* **1957**, *79*, 5441-5444.

22. Watson, D.G. Amines. In *Pharmaceutical Chemistry*; Watson, D.G., Ed.; Elsevier Ltd: New York, 2011; pp 35-56.
23. Uthagrove, A.L.; Nelson, W.L. "Importance of Amine pK_a and Distribution Coefficient in the Metabolism of Fluorinated Propranolol Derivatives. Preparation, Identification of Metabolite Regioisomers, and Metabolism by CYP2D6." *Drug Metab. Dispos* **2001**, *29*, 1377-1388.
24. McKerrall, S.J. et. al. "Structure- and Ligand-Based Discovery of Chromane Arylsulfonamide Na_v1.7 Inhibitors for the Treatment of Chronic Pain." *J. Med. Chem.* **2019**, *62*, 4091-4109.
25. Staveness, D.; Sodano, T.M.; Li, K.; Burnham, E.A.; Jackson, K.D.; Stephenson, C.R.J. "Providing a New Aniline Bioisostere through the Photochemical Production of 1-Aminonorbornanes." *Chem*, **2019**, *5*, 215-226.
26. Haghshenas, P; Quail, J.W.; Gravel, M. "Substrate-Controlled Diastereoselectivity Reversal in NHC-Catalyzed Cross-Benzoin Reactions Using *N*-Boc-*N*-Bn-Protected α -Amino Aldehydes." *J. Org. Chem.* **2016**, *81*, 12075-12083.
27. Meth-Cohn, O.; Taylor, D.L. "The reverse vilsmeier approach to the synthesis of quinolines, quinolinium salts, and quinolones." *Tetrahedron*, **1995**, *51*, 12869-12882.
28. Zhang, X.; Weng, G.; Zhang, Y.; Li, P. "Unique chemoselective Paal-Knorr reaction catalyzed by Mg₂I etherate under solvent-free conditions." *Tetrahedron*, **2015**, *71*, 2595-2602.
29. Zhang, Z.; Widenhoefer, R.A. "Regio- and Stereoselective Synthesis of Alkyl Allylic Ethers via Gold(I)-Catalyzed Intermolecular Hydroalkoxylation of Allenes with Alcohols." *Org. Lett.* **2008**, *10*, 2079-2081.
30. Carreras, J.; Kirillova, M.S.; Echavarren, A.M. "Synthesis of (-)-Cannabimovone and Structural Reassignment of Anhydrocannabimovone through Gold(I)-Catalyzed Cycloisomerization." *Angew. Chem. Int. Ed.* **2016**, *55*, 7121-7125.

Chapter 5

Evaluation of Metabolic Stability and KCNQ Agonism Activity of 1-Aminonorbornane Analogs

A portion of the work in this chapter appeared in the following publication (no permissions required): Staveness, D.; Sodano, T.M.; Li, K.; Burnham, E.A.; Jackson, K.D.; Stephenson, C.R.J. “Providing a New Aniline Bioisostere through the Photochemical Production of 1-Aminonorbornanes.” *Chem*, **2019**, 5, 215-226. Unpublished results have been completed in collaboration with Dr. Daryl Staveness (University of Michigan), Prof. Klarissa Jackson (University of North Carolina – Chapel Hill), Dasean Nardone-White (University of North Carolina – Chapel Hill), and Prof. R. Keith Duncan (University of Michigan).

5.1 Metabolic Behavior of Anilines

Within small molecule drug development, some functional groups have been designated as “structural alerts” due to a high propensity for bioactivation into undesired reactive species.^{1,2} One

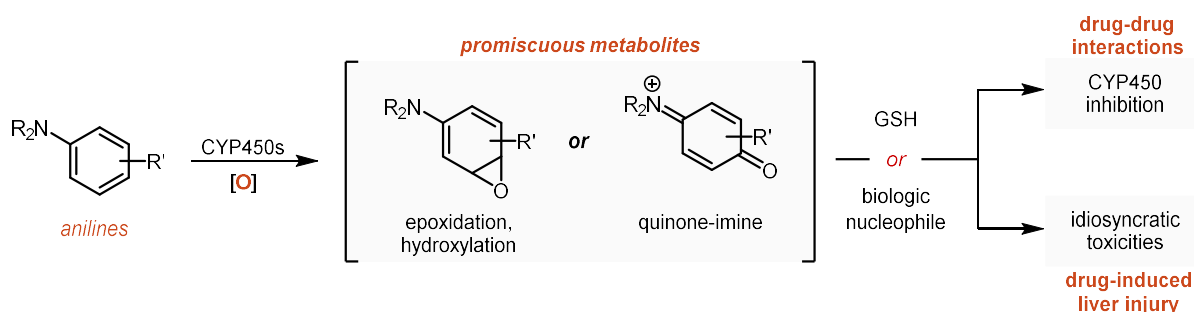


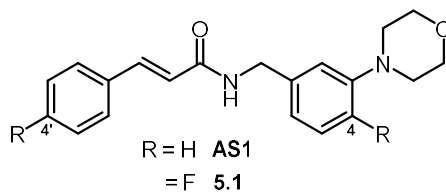
Figure 5.1. General scheme for the metabolic processing of anilines by CYP450s

such molecular fragment with a well-earned reputation for toxicity issues is the aniline. The electron-rich arene undergoes oxidation by cytochrome P450 enzymes (CYP450s) in the liver,

forming highly electrophilic intermediates such as epoxides or quinone-imines (Figure 5.1).³ These promiscuous metabolites then indiscriminately alkylate biological nucleophiles, leading to CYP450 inhibition or idiosyncratic toxicities that clinically manifest as drug-induced liver injury. The main strategy that the pharmaceutical industry has adopted to overcome this deleterious metabolic processing within the drug discovery process is strict avoidance of anilines and other structural alerts in lead compounds.⁴ However, several drugs, including the blockbuster Lipitor, contain structural alerts that undergo bioactivation to reactive metabolites, but do not lead to toxicity issues or other adverse outcomes for patients. The disadvantage then, with complete avoidance of structural alerts in drug development, is that many safe and effective therapies may be overlooked. Instead, efforts should be focused on identifying the source of reactive metabolite formation and making informed structural modifications to prevent harmful bioactivation.

5.1.1 Metabolic Processing of Acrylamide S1

Acrylamide S1 (**AS1**) is a KCNQ agonist disclosed by Bristol-Myers Squibb (BMS) in the early 2000s with promising activity in a cortical spreading depression model of migraine.⁵ The initial investigations of the pharmacokinetic (PK) properties of **AS1** showed excellent bioavailability (93%) upon oral dosing in Sprague-Dawley rats (Table 5.1). When probing metabolic activity, it was found that **AS1** moderately inhibits recombinant CYP2C9 with an IC₅₀ of 5.3 μM (Table 5.2A).⁶ However, when **AS1** was evaluated against the same panel of rCYP450s in a time-dependent inhibition (TDI) assay, no TDI was observed with rCYP2C9. Instead, **AS1** was shown to be a significant inhibitor of rCYP3A4, with a 4-fold decrease in IC₅₀ (96 μM to 22



	PK Parameter	AS1	5.1
IV	dose (mg/kg)	5	1
	$t_{1/2}$ (h)	2.1	3.5
	clearance (mL/min·kg)	41	18
PO	dose (mg/kg)	11	10
	oral absorption (h)	5	0.7
	oral bioavailability (%)	93	84

Table 5.1. Side-by-side comparison of pharmacokinetic parameters of **AS1** and **5.1**

μM) between 5 and 45 min timepoints (Table 5.2B).⁷ For comparison, troleandomycin, a potent metabolism dependent inhibitor of CYP3A4, was included as a control, showing a 3.8-fold decrease in IC_{50} from 5 to 45 min. As CYP3A4 comprises 30% of CYP450s in the liver and is estimated to be responsible for the metabolism of half of all drug used in humans, the inhibition displayed by **AS1** causes serious concern for drug-drug interactions and other toxicity issues.

A. Inhibition of Recombinant Human CYP450s by AS1

CYP	1A2	2C9	2C19	2D6	3A4
IC_{50} (μM)	78	5.3	13	>100	27

B. Time-Dependent Inhibition of rCYP3A4 by AS1 (IC_{50} , μM)

compound	5 min	15 min	30 min	45 min
AS1	96	62	33	22
5.1	18	21	19	19
troleandomycin	61	33	20	16

Table 5.2. (A) CYP450 inhibitory potential of **AS1**; (B) Results of TDI studies of **AS1** and **5.1**

The mechanism of CYP3A4 inhibition by **AS1** was determined to be irreversible enzyme inactivation, likely a result of a reactive metabolite species covalently binding to the CYP450 enzyme. The basis for this conclusion arose from the observation that the addition of modifiers, such as glutathione (GSH), did not affect **AS1**-mediated inhibition of CYP3A4, suggesting the

inactivation was occurring in or near the enzyme active site. While not contradictory to these findings, preliminary metabolite identification efforts in the Jackson lab have characterized **AS1**-GSH conjugates (not shown). To determine the functionality responsible for the TDI, structure-metabolism relationship studies were performed (Figure 5.2). Reduction of the olefin (**5.2**) or variable fluorination of the acrylamide arene (**5.3**) did not impede inhibition. However, when the morpholine was removed from the scaffold (**5.4**), inhibition of rCYP3A4 was not observed.

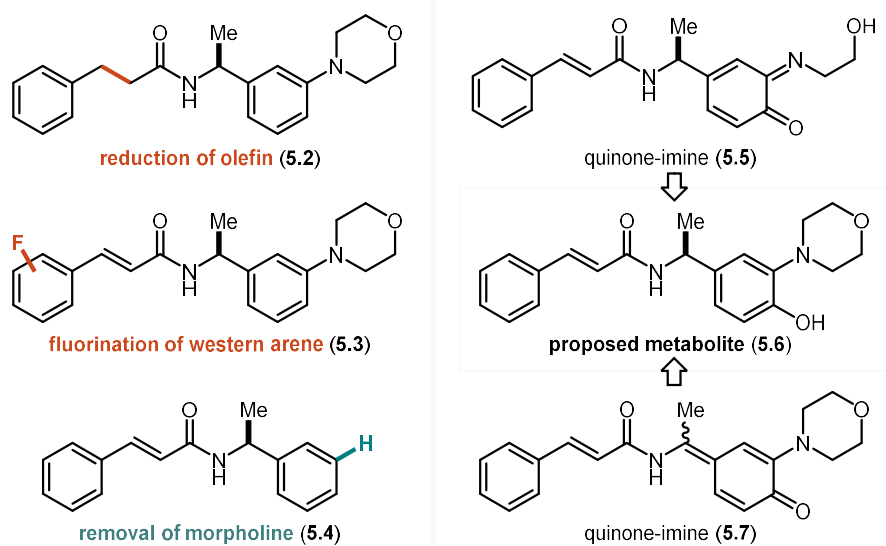


Figure 5.2. Structure-metabolism studies of **AS1** identifies aniline as source of reactive metabolite formation

Further studies in rat and human liver microsomes identified a monohydroxylated metabolite (**5.6**), hypothesized to arise from para-quinoneimines **5.5** and **5.7**.^{8,9} To prevent this oxidation, this position was blocked by incorporation of a fluorine.¹⁰ Further optimization for KCNQ2 agonism potency identified **5.1** as a new lead compound. Compound **5.1** has rapid oral absorption (peak concentration at 0.7 h), a longer half-life than **AS1** (3.5 h), and excellent oral bioavailability (84%) (Table 5.1). Additionally, the TDI was completely ameliorated (Table 5.2B), and **5.1** showed comparable KCNQ2 agonism activity to **AS1** (1.2 μ M vs. 3.0 μ M, respectively).

5.2 Evaluation of AminoNB Metabolic Stability

5.2.1 Microsomal Stability Assays and Metabolite Identification on AminoNB Model Systems

Preliminary assessment of metabolic susceptibility of aminoNBs was achieved through microsomal stability assays and identification of prominent metabolites. Selected compounds at 10 μ M concentration were incubated for 45 min with either rat or human liver microsomes (RLMs or HLMs, respectively), and the percent compound retention was determined relative to an untreated control (Figure 5.3). In general, the RLMs were more efficient in processing both the anilines and aminoNBs relative to the HLMs. Interestingly, aniline stability was highly dependent on the pattern of methyl substitution (**5.8**: H > **5.10**: 3,5-diMe > **5.9**: 4-Me > **5.11**: 2,6-diMe), with the 2,6-dimethyl system (**5.11**) being all but entirely decomposed in both trials. *N*-Phenylmorpholine (**5.8**) appeared to be the most stable aniline system, likely due to the lack of potential benzylic oxidation sites and reduced hydrophobicity. The decomposition of the aminoNBs was more consistent overall across the selected substitution patterns, especially in HLMs (all four compounds between 55-75% retention). In both RLMs and HLMs, the aminoNB panel outperformed or was on par with the most robust aniline compounds. One notable exception was C4-Me aminoNB **5.14** in the RLM assay, in which it was entirely decomposed in the 45 min. This is presumably an isoform-specific and/or species-dependent result given the 58% retention measured in HLMs. CYP450 active sites tend to be hydrophobic in nature,¹¹ thus the trimethylated norbornane core of **5.14** could be serving as an optimal lipophilic anchor for a specific RLM-derived CYP450 isoform. Any given aminoNB-based drug lead is likely to have additional polar functionality that would disrupt this anchoring effect, and unsurprisingly, the C3-axial acetamide aminoNB **5.15** offered the best overall retention profile between the two species (RLMs - 67% and HLMs - 73%).

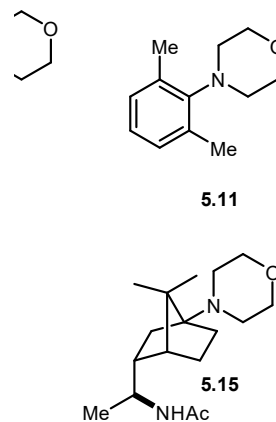
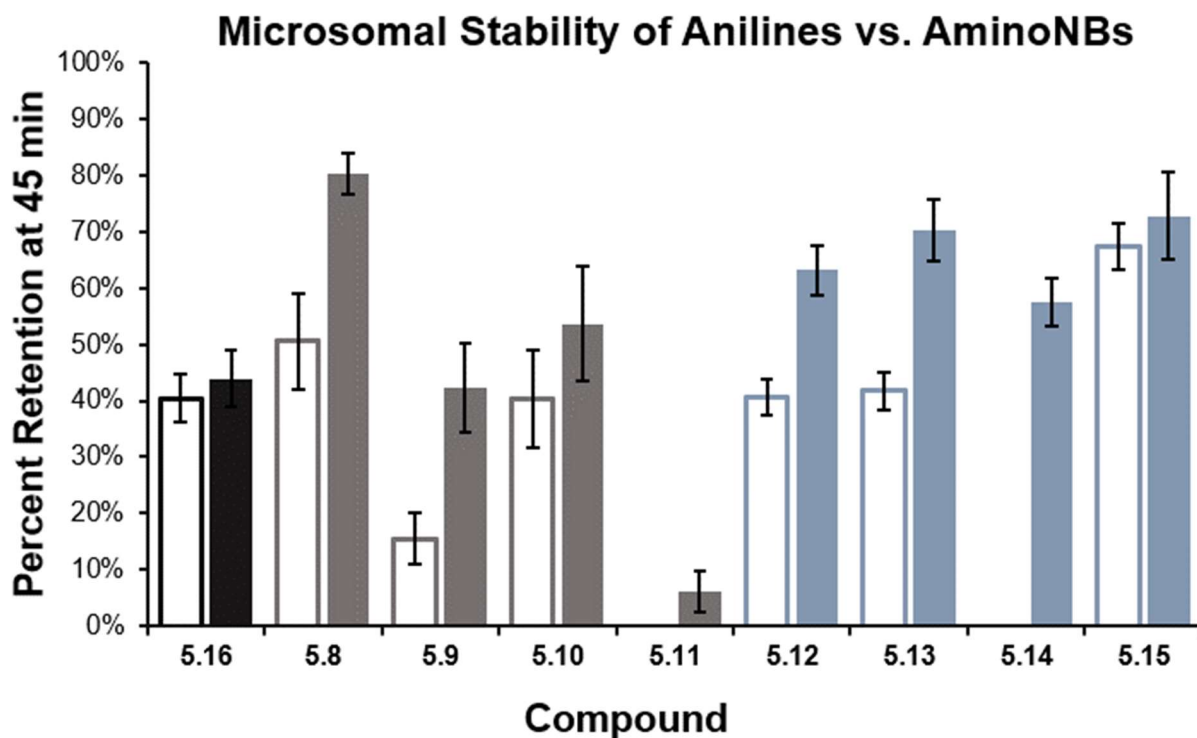


Figure 5.3. Panel of anilines and aminoNBs evaluated in microsomal stability assays; graphical depiction of compound retention after 45 min incubation in the presence of RLMs or HLMs. Empty bars = RLMs, Filled bars = HLMs, **5.16** = verapamil·HCl, positive control

Importantly, the aniline bioisostere concept does not hinge on imbuing complete inertness to metabolic processing, rather the avoidance of reactive metabolite generation is the true goal. The norbornane core provides no obvious path towards the generation of reactive metabolites, and this hypothesis was supported with metabolite profiling. Using LC-MS/MS, formamide **5.17** and

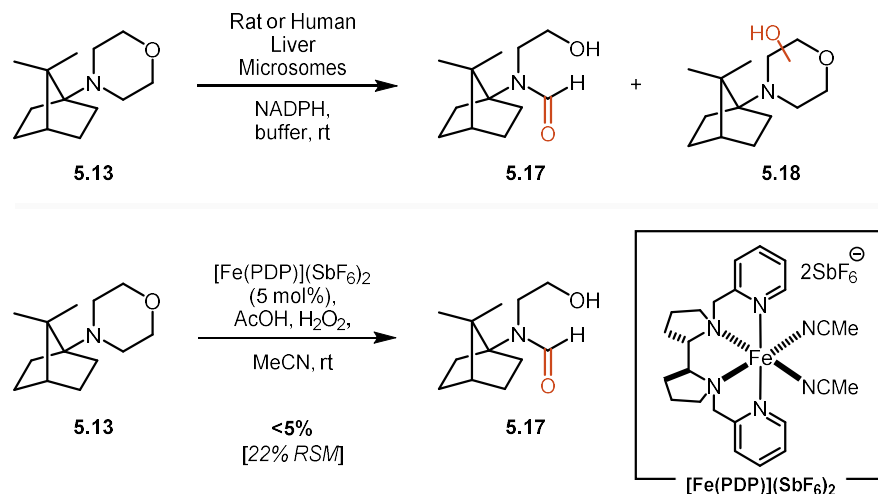


Figure 5.4. Metabolite identification of **5.13**

a monohydroxylated morpholine **5.18** were identified as the primary metabolites arising from aminoNB **5.13** (Figure 5.4). The identity of the formamide was verified through chemical synthesis of an authentic standard of the proposed metabolite. Oxidation of aminoNB **5.13** with a non-heme iron catalyst developed by White and co-workers for C-H hydroxylation^{12,13} generated formamide **5.17** as the major isolable product. Other oxidation products were formed in this reaction, postulated as mono- and poly-hydroxylated morpholine species, but were not readily isolable. However, no products of core oxidation were directly observed in RLMs, HLMs, or with chemical oxidants, likely owing to the increased *s*-character of the norbornane C-H bonds. Addition of glutathione to the microsomal incubations of **5.13** led to no discernable change in the metabolite profile, demonstrating that the aminoNB systems show no inherent propensity to the glutathione adduction that is often representative of reactive metabolite formation.

5.2.2 Microsomal Stability Assay and Metabolite Identification of AminoNB Analogs

With the promising results from the metabolic profiling on model aminoNB systems, we moved towards evaluating the more complex aminoNB analogs in a microsomal stability assay employing male Sprague-Dawley rat microsomes (Figure 5.5). **RTG** showed minor CYP450

processing (matching closely to previous reports),¹⁴ while more than 60% of aniline-based compounds **AS1** and **5.19** were cleared in 45 min. Importantly, more than 80% of C3-substituted analogs **5.20** and **5.21** was retained in the same time course, providing initial evidence that the aminoNB substitution did in fact impart inertness to CYP450-mediated processing. Interestingly, the 7*S* C7 analog (**4.10**, data not shown) readily decomposed, though this system adopts a unique

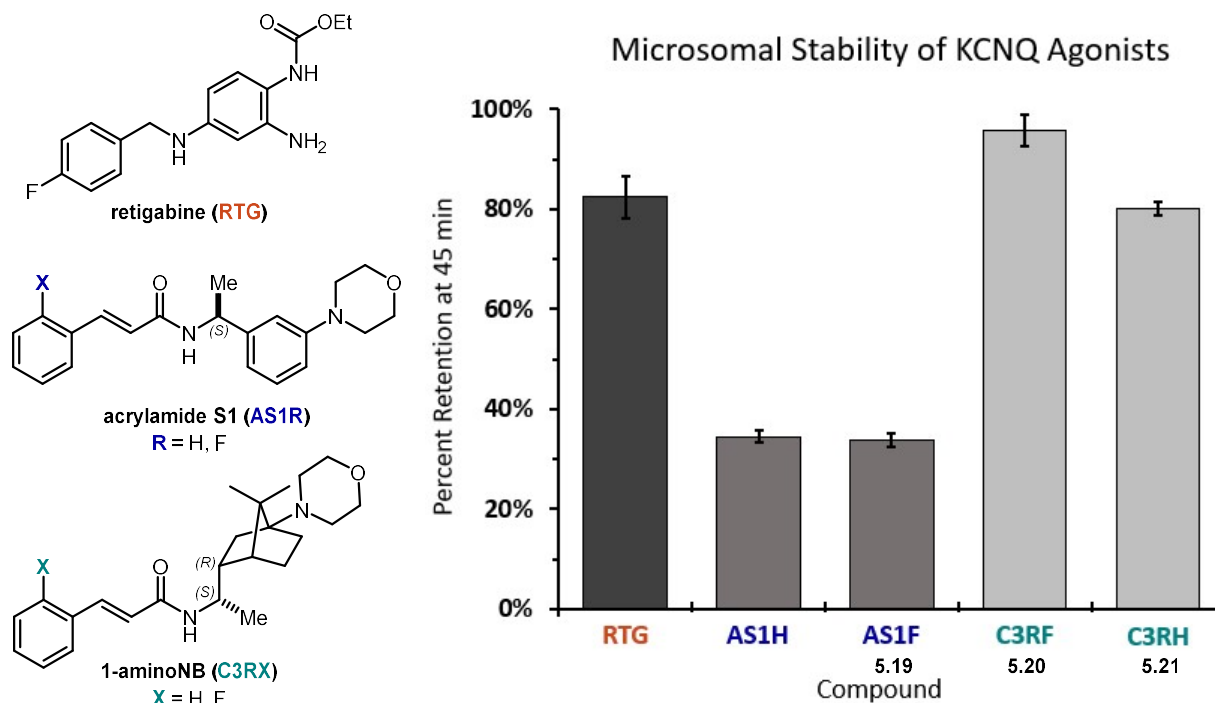


Figure 5.5. Results of microsomal stability assay of **RTG**, **AS1** scaffolds, and C3-axial aminoNB analogs

conformation in which the cinnamamide and morpholine are engaged in an intramolecular H-bonding interaction, a conformation that assuredly cannot be adopted by the parent analogs and likely alters the reactivity of the morpholine and cinnamamide motifs. As the aniline-based compounds are known to generate reactive metabolites that lead to a time-dependent inhibition of CYP3A4 (and other isoforms), it will be critical to evaluate the analogs in a time-dependent inhibition assay with different isoforms of CYP450s in future studies.

In addition to determining metabolic stability ($t_{1/2}$, kinetics of decay), isoform specificity, propensity for TDI of CYP450s, and hepatotoxicity, metabolite identification on final analogs will be performed to establish a full metabolic profile on any aminoNB lead compounds. Towards this end, C3-axial aminoNB analog **5.22** was incubated in the presence of RLMs and HLMs, and major metabolites were identified using LC-MS/MS analysis (Figure 5.6). Two metabolites with morpholine oxidation were identified, ethanolamine **5.23** and formamide **5.24**, both of which are commonly reported metabolites of *N*-alkyl morpholines.^{15,16} Interestingly, reduction of the acrylamide olefin was observed as in metabolite **5.25**. While the formation of this species was found to be NADPH-dependent, olefin reduction is a transformation not commonly attributed to CYP450 activity. Instead, this metabolite may arise from an α,β -ketoalkene C=C reductase present

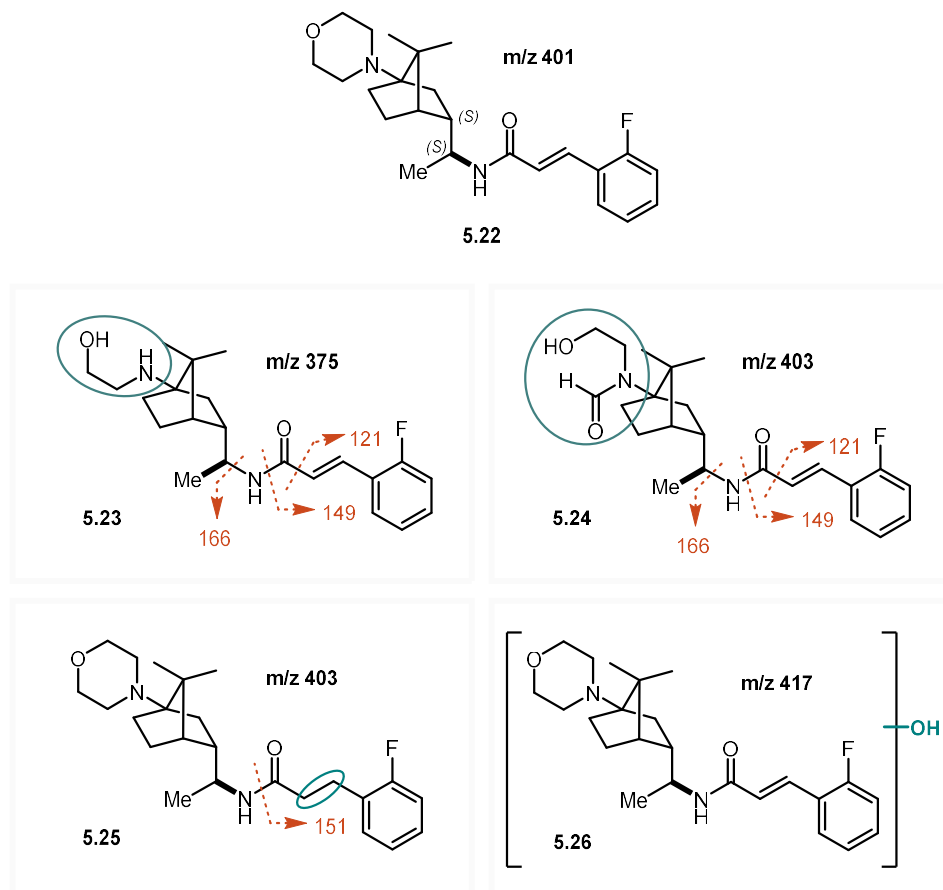


Figure 5.6. Metabolite identification of aminoNB analog **5.22**

in liver microsomes, as similar reactivity was reported in 2013 by Zeng *et al.*¹⁷ The formation of **5.23**, **5.24**, and **5.25** were consistent across RLMs and HLMs, but three hydroxylated species (generically represented as **5.26**) were detected in RLMs whereas only two were formed with HLMs. The position of hydroxylation has not yet been determined, but two of these intermediates are postulated to be α -*O* and α -*N* functionalization on the morpholine (as in **5.18**). These results are consistent with the studies on the model systems, with morpholine being the primary location of metabolism, and functionalization of the norbornane core was not observed. Future efforts will include GSH as an additive in the microsomal stability assays to trap any reactive metabolite species that form and allow for identification of the site of functionalization. If the metabolism of the morpholine proves to be detrimental and generate concern for future toxicity issues, this fragment can be modified with electron-withdrawing substituents to deactivate the ring and block sites of oxidation as suggested in Chapter 4.8.

5.3 Evaluating AminoNB Analogs for KCNQ Agonism Activity

5.3.1 Background on KCNQ Ion Channels: Physiology and Role in Disease

Ion channels are a diverse class of signaling proteins and have long been attractive targets for drug development due to the wide spectrum of physiological processes they are responsible for regulating.^{18,19} One category of ion channels is voltage-gated potassium channels (K_v) which are encoded by 40 different genes and further divided into 12 subfamilies. K_v channels are characterized by six transmembrane segments, divided into a voltage-sensing region (segments 1-4) and a pore region containing a selectivity filter (segments 5-6) (Figure 5.7). The fully functional form of K_v channels is comprised of four, six segment domains (I-IV), but unlike sodium and calcium ion channels, each domain is expressed separately and later assembled into the tetrameric

structure with (pseudo)-C₄ symmetry around the ion conducting pore. This feature of K_v channels allows for increased diversity in that the four domains need not arise from the same gene, yielding either homo- or heterotetramer ion channels.

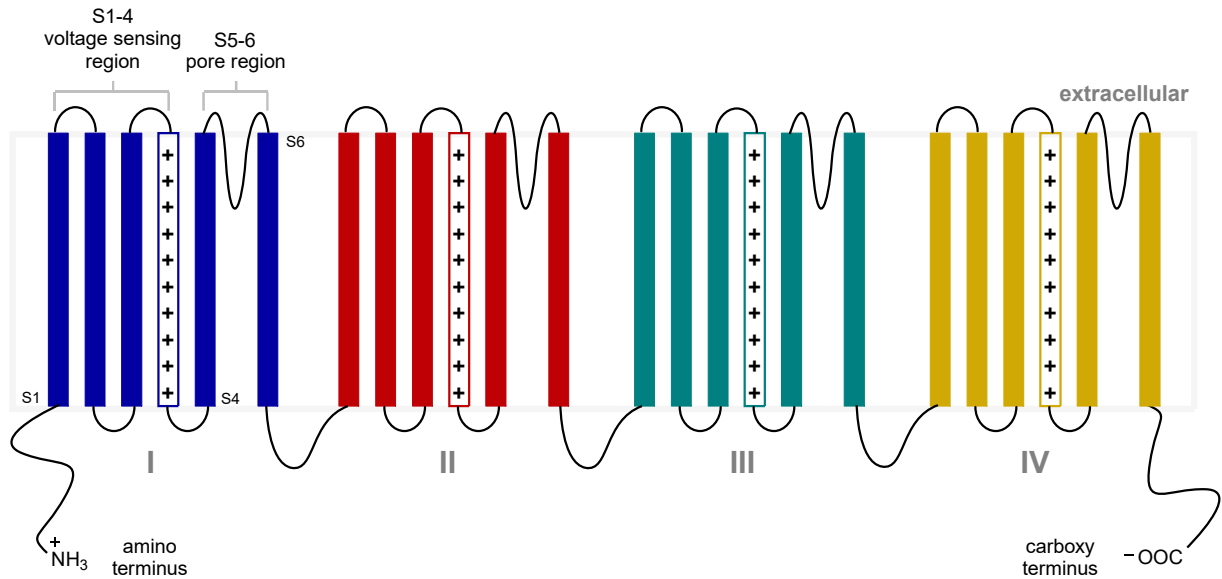


Figure 5.7. Schematic representation of a generic potassium ion channel

One subfamily of K_v channels are designated as K_v7, and as they are encoded by the KCNQ gene, are often referred to as KCNQ ion channels. The KCNQ family are voltage-gated, non-inactivating ion channels comprised of 5 isoforms, KCNQ1-5 (Figure 5.8), and assemble as either homo- or heterotetramers (KCNQ2/3, KCNQ3/5, KCNQ4/5). Each isoform has variable distribution within the body, and specific mutations within the gene family have been implicated in disease.²⁰ As a few representative examples, KCNQ1 is present in cardiac myocytes, and dysfunction of these channels is associated with long QT syndrome (a dangerous, irregular heartbeat).²¹ KCNQ2 can associate as either a homotetramer or a heterotetramer with KCNQ3; both of these channels are found in the CNS, and genetic abnormalities result in a number of hyperexcitability disorders, such as epilepsy,²² neuropathic pain,²³ and mood disorders.²⁴ The

KCNQ4 homotetramer is localized in the inner ear in hair cells, and disruption of function causes hearing loss²⁵ and has been implicated in tinnitus.²⁶

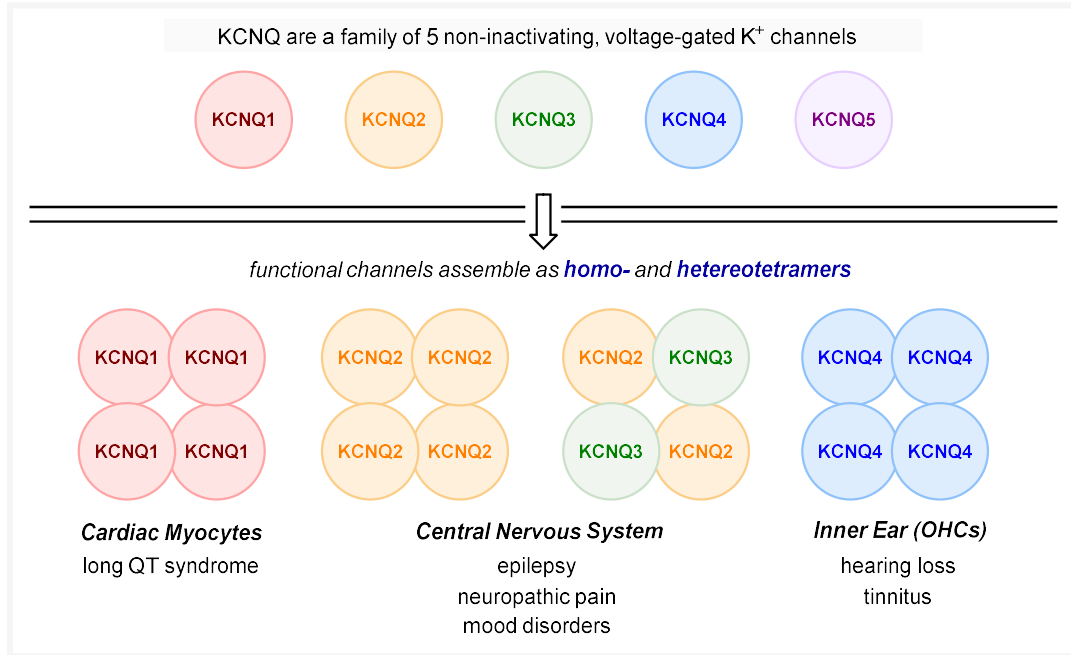


Figure 5.8. Introduction to the KCNQ family of voltage-gated potassium ion channels

In terms of their physiology, KCNQ channels have been referred to as an action potential “break pedal.” In order to understand how KCNQ channel activity modulates cellular excitability, a generic description of an action potential is described below. The resting membrane potential of many cells is polarized to around -60 mV (Figure 5.9, left). When a depolarizing stimulus arrives at the cell membrane, sodium ion channels begin to open, allowing sodium ions (positive charge) to flow into the cell and depolarize the membrane (A). The magnitude of the depolarization in mV is denoted as variable X. If the magnitude of X is large enough ($X \geq X_1$) such that the membrane potential reaches what is known as the threshold potential (B), then an action potential will occur in which a rapid influx of sodium ions increases the membrane potential to around +40 mV (C). At these positive potentials, sodium channels inactivate, preventing additional sodium ions from entering the cell, and voltage-gated potassium ion channels will open, transporting potassium ions

out of the cell. The efflux of potassium ions hyperpolarizes (**D**) the membrane potential, which then equilibrates (**E**) back to the resting potential. If the threshold potential is not attained with the arrival of a depolarizing stimulus (i.e. $X < X_1$), the action potential will fail to initiate, and the membrane potential will equilibrate back to the resting potential (not shown).

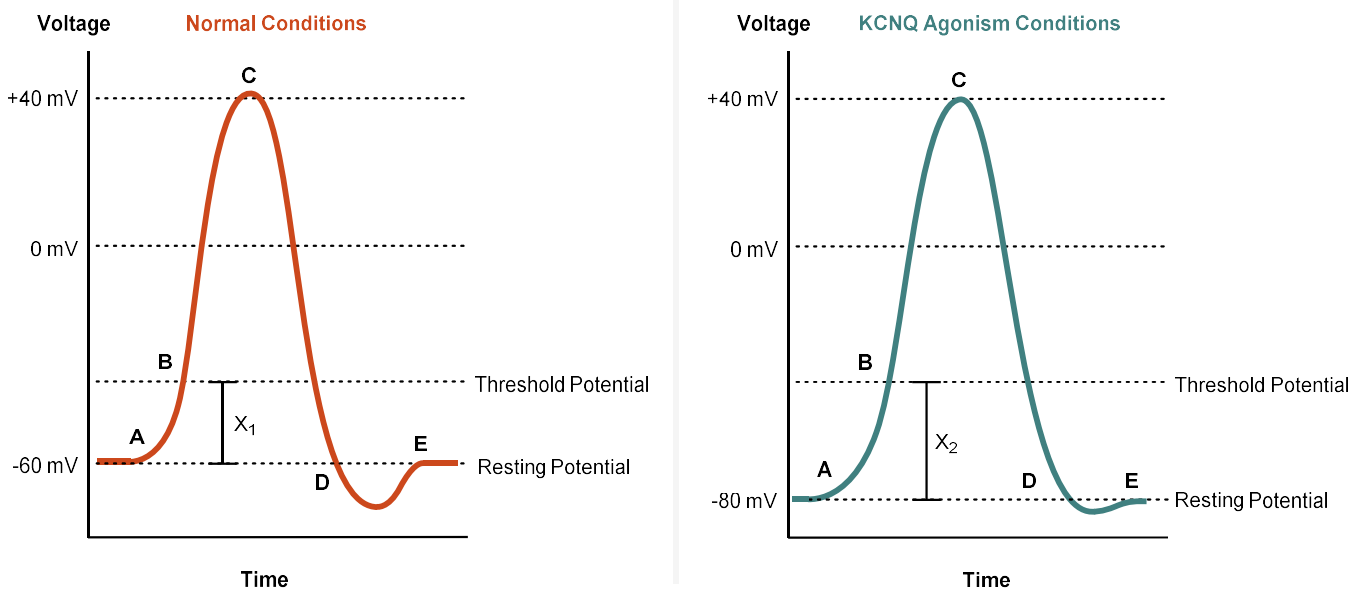
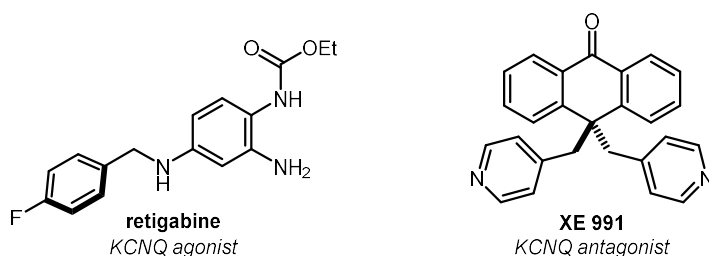


Figure 5.9. Graph of cell membrane potential over the course of an action potential

While some K_v ion channels activate at positive potentials, KCNQ channels operate around the negative resting membrane potential. Therefore, at potentials of ca. -60 mV, a small population of KCNQ channels will be open, defusing potassium ions out of the cell. When KCNQ is agonized, there is a larger potassium efflux that hyperpolarizes the membrane prior to the depolarizing stimulus (**A**), thus increasing the magnitude of X (Figure 5.9, right). In many hyperexcitability disorders, action potentials occur either too frequently or too rapidly in succession. One way to attenuate this activity is through hyperpolarization the membrane, such that $X_2 > X_1$, and only large stimuli will trigger an action potential.

Only two drugs have been approved by regulatory agencies and marketed with KCNQ agonism as the mechanism of action; retigabine (USA) and a closely-related pyridal analog, flupirtine (EU). Retigabine (**RTG**) is non-selective across KCNQ channels, but its ability to reduce neuronal hyperexcitability is clearly illustrated in an experiment described by Grunnet *et. al.*²⁴ Action potentials in normal rat hippocampal CA1 neuron slices were recorded after application of depolarizing current, and six action potentials were documented over the 600 ms time course (Figure 5.10). When 10 μM of **RTG** was applied, the number of action potentials decreased by half, and this effect was reversible upon wash-out. In contrast, when KCNQ antagonist XE 991 was dosed at a 10 μM concentration and the KCNQ channels were prevented from functioning, there is a dramatic increase in the number of action potentials firing.

Despite its efficacy, **RTG** was withdrawn from the market in 2017 due to off-target effects such as blue skin discoloration and eye abnormalities.²⁷ In 2018, the European Medicines Agency



Recorded action potentials from rat hippocampal CA1 neurons

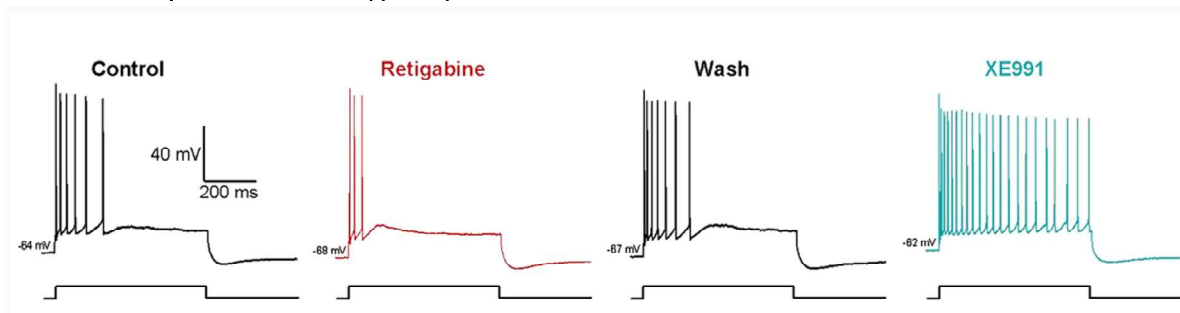


Figure 5.10. The effect of a KCNQ agonist (**RTG**) and antagonist (**XE 991**) on neuronal excitability. Figure reproduced from *Ref. 24*

recommended discontinuing flupirtine because of the risk for serious liver injury. There is now a substantial void in the treatment of drug-resistant epilepsies and other hyperexcitability disorders despite the broad biomedical relevance and therapeutic potential KCNQ agonists.²⁸

5.3.2 Overview of Whole Cell Electrophysiology

Electrophysiology is one common analytical technique used to assess ion channel activity as it allows for direct measurement of current across the cellular membrane. Experimentally, a borosilicate glass pipette shaped to have an opening approximately 1 μm in size is filled with an

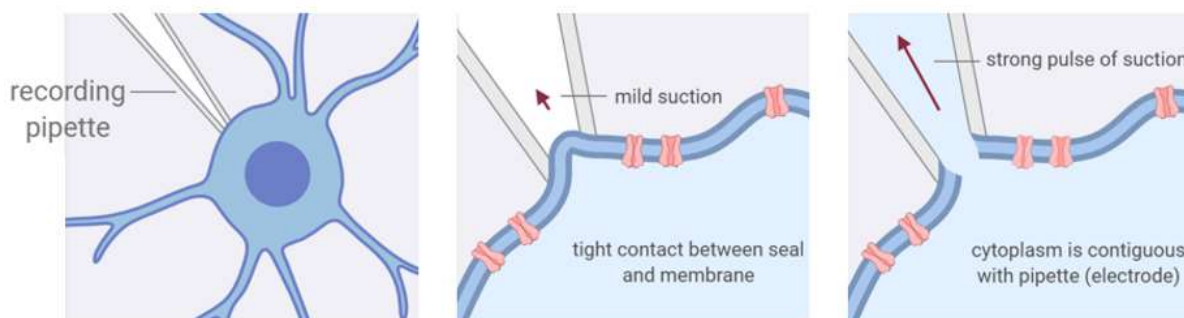


Figure 5.11. Overview of electrophysiology – whole cell configuration. Redrawn from Leica Microsystems⁵⁰

electrolyte solution mimicking the composition of the cytosol. Into this solution is submerged a Ag/AgCl wire to serve as the electrode. Cells expressing the voltage-gated ion channel of interest are plated in a bath composed of extracellular solution with a ground wire, and an isolated cell is carefully approached with the recording pipette (Figure 5.11). Once the pipette is in close proximity to the cell, mild suction is applied such that a tight ($\sim 1 \text{ G}\Omega$) seal is formed between the glass and the cell membrane. After this seal forms, a strong pulse of suction selectively ruptures the cell membrane, such that the cytoplasm and the interior of the pipette are contiguous. This configuration is known as a whole cell recording in that current passing through the entirety of the cell membrane is measured.

Once this configuration is achieved, the electrode controls the membrane potential, and a series of voltage steps (e.g. -100 mV to +40 mV, 10 mV increments) are applied and current output is measured. Data are plotted from tail currents as current (I) against voltage (V), generating an S-shaped curve (Figure 5.12) that is fit to a charge-voltage Boltzmann distribution

$$f(V) = \frac{I_{max}}{1 + e^{(V_{1/2} - V)/V_C}} + C \quad (\text{Eq. 5.1})$$

where $f(V)$ is the peak current density at the applied voltage, I_{max} is the maximum current, $V_{1/2}$ is the voltage at which the current is at a half-maximum, V_C is the slope factor, and C is the capacitance.

In the idealized examples of Boltzmann distributions presented in Figure 5.12, at negative potentials (e.g. -80 mV), the current output is approximately zero, representative of ion channels in a closed state. As the membrane is depolarized, ion channels open and conduct current until saturation is achieved at more positive potentials (e.g. +10 mV). The voltage at which the current is half maximal is defined as $V_{1/2}$. One mechanism by which a KCNQ agonist hyperpolarizes the membrane is by opening KCNQ channels at more negative potentials, manifesting as a leftward shift in the $V_{1/2}$ value (Figure 5.11A). KCNQ agonists may also, independently or in conjunction

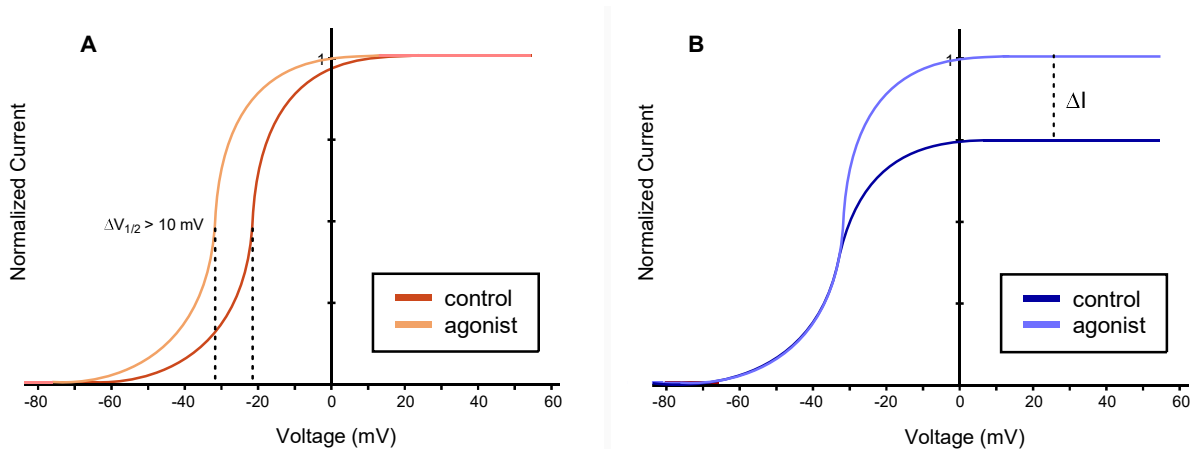


Figure 5.12. Mechanism of KCNQ agonism by (A) leftward shift of $V_{1/2}$ and/or (B) increase in conductance

with shifting the $V_{1/2}$, increase channel conductance and the overall current output (Figure 5.11B). The agonistic activity displayed by both **RTG** and **AS1** are a result of shifting $V_{1/2}$ (*vide infra*).

5.3.3 KCNQ Agonism Activity of Acrylamide S1

The **AS1** scaffold was identified in a high-throughput FLIPR screen using a fluorescent dye, and its activity was fully validated by two-electrode voltage clamp recordings from *Xenopus laevis* oocytes expressing mKCNQ2.⁵ From these experiments, an EC_{50} of 6.0 μ M was extrapolated. At 20 μ M concentration, the $V_{1/2}$ was shifted from -70 to -85 mV ($\Delta V_{1/2} = -15$ mV). **AS1** was also shown to increase current output in the range of -70 to +10 mV, but partially inhibited channel conductance at more positive voltages ($> +20$ mV); similar activity has also been reported for **RTG**. As *Xenopus laevis* oocytes have endogenous KCNQ1 channels (and potentially other KCNQ family members), to ensure the observed activity of **AS1** could solely be attributed to KCNQ2 agonism, an alternative expression system was evaluated. HEK239 cells stably expressing mKCNQ2 were analyzed, and under conditions employing local superfusion of 10 μ M **AS1**, the $V_{1/2}$ shifted from -18.3 to -52.1 mV ($\Delta V_{1/2} = -33.8$ mV). The agonism was found to be reversible upon wash-out. More rigorous studies supplied an EC_{50} of 3.3 ± 0.6 μ M in the HEK293 expression system, and hKCNQ2 gave similar results to mKCNQ2.

The FLIPR-based assay showed promiscuity of **AS1** across KCNQ family members, and further electrophysiological evaluation by Olesen *et. al.* showed that **AS1** displayed different activities based on the identity of the channel.²⁹ KCNQ1 is the only member of the family that is inhibited by **AS1**. Hyperpolarizing shifts of the activation curves for KCNQ2, KCNQ2/3, KCNQ4, and KCNQ5 were observed, and the voltage-dependent block that BMS reported for KCNQ2 was also present in KCNQ2/3. In contrast, KCNQ4 and KCNQ5 displayed uniform increases in maximal current amplitude across all voltages.

Several groups have now reported on the key binding interaction responsible for the agonistic affect of **AS1**, which has been identified as a tryptophan residue in a hydrophobic pocket on the intracellular side of S5, close to the gating hinge of the pore.²⁹ This residue is also important for **RTG** agonism,³⁰⁻³² although additional residues important for **RTG** activity have also been identified. Work by Kurata *et. al.* has demonstrated that the tryptophan and amide carbonyl of **RTG** (and presumably, **AS1**) engage in a hydrogen-bonding interaction, and analogs of **RTG** with increased negative electrostatic surface potentials around the carbonyl functionality increase potency.³³

5.3.4 Preliminary Evaluation of AminoNB Analogs as KCNQ Agonists

The agonism activity of **RTG**, **AS1**, **F-AS1 (5.19)** and C3-axial aminoNB analogs **5.20** and **5.21** was evaluated by whole cell electrophysiology in HEK239A cells transiently expressing hKCNQ2. To validate the transfection protocol and ensure hKCNQ2 was being expressed, transported to the membrane, and assembled as a functional tetramer, untransfected HEK293A cells were compared against HEK293A cells transfected with hKCNQ2 wt cDNA. HEK293A cells endogenously express voltage-gated ion channels, so it was also important to assess whether these native channels would interfere with analysis of heterologous potassium channels such as KCNQ.³⁴ The untransfected control was evaluated in a bath of extracellular solution, and the stimulation protocol consisted of a holding potential of -60 mV before applying squared test pulses from -100 to +60 mV lasting 1000 ms each (Figure 5.13A). Under these conditions, the overall current is low with a visible non-inactivating component (IKN). In contrast, cells transfected with hKCNQ2 cDNA showed 1 nA (typical best) of a slowly activating outward current representative

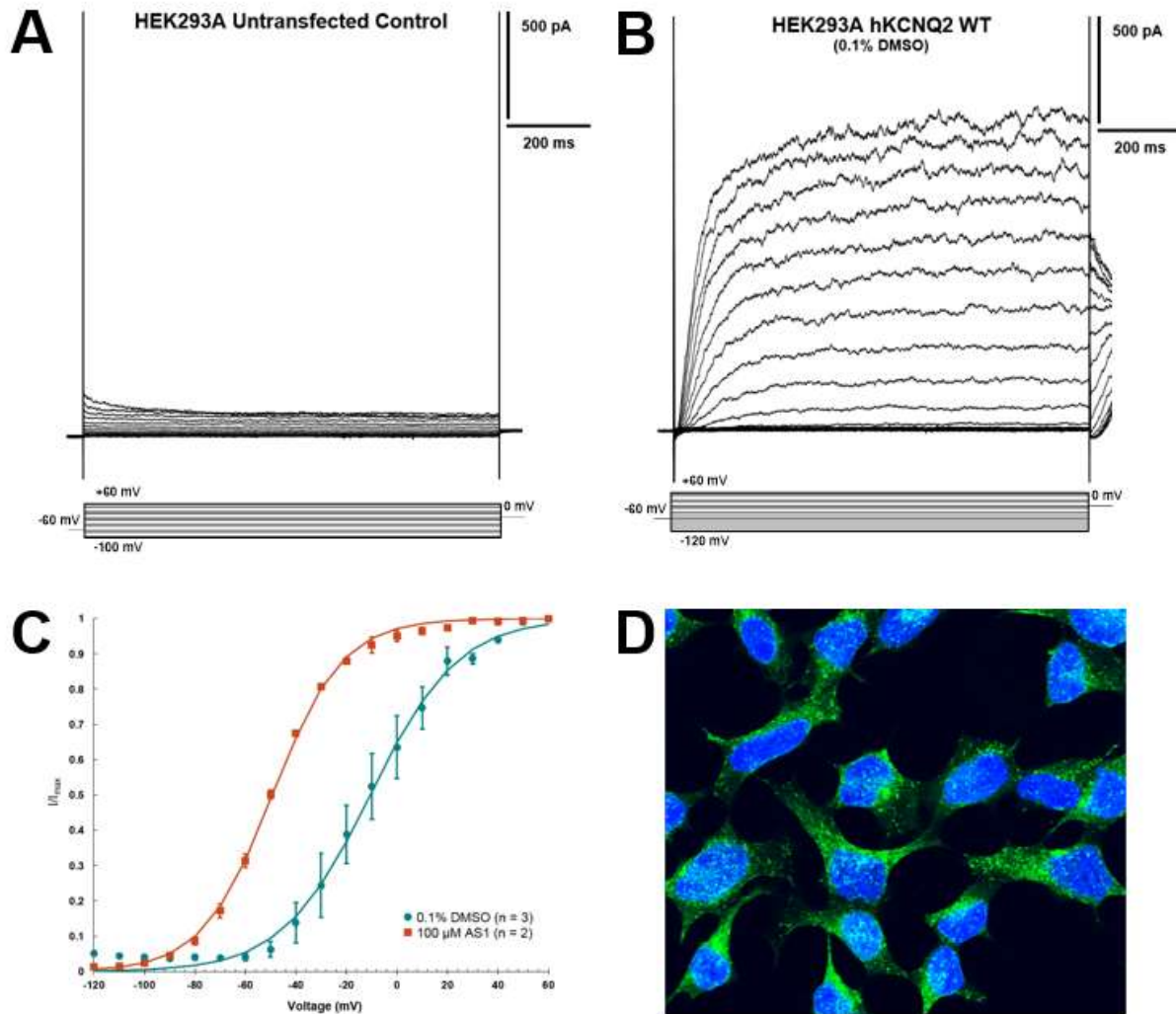


Figure 5.13. Representative whole cell recording from an (A) untransfected HEK293A cell in extracellular solution or (B) HEK293A cell transiently transfected with hKCNQ2 wt in 0.1% DMSO. Leak currents were subtracted off-line and capacitance is uncorrected; (C) Analysis of tail currents from the final voltage step to 0 mV against the preceding test potentials as a normalized I-V Boltzmann curve for 0.1% DMSO (n = 3, teal) and 100 μ M AS1 (n = 2, orange); (D) Immunohistochemistry results staining fixed preparations for anti-KCNQ2 (green) and counterstained with Hoechst to reveal cell nuclei (blue). The images show robust KCNQ expression with high efficiency between cells (~95% of cells labeled in 9 independent random fields).

of KCNQ ion channels (Figure 5.13B). The pulse protocol had been expanded to voltage steps from -120 to +60 mV with tail currents elicited at 0 mV, and the cells were instead submerged in a bath consisting of extracellular solution containing 0.1% DMSO as a vehicle control.

Importantly, the native IKN is not visible, suggesting that with large amounts of current, the contributions from HEK endogenous current is negligible and will not interfere with the analysis of KCNQ currents.

Cells expressing hKCNQ2 wt were then separated into different treatment groups and analyzed for KCNQ functional responses. Figure 13C shows the relationship between average normalized current (I/I_{\max} , \pm SEM) and the applied voltage (V) fitted to a Boltzmann distribution for two conditions – 0.1% DMSO vehicle control and 100 μ M AS1. For 0.1% DMSO, the $V_{1/2}$ was determined to be -10.6 mV ($n = 3$). However, under this pulse protocol (-120 to +60 mV), steady state was not achieved and for future experiments the voltage steps should be expanded to -120 to +80 mV. Under otherwise the same conditions, cells treated with 100 μ M AS1 showed a substantial negative shift in $V_{1/2}$ to -49.3 mV ($n = 2$) and a $\Delta V_{1/2}$ of -38.7 mV from the control.

The $V_{1/2}$ (Figure 14A) and I_{\max} (Figure 14B) were then compared for 7 different treatment groups – extracellular solution, 0.1% DMSO, 10 μ M RTG, 100 μ M AS1, 100 μ M F-AS1, 100 μ M **5.21**, and 100 μ M **5.20**. All data is presented as mean values \pm SEM unless otherwise noted. The extracellular solution ($n = 8$) and 0.1% DMSO ($n = 3$) gave comparable $V_{1/2}$ values of -14.5 ± 1.2 mV and -10.1 ± 6.7 mV, respectively. The I_{\max} values were also similar (342 ± 90 and 528 ± 229 , respectively). **RTG** ($n = 9$), **5.21** ($n = 5$), and **5.20** ($n = 6$) at the doses indicated did not represent statistically significant shifts in $V_{1/2}$ ($p > 0.05$). However, 10 μ M is known to be an effective concentration of RTG against KCNQ2 in CHO cells.^{35,36} The limited number of cells analyzed under each treatment group and unpaired experimental conditions likely led to the relatively large error. **AS1** ($n = 2$) and **F-AS1** ($n = 5$) did give statistically significant negative shifts of $V_{1/2}$ to -50.0 ± 1.0 mV ($p < 0.05$) and -82.7 ± 5.4 mV ($p < 0.01$), respectively. Of note, based on visual inspection of the raw traces for 100 μ M doses of **F-AS1** (not shown), the channels were beginning

to open at the first voltage pulse of -120 mV and were already conducting at the half maximal current at the holding potential of -60 mV. Changing the pulse protocol to potentials more negative than -120 mV is likely to have a negative effect on the health of the cells, and therefore 100 μ M concentrations of **F-AS1** should be avoided in the future. It is interesting that **F-AS1** is more potent than **AS1** under these conditions, as a recent report by Wipf *et. al.* illustrates the importance of fluorination on potency and selectivity for **RTG** analogs.³⁷

Perturbation of I_{\max} for each treatment group was not rigorously evaluated due to low sampling and high variability in expression of hKCNQ2 wt between cells (Figure 5.14B). However, 100 μ M **F-AS1** shows statistical significance ($p < 0.01$) compared to the 0.1% DMSO

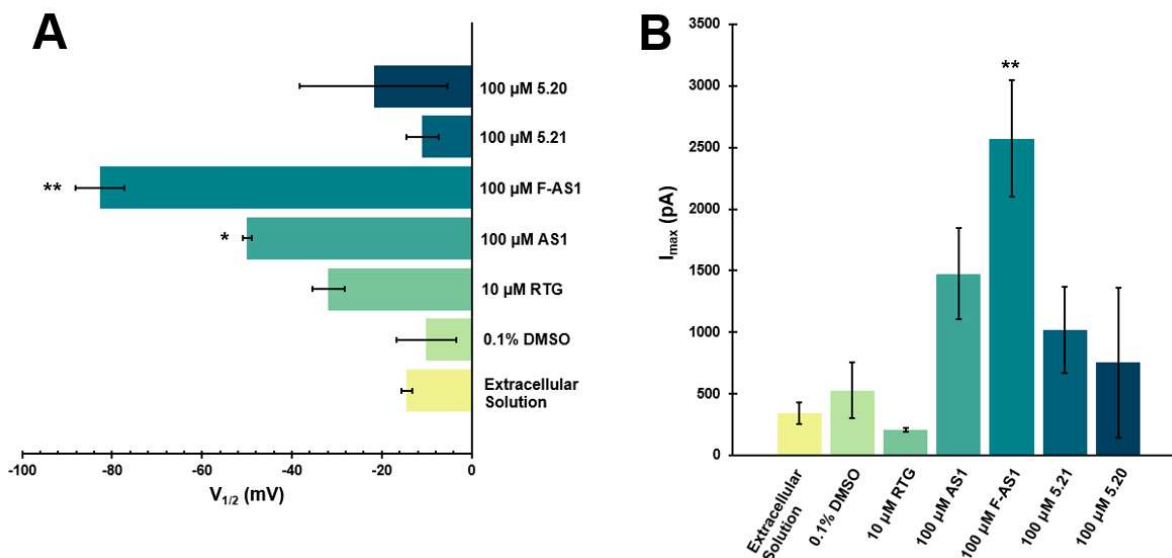


Figure 5.14. Summary bar graphs representing (A) half-activation ($V_{1/2}$) and (B) I_{\max} of hKCNQ2 wt currents calculated from I-V Boltzmann curves at controls and compound treatment groups. Error bars represent the mean \pm SEM. * $p < 0.05$, ** $p < 0.01$ Statistical significance between 0.1% DMSO control and test conditions was determined using Student's *t*-test (unpaired, two sample unequal variances, two-tailed distribution)

control, but this may be another artifact of the high doses being employed and unoptimized pulse sequence protocol.

5.3.5 Future Directions

The initial investigation of KCNQ agonism activity of the aminoNB analogs is promising. While the two analogs evaluated, **5.20** and **5.21**, did not show statistically significant shifts in $V_{1/2}$ when compared to the 0.1% DMSO control, these results also represent only one aminoNB substitution pattern against one isoform of KCNQ. The first-generation library of analogs seeks to evaluate 13 differentially substituted aminoNBs against seven KCNQ ion channels, and other properties aside from substitution pattern (such as amine identity, amine pK_a , and electronic properties of the acrylamide) are unoptimized. Due to the large volume of data desired and the low throughput pace of manual electrophysiology, preliminary evaluation of the analog library will move to a fluorescence-based assay to allow for rapid identification of lead compounds to be later verified by more rigorous methods. Many commercial fluorescence reporter assays are available for the purpose of detecting small molecule modulators of ion channels, and the thallium flux assay was developed to specifically target voltage- and ligand-gated potassium ion channels.³⁸ The plate-based format of the assay allows for analysis of 96- or 384-well plates in a Functional Drug Screening System (FDSS), and the HTE capabilities of the Center for Chemical Genomics (CCG) at Michigan will expedite collection of data. While this platform will provide information on KCNQ agonism activity and selectivity across isoforms, the mechanism of agonism cannot be determined through this method. Subsequent electrophysiology on lead compounds will be critical in elucidating these details.

The other main limitation of the initial whole cell electrophysiology studies was the high variability of expression between cells. Concerns of channel run down due to depletion of PIP2

over time and repeated depolarizing cycles precluded analysis of multiple conditions within a single cell.³⁹⁻⁴⁰ Therefore, each experimental condition was applied separately to individual cells, increasing the statistical variance. At the same time, inconsistent levels of hKCNQ2 wt expression between cells as a result of transient transfection introduced additional variability in parameters such as I_{\max} . In an effort to increase reproducibility between recordings, stably expressing, monoclonal HEK239A cell lines were obtained of each of the desired isoforms of KCNQ (KCNQ1, KCNQ2, KCNQ2/3, KCNQ3, KCNQ4, KCNQ4/5, KCNQ5). Additionally, a KNCQ2 W236L mutant cell line was generated to confirm that the aminoNB analogs are enacting on the same key residue proposed to be responsible for **AS1** and **RTG** agonism activity. The cDNA from which each cell line was derived has been validated by Sanger sequencing. Functional expression has been assessed by the fluorescence-based TI^+ flux assay or via an automated electrophysiology platform. Recently, immunohistochemistry results show robust hKCNQ2 wt expression with high efficiency between cells (Figure 13D).

While the biological evaluation of the aminoNB analogs is still in the early stages, the preliminary results are encouraging, and this research program has significant potential to impact areas of unmet medical need. There are currently no small molecule therapies on the market with KCNQ agonism as the mechanism of action despite the abundance of proposed clinical applications, some of which already face a scarcity of treatment options. While the initial goal of this project was to provide proof of concept for aminoNBs to serve as metabolically innocuous aniline isosteres, the capacity of this research to impact new synthetic methodologies, drug development, and fundamental knowledge on KCNQ physiology has greatly expanded the impact of this program.

5.4 Experimental Procedures and Characterization of Compounds

5.4.1 Preparation of Compounds

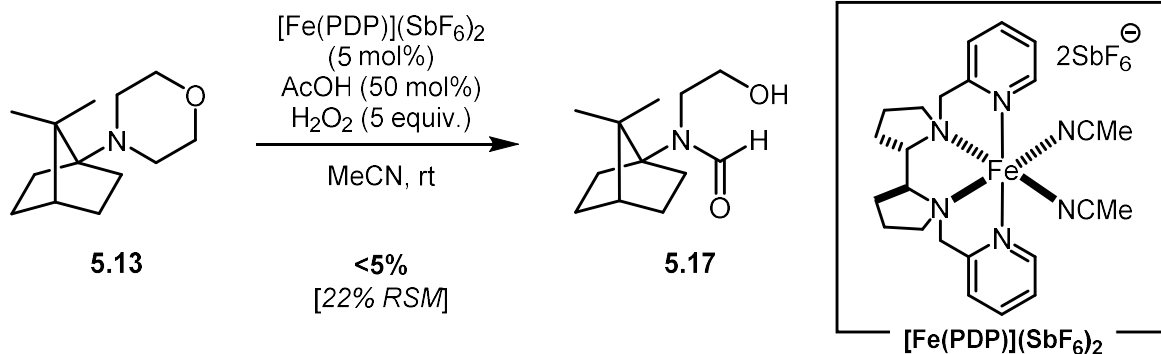
Unless otherwise noted, all reactions were run under a nitrogen or argon atmosphere in flame-dried or oven-dried (150 °C, 24 h) glassware. Reactions were stirred with Teflon-coated magnetic stir bars. Reactions were monitored by thin layer chromatography (TLC) using glass-backed plates pre-coated with 230-400 mesh silica gel (250 µm thickness) with fluorescent indicator F254 (MilliporeSigma Cat. No. 1.05715.0001). Plates were visualized with dual short wave/long wave UV light and/or by treatment with acidic *p*-anisaldehyde stain or KMnO₄ stain with gentle heating. Products were purified by manual or automated flash column chromatography over 230-400 mesh silica (SiliCycle Cat No. R12030B) unless otherwise noted using the solvent systems indicated.

All chemicals were used as received unless otherwise noted and stored as recommended by the supplier. Organic solvents (acetonitrile, dichloromethane, diethyl ether, dimethylformamide, dimethyl sulfoxide, methanol, tetrahydrofuran, toluene) and amine bases (triethylamine, pyridine, *N,N*-diisopropylethylamine, and diisopropylamine) were purified prior to use by the method of Grubbs using a Phoenix Solvent Drying System (available from JC-Meyer Solvent Systems) or PureSolv Micro Amine Drying Column (available from Innovative Technology/Inert) under positive argon pressure. Morpholine was distilled periodically as needed if reagent discolored.

Reactions conducted with microwave irradiation were performed in a Biotage Initiator+ Microwave Synthesizer. NMR spectra were measured on Varian MR400, Varian Inova 500, Varian VNMRs 500, or Varian VNMRs 700 magnetic resonance spectrometers. Deuterated solvents were obtained from Cambridge Isotopes, Inc. Chemical shifts for ¹H NMR were reported

as δ , parts per million, relative to the signal of CHCl_3 at 7.26 ppm. Chemical shifts for ^{13}C NMR were reported as δ , parts per million, relative to the center line signal of the CHCl_3 triplet at 77.16 ppm. Chemical shifts for ^{19}F NMR were uncorrected and reported as δ , parts per million. Abbreviations for chemical shifts are as follows: singlet (s), broad singlet (br s), doublet (d), triplet (t), quartet (q), quintet (quint.), septet (sept.), multiplet (m), apparent (app.). Infrared spectra were recorded on a Thermo-Nicolet IS-50 spectrophotometer and ATR accessory with diamond crystal and are reported in wavenumbers (cm^{-1}). High resolution mass spectra were obtained using an Agilent Q-TOF HPLC-MS using electrospray ionization (ESI) positive ion mode. We thank Dr. James Windak and Dr. Paul Lennon at the University of Michigan Department of Chemistry for assisting with these experiments.

Retigabine was purchased from Cayman Chemical (Ann Arbor, MI). Anilines **5.9**, **5.10**, and **5.11** were prepared according to known procedures⁴¹ and their spectral properties matched those previously reported in the literature.^{42,43} The syntheses of aminoNBs **5.12-5.15** and final analogs **5.20-5.22** are outline in Chapter 2 and Chapter 4, respectively. All final analogs were purified by HPLC prior to biological evaluation and were stored as 10 mM or 100 μM solutions in anhydrous, molecular biology-grade DMSO.



***N*-((1*r*,4*r*)-7,7-dimethylbicyclo[2.2.1]heptan-1-yl)-*N*-(2-hydroxyethyl)formamide (**5.17**)**

In dry vial under nitrogen, 1-aminoNB **5.13** (109 mg, 521 μmol , 1 equiv.) was dissolved in 5.2 mL dry MeCN. Acetic acid (15 μL , 260 μmol , 50 mol%) was added in one portion, followed by bolus addition of $[\text{Fe}(\text{PDP})](\text{SbF}_6)_2$ (24 mg, 26 μmol , 5 mol%; purchased from Strem). The reaction mixture was cloudy brown/orange. Hydrogen peroxide (30 wt% in water, 270 μL , 2.6 mmol) was added down the side of vial over 5 min. At the outset of the addition, the reaction turned purple, then steadily reverted to the brown/orange color. After stirring for 4 h at room temperature, the reaction was quenched with 10 mL sat. sodium bicarbonate, 0.5 mL 6 M NaOH, and 10 mL sat. Na₂S₂O₃. The mixture was further diluted with 10 mL ethyl acetate, and the layers were separated. The aqueous layer was extracted 3x 10 mL ethyl acetate. The combined organic layers were washed with 10 mL brine, dried over anhydrous Na₂SO₄, filtered, and concentrated *in vacuo*. The crude material was purified by flash column chromatography over silica pre-neutralized with 1% NEt₃ (eluting with 30, 40, 50, 60, 80, 100% EtOAc/hexanes), and 24.4 mg (116 μmol , 22% yield) of starting material **5.13** was recovered along with 8.2 mg of **5.17** as a ~50 wt% mixture with an unidentified by-product. The mixture required further purification (2x) by flash column chromatography over silica pre-neutralized with 1% NEt₃ (eluting with 50, 75, 100% EtOAc/pentane) and formamide **15** was collected as 2 mg (9.5 μmol , <5% yield) of a clear, colorless oil.

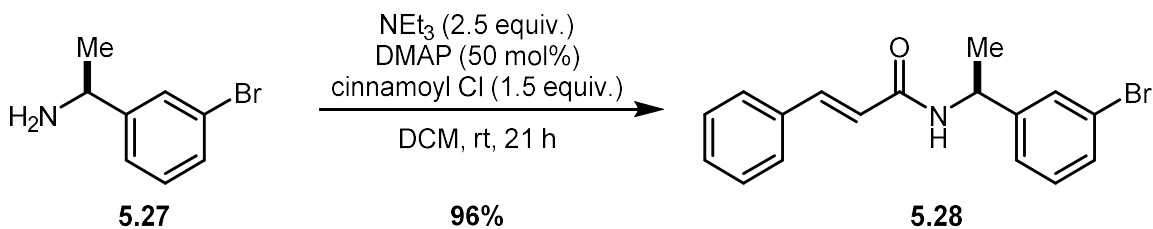
R_f = 0.20 (80% EtOAc/hexanes + 1% NH₄OH), stains red in *p*-anisaldehyde

¹H NMR (700 MHz, CDCl₃): δ 8.45 (s, 1H), 3.75 (t, *J* = 4.8 Hz, 1H), 3.73 (*app.* dt, *J* = 16.4, 5.2 Hz, 2H), 3.60 (*app.* t, *J* = 5.0 Hz, 2H), 2.13-2.08 (m, 2H), 1.96-1.90 (m, 2H), 1.69 (*app.* t, *J* = 4.5 Hz, 1H), 1.69-1.64 (m, 2H), 1.36 (ddd, *J* = 11.5, 10.1, 4.0 Hz, 2H), 1.09 (s, 6H) ppm

¹³C NMR (176 MHz, CDCl₃): δ 165.1, 69.7, 63.9, 47.7, 46.5, 45.9, 34.0, 27.3, 20.4 ppm

IR (neat): 3396, 2959, 2941, 1725, 1643, 1456, 1368, 1323, 1293, 1186, 1053 cm⁻¹

HRMS (ESI+, *m/z*) calculated for C₁₂H₂₂NO₂⁺ 212.1645; found: 212.1644



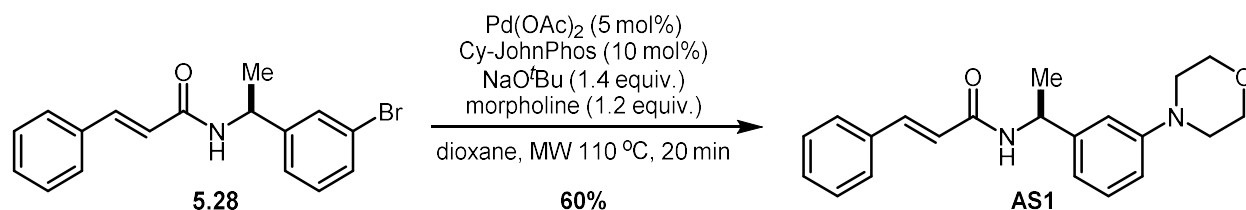
(S)-N-(1-(3-bromophenyl)ethyl)cinnamamide (5.28)

Cinnamoyl chloride (250 mg, 1.50 mmol, 1.5 equiv.) was dissolved in 6 mL dry DCM. NEt_3 (0.35 mL, 2.50 mmol, 2.5 equiv.) was added dropwise, turning the reaction mixture yellow and evolving a white mist. Next, amine **5.27** (0.15 mL, 1.00 mmol, 1 equiv.) was added, followed by DMAP (61.1 mg, 500 μmol , 50 mol%). The reaction was stirred at room temperature for 21 h. The reaction was poured into 20 mL 1 M HCl and further diluted with 20 mL diethyl ether. The layers were separated, and the aqueous layer was extracted 3x 20 mL diethyl ether. The combined organic layers were washed with 20 mL brine, dried over anhydrous MgSO_4 , filtered, and concentrated *in vacuo*. The crude material was purified by flash column chromatography over silica (eluting 8-48% EtOAc/hexanes, 8% increments) and acrylamide **5.28** was collected as 317 mg (959 μmol , 96% yield) of an off-white solid.

R_f = 0.70 (50% EtOAc/hexanes)

$^1\text{H NMR}$ (500 MHz, CDCl_3) δ 7.64 (d, J = 15.6 Hz, 1H), 7.49 (m, 2H), 7.44 – 7.32 (m, 3H), 7.30 (d, J = 7.7 Hz, 1H), 7.22 (t, J = 7.8 Hz, 1H), 6.39 (d, J = 15.6 Hz, 1H), 5.80 (br s, 1H), 5.24 (p, J = 7.1 Hz, 1H), 1.55 (d, J = 7.0 Hz, 3H) ppm

$^{13}\text{C NMR}$ (176 MHz, CDCl_3) δ 165.12, 145.72, 141.77, 134.84, 130.62, 130.42, 129.91, 129.35, 128.96, 127.95, 125.23, 122.93, 120.44, 48.67, 21.92 ppm

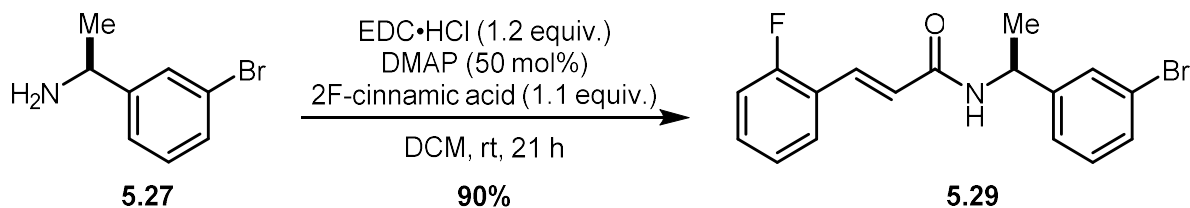


(S)-N-(1-(3-morpholinophenyl)ethyl)cinnamamide (AS1)

Aryl bromide **5.28** (50 mg, 151 μmol , 1 equiv.) was dissolved in 1.5 mL 1,4-dioxane. Sequentially, CyJohnPhos (5.3 mg, 15.1 μmol , 10 mol%), Pd(OAc)_2 (1.7 mg, 7.6 μmol , 5 mol%), NaO^tBu (20.4 mg, 212 μmol , 1.4 equiv.), and freshly distilled morpholine (16 μL , 182 μmol , 1.2 equiv.) were added. The light-yellow heterogeneous reaction mixture was degassed by 3x freeze-pump-thaw cycles. Under inert atmosphere, the reaction mixture was transferred to a 0.5 – 2 mL microwave vial. The vial was securely capped and irradiated in a Biotage Initiator+ microwave at 110 °C for 20 min. After cooling to room temperature, the reaction mixture was diluted 5 mL diethyl ether and 5 mL water. The layers were separated, and the aqueous layer was extracted 3x 5 mL diethyl ether. The combined organic layers were washed with 5 mL brine, dried over anhydrous MgSO_4 , filtered through Celite, and concentrated *in vacuo* to a yellow oil. The crude material was purified by flash column chromatography over silica (eluting 20-60% EtOAc/hexanes, 10% increments) and **AS1** was collected as 30.3 mg (90.1 μmol , 60% yield) of an off-white foam. The spectroscopic properties matched those previously reported.⁵

R_f = 0.30 (50% EtOAc/hexanes)

$^1\text{H NMR}$ (500 MHz, CDCl_3) δ 7.63 (d, J = 15.6 Hz, 1H), 7.49 (dd, J = 7.4, 1.7 Hz, 2H), 7.40 – 7.32 (m, 3H), 7.31 – 7.25 (m, 1H), 6.92 (s, 1H), 6.89 (d, J = 7.6 Hz, 1H), 6.83 (dd, J = 8.2, 2.1 Hz, 1H), 6.36 (d, J = 15.6 Hz, 1H), 5.77 (d, J = 7.8 Hz, 1H), 5.24 (p, J = 7.0 Hz, 1H), 3.92 – 3.79 (m, 4H), 3.23 – 3.12 (m, 4H), 1.56 (d, J = 6.9 Hz, 3H) ppm



(S,E)-N-(1-(3-bromophenyl)ethyl)-3-(2-fluorophenyl)acrylamide (5.29)

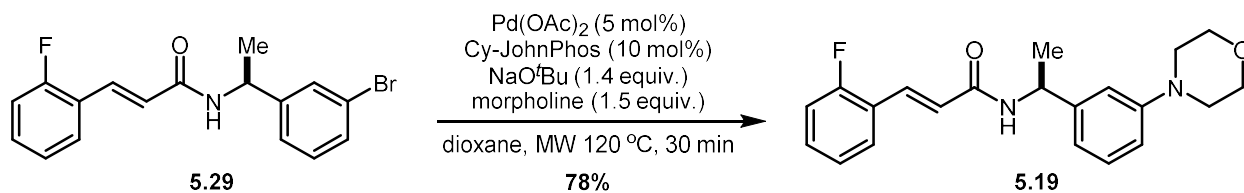
To a flask was added 2-fluorocinnamic acid (183 mg, 1.10 mmol, 1.1 equiv.) and 20 mL dry DCM. Next, amine **5.27** (200 mg, 1.00 mmol, 1 equiv.) was added, followed by EDC·HCl (230 mg, 1.20 mmol, 1.2 equiv.) and DMAP (61.1 mg, 500 μmol , 50 mol%), each as one portion. The reaction was stirred at room temperature for 21 h, then poured into 20 mL 1 M HCl and further diluted with 20 mL diethyl ether. The layers were separated, and the aqueous layer was extracted 3x 20 mL diethyl ether. The combined organic layers were washed with 20 mL brine, dried over anhydrous MgSO_4 , filtered, and concentrated *in vacuo*. The crude material was purified by flash column chromatography over silica (eluting 8-48% EtOAc/hexanes, 8% increments) and acrylamide **5.29** was collected as 313 mg (898 μmol , 90% yield) of an off-white solid.

$R_f = 0.60$ (50% EtOAc/hexanes)

$^1\text{H NMR}$ (500 MHz, CDCl_3) δ 7.70 (d, $J = 15.8$ Hz, 1H), 7.50 (s, 1H), 7.51 – 7.44 (t, $J = 7.5$ Hz, 1H), 7.40 (d, $J = 7.9$ Hz, 1H), 7.35 – 7.28 (m, 2H), 7.22 (t, $J = 7.8$ Hz, 1H), 7.14 (t, $J = 7.5$ Hz, 1H), 7.09 (dd, $J = 10.4, 8.8$ Hz, 1H), 6.54 (d, $J = 15.8$ Hz, 1H), 5.83 (s, 1H), 5.24 (p, $J = 7.1$ Hz, 1H), 1.55 (d, $J = 7.0$ Hz, 3H) ppm

$^{13}\text{C NMR}$ (176 MHz, CDCl_3) δ 165.07, 161.52 (d, $J = 253.4$ Hz), 145.68, 134.85, 131.15 (d, $J = 8.7$ Hz), 130.61, 130.41, 129.98 (d, $J = 3.2$ Hz), 129.36, 125.22, 124.52 (d, $J = 3.5$ Hz), 123.46 (d, $J = 7.9$ Hz), 122.91, 122.85, 116.28 (d, $J = 22.0$ Hz), 48.73, 21.90 ppm

HRMS (ESI+, m/z) calculated for $\text{C}_{17}\text{H}_{15}\text{BrFNNaO}^+$ 370.0219; found 370.0220



(S,E)-3-(2-fluorophenyl)-N-(1-(3-morpholinophenyl)ethyl)acrylamide (5.19, F-AS1)

Aryl bromide **5.29** (143 mg, 409 μmol , 1 equiv.), CyJohnPhos (14.3 mg, 40.9 μmol , 10 mol%), Pd(OAc)₂ (4.6 mg, 20.5 μmol , 5 mol%), morpholine (54 μL , 614 μmol , 1.5 equiv.), and NaO^tBu (55.1 mg, 573 μmol , 1.4 equiv.) were each added sequentially to a 2-5 mL microwave vial. The solids were dissolved in 4.1 mL 1,4-dioxane. The heterogeneous, orange reaction mixture was vigorously stirred on the benchtop for 10 min and the headspace was thoroughly flushed with argon. The vial was securely capped and irradiated in a Biotage Initiator+ microwave at 120 °C for 30 min. After cooling to room temperature, the reaction mixture was diluted 10 mL diethyl ether and 10 mL water. The layers were separated, and the aqueous layer was extracted 3x 10 mL diethyl ether. The combined organic layers were washed with 10 mL brine, dried over anhydrous MgSO₄, filtered, and concentrated *in vacuo*. The crude material was purified by automated flash column chromatography over silica (25 g column, eluting 25-80% EtOAc/hexanes over 15 CVs) and **5.19 (F-AS1)** was collected as 112.9 mg (319 μmol , 78% yield) of an off-white foam.

R_f = 0.50 (50% EtOAc/hexanes)

¹H NMR (500 MHz, CDCl₃) δ 7.69 (d, *J* = 15.8 Hz, 1H), 7.47 (t, *J* = 7.1 Hz, 1H), 7.30 (dd, *J* = 11.5, 5.7 Hz, 1H), 7.28 – 7.22 (m, 3H), 7.14 (t, *J* = 7.4 Hz, 1H), 7.08 (dd, *J* = 10.5, 8.7 Hz, 1H), 6.92 (s, 1H), 6.89 (d, *J* = 7.6 Hz, 1H), 6.83 (dd, *J* = 8.2, 1.9 Hz, 1H), 6.51 (d, *J* = 15.8 Hz, 1H), 5.82 (d, *J* = 7.2 Hz, 1H), 5.24 (p, *J* = 6.9 Hz, 1H), 3.91 – 3.71 (m, 4H), 3.23 – 3.08 (m, 4H), 1.56 (d, *J* = 6.3 Hz, 3H) ppm

HRMS (ESI+, *m/z*) calculated for C₂₁H₂₄FN₂O₂⁺ 355.1816; found 355.1849

5.4.2. Evaluation of Metabolic Stability

Materials

Test compounds were dissolved in DMSO (biochemical grade, sterile-filtered) immediately following purification to generate 10 mM stock solutions; stock solutions were stored under Ar in a -20 °C freezer. Microsomes were purchased from ThermoFisher Scientific; Rat (Sprague-Dawley) Catalog No.: RTMCPL [Lot No.: RT0541-B and RT0541-C], Human (50 Donor Pool) Catalog No.: HMMCPL [Batch No.: PL050C-B]. NADPH regenerating solution components were purchase from Corning (Gentest NADPH Regenerating System); Solution A [NADP⁺/Glc-6-PO₄] Product No.: 451220, Solution B [G6PDH] Product No.: 451200. Solvents (HPLC-grade), buffer components (biochemical grade), and positive control (verapamil·HCl, **5.16**) were purchased from Sigma-Aldrich. The 0.1 M potassium phosphate buffer listed below (henceforth “phosphate buffer”) was prepared in the following manner: 1) 0.1 M KH₂PO₄ solution was prepared from 3.40 g KH₂PO₄ in 250 mL water (18 MΩ); 2) 0.1 M KH₂PO₄ solution was prepared from 17.42 g K₂HPO₄ in 1.0 L water; 3) 190 mL of 0.1 M KH₂PO₄ solution was added to 810 mL of 0.1 M KH₂PO₄ solution, and the pH was adjusted to 7.4 using 1.0 M KOH (aq.); 4) 0.1 M phosphate buffer was sterile-filtered and stored at room temperature. Sterile filters were purchased from Corning; 500 mL bottle top vacuum filter, 0.2 μm pore size, 33.2 cm² Nylon membrane [Product No.: 430049]. Filter plates were purchased from Pall Corporation; AcroPrep Advance 96-well filter plates, 350 μL, 0.2 μm GHP membrane [Part No.: 8082]; wells not containing microsomes could be re-used by flushing with water then methanol (2x) and air-drying before re-use. Plates were purchased from Waters; Acquity 700 μL round 96-well sample plates [Part No.: 186005837]. Samples were analyzed on an Agilent Q-TOF HPLC-MS (Infinity 1290 Series HPLC; Agilent 6520 Accurate-Mass Q-TOF LC/MS) using an Agilent Zorbax Eclipse Plus

C18 column (2.1 x 50 mm); each sample (10 μ L injection) was run on a 5% to 100% A:B gradient (A=95:5 water:MeCN + 0.1% formic acid; B=MeCN + 0.1% formic acid) at 0.4 mL/min for 4.5 min before holding at 100% B for 0.5 min, then re-equilibrating to 5% A:B over 1 min; data was analyzed using Agilent MassHunter software by extracting mass data for analyte in question and integration of peak.

Protocol

Microsomal stability assay protocol was adapted from literature sources^{44,45} as well as supplier protocols. Verapamil·HCl (**5.16**) was included as a positive control and metric for assay consistency in all runs. RLMs and HLMs were generally run side by side, with the negative controls serving for both trials. All compounds were evaluated in five individual assays in either singlicate or triplicate; final retention values are reported as averaged percent retained relative to the negative control (no incubation) \pm SEM. Amounts below are specific to the analysis of 6 samples per experiment, but these values can be scaled to include additional compounds. Trials were run directly in the filter plates listed above, thus necessitating only centrifugation into the final analysis plate before placement in the HPLC.

1) Pre-incubation preparation

- Cooled 1.135 mL phosphate buffer on ice in microcentrifuge tube; once cool, added 31 μ L microsomes and mixed by gentle inversion over the course of 1 min; returned to ice for later use; microsomes were thawed immediately before use and stored at -80 °C
- Cooled 12-15 mL MeCN on ice in Falcon tube
- Thawed 10 mM DMSO stocks of compounds; in separate vials (one for each compound), mixed 9 μ L MeCN and 9 μ L water; added 2 μ L 10 mM to generate a 1 mM stock of each compound

(100x). This mixture allows final assay composition to remain $\leq 0.1\%$ DMSO and $\leq 0.5\%$ MeCN while still ensuring compound solubility pre-assay.

- Plate Setup:

- Edge wells: 200 μL water were added to each well bordering the wells to be analyzed.
- Microsome trial wells: 188 μL of diluted RLM or HLM suspension were added to each well.
- Negative control wells: 198 μL of phosphate buffer were added to each well

2) Incubation

- Immediately before incubation, 2 μL of 100x compound stock was added to the corresponding RLM/HLM well.
- Transferred plate into shaker pre-heated to 37 °C [Orbital SSI3 benchtop shaking incubator].
- Incubated 10 min at 37 °C while shaking at 100 rpm.
- NADPH regenerating solution was prepared by mixing 55 μL solution A with 11 μL solution B (pipet mix), then cooling on ice; these volumes were doubled if running RLMs and HLMs concurrently; both solutions A and B were thawed immediately before use and stored at -20 °C;
- Plate was removed from shaker, and 10 μL NADPH regenerating solution was added to each microsome trial well (200 μL final assay volume).
- Incubated 45 min at 37 °C while shaking at 100 rpm.
- Plate was removed from shaker, and 100 μL of cold MeCN was jetted into each well (microsome trial and negative control) to quench reaction. Of note, quenching reaction by pipetting cold MeCN up and down led to highly inconsistent data. Jetting the MeCN directly into the center of the well and allowing diffusion to cool and quench the mixture has offered the most consistent and reproducible results in our experience.

- To each negative control well, 2 μL 100x compound stock was added.

3) Centrifugation/Analysis

- Plate was centrifuged for 45 min at 3500 rpm at 20 $^{\circ}\text{C}$ [Eppendorf 5804 R tabletop centrifuge with a A-2-DWP swinging basket rotor]; for RLMs, only 4 min of centrifugation are required.

- Plate was transferred into Agilent HPLC, analyzing 10 μL injections of each well.

- Compound retention was assessed using MassHunter software, and the average percent retention after 45 min of incubation across 5 experiments is listed below (and provided in the text in graphical format; presented as \pm SEM).

Validation of Microsomal Activity

In order to validate the performance of the microsomes, each batch was run through a series of control experiments. Volumes of solutions were scaled from above based on need within the assay. For each run, a single experiment was performed with each of the following controls being run in triplicate:

- [+]: standard microsomal mixture

- **HI**: standard microsomal mixture, but with heat-inactivated microsomes (188 μL taken from 200 μL aliquot that was exposed to 80 $^{\circ}\text{C}$ water bath for 10 min in separate tube before cooling back to 0 $^{\circ}\text{C}$).

- **blank**: buffer control, in which 188 μL RLM/HLM aliquot is replaced with 188 μL phosphate buffer.

- **0 min**: standard microsomal mixture, but with NADPH regenerating solution being added after 45 min incubation.

- [-]: standard negative control (i.e. 198 μL phosphate buffer, compound added after incubations).

Representative plots for both RLMs and HLMs are shown below. Verapamil·HCl (**5.16**) is not highly stable in solution, hence the discrepancy between the [-] run and the other negative controls; this was not observed nor is it expected for the aniline and aminoNB compounds. The consistency of the other three negative controls validates that the effectiveness of the microsomes, NADPH regenerating solution, and assay setup.

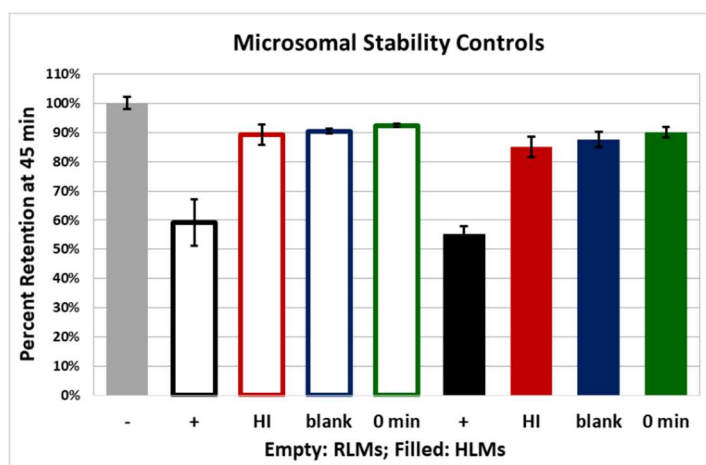


Figure 5.15. Validation of Microsome Source

Empty bars: Percent retention of verapamil relative to standard negative control \pm SD (RLM batch RT0541-C); Filled bars: Percent retention of verapamil relative to standard negative control \pm SD (HLM batch PL050C-B).

Data Summary

Rat (Sprague-Dawley) Liver Microsomes							
	Exp 1	Exp 2	Exp 3	Exp 4	Exp 5	Avg (N=5)	SEM (N=5)
14	56%	39%	32%	34%	41%	40%	4%
10	35%	31%	47%	65%	75%	51%	8%
11	31%	20%	7%	15%	5%	15%	5%
12	65%	51%	24%	18%	45%	40%	9%
13	0%	0%	0%	0%	0%	0%	0%
2m	40%	48%	34%	34%	47%	41%	3%
2a	47%	52%	37%	35%	38%	42%	3%
2l	0%	0%	0%	0%	0%	0%	0%
2x	64%	73%	53%	74%	74%	67%	4%

Human Liver Microsomes							
	Exp 1	Exp 2	Exp 3	Exp 4	Exp 5	Avg (N=5)	SEM (N=5)
14	49%	54%	53%	37%	28%	44%	5%
10	73%	.	74%	89%	86%	80%	4%
11	38%	53%	60%	46%	15%	42%	8%
12	49%	78%	65%	57%	18%	54%	10%
13	0%	15%	15%	0%	0%	6%	4%
2m	74%	67%	68%	58%	49%	63%	4%
2a	82%	51%	73%	79%	66%	70%	5%
2l	62%	52%	44%	62%	68%	58%	4%
2x	87%	50%	59%	84%	84%	73%	8%

Figure 5.16. Complete Microsomal Stability Data Set

Top: Individual percent retention measurements and averaged data for RLM trials; Bottom: Individual percent retention measurements and averaged data for HLM trials; *for **10**, a point is deleted due to errors in the HPLC data collection software. For compound labeling, see: *Chem.* **2019**, *5*, 215-226.

Metabolite Identification - Materials and Instrumentation (Figure 5.3 and Figure 5.5)

As described above, 10 mM stock solutions of test compounds **5.9** and **5.13** dissolved in DMSO were stored at -20 °C. Pooled HLM (150 donor pool, mixed gender) were purchased from Corning Discovery Labware (Catalog No.: 452117) and stored at -80 °C; the same batch of RLMs as used above were employed here. NADPH-regenerating system solutions (Solution A: 26 mM NADP⁺, 66 mM glucose 6-phosphate, 66 mM MgCl₂ in water; Solution B: 40 U/mL glucose 6-phosphate dehydrogenase in 5 mM sodium citrate) were purchased from Corning Discovery Labware (Catalog No.: 451220 and 451200, respectively) and stored at -20°C. Potassium phosphate buffer (0.1 M, adjusted to pH 7.4) was prepared according to standard protocols and stored at room temperature. L-Glutathione reduced (GSH) was purchased from SigmaAldrich. Metabolic incubations were carried out in a temperature-controlled shaking water-bath. LC-MS/MS analysis of parent compounds and metabolites was carried out using two different systems, similar to that described previously.⁴⁶ System A: The first system consisted of two Shimadzu LC-20ADXP pumps, a CTC PAL autosampler, and a CTO-20A column oven coupled to an AB Sciex Q-Trap 6500. System B: The second system consisted of two Shimadzu LC-20ADXP pumps, a

SIL-20ACXR autosampler, and a CTO-20A column oven coupled to a Shimadzu LC-MS/MS 8030 triple quadrupole mass spectrometer. For both systems, a Kinetex EVO C18 (2.6 mm, 50 μ m x 2.1 mm) heated to 32 °C was used for analyte separation with a flow rate of 0.3 mL/min. Mobile phase A was 0.1 % formic acid in LC/MS-grade water, and mobile phase B was 0.1% formic acid in LC/MS-grade acetonitrile. Two LC gradients were used for the separation of compound metabolites. LC gradient program 1: linear gradient of 5-25% B from 0-8 min; 25-95% B from 8-9 min; 95% B 9-9.5 min; 95-5% B from 9.5-9.6 min; and re-equilibration at 5% B from 9.6-11.0 min. LC gradient program 2: linear gradient of 5-40% B from 0-8 min; 40-95% B from 8-9 min; 95% B 9-9.5 min; 95-5% B from 9.5-9.6 min; and re-equilibration at 5% B from 9.6-11.0 min. The total run time for both methods was 11 min. Samples (injection volume 10-20 μ L) were injected into the equilibrated LC-MS system. MS/MS analysis was conducted using electrospray ionization in positive ion mode. Analysis using the Sciex Q-Trap 6500 employed information-dependent acquisition with two survey scans: 1) multiple reaction monitoring (MRM) for predicted biotransformation products based on the MS/MS spectrum of the parent compound, and 2) enhanced product ion (EPI) analysis. Collision induced dissociation of selected precursor ions was performed at collision energy 25-36 V. Shimadzu LabSolutions and Sciex Acquisition, PeakView, and MassQuant Software were used to acquire and analyze MS spectral data.

Protocol

Microsomal incubations were performed analogously to those listed above; the exact methods are listed below for sake of completeness.

Working solutions (1 mM) of test compounds were prepared from 10 mM stock solutions in DMSO. In a 1.5 mL microcentrifuge tube, 4 μ L of 1000x test compound was added to a 1:1

mixture of de-ionized water and acetonitrile (36 μ L). The final volume was 40 μ L (1 mM test compound; 10% DMSO; 45% water; 45% acetonitrile). Glutathione (5 mM) was prepared in potassium phosphate buffer (0.1 M, pH 7.4). Immediately before incubation, pooled RLM (20 mg/mL) were thawed rapidly at 37 °C and stored on ice. Aliquots of pooled RLM (1:40 dilution) were added to the reaction mixture for a final concentration of 0.5 mg protein/ml. Samples were mixed gently by inverting 3-4 times. NADPH solution B was added (1:100 dilution) to the experimental samples, and an equivalent volume of potassium phosphate buffer was added to control incubations. Samples were pre-incubated for 5 min at 37°C. Reactions were initiated by addition of NADPH solution A (1:20 dilution). The final reaction volume was 0.2 mL. Incubations were carried out for 45 min at 37 °C in a shaking water-bath (45 rpm). Reactions were terminated with the addition of an equal volume of ice-cold acetonitrile (0.2 mL) to pellet proteins. Controls: 1) Time 0-min controls were prepared without addition of NADPH until after the 45-min incubation and addition of an equal volume of ice-cold acetonitrile (0.2 mL); 2) blank control samples were prepared without RLM; 3) negative controls were prepared without NADPH-regenerating system and without RLM. Each reaction condition was performed in triplicate. Following the incubation and addition of an equal volume of ice-cold acetonitrile, samples were mixed with a vortex device for 10 s, placed on ice for 5-10 min, and centrifuged at 14,000 rpm for 20 min at 4°C. The clear supernatant was transferred to LC-MS vials and stored at -20°C prior to LC-MS/MS analysis.

Results Summary

The structures, retention times, and fragmentations patterns of the parent compound aminoNB **5.13** and the identified metabolites are provided below. Formamide **5.17** was confirmed

with an authentic sample. The fragmentation pattern of hydroxylated metabolite **5.18** was consistent with morpholine oxidation (unknown whether this is adjacent to the nitrogen or oxygen). No additional hydroxylation products or alternative oxidation states (e.g. ketones, amides, esters) were detected upon explicit mass-directed searches. For GSH trials, samples were analyzed for the neutral loss of 129 Da, which is characteristic of loss of the pyroglutamic acid moiety of GSH;⁴⁷ no metabolites corresponding to this mass (or the full GSH adduct mass) were detected across multiple runs with 1-aminoNB **5.13**.

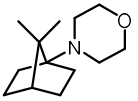
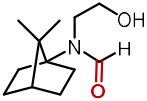
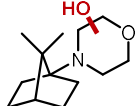
Compound	[M+H] ⁺ (<i>m/z</i>)	Fragmentation Ions (<i>m/z</i>)	Residence Time (min)
 5.13	210.1852	123, 81	1.21
 5.17	212.1645	194, 184, 123, 81	6.32
 5.18	226.1802	208, 166, 152, 123, 81	1.17

Figure 5.17. Tabular Metabolite Fragmentation Data

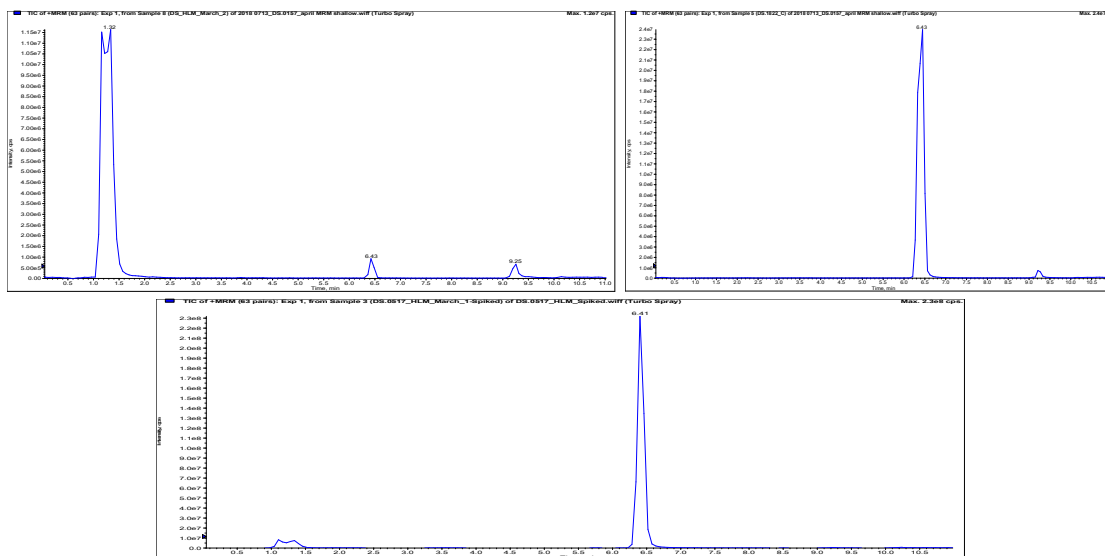


Figure 5.18. HPLC traces of aminoNB **5.13** upon incubation with RLMs and validation of formamide **5.17** identity

Top Left) Total ion chromatogram from LC-MS/MS analysis of microsomal incubations containing HLM + NADPH + aminoNB **5.13**; Top Right) Total ion chromatogram from LC-MS/MS analysis of formamide **5.17** synthetic standard alone; Bottom) Total ion chromatogram from LC-MS/MS analysis of metabolic incubations containing HLM + NADPH + aminoNB **5.13** spiked with formamide **5.17** synthetic standard.

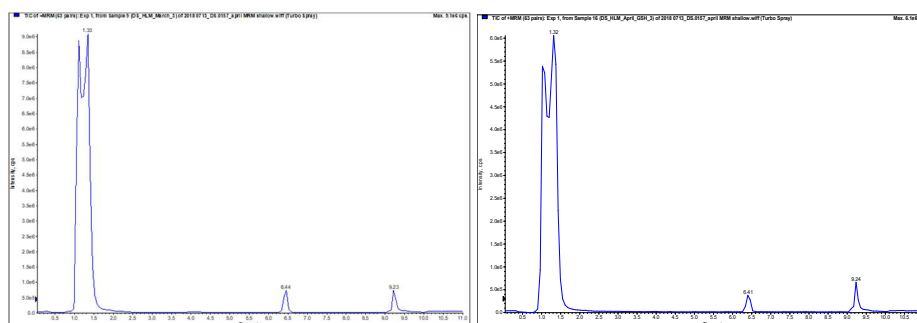


Figure 5.19. Glutathione trials with aminoNB **5.13**

Left) Total ion chromatogram from LC-MS/MS analysis of microsomal incubations containing HLM + NADPH + aminoNB **5.13** [no GSH]; Right) Total ion chromatogram from LC-MS/MS analysis of microsomal incubations containing HLM + NADPH + aminoNB **5.13** + 5 mM GSH.

Metabolite Identification - Procedure (Figure 5.6)

- Prepare 1 mM working solution of each test compound from 10 mM stock in DMSO. (1:10 dilution)
 - In a 1.5 mL microcentrifuge tube, add 45 μ L of de-ionized water + 45 μ L of acetonitrile + 10 μ L of 10 mM test compound. Vortex 10 s.
 - Final volume and concentration = 100 μ L of 1 mM test compound (10% DMSO; 40% water; 40% acetonitrile)
- Prepare 5 mM GSH in 100 mM KPi: (GSH MW = 307.32 g/mol)

5 mM GSH = 1.537 mg/ml

Prepare for 5.6 ml total incubation: 8.61 mg GSH + 5.138 mL of 100 mM KPi.

This is a 14x mix (367 μ L x 14 = 5138 μ L).
- Prepare the following Reaction Mix:

Reagent	Dilution Factor	Volume (μ L)	14X Master Mix (μ L)
5 mM GSH in 100 mM potassium phosphate	NA	367	5138
1 mM test compound (working solution)	100	4	56
Total		371	5194

Table 5.3. Reaction mix for metabolite identification

- Aliquot 371 μ L each of reaction mix into labeled sample vials: 6 vials total for HLM and 6 vials total for RLM (run experiment in parallel with HLM and RLM). See table below.

Vial #	Sample	HLM (20 m/ml)	NADPH Sol B (μ L)	NADPH Sol A (μ L)	Final Volume (μ L)
1	+HLM +NADPH	+5	+4	+20	400
2	+HLM +NADPH	+5	+4	+20	400
3	+HLM +NADPH	+5	+4	+20	400
4	-HLM +NADPH (control)	+5 of buffer	+4	+20	400
5	+HLM – NADPH (control)	+5	+4 μ L of buffer	+20 μ L of buffer	400

6	- HLM - NADPH (control)	+5 of buffer	+4 μ L of buffer	+20 μ L of buffer	400
7	+RLM +NADPH	+5	+4	+20	400
8	+RLM +NADPH	+5	+4	+20	400
9	+RLM +NADPH	+5	+4	+20	400
10	-RLM +NADPH (control)	+5 of buffer	+4	+20	400
11	+RLM - NADPH (control)	+5	+4 μ L of buffer	+20 μ L of buffer	400
12	- RLM - NADPH (control)	+5 of buffer	+4 μ L of buffer	+20 μ L of buffer	400

Table 5.4. Summary of metabolite identification trials in RLMs, HLMs, and control experiments

- Add 5 μ L **HLM** (20 mg/ml) to vials **1-3** and vial **5** (+HLM); add 5 μ L **RLM** (20 mg/ml) to vials **7-9** and vial **11** (+RLM); add 5 μ L buffer to control vials **4, 6** (-HLM) and vials **10, 12** (-RLM).
- Add 4 μ L NADPH Solution B to vials **1-4** and **7-10**; add 4 μ L buffer to (-NADPH) control vials **5-6** and **11-12**.
- Pre-warm reaction mix for 5 min before adding NADPH solution A.
- For time 0 min:** Remove 190 μ L from vials **1-12**, and transfer to a separate vial. Add 200 μ L of ice-cold MeCN. Vortex for 10 seconds. Add 10 μ L NADPH Solution A to vials **1-4** and **7-10**. Repeat vortex, and place on ice. Add 10 μ L of buffer to (-NADPH) control vials **5-6** and **11-12**.
- For remaining reaction mix:** Initiate reaction by adding 10 μ L NADPH Solution A to vials **1-4** and **7-10**; add 10 μ L of buffer to (-NADPH) control vials **5-6** and **11-12**.
- Incubate in 37 $^{\circ}$ C water-bath for 45 min.
- After 45 min, add 200 μ L of ice-cold MeCN containing to reaction vials. Vortex for 10 seconds and place on ice.
- Place samples on wet ice for 5-10 min. Centrifuge at 14,000 rpm, 20 min (table-top centrifuge).

13. Transfer 300 μL of supernatant to separate LC-MS vials for analysis by LC-MS (liquid chromatography – mass spectrometry).

Total Samples: 1 compound X 6 reactions X 2 time points X 2 species (rat/human) = 24

samples

Final Reaction Mix:

Reagent	Dilution Factor	Final Concentration	Volume (μL)	14X Master Mix (μL)
5 mM GSH in 100 mM potassium phosphate	NA	100 mM KPi, 5 mM GSH	367	5138
1 mM test compound (working solution)	100	10 μM	4	56
HLM or RLM (20 mg/ml)	80	0.25 mg/ml	5	each
NADPH solution B	100		4	each
<i>~Pre-warm for 5 min before adding NADPH solution A to initiate reaction~</i>				
NADPH solution A	20		20	each
Total			400	

Table 5.5. Final reaction mix for metabolite identification experiments

1/10/20_TMS0595: 10 uM TMS0595 in RLM; 5 mM GSH_45 min:
 +NADPH
 Product Ion Scan m/z 375 (CE 31V)

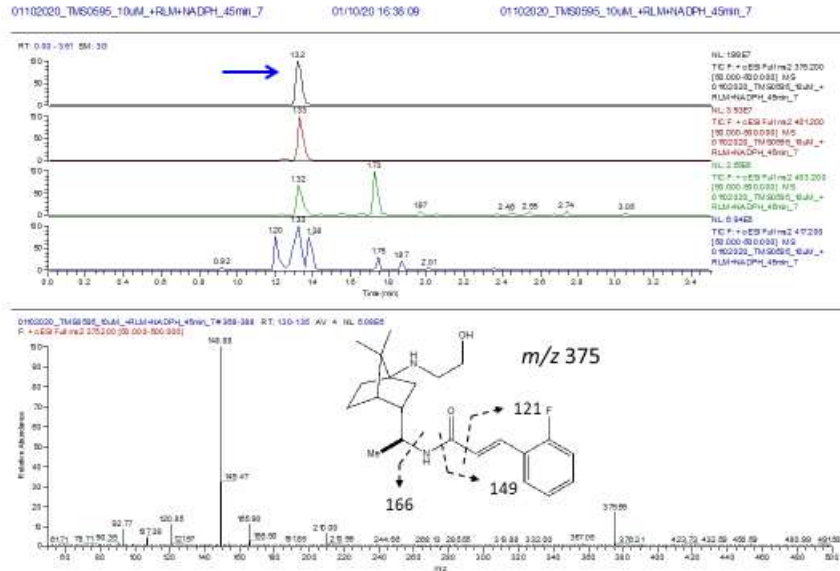


Figure 5.20. LC/MS/MS trace identifying metabolite 5.23 in RLMs

1/10/20_TMS0595: 10 uM TMS0595 in RLM; 5 mM GSH_45 min:
 +NADPH
 Product Ion Scan m/z 401 (CE 31V)

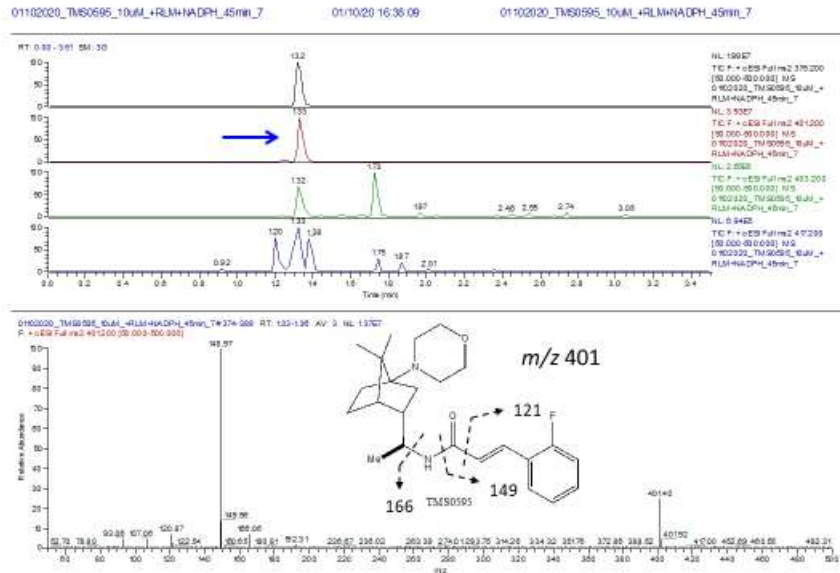


Figure 5.21. LC/MS/MS trace identifying metabolite 5.22 in RLMs

1/10/20_TMS0595: 10 uM TMS0595 in RLM; 5 mM GSH_45 min:
 +NADPH
 Product Ion Scan m/z 403 (CE 31V)

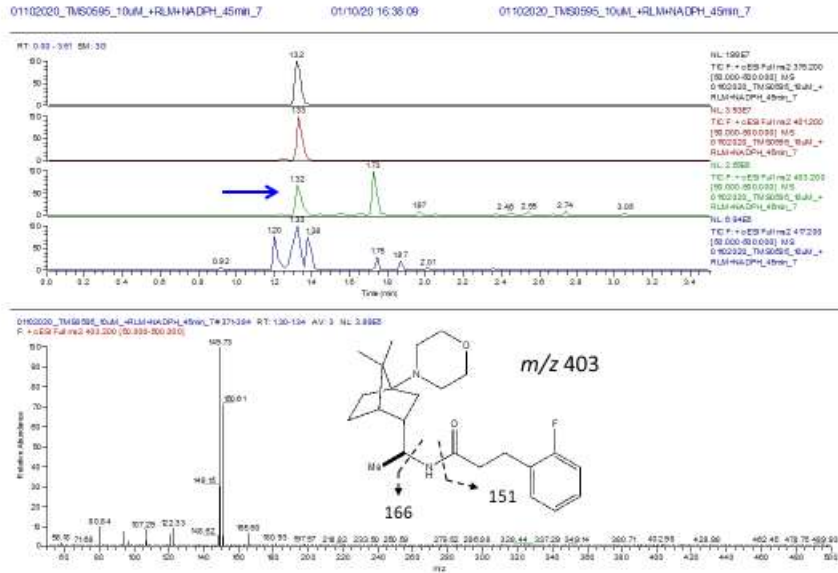


Figure 5.22. LC/MS/MS trace identifying metabolite 5.25 in RLMs

1/10/20_TMS0595: 10 uM TMS0595 in RLM; 5 mM GSH_45 min:
 +NADPH
 Product Ion Scan m/z 403 (CE 31V)

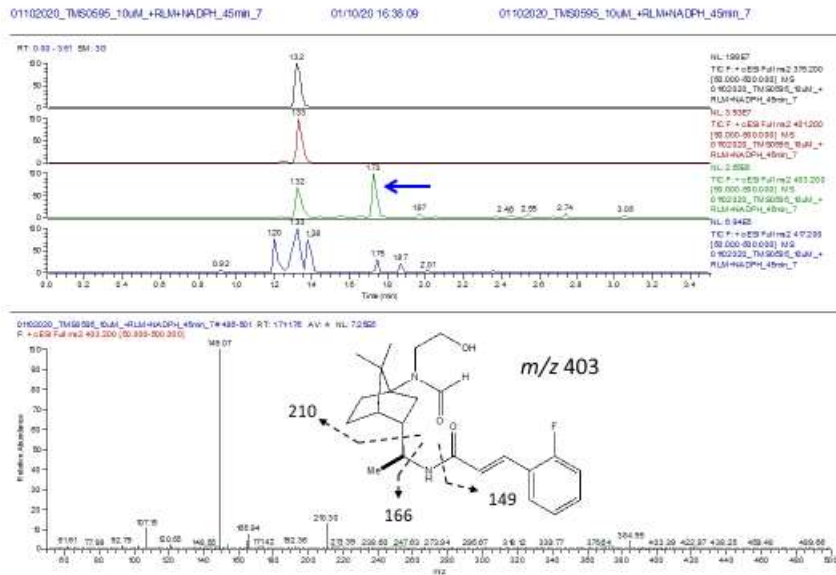


Figure 5.23. LC/MS/MS trace identifying metabolite 5.24 in RLMs

5.4.3 Manual Whole Cell Electrophysiology

Constructs and Chemicals

The hKCNQ2 construct was a generous gift from Mark Shapiro (University of Texas – San Antonio). cDNA was prepared by transformation in competent *E. coli* bacteria (New England BioLabs, NED 10-beta Competent *E. coli* High Efficiency), purified using EndoFree Plasmid Kits (Qiagen), and cDNA suspensions in nuclease-free water were quantified using a NanoDrop Spectrophotometer (ThermoFisher).

Stock solutions of compounds were stored as 10 mM or 100 μ M solutions in molecular biology-grade DMSO at -20 °C. Working solutions of compounds were prepared from fully thawed stocks by dissolving in the appropriate physiological buffer on the day of the experiment. Working solution DMSO content did not exceed 0.1%.

Cell Culture and Transfection

HEK293A cells (a gift of Prof. Anatoli Lopatin,⁴⁸ UMich) were grown continuously as a monolayer at humidified 37 °C and 5% CO₂ in Dulbecco's Modified Eagle's Medium (DMEM) + GlutaMAX (Gibco, Ref. 10569-101) supplemented with 10% fetal bovine serum (FBS) (Corning, Ref. 35-010-CV). Cells were transfected with Lipofectamine LTX with PLUS Reagent (Invitrogen, Ref. 152338-030) according to the manufacturer's instructions. Cells were split and plated in 35 mm culture dishes onto untreated glass coverslips 24 hours post-transfection, allowed to adhere for a minimum of 4 h, and used for recordings after a further 20-72 h. Cells were analyzed before 15 passages.

Whole Cell Electrophysiology

Whole cell electrophysiology recordings were used to assess the effects of **RTG**, **AS1**, **F-AS1**, and the aminoNB analogs (**5.20**, **5.21**) on hKCNQ wt channel current. All buffers and salts

were purchased from Sigma Aldrich or Fisher Scientific. Patch pipettes were filled with an intracellular solution composed of 132 mM K-gluconate, 10 mM KCl, 4 mM Mg·ATP, 20 mM HEPES, and 1 mM EGTA; pH was adjusted to 7.2-7.3 with KOH and osmolarity was 275 mOsm. A low concentration of EGTA was used (compared to other reports employing 10 mM EGTA) due to the observation that “concentrations of calcium chelators above 1 mM lead to a very rapid diminution of KCNQ currents.”⁴⁰ To minimize contributions from anion currents, KCl was largely replaced with K-gluconate. Extracellular solutions were prepared from 140 mM NaCl, 5 mM KCl, 2 mM CaCl₂·2H₂O, 1.5 mM MgCl₂·6H₂O, 10 mM HEPES, and 10 mM D(+)-glucose; pH was adjusted to 7.35-7.45 and osmolarity was measured to be 295-305 mOsm.⁴⁹ All solutions were sterile-filtered through a syringe filter before use.

Electrodes were pulled from borosilicate glass capillaries (World Precision Instruments, Cat. No. 1B100F-4) to a tip resistance of 4-8 MΩ when filled with intracellular solution. Experiments were performed at room temperature (20-25 °C). Coverslips containing cultured cells were rinsed with extracellular solution to remove growth media, placed in a recording chamber on the stage of an inverted microscope, and gently covered in extracellular solution containing the desired concentration of drug compound. Only isolated cells were analyzed as HEK239A cells form gap junctions with each other. Recordings were performed 2 min after achieving whole cell configuration. After no more than 60 min submerged in the drug concentration being analyzed, the coverslip was discarded.

The cells were clamped at -60 mV for 38 ms before eliciting currents by 1,000 ms depolarizing potentials in 10 mV increments (-120 mV or -100 mV to +60 mV, 17-19 total steps), followed by a return step to 0 mV for 60 ms. Data was collected using an AxoPatch-200B amplifier

(Molecular Devices) and digitized using DigiData 1440A with pClamp software (Axon Instruments).

Data Analysis and Statistics

Only cells that fell within acceptable recording parameters (Membrane resistance $R_m > 300$ m Ω , Access Resistance $R_A < 20$ M Ω) and displayed slow activating currents were analyzed. Cells most often had C_m between 10-20 pF but ranged from 6.3-26.4 pF. Whole cell currents elicited by each voltage step were measured from the amplitudes of the deactivation tails after capacitance had diminished. Leak was subtracted offline, and capacitance was uncorrected. Conductance-Voltage (I-V) curves were generated in ClampFit software, and single Boltzmann distribution (Eq. 5.1) was used to fit the I-V curves to determine the maximal current (I_{max}) and half-maximal activation voltage ($V_{1/2}$) of KCNQ currents in ClampFit or Microsoft Excel. All data are quoted as mean \pm SEM unless otherwise specified. Statistical significance between control and test conditions were determined using Student's *t*-test (unpaired, two sample unequal variances, two-tailed distribution) and differences were significant at $p < 0.05$.

5.5 References

1. Limban, C.; Nuta, D.C.; Chirita, C.; Negres, S.; Arsene, A.L.; Goumenou, M.; Karakitsios, S.P.; Tsatsakis, A.M.; Sarigiannis, D.A. "The use of structural alerts to avoid the toxicity of pharmaceuticals." *Toxicol. Rep.* **2018**, *5*, 943-953.
2. Claesson, A.; Minidis, A. "Systematic Approach to Organizing Structural Alerts for Reactive Metabolite Formation from Potential Drugs." *Chem. Res. Toxicol.* **2018**, *31*, 389-411.
3. Kalgutkar, A.; Dalvie, D. "Predicting Toxicities of Reactive Metabolite-Positive Drug Candidates." *Annu. Rev. Pharmacol. Toxicol.* **2015**, *55*, 35-54.
4. Kalgutkar, A.S. "Designing around Structural Alerts in Drug Discovery." *J. Med. Chem.* **2019**, DOI:10.1021/acs.jmedchem.9b00917
5. Wu, Y-J.; Boissard, C.G.; Greco, C.; Gribkoff, V.K.; Harden, D.G.; He, H.; L'Heureux, A.; Kang, S.H.; Kinney, G.G.; Knox, R.J.; Natale, J.; Newton, A.E.; Lehtinen-Oboma, S.; Sinz, M.W.; Sivarao, D.V.; Starrett Jr., J.E.; Sun, L-Q.; Tertyshnikova, S.; Thompson, M.W.; Weaver, D.; Wong, H.S.; Zhang, L.; Dworetzky, S.I. "(S)-N-[1-(3-Morpholin-4-ylphenyl)ethyl]-3-phenylacrylamide: An Orally Bioavailable KCNQ2 Opener with Significant Activity in a Cortical Spreading Depression Model of Migraine." *J. Med. Chem.* **2003**, *46*, 3197-3200.
6. Wu, Y-J.; Davis, C.D.; Dworetzky, S.; Fitzpatrick, W.C.; Harden, D.; He, H.; Knox, R.J.; Newton, A.E.; Philip, T.; Polson, C.; Sivarao, D.V.; Sun, L-Q.; Tertyshnikova, S.; Weaver, D.; Yeola, S.; Zoeckler, M.; Sinz, M.W. "Fluorine Substitution Can Block CYP3A4 Metabolism-Dependent Inhibition: Identification of (S)-N-[1-(4-Fluoro-3-morpholin-4-ylphenyl)ethyl]-3-(4-fluorophenyl)acrylamide as an Orally Bioavailable KCNQ2 Opener Devoid of CYP3A4 Metabolism-Dependent Inhibition." *J. Med. Chem.* **2003**, *46*, 3778-3781.
7. In this assay, time-dependent inhibition is defined as a 2-fold decrease in IC₅₀ between 5 and 45 min
8. Shaikh, A.R.; Del Carpio, C.A.; Tsuboi, H.; Koyama, M.; Hatakeyama, N.; Endou, A.; Takaba, H.; Kubo, M.; Broclawik, E.; Miyamoto, A.; "Does Metabolism of (S)-N-[1-(3-Morpholin-4-ylphenyl)ethyl]-3-phenylacrylamide Occur at the Morpholine Ring? Quantum Mechanical and Molecular Dynamics Studies." *Mater. Trans.* **2007**, *48*, 740-744.
9. Shaikh, A.R.; Broclawik, E.; Ismael, M.; Tsuboi, H.; Koyama, M.; Kubo, M.; Del Carpio, C.A.; Miyamoto, A. "Hyperconjugation with lone pair of morpholine nitrogen stabilizes transition state for phenyl hydroxylation in CYP3A4 metabolism of (S)-N-[1-(3-morpholin-4-yl phenyl) ethyl]-3-phenylacrylamide." *Chem. Phys. Lett.* **2006**, *419*, 523-527.
10. Wu, Y-J.; He, H.; Sun, L-Q.; Wu, D.; Gao, Q.; Li, H-Y. "Synthesis of Fluorinated 1-(3-Morpholin-4-yl-phenyl)-Ethylamines." *Bioorg. Med. Chem. Lett.* **2003**, *13*, 1725-1728.

11. Munro, A.; Girvan, H.; Mason, A.; Dunford, A.; McLean, K. "What makes a P450 tick?" *Trends Biochem. Sci.* **2013**, *28*, 140-150.
12. Chen, M.; White, M.C. "A predictably selective aliphatic C-H oxidation reaction for complex molecule synthesis." *Science* **2007**, *318*, 783-788.
13. Howell, J.; Feng, K.; Clark, J.; Tzrepkowski, L.; White, M.C. "Remote oxidation of aliphatic C-H bonds in nitrogen-containing molecules." *J. Am. Chem. Soc.* **2015**, *137*, 14590-14593.
14. Wickenden, A.D.; Yu, W.; Zou, A.; Jegla, T.; Wagoner, P.K. "Retigabine, A Novel Anti-Convulsant, Enhances Activation of KCNQ2/3 Potassium Channels." *Mol. Pharmacol.* **2000**, *58*, 591-600.
15. Bolleddula, J.; DeMent, K.; Driscoll, J.P.; Worboys, P.; Brassil, P.J.; Bourdet, D.L. "Biotransformation and bioactivation reactions of alicyclic amines in drug molecules." *Drug Metab Rev.* **2014**, *46*, 379-419.
16. Denissen, J.F.; Grabowski, B.A.; Johnson, M.K.; Boyd, S.A.; Uchic, J.T.; Stein, H.; Cepa, S.; Hill, P. "The orally active renin inhibitor A-74273. *In vivo* and *in vitro* morpholine ring metabolism in rats, dogs, and humans." *Drug Metab. Dispos* **1994**, *22*, 880-888.
17. Yu, L.; Jiang, Y.; Wang, L.; Sheng, R.; Hu, Y.; Zeng, S. "Metabolism of BYZX in Human Liver Microsomes and Cytosol: Identification of the Metabolites and Metabolic Pathways of BYZX." *PLoS One* **2013**, *8*, e59882.
18. Kaczorowski, G.J.; McManus, O.B.; Priest, B.T.; Garcia, M.L. "Ion Channels as Drug Targets: The Next GPCRs." *J. Gen. Physiol.* **2008**, *131*, 399-405.
19. Wulff, H.; Castle, N.A.; Pardo, L.A. "Voltage-gated potassium channels as therapeutic targets." *Nat. Rev. Drug Discov.* **2009**, *8*, 982-1001.
20. Jentsch, T.J. "Neuronal KCNQ Potassium Channels: Physiology and Role in Disease." *Nat. Rev. Neurosci.* **2000**, *1*, 21-30.
21. Boulet, I.R.; Raes, A.L.; Ottschytsch, N.; Snyders, D.J. "Functional effects of a KCNQ1 mutation associated with the long QT syndrome." *Cardiovasc. Res.* **2006**, *70*, 466-474.
22. Schwake, M.; Pusch, M.; Kharkovets, T.; Jentsch, T.J. "Surface Expression and Single Channel Properties of KCNQ2/KCNQ3, M-type K⁺ Channels Involved in Epilepsy." *J. Biol. Chem.* **2000**, *275*, 13343-13348.
23. Munro, G.; Dalby-Brown, W. "Kv7 (KCNQ) Channel Modulators and Neuropathic Pain." *J. Med. Chem.* **2007**, *50*, 2576-2582.
24. Grunnet, M.; Strøbæk, D.; Hougaard, C.; Christophersen, P. "K_v7 channels as targets for anti-epileptic and psychiatric drug-development." *Eur. J. Pharmacol.* **2014**, *726*, 133-137.

Reprinted from Kv7 channels as targets for anti-epileptic and psychiatric drug-development, 726, Morton Grunnet, Dorte Strøbæk, Charlotte Hougaard, Palle Christophersen, 133-137, 2014, with permission from Elsevier Ltd. License Number 4865160518097

25. Beisel, K.W.; Nelson, N.C.; Delimont, D.C.; Fritzsche, B. “Longitudinal gradients of KCNQ4 expression in spiral ganglion and cochlear hair cells correlate with progressive hearing loss in DFNA2.” *Mol. Brain Res.* **2000**, *82*, 137-149.

26. Langguth, B.; Elgoyhen, A.; Schlee, W. “Potassium channels as promising new targets for pharmacologic treatment of tinnitus: can internet-based ‘crowd sensing’ initiated by patients speed up the transition from bench to bedside?” *Exp. Opin. Ther. Targets* **2016**, *20*, 251-254.

27. Clark, S.; Antell, A.; Kaufman, K. “New antiepileptic medication linked to blue discoloration of the skin and eyes.” *Ther Adv Drug Saf* **2015**, *6*, 15-19.

28. Xiong, Q.; Gao, Z.; Wang, W.; Li, M. “Activation of Kv7 (KCNQ) voltage-gated potassium channels by synthetic compounds.” *Trends Pharmacol. Sci.* **2007**, *29*, 99-107.

29. Bentzen, B.H.; Schmitt, N.; Calloe, K.; Brown, W.D.; Grunnet, M.; Olesen, S-P. “The acrylamide (S)-1 differentially affects Kv7 (KCNQ) potassium channels.” *Neuropharmacology* **2006**, *51*, 1068-1077.

30. Schenzer, A.; Friedrich, T.; Pusch, M.; Saftig, P.; Jentsch, T.J.; Grötzinger, J.; Schwake, M. “Molecular Determinants of KCNQ (Kv7) K⁺ Channel Sensitivity to the Anticonvulsant Retigabine.” *J. Neurosci.* **2005**, *25*, 5051-5060.

31. Wuttke, T.V. Seebohm, G.; Bail, S.; Maljevic, S.; Lerche, H. “The New Anticonvulsant Retigabine Favors Voltage-Dependent Opening of the Kv7.2 (KCNQ2) Channel by Binding to Its Activation Gate.” *Mol. Pharmacol.* **2005**, *67*, 1009-1017.

32. ¹ Lange, W.; Geißendörfer, J.; Schenzer, A.; Grötzinger, J.; Seebohm, G.; Friedrich, T.; Schwake, M. “Refinement of the Binding Site and Mode of Action of the Anticonvulsant Retigabine on KCNQ K⁺ Channels.” *Mol. Pharmacol.* **2009**, *75*, 272-280.

33. Kim, R.Y.; Yau, M.C.; Galpin, J.D.; Seebohm, G.; Ahern, C.A.; Pless, S.A.; Kurata, H.T. “Atomic basis for therapeutic activation of neuronal potassium channels.” *Nat. Commun.* **2015**, DOI:10.1038/ncomms9116

34. Ponce, A.; Castillo, A.; Hinojosa, L.; Martinez-Rendon, J.; Cerejido, M. “The Expression of Endogenous Voltage-Gated Potassium Channels in HEK293 Cells Is Affected by Culture Conditions.” *Physiol. Rep.* **2018**, *6*, e13663.

35. Kumar, M.; Reed, N.; Liu, R.; Aizenman, E.; Wipf, P.; Tzounopoulos, T. “Synthesis and Evaluation of Potent KCNQ2/3-specific Channel Activators.” *Mol. Pharmacol.* **2016**, *89*, 667-677.

36. Tatulian, L.; Delmas, P.; Abogadie, F.C.; Brown, D.A. "Activation of Expressed KCNQ Potassium Currents and Native Neuronal M-Type Potassium Currents by the Anti-Convulsant Drug Retigabine." *J. Neurosci.* **2001**, *21*, 5535-5545.
37. Liu, R.; Tzounopoulos, T.; Wipf, P. "Synthesis and Optimization of Kv7 (KCNQ) Potassium Channel Agonists: The Role of Fluorines in Potency and Selectivity." *ACS Med. Chem. Lett.* **2019**, *10*, 929-935.
38. Weaver, C.D.; Harden, D.; Dworetzky, S.I.; Robertson, B.; Knox, R.J. "A Thallium-Sensitive, Fluorescence-Based Assay for Detecting and Characterizing Potassium Channel Modulators in Mammalian Cells." *J. Biomol Screen.* **2004**, *9*, 671-677.
39. Li, Y.; Gamper, N.; Hilgemann, D.W.; Shapiro, M.S. "Regulation of Kv7 (KCNQ) K⁺ Channel Open Probability by Phosphatidylinositol 4,5-Bisphosphate." *J. Neurosci.* **2005**, *25*, 9825-9835.
40. Kim, K.S.; Duignan, K.M.; Hawryluk, J.M.; Soh, H.; Tzingounis, A.V. "The Voltage Activation of Cortical KCNQ Channels Depends on Global PIP2 Levels." *Biophys. J.* **2016**, *110*, 1089-1098.
41. Wolfe, J.P.; Tomori, H.; Sadighi, J.P.; Yin, J.; Buchwald, S.L. "Simple, Efficient Catalyst System for the Palladium-Catalyzed Amination of Aryl Chlorides, Bromides, and Triflates." *J. Org. Chem.* **2000**, *65*, 1158-1174.
42. Wolfe, J.P.; Buchwald, S.L. "Palladium-Catalyzed Amination of Aryl Iodides." *J. Org. Chem.* **1996**, *61*, 1133-1135.
43. Komaromi, A.; Novak, Z. "Examination of the Aromatic Amination Catalyzed by Palladium on Charcoal." *Adv. Synth. Catal.* **2010**, *352*, 1523-1532.
44. Jia, L.; Liu, X. "The conduct of drug metabolism studies considered good practice (II): *In vitro* experiments." *Curr. Drug Metab.* **2007**, *8*, 822-829.
45. Knights, K.; Stresser, D.; Miners, J.; Crespi, C. "In vitro drug metabolism using liver microsomes." *Curr. Protoc. Pharmacol.* **2016**, *74*, 7.8.1-7.8.24.
46. Patras, A.; Julakanti, S.; Yannam, S.; Bansode, R.R.; Burns, M.; Vergne, M.J. "Effect of UV irradiation on aflatoxin reduction: a cytotoxicity evaluation study using human hepatoma cell line." *Mycotoxin Res.* **2017**, *33*, 343-350.
47. Baillie, T.; Davis, M. "Mass spectrometry in the analysis of glutathione conjugates." *Biol. Mass Spectrom.* **1993**, *22*, 319-325.
48. Chen, J.; Hessler, J.A.; Putchakayala, K.; Panama, B.K.; Khan, D.P.; Hong, S.; Mullen, D.G.; DiMaggio, S.C.; Som, A.; Tew, G.N.; Loptain, A.N.; Baker Jr., J.R.; Banaszak Holl, M.M.; Orr, B.G. "Cationic Nanoparticles Induce Nanoscale Disruption in Living Cell Plasma Membranes." *J. Phys. Chem. B* **2009**, *113*, 11179-11185.

49. Gao, Z.; Zhang, T.; Wu, M.; Xiong, Q.; Sun, H.; Zhang, Y.; Zu, L.; Wang, W.; Li, M. “Isoform-specific Prolongation of Kv7 (KCNQ) Potassium Channel Opening Mediated by New Molecular Determinants for Drug-Channel Interactions.” *J. Biol. Chem.* **2010**, *285*, 28322-28332.

50. Veitinger, S. The Patch-Clamp Technique. Figure 3. <https://www.leica-microsystems.com/science-lab/the-patch-clamp-technique/> (accessed July 10, 2020).